Master Thesis in Geographical Information Science nr 138

Assessing the suitability of using Sentinel-1A SAR multi-temporal imagery to detect fallow periods between rice crops

Lukasz Langowski

2021
Department of
Physical Geography and Ecosystem Science
Centre for Geographical Information Systems
Lund University
Sölvegatan 12
S-223 62 Lund
Sweden

Lukasz Langowski (2021). Assessing the suitability of using Sentinel-1A SAR multi-temporal imagery to detect fallow periods between rice crops
Master degree thesis, 30 credits in Master in Geographical Information Science
Department of Physical Geography and Ecosystem Science, Lund University

Assessing the suitability of using Sentinel-1A SAR multi-temporal imagery to detect fallow period between rice crops

---

Lukasz Langowski

Master thesis, 30 credits, in Geographical Information Sciences

Supervisor

Prof. Andy Nelson

University of Twente

Acknowledgements

First of all, I would like to thank my supervisor, Andy Nelson, for his support, advice, feedback and reassurance, which were invaluable and helped me throughout all the aspects of this thesis.

Many thanks to my family, especially to Piotr, for their support, warm words, and encouraging me to complete the thesis. Also, for putting up with me throughout the ups and downs that I experienced during the research and the writing process.

I would also like thank the Pest Risk Identification and Management (PRIME) project team for sharing the field data and Sentinel-1A imagery, without which this research would have been impossible.

Abstract

Fallow, understood as a period where no crop is cultivated during a growing season, is an important crop management practice. Fallow plays an important role in pest and disease management, and monitoring the presence and duration of fallow can have implications for understanding the extent and effectiveness of this agricultural practice. Therefore, fallow period mapping using remotely sensed data is a widely researched topic. However, its identification using remotely sensed data is often problematic due to the fallow backscatter values being similar to other land cover classes. SAR data tends to be applied to crop identification, paying little to no attention to fallow. This thesis investigated fallow backscatter characteristics and detection methods that could be used for identification of fallow periods between rice crops. Timeseries of backscatter from Sentinel-1A data were plotted for 83 fields in two areas in the Philippines. Rice crop and fallow temporal characteristics were derived from field data and correlated with the plotted backscatter.

The start and end of fallow showed significant differences that could be used for detecting fallow periods. However, the detection gave acceptable results only using VH polarisation and the VV/VH ratio, while VV polarisation resulted in the lowest accuracy. A backward fallow detection method was also employed, where the end of the rice season indicated the fallow start, and the start of the rice season marked the fallow end. This method proved more successful in determining fallow duration than using the fallow itself. Fallow duration was also categorised according to its length into short and long fallow. In short fallow periods, backscatter was mainly decreasing during the whole fallow period, while in long fallow periods, some variation was observed approximately halfway through the fallow duration, which were attributed to short-term drought tolerant crops. Fallow backscatter values for irrigated and rainfed fields were also compared. Ecosystem type was found to have a significant effect on fallow backscatter only in one of the two study areas, indicating that water availability may affect fallow duration. The study found that SAR backscatter can be used to map fallow by detecting rice seasons, although the detected fallow duration was slightly overestimated. The study lacked information about the conditions of the fields during the fallow periods; therefore, future studies could benefit from more information about weed prevalence, planting of non-rice crops, water or rainfall deficit, and flooding/tillage activities during or after fallow.

Keywords: Geography, Geographical Information System, GIS, Remote Sensing, Fallow, Detection, Sentinel-1A, Synthetic-aperture radar, SAR

Table of contents

Acknowledgements iv
Abstract v
Table of contents vi
List of figures ix
List of tables xi
List of abbreviations xii
1 Introduction 1
1.1 Problem statement 2
1.2 Research aim and objectives 3
1.3 Research questions 3
2 Background 5
2.1 Fallow duration 5
2.2 Remote sensing 5
2.3 SAR 7
2.4 Polarisation 9
2.5 Rice recognition 10
2.6 Fallow recognition 12
3 Study areas and data 15
3.1 Study area selection 15
3.2 Study areas 15
3.3 Data 17
3.3.1 Field data 17
3.3.2 Sentinel-1A data and pre-processing 17
3.3.3 Rainfall data 18
4 Methodology 19
4.1 Sentinel-1A mean backscatter value extraction 19
4.2 Computation of VV/VH polarisation ratio 20
4.3 Savitzky-Golay smoothing filter 20
4.4 Phenological/cropping features estimation 21
4.5 Backscatter plotting (exploratory analysis) 22

4.6 Estimation of additional fallow periods 23
4.7 Estimation of reliability of the farmer reported dates 23
4.8 Selected rice crops and fallow periods 25
4.9 Fallow duration 27
4.10 Statistical tests 27
4.11 Fallow detection 28
4.12 Extraction of rainfall data 28
5 Results 29
5.1 Temporal backscatter characteristics of rice and fallow 29
5.2 Polarisation significance tests 36
5.3 Fallow and rice detection 38
5.3.1 Fallow periods detection 38
5.3.2 Rice season detection 40
5.3.3 Between crops fallow detection 42
5.4 Rainfall 44
6 Discussion 47
6.1 Fallow and rice SAR backscatter characteristics and fallow duration 47
6.1.1 Fallow start 48
6.1.2 Mid-fallow 49
6.1.3 Fallow end 50
6.2 Fallow duration 51
6.3 Fallow differences based on ecosystem types 52
6.4 Fallow and rice detection using SAR time-series 53
6.5 Fallow detection between rice crops 54
6.6 Discussion of the data used in the study 55
6.7 Limitations and recommendations 56
7 Conclusion 57
References 59
Appendix A. IRRI's Field Survey Protocol for Pangasinan and Iloilo provinces 69
Appendix B. Brief list of Sentinel-1A pre-processing staps 71
Appendix C. Boxplots showing differences of backscatter values between the fallow start and end 72
Appendix D. Boxplots of rice and fallow temporal backscatter separated by ecosystem type 73
Appendix E. Average dekad rainfall separated by ecosystem type 77

Appendix F. Fallow detection with ratoon fields removed.....78
Appendix G. Time-series for each field in Pangasinan and Iloilo.....80
Series from Lund University.....247

List of figures

Figure 1. SAR backscattering mechanisms in a) flooded fields; b) paddy rice; c) dry smooth soil; d) wet smooth soil; e) dry rough soil; and f) wet rough soil. 8

Figure 2. Map of the selected fields in Pangasinan and Iloilo provinces. 16

Figure 3. Examples of the Sentinel-1A image pixels (DN) in VH polarisation (upper) and VV polarisation (lower) within field 106 at a) crop establishment, b) flowering, c) harvest, d) fallow start and e) fallow end. Size of each pixel is 20x20m. 19

Figure 4. Example of the original unsmoothed temporal backscatter data (grey) overlayed with the Savitzky-Golay filtered/smoothed data (orange). 21

Figure 5. Example of potential recall bias in the timeseries data in last rice crop establishment (CE1) date. 24

Figure 6. Distribution of the accepted fields in Pangasinan (top) and Iloilo (bottom). 26

Figure 7. Boxplots of the backscatter coefficient derived from Sentinel-1A for rice planting activities, cropping stages and fallow in Pangasinan for VH (top), VV (middle) and VV/VH polarisation ratio (bottom). Fallow number relates to Sentinel-1A revisit time since the start of fallow. Shades of green indicate rice cropping phases and shades of grey are fallow durations (at 12-day intervals) from harvest. 32

Figure 8. Boxplots of the backscatter coefficient derived from Sentinel-1A for rice planting activities, cropping stages and fallow in Iloilo for VH (top), VV (middle) and VV/VH polarisation ratio (bottom). Fallow number relates to Sentinel-1A revisit time since the start of fallow. Shades of orange indicate rice cropping phases and shades of grey are fallow durations (at 12-day intervals) from harvest. 33

Figure 9. Boxplots of the backscatter coefficients for fallow separated by fallow duration (short and long) in Pangasinan for VH (top), VV (middle) and VV/VH ratio (bottom). Fallow number relates to Sentinel-1A revisit time since start of fallow. 34

Figure 10. Boxplots of the backscatter coefficients for fallow separated by fallow duration (short and long) in Iloilo for VH (top), VV (middle) and VV/VH ratio (bottom). Fallow number relates to Sentinel-1A revisit time since the start of fallow. 35

Figure 11. Boxplots of the temporal differences between the observed fallow start (FS) date and the obtained VH and VV local maxima, and VV/VH ratio minima in a) Pangasinan and b) Iloilo. RMSE is expressed in days. 39

Figure 12. Boxplots of the temporal differences between the observed fallow end date (FE) and the obtained VH and VV local maxima, and VV/VH ratio minima in a) Pangasinan and b) Iloilo. RMSE is expressed in days. 40

Figure 13. Boxplots of the temporal differences between the reported crop establishment date and the VH and VV local minima, and VV/VH ratio maxima in a) Pangasinan and b) Iloilo. RMSE is expressed in days. 41

Figure 14. Boxplots of the temporal differences between the reported harvest date and the VH and VV local maxima, and VV/VH ratio minima in a) Pangasinan and b) Iloilo. RMSE is expressed in days. 42

Figure 15. Boxplots of the temporal differences between the reported harvest date (fallow start) and the detected VH and VV local maxima, and VV/VH ratio minima in a) Pangasinan and b) Iloilo. RMSE is expressed in days. 43

Figure 16. Boxplots of the temporal differences between the reported crop establishment date (fallow end) and the detected VH and VV local minima, and VV/VH ratio maxima in a) Pangasinan and b) Iloilo. RMSE is expressed in days. 44

Figure 17. Average rainfall per dekad covering the duration of the fallow periods in Pangasinan (upper) and Iloilo (lower). Dekad1 corresponds to the start of fallow in each field. Duration based on fallow occurrence with Dekad16 containing rainfall data only for the longest fallow periods. 45

List of tables

Table 1. The specifications of the Sentinel-1A data and acquisition periods. 18

Table 2. Number of accepted samples based on the cropping type. 25

Table 3. Fallow duration per number of fields in Pangasinan and Iloilo. 27

Table 4. p-values for Kruskal-Wallis test between crop establishment, harvest and fallow start and end at VH, VV and VV/VH polarisation ratio. Pangasinan *n*=128; Iloilo *n*=157. 36

Table 5. p-values for post hoc pairwise comparison from Kruskal-Wallis test between crop establishment, harvest, fallow start and fallow end at VH, VV and VV/VH polarisation ratio. Pangasinan *n*=128; Iloilo *n*=157. 37

Table 6. p-values between fallow start and end separated by the fallow duration (short and long) from Mann-Whitney U test. Pangasinan *n*=20; Iloilo *n*=21. 37

Table 7. p-values of Mann-Whitney U test between fallow occurring in the irrigated and rainfed fields. Pangasinan *n*=172; Iloilo *n*=134. 38

Table 8. Root mean square error (RMSE) result for the start and end of fallow. The RMSE was performed for derived minima and maxima dates from fallow backscatter and the farmer reported fallow periods. Pangasinan *n*=20; Iloilo *n*=21. 39

Table 9. Root mean square error (RMSE) result for detecting the start and end of rice season. The RMSE was performed for derived minima and maxima dates from the rice backscatter and the farmer reported rice season dates. Pangasinan *n*=44; Iloilo *n*=57. 41

Table 10. Root mean square error (RMSE) result for detecting the start and end of between crops fallow periods. The RMSE was performed for derived minima and maxima dates from the rice backscatter and farmer reported dates. Pangasinan *n*=9; Iloilo *n*=9. 43

Table 11. Average amount of rainfall during the fallow periods received in the fallowed fields in Pangasinan and Iloilo. 44

Table 12. Average fallow duration observed from the farmer questionnaires and detected between crops. Pangasinan *n*=9; Iloilo *n*=9. 55

List of abbreviations

AOI	Area of interest
CE	Crop establishment (rice-growth stage)
CE#	Day after crop establishment – number indicating days after crop establishment
dB	Decibel (measure of SAR backscatter intensity)
EOS	End of rice season
F#	Fallow - number indicating consecutive 12th day after harvest
FE	End of fallow
FLW	Flowering (rice-growth stage)
FS	Start of fallow
H	Harvest (rice cropping activity)
IRRI	International Rice Research Institute
LP	Land preparation (rice cropping activity)
NDVI	Normalised difference vegetation index
PRIME	Pest Risk Identification and Management project
PRISM	Philippine Rice Information System
PSA	Philippine Statistics Authority
RMSE	Root mean square error
SAR	Synthetic-aperture radar
SG	Savitzky-Golay filter
SOS	Start of rice season
VH	Vertical transmit and horizontal receive (cross-polarised) SAR polarisation
VV	Vertical transmit and vertical receive (co-polarised) SAR polarisation
VV/VH	Depolarisation VV/VH ratio
σ^0	Backscatter scattering coefficient expressed in dB

1 Introduction

Rice is one of the most important staple crops in the world and is the biggest "single source of calories for more than 3.7 billion people" (Nelson et al., 2014, p. 10775), which accounts for approximately 50% of the global population. Over 90% of the global rice production is based in Asia (Clauss et al., 2018a), and projections suggest that the overall agricultural production will have to increase by 70% by 2050 to satisfy the global demand for food (Carvajal-Yepes et al., 2019), putting more pressure on improving rice yields.

Rice is an annual crop that is adapted to grow in wetland environments (paddy fields). Therefore, in tropical areas of the South-East Asia rice is typically grown during the wet season. However, places with good irrigation management, e.g., areas with dams or other man-made water retaining structures, can grow rice during the dry seasons (Litsinger et al., 2009).

In areas with relatively stable temperatures during the whole year, high levels of rainfall and good irrigation systems, such as in the Philippines, up to three rice crops can be planted and harvested during a year (Bégué et al., 2018). However, constant presence of rice crops throughout the year, together with other habitats in the neighbouring fields, create favourable conditions for pest and rice disease development and allows pests to carry over from crop to crop, which can lead to yield losses (Rola and Pingali, 1993; Litsinger et al., 2009). Savary et al. (2019) estimate the average global loss of rice yields due to pest and crop disease to be approximately 30%. Application of pesticides is one of the solutions to reduce pest or disease outbreaks and increase rice yields (Rola and Pingali, 1993). However, persistent use of pesticides has been linked to negative effects upon the health of farmers and consumers; contamination of ground and surface water that leads to reduction of inland fishing resources (Parveen and Nakagoshi, 2001); secondary pest outbreaks due to removal of their natural enemies by the pesticides (Litsinger et al., 2009); and/or to disproportionally higher energy and pesticide use in relation to much lower increase of rice yields over time (Rola and Pingali, 1993, Chapter 3). Due to this, more recognition is given to more natural crop management methods, such as fallowing (Schoenly et al., 2010).

Fallow period is part of crop rotation or succession practice that takes place after crop harvest and is a non-productive period of varying duration when no crop is purposely cultivated during a growing season (Wojtkowski, 2008).

The primary purposes of fallow periods are to restore soil and ecosystem fertility, conserve soil moisture, and remove toxic substances from pesticides and pathogens. Fallow is also used as a natural way of pest management that disrupts the pest or disease growth conditions and habitats by the absence of crops/habitat (Mertz, 2002; Litsinger et al., 2009; Schoenly et al., 2010; Bégué et al., 2018; Minh et al., 2019). However, in the eyes of farmers, fallow can be seen as the least favourable option, as it removes potential income that planting other crops, for example drought tolerant plants such as garlic, could bring (FAO, 2013). Therefore, fallow is often not a deliberate choice, but rather a result of limited waster availability, especially in areas with lack of irrigation systems (Nguyen et al., 2015), such as hilly terrains where rice fields are in the form of terraces. However, Mertz (2002) and Wojtkowski (2008) argued that

well cultivated post-fallowed fields are overall cost-effective by bringing higher yields and requiring lower amounts of pesticides and insecticides.

Successful insect pest management requires the fallowing practice to last long enough, usually more than one pest generation, and to be spread over multiple neighbouring fields in order to be effective (Schoenly et al., 2010). This is due to the fact that habitats which neighbour the rice fields provide refuge for certain rice pests and their natural enemies throughout the year. Therefore, there is an organisational problem where farmers and local governments have to synchronise the fallowing period to start at the same time (Schoenly et al., 2010). Yet, most of the rice fields in the world are smallholders that are smaller than two hectares (Nelson et al., 2014), which increases the problem for synchronising and monitoring fallow periods over large areas. However, spatial image analysis could help with this issue.

Remote sensing (RS) is effective in observing temporal and spatial changes in cropping practices over a wide variety of crops (Bégué et al., 2018). In tropical regions, where the cloud coverage is high, optical sensors have limited application (Clauss et al., 2018a). Alternatively, active microwave sensors, also known as a synthetic-aperture radar (SAR), are able to penetrate clouds and collect the data during day and night. Moreover, SAR has been proven to be very good at detecting changes in the lowland rice growth stages, and with the right understanding of backscatter values (dB) it can act as a cheaper alternative to time consuming land surveys (Nelson et al., 2014). However, most RS studies have focused on crop mapping, paying little attention to the fallow periods.

Moreover, Bégué et al. (2018) observed that in mapping applications fallow periods are often classified as cropped land instead of as a separate class. They concluded that this may be due to the difficulties in differentiating short fallow fields from cropped fields that may be due to "climatic and soil conditions, cropping techniques, crop failure, or may be confused with surrounding ecosystems due to its natural regeneration" (p. 103).

1.1 Problem statement

In the tropical regions of Asia, synchronous rice cultivation creates fallow periods of about 1 to 3 months, mostly between the dry and wet seasons, due to the need to limit water usage in the dry season (Schoenly et al., 2010). Those instances create a possibility for natural management of insect pests, diseases, and weeds. The present research focuses on fallow practices in the Philippines, and the detailed description of the study areas, along with the justification for their choice, can be found in Chapter 3.

Timely mapping of the rice fields in the Philippines can be challenging due to high cloud coverage, especially during the wet season. However, SAR images, thanks to their cloud penetration capabilities, have been successfully employed in various rice observations studies (Nelson et al., 2014). Additionally, improved spatial and temporal resolution, as well as the dual polarisation capabilities of the Sentinel-1A satellite open new prospects for more detailed exploration of temporal changes in the rice field monitoring (Minh et al., 2019). Hence, Sentinel-1A's SAR data, together with ancillary information, could be used to improve the understanding of the fallow backscatter characteristics, duration, and to indicate the occurrence

factors, e.g., due to type or lack of irrigation system, and help monitor potential pest outbreaks over large areas, all of which would be beneficial to improving food security.

Many studies that utilised SAR images for application in rice crop analysis usually concentrated on detecting or monitoring rice types and rice growth stages, or predicting rice yields, whereas fallow analysis received very little attention by either classifying it as part of the early rice growth stage or not considering it at all (for example Asilo et al., 2014; Nelson et al., 2014; Nguyen et al., 2015; Mansaray et al., 2017; Nguyen and Wagner, 2017; Clauss et al., 2018a), leaving a knowledge gap, which the present research aims to address, with the aims and objectives described below.

1.2 Research aim and objectives

The overall aim of this study is to detect fallow periods using Sentinel-1A and field data in the Philippines.

The specific objectives of this study are to:

1. Describe the SAR C-band temporal backscatter behaviour over fallow periods;
2. Measure the differences in multi-temporal SAR backscatter values between fallow in irrigated and rainfed fields;
3. Derive backscatter values over rice seasons and fallow periods that can be used for fallow identification;
4. Determine which polarisation in multi-temporal SAR images is best at discriminating between fallow and rice.

1.3 Research questions

The above objectives will be achieved by answering the following research questions:

1. What are the characteristics of SAR backscatter during fallow period?
2. Are fallow backscatter values different for irrigated and rainfed fields?
3. Can fallow be detected using SAR time-series?
4. Which polarisation (VV, VH or VV/VH polarisation ratio) is best at detecting fallowing?

2 Background

2.1 Fallow duration

The duration of a fallow period can vary from a few weeks to a few years and usually depends on crop type and reason for entering fallow practice. For example, in dry areas of bush/fallow swidden landscapes that are cultivated for a few years and later cleared by fire (where fallow is classed as an unmanaged land), fallow can last from a few to approximately ten years, during which natural shrub vegetation has enough time to develop (Leisz and Rasmussen, 2012). However, in tropical Asia, fallow within rice fields typically lasts from several days to three months between dry and wet seasons (Schoenly et al., 2010; Sander et al., 2018) usually during the dry season when farmers with limited water availability (e.g., with no access to irrigation) are no longer able to grow rice or have no access to other drought-tolerant crops (Schoenly et al., 2010), such as garlic (FAO, 2013). Another common reason for fallow, typically of a shorter duration, is the period between crops during which some type of land preparation can take place, such as tillage or irrigation (Sander et al., 2018). There are therefore many definitions of fallow, but for the purpose of this research fallow will be classed as any period after harvest where no crop was being grown nor land preparation was taking place, but could have had some vegetation coverage (e.g., weeds or naturally ratooned crop, which is where crop grows again from stubble left in the field after harvest [Boschetti et al., 2017]) that was not purposely planted for harvest, as previously mentioned in the Introduction.

In tropical Asia, where up to three rice harvests can be achieved throughout the year, the fallow length is becoming shorter (Litsinger et al., 2009). Therefore, it is important to understand how this shortening period of shifting cropping type can be identified with remote sensing. Similar trends of shortening fallow periods were observed in other crop types and across various locations (e.g., Dalle and de Blois, 2006; Delang et al., 2016). Shortening fallow periods pose potential problems for enhancing environmental management efforts. The management of paddy rice fields affect various environmental aspects, which are characterised by an increased water usage due to the need for a profuse amount of water during growing stages (when compared to other staple crops), increased greenhouse gases emissions through significant release of methane (CH_4) and CO_2 gases, as well as being a key location of transmission for some diseases, for example avian influenza A (H5N1) disease (Dong and Xiao, 2016). Therefore, mapping and monitoring of rice at local and intra-national scales could aid wide-scale decision making, improve environmental management practices (Dong and Xiao, 2016) and can lead to better use of pesticides and fertilisers (Vreugdenhil et al., 2018).

2.2 Remote sensing

Remotely sensed data has been widely used for mapping and monitoring agricultural environments with various types of sensors (Kuenzer and Knauer, 2013; Bégué et al., 2018; Tong et al., 2020). However, mapping of fallow has been given much less consideration. Fallow classification and mapping is often omitted from the agricultural classification as a separate land cover type. Tong et al. (2020) went as far as to call fallow the “forgotten land use class” in mapping agricultural lands of some parts of the world, especially the grass fallow systems in semi-arid regions.

The limited use of remote sensing to detect fallow is not without good reason. One of the main challenges in mapping rice fields stems from the fact that most of them are smallholders of a size smaller than two hectares (Nelson et al., 2014). Therefore, mapping with coarser resolution sensors can be limited in application for fallow observation where not every field or the entirety of a field may be fallowed.

During the 80's and early 90's Landsat MSS/TM was the main image type utilised for mapping paddy rice (Kuenzer and Knauer, 2013; Dong and Xiao, 2016). This, however, has changed with the launch of the SAR-C radar in the mid-90s, when mapping of rice fields from SAR derived images was gaining in popularity, for example ERS-1 and RADARSAT-1 C-band, and JERS L-band data (Liew et al., 1997; Le Toan et al., 1997; McNairn and Brisco, 2004; Clauss et al., 2018b). However, due to restricted accessibility, the coarseness of early SAR images, the complexity of SAR scattering applicability, and small paddy rice field sizes, which were limited by the requirement for good drainage and irrigation conditions, SAR data for paddy rice mapping was not as prevalent as was the case with multispectral images (Inoue and Sakaiya, 2013; Dong and Xiao, 2016; Steele-Dunne et al., 2017). Additionally, early SAR sensors recorded information about a target in a single polarisation and frequency that hampered the interpretation of SAR data. To alleviate this problem and achieve similar classification results to multichannel optical sensors, acquisition of multitemporal SAR data was required (McNairn and Brisco, 2004). Enhanced application of SAR for rice field mapping increased between 2000 and 2020, which was correlated with wider availability of SAR satellites, improved image resolution and application of various SAR bands and polarisations (e.g., ENVISAT ASAR, RADARSAT-2, ALOS, COSMO-SkyMed or TerraSAR-X; Chen et al., 2007; Bouvet et al., 2009; Zhang et al., 2009; Lopez-Sanchez et al., 2011; Torbick et al., 2011a; Li et al., 2012; Lopez-Sanchez et al., 2012; Inoue and Sakaiya, 2013; Inoue et al., 2014; Nelson et al., 2014).

Even then, some of the main limitations that potentially reduced classification accuracy were poor image acquisition frequency, reliance on temporal averaging and incidence angle normalisation algorithms to make the data usable in the temporal cropping classification or crop identification (Inoue et al., 2014; Bégué et al., 2018). All of those aspects potentially reduce classification accuracy. However, since the launch of ESA's Sentinel-1A satellite those problems have mostly been eliminated or at least reduced because the Sentinel-1A satellite offers a regular temporal revisit frequency, acquires images at a constant incidence angle and has improved spatial resolution (Geudtner et al., 2013; Veloso et al., 2017; Bégué et al., 2018; Vreugdenhil et al., 2018)

Despite the recent improvements of radar sensors and increased availability of SAR data, the use of SAR data for agricultural applications is still lagging behind when compared with optical data. Reasons for this include a higher level of complexity involved in interpretation of such data, but also a diversity of SAR frequencies/polarisations that have various canopy penetration capabilities (Veloso et al., 2017). Additionally, intense rainfalls and high winds negatively impact SAR data by generating random scatterings that are characterised by strong backscatter increases during such events (Lopez-Sanchez et al., 2012; Holecz et al., 2013; Nelson et al., 2014). Nelson et al. (2014) noted that those effects can be corrected for but require knowledge of the weather conditions at the time of image acquisition. Another aspect that could have

hampered the spread of SAR for crop mapping is a greater requirement for field visits and/or farmer interviews than in the case of optical data, to help interpret what is being observed by SAR backscatter at given date (Asilo et al., 2014; Clauss et al., 2018a; Onojeghuo et al., 2018). To eliminate this problem some studies correlated SAR data with optical images to visually identify or validate which fields were fallowed and planted with what type of crop, and as a result reduced the need for field visits (Gumma et al., 2011; Torbick et al., 2011a; Nguyen and Wagner, 2017; Das and Pandey, 2019; Dirgahayu et al., 2019; Minh et al., 2019; Muthukumarasamy et al., 2019; Rudiyanto et al., 2019; Chandna and Mondal, 2020; Mohammed et al., 2020; Pasha et al., 2020). This approach showed good results, but its application required a level of priori knowledge about the studied area and does not always eliminate the need for a field visit. Laborte et al. (2010) trialled a signature generalisation technique where agricultural signatures derived from multiple images within one season were applied for classifying historical LANDSAT images for which there was no field data available. Their study gave promising results but based on the reviewed literature this approach was not expanded to SAR data classification. In the past few years many studies have utilised machine and deep learning for mapping and monitoring rice fields where multitemporal data from multiple sensors can be combined for improved rice classification accuracy (Onojeghuo et al., 2018; Setiyono et al., 2018; Tian et al., 2018; Bazzi et al., 2019; Cai et al., 2019; Mansaray et al., 2019; Zhou et al., 2019). However, this approach did not fully remove the requirement for some level of a priori knowledge about the studied areas and often involved large input datasets (Bazzi et al., 2019; Weiss et al., 2020). Despite many limitations, SAR remains one of the most favourable options for mapping cropping activities, as will be described below.

2.3 SAR

In the past decade, SAR has become a popular method for crop mapping and detection in the tropical regions, such as Philippines, because of its cloud penetration capabilities (Le Toan et al., 1997; Nelson et al., 2014). SAR is able to observe crop development stages, from planting to harvest, thanks to the interaction of radar backscatter with vegetation that is determined by dielectric properties (affected by water content), size/height, shape, orientation and roughness of foliage, stems and grains that change at each crop development stage (Oh et al., 2009; Asilo et al., 2014; Inoue et al., 2014; Nelson et al., 2014). Moreover, SAR is also useful for detecting fallow because of SAR behaviour that is affected by soil roughness and moisture (dielectric properties; Steele-Dunne et al., 2017). Therefore, wet rough/tilled soil reflects or diffuses more microwave signal (appearing lighter in the SAR images) than dry tilled ground (appearing slightly darker than wet soil), and even more than settled/unploughed dry or wet soil because in the latter cases more signal is specularly reflected. Similarly, with flooded soils, water exposed during early rice development, where specular reflection is the highest, most signal is reflected away from the SAR sensor (Brogioni et al., 2010). See Figure 1 for illustration of the backscattering mechanisms.

Additionally, SAR sensors provide unique capabilities for observing cropping events because different bands have various vegetation penetration capabilities. Radar frequency results in different soil or crop canopy penetration capabilities of the microwave wavelengths. Shorter wavelengths, such as C- and X-band sensors, are most widely used in agricultural applications

(Lopez-Sanchez et al., 2011; Inoue et al., 2014) because they are better at detecting crop types and discriminating between vegetated and bare soils thanks to a good balance of canopy penetration abilities and also because they can detect residue cover after harvest (McNairn et al., 1998). However, X-band is limited to detecting only vegetation canopy making it difficult to use for distinguishing between plants and other objects (Suga and Konishi, 2008; Minh et al., 2019). In contrast, C- and L-bands are sensitive to water and crop geometry, making them better suited for differentiating between vegetated and non-vegetated fields, than shorter wavelengths (e.g., X-band), which are more suited for detecting smaller or younger vegetation (McNairn et al., 2002; Suga and Konishi, 2008; Inoue et al., 2014; Dong and Xiao, 2016; Minh et al., 2019). Moreover, L-band proved to be better at detecting variations in bare soils and observing soil-conditions in vegetated areas (McNairn and Brisco, 2004), but have more limited application in detecting vegetated and non-vegetated fields than C-band sensors.

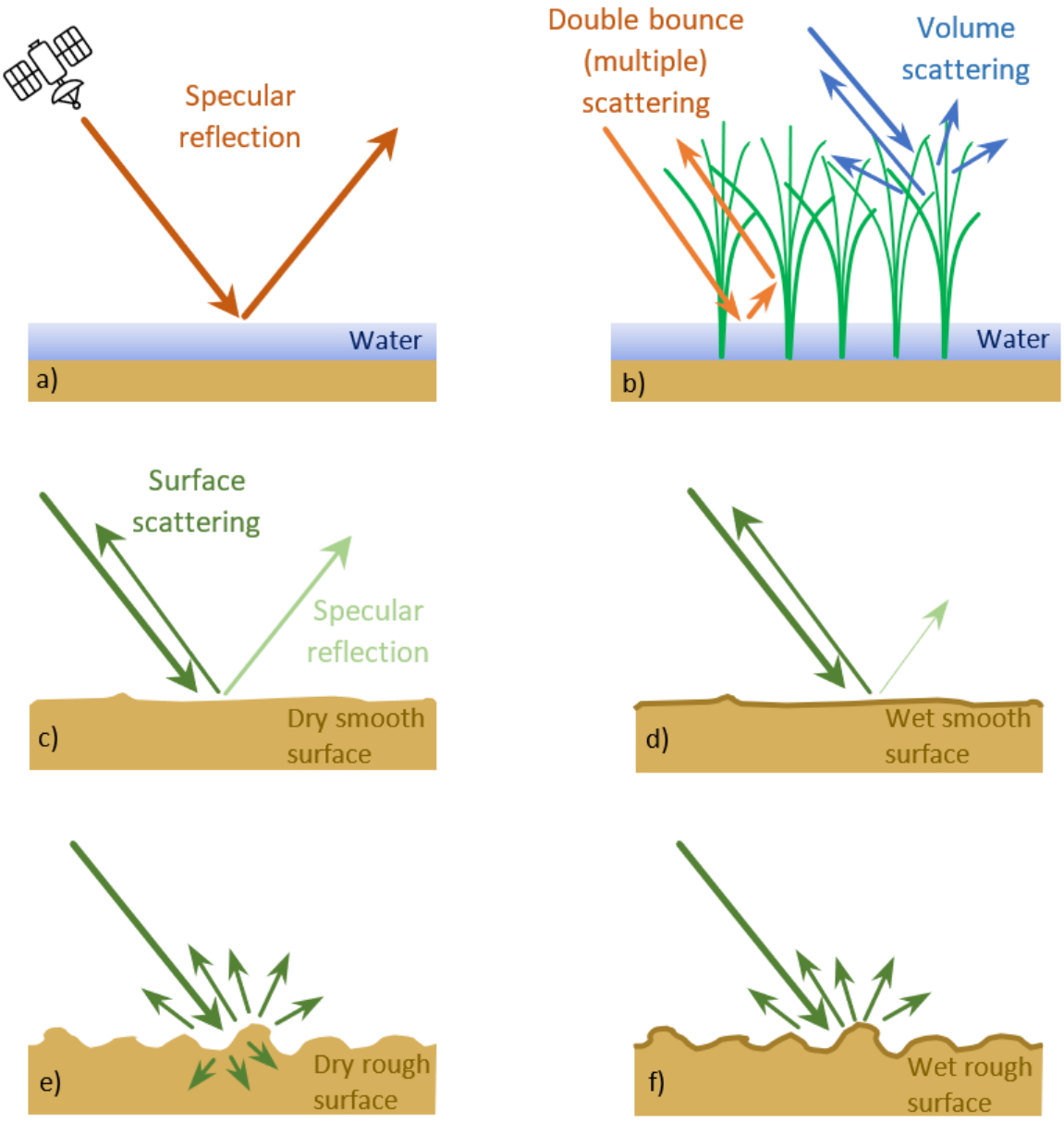

Figure 1. SAR backscattering mechanisms in a) flooded fields; b) paddy rice; c) dry smooth soil; d) wet smooth soil; e) dry rough soil; and f) wet rough soil.

2.4 Polarisation

Polarisation is an indication of transmitted and received electromagnetic wave geometrical travel direction (horizontal, vertical or circular) which is perpendicular to the magnetic field (NASA, 2020). Polarisations are represented by signatures or backscatter values which are a sum of multiple individual scatterers within a pixel (McNairn et al., 2002). Various polarisations reveal different details about the observed surface that depend on the land cover type properties (e.g., surface roughness or volume scattering) that result in different scattering mechanisms. Cross-polarisations detect the repolarisation (orthogonal H or V) – change in the degree of polarisation vector after interaction with a target – from the transmitted linear wave (V or H). Whereas co-polarisations detect the intensity between identical transmitted (V or H) and received (V or H) polarisations (McNairn et al., 2002).

In SAR's C-band spectrum, the VV polarisation has been shown to be better at detecting small grain crops, such as rice, than larger crops, because the VV polarisation is less susceptible to volume scattering than the VH polarisation as more signal can penetrate through the canopy (Oh et al., 2009; Gherboudj et al., 2011; Nelson et al., 2014; Xu et al., 2019). On the other hand, cross-polarised SAR signal, such as VH, is more receptive to the canopy overall structure and provide different information of the canopy or surface area than the co-polarised VV measurements (McNairn and Brisco, 2004). Therefore, VH polarisation increases faster during crop hight increases than the VV polarisation (Gherboudj et al., 2011). Reasons for this can be accredited to the lower attenuation by leaves and stems at the VH polarisation (Oh et al., 2009; Mansaray et al., 2017). The VV polarisation, on the other hand, could be a better indicator of fallow because of low depolarising properties of bare ground (NASA, 2020).

In terms of moisture content, both C-band polarisations (VV and VH) provide more information about soil moisture content during crop season than after harvest or in the exposed soil because of multiple/increased volume scattering mechanisms that occur in vegetation canopy (Khabbazan et al., 2019), as opposed to only volume scattering present in bare soils. Whereas the co-polarised (VV) L-band wavelengths are most sensitive to soil moisture content. This property is slightly less prominent in the C-band wavelength due to a higher sensitivity to small vegetation that can grow within bare fields, especially at the VV polarisation (Brogioni et al., 2010). However, a higher sensitivity to even minimal vegetation coverage makes the C-band better suited for application in crop monitoring.

Additionally, a polarimetric channel ratio of the C-band backscatter, such as VH/VV or VV/VH, has been found to be a good indicator for vegetation densities and their structure, monitoring crop growth stages (Vreugdenhil et al., 2018) and vegetation water content (Kim et al., 2012) of various crop types. Gherboudj et al. (2011) observed that the VH/VV depolarisation ratio tends to increase with crop height, which they accredited to higher sensitivity of the VH polarisation to vegetation height than the VV polarisation.

Furthermore, soil roughness differs based on the type of tillage method used (McNairn and Brisco, 2004), which can be helpful for observing the start of land preparation after harvest or fallow. For example, the VH polarisation has been shown to have clearest separation of backscatter values between bare soils and grounds with residue standing after harvest at various incidence angles when compared to the VV polarisation, which experiences a lot of backscatter

value mixing (McNairn and Brisco, 2004). Those findings suggest that tilled fields could be distinguished from the fallowed lands that are left untouched for prolonged periods. Moreover, polarisation ratios, such as VV/VH, VV/HH and VH/VV, have been suggested to be better indicators for measuring soil roughness, because smooth surfaces differed significantly between each polarisation, whereas very rough surfaces did not show any distinction (McNairn and Brisco, 2004). In bare soils depolarised VH/VV ratio decreases with increasing soil roughness, as opposed to VH/VV increases observed in vegetation growth stages (Gherboudj et al., 2011). In the VV/VH polarisation ratio the trend is expected to resemble this but in the reverse direction. Additionally, water alters the dielectric properties of soil backscatter (McNairn and Brisco, 2004) by decreasing soil roughness sensitivity in the VH polarisation in very moist soils (Oh, 2004).

As mentioned above, the cross-polarisations (e.g., VH) have been shown to be better at distinguishing bare fields from vegetated fields (Steele-Dunne et al., 2017); however, Baronti et al. (1995) reported good discrimination results between bare surfaces and vegetated fields by using linear HV polarisation together with circular RL polarisation. In this case, bare surfaces were represented by significantly higher RL backscatter values than the cross-polarised HV backscatters. Comparable results were also achieved by Ferrazzoli et al. (1997) where circular RL, RR, HV-HH and HV-VV C-band polarisations were applied to distinguish cropped areas from bare soils, which also resulted in bare fields having higher backscatter values than the vegetated areas.

To summarise, discrimination between canopy cover and fallow fields can be distinguished in SAR backscatter data thanks to the sensitivity of spatial radar signal to the variations in soil roughness, soil and vegetation water content as well as vegetation structure and height (Vreugdenhil et al., 2018).

2.5 Rice recognition

“Paddy rice is the only staple grain that needs to be transplanted” (Dong and Xiao, 2016, p. 216), and the beginning of the rice crop season can vary by a few weeks across fields located within the same region (Le Toan et al., 1997), even if planting was done by direct seeding (Boschetti et al., 2017). For this reason, mapping and monitoring of paddy rice has always had to be done with the use of multitemporal images (Kuenzer and Knauer, 2013). Early paddy rice mapping and monitoring relied on spectral bands from optical imagery, such as SPOT, MODIS or Landsat, that were sensitive to water bodies, soil and vegetation (Dong and Xiao, 2016). Common classification approaches included on-screen digitization, supervised and unsupervised classifiers, knowledge-based and phenology-based approaches, and maximum likelihood classifier (MLC), as well as vegetation indices (VI), such as normalised vegetation index (NDVI; Kuenzer and Knauer, 2013; Mosleh et al., 2015; Dong and Xiao, 2016). Since the 2000s paddy rice mapping improved, thanks to the advances in the optical satellite imagery, increased revisit times, a better spatial resolution, the involvement of more images and the development of new classifiers, such as neutral network (NN), change detection (CD), and object-based image analysis (Dong and Xiao, 2016). Additionally, technological advances in the optical sensors also improved rice mapping with vegetation indices, out of which the normalised difference vegetation index (NDVI), enhanced vegetation index (EVI) and land

surface water index (LSWI) have been one of the most commonly used VI for rice crop mapping (Chen et al., 2004; Torbick et al., 2011b; Torbick and Salas, 2014; Bégué et al., 2018; Mansaray et al., 2019). However, as previously noted, the use of optical data is limited in tropical areas where cloud cover might continue for more than 70% of the rice growing season (Le Toan et al., 1997; Kuenzer and Knauer, 2013; Bazzi et al., 2019). Le Toan et al. (1997) observed that thanks to cloud penetration capabilities SAR satellites are the only system that can be used for regular rice mapping and monitoring. Rice mapping and monitoring has been done with various SAR frequencies (C-, L-, and X-band) (Inoue et al., 2002; Suga and Konishi, 2008; Kim et al., 2009; Oh et al., 2009; Inoue and Sakaiya, 2013; Nelson et al., 2014; Mansaray et al., 2017; Son et al., 2021), each of which have different canopy penetration capabilities. The most common bands for mapping paddy rice are the C- and L-band (lower frequency) because they penetrate deeper into canopy, making them more sensitive to the changes in canopy structure and differences detected between exposed soil and vegetation development (Suga and Konishi, 2008), while X-band (higher frequency) was successfully used for rice monitoring, however, their application was more limited due to lower temporal changes observed in the X-band backscatter that reach saturation at rice heading stage, plateau and increase slightly more near the harvest season (Inoue et al., 2002; Suga and Konishi, 2008; Kim et al., 2009). However, the rice growth cycle in X- and L-band is not as well defined as in C-band backscatter, which from the reviewed literature, recently was the most widely used frequency for paddy rice mapping and monitoring (Le Toan et al., 1997; Mansaray et al., 2017; Torbick et al., 2017; Veloso et al., 2017; Clauss et al., 2018b; Tian et al., 2018; Bazzi et al., 2019; Dirgahayu et al., 2019; Minh et al., 2019; Xu et al., 2019; Son et al., 2021). One of the main obstacles that has been mentioned in SAR mapping is the spatial resolution of SAR images and revisit time, but those limitations have been improving in recent years, especially since the launch of the Sentinel-1A satellite.

Moreover, early studies of Rosenthal and Blanchard (1984) and Brisco et al. (1989) indicated that agricultural type detection can be enhanced by combining SAR and visible or infrared data, which improved the classification by 20% to 25% when compared to SAR alone. Since then this approach has been adopted by many other studies, especially those employing machine learning (Torbick et al., 2011a; Asilo et al., 2014; Karila et al., 2014; Torbick et al., 2017; Veloso et al., 2017; Setiyono et al., 2018; Cai et al., 2019; Muthukumarasamy et al., 2019; Zhou et al., 2019).

Identification and mapping of paddy rice fields with SAR data is based on strong temporal changes of the rice growth stages in the composition of water content, canopy height and structure, and soil exposure observed in remotely sensed images (Torbick et al., 2011b; Inoue et al., 2014; Dong and Xiao, 2016; Chandna and Mondal, 2020). Backscatter behaviour at each rice growth stage has been extensively studied (see Le Toan et al., 1997; Inoue et al., 2002; Oh et al., 2009; Lopez-Sanchez et al., 2011; Lopez-Sanchez et al., 2012; Inoue and Sakaiya, 2013; Inoue et al., 2014; Nelson et al., 2014; Nguyen and Wagner, 2017; Steele-Dunne et al., 2017 for an extensive review of rice crop behaviour) and enables phenology-based classification of rice from non-rice. Based on known temporal changes in the SAR backscatter during the vegetative stage (after sowing or transplanting), when the rice canopy increases, the SAR backscatter also increases gradually because the microwave signal becomes more affected by

vegetation and less by exposed ground. During the reproduction and ripening stages, when the rice canopy is significant, more SAR signal is reflected back by the rice tillage than the soil. At those stages backscatter reaches its peak and some signal fluctuations are observed that are captured differently by the VV and VH polarisations (Inoue et al., 2002; Oh et al., 2009; Lopez-Sanchez et al., 2011). In general, the VV polarisation reaches saturation at the reproductive stage (around the flowering), which is followed by a decrease at the ripening stage due to canopy attenuation (Le Toan et al., 1997; Oh et al., 2009; Nelson et al., 2014). In terms of the VH polarisation, the signal reaches saturation at the ripening stage (between the flowering and harvest; Oh et al., 2009; Nguyen and Wagner, 2017) After harvest there is a significant decrease of backscatter value that is once more affected by increased reflection of soil (Asilo et al., 2014). This change could potentially be used as a marker for the start of a fallow period.

Fallow recognition would be based on a similar principle as it is done for crops, where temporal changes in the SAR backscatter after harvest would differ from that of rice or other crops. However, from the reviewed literature the fallow backscatter behaviour has not been very well researched, and this study will provide some analysis to fill in this knowledge gap.

2.6 Fallow recognition

Fallow mapping with remotely sensed data is a widely researched topic, often included in crop observation research. The majority of analysed studies used normalised difference vegetation index (NDVI) to map and monitor fallow periods obtained from optical (visible and infrared) bands of multispectral satellite imagery (Girard et al., 1994; Folving and Christensen, 2007; Yamamoto et al., 2009; Leisz and Rasmussen, 2012; Wu et al., 2014; Bandyopadhyay et al., 2015; Gumma et al., 2016; Ghosh et al., 2017; Wallace et al., 2017; Chandna and Mondal, 2020; Pasha et al., 2020; Tong et al., 2020), and a few utilised panchromatic bands from multispectral sensors (for example, Elmqvist and Khatir, 2007). Other research utilising radar signals that concentrated on non-vegetated areas has been based on sensors with coarse single frequency and polarisations (McNairn et al., 2002).

NDVI is a good indicator of vegetation coverage because it measures photosynthetic activity in a form of reflectance profile where more vegetated areas are represented by increased absorption of red wavelengths and higher reflection of near-infrared wavelengths (Yamamoto et al., 2009). For instance, it has been used to map agricultural crop types and fallow occurrence and duration in India (Ghosh et al., 2017) or to identify fallow practices in Laos (Yamamoto et al., 2009). However, using NDVI for fallow detection can prove problematic in vegetated (e.g. weeded) fallow where marking the distinction between cropped field and vegetated fallow fields can create confusion and give less accurate classification (Wu et al., 2014; Wallace et al., 2017). Additionally, NDVI is also affected by cloud coverage which obstructs view, limiting regular observation capabilities, especially in high cloud coverage areas. This is where SAR sensors could be more useful for observing fallow periods thanks to the collection of information with different wavelengths and its cloud penetration capabilities.

Torbick and Salas (2014) found fallow classification within paddy rice environments to be the most problematic land cover type to classify due to temporal fluctuations or mixing of the fallow backscatter values that was similar to other land cover classes. Similar conclusions were also drawn by other studies (Bégué et al., 2018). Despite previous research, backscatter

behaviour and mixing of fallowed fields with other cropping types in SAR imagery is not well understood (Yesou et al., 1996; Schieche et al., 1999). From the majority of the analysed literature, fallow was briefly mentioned in crop mapping studies without any detailed analysis of SAR signal behaviour (Brisco et al., 1989; Asilo et al., 2014; Nelson et al., 2014; Stefanski et al., 2014; Torbick and Salas, 2014; Uppala et al., 2015; Boschetti et al., 2017; Torbick et al., 2017; Minh et al., 2019) even though it could be detected with a single-date hybrid polarimetric SAR data (Uppala et al., 2015). Banqué et al. (2015) observed that bare soils stay relatively low in co- and cross-polarised SAR signal; however, in unmanaged fallow fields variations of backscatter can be observed from developing vegetation or weeds (Wallace et al., 2017). Additionally, there can be other variation of the SAR signal affected by soil moisture (Gherboudj et al., 2011) and soil roughness (Oh, 2004).

This lack of understanding of backscatter characteristics poses a challenge for developing automated fallow classification method in a similar way as was attempted for rice (Nelson et al., 2014). Therefore, this research aims to identify fallow periods using SAR backscatter behaviour from Sentinel-1A data. Backscatter variations observed during the rice growth stages and fallow periods have been used. The detection of rice cropping seasons has been successfully applied by identifying local maxima and local minima (Boschetti et al., 2017; Zhang et al., 2019; Zhou et al., 2019). This study will apply a similar approach to fallow backscatter to assess if detection using local minima and maxima can be applied to fallow periods. Additionally, as rice has more consistent temporal backscatter behaviour than fallow, this study will compare if detection of rice seasons results in higher accuracy than detection of fallow periods.

3 Study areas and data

This chapter will first explain site selection, then will briefly describe study areas and will provide a brief description of the types of data used in the analysis.

3.1 Study area selection

The choice of the study areas was made according to criteria specified by regional officers of the Pest Risk Identification and Management (PRIME) project in the Philippines. The selection criteria considered factors such as individual field size, accessibility, distance from buildings and other roads (see Appendix A for a reproduced Fields Survey Protocol). Out of those criteria, eight municipalities in Pangasinan and Iloilo provinces were selected.

3.2 Study areas

The Philippines is an archipelago of approximately 7100 islands located in south-east Asia. The climate in the Philippines is tropical marine with two prominent seasons, dry and wet; however, due to complex topography and rainfall distribution the Philippine Atmospheric, Geophysical and Astronomical Services Administration (PAGASA) categorised it into four climatic types (Maclean et al., 2013; PAGASA, 2021). Type I is characterised by a distinctive summer monsoonal wet season from April to October and a dry season for the rest of the year, and it covers most western regions of the Philippines (Central Luzon, western Visayas). Type II has no dry season with highest rainfall occurring between November-February. It covers most of the eastern regions. Type III has no apparent maximum rainfall period with a short dry season from November to February, and it covers central Visayas, western Bicol and northern Mindanao. Type IV covers central and south Mindanao where rainfall is evenly distributed throughout the year and has no dry season.

The Philippines is the eighth top rice producing country, with approximately 4.4 million ha of land occupied by rice fields in 2010, of which 69% are equipped for irrigation (majority located in the central plain of Luzon). The remaining rice fields are rainfed and upland (Maclean et al., 2013), which are prone to water availability shortages, especially in the dry season. This provides the opportunity for detection of fallow behaviour over larger areas.

The two research areas are located in the rolling terrain of Pangasinan province (Ilocos Region) in the centre-west part of the Luzon Island and sloping Iloilo province (Western Visayas region) in the centre-west part of the Philippines (see Figure 2). Both areas are located in the same climatic type I – dry from November to April and wet in the rest of the year (Maclean et al., 2013; PAGASA, 2021). They also lie in some of the major rice-producing regions of the Philippines, of which Western Visayas region ranks second (Maclean et al., 2013) and Pangasinan province third (Asilo et al., 2014). Additionally, the areas provide a good comparison of fallow behaviour in rainfed and irrigated rice areas, as both provinces have mixed water sources (Philippine Statistics Authority (PSA), 2019).

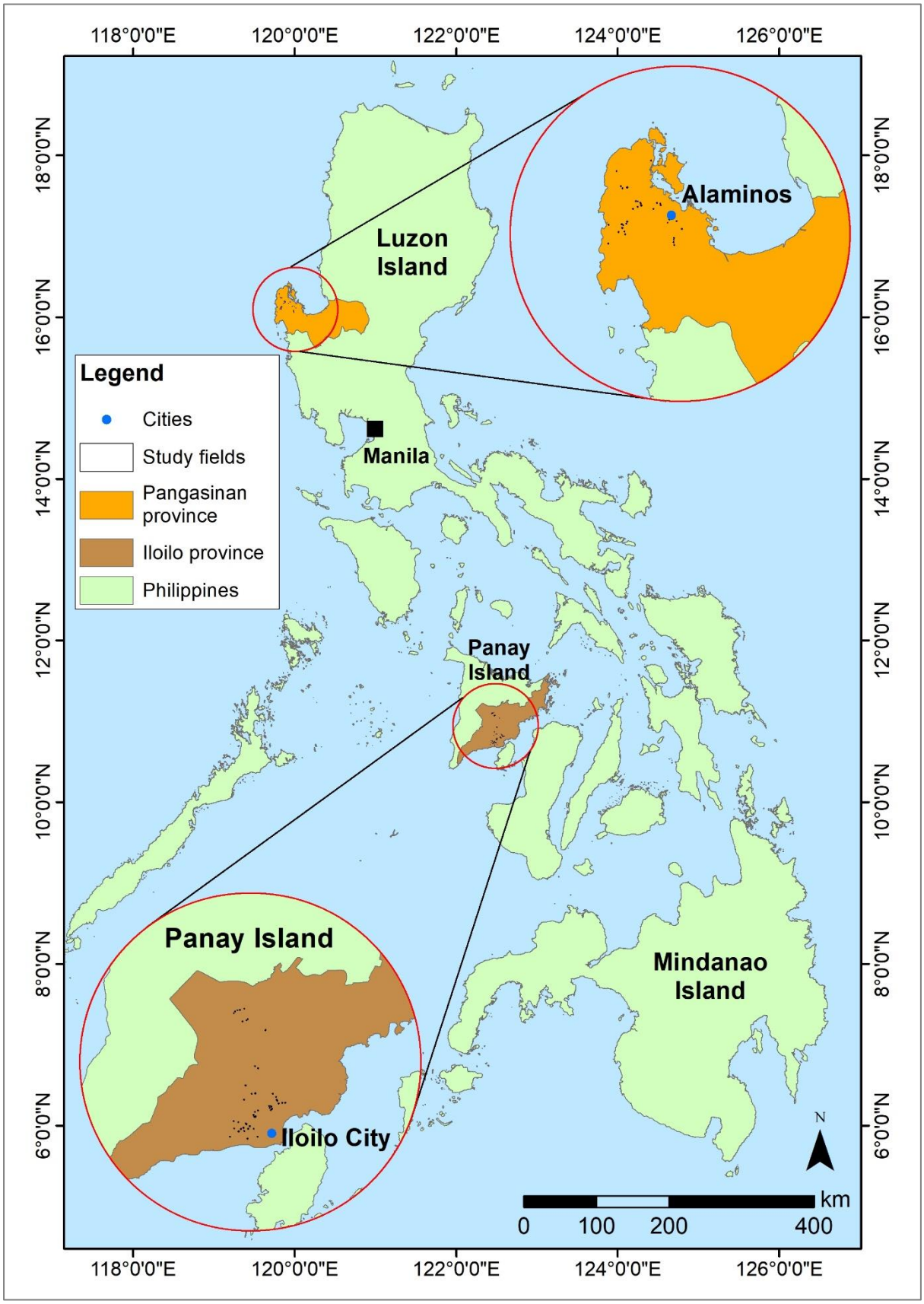

Figure 2. Map of the selected fields in Pangasinan and Iloilo provinces.

3.3 Data

This study utilised secondary data from farmer questionnaires collected in Pangasinan and Iloilo provinces in the Philippines and SAR backscatter data from time-series of Sentinel-1A satellite images over the same areas. The following sections provide a brief description of each dataset and step taken in field data collection and pre-processing of the secondary data.

3.3.1 Field data

The field survey data was collected by the Pest Risk Identification and Management (PRIME) project staff between February and March 2019 (see Appendix A for dates based on visited municipality). In Pangasinan and Iloilo provinces, 72 and 75 fields, respectively, were visited for which GPS coordinates of each field extent were recorded and farmers interviewed. The farmer questionnaires contained information about the farmer recalled dates of the land, water and crop management activities covering dry and wet seasons between late 2017 and early 2019. However, the reported fallow and rice cropping dates, and rice ecosystem types were of interest for this study, which were used in relation to interpretation of the multi-temporal backscatter values in each field. Additionally, the field extents were used as areas of interest (AOI) for extracting data from spatial imagery used in this study.

3.3.2 Sentinel-1A data and pre-processing

The multi-temporal SAR image backscatter values that were used in this study were downloaded, processed and SAR values extracted by the IRRI (PRIME project) team – a brief description of the pre-processing steps (adapted from Nelson et al., 2014) is provided in Appendix B. The remaining manipulation, backscatter calculation and plotting of the data was completed by the author.

The Sentinel-1A images (distributed as a single-look complex [SLC] product) from Interferometric Wide (IW) swath mode and descending orbit were used to generate time-series data over the study sites – see Table 1 for specifications of the Sentinel-1A data. However, unprocessed time-series SAR data is not instantly usable, as various geometric and radiometric corrections datasets captured over time are required for analysis of the temporal data. Only then the produced terrain geocoded backscatter coefficients (σ°) data can be used for analysis.

Pre-processing of the SAR image sets were completed separately for three seasons or stacks of images (2018 season one [dry season], 2018 season two [wet season] and 2019 season one [dry season] – see Table 1 for the acquisition periods of the Sentinel-1A images, where two acquisitions in Iloilo and one in Pangasinan were missing). Pre-processing was done using an automated processing routine set within the *MAPscape-RICE* software (Holecz et al., 2013; Nelson et al., 2014) that involved separate processing for VH and VV polarisations.

Table 1. The specifications of the Sentinel-1A data and acquisition periods.

Parameter	Specification	
Satellite	Sentinel-1A	
Wavelength / frequency	SAR-C (3.75 - 7.5 cm) / 5.405 GHz	
Orbit	Sun-synchronous (descending pass)	
Level data	Level-1 Ground Range Detected (GRD)	
Image mode	Interferometric Wide swath (IW – 250 km)	
Spatial resolution	20 m	
Incidence angle	29.1° - 46.0°	
Polarisation	Dual polarisation (VV and VH)	
Revisit cycle	12 days	
Acquisition periods	Iloilo	16 Sep 2017 - 22 Mar 2019 (46 images)
	Pangasinan	26 Sep 2017 - 20 Mar 2019 (45 images)
Missing acquisitions	Iloilo	15 Mar 2018 and 14 Feb 2019
	Pangasinan	28 Aug 2018

3.3.3 Rainfall data

Rainfall data was used to help interpret changes observed in the backscatter values over the fallow periods.

Rainfall data could be obtained from NOAA (National Oceanic and Atmospheric Administration) that provides freely available daily rainfall amounts. However, because of the large distances between the weather observation stations and studied fields (45km in the closest example), the actual rainfall volume and occurrence at the studied locations may have been misrepresented. Therefore, a decision has been made to obtain rainfall data from high special and temporal weather observation satellites, such as TRMM (Tropical Rainfall Mapping Mission) and CHIRPS (Climate Hazards Group Infrared Precipitation with Stations), which are one of the most popular and globally accepted satellite-based daily precipitation datasets (Gupta et al., 2019). Their spatial (grid) resolution ranges from approx. 0.05° for CHIRPS and 0.25° for TRMM, and both have daily coverage (Sun et al., 2018; Gupta et al., 2019).

Both systems have been shown to provide fairly reliable rainfall estimates in various regions, for instance, in Brazil (Nogueira et al., 2018), Burkina Faso (Dembélé and Zwart, 2016) and India (Gupta et al., 2019). In the Philippines, Jamandre and Narisma (2013) validated two satellite derived datasets, one of which was TRMM. They suggested that in general TRMM did not perform well in the country. Although they acknowledged that performance is slightly better in the northern regions, a decision was made to choose CHIRPS satellite rainfall data given the evidence against TRMM. Nevertheless, it is acknowledged that all satellite weather observation systems have their own limitations in predicting rainfall amounts over various regions (Sun et al., 2018).

For this study, daily CHIRPS rainfall estimation was collected for all the dekads from June 2018 to March 2019 (covering the farmer reported rice cropping dates) and rainfall data exported over the studied fields. CHIRPS was accessed from the Climate Hazards Center at the University of California, Santa Barbara's repository under the following URL: ftp://ftp.chg.ucsb.edu/pub/org/chg/products/CHIRPS-2.0.

4 Methodology

This section will describe steps undertaken to answer the research questions listed in Chapter 1.3.

4.1 Sentinel-1A mean backscatter value extraction

Sentinel-1A images were pre-processed separately for each season/stack of the images. The three stacks of the Sentinel-1A images had two overlapping images covering the same dates between each stack (season) that, due to radiometric temporal filters applied to each stack, there were slightly different backscatter values. To create one continuous time-series that covered all three seasons an average (of the linear scaling) of each overlapping image was taken. After this, the Sentinel-1A values for VH and VV polarisations were calibrated from linear scaling (DN) to sigma naught (σ^0) backscatter coefficient (dB) for use in the analysis using the following equation (Mansaray et al., 2019):

$$\sigma^0(dB) = 10 \times \log_{10}(DN)$$

Figure 3 presents examples of the Sentinel-1A pixels (DN) for selected cropping stages and activities in field 106 in Pangasinan.

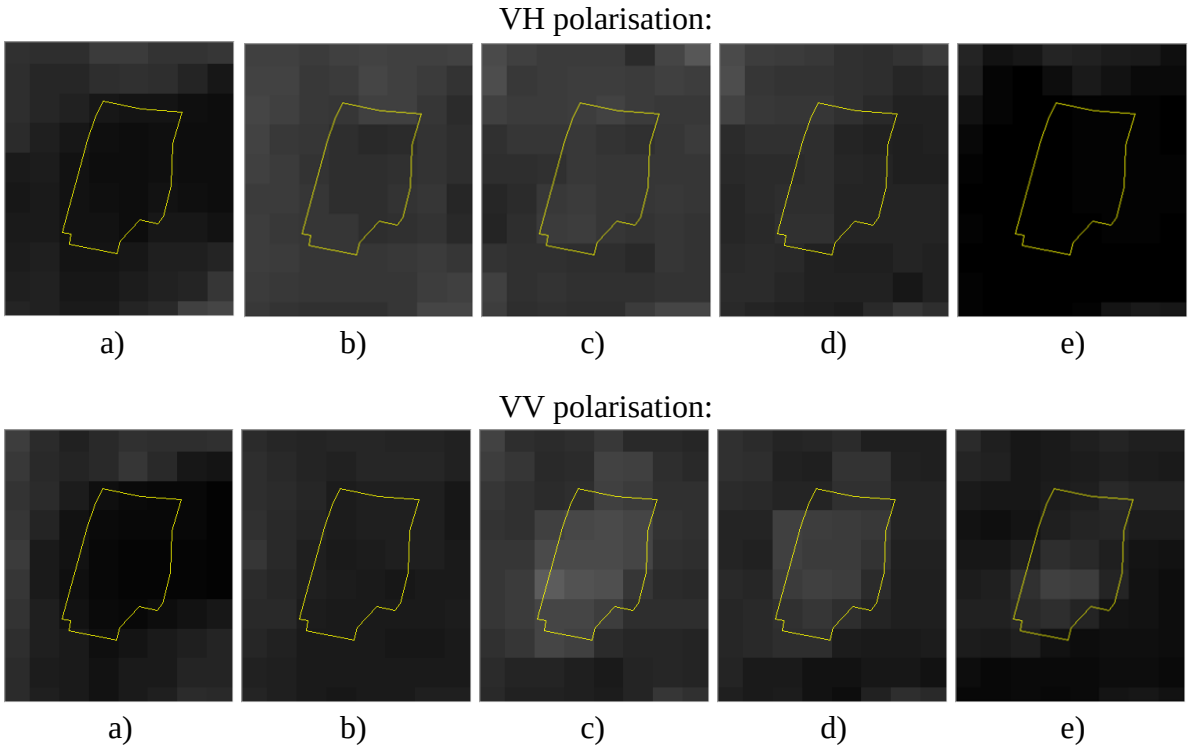

Figure 3. Examples of the Sentinel-1A image pixels (DN) in VH polarisation (upper) and VV polarisation (lower) within field 106 at a) crop establishment, b) flowering, c) harvest, d) fallow start and e) fallow end. Size of each pixel is 20x20m.

Backscatter value extraction was performed for each field using GPS field boundary extents recorded during field surveys. Each field was assigned a unique ID number that also corresponded to the farmer questionnaires.

Temporal backscatter value (dB) extraction was done for each pixel within the field polygons in *R* software for VV and VH polarisations separately. During this process each pixel was assigned its position within the field boundary (either field or boundary), which allowed for exclusion of the pixels at the field borders. This was to eliminate potential edge effect that can affect the accuracy of the extracted data due to signature/backscatter value mixing at edges of the fields (Zhou et al., 2019; Son et al., 2021).

From the extracted data, the mean backscatter of each field was calculated by first converting the backscatter (dB) values to linear scaling (DN), then computing the average of individual fields and then converting the mean DN back to dB values.

The mean backscatters covered time period from mid-September 2017 through to the end of March 2019 using a 12-day interval, which is the revisit time of the Sentinel-1A satellite. However, the analysis was based on two seasons (2018 wet and 2019 dry seasons – April 2018 to March 2019), due to low number of fields (only eight fields in Iloilo) for which cropping activities were reported for the 2018 dry season.

4.2 Computation of VV/VH polarisation ratio

Polarimetric channel mixing (also known as depolarisation ratio), such as VV/VH polarisation ratio, can provide additional insight into the standard cross-polarised (VH) and co-polarised (VV) backscatter (Bégué et al., 2018). Additionally, the depolarisation ratio was shown to improve the identification accuracy of paddy rice crops (Lasko et al., 2018). Therefore, the VV/VH ratio was examined to assess if it provided additional information for distinguishing between rice crops and fallow periods.

The VV/VH polarisation ratio was derived from the VV and VH polarisation backscatter values before the mean values for each polarisation were calculated. The formula for ratio computation is modelled on the linear domain cross ratio calculation (Vreugdenhil et al., 2018), but because the exported backscatter coefficients were in a $10xlog_{10}$ (dB) form, the ratio was calculated according to the following formula:

$$VV/VH\ ratio\ =\ VV\ dB - VH\ dB$$

where VV dB is the backscatter coefficient (σ^0) at VV polarisation and VH the backscatter coefficient (σ^0) at VH polarisation.

In the end, mean VV/VH ratio for each set of study fields was computed in the same way as for the linear polarisations.

4.3 Savitzky-Golay smoothing filter

After extracting the temporal mean backscatter values (σ^0) for each field from the post-processed SAR data, some noise was still observed in the plotted time-series. The noise was characterised by variations in the backscatter values throughout the time-series (see the grey line in Figure 4), which could be due to the interference of the waves from various scatterers

that affect the SAR backscatter/signal (Son et al., 2021) and atmospheric attenuation (Nelson et al., 2014). Similar SAR signal interference was observed in previous studies (Li et al., 2018; Son et al., 2021) that dealt with the issue by applying a filter to the original SAR data.

A popular filter used to reduce remaining noise in temporal SAR backscatter is the Savitzky-Golay (SG) filter (Son et al., 2021). SG is a least-squares polynomial approximation that smooths temporal signal while preserving shape and height of waveform peaks (Schafer, 2011; Gir et al., 2015). One of the most important aspects/factors of the SG filter is the half-width of the smoothing window – setting it too high can remove variations in the data, whereas setting it too low can over fit the filtered data (Chen et al., 2004).

The SG filter was applied to the original mean SAR backscatter in all polarisations (VH, VV and VV/VH ratio) for each field separately. To prevent any over and undersmoothing of the temporal backscatter, the filter order was set to four and length was set to nine SAR images. The SG filter produced smooth temporal backscatters (see the orange line in Figure 4) that made evaluating the reliability of the farmer reported cropping dates easier. The SG filtered temporal backscatter values were used in the final analysis.

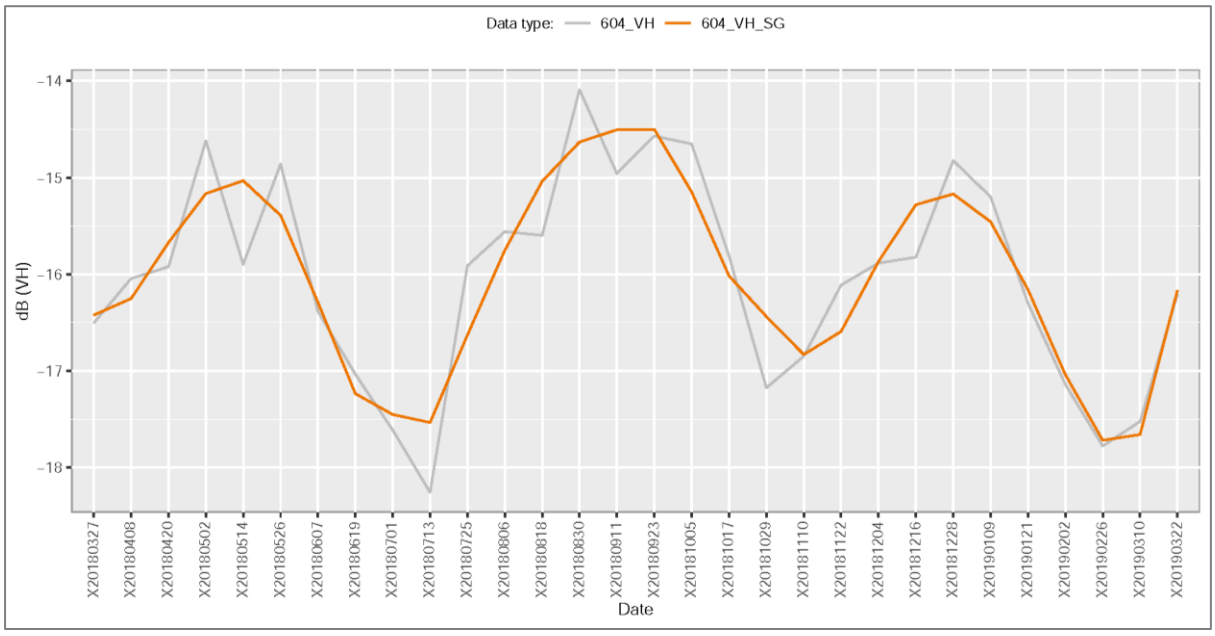

Figure 4. Example of the original unsmoothed temporal backscatter data (grey) overlayed with the Savitzky-Golay filtered/smoothed data (orange).

4.4 Phenological/cropping features estimation

Analysis of the phenological/cropping features was based on temporal changes observed in the extracted backscatter data over rice crops and fallow periods. The classification was based on IRRI's main rice crop growth and planting stages (IRRI, 2015) that start from land preparation (LP), followed by crop establishment (CE), flowering (FLW) and harvest (H). Out of the listed cropping stages and activities, crop establishment and harvest were used in this study, as they

indicated the start and end of the rice growth season. Fallow (F) was one class, which had no subdivisions, and was assigned to the first Sentinel-1A acquisition date after harvest. Additionally, two main ecosystem types (irrigated and rainfed; IRRI, 2007) for each field were used for observation of differences between fallow coming from irrigated and rainfed fields.

The timings of the main cropping features (rice crop establishment, flowering, harvest, and fallow) were obtained from the farmer questionnaires, which contained mid-week dates of cropping stages and activities. In order to obtain backscatter profile for each phenological stage and activity the reported mid-week dates were converted to the nearest SAR image acquisition dates that were captured after the reported cropping stage or activity took place. This was to avoid situations where Sentinel-1A data preceded the reported cropping activity even by a short amount of time, such as one day. Otherwise, the SAR backscatter would not have had the opportunity to record any cropping activity yet to take place.

Moreover, based on the rice cropping calendar, the flowering stage occurs approximately 30 days before harvest (IRRI, 2015; Liu et al., 2016). However, in the farmer questionnaires some flowering stages were reported to last more than four weeks, which may be due to misremembering of the start of rice flowering by the farmers. This could be due to the fact that flowering is not as significant an event to the farmers as crop establishment or harvest is, or because flowering is classified by some farmers at different (earlier or later) rice growth stage than the classification used in this research, where flowering takes place 30 days before harvest. Therefore, the flowering dates for all the rice crops were adjusted to occur 30 days before harvest and matched to the nearest SAR acquisition day after the new date.

Additionally, due to the 12-day revisit period of the Sentinel-1A satellite, there were cases where multiple cropping activities, such as harvest and land preparation or crop establishment, occurred within the 12-day window and were recorded within the same SAR image. In those instances, the same backscatter values were used for both of the affected cropping stages or activities. A similar approach was employed for times where there was a missing SAR image acquisition date (28 August 2018 in Pangasinan; and 14 February 2019 in Iloilo). In such cases, the backscatter value from the next available SAR date was assigned for the affected cropping activities.

4.5 Backscatter plotting (exploratory analysis)

Time-series plots of backscatter values correlated with selected cropping practices were created for exploration of the backscatter behaviour during selected rice-development phases and fallow periods. Produced plots were also employed in defining the accuracy of the farmer reported activities and phenological dates, and determining types of statistical tests needed for answering the research questions.

Additionally, time-series plots showed different temporal behaviour of fallow backscatter that varied depending on fallow duration. A distinction was observed between fallow periods that lasted up to 84 days – defined as short fallow – and over 84 days – defined as long fallow. The decision to distinguish the two types of fallows along the axis of 84 days was based on the analysis of fallow plots, which showed clear backscatter differentiation at this point of time. Short fallow periods had mostly a descending backscatter pattern, whereas many of the long

fallow periods experienced varying temporal behaviour after approximately 60 days since harvest, which could have been affected by unreported crops being planted at that time. To examine those variations in fallow's backscatter additional time-series plots were produced separated by long and short fallow duration.

4.6 Estimation of additional fallow periods

During the field visits farmers reported 101 rice crops and 37 fallow periods in Pangasinan, and 149 rice crops and 21 fallow periods in Iloilo, with the shortest lasting 48 days (equivalent to the period of collection of 4 SAR images) in Pangasinan and Iloilo. All the reported fallow periods were for the most recent dates after the last harvest, which could be due to the farmers' not remembering any previous fallows between earlier planted crops. However, in the extracted SAR time-series there were periods between crops or after the last harvest that were not assigned to any cropping activity but were meeting the fallow criteria – any period where no crop was being planted. In those cases, additional fallow practices were identified for periods of at least 48 days where no cropping activity was being reported. To keep in line with the shortest reported fallow periods, any periods shorter than 48 days were not included. Additionally, several of those shorter fallows experienced some variations/increases in the backscatter behaviour that could suggest that some unreported cropping activity, such as land preparation for the next crop, was taking place, which was another reason for not including them in the analysis. Longer additional fallow periods (the longest lasting 72 days), on the other hand, were deemed to be better suited for the fallow temporal analysis and had higher chances of fields being left fallowed. The additional fallow periods, included as the result of the SAR time-series analysis, accounted for another twelve fallow data points in Pangasinan and eight in Iloilo and were included in the further analysis together with the farmer reported fallow.

4.7 Estimation of reliability of the farmer reported dates

The phenological stages of crop development and fallow occurrence were obtained from the farmer questionnaires, which relied on the farmer recollection of dates of each cropping stage and activity. However, as the field data was collected at the beginning of 2019, but the cropping dates went as far back as April 2018, there was a possibility of recall bias (Wollburg et al., 2020) that may have resulted in cropping activities being assigned to the wrong dates and hence the wrong backscatter values. This can in fact be observed in some timeseries graphs. For instance, Figure 5 shows that the crop establishment reported by the farmer in the last rice crop (Rice1) falls at a stage where the signal is well past the lowest point and heads towards the peak. Rice signal is well researched and has a clear growth profile, especially in the C-band SAR data (Le Toan et al., 1997; Inoue et al., 2002; Suga and Konishi, 2008; Bouvet et al., 2009; Kim et al., 2009; Oh et al., 2009; Nelson et al., 2014; Nguyen et al., 2016; Mansaray et al., 2017; Nguyen and Wagner, 2017; Lasko et al., 2018; Bazzi et al., 2019; Dirgahayu et al., 2019; Minh et al., 2019; Xu et al., 2019). Therefore, it is unlikely that the reported date was accurate, as crop establishment is expected to correspond to the signal minima, and the reported crop establishment date (CE1) falls at the rice tillering stage.

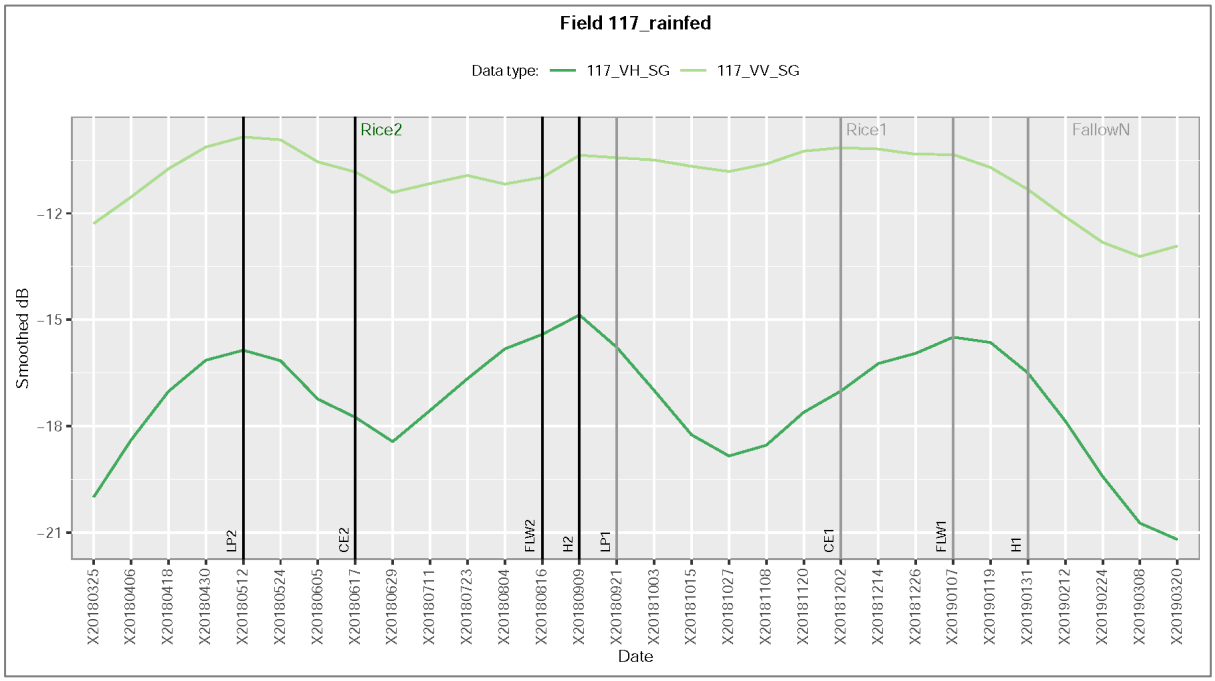

Figure 5. Example of potential recall bias in the timeseries data in last rice crop establishment (CE1) date.

To reduce recall bias, the following steps were taken to identify and filter out potential misreported cropping dates. SAR backscatter is sensitive to rice crop phenological stages and the VH polarisation was selected for establishing the recall bias because it was characterised by the most sustained increase in rice growth backscatter out of the three polarisations used in this research (Liu et al., 2016; Mansaray et al., 2017; Chandna and Mondal, 2020). The temporal rice profile in the VV polarisation was also expected to follow a similar behaviour to the one observed in VH; however, in the analysed data some inconsistencies in rice temporal SAR behaviour were observed, especially in Iloilo province, which is shown in Figure 8, and were attributed to stronger attenuation by leaves and stems in the VV polarisation (Mansaray et al., 2017). Therefore, the rejection was based solely on the VH polarisation in both provinces.

During rice planting, the SAR signal at the VH polarisation is at or near minima because fields are flooded with water, which is due to specular reflection of water bodies. Whereas, during rice heading the stems and canopy increases causing higher backscattering of the VH polarisation reaching maxima values near the rice harvest (Asilo et al., 2014; Nelson et al., 2014; Lasko et al., 2018; Onojeghuo et al., 2018; Bazzi et al., 2019; Mansaray et al., 2019). Based on this backscatter behaviour an estimate of the reliability of the farmer recollected dates for each reported rice season was made. The dates and backscatter values that did not align with the above criteria were deemed unreliable and rejected from further analysis.

Moreover, after rejecting rice crops where the reported dates were deemed inaccurate, fallow that followed or preceded the rejected rice crop was also removed from the analysis, as the date of fallow occurrence (normally after harvest) was deemed inaccurate. Therefore, the final

analysis included only fallow from fields with accepted crop start and end dates. The selected rice crops and fallow periods are listed in the section below.

4.8 Selected rice crops and fallow periods

Based on the rice backscatter analysis mentioned in section 4.7, only the rice crops that were deemed as accurate were accepted for further analysis. In addition, some of the fallow periods that preceded or followed the rejected rice crops had to be discarded. This was due to an inability to determine the start or finish of the fallow period, and due to uncertainty whether such fallow seasons were genuinely fallow. Based on this, the number of the accepted rice and fallowed fields in each province is listed in Table 2 and presented in Figure 6.

Table 2. Number of accepted samples based on the cropping type.

Province	Cropping Type	Number of selected fields
Pangasinan	Rice	44
	Fallow	20
Iloilo	Rice	57
	Fallow	21

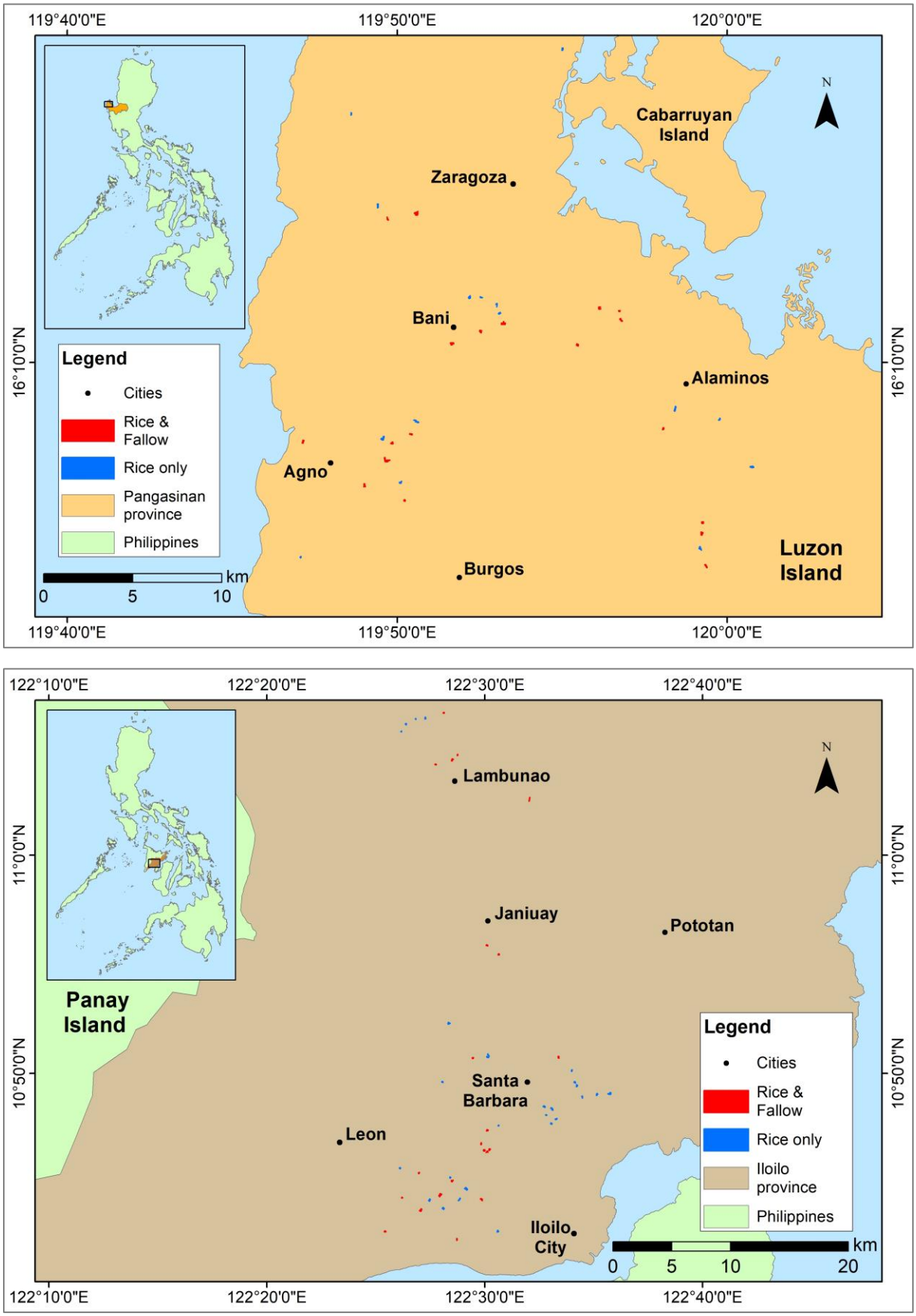

Figure 6. Distribution of the accepted fields in Pangasinan (top) and Iloilo (bottom).

4.9 Fallow duration

In the selected/filtered fields fallow was reported by the farmers to last at least 48 days (as a minimum established for inclusion in the study) in Pangasinan and at least 60 days in Iloilo, out of which 60- and 84-day fallow were the most prevailing durations in Iloilo and 144-day fallow was most prevailing in Pangasinan. The longest fallow periods in the analysed fields lasted for 156 days in Pangasinan and 168 days in Iloilo; however, the number of fields which were kept fallowed for such long periods was very low – two fields in Pangasinan and three fields in Iloilo (see Table 3).

Table 3. Fallow duration per number of fields in Pangasinan and Iloilo.

Fallow duration (days)	Number of fields	
	Pangasinan	Iloilo
48	3	-
60	2	6
72	3	4
84	-	7
96	2	-
108	1	-
120	1	1
132	1	-
144	5	-
156	2	-
168	-	3

4.10 Statistical tests

To determine statistical differences between the backscatter from various rice and fallow stages or activities, non-parametric tests were performed, as they do not need the assumption of a normal distribution of the data (Ebdon, 1985). The tests were applied to differences in backscatter values between rice crops and fallow, as well as between fallow occurring in irrigated and rainfed fields. The type of non-parametric tests employed was governed by the number of independent samples of equal or different sample sizes involved in the test. The Mann-Whitney U test was selected to compare two sets of samples, whereas the Kruskal-Wallis H test was selected for testing more than two independent samples (Ebdon, 1985).

The Kruskal-Wallis H test was selected to compare backscatter values that occurred during the selected cropping stages/activities – rice establishment (start of season) and rice harvest (end of season) and fallow start and end. From the rice development phases, the crop establishment and harvest were selected because produced boxplots indicated that those phases could be good indicators of the rice-growing season. This test was then followed by a post hoc pairwise comparison to try to determine which of the selected cropping types between rice and fallow were significantly different.

On the other hand, the Mann-Whitney U test was employed in two scenarios. Firstly, it was used to determine statistical differences between the start and end of fallow periods separated by fallow duration (short and long). The test was performed separately for each polarisation (VH, VV and VV/VH ratio). Secondly, the Mann-Whitney U test was also applied to mean fallow backscatter values from each field based on the ecosystem types (irrigated and rainfed). This was in order to determine whether the overall fallow behaviour changes in fields with access to irrigation compared to rainfed ones. For this test the assumption was that in the irrigated ecosystems fields would have access to water, especially during the dry season, if the neighbouring fields were planted/flooded for rice cropping. However, it is not known from the farmers questionnaires if this was the case. All tests were performed in SPSS software and were ran separately for VH, VV and VV/VH polarisations.

4.11 Fallow detection

Following the analysis mentioned in the above subsections, fallow detection was based on a backward approach of the rice season identification, where periods that occurred between rice crops were classified as fallow. For this step, dates that corresponded to rice local minima and maxima backscatter were obtained (Nelson et al., 2014; Chang et al., 2020). This approach relies on the high backscatter variations that result in temporal differences at the start and end of rice-growth cycles (Holecz et al., 2013; Nelson et al., 2014; Chang et al., 2020), which are characterised by rice establishment being at or near minima backscatter value and rice harvest occurring at or near maxima backscatter in VH polarisation. The behaviour of rice-development phases change in VV polarisation, and is near minima around rice establishment, but reaches saturation near tillering (Mansaray et al., 2019), making this polarisation less suitable for fallow detection. In the case of VV/VH ratio the pattern is expected to resemble the inverted VH polarisation (Veloso et al., 2017), where minima and maxima would reflect the start and end of the rice season, respectively.

To evaluate the accuracy of the start and end of the rice season a root mean square error (RMSE) was calculated between the observed (the farmer reported) dates and estimated dates from rice's local maximum and minimum backscatter (Asilo et al., 2014). The lower the RMSE, the closer the estimated dates were to the reported ones. In this step separate estimates and calculations were performed for the three polarisations in R v3.6.3 statistical software.

4.12 Extraction of rainfall data

Rainfall data covering the dates of SAR images were used to detect whether the changes in the fallow backscatter corresponded to rainfall presence. Dekadal rainfall was extracted for each fallowed field from the CHIRPS images. Rainfall analysis was performed by plotting the dekadal rainfall on bar plots and correlating them with the fallow SAR time-series. In the end combined bar plots were created for all the fallowed fields in each studied location that showed average rainfall per dekad in each studied location. To achieve this, dekadal rainfalls that were nearest to/covering the start and end of each fallow were used and assigned consecutive numbers, where *Dekad1* was the first dekad of rainfall that corresponded to the start of each fallow period. From that, average dekadal rainfall was calculated for each consecutive dekad.

The dekadal rainfall extraction for each field was done in R and graphs were produced in Excel.

5 Results

This section contains the main findings from the research, including temporal backscatter plots correlated with the cropping types; boxplots of the backscatter values for selected cropping types, results of statistical significance tests, and outcomes and accuracy of detecting fallow periods based on the start and end of fallow and rice crop season.

5.1 Temporal backscatter characteristics of rice and fallow

Extracted SAR backscatter data for selected rice development phases and fallow periods are illustrated in boxplots presented in Figure 7 and Figure 8. Fallow was split into short and long duration fallow periods and is presented in Figure 9 and Figure 10. The trend used for the analysis was selected from the median of each boxplot and range/magnitude was based on the lowest and highest values of the boxplot whiskers.

The selected rice development stages and activities consisted of land preparation, crop establishment, the 12^{th}, 24^{th}, 36^{th} and 48^{th} day after crop establishment, flowering, and harvest. Fallow stages were based on the length of fallow that started from the first SAR image acquisition date after the crop harvest. At land preparation, the backscatter values cover the widest range of all the rice development phases in VH polarisation in Pangasinan and VV in Iloilo. At the crop establishment some of the fields reported the lowest VH backscatter values of all rice development phases in both provinces, however, they did not reach the lowest median value. The overall lowest VH median was observed 12 days after the crop establishment (CE12). After that the VH backscatter gradually increased, reaching the highest median value at the flowering stage in Pangasinan and at harvest in Iloilo.

In VV polarisation the differences between Pangasinan and Iloilo provinces were greater than in VH polarisation. In Pangasinan the VV backscatter curve resembles the behaviour of VH polarisation which achieved the lowest median value at the crop establishment and the highest median value at the flowering stage, which corresponds to the peak of the vegetation cover. At harvest, when the vegetation coverage started to reduce, the median value was lower than at the flowering stage and continued to steadily decrease with the development of the fallow periods. In Iloilo at VV polarisation the rice growth backscatter curve was less pronounced and whiskers at each rice-growth stage had a wide range of backscatter values at most phenological stages. The crop establishment had the greatest magnitude between the maximum and minimum VV backscatter values. Also, the median peaked 24 days after crop establishment (CE24) and from that point started to decrease. Additionally, the flowering stage had the lowest VV median and lowest overall backscatter values out of all rice cropping phases in Iloilo. Harvest also had a lower median, but the VV backscatter extrema (minimum and maximum) were not as extreme as at the flowering stage. The overall VV behaviour of the rice season in Iloilo differed to the one recorded at VH polarisation and in Pangasinan in both, VV and VH polarisations.

Fallow, on the other hand, began after harvest and was marked by a gradual drop in the median backscatter in both polarisations in both provinces due to increased surface scattering owing to the lack of vegetation coverage and decaying vegetation residue (e.g., rice stalks; McNairn et

al., 2002). The decrease of the medians lasted for approximately 60 days in both locations after which some changes were observed. In Pangasinan after approximately 72 days of fallow (F6), the median started to fluctuate gently, whereas in Iloilo the backscatter increased sharply and was substantially greater than the backscatter soon after harvest. This unusual behaviour could imply a quick increase in vegetation coverage (Bégué et al., 2018) followed by a decline. However, those changes appeared at a point where a number of fields with fallow of over 60 days started to reduce, especially in Iloilo, which could also explain why the change in the boxplots was more pronounced in Iloilo.

Figure 9 and Figure 10 confirmed that the decrease and fluctuations in both polarisations varied with fallow duration where longer fallow periods (over 72 days in Pangasinan and 84 days in Iloilo) had a more gradual decrease than short fallow periods. This decrease during fallow in VV and VH polarisations was followed for the first 60 days (five SAR images) since harvest in Pangasinan and 48 days (four SAR images) in Iloilo, after which some fluctuations were observed in the median dB values in both provinces (characterised by overall decreasing trend). Additionally, Pangasinan was represented by a more pronounced overall decreasing trend, especially after harvest, in which the maximum value during fallow was lower than the maximum backscatter value during harvest. In Iloilo the situation was markedly different, in that most fallow median values were lower than the accompanying harvest median, but the maximum values were much higher than maximum backscatter values during all rice development points. Additionally, over the progression of the fallow periods, the minimum values were also lower than any of the rice-development phases in both provinces. Moreover, in Pangasinan, the fallow's median backscatters were also lower than medians at any rice cropping stage or activity. This, however, was not the case in Iloilo, where the lowest fallow median never surpassed the lowest rice median on the 12th day after the crop establishment (CE12). Slight increases were observed at the end of many fallow periods, which were more evident in Iloilo. In Pangasinan, on the other hand, the increase was milder and followed a downward trend.

Additionally, fallow duration lasted longer in Pangasinan than in Iloilo (up to 156 and 168 days, respectively). Those differences, together with backscatter behaviour, are likely affected by differences in farming practices in both provinces, with Iloilo being renowned for having one of the most intense farming regions in the Philippines, where up to three rice crops are commonly planted in one year (Villano et al., 2019).

In addition to the analysis of the VH and VV polarisations, the polarisation ratio was also used in the analysis. Polarisation ratio is not a new polarisation per se, as it is derived from mathematical calculations and not obtained in situ. Nevertheless, the polarisation ratio can better distinguish between various crop cycles (Vreugdenhil et al., 2018; Khabbazan et al., 2019) as it combines cross- and co-polarised polarisations together. In this research the VV/VH ratio was used to determine whether there were any significant differences between VV/VH with respect to the VH and VV polarisations, which would identify fallow periods with better accuracy.

The plotted VV/VH ratio curve appeared inverted in both provinces, with positive backscatter values due to the VV/VH ratio calculation, which reversed the shape and sign of the curve. In

Pangasinan and Iloilo magnitude of the ratio at short n=8 and long n=12 at the crop establishment was lower than in the individual polarisations. The VV/VH rice trend in Pangasinan (Figure 7) was gentler than in Iloilo (Figure 8), but in both instances, saturation was attained on the 12th day after the crop establishment (CE12). After that, the backscatter began to decline until the end of the reproductive stage (flowering), when the SAR signal reached its lowest point and was followed by a slight signal increase at harvest. However, it should be noted that some longer fallows have a very small number of observations, with as few samples as two in one instance. Additionally, the rice-growth trend of VV/VH ratio in Iloilo was better defined compared to what was obtained in VV co-polarisation.

During the first 60 days of fallow in Pangasinan, there was a continuous increase in backscatter, possibly due to increasing soil exposure as any remaining crop residue continued to decay. After 72 days (F6) in both locations, the ratio began to fluctuate slightly, but the overall pattern remained constant, with the most substantial change occurring on the 96th day of fallow (F8). These oscillations were only seen in longer fallows (see Figure 9) and could relate to developments of vegetation. In Iloilo after harvest the backscatter values also were increasing for the first 60 days, but the change was greater during the first 36 days of fallow, especially during shorter fallows (see Figure 10), after which the dB ratio began to stabilise. On 72nd and 84th day of fallow (F6 and F7) there was a steep decline of the ratio, after which the values began to increase once again after the 96th day (F8). This drop happened when the shorter fallow periods ended, which were characterised by significantly higher backscatter than the longer fallows. Therefore, this change may not necessarily indicate significant changes taking place in the fields, but could be due to the differences observed between shorter and longer fallow durations.

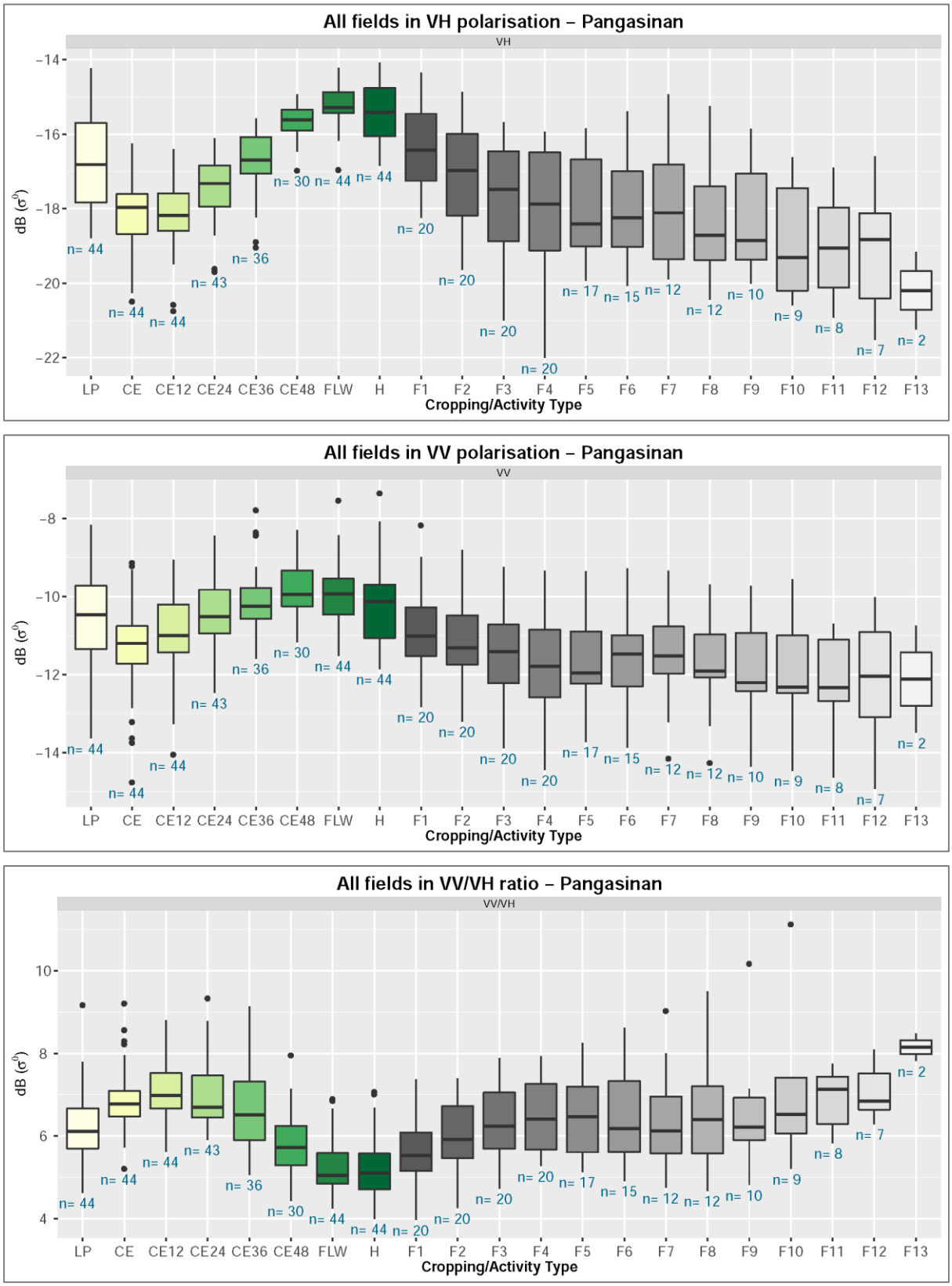

Figure 7. Boxplots of the backscatter coefficient derived from Sentinel-1A for rice planting activities, cropping stages and fallow in Pangasinan for VH (top), VV (middle) and VV/VH polarisation ratio (bottom). Fallow number relates to Sentinel-1A revisit time since the start of fallow. Shades of green indicate rice cropping phases and shades of grey are fallow durations (at 12-day intervals) from harvest.

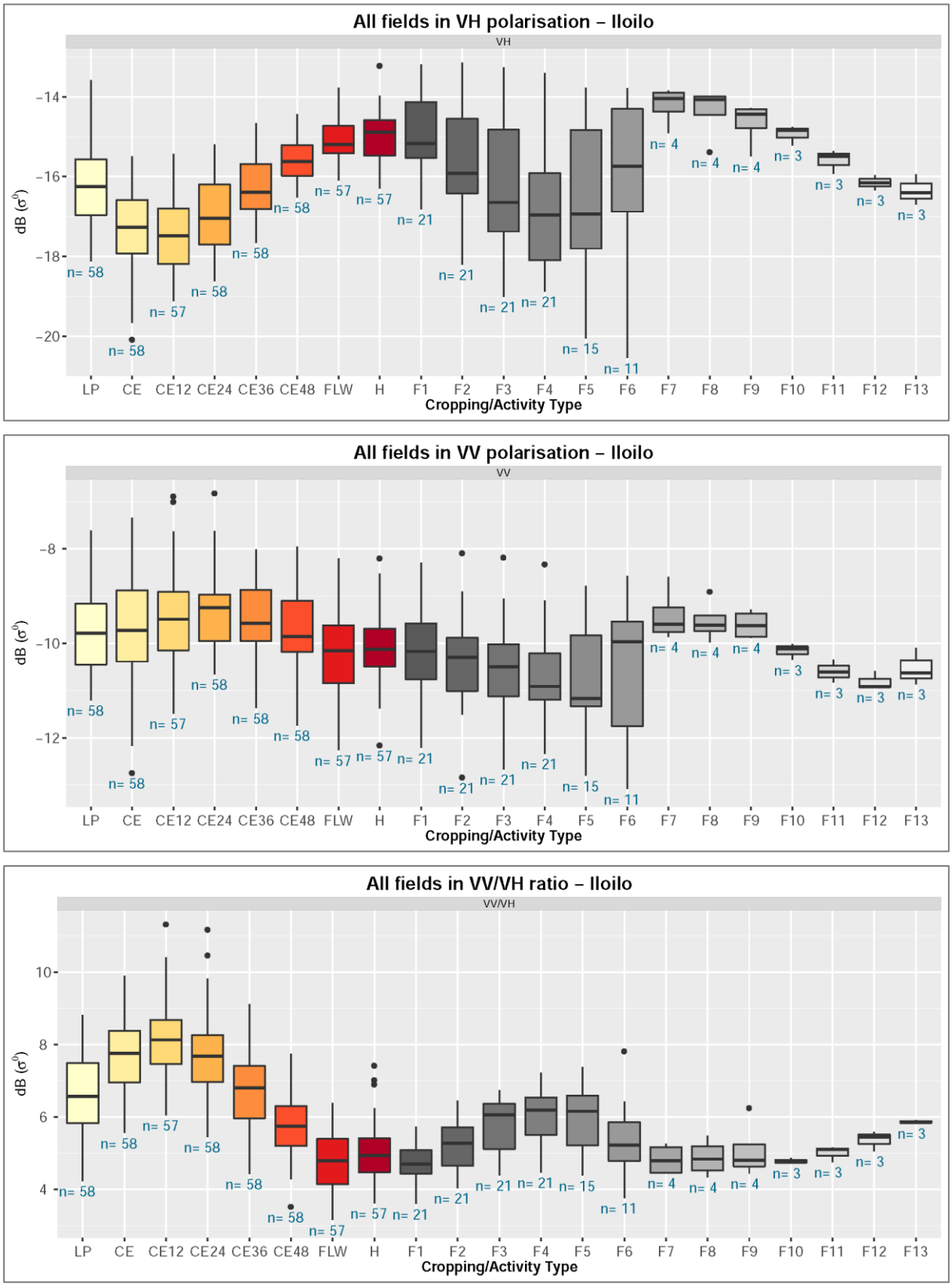

Figure 8. Boxplots of the backscatter coefficient derived from Sentinel-1A for rice planting activities, cropping stages and fallow in Iloilo for VH (top), VV (middle) and VV/VH polarisation ratio (bottom). Fallow number relates to Sentinel-1A revisit time since the start of fallow. Shades of orange indicate rice cropping phases and shades of grey are fallow durations (at 12-day intervals) from harvest.

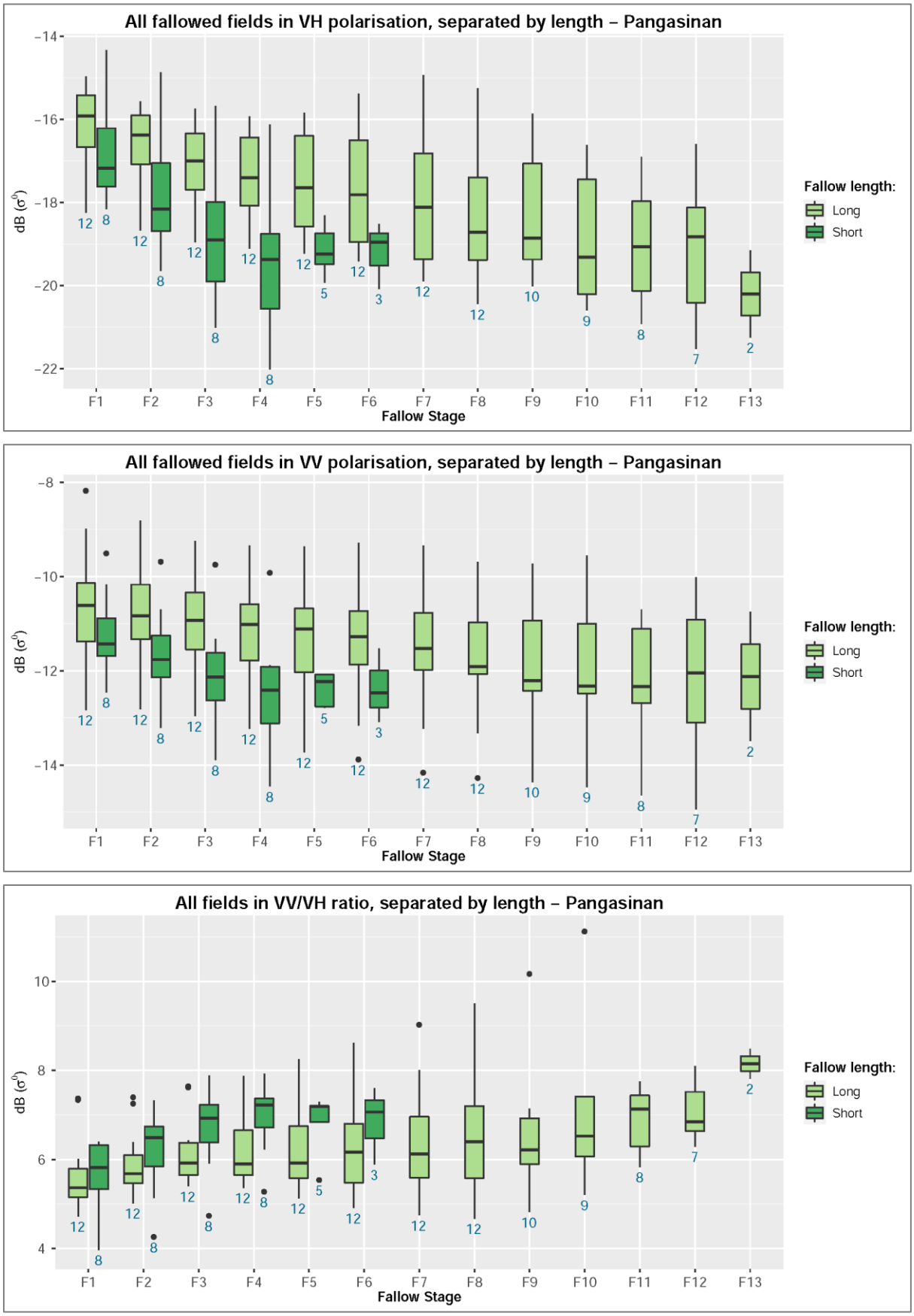

Figure 9. Boxplots of the backscatter coefficients for fallow separated by fallow duration (short and long) in Pangasinan for VH (top), VV (middle) and VV/VH ratio (bottom). Fallow number relates to Sentinel-1A revisit time since start of fallow.

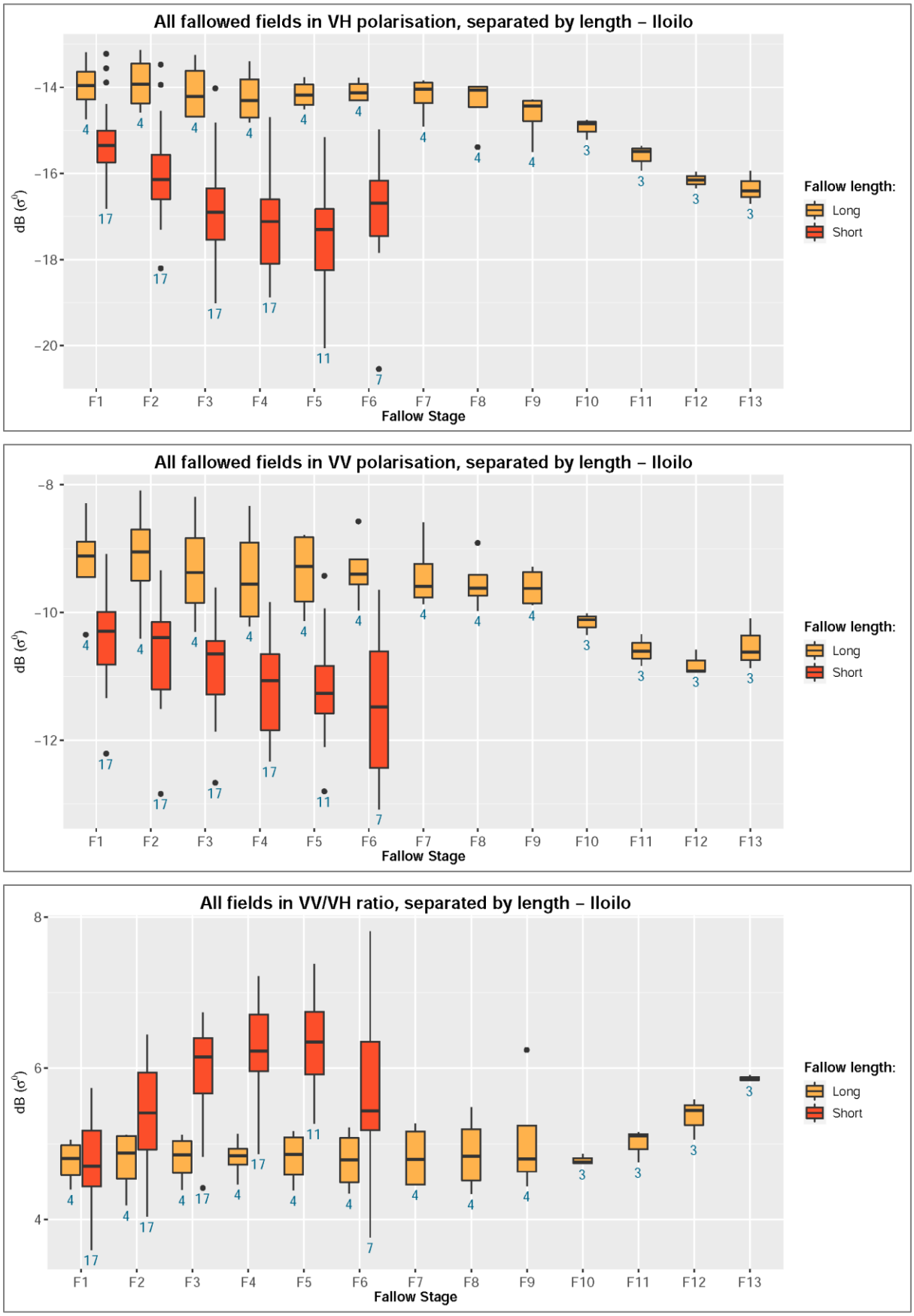

Figure 10. Boxplots of the backscatter coefficients for fallow separated by fallow duration (short and long) in Iloilo for VH (top), VV (middle) and VV/VH ratio (bottom). Fallow number relates to Sentinel-1A revisit time since the start of fallow.

5.2 Polarisation significance tests

Nonparametric tests were applied to the backscatter data to determine distinctions between various rice and fallow stages using the VH, VV polarisations and the VV/VH ratio. The boxplots covered in section 5.1 showed that there were temporal differences between the start and end of the rice season and fallow periods. The Kruskal-Wallis H test was performed to assess whether there were significant differences between backscatter values at the rice crop establishment, harvest, fallow start and fallow end. Table 4 shows the p-values from the Kruskal-Wallis test, which indicated that there were significant differences ($p<0.05$) between the means of the selected cropping types at each polarisation in data from Pangasinan and Iloilo.

Table 4. p-values for Kruskal-Wallis test between crop establishment, harvest and fallow start and end at VH, VV and VV/VH polarisation ratio. Pangasinan *n*=128; Iloilo *n*=157.

Province	p-value		
	VH	VV	VV/VH
Pangasinan	0.000*	0.000*	0.000*
Iloilo	0.000*	0.000*	0.000*

(* statistically significant at 0.001 level)

To indicate which cropping types were significantly different, a post hoc pairwise comparison was done, with results shown in Table 5. The results showed that in Pangasinan significant differences were between crop establishment-harvest, fallow start-fallow end and fallow end-harvest in the three polarisations. Additionally, fallow start-crop establishment was significantly different using the VH polarisation and the VV/VH ratio. Whereas in Iloilo, significant differences were observed between crop establishment-harvest, fallow start-fallow end, fallow start-crop establishment and fallow end-harvest using the VH polarisation and the VV/VH ratio. Fallow end-crop establishment differed when using the VV polarisation and the VV/VH ratio. Moreover, fallow end-harvest were the only cropping types that were significantly different in the three polarisations in Iloilo.

Therefore, the results showed that, as observed in the boxplots, among the three polarisations there were statistical differences between the start and end of the rice season and fallow periods only in Pangasinan. In Iloilo the differences between the start/end of fallow and the rice season are not as robust and more mixing of the backscatter values occurred.

Table 5. p-values for post hoc pairwise comparison from Kruskal-Wallis test between crop establishment, harvest, fallow start and fallow end at VH, VV and VV/VH polarisation ratio. Pangasinan *n*=128; Iloilo *n*=157.

Province	Cropping stage/activity	p-value		
		VH	VV	VH/VV
Pangasinan	CE-H	0.000	0.001	0.000
	FS-FE	0.000	0.034	0.000
	FS-CE	0.002	1.000	0.000
	FS-H	0.121	0.305	0.766
	FE-CE	0.301	0.156	1.000
	FE-H	0.000	0.000	0.000
Iloilo	CE-H	0.000	0.134	0.000
	FS-FE	0.000	0.064	0.001
	FS-CE	0.000	0.244	0.000
	FS-H	1.000	1.000	0.613
	FE-CE	1.000	0.000	0.000
	FE-H	0.000	0.003	0.001

Highlighted cells correspond to polarisations with sig. difference ($p<0.05$, $\alpha=95\%$)

In the post hoc pairwise comparison, the start and end of fallow showed good separability in at least two polarisations that could be used for detecting fallow. An additional test, the Mann-Whitney U test, was performed to assess whether there were significant differences between backscatter of the fallow start and end separated by the fallow duration (short and long fallows).

The results in Table 6 showed that in Pangasinan there were no significant differences ($p<0.05$) between fallow stages in the short and long fallow periods. In Iloilo, backscatter difference was significant between fallow durations at the fallow start in VH and VV polarisations and at the fallow end in VV polarisation. This was also supported by boxplots presented in Appendix C.

Table 6. p-values between fallow start and end separated by the fallow duration (short and long) from Mann-Whitney U test. Pangasinan *n*=20; Iloilo *n*=21.

Province	Fallow stage & duration	p-value		
		VH	VV	VH/VV
Pangasinan	Start Short - Start Long	0.305	0.238	0.624
	End Short - End Long	0.910	0.624	0.521
Iloilo	Start Short - Start Long	0.024	0.040	1.000
	End Short - End Long	0.081	0.024	0.698

Highlighted cells correspond to polarisations with sig. difference ($p<0.05$, $\alpha=95\%$)

Another Mann-Whitney U test was conducted to determine whether there were differences in the fallow backscatter characteristics based on the ecosystem type (irrigated and rainfed). Table 7 presents the p-values from Man-Whitney U test, which indicated that in Pangasinan there were significant differences in the fallow backscatter values among the three polarisation channels, whereas in Iloilo there were no significant differences.

Table 7. p-values of Mann-Whitney U test between fallow occurring in the irrigated and rainfed fields. Pangasinan *n*=172; Iloilo *n*=134.

Province	Fallow separated by ecosystem type	p-value		
		VH	VV	VV/VH
Pangasinan	Irrigated - Rainfed	0.001	0.002	0.015
Iloilo	Irrigated - Rainfed	0.590	0.459	0.644

(Highlighted cells correspond to polarisations with sig. difference ($p<0.05$, $\alpha=95\%$))

5.3 Fallow and rice detection

5.3.1 Fallow periods detection

The backscatter behaviour and statistical tests indicated differences between the start and end of rice and fallow periods. These differences were used to detect fallow by finding local minima and maxima of rice and fallow backscatter.

The accuracy assessment of the start and end of fallow periods was performed for each polarisation separately between the observed and detected highest and lowest point in the backscatter. At the fallow start (FS), maximum backscatter was detected in VV and VH polarisations and the minimum value in VV/VH ratio. Whereas at the fallow end (FE), minimum backscatter was detected in VH and VV polarisations and maximum in VV/VH ratio. The accuracy of this model was assessed by root mean square error (RMSE), which is widely used for evaluating time-series forecasting (Schlund and Erasmi, 2020). The RMSE results are shown in Table 8 and differences between the detected and observed FS and FE dates are displayed in Figure 11 and Figure 12.

VH had the highest overall detection accuracy, but the detection varied between the FS and the FE. Identification of the FS was most accurate in VH and VV/VH ratio in both locations (RMSE between 22.4 and 39.3 days); however, in Iloilo, the VV/VH ratio was most accurate (RMSE of 22.4 days or 1.9 Sentinel-1A revisit time) out of both locations. The VV polarisation resulted in the lowest detection accuracy (RMSE between 52.6 and 58.8 days). Whereas detection of the FE was most accurate in the three polarisations in both locations (RMSE between 9.7 and 11.4 days) that resulted in accuracy of less than one Sentinel-1A revisit time.

Table 8. Root mean square error (RMSE) result for the start and end of fallow. The RMSE was performed for derived minima and maxima dates from fallow backscatter and the farmer reported fallow periods. Pangasinan *n*=20; Iloilo *n*=21.

Province	SAR channel	RMSE - Fallow			
		Start of fallow		End of fallow	
		RMSE (days)	Sentinel-1A revisits	RMSE (days)	Sentinel-1A revisits
Pangasinan	VH	36.9**	3.1	9.7*	0.8
	VV	58.8**	4.9	9.7*	0.8
	VV/VH	39.3*	3.3	11.4**	0.9
Iloilo	VH	33.3**	2.8	9.4*	0.8
	VV	52.6**	4.4	10.5*	0.9
	VV/VH	22.4*	1.9	10.5**	0.9

(RMSE based on reported FS/FE and derived date from backscatter: * local minima; and ** local maxima)

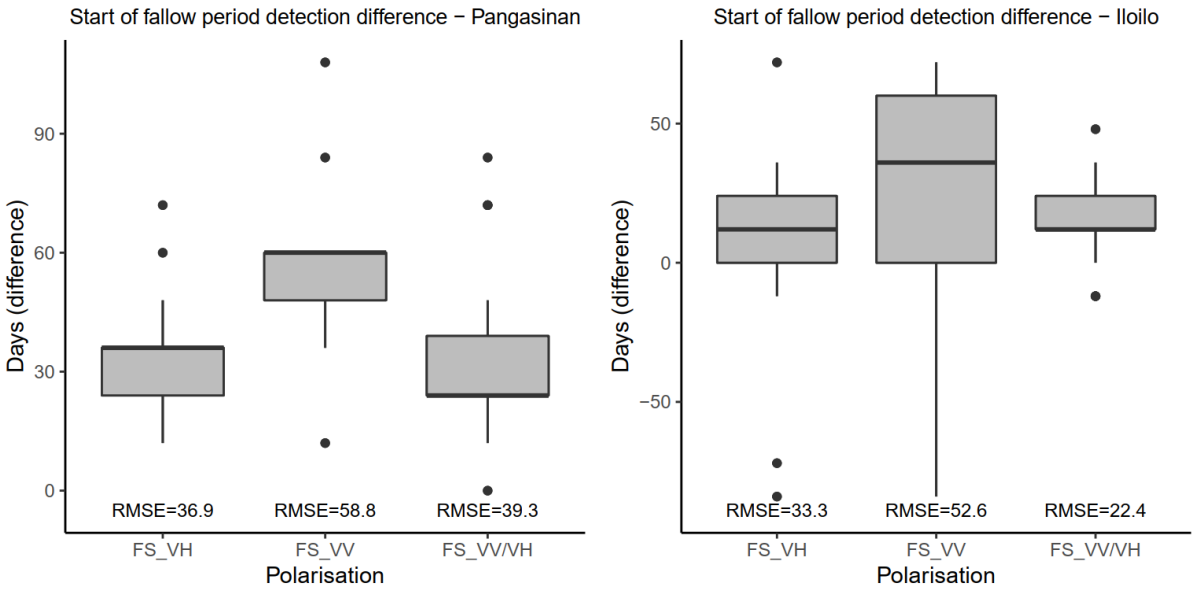

a) b)

Figure 11. Boxplots of the temporal differences between the observed fallow start (FS) date and the obtained VH and VV local maxima, and VV/VH ratio minima in a) Pangasinan and b) Iloilo. RMSE is expressed in days.

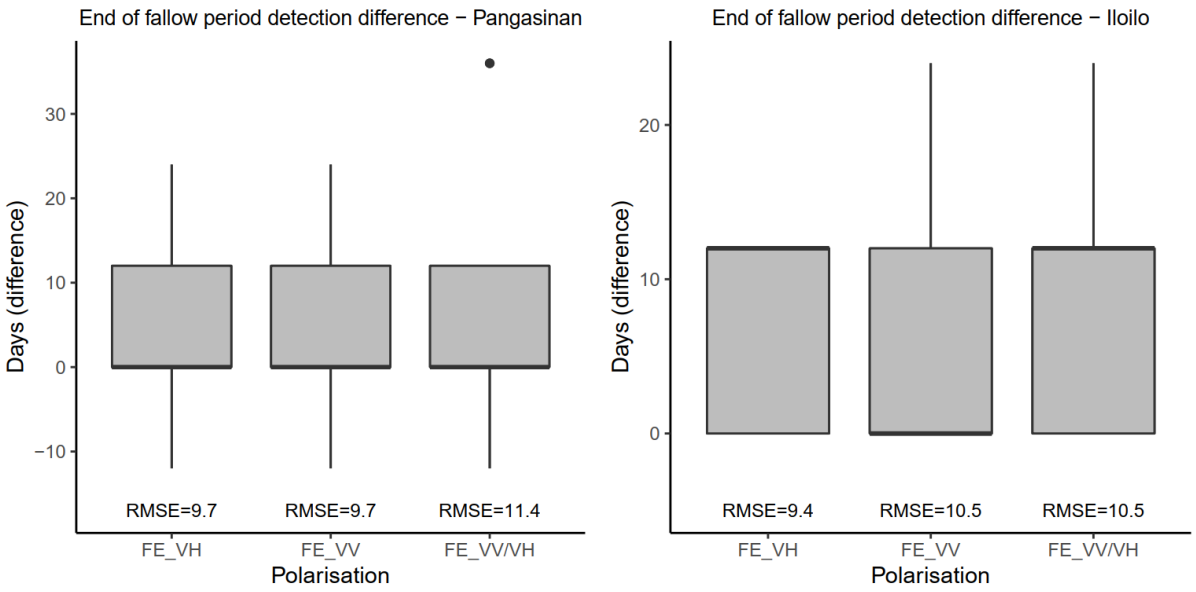

a) b)

Figure 12. Boxplots of the temporal differences between the observed fallow end date (FE) and the obtained VH and VV local maxima, and VV/VH ratio minima in a) Pangasinan and b) Iloilo. RMSE is expressed in days.

5.3.2 Rice season detection

In the case of the rice season detection, minima values were used for detecting the crop establishment in VH and VV polarisations, whereas for the VV/VH ratio, the maxima backscatter was identified. At harvest, the order was reversed, and maxima VH backscatter was used and the minima for the VV/VH ratio. Table 9 lists the RMSE results, with disparities between the detected and observed crop establishment and harvest dates plotted in Figure 13 and Figure 14.

The root mean squared difference between the crop establishment and local minima (maxima for VV/VH ratio) was lowest in Pangasinan (12 days in VH and 42.7 days in VV polarisations), whereas in Iloilo the RMSE difference was lowest in VV/VH ratio (16.4 days). At the end of the season, the RMSE difference between the reported harvest and local minima was lowest in Iloilo (20.2 days in VH and 21.5 days in VV/VH ratio), whereas in Pangasinan the difference was lowest in VV polarisation (45.6 days).

Based on the fact that Sentinel-1A's revisit time was 12 days, overall, the lowest RMSE differences at the start and end of the rice season were recorded in VH polarisation in both study locations. It is worth noting that the ratio resulted in second best detection difference, much closer to the results obtained in VH polarisation rather than the VV.

Table 9. Root mean square error (RMSE) result for detecting the start and end of rice season. The RMSE was performed for derived minima and maxima dates from the rice backscatter and the farmer reported rice season dates. Pangasinan *n*=44; Iloilo *n*=57.

Province	SAR channel	RMSE – Rice season			
		Start of season		End of season	
		RMSE (days)	Sentinel-1A revisits	RMSE (days)	Sentinel-1A revisits
Pangasinan	VH	12.0*	1.0	22.9**	1.9
	VV	42.7*	3.6	45.6**	3.8
	VV/VH	22.4**	1.9	30.3*	2.5
Iloilo	VH	13.1*	1.1	20.2**	1.7
	VV	68.3*	5.7	73.1**	6.1
	VV/VH	16.4**	1.4	21.5*	1.8

(RMSE based on reported SOS/EOS and derived date from backscatter: * local minima; and ** local maxima)

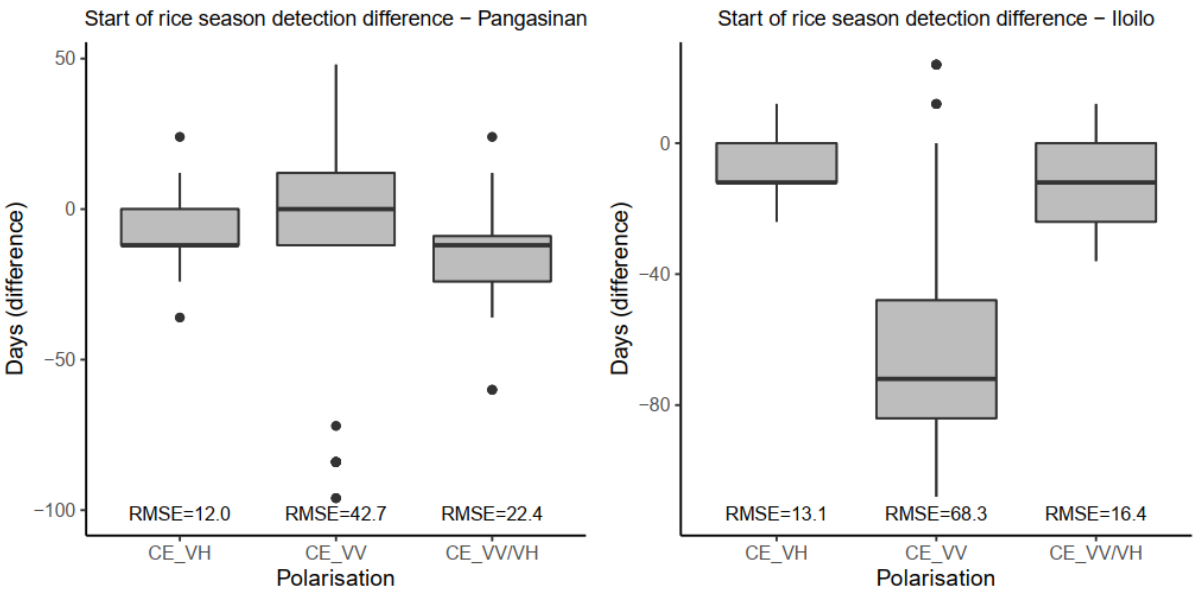

a) b)

Figure 13. Boxplots of the temporal differences between the reported crop establishment date and the VH and VV local minima, and VV/VH ratio maxima in a) Pangasinan and b) Iloilo. RMSE is expressed in days.

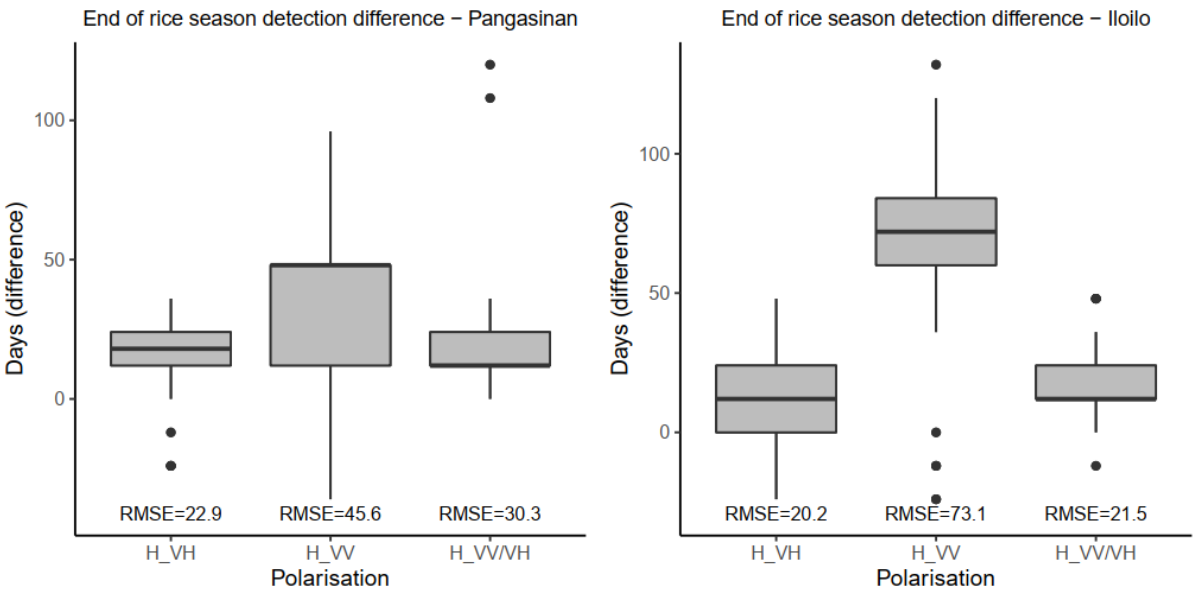

a) b)

Figure 14. Boxplots of the temporal differences between the reported harvest date and the VH and VV local maxima, and VV/VH ratio minima in a) Pangasinan and b) Iloilo. RMSE is expressed in days.

5.3.3 Between crops fallow detection

Between crops, fallow detection was performed on data from 18 fields (nine in each location) where two successive rice crops were present. As detection of the rice season performed better than detection of fallow seasons, a backward approach was applied for this task, where crop establishment was used as the end of fallow and harvest as the start of fallow. The results are shown in Table 10 and plotted in Figure 15 and Figure 16.

The results indicated that the detection of fallow periods (FS and FE) best performed in the VH polarisation (RMSE between 15.0 and 18.8 days in both locations). The accuracy was also good using the VV/VH ratio (RMSE between 11.3 and 22.3 days), however, resulted in low detection of the FS in Pangasinan (RMSE of 43.6). The VV polarisation performed the worst in detecting the FS in Iloilo and the FE in both locations (RMSE of a range from 74.2 to 79.8 days. RMSE of 27.4 days was recorded only for the FS detection in Pangasinan.

Table 10. Root mean square error (RMSE) result for detecting the start and end of between crops fallow periods. The RMSE was performed for derived minima and maxima dates from the rice backscatter and farmer reported dates. Pangasinan *n*=9; Iloilo *n*=9.

Province	SAR channel	RMSE - Fallow detected between crops			
		Start of fallow		End of fallow	
		RMSE (days)	Sentinel-1A revisits	RMSE (days)	Sentinel-1A revisits
Pangasinan	VH	18.8*	1.6	16.0**	1.3
	VV	27.4*	2.3	79.8**	6.6
	VV/VH	43.6**	3.6	11.3*	0.9
Iloilo	VH	15.0*	1.2	15.5**	1.3
	VV	77.6*	6.5	74.2**	6.2
	VV/VH	22.3**	1.9	18.8*	1.6

(RMSE based on reported SOS/EOS and derived date from backscatter: * local minima; and ** local maxima)

The boxplots indicated that the FS detection (Figure 15) was skewed towards 12 days before harvest, whereas dip of the SAR signal or its saturation in the band ratio (indicating the FE; Figure 16) was detected mostly 12 days after the crop establishment in VH and VV/VH ratio. In VV polarisation detection of local maxima was mostly occurring 84 days after the crop establishment.

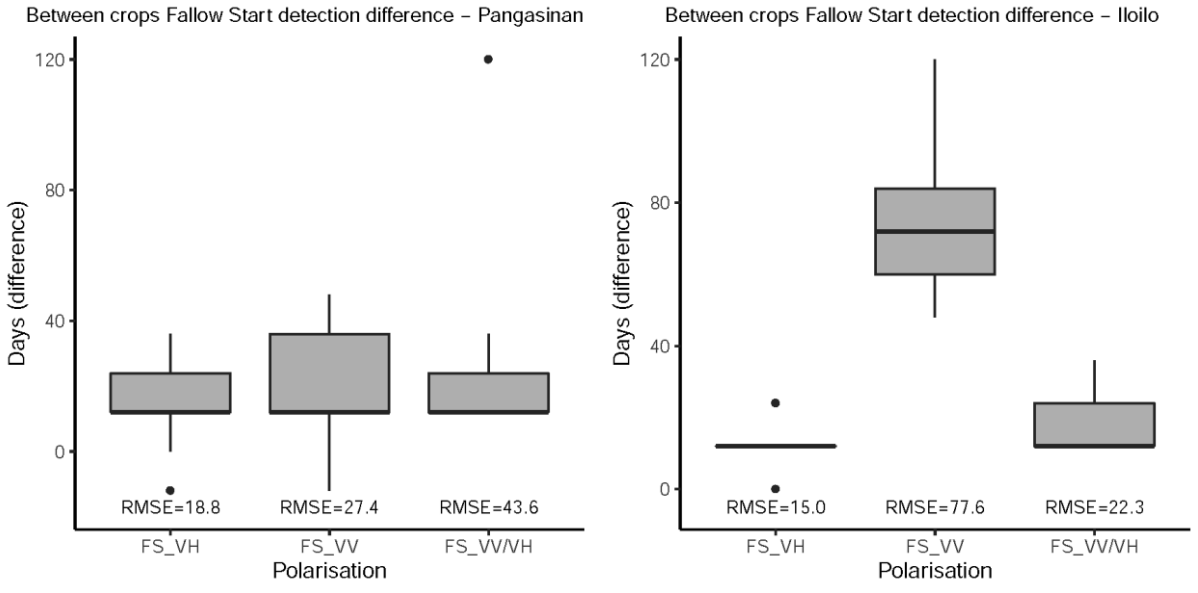

a) b)

Figure 15. Boxplots of the temporal differences between the reported harvest date (fallow start) and the detected VH and VV local maxima, and VV/VH ratio minima in a) Pangasinan and b) Iloilo. RMSE is expressed in days.

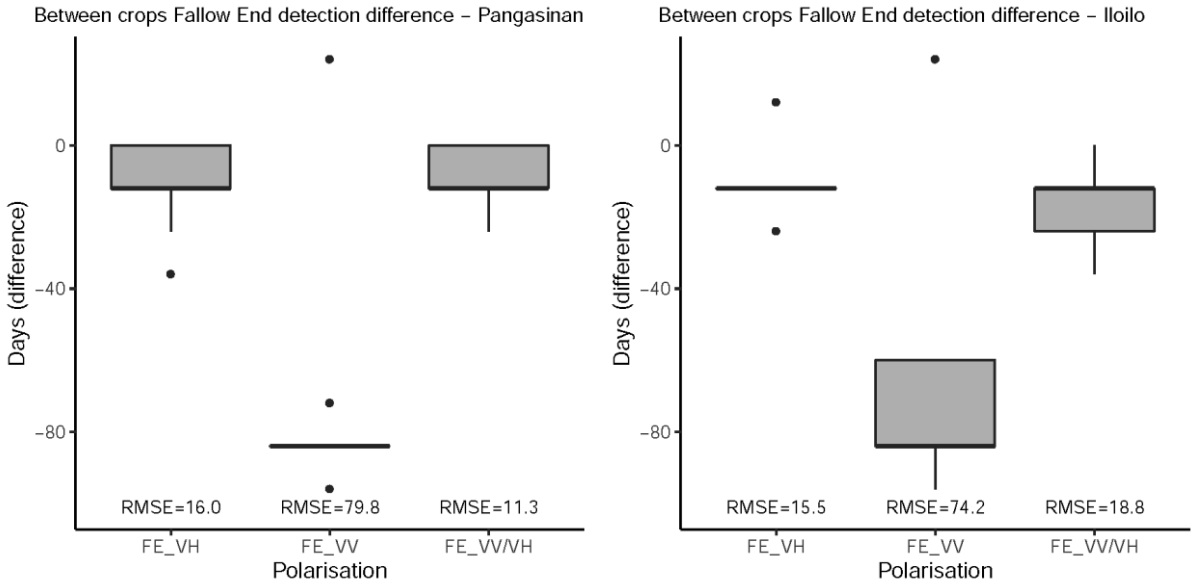

Figure 16. Boxplots of the temporal differences between the reported crop establishment date (fallow end) and the detected VH and VV local minima, and VV/VH ratio maxima in a) Pangasinan and b) Iloilo. RMSE is expressed in days.

5.4 Rainfall

Rainfall data was used for observing if precipitation, or lack thereof, impacted fallow behaviour. Table 11 presents average rainfall received per field over the fallow periods in the study sites. Pangasinan received the least rainfall (45.2 mm) while Iloilo experienced 2.5 time more rainfall (116.6 mm) over the fallow periods.

Table 11. Average amount of rainfall during the fallow periods received in the fallowed fields in Pangasinan and Iloilo.

Province	Average fallow rainfall per field (mm)
Pangasinan	45.20
Iloilo	116.56

Figure 17 shows average dekadal distribution of rainfall over the fallow periods in Pangasinan and Iloilo extracted from CHIRPS data. Each column in the graph corresponds to the average amount of rainfall that was obtained from the start of fallow in each studied field and distributed depending on fallow duration. Pangasinan received an overall low amount of rainfall in each dekad, except an increase in average rainfall in the first fallow dekad; however, this peak was affected by substantial rainfall experienced on 27/10/2018, at which point fallow started in only three fields (110, 116 and 131). The remaining fields received a significantly lower amount of rainfall in the first dekad, not exceeding 27.6 mm. Therefore, the peaked value will not be

considered as significant in the overall analysis of rainfall at the start of fallow periods in the Pangasinan province. Rainfall distribution in Iloilo was more spread out throughout the year that has not exceeded 25mm in any of the dekads.

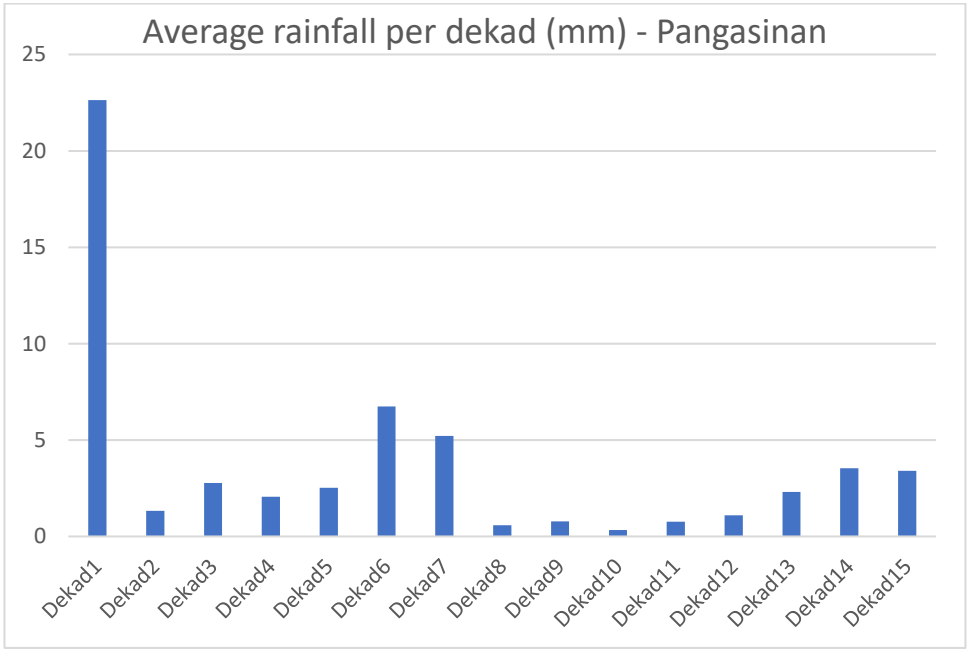

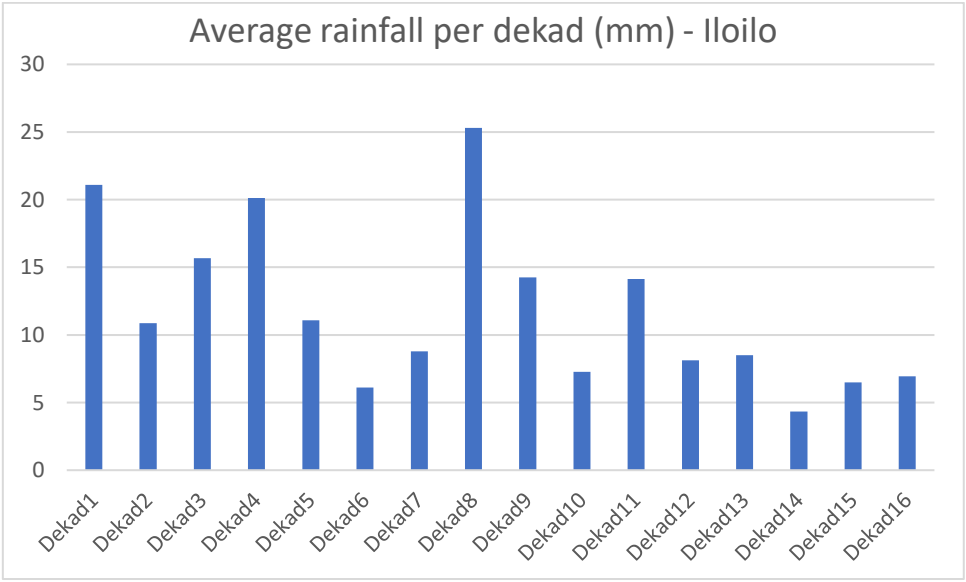

Figure 17. Average rainfall per dekad covering the duration of the fallow periods in Pangasinan (upper) and Iloilo (lower). Dekad1 corresponds to the start of fallow in each field. Duration based on fallow occurrence with Dekad16 containing rainfall data only for the longest fallow periods.

6 Discussion

This study looked at the temporal SAR backscatter characteristics of fallow within rice fields. Addressing a gap in the reviewed literature, this study described temporal characteristics of fallow periods and compared them to rice backscatter behaviour. In addition, fallow duration and ecosystem types – irrigated and rainfed fields – were compared to identify potential differences in fallow or land management based on interpretation of the backscatter values. Furthermore, the study aimed to establish whether fallow can be detected using Sentinel-1A data, and which polarisation best showed significant differences between fallow and rice.

6.1 Fallow and rice SAR backscatter characteristics and fallow duration

The results indicate that analysed rice fields have a well-defined temporal profile from the crop establishment until harvest. The profile is characterised by overall increasing trend from crop establishment until flowering or harvest in VH polarisation; increasing at the reproductive stage and decreasing at the ripening stage in VV polarisation; and decreasing in VV/VH polarisation ratio, which is in line with findings from other studies (Chen et al., 2007; Oh et al., 2009; Asilo et al., 2014; Nelson et al., 2014; Mansaray et al., 2017; Bazzi et al., 2019; Chang et al., 2020). The backscatter profile was lowest 12 days after the crop establishment in the VH polarisation, which was ascribed to increased flooding after the crops were well established (Nelson et al., 2014) resulting in more spectral reflection. Saturation of the SAR signal was reached between flowering and harvest using VH polarisation in Pangasinan and Iloilo, and using the VV polarisation in Pangasinan. The saturation of the signal was attributed to the peak in plant height and canopy around flowering stage, which was followed by a slight decline near harvest when leaves began to wither and ground exposure increased (Li et al., 2018; Son et al., 2018). However, in the case of VV polarisation in Iloilo, after initial increases, the signal reached its peak at the mid-point of the vegetative phase and then carried on decreasing. This pattern may appear unexpected because, even though VV polarisation is more sensitive to small canopy reductions than VH polarisation (McNairn and Brisco, 2004; Oh et al., 2009; Nelson et al., 2014), rice canopy increases at the vegetative stage, and this should be reflected by backscatter increases due to more double-bounce reflections (McNairn and Brisco, 2004). Mansaray et al. (2017), however, experienced similar results, which they attributed to increased attenuation by leaves and stems using the VV polarisation. Moreover, no such behaviour was observed using the VH polarisation in Iloilo, which resulted in a more sustained increase in backscatter that resembled rice-growth pattern observed in Pangasinan, nor was it observed using the VV polarisation in Pangasinan. However, this divergence between the VV and VH polarisations in Iloilo resulted in a more pronounced temporal profile of VV/VH ratio, than in Pangasinan, that showed better separability between the crop establishment and harvest.

The statistical tests and boxplots (see Appendix C) indicated that, except for VV polarisation in Iloilo, the start and end of the rice season can be detected in Sentinel-1A imagery using local minima and maxima backscatter values in the remaining polarisations. As for fallow signal, the analysis indicated some temporal changes during fallow events, which differed slightly between Pangasinan and Iloilo provinces. These changes were not as well-defined as they were for rice, but an attempt was made to segregate them into three phases – the start of fallow (FS);

the mid fallow (FM) and the end of fallow (FE). The classification into three phases was made more difficult by the lack of information about specific fallow conditions in the farmer questionnaires. This limitation was overcome thanks to the application of findings from previous studies that analysed backscatter behaviour in exposed soils and vegetated areas.

6.1.1 Fallow start

Fallow periods began with higher backscatter coefficients, but with values normally lower than at the rice harvest, and in general they decreased over a few consecutive weeks in VH and VV polarisations in both provinces. This indicated that the soils were not fully exposed after harvest as the values were too high, which can be attributed to the crop residues, such as stubble and cut straw, remaining on the field after harvest and their decay over time. This was also supported by a gentler decline in backscatter coefficients in VV polarisation, than in VH polarisation in both provinces, because VV is more sensitive to remaining biomass (McNairn et al., 2002; Schlund and Erasmi, 2020), but is unaffected by residue structural characteristics (McNairn and Brisco, 2004). VH polarisation, on the other hand, is more sensitive to crop structure that results in multiple volume scattering of vegetation canopy and scattering from rough surfaces and thus, results in steeper decreases in the post-harvest conditions (McNairn and Brisco, 2004). These results are supported by questionnaire data, which suggested that the most prevailing harvest practice was leaving straws in the fields to decompose, as reported by majority of farmers in both provinces. In Pangasinan, the majority of harvests were done using machinery, whereas in Iloilo, manual harvest was the prevailing method, with the former typically leaving more standing crop residue and cut straws in the field (Bijay-Singh et al., 2008). The data shows that in Pangasinan there was a bigger drop in backscatter values after harvest than in Iloilo. However, as the majority of crops in Pangasinan were mechanically harvested, it would be expected for the backscatter to decrease more slowly than in mainly manual harvested fields in Iloilo. Perhaps this difference could be attributed to weed presence during and after the rice season (Minh et al., 2019) in Iloilo that then was characterised by higher backscatter coefficients in VH polarisation until mid-fallow. Nevertheless, it is unclear if weed growth would have enough time to appear, especially in areas such as Iloilo, where up to three rice seasons can be grown in a year. Alternatively, Li et al. (2012) noted that the difference could be attributed to increased surface scattering from wet soils and rice residue after harvest which resulted in gentler temporal decrease, especially since Iloilo experienced higher rainfall during the dry season. However, this would require further investigation.

Other stubble management methods presented differences in the fallow backscatter behaviour. In Pangasinan there was one field (120) where rice residues were burnt in the field. Fallow at that location (see Appendix G) was characterised by very low backscatter values from its start (-18.24 in VH and -12.83 in VV) and a gradual decrease over time due to dominance of bare soils directly after harvest (Bégué et al., 2018). Similar behaviour was observed in fallow where crop residues were removed after harvest (fields 118 and 151 in Pangasinan; and 654 in Iloilo), but backscatter in those locations resembles more the overall fallow behaviour, which was at first relatively high due to stubble scattering (Schlund and Erasmi, 2020), but on average lower than in the fields with residues left in the field, with a gradual reduction over time. Furthermore, none of the fields' backscatter coefficients increased with time, indicating that the conditions and duration were not favourable for significant vegetation development. However, certain

changes in backscatter behaviour were observed in fields with residue remaining in the fields, which are thought to be related to vegetation development mid-fallow, although these were linked to fallow duration rather than stubble management method.

It should be noted that vegetation development is not solely linked to the presence of crop residue, but rather to the conditions, soil organic levels and water availability that the uncleared fields generate after harvest, which permit for faster regeneration of vegetation, such as weeds or crops, than in managed or burnt fields (Nielsen and Calderón, 2011). Additionally, higher backscatter values at the FS also indicate that soils were drained before the rice harvest (Bégué et al., 2018), which creates desirable conditions for decomposing of the crop residues.

6.1.2 Mid-fallow

In the longer fallow events (over 72 days or six Sentinel-1A revisits in Pangasinan and over 84 days or seven Sentinel-1A revisits in Iloilo) mid fallow was observed. It was characterised by signal fluctuations following a descending trend since the FS, but this characteristic was not present in all fields with longer fallow. Additionally, no such behaviour was seen in fallow shorter than 84 days. It should be noted that the number of shorter and longer fallow durations was different in both provinces – short n=8 and long n=12 in Pangasinan, and short n=17 and long n=4 in Iloilo.

Halfway through fallow in Pangasinan, on average between 60-72 days since harvest, some subtle changes in the backscatter values were observed, characterised by short increases of the upper boxplot quartiles lasting for 24-36 days followed by further decrease towards the end of fallow periods. Those were assumed to indicate wild vegetation development or cropping of drought tolerant non-rice crops, especially since such changes were more prominent in VV polarisation that is more sensitive to volume scattering of even small vegetation (McNairn et al., 2002; Brogioni et al., 2010). In Iloilo, the changes in fallow backscatter were observed at similar times but lasted between 24-48 days; however, the increase of median backscatter in both polarisations was more substantial than in Pangasinan (possibly due to lower number of samples available at that time in Iloilo), suggesting that vegetation growth was more prominent in Iloilo and lasted for approximately 48 days before starting to decline. This temporal break between harvest and the start of fluctuations in backscatter was more likely affected by unreported non-rice crops rather than weed development (Chang et al., 2020). This also correlates with rainfall data that was over twice as high and more spread-out in Iloilo than in Pangasinan, making conditions for growth more favourable in Iloilo.

Moreover, mid-fallow in Iloilo, a significant jump in the backscatter median (Figure 8) was observed and occurred at a point where the number of fields with fallow over 84 days was declining (from n=15 to n=4). It was characterised by the largest magnitude using the VH and VV polarisations, out of all boxplots in the time-series, and is also clearly observable when the backscatter was separated by fallow length. This may have important implications for understanding management practices, which were typically not reported in the farmer data, except in a few cases where some ratooning during fallow was reported. It was therefore assumed that the fields were kept unmanaged. However, since the conditions for vegetation development were more favourable in Iloilo, it was expected that some development of wild vegetation might also take place in shorter fallows before they are disrupted by the land

preparation for planting of the next crop. The argument is also valid for Pangasinan, but the separation of backscatter between short and long fallow was less pronounced. Therefore, the observed changes suggest that in the study, a location's fallow duration was linked to management practices, where shorter fallows were left unmanaged and longer fallows were managed and used for planting short-term crops, such as garlic and mung bean, which are characterised by short and gentle peaks of the SAR signal (Gumma et al., 2016; Chang et al., 2020).

Moreover, strong rain events can also affect interpretation of fallow backscatter (Bégué et al., 2018) by changing the depolarisation of the wet soils defined by higher backscatter intensity using the VV and VH polarisations (Gherboudj et al., 2011; Khabbazan et al., 2019). Therefore, drying, and wetting conditions lead to temporal fluctuations of the SAR signal. However, rainfall data for the fallowed fields indicate that, except at the beginning of fallow, no substantial rainfalls were experienced in either of the study sites, particularly in the Pangasinan province, which was defined by largely low dekadal rainfall (<7mm per dekad). Iloilo received on average two and a half times more rain than Pangasinan, but the rainfall was typically low and spread-out throughout the fallow periods. Some level of wetting effect is, however, expected within intensely cultivated areas, such as Iloilo (Villano et al., 2019), where continuous irrigation can take place (Sander et al., 2018). However, harvest reduces sensitivity of VH and VV polarisation to soil moisture that prevails throughout cropping season (Khabbazan et al., 2019). Therefore, any changes in the signal mid-fallow were assumed to be linked to the vegetation coverage and crop residue post-harvest rather than soil moisture content.

6.1.3 Fallow end

The end of fallow (FE) was assigned to the last phase of fallow periods, which was represented by accelerated declining of signal in the VH and VV polarisations, and reached a minimal point near the last day of fallow occurrence. This stage was observed in all fallowed fields irrespective of fallow length, although the time-series showed a distinctive behaviour dependant on fallow length and location.

In Iloilo shorter fallows (<84 days) were characterised by a faster decrease and lower backscatter coefficients at the FE, especially in the VV polarisation. Longer fallows (>84 days) decreased at a similar pace after mid-fallow fluctuations, but the last backscatter values were significantly higher than in short fallows. Whereas, in Pangasinan the distinction between fallow lengths was lower with coefficient at the FE in VH higher than at the end of longer fallows. Those differences can be attributed to Iloilo having lower number of fields with long fallow periods (Pangasinan n=12 and Iloilo n=4) and higher signal saturation from probably short-term crops during the mid-fallow phase, especially since more fields had access to irrigation in Iloilo than in Pangasinan, shortening fallow duration in favour of planting more rice crops. Moreover, varying declines in the FE backscatter values indicated varying level of surface scattering, especially using the VV polarisation (McNairn et al., 2002), characterised by quicker and greater soil exposure due to the land preparation for the next crop in the shorter fallows, and a gentler gradual exposure in the longer fallows, due to weed and crop residue decay and drying of the land (McNairn et al., 2002; Bégué et al., 2018). Additionally, several

fields in Pangasinan reported dips below -20dB of VH polarisation observed in the shortest (48 days) and several longer (>84 days) fallows, which were not observed in Iloilo. The dips were lower than the lowest point during the rice growing season (crop establishment) and were connected to potentially standing water in preparation for the next planting of rice (Asilo et al., 2014; Nelson et al., 2014; Minh et al., 2019).

Furthermore, the very end (the last day of available SAR data) of some fallowed areas in both locations were characterised by rises in the VH and VV backscatter. Because the changes happened at the end of dry season, when the surface scattering of bare soil was most dominant (McNairn et al., 2002), those changes were linked to preparation/tillering of land for the next crop.

6.2 Fallow duration

Analysed data covered wet and dry seasons (March 2018 to March 2019), but fallow periods occurred only during dry season, between October 2018 and March 2019. All the farmer reported fallow periods took place after the last crop, when field surveys were collected (February-March 2019). This was also the case for the additional identified fallow periods in Iloilo and Pangasinan, when no cropping activity was reported for at least 48 days. Only Pangasinan had one additional fallow period that happened between crops (between rice and mung bean), but it also occurred at the beginning of the dry season. This indicates that in the studied locations unmanaged fallow of at least 48 days occurs during the dry season when water availability is lowest, even in the irrigated fields.

Fallow duration in the studied locations varied among most of the fields, with the shortest periods lasting from 48 days in Pangasinan and 60 days in Iloilo, and up to 156 days and 168 days in Pangasinan and Iloilo, respectively. It should be noted that the shortest fallow was limited to the fallow periods reported by the farmers and the study did not look at any other/shorter periods between crops that were fallowed.

Additionally, the availability of SAR data, which was collected and processed up until the end of March 2019, could have influenced the end of some fallow periods. Therefore, it is possible that several fields were left fallow for longer. However, as this was at the end of the dry season, and some backscatter suggested field preparation activities, it is assumed that data availability had little impact on the analysed duration of the fallow periods.

Moreover, the temporal series revealed that fallow behaviour differed depending on its duration, which was categorised into short (<72 days in Pangasinan and <84 days in Iloilo) and long fallow (>72 days in Pangasinan and >84 days in Iloilo). In Iloilo short fallow was most common (17 short and 4 long fallow periods), whilst in Pangasinan long fallow was predominant (8 short and 12 long fallow periods). This disparity was attributed to varying cropping intensities in both locations, out of which Iloilo is known as one of the most intensely cultivated monocropping areas in the Philippines, where up to three rice crops are grown within one year (Villano et al., 2019) resulting in shorter fallow durations.

6.3 Fallow differences based on ecosystem types

Ecosystem type was thought to have impact on the overall fallow backscatter behaviour. As fallow occurred during the dry season (between the end of November 2018 to the end of March 2019), an assumption was made that fallow occurring in fields with access to irrigation was going to experience more vegetation growth than the rainfed fields, as water availability could have been greater if the neighbouring fields were flooded with water. However, statistical analysis for Iloilo indicated that there was no difference between fallow ecosystem type in all polarisations. In contrast, in Pangasinan the Mann-Whitney test suggested that there was a difference between ecosystem types. Those findings are also supported by comparing the time-series of fallow backscatter in irrigated and rainfed ecosystems (see Appendix D), which demonstrated differences in fallow behaviour in the two ecosystem types. In Pangasinan, backscatter decreased significantly at the FS in all polarisations, whereas such a steep change was not observed in Iloilo.

Moreover, fallow in the irrigated fields in Pangasinan started later than in a rainfed ecosystem – mid January-February in irrigated and November-December in rainfed fields. Occurrence of fallow mid-term of the dry season was characterised by a dynamic decrease at the start of fallow in irrigated fields as exposure to barren land and drying of the crop residue accelerated at that time. In Iloilo, fallow in irrigated ecosystems also began between the end of December-February, but three fields had ratoon crops growing in portions of the fields, which could explain why the FS had higher backscatter in VH polarisation and gentler decrease over the fallow periods in irrigated fields in Iloilo. Additionally, the temporal variation observed between both ecosystems was despite irrigated fields receiving lower rainfall during fallow than rainfed ones (see Appendix E). This suggests that cropping of rice and/or non-rice crops can be done for longer in irrigated ecosystems despite receiving lower rainfall than in rainfed ones. Therefore, in rainfed ecosystems the farmers were possibly forced to enter fallow earlier than in areas with access to irrigation.

In summary, fallow behaviour mainly differed at the start of fallow between irrigated and rainfed ecosystems, but the overall difference between the ecosystems was statistically significant only in Pangasinan province. Pangasinan experienced steeper deterioration of the backscatter in all polarisations after harvest, with gradual increases towards the end of fallow in irrigated ecosystems. Additionally, fallow in irrigated fields occurred mid-dry season and had a shorter duration compared to rainfed locations. In Iloilo irrigated fallow was also shorter but had a more mixed response represented by higher backscatter coefficients in VH than during the rice season which can be linked to higher multiple scattering (Mansaray et al., 2017) from the secondary crop growth reported in parts of some fields. In VV and VV/VH ratio the variation between the ecosystems was not as noticeable, represented by lower σ^0 from the FS, which can be linked to VV's lower receptiveness to volume scattering (Xu et al., 2019). This was also reflected in VV/VH ratio. Apart from that, the signal variation remained consistent among all polarisations towards the FE in irrigated and half term of fallow duration in rainfed ecosystem, which may explain lack of statistical differences between all polarisations reported in Iloilo.

6.4 Fallow and rice detection using SAR time-series

In the studied locations, fallow occurred during the dry season after last crop was harvested. There were no reported fallows between crops, which affected identifying fallow in continuous data that had rice crops before and after fallow periods. Additionally, analysis of the temporal SAR data showed that the high variability of fallow backscatter can make fallow detection problematic. However, the statistical tests indicated that the FS and the FE were significantly different among all polarisations. Similar results were observed in rice development points where significant differences were observed between the crop establishment and harvest. Those points could be used for detecting local maxima and minima as the start and end of fallow.

Therefore, two approaches for detecting fallow were proposed. One was detecting fallow during actual fallow periods; another method was a backward approach where the start and end of the rice season would be used as the end and start of fallow. The former method was based on backscatter between rice reproductive stage and the fallow end, whereas the latter method used rice backscatter that contained backscatter before, during and after rice crops.

The FS detection using fallow backscatter had a mixed results with best accuracy observed only in VV/VH ratio in Iloilo (RMSE of 22.4 days) followed by VH polarisation (RMSE between 33.3 - 36.9 days) in both provinces, and VV polarisation having the worst detection accuracy (RMSE between 52.6 - 58.8 days). The boxplots (Figure 11) indicated that higher RMSE at the FS resulted from detection of backscatter between the flowering stage and harvest where signal reached its peak, except in the VV polarisation where signal saturation occurred closer to the vegetative stages than harvest. Moreover, three fields in Pangasinan and three in Iloilo were ratooned before fallow commenced. Ratoon had lower backscatter than the rice harvest, which affected the FS detection accuracy by increasing the temporal break between backscatter peak near harvest and fallow. Alternative analysis was performed with ratoon fields removed. The accuracy (see Appendix F) increased slightly in Pangasinan to RMSE of 28.2 and 31.7 days in VV/VH ratio and VH, respectively. In Iloilo accuracy had not changed except for VH, for which the RMSE increased to 2.6 days. Overall, the FS detection performed best in VH and VV/VH ratio, and was between 23.4 and 31.7 days, which is below two and a half Sentinel-1A revisit times. Detection of the end of the rice season (harvest – fallow commencement indicator) resulted in better accuracy than the FS detection – ranging between 20.2-22.8 days in VH polarisation, followed by VV/VH ratio of accuracy between 21.5-30.3 days. This was because the signal reached saturation between the rice flowering and harvesting in VH and VV/VH ratio, which was the same as in the case of FS detection.

Detection of the FE performed particularly well using fallow backscatter with RMSE accuracy best between 9.4 and 11.4 days, which was less than 12 days or one Sentinel-1A revisit time, in both locations over the three polarisations. It also resulted in better accuracy than detection of rice establishment (the start of the rice season - alternative marker for the end of fallow), where detection accuracy was only slightly poorer and was near the temporal resolution of Sentinel-1A at 12-day revisit time in VH polarisation and less than two Sentinel-1A revisit times in VV/VH ratio. Better performance of fallow detection than the start of the rice season may have been affected by the fact that used datasets finished before the next crop was recorded. However, as the backscatter was at its lowest at the FE, which in many instances was

lower than at the crop establishment observed over preceding rice crops, it is unlikely that the detection would have been significantly different. This reasoning is supported the fact that the lowest backscatter values possible reflected flooding of the fields (Asilo et al., 2014; Clauss et al., 2018a; Minh et al., 2019) that were then followed by gentle backscatter increases observed in a number of fields at the end of the used data, which were connected to tillering practices taking place in preparation for the next crop.

To summarise, the fallow and rice season detection was weakest using VV polarisation. This was related to VV sensitivity to canopy attenuation at a much earlier stage than when using VH polarisation (Oh et al., 2009; Nelson et al., 2014; Li et al., 2018; Son et al., 2018), which in the studied fields VV on average started to decrease 48 days since the crop establishment. Furthermore, VV experienced more backscatter values mixing between fallow and the start of the rice season than the other two polarisations. Therefore, VH and VV/VH ratio have much better potential for detecting fallow periods based on the start and end of rice seasons. Similar conclusions were also reported by (McNairn and Brisco, 2004; Onojeghuo et al., 2018).

Additionally, the detection methods used in this study were not affected by missing image acquisition in either of the provinces. This was because the missing data occurred mid-rice and -fallow seasons. Furthermore, the Savitzky-Golay filter applied to the original data should have minimised the impact of missing values (Estel et al., 2015). However, should the missing date occur at the beginning or the end of the fallow or rice season, or if more acquisitions were missing, then the detection would have been affected.

6.5 Fallow detection between rice crops

Between crops fallow detection was performed using a "backward" approach to fields with two rice crops to identify fallow periods between harvest and rice establishment. The detection results showed that this method had similar accuracy to rice cropping season recognition and was most accurate using the VH polarisation (RMSE between 15,0 and 18,8 days at the FS and 15,5 and 15,0 days at the FE). The FE had the best accuracy in VH and VV/VH ratio (RMSE between 15.5 and 16.0 days in VH and 11.3 and18.8 days in VV/VH ratio). The boxplots (Figure 13 and Figure 14) indicated that the FS were identified 12 days before the rice harvest in the three polarisations in Pangasinan and VH and VV/VH ratio in Iloilo. In Iloilo, VV polarisation had the worst recognition of the FS, which resulted in detection error of RMSE 77.6 days. The results were due to the highest points in the backscatter occurring before flowering stages, and not near harvest, as was the case with VH. Similar skewedness of the detection was observed at the FE in both study locations, where lowest points were detected around the flowering stage. The low detection accuracy in VV was in line with rice backscatter behaviour observed in VV, especially in Iloilo, which was discussed in Section 6.1. Additionally, detection of fallow between crops resulted in longer fallow durations than reported by the farmers (see Table 12). The average overestimation ranged from 17.3 days in VH in Pangasinan, which is relatively low considering that Sentinel-1A revisit time is 12 days, to 133.3 days in VV in Iloilo, which further confirms the low accuracy of the VV polarisation also detected in the fallow and rice season recognition.

Table 12. Average fallow duration observed from the farmer questionnaires and detected between crops. Pangasinan *n*=9; Iloilo *n*=9.

Province	Average fallow duration (days)			
	Observed	Detected		
		VH	VV	VV/VH
Pangasinan	48.0	65.3	130.7	77.3
Iloilo	26.7	52.0	160.0	62.7

6.6 Discussion of the data used in the study

In the stacks of images used in this study, there were a few Sentinel-1A images that were not available due to missing acquisitions. In Iloilo, the acquisition was missing on 14/02/2019 and this mostly impacted fallow periods and some rice crops near flowering stages. Due to this, calculations of fallow duration in Iloilo were adjusted to reflect true fallow lengths. Moreover, the missing acquisition could explain why the median at the flowering stage in Iloilo was lower than expected, compared to harvest. Whereas, in Pangasinan the missing acquisition on 28/08/2018 had no bearing on fallow because it happened before the commencement of the earliest fallowing period. However, it occurred between the late vegetative and early rice ripening stages, affecting data primarily at the flowering stage, for which next available acquisition date was assigned. However, because the start of the rice season in Pangasinan was more varied, it is assumed that the missing date had a lesser impact on rice backscatter interpretation than in Iloilo.

This study extracted backscatter data for fallow and selected rice-development phases to show a continuous trend profile during the rice season and fallow. However, the original SAR data contained temporal noise, which was characterised by variations in backscatter values, that according to previous studies (Nelson et al., 2014; Clauss et al., 2018b; Son et al., 2018; Chang et al., 2020) were not expected to appear as part of the gradual process of vegetation change. The Savitzky-Golay (SG) filter provided an effective smoothing method for reducing temporal noise in the original temporal time-series while maintaining the shape and height of the waveform peaks. Furthermore, rice development stages and activities were useful for establishing SG filter smoothing parameters that did not under or over fit the filtered data that otherwise could have impacted interpretation of the temporal trends (Chen et al., 2004).

Additionally, the behaviour of known rice temporal characteristics and cropping dates were found to be misaligned for a number of rice seasons when the farmer reported dates were compared to temporal backscatter. Rice seasons deemed inaccurate were removed from the analysis. This demonstrates a difficulty that can arise from relying solely on the farmer reported dates and the need for some sort of verification. Regular field visits around the period of SAR image acquisition could be one solution, however, this procedure is inconvenient and costly. Nevertheless, the verification used in this study proved a viable option for alleviating such issue.

6.7 Limitations and recommendations

The field data used in the research lacked information about the conditions during fallow periods. Due to this, interpretation of fallow behaviour was limited to the temporal changes observed in backscatter values and assumptions made about water availability and cropping practices reported for rice cropping seasons, such as ecosystem harvesting method and copping of non-rice crops, as well as dekadal rainfall data extracted from CHIRPS images. Consequently, the analysis was restricted to what was known from previous research about after rice harvest and stubble management, fallow conditions, soil and vegetation impacts on the C-band SAR sensors, flooding events, etc. Therefore, future studies could benefit from more information about the conditions over fallows, weed prevalence, planting of non-rice crops, water shortage or rainfall, and flooding/tillage activities during or after fallow, which could further elaborate on the findings of this study.

The studied sites were located far from weather stations and an attempt was made to extract rainfall data from CHIRPS (Climate Hazards Group Infrared Precipitation with Stations) imagery which provides predicted rainfall amounts. However, due to the coarseness of the images, this had limited application for comparing rainfall data with fallow changes.

In the analysed data, fallow events were not always practiced after the rice harvest. Several fallows, occurred after the ratoon harvest or non-rice crops, which had different backscatter behaviour at their harvest or crop establishment than rice crop. This created problems for application/identification of fallows' minima and maxima on a continuous time-series data. Therefore, further studies could benefit from analysing the application of the used detection method for more fields/sites with continuous rice-fallow-rice cropping pattern.

Additionally, based on the backscatter variations observed during fallow periods, increasing the revisit time over the fallowed fields, by combining data from Sentinel-1A and the recently introduced Sentinel-1B satellites, would be beneficial to observe the changes in the fallow periods, especially for detecting any unreported short-term crops which experience faster temporal changes than rice crops.

The accuracy of the applied fallow detection method (using local minima and maxima method) could be affected in areas where vegetation development was taking place mid-fallow. Depending on the vegetation type and their density present during fallow, it could result in significant backscatter value increases. In such cases, identification of the fallow start could be affected. However, in the studied areas vegetation/non-rice crops did not have a significant effect as many fields had no or limited vegetation/crops growth mid-fallow, and observed peaks were negligible. Additionally, detection of fallow based on the rice season recognition has limited application in non-rice crops, where backscatter behaviour is different to that of rice (Chang et al., 2020).

In the analysed data there was one field where crop residue was burned after harvest and showed that this practice had different backscatter behaviour than other stubble management practices. This indicated that SAR data, such as Sentinel-1A and -1B could be used for detecting agricultural burning practices, which unlike wildland and forest fire detection, have been subject to little research to date.

7 Conclusion

The analysis performed in this study aimed to answer four research questions, the conclusions of which are summarised in following points.

1. What are the characteristics of SAR backscatter during fallow period?

Differences in backscatter behaviour were observed, based on fallow duration – short and long fallow – and differed slightly between the study locations. In short fallows, two phases dominated (the fallow start and the fallow end). Whereas, in long fallow another phase – mid-fallow – was observed approximately halfway through fallow duration.

At the start of fallow, backscatter was characterised by higher values, which decreased with time. The decrease was steeper in shorter fallows, whereas longer fallows saw a more gradual decrease. Near the end of fallow, in both fallow durations, backscatter values reached lowest points. This temporal change was attributed to the crop residues left after harvest that decayed over time and provided more exposure from the soils, and in some fields, this was followed by flooding in preparation for next crop. Additionally, a number of fields, in both locations, after prolonged backscatter decrease, showed some increases at the very end of fallow periods. This change happened at the end of the dry season and was accredited to tillering practices for the next crop.

Furthermore, in longer fallows, some variation of backscatter was observed after 60 days from the rice harvest, which saw subtle increases that lasted between 24 and 36 days in Pangasinan, and between 24 and 48 days in Iloilo. This variation was linked to vegetation development that resulted potentially from shot-term drought tolerant crops. This variation of backscatter was higher in Iloilo that also saw a gentler decrease of the backscatter after the mid-fallow variation.

The decreasing backscatter coefficient during fallows indicated that exposed soils dominated towards the end of fallow periods, despite fallow length, which implied that any vegetation growth/presence ceased towards the end and/or that land was managed, e.g., in preparation for the next crop. Additionally, in Pangasinan, the end of fallow had a more stable decreasing backscatter, suggesting that fields were mostly kept unmanaged which can be related to waster scarcity as most fields in the area were reliant on rainfall for its water source.

Additionally, fallow periods were characterised by declining trend with higher variation of the backscatter ranges than in rice. Most of fallow backscatter values mixed/overlayed with rice backscatter values making distinction between rice and fallow problematic. However, similarly to the rice season, fallow periods showed biggest difference between the start and the end of fallow, which could be used for detecting fallow duration.

Moreover, rainfall data extracted from CHIRPS images showed that, on average, Iloilo received over twice as much rainfall as Pangasinan (116.56mm and 45.20mm, respectively) throughout the fallow seasons. This may explain why longer fallows in Iloilo had overall higher backscatter coefficient than Pangasinan, which were linked to more favourable conditions for cropping short-term crops.

2. Are fallow backscatter values different for irrigated and rainfed fields?

The results indicated that there was no significant difference in fallow characteristics in the SAR backscatter values between ecosystem types in Iloilo across all polarisations. Pangasinan, on the other hand, was the only province with statistically significant variations in the three polarisations (VH, VV, and VV/VH ratio) represented by a higher decrease in backscatter after harvest, and slight increases observed near the end of fallow periods in irrigated ecosystems. Furthermore, long fallow only occurred in rainfed ecosystems in Pangasinan, and just one long fallow happened in an irrigated ecosystem in Iloilo. This suggests that water source affects the duration that land was kept fallowed.

3. Can fallow be detected using SAR time-series?

The study indicated that the fallow period in rice cropping systems can exhibit more temporal fluctuations than during the rice growing season. However, the start and the end of fallow were not affected by the variations and these stages were used to detect fallow by finding local minima and maxima. The FS detection accuracy was much lower than the FE detection, as peaks in the signal (indicating the FS) were reached before harvest. Additionally, the detection of the rice season provided another alternative for detecting fallow, where anything non-rice was classed as fallow. The results were overall better than using the same method over fallow periods but resulted in overestimation of the fallow duration in the three polarisations that was lowest using the VH polarisation (between 13.3 and 25.3 days in Pangasinan and Iloilo, respectively). Moreover, fallow detection methods used in this research may have somewhat limited application, as they may not work as well for non-rice crops, especially short maturing crops (Defourny, 2017)

4. Which polarisation (VV, VH or VV/VH polarisation ratio) is better at detecting fallowing?

The VH polarisation was best at detecting the start and the end of fallow and the rice season in both locations. Similarly, the VV/VH ratio produced acceptable results. The VV polarisation, in turn, resulted in the lowest overall accuracy in detecting the start and end of the rice season and fallow periods.

References

Asilo, S., K. de Bie, A. Skidmore, A. Nelson, M. Barbieri, and A. Maunahan. 2014. Complementarity of two rice mapping approaches: Characterizing strata mapped by hypertemporal MODIS and rice paddy identification using multitemporal SAR. *Remote Sensing* 6: 12789–12814. doi:10.3390/rs61212789.

Bandyopadhyay, K. K., R. N. Sahoo, R. Singh, S. Pradhan, S. Singh, G. Krishna, S. Pargal, and S. K. Mahapatra. 2015. Characterization and crop planning of rabi fallows using remote sensing and GIS. *Current Science* 108: 2051–2062. doi:10.18520/cs/v108/i11/2051-2062.

Banqué, X., J. M. Lopez-sanchez, D. Monells, D. Ballester, and J. Duro. 2015. Polarimetry-Based Land Cover Classification With Sentinel-1 Data. In *ESA SP*, ed. L. Ouwehand, 729:1–5. ESA Communications.

Baronti, S., F. Del Frate, P. Ferrazzoli, S. Paloscia, P. Pampaloni, and G. Schiavon. 1995. SAR polarimetric features of agricultural areas. *International Journal of Remote Sensing* 16: 2639–2656. doi:10.1080/01431169508954581.

Bazzi, H., N. Baghdadi, M. El Hajj, M. Zribi, D. H. T. Minh, E. Ndikumana, D. Courault, and H. Belhouchette. 2019. Mapping paddy rice using Sentinel-1 SAR time series in Camargue, France. *Remote Sensing* 11: 887–902. doi:10.3390/RS11070887.

Bégué, A., D. Arvor, B. Bellon, J. Betbeder, D. de Abelleyra, R. P. D. Ferraz, V. Lebourgeois, C. Lelong, et al. 2018. Remote Sensing and Cropping Practices: A Review. *Remote Sensing* 10: 99. doi:10.3390/rs10010099.

Bijay-Singh, Y. H. Shan, S. E. Johnson-Beebout, Yadvinder-Singh, and R. J. Buresh. 2008. Chapter 3 Crop Residue Management for Lowland Rice-Based Cropping Systems in Asia. In *Advances in Agronomy*, 98:117–199. doi:10.1016/S0065-2113(08)00203-4.

Boschetti, M., L. Busetto, G. Manfron, A. Laborte, S. Asilo, S. Pazhanivelan, and A. Nelson. 2017. PhenoRice: A method for automatic extraction of spatio-temporal information on rice crops using satellite data time series. *Remote Sensing of Environment* 194. Elsevier Inc.: 347–365. doi:10.1016/j.rse.2017.03.029.

Bouvet, A., T. Le Toan, and Nguyen Lam-Dao. 2009. Monitoring of the Rice Cropping System in the Mekong Delta Using ENVISAT/ASAR Dual Polarization Data. *IEEE Transactions on Geoscience and Remote Sensing* 47. IEEE: 517–526. doi:10.1109/TGRS.2008.2007963.

Brisco, B., R. J. Brown, and M. J. Manore. 1989. Early season crop discrimination with combined SAR and TM data. *Canadian Journal of Remote Sensing* 15: 44–54.

Brogioni, M., S. Pettinato, G. Macelloni, S. Paloscia, P. Pampaloni, N. Pierdicca, and F. Ticconi. 2010. Sensitivity of bistatic scattering to soil moisture and surface roughness of bare soils. *International Journal of Remote Sensing* 31: 4227–4255. doi:10.1080/01431160903232808.

Cai, Y., H. Lin, and M. Zhang. 2019. Mapping paddy rice by the object-based random forest method using time series Sentinel-1/Sentinel-2 data. *Advances in Space Research* 64. COSPAR: 2233–2244. doi:10.1016/j.asr.2019.08.042.

Carvajal-Yepes, M., K. Cardwell, A. Nelson, K. A. Garrett, B. Giovani, D. G. O. Saunders, S.

Kamoun, J. P. Legg, et al. 2019. A global surveillance system for crop diseases. *Science* 364: 1237–1239. doi:10.1126/science.aaw1572.

Chandna, P. K., and S. Mondal. 2020. Analyzing multi-year rice-fallow dynamics in Odisha using multi-temporal Landsat-8 OLI and Sentinel-1 Data. *GIScience and Remote Sensing* 57. Taylor & Francis: 431–449. doi:10.1080/15481603.2020.1731074.

Chang, L., Y.-T. Chen, J.-H. Wang, and Y.-L. Chang. 2020. Rice-Field Mapping with Sentinel-1A SAR Time-Series Data. *Remote Sensing* 13: 103–130. doi:10.3390/rs13010103.

Chen, J., P. Jönsson, M. Tamura, Z. Gu, B. Matsushita, and L. Eklundh. 2004. A simple method for reconstructing a high-quality NDVI time-series data set based on the Savitzky-Golay filter. *Remote Sensing of Environment* 91: 332–344. doi:10.1016/j.rse.2004.03.014.

Chen, J., H. Lin, and Z. Pei. 2007. Application of ENVISAT ASAR data in mapping rice crop growth in southern China. *IEEE Geoscience and Remote Sensing Letters* 4: 431–435. doi:10.1109/LGRS.2007.896996.

Clauss, K., M. Ottinger, P. Leinenkugel, and C. Kuenzer. 2018a. Estimating rice production in the Mekong Delta, Vietnam, utilizing time series of Sentinel-1 SAR data. *International Journal of Applied Earth Observation and Geoinformation* 73. Elsevier: 574–585. doi:10.1016/j.jag.2018.07.022.

Clauss, K., M. Ottinger, and C. Kuenzer. 2018b. Mapping rice areas with Sentinel-1 time series and superpixel segmentation. *International Journal of Remote Sensing* 39. Taylor & Francis: 1399–1420. doi:10.1080/01431161.2017.1404162.

Dalle, S. P., and S. de Blois. 2006. Shorter Fallow Cycles Affect the Availability of Noncrop Plant Resources in a Shifting Cultivation System. *Ecology and Society* 11: 1–26. doi:10.5751/ES-01707-110202.

Das, P., and V. Pandey. 2019. Use of Logistic Regression in Land-Cover Classification with Moderate-Resolution Multispectral Data. *Journal of the Indian Society of Remote Sensing* 47. Springer India: 1443–1454. doi:10.1007/s12524-019-00986-8.

Defourny, P. 2017. Land cover mapping and monitoring. In *Handbook on Remote Sensing for Agricultural Statistics*, ed. J. Delincé. Rome: Handbook of the Global Strategy to improve Agricultural and Rural Statistics (GSARS).

Delang, C. O., X. Weiyi, B. Brooke, and K. P. Chun. 2016. The Effect of Fallow Period Length on the Abundance and Diversity of Usable Plant Assemblages in Shifting Cultivation System (Swidden Agriculture) in Northern Laos. *Polish Journal of Ecology* 64: 350–356. doi:10.3161/15052249PJE2016.64.3.005.

Dembélé, M., and S. J. Zwart. 2016. Evaluation and comparison of satellite-based rainfall products in Burkina Faso, West Africa. *International Journal of Remote Sensing* 37. Taylor & Francis: 3995–4014. doi:10.1080/01431161.2016.1207258.

Dirgahayu, D., I. M. Parsa, and S. Harini. 2019. Detection Paddy Field using dual Polarization SAR Sentinel-1 Data. *IOP Conference Series: Earth and Environmental Science* 280: 1–12. doi:10.1088/1755-1315/280/1/012022.

Dong, J., and X. Xiao. 2016. Evolution of regional to global paddy rice mapping methods: A review. *ISPRS Journal of Photogrammetry and Remote Sensing* 119. International Society for Photogrammetry and Remote Sensing, Inc. (ISPRS): 214–227. doi:10.1016/j.isprsjprs.2016.05.010.

Ebdon, D. 1985. *Statistics in Geography*. 2nd ed. Oxford: Blackwell.

Elmqvist, B., and A. R. Khatir. 2007. The possibilities of bush fallows with changing roles of agriculture-An analysis combining remote sensing and interview data from Sudanese drylands. *Journal of Arid Environments* 70: 329–343. doi:10.1016/j.jaridenv.2006.12.018.

Estel, S., T. Kuemmerle, C. Alcántara, C. Levers, A. Prishchepov, and P. Hostert. 2015. Mapping farmland abandonment and recultivation across Europe using MODIS NDVI time series. *Remote Sensing of Environment* 163. Elsevier Inc.: 312–325. doi:10.1016/j.rse.2015.03.028.

FAO. 2013. Fallow Cropping: Garlic after Rice, Philippines. *Technologies and practices for small agricultural producers (TECA)*: 1–4.

Ferrazzoli, P., S. Paloscia, P. Pampaloni, G. Schiavon, S. Sigismondi, and D. Solimini. 1997. The potential of multifrequency polarimetric SAR in assessing agricultural and arboreous biomass. *IEEE Transactions on Geoscience and Remote Sensing* 35: 5–17. doi:10.1109/36.551929.

Folving, R., and H. Christensen. 2007. Farming system changes in the Vietnamese uplands - Using fallow length and farmers' adoption of Sloping Agricultural Land Technologies as indicators of environmental sustainability. *Geografisk Tidsskrift* 107: 43–58. doi:10.1080/00167223.2007.10801374.

Geudtner, D., R. Torres, P. Snoeij, I. Navas-traver, A. Ostergaard, and B. Rommen. 2013. Sentinel-1 System Overview. In *Proc. "ESA Living Planet Symposium 2013", Edinburgh, UK*, 2013:1–5.

Gherboudj, I., R. Magagi, A. A. Berg, and B. Toth. 2011. Soil moisture retrieval over agricultural fields from multi-polarized and multi-angular RADARSAT-2 SAR data. *Remote Sensing of Environment* 115: 33–43. doi:10.1016/j.rse.2010.07.011.

Ghosh, S. M., S. Saraf, M. D. Behera, and C. Biradar. 2017. Estimating Agricultural Crop Types and Fallow Lands Using Multi Temporal Sentinel-2A Imageries. *Proceedings of the National Academy of Sciences India Section A - Physical Sciences* 87. Springer India: 769–779. doi:10.1007/s40010-017-0447-5.

Gir, R., L. Jain, and R. Rai. 2015. Speckle Reduction of Synthetic Aperture Radar Images using Median Filter and Savitzky-Golay Filter. *International Journal of Computer Applications* 113: 38–43. doi:10.5120/19874-1877.

Girard, C. M., C. Le Bas, W. Szujecka, and M. C. Girard. 1994. Remote sensing and fallow land. *Journal of Environmental Management* 41: 27–38. doi:10.1006/jema.1994.1031.

Gumma, M. K., P. S. Thenkabail, I. V. Muralikrishna, M. N. Velpuri, P. T. Gangadhararao, V. Dheeravath, C. M. Biradar, S. A. Nalan, et al. 2011. Changes in agricultural cropland areas between a water-surplus year and a water-deficit year impacting food security, determined using MODIS 250 m time-series data and spectral matching techniques, in the Krishna river basin (India). *International Journal of Remote Sensing* 32: 3495–3520. doi:10.1080/01431161003749485.

Gumma, M. K., P. S. Thenkabail, P. Teluguntla, M. N. Rao, I. A. Mohammed, and A. M. Whitbread. 2016. Mapping rice-fallow cropland areas for short-season grain legumes intensification in South Asia using MODIS 250 m time-series data. *International Journal of Digital Earth* 9: 981–1003. doi:10.1080/17538947.2016.1168489.

Gupta, V., M. K. Jain, P. K. Singh, and V. Singh. 2019. An assessment of global satellite-based precipitation datasets in capturing precipitation extremes: A comparison with observed precipitation dataset in India. *International Journal of Climatology*: 1–22. doi:10.1002/joc.6419.

Holecz, F., M. Barbieri, F. Collivignarelli, L. Gatti, A. Nelson, T. D. Setiyono, M. Boschetti, G. Manfron, et al. 2013. An Operational Remote Sensing Based Service for Rice Production Estimation at National Scale. *ESA Living Planet Symposium* 2013. doi:10.13140/2.1.1492.8643.

Inoue, Y., and E. Sakaiya. 2013. Relationship between X-band backscattering coefficients from high-resolution satellite SAR and biophysical variables in paddy rice. *Remote Sensing Letters* 4: 288–295. doi:10.1080/2150704X.2012.725482.

Inoue, Y., T. Kurosu, H. Maeno, S. Uratsuka, T. Kozu, K. Dabrowska-Zielinska, and J. Qi. 2002. Season-long daily measurements of multifrequency (Ka, Ku, X, C, and L) and full-polarization backscatter signatures over paddy rice field and their relationship with biological variables. *Remote Sensing of Environment* 81: 194–204. doi:10.1016/S0034-4257(01)00343-1.

Inoue, Y., E. Sakaiya, and C. Wang. 2014. Capability of C-band backscattering coefficients from high-resolution satellite SAR sensors to assess biophysical variables in paddy rice. *Remote Sensing of Environment* 140. Elsevier Inc.: 257–266. doi:10.1016/j.rse.2013.09.001.

IRRI. 2007. The rice environments or ecosystems.

IRRI. 2015. *IRRI Rice Production Manual: Steps to successful rice production*. Los Baños, Philippines.

Jamandre, C. A., and G. T. Narisma. 2013. Spatio-temporal validation of satellite-based rainfall estimates in the Philippines. *Atmospheric Research* 122. Elsevier B.V.: 599–608. doi:10.1016/j.atmosres.2012.06.024.

Karila, K., O. Nevalainen, A. Krooks, M. Karjalainen, and S. Kaasalainen. 2014. Monitoring Changes in Rice Cultivated Area from SAR and Optical Satellite Images in Ben Tre and Tra Vinh Provinces in Mekong Delta, Vietnam. *Remote Sensing* 6: 4090–4108. doi:10.3390/rs6054090.

Khabbazan, S., P. Vermunt, S. Steele-Dunne, L. Ratering Arntz, C. Marinetti, D. van der Valk, L. Iannini, R. Molijn, et al. 2019. Crop Monitoring Using Sentinel-1 Data: A Case Study from The Netherlands. *Remote Sensing* 11: 1887–1910. doi:10.3390/rs11161887.

Kim, Y., J. Thomas, B. Rajat, H. Lee, and S. Hong. 2012. Radar Vegetation Index for Estimating the Vegetation Water Content of Rice and Soybean. *IEEE Geoscience and Remote Sensing Letters* 9. IEEE: 564–568. doi:10.1109/LGRS.2011.2174772.

Kim, Y. H., S. Y. Hong, and Y. H. Lee. 2009. Estimation of paddy rice growth parameters using L, C, X-bands polarimetric scatterometer. *Korean Journal of Remote Sensing* 25: 31–44.

Kuenzer, C., and K. Knauer. 2013. Remote sensing of rice crop areas. *International Journal of Remote Sensing* 34: 2101–2139. doi:10.1080/01431161.2012.738946.

Laborte, A. G., A. A. Maunahan, and R. J. Hijmans. 2010. Spectral Signature Generalization and Expansion Can Improve the Accuracy of Satellite Image Classification. Edited by

Wendy A. Peer. *PLoS ONE* 5: e10516. doi:10.1371/journal.pone.0010516.

Lasko, K., K. P. Vadrevu, V. T. Tran, and C. Justice. 2018. Mapping Double and Single Crop Paddy Rice with Sentinel-1A at Varying Spatial Scales and Polarizations in Hanoi, Vietnam. *IEEE Journal of Selected Topics in Applied Earth Observations and Remote Sensing* 11. IEEE: 498–512. doi:10.1109/JSTARS.2017.2784784.

Le Toan, T., F. Ribbes, Li-Fang Wang, N. Floury, Kung-Hau Ding, Jin Au Kong, M. Fujita, and T. Kurosu. 1997. Rice crop mapping and monitoring using ERS-1 data based on experiment and modeling results. *IEEE Transactions on Geoscience and Remote Sensing* 35: 41–56. doi:10.1109/36.551933.

Leisz, S. J., and M. S. Rasmussen. 2012. Mapping fallow lands in Vietnam's north-central mountains using yearly Landsat imagery and a land-cover succession model. *International Journal of Remote Sensing* 33: 6281–6303. doi:10.1080/01431161.2012.681712.

Li, H., K. Li, Y. Shao, P. Zhou, X. Guo, C. Liu, and L. Liu. 2018. Retrieval of Rice Phenology Based on Time-Series Polarimetric SAR Data. In *IGARSS 2018 - 2018 IEEE International Geoscience and Remote Sensing Symposium*, 4463–4466. Valencia, Spain: IEEE. doi:10.1109/IGARSS.2018.8519204.

Li, K., B. Brisco, S. Yun, and R. Touzi. 2012. Polarimetric decomposition with RADARSAT-2 for rice mapping and monitoring. *Canadian Journal of Remote Sensing* 38: 169–179. doi:10.5589/m12-024.

Liew, S. C., S. P. Kam, T. P. Tuong, P. Chen, V. Q. Minh, and H. Lim. 1997. Landcover classification over the Mekong river delta using ERS and RADARSAT SAR images. In *IGARSS'97. 1997 IEEE International Geoscience and Remote Sensing Symposium Proceedings. Remote Sensing - A Scientific Vision for Sustainable Development*, 4:2038–2040. IEEE. doi:10.1109/IGARSS.1997.609209.

Litsinger, J. A., B. L. Canapi, J. P. Bandong, M. D. Lumaban, F. D. Raymundo, and A. T. Barrion. 2009. Insect pests of rainfed wetland rice in the Philippines: Population densities, yield loss, and insecticide management. *International Journal of Pest Management* 55: 221–242. doi:10.1080/09670870902745070.

Liu, Y., K. S. Chen, P. Xu, and Z. L. Li. 2016. Modeling and Characteristics of Microwave Backscattering From Rice Canopy Over Growth Stages. *IEEE Transactions on Geoscience and Remote Sensing* 54. IEEE: 6757–6770. doi:10.1109/TGRS.2016.2590439.

Lopez-Sanchez, J. M., J. D. Ballester-Berman, and I. Hajnsek. 2011. First Results of Rice Monitoring Practices in Spain by Means of Time Series of TerraSAR-X Dual-Pol Images. *IEEE Journal of Selected Topics in Applied Earth Observations and Remote Sensing* 4. IEEE: 412–422. doi:10.1109/JSTARS.2010.2047634.

Lopez-Sanchez, J. M., S. R. Cloude, and J. D. Ballester-Berman. 2012. Rice Phenology Monitoring by Means of SAR Polarimetry at X-Band. *IEEE Transactions on Geoscience and Remote Sensing* 50. IEEE: 2695–2709. doi:10.1109/TGRS.2011.2176740.

Maclean, J. L., B. Hardy, and G. P. Hettel. 2013. *Rice almanac*. 4th ed. Los Baños (Philippines): International Rice Research Institute.

Mansaray, L. R., D. Zhang, Z. Zhou, and J. Huang. 2017. Evaluating the potential of temporal Sentinel-1A data for paddy rice discrimination at local scales. *Remote Sensing Letters* 8.

Taylor & Francis: 967–976. doi:10.1080/2150704X.2017.1331472.

Mansaray, L. R., L. Yang, V. T. S. Kabba, A. S. Kanu, J. Huang, and F. Wang. 2019. Optimising rice mapping in cloud-prone environments by combining quad-source optical with Sentinel-1A microwave satellite imagery. *GIScience and Remote Sensing* 56. Taylor & Francis: 1333–1354. doi:10.1080/15481603.2019.1646978.

McNairn, H., and B. Brisco. 2004. The application of C-band polarimetric SAR for agriculture: A review. *Canadian Journal of Remote Sensing* 30: 525–542. doi:10.5589/m03-069.

McNairn, H., D. Wood, Q. H. J. Gwyn, R. J. Brown, and F. Charbonneau. 1998. Mapping Tillage and Crop Residue Management Practices with RADARSAT. *Canadian Journal of Remote Sensing* 24: 28–35. doi:10.1080/07038992.1998.10874688.

McNairn, H., C. Duguay, B. Brisco, and T. . Pultz. 2002. The effect of soil and crop residue characteristics on polarimetric radar response. *Remote Sensing of Environment* 80: 308–320. doi:10.1016/S0034-4257(01)00312-1.

Mertz, O. 2002. The relationship between length of fallow and crop yields in shifting cultivation: A rethinking. *Agroforestry Systems* 55: 149–159. doi:10.1023/A:1020507631848.

Minh, H. V. T., R. Avtar, G. Mohan, P. Misra, and M. Kurasaki. 2019. Monitoring and mapping of rice cropping pattern in flooding area in the Vietnamese Mekong delta using Sentinel-1A data: A case of an Giang province. *ISPRS International Journal of Geo-Information* 8: 211–232. doi:10.3390/ijgi8050211.

Mohammed, I., M. Marshall, K. de Bie, L. Estes, and A. Nelson. 2020. A blended census and multiscale remote sensing approach to probabilistic cropland mapping in complex landscapes. *ISPRS Journal of Photogrammetry and Remote Sensing* 161. Elsevier: 233–245. doi:10.1016/j.isprsjprs.2020.01.024.

Mosleh, M., Q. Hassan, and E. Chowdhury. 2015. Application of Remote Sensors in Mapping Rice Area and Forecasting Its Production: A Review. *Sensors* 15: 769–791. doi:10.3390/s150100769.

Muthukumarasamy, I., R. S. Shanmugam, and T. Usha. 2019. Incorporation of textural information with SAR and optical imagery for improved land cover mapping. *Environmental Earth Sciences* 78. Springer Berlin Heidelberg: 643–653. doi:10.1007/s12665-019-8654-9.

NASA. 2020. Polarimetry. *NASA-ISRO SAR Mission (NISAR)*. https://nisar.jpl.nasa.gov/mission/get-to-know-sar/polarimetry/. Accessed July 12.

Nelson, A., T. Setiyono, A. B. Rala, E. D. Quicho, J. V. Raviz, P. J. Abonete, A. A. Maunahan, C. A. Garcia, et al. 2014. Towards an operational SAR-based rice monitoring system in Asia: Examples from 13 demonstration sites across Asia in the RIICE project. *Remote Sensing* 6: 10773–10812. doi:10.3390/rs61110773.

Nguyen, D. B., and W. Wagner. 2017. European rice cropland mapping with Sentinel-1 data: The mediterranean region case study. *Water* 9: 392–412. doi:10.3390/w9060392.

Nguyen, D. B., K. Clauss, S. Cao, V. Naeimi, C. Kuenzer, and W. Wagner. 2015. Mapping Rice Seasonality in the Mekong Delta with multi-year envisat ASAR WSM Data. *Remote Sensing* 7: 15868–15893. doi:10.3390/rs71215808.

Nguyen, D. B., A. Gruber, and W. Wagner. 2016. Mapping rice extent and cropping scheme

in the Mekong Delta using Sentinel-1A data. *Remote Sensing Letters* 7. Taylor & Francis: 1209–1218. doi:10.1080/2150704X.2016.1225172.

Nielsen, D. C., and F. J. Calderón. 2011. Fallow Effects on Soil. In *Soil Management: Building a Stable Base for Agriculture*, ed. J. L. Hatfield and T. J. Sauer, 287–300. Madison, WI, USA: Soil Science Society of America. doi:10.2136/2011.soilmanagement.c19.

Nogueira, S. M. C., M. A. Moreira, and M. M. L. Volpato. 2018. Evaluating precipitation estimates from Eta, TRMM and CHRIPS data in the south-southeast region of Minas Gerais state-Brazil. *Remote Sensing* 10: 313–328. doi:10.3390/rs10020313.

Oh, Y. 2004. Quantitative Retrieval of Soil Moisture Content and Surface Roughness From Multipolarized Radar Observations of Bare Soil Surfaces. *IEEE Transactions on Geoscience and Remote Sensing* 42: 596–601. doi:10.1109/TGRS.2003.821065.

Oh, Y., S. Y. Hong, Y. Kim, J. Y. Hong, and Y. H. Kim. 2009. Polarimetric backscattering coefficients of flooded rice fields at L- and C-bands: Measurements, modeling, and data analysis. *IEEE Transactions on Geoscience and Remote Sensing* 47. IEEE: 2714–2721. doi:10.1109/TGRS.2009.2014053.

Onojeghuo, A. O., G. A. Blackburn, Q. Wang, P. M. Atkinson, D. Kindred, and Y. Miao. 2018. Mapping paddy rice fields by applying machine learning algorithms to multi-temporal sentinel-1A and landsat data. *International Journal of Remote Sensing* 39. Taylor & Francis: 1042–1067. doi:10.1080/01431161.2017.1395969.

PAGASA. 2021. Climate of the Philippines. *The Philippine Atmospheric, Geophysical and Astronomical Services Administration*. http://bagong.pagasa.dost.gov.ph/information/climate-philippines. Accessed August 6.

Parveen, S., and N. Nakagoshi. 2001. An analysis of pesticide use for rice pest management in Bangladesh 【Article】. *Journal of International Development and Cooperation* 8: 107–126. doi:10.15027/14370.

Pasha, S. V., M. D. Behera, S. K. Mahawar, S. K. Barik, and S. R. Joshi. 2020. Assessment of shifting cultivation fallows in Northeastern India using Landsat imageries. *Tropical Ecology* 61. Springer India: 65–75. doi:10.1007/s42965-020-00062-0.

Philippine Statistics Authority (PSA). 2019. Palay and Corn: Area Harvested by Ecosystem/Croptype, by Quarter, by Semester, by Region and by Province, 1987-2019 by Ecosystem/Croptype, Geolocation, Year and Period.

Rola, A. C., and P. L. Pingali. 1993. *Pesticides, rice productivity, and farmers' health: an economic assessment*. Edited by Agnes Rola and Prabhu L. Pingali. International Rice Research Institute.

Rosenthal, W. D., and B. J. Blanchard. 1984. Active microwave responses: an aid in improved crop classification. *Photogrammetric Engineering & Remote Sensing* 50: 461–468.

Rudiyanto, B. Minasny, R. M. Shah, N. C. Soh, C. Arif, and B. I. Setiawan. 2019. Automated near-real-time mapping and monitoring of rice extent, cropping patterns, and growth stages in Southeast Asia using Sentinel-1 time series on a Google Earth Engine platform. *Remote Sensing* 11: 1–27. doi:10.3390/rs11141666.

Sander, B. O., M. Samson, P. B. Sanchez, K. P. Valencia, E. A. M. Demafelix, and R. J. Buresh. 2018. Contribution of fallow periods between rice crops to seasonal GHG emissions: effect of water and tillage management. *Soil Science and Plant Nutrition* 64. Taylor &

Francis: 200–209. doi:10.1080/00380768.2018.1440937.

Savary, S., L. Willocquet, S. J. Pethybridge, P. Esker, N. McRoberts, and A. Nelson. 2019. The global burden of pathogens and pests on major food crops. *Nature Ecology & Evolution* 3. Springer US: 430–439. doi:10.1038/s41559-018-0793-y.

Schafer, R. W. 2011. What is a savitzky-golay filter? [Lecture Notes]. *IEEE Signal Processing Magazine* 28. IEEE: 111–117. doi:10.1109/MSP.2011.941097.

Schieche, B., S. Erasmi, T. Schrage, and P. Hurlemann. 1999. Monitoring and registering of grassland and fallow fields with multitemporal ERS data within a district of lower Saxony, Germany. In *IEEE 1999 International Geoscience and Remote Sensing Symposium. IGARSS'99 (Cat. No.99CH36293)*, 2:759–761. IEEE. doi:10.1109/IGARSS.1999.774431.

Schlund, M., and S. Erasmi. 2020. Sentinel-1 time series data for monitoring the phenology of winter wheat. *Remote Sensing of Environment* 246. Elsevier: 111814–111824. doi:10.1016/j.rse.2020.111814.

Schoenly, K. G., J. E. Cohen, K. L. Heong, J. A. Litsinger, A. T. Barrion, and G. S. Arida. 2010. Fallowing did not disrupt invertebrate fauna in Philippine low-pesticide irrigated rice fields. *Journal of Applied Ecology* 47: 593–602. doi:10.1111/j.1365-2664.2010.01799.x.

Setiyono, T. D., E. D. Quicho, L. Gatti, M. Campos-Taberner, L. Busetto, F. Collivignarelli, F. J. García-Haro, M. Boschetti, et al. 2018. Spatial rice yield estimation based on MODIS and Sentinel-1 SAR data and ORYZA crop growth model. *Remote Sensing* 10: 1–20. doi:10.3390/rs10020293.

Son, N. T., C. F. Chen, C. R. Chen, and V. Q. Minh. 2018. Assessment of Sentinel-1A data for rice crop classification using random forests and support vector machines. *Geocarto International* 33. Taylor & Francis: 587–601. doi:10.1080/10106049.2017.1289555.

Son, N. T., C. F. Chen, C. R. Chen, P. Toscano, Y. S. Cheng, H. Y. Guo, and C. H. Syu. 2021. A phenological object-based approach for rice crop classification using time-series Sentinel-1 Synthetic Aperture Radar (SAR) data in Taiwan. *International Journal of Remote Sensing* 42. Taylor & Francis: 2722–2739. doi:10.1080/01431161.2020.1862440.

Steele-Dunne, S. C., H. McNairn, A. Monsivais-Huertero, J. Judge, P. W. Liu, and K. Papathanassiou. 2017. Radar Remote Sensing of Agricultural Canopies: A Review. *IEEE Journal of Selected Topics in Applied Earth Observations and Remote Sensing* 10. IEEE: 2249–2273. doi:10.1109/JSTARS.2016.2639043.

Stefanski, J., T. Kuemmerle, O. Chaskovskyy, P. Griffiths, V. Havryluk, J. Knorn, N. Korol, A. Sieber, et al. 2014. Mapping land management regimes in western Ukraine using optical and SAR data. *Remote Sensing* 6: 5279–5305. doi:10.3390/rs6065279.

Suga, Y., and T. Konishi. 2008. Rice crop monitoring using X, C and L band SAR data. In *32nd Asian Conference on Remote Sensing 2011, ACRS 2011*, ed. C. M. U. Neale, M. Owe, and G. D'Urso, 3:710410. doi:10.1117/12.800051.

Sun, Q., C. Miao, Q. Duan, H. Ashouri, S. Sorooshian, and K. L. Hsu. 2018. A Review of Global Precipitation Data Sets: Data Sources, Estimation, and Intercomparisons. *Reviews of Geophysics* 56: 79–107. doi:10.1002/2017RG000574.

Tian, H., M. Wu, L. Wang, and Z. Niu. 2018. Mapping early, middle and late rice extent using

Sentinel-1A and Landsat-8 data in the poyang lake plain, China. *Sensors (Switzerland)* 18: 185–199. doi:10.3390/s18010185.

Tong, X., M. Brandt, P. Hiernaux, S. Herrmann, L. V. Rasmussen, K. Rasmussen, F. Tian, T. Tagesson, et al. 2020. The forgotten land use class: Mapping of fallow fields across the Sahel using Sentinel-2. *Remote Sensing of Environment* 239. doi:10.1016/j.rse.2019.111598.

Torbick, N., and W. Salas. 2014. Mapping agricultural wetlands in the Sacramento Valley, USA with satellite remote sensing. *Wetlands Ecology and Management* 23: 79–94. doi:10.1007/s11273-014-9342-x.

Torbick, N., W. Salas, X. Xiao, P. Ingraham, M. Fearon, C. Biradar, D. Zhao, Y. Liu, et al. 2011a. Integrating SAR and optical imagery for regional mapping of paddy rice attributes in the Poyang Lake Watershed, China. *Canadian Journal of Remote Sensing* 37: 17–26. doi:10.5589/m11-020.

Torbick, N., W. A. Salas, S. Hagen, and X. Xiao. 2011b. Monitoring Rice Agriculture in the Sacramento Valley, USA With Multitemporal PALSAR and MODIS Imagery. *IEEE Journal of Selected Topics in Applied Earth Observations and Remote Sensing* 4. IEEE: 451–457. doi:10.1109/JSTARS.2010.2091493.

Torbick, N., D. Chowdhury, W. Salas, and J. Qi. 2017. Monitoring Rice Agriculture across Myanmar Using Time Series Sentinel-1 Assisted by Landsat-8 and PALSAR-2. *Remote Sensing* 9: 119. doi:10.3390/rs9020119.

Uppala, D., R. V. Kothapalli, S. Poloju, S. S. V. Rama Mullapudi, and V. K. Dadhwal. 2015. Rice crop discrimination using single date RISAT1 Hybrid (RH, RV) polarimetric data. *Photogrammetric Engineering and Remote Sensing* 81: 557–563. doi:10.14358/PERS.81.7.557.

Veloso, A., S. Mermoz, A. Bouvet, T. Le Toan, M. Planells, J. F. Dejoux, and E. Ceschia. 2017. Understanding the temporal behavior of crops using Sentinel-1 and Sentinel-2-like data for agricultural applications. *Remote Sensing of Environment* 199: 415–426. doi:10.1016/j.rse.2017.07.015.

Villano, L., J. Raviz, N. M. Paguirigan, M. A. Gutierrez, M. R. Mabalay, and A. Laborte. 2019. SEPARABILITY OF TRANSPLANTED AND DIRECT SEEDED RICE USING MULTI-TEMPORAL SENTINEL-1A DATA. *ISPRS - International Archives of the Photogrammetry, Remote Sensing and Spatial Information Sciences* XLII-4/W19: 471–478. doi:10.5194/isprs-archives-XLII-4-W19-471-2019.

Vreugdenhil, M., W. Wagner, B. Bauer-Marschallinger, I. Pfeil, I. Teubner, C. Rüdiger, and P. Strauss. 2018. Sensitivity of Sentinel-1 Backscatter to Vegetation Dynamics: An Austrian Case Study. *Remote Sensing* 10: 1396–1414. doi:10.3390/rs10091396.

Wallace, C. S. A., P. Thenkabail, J. R. Rodriguez, and M. K. Brown. 2017. Fallow-land Algorithm based on Neighborhood and Temporal Anomalies (FANTA) to map planted versus fallowed croplands using MODIS data to assist in drought studies leading to water and food security assessments. *GIScience and Remote Sensing* 54. Taylor & Francis: 258–282. doi:10.1080/15481603.2017.1290913.

Weiss, M., F. Jacob, and G. Duveiller. 2020. Remote sensing for agricultural applications: A meta-review. *Remote Sensing of Environment* 236. Elsevier: 111402–111420. doi:10.1016/j.rse.2019.111402.

Wojtkowski, P. A. 2008. Temporal Economics. In *Agroecological Economics*, ed. P. A. Wojtkowski, 1st ed., 97–114. London: Elsevier. doi:10.1016/B978-012374117-2.50008-X.

Wollburg, P., M. Tiberti, and A. Zezza. 2020. Recall length and measurement error in agricultural surveys. *Food Policy*. Elsevier Ltd: 1–14. doi:10.1016/j.foodpol.2020.102003.

Wu, Z., P. S. Thenkabail, R. Mueller, A. Zakzeski, F. Melton, L. Johnson, C. Rosevelt, J. Dwyer, et al. 2014. Seasonal cultivated and fallow cropland mapping using MODIS-based automated cropland classification algorithm. *Journal of Applied Remote Sensing* 8: 1–14. doi:10.1117/1.JRS.8 .083685.

Xu, L., H. Zhang, C. Wang, B. Zhang, and M. Liu. 2019. Crop classification based on temporal information using Sentinel-1 SAR time-series data. *Remote Sensing* 11: 53–70. doi:10.3390/rs11010053.

Yamamoto, Y., T. Oberthür, and R. Lefroy. 2009. Spatial identification by satellite imagery of the crop-fallow rotation cycle in northern Laos. *Environment, Development and Sustainability* 11: 639–654. doi:10.1007/s10668-007-9134-z.

Yesou, H., C. Meyer, and P. De Fraipont. 1996. Assessment of ERS SAR data for fallow land monitoring: A radiometric and textural approach. *European Space Agency, (Special Publication) ESA SP*: 473–478. doi:10.1117/12.227205.

Zhang, B., X. Lui, M. Lui, and Y. Meng. 2019. Detection of Rice Phenological Variations under Heavy Metal Stress by Means of Blended Landsat and MODIS Image Time Series. *Remote Sensing* 11: 13–29. doi:10.3390/rs11010013.

Zhang, Y., C. Wang, J. Wu, J. Qi, and W. A. Salas. 2009. Mapping paddy rice with multitemporal ALOS/PALSAR imagery in southeast China. *International Journal of Remote Sensing* 30: 6301–6315. doi:10.1080/01431160902842391.

Zhou, Y., J. Luo, L. Feng, and X. Zhou. 2019. DCN-Based Spatial Features for Improving Parcel-Based Crop Classification Using High-Resolution Optical Images and Multi-Temporal SAR Data. *Remote Sensing* 11: 1619–1637. doi:10.3390/rs11131619.

Appendix A. IRRI's Field Survey Protocol for Pangasinan and Iloilo provinces

The descriptions below were reproduced/amended from IRRI's report that listed criteria for selecting survey sites.

Survey area selection

1. The selection of the survey sites *(region and province)* was primarily based on the top 20 rice growing provinces. IRRI used the 5-year average (2013-2017) from Philippine Statistics Authority (PSA) report of harvested area, aggregated by semester (Jan-Jun and Jul-Dec) and by ecosystem (irrigated and rainfed). Aside from the PSA report, the available data collected from the Pest Risk Identification and Management (PRIME) monitoring fields, Philippine Rice Information System (PRISM) monitoring fields (2016-2018), and other sources (e.g., points collected as part of Villano's thesis) were also considered in the selection. The provinces with larger area planted to rice in rainfed ecosystem and without or with lesser number of field observations from PRIME and PRISM were given high priority.

2. Based on the above considerations, the following areas have been shortlisted:

   - Luzon: Pangasinan (Region I), Palawan (MIMAROPA), Cagayan (Region II), Camarines Sur (Region V)
   - Visayas: Capiz, Negros Occidental, and Antique (Region VI), Samar and Leyte, priority in rainfed areas (Region VIII), and Bohol (Region VII).
   - Mindanao: Maguindanao and Lanao del Sur (ARMM), Agusan del Sur (Caraga), and North Cotabato (SOCCSKSARGEN)
   - 3. Finally, in the interest of time, budget, and safety and security, IRRI have selected Pangasinan, Region I and Iloilo, Region VI, among three other provinces for which data was not utilised in this study.

3. Within each of the selected provinces, IRRI identified the top rice growing municipalities (e.g., top 5 to 10 depending on the size of the areas) based on the local government unit (LGU) report. The reported statistics was aggregated by season (wet and dry) and by ecosystem (irrigated and rainfed). The PRIME and PRISM monitoring sites were again considered in the selection of the municipalities, such that areas without or with small number of sites were prioritized. Due to limited time and resources, accessibility, and proximity of the municipalities with each other were also considered in the selection criteria. The sample fields had to represent diversity in the rice-based cropping areas in terms of ecosystems (rainfed and irrigated) and the crop establishment practices/methods (transplanted, wet direct-seeded, and dry direct-seeded).

4. Below is a list of selected provinces and municipalities and target number of survey fields. IRRI aimed to collect 80 survey fields per province.

Provinces (REGIONS) and municipalities	Number of surveyed fields	Dates of field visit
Pangasinan (REGION 1)	72	
Agno	17	26 - 27 Feb 2019
Alaminos City	18	20 - 21 Feb 2019
Bani	20	22 - 23 Feb 2019
Bolinao	17	28 Feb - 1 Mar 2019
Iloilo (REGION VI)	75	
Cabatuan	16	4 - 5 Feb 2019
Lambunao	19	12 - 13 Feb 2019
Oton	20	6 - 7 Feb 2019
Sta Barbara	20	8 and 11 Feb 2019

Criteria for field selection

To identify survey fields, the IRRI team coordinated with the corresponding DA-Regional Field Office (RFO) PRIME focal persons/team and LGUs. The selected field had to satisfy the following criteria:

1. Should be rice-based (e.g., planted with rice at least once in 2018), and could be planted with rice or non-rice crop(s) or fallow in the current season;
2. Should be at least 4,000 sq. m in size and regular in shape (4 sides, rectangular or square). In case the parcel is small, the field could consist of more than one parcel as long as the parcels are contiguous;
3. Surrounded by at least 1 ha of rice fields of the same ecosystem, if currently planted with rice;
4. Should be at least 60 m away from paved roads, built up areas (e.g., cluster of houses and buildings) and other structures (e.g., electric towers);
5. Survey fields should at least be 500 m away from each other; and
6. Survey fields should be accessible.

Appendix B. Brief list of Sentinel-1A pre-processing staps

Below is a brief list of steps (adapted from Nelson et al., 2014) involved in the pre-processing stages:

1. Strip mosaicking: Mosaicking of the images from the same accusation day and orbit to produce single image strips in slant range geometry.
2. Co-registering: Co-registering of images in slant range geometry involved:
    a. Application of the orbit shift correction shift from orbit file (based on accurate satellite position and velocity);
    b. Identification of pixel shifts between referenced and co-registered images and elevation, and their correction based on cross-correlation;
    c. Calculation and geometric correction of azimuth and range direction shifts.
3. Speckle filtering: Time-series speckle filtering of image stacks to improve discrepancies that may result from temporal dielectric and geometrical properties of the scatters.
4. Terrain geocoding: In this step range-Doppler calculations were performed to transform two-dimensional coordinates of the slant range image into three-dimensional object coordinates in a specified cartographic reference system.
5. Radiometric calibration and normalisation: Radiometric calibration was calculated using scattering area, antenna gain patterns and range spread loss. Then, the cosine law of the incidence angle was applied to the backscatter coefficient to compensate for range dependency.
6. Anisotropic Non-Linear Diffusion (ANLD) filtering: The ANLD was applied to improve differences between linear structures by smoothing homogenous areas.
7. Removal of atmospheric effects: C-band wavelengths can be affected by atmospheric vapour content, which after tropical storms can be characterised by weakened backscatter values soon after the event. Whereas the signal can increase during intense rainfall and a significant decrease in of the signal after the event. Removal of the atmospheric effects was achieved by interpolation of anomalous peaks and troughs. However, “this process relies strongly on a priori knowledge of the rice crop calendar and the weather conditions when the image was acquired” (Nelson et al., 2014, p. 10788).

Appendix C. Boxplots showing differences of backscatter values between the fallow start and end

The boxplots are for VH, VV and VV/VH ratio in a) Pangasinan and b) Iloilo provinces.

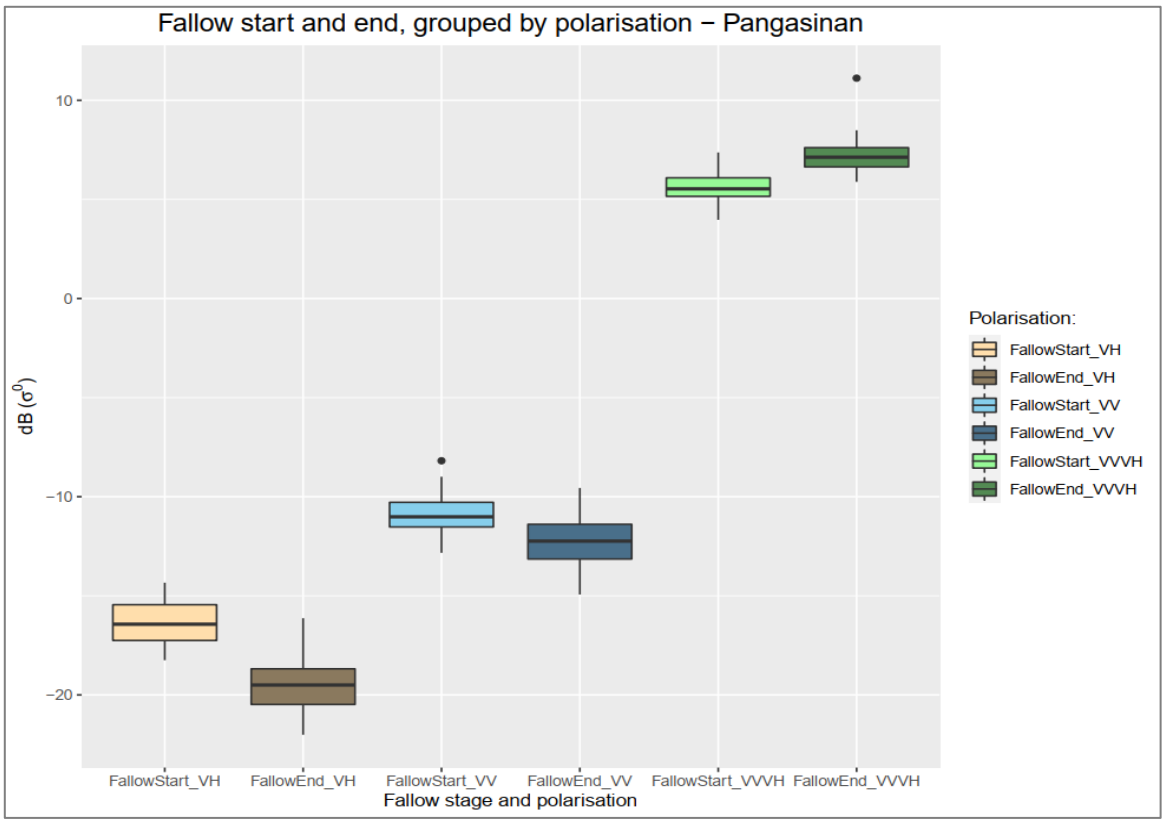

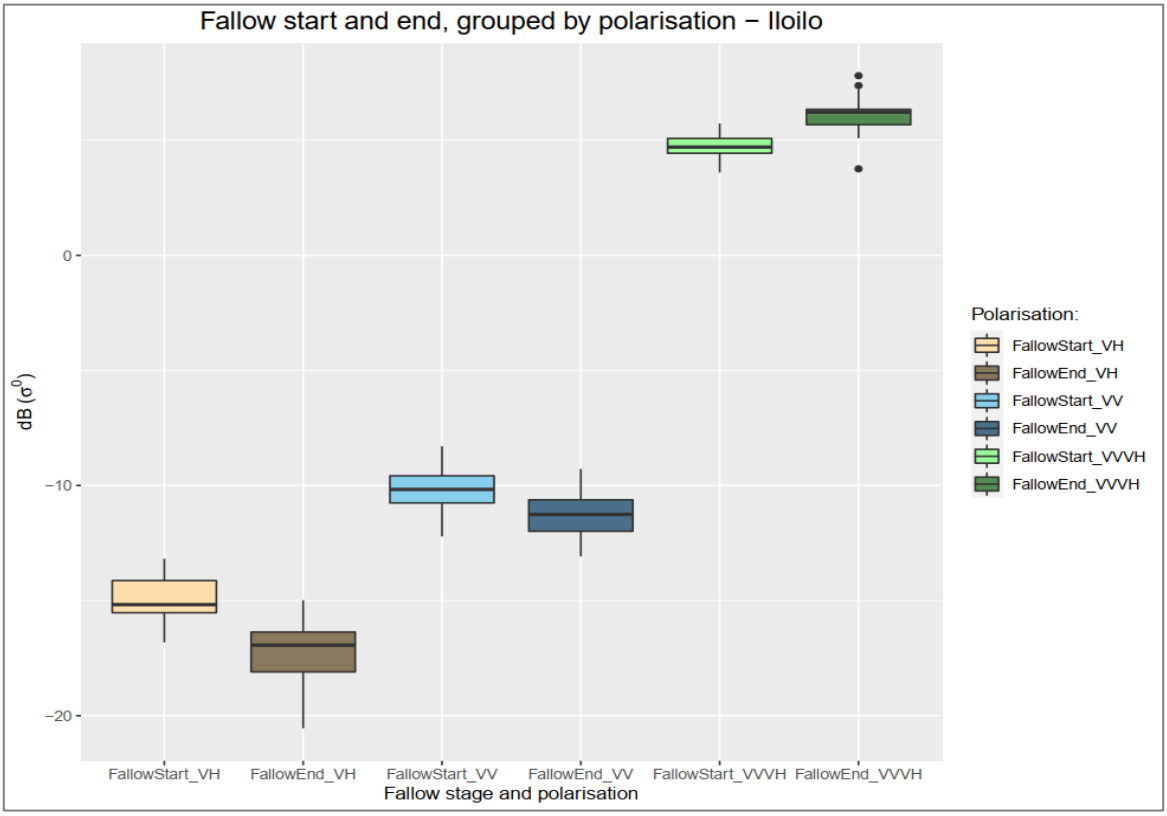

Appendix D. Boxplots of rice and fallow temporal backscatter separated by ecosystem type

Boxplots show temporal backscatter for irrigated (left) and rainfed (right) fields in Pangasinan in a) VH, b) VV and c) VV/VH polarisation ratio, and Iloilo in d) VH, e) VV and F) VV/VH polarisation ratio.

a) Pangasinan – VH polarisation

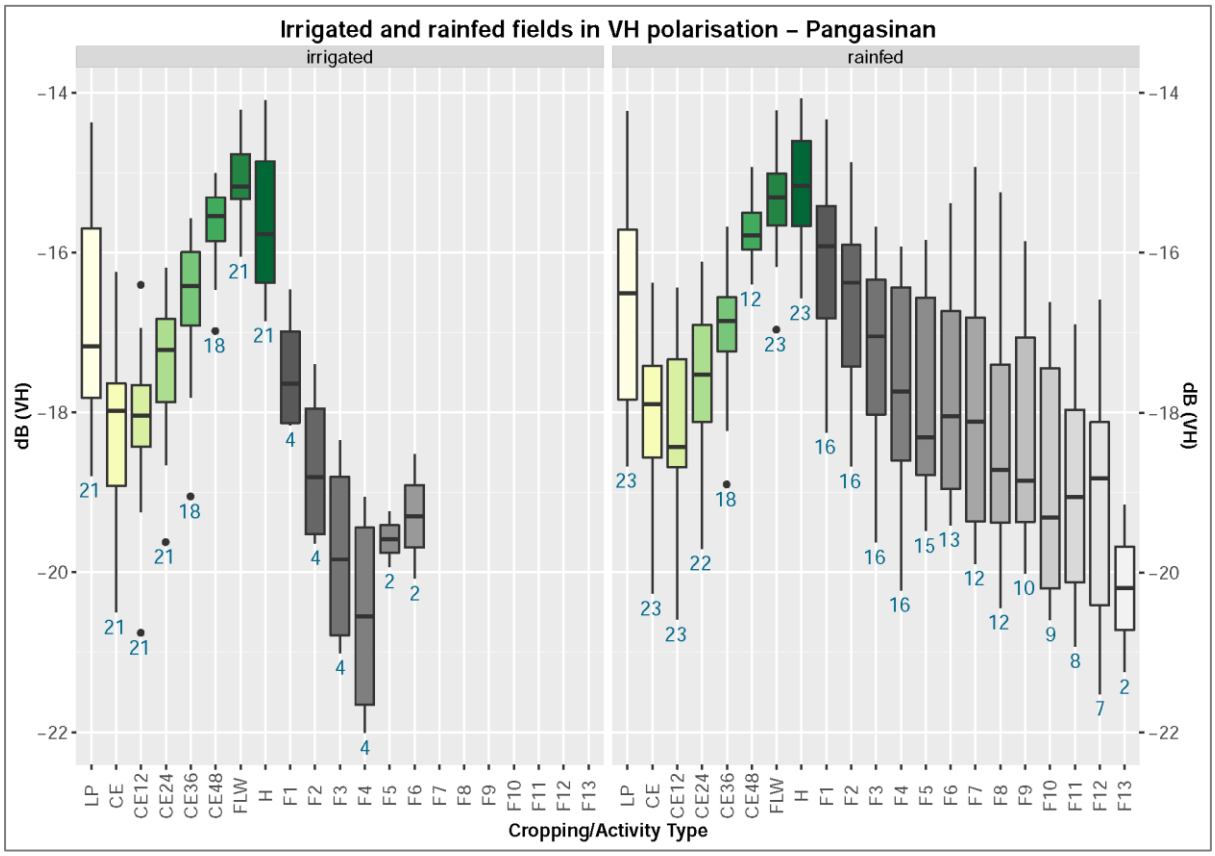

b) Pangasinan – VV polarisation

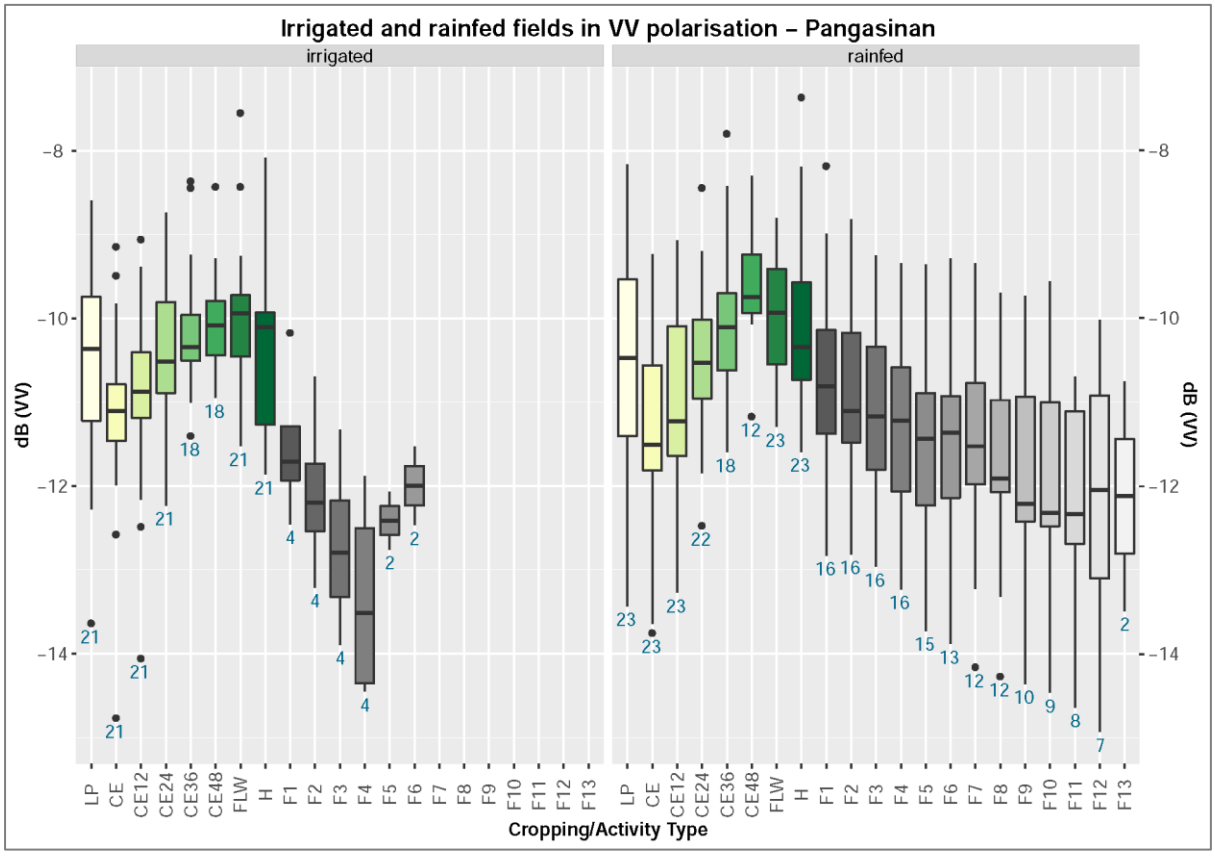

c) Pangasinan – VV/VH polarisation ratio

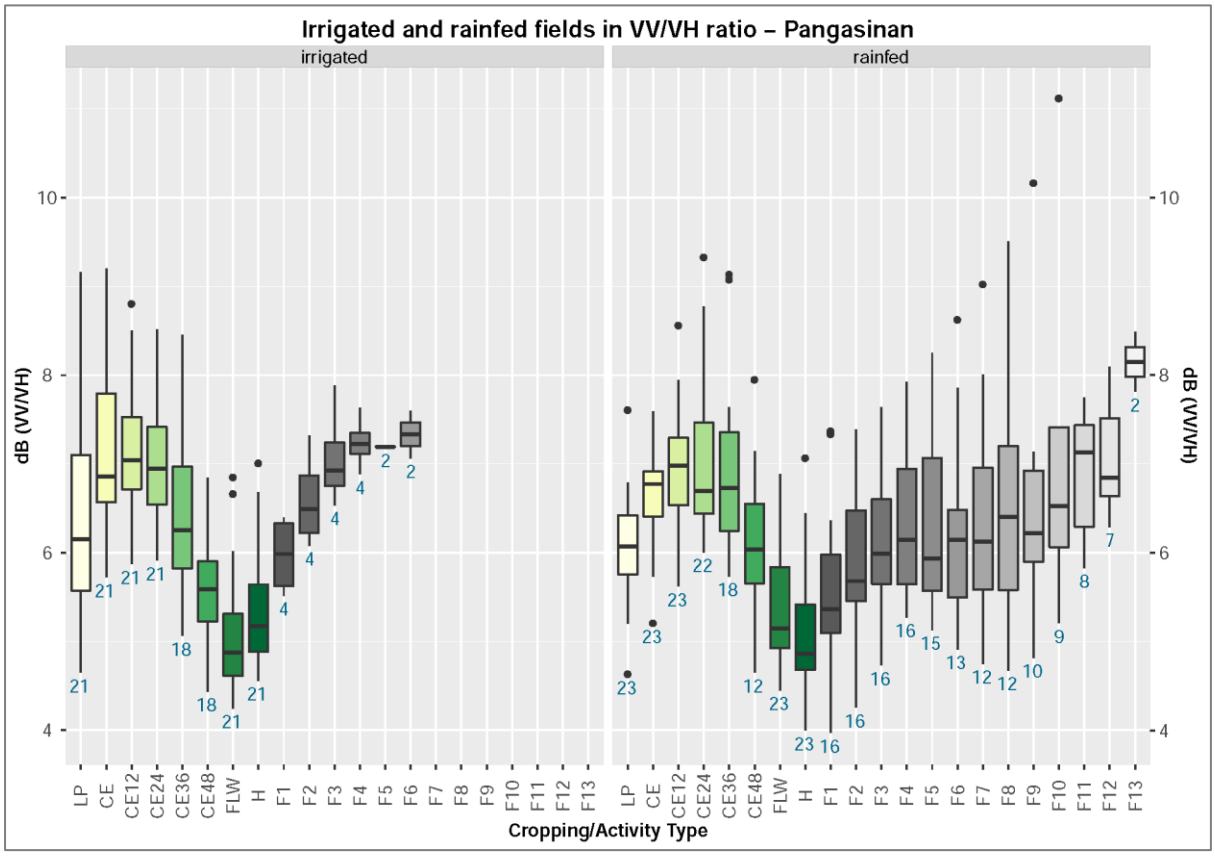

d) Iloilo – VH polarisation

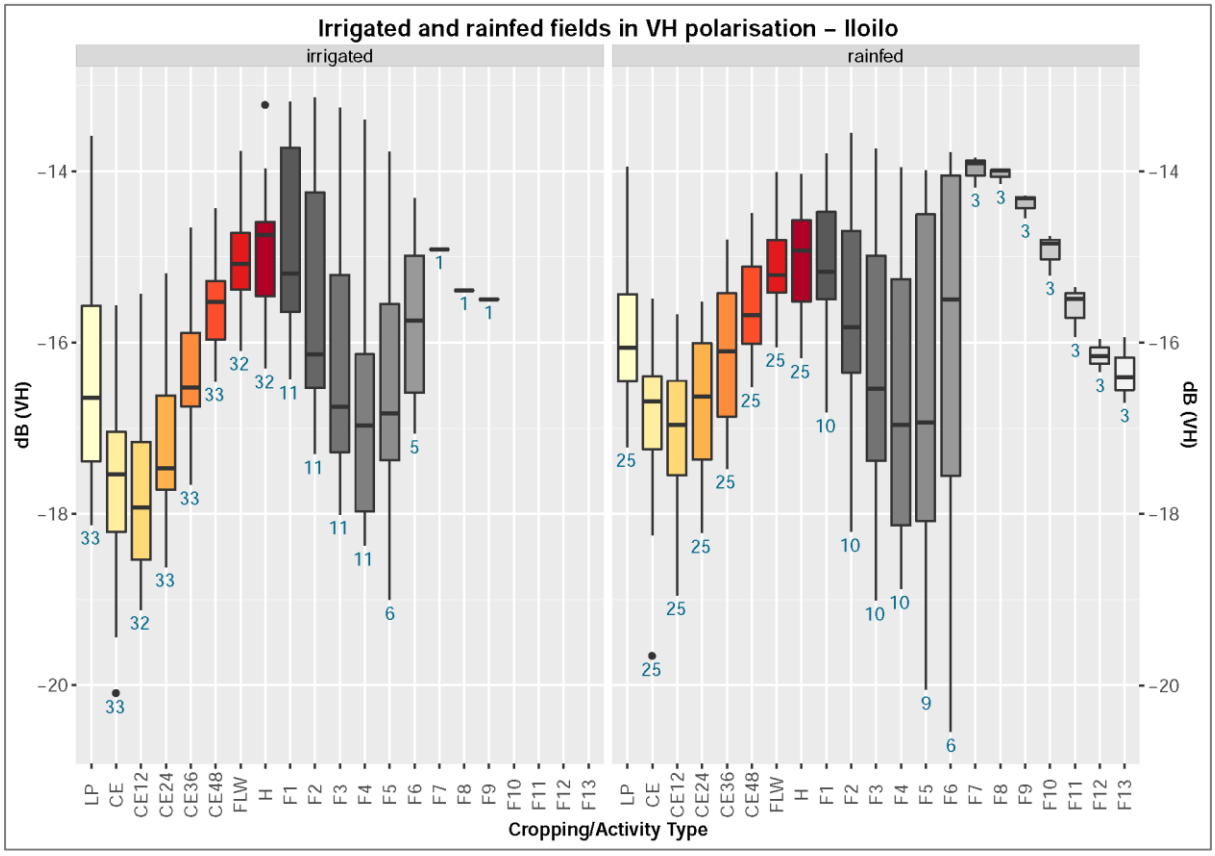

e) Iloilo – VV polarisation

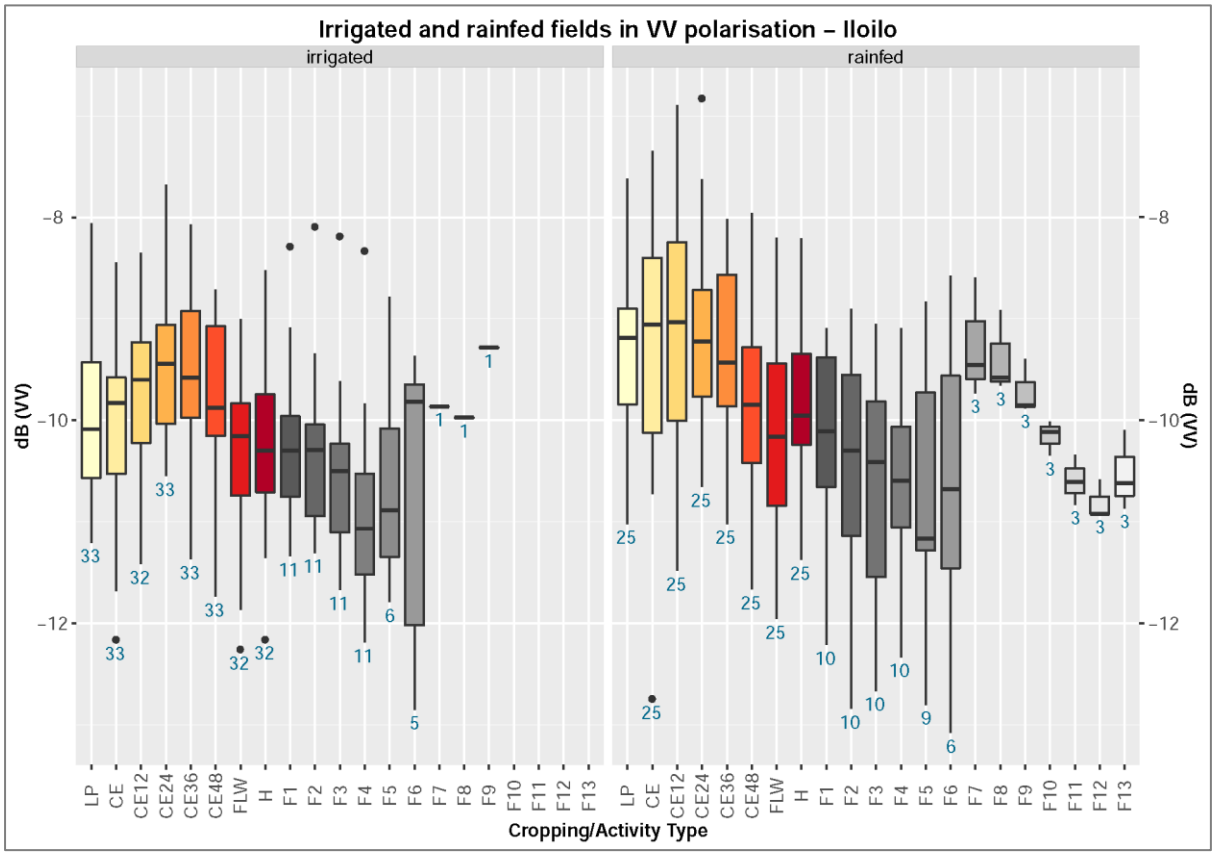

f) Iloilo – VV/VH polarisation ratio

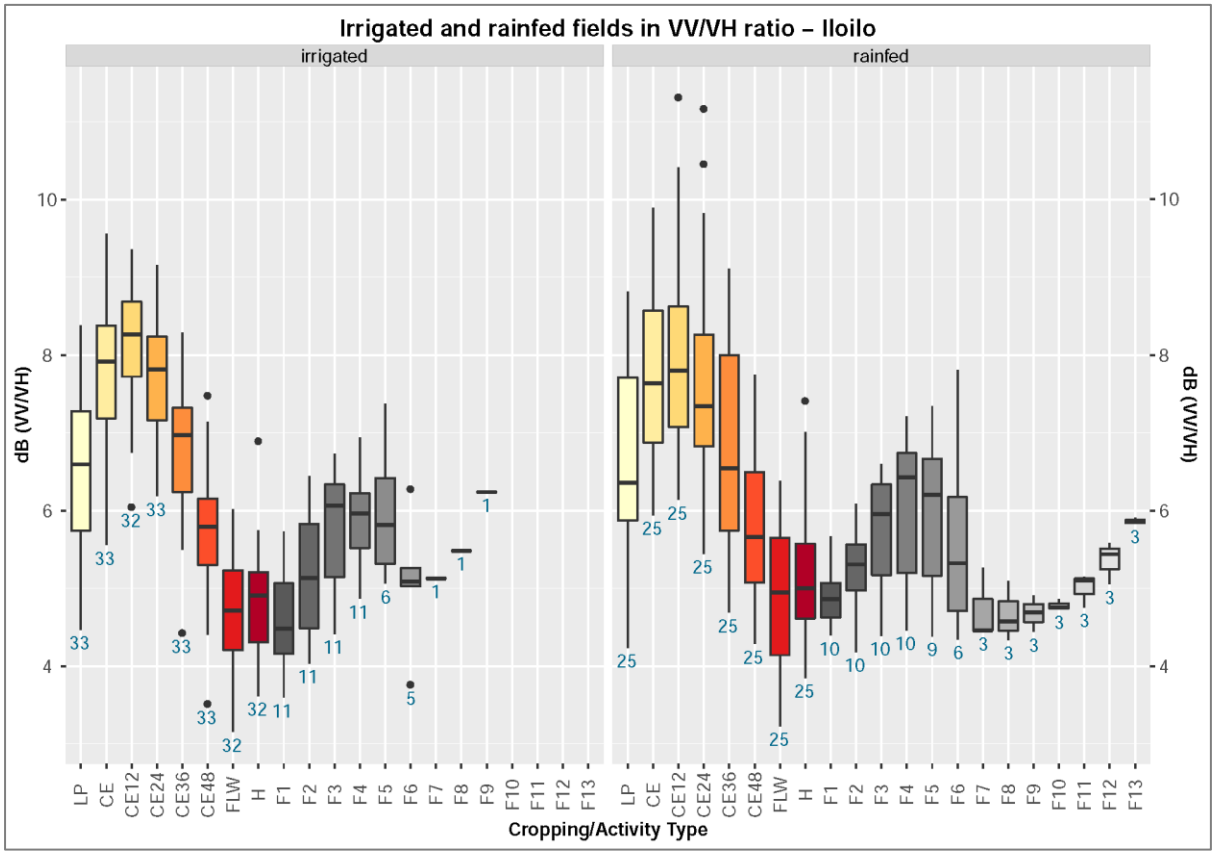

Appendix E. Average dekad rainfall separated by ecosystem type

The boxplots cover the duration of fallow periods in Pangasinan (upper) and Iloilo (lower).

Dekad1 corresponds to the start of fallow in each field. Duration based on fallow occurrence with Dekad16 containing rainfall data only for the longest fallow periods.

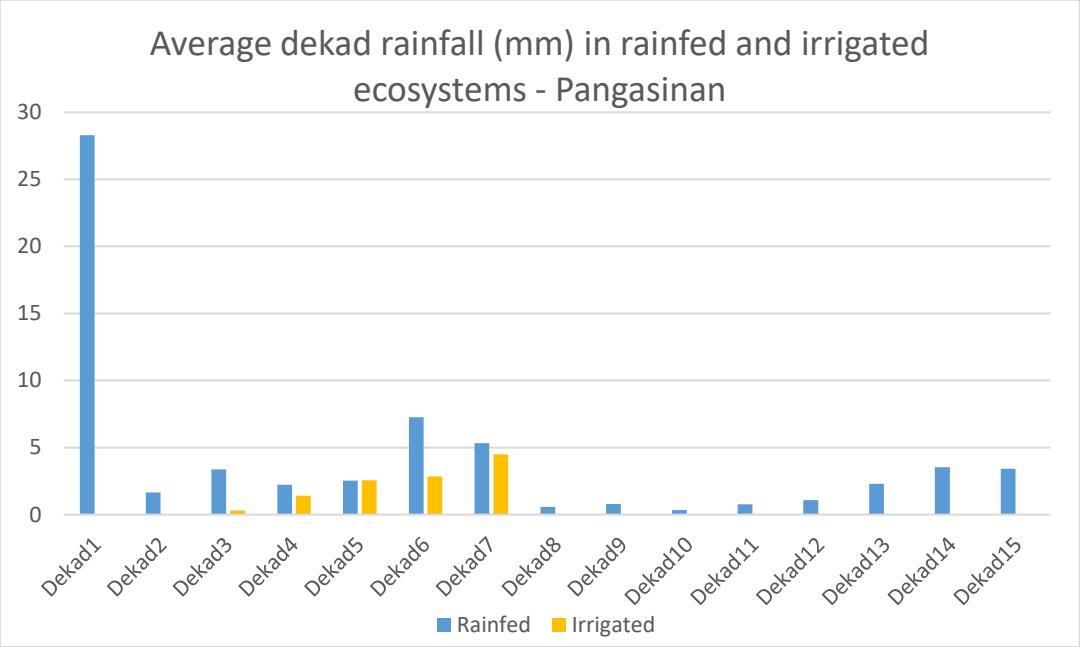

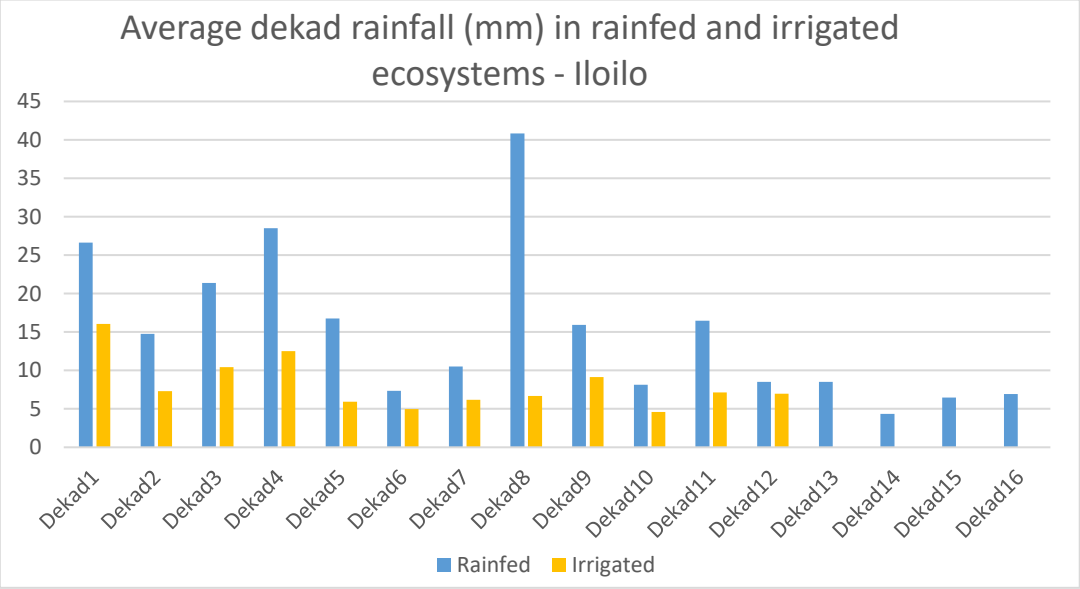

Appendix F. Fallow detection with ratoon fields removed

Table below shows root mean square error (RMSE) result for the start and end of fallow with ratoon fields removed. The RMSE was performed for derived minima and maxima dates from fallow backscatter and the farmer reported fallow periods.

Province	SAR channel	RMSE - Fallow			
		Start of fallow		End of fallow	
		RMSE (days)	Sentinel-1A revisits	RMSE (days)	Sentinel-1A revisits
Pangasinan	VH	31.7**	2.6	8.7*	0.7
	VV	55.1**	4.6	10.1*	0.8
	VV/VH	28.2*	2.4	8.7**	0.7
Iloilo	VH	30.9**	2.6	9.1*	0.8
	VV	52.5**	4.4	10.7*	0.9
	VV/VH	23.4*	1.9	10.7**	0.9

(RMSE based on reported FS/FE and derived date from backscatter: * local minima; and ** local maxima)

Boxplots below show the of the temporal differences between the observed fallow start date (upper) and the fallow end date (lower) in a) Pangasinan and b) Iloilo. RMSE is expressed in days.

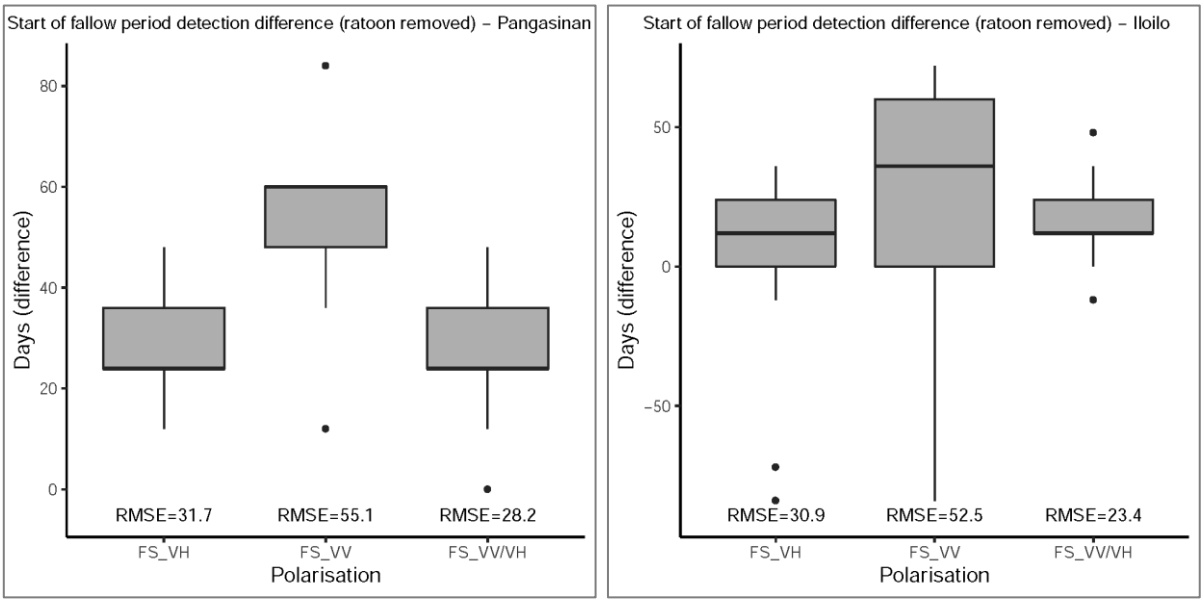

a) b)

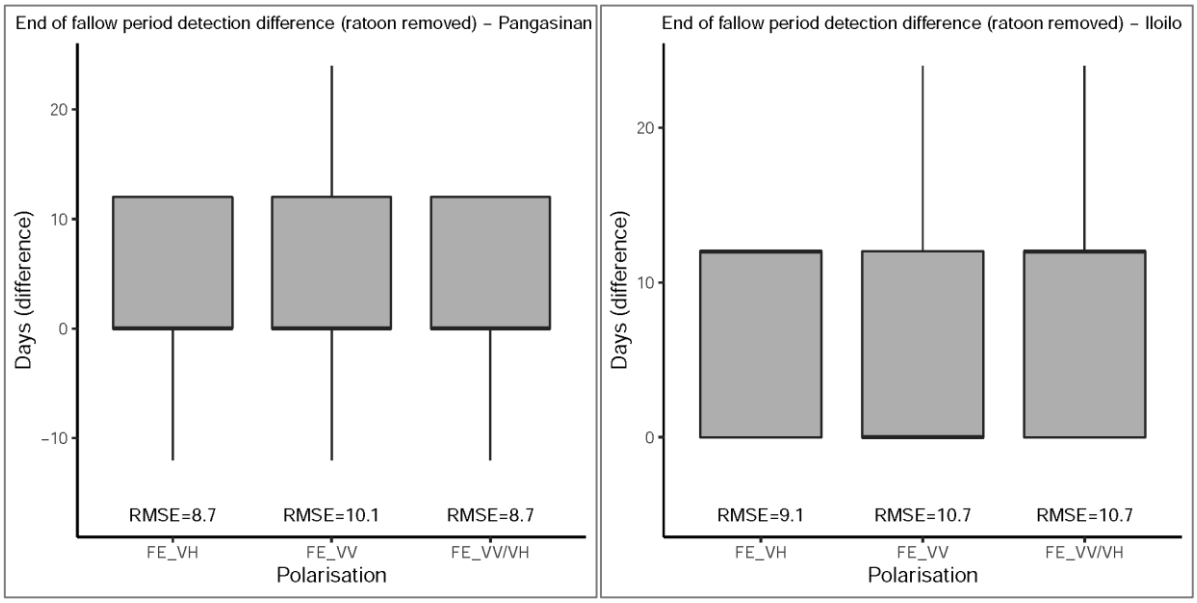
End of fallow period detection difference (ratoon removed) – Pangasinan
Days (difference)
20
10
0
−10
RMSE=8.7
RMSE=10.1
RMSE=8.7
FE_VH
FE_VV
FE_VV/VH
Polarisation
End of fallow period detection difference (ratoon removed) – Iloilo
Days (difference)
20
10
0
RMSE=9.1
RMSE=10.7
RMSE=10.7
FE_VH
FE_VV
FE_VV/VH
Polarisation

a) b)

Appendix G. Time-series for each field in Pangasinan and Iloilo.

The time-series contain Savitzky-Golay filtered SAR data for fields with accepted rice cropping patterns. Accepted rice cropping stages and activities are marked with black text and lines, whereas rejected rice crops were marked by grey horizontal lines.

Abbreviations of the cropping stages and activities used in the graphs are as follows: LP = Land preparation; CE = Crop Establishment; FLW = Flowering; H= harvest; and RH = Ratoon Harvest. The numbers next to the cropping phases indicate the crop number each stage and activity relates to. FallowN indicates additional fallow periods not previously reported by the farmers.

To differentiate between both locations, the data for the fields in Pangasinan were plotted in green, whereas Iloilo data was plotted in orange. Also, the three-digit field numbers starting with 1 are for Pangasinan, whereas fields in Iloilo start with 6.

Time series for Pangasinan VH and VV polarisations:

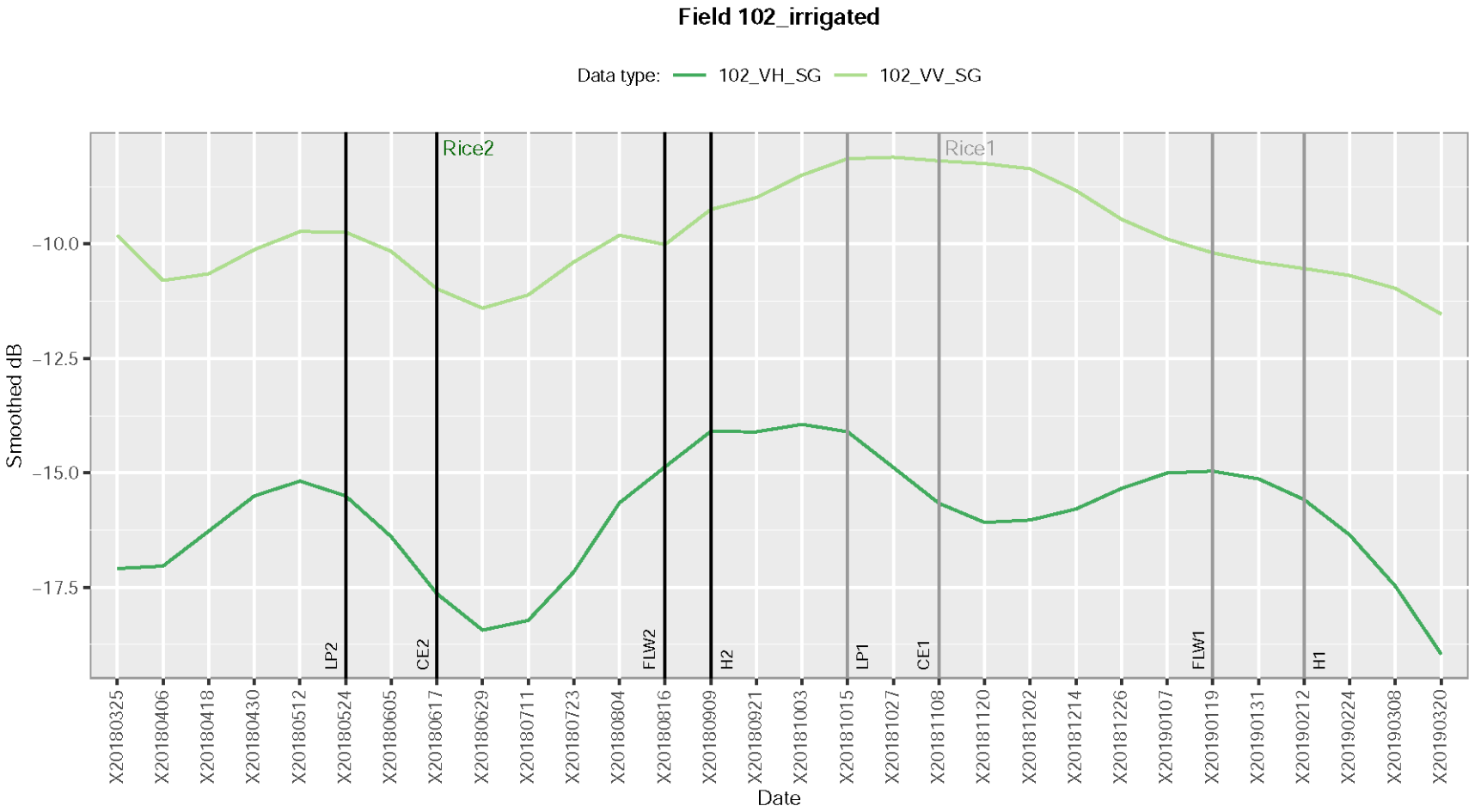

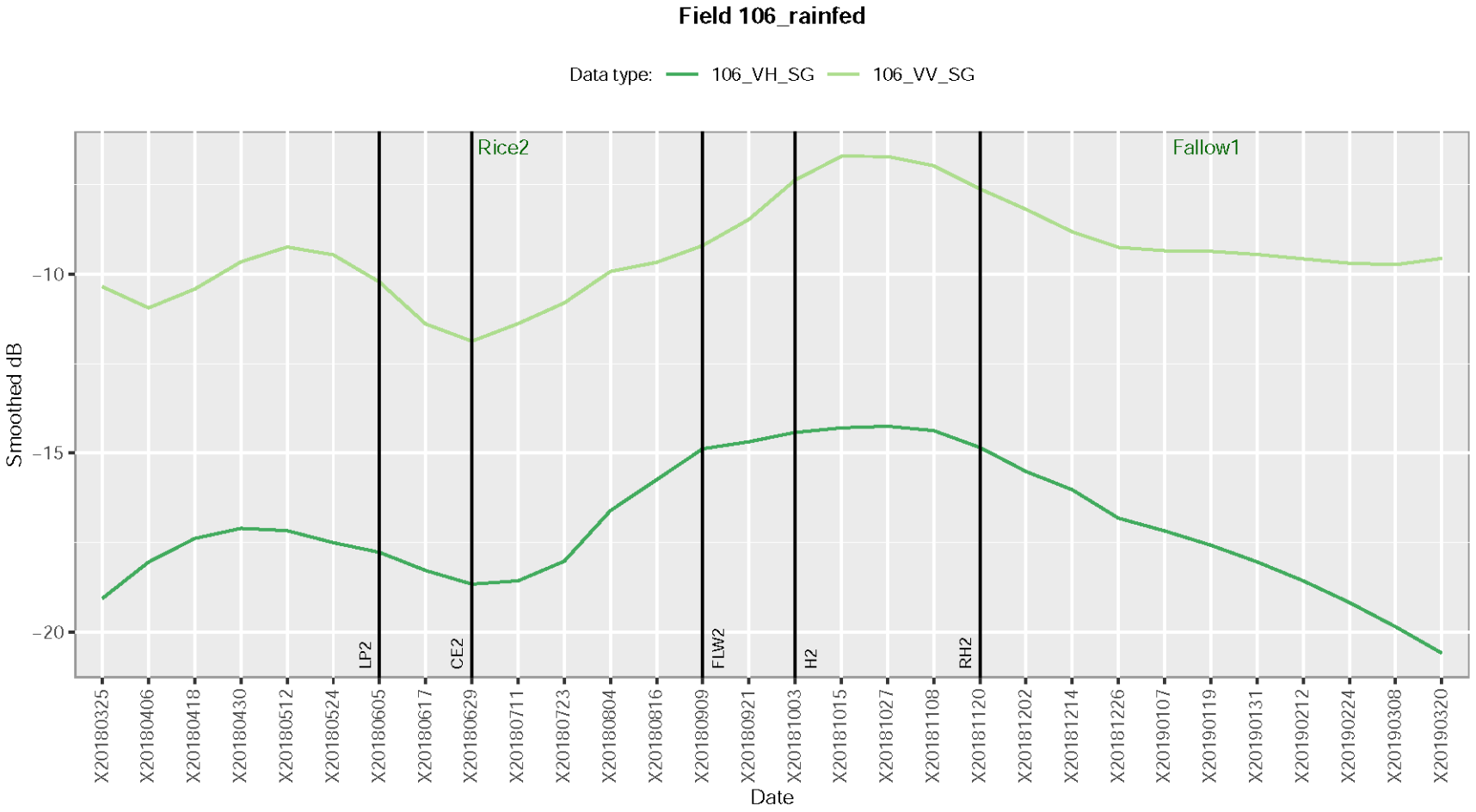
Field 106_rainfed
Data type: 106_VH_SG 106_VV_SG
Rice2
Fallow1
LP2
CE2
FLW2
H2
RH2
Smoothed dB
−10
−15
−20
X20180325
X20180406
X20180418
X20180430
X20180512
X20180524
X20180605
X20180617
X20180629
X20180711
X20180723
X20180804
X20180816
X20180909
X20180921
X20181003
X20181015
X20181027
X20181108
X20181120
X20181202
X20181214
X20181226
X20190107
X20190119
X20190131
X20190212
X20190224
X20190308
X20190320
Date

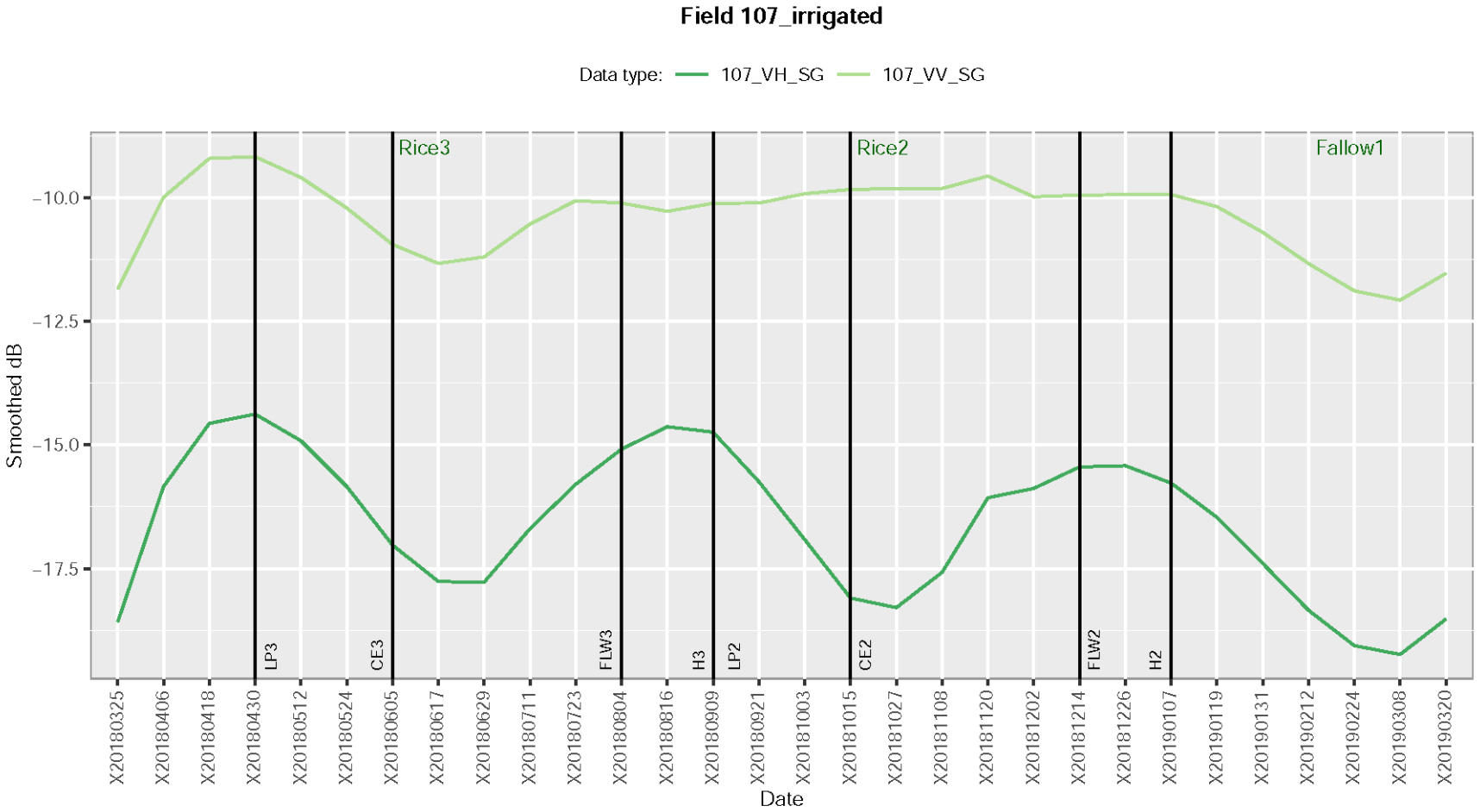
Field 107_irrigated
Data type: 107_VH_SG 107_VV_SG
Rice3
Rice2
Fallow1
Smoothed dB
−10.0
−12.5
−15.0
−17.5
LP3
CE3
FLW3
H3
LP2
CE2
FLW2
H2
X20180325
X20180406
X20180418
X20180430
X20180512
X20180524
X20180605
X20180617
X20180629
X20180711
X20180723
X20180804
X20180816
X20180909
X20180921
X20181003
X20181015
X20181027
X20181108
X20181120
X20181202
X20181214
X20181226
X20190107
X20190119
X20190131
X20190212
X20190224
X20190308
X20190320
Date

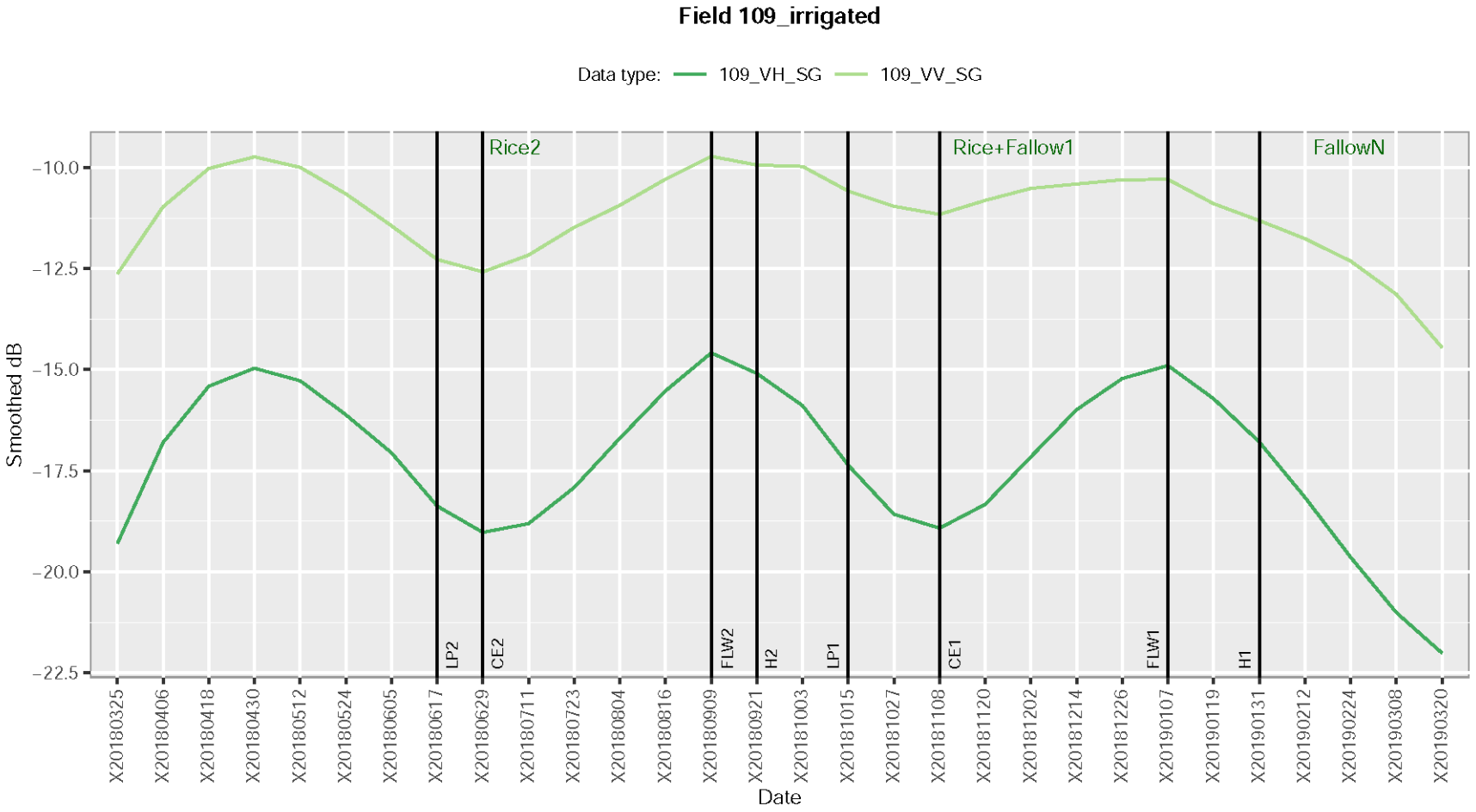
Field 109_irrigated
Data type: 109_VH_SG 109_VV_SG
Rice2
Rice+Fallow1
FallowN
Smoothed dB
−10.0
−12.5
−15.0
−17.5
−20.0
−22.5
LP2
CE2
FLW2
H2
LP1
CE1
FLW1
H1
X20180325
X20180406
X20180418
X20180430
X20180512
X20180524
X20180605
X20180617
X20180629
X20180711
X20180723
X20180804
X20180816
X20180909
X20180921
X20181003
X20181015
X20181027
X20181108
X20181120
X20181202
X20181214
X20181226
X20190107
X20190119
X20190131
X20190212
X20190224
X20190308
X20190320
Date

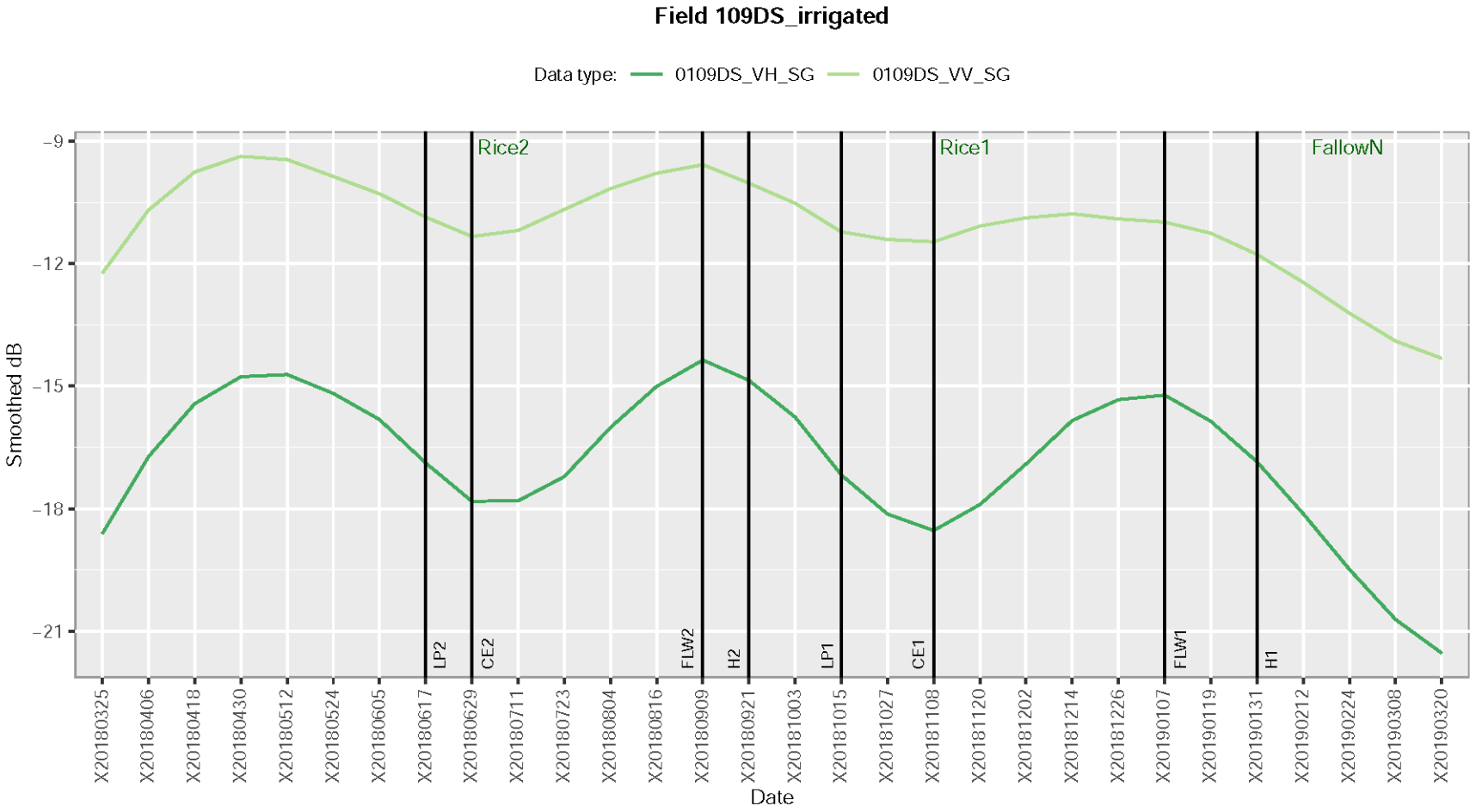
Field 109DS_irrigated
Data type:
0109DS_VH_SG
0109DS_VV_SG
Rice2
Rice1
FallowN
LP2
CE2
FLW2
H2
LP1
CE1
FLW1
H1
Smoothed dB
−9
−12
−15
−18
−21
X20180325
X20180406
X20180418
X20180430
X20180512
X20180524
X20180605
X20180617
X20180629
X20180711
X20180723
X20180804
X20180816
X20180909
X20180921
X20181003
X20181015
X20181027
X20181108
X20181120
X20181202
X20181214
X20181226
X20190107
X20190119
X20190131
X20190212
X20190224
X20190308
X20190320
Date

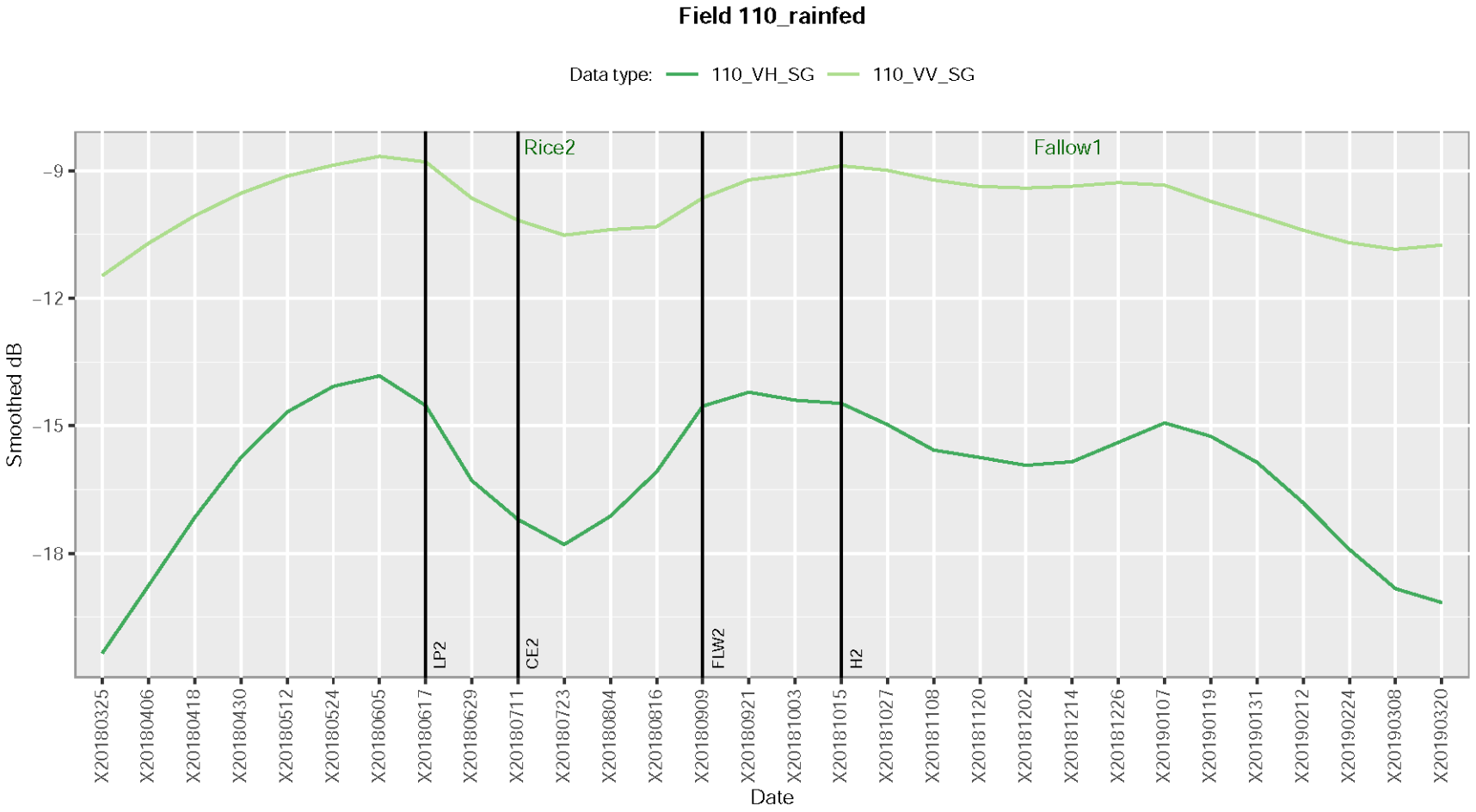
Field 110_rainfed
Data type: 110_VH_SG 110_VV_SG
Rice2
Fallow1
LP2
CE2
FLW2
H2
Smoothed dB
-9
-12
-15
-18
X20180325
X20180406
X20180418
X20180430
X20180512
X20180524
X20180605
X20180617
X20180629
X20180711
X20180723
X20180804
X20180816
X20180909
X20180921
X20181003
X20181015
X20181027
X20181108
X20181120
X20181202
X20181214
X20181226
X20190107
X20190119
X20190131
X20190212
X20190224
X20190308
X20190320
Date

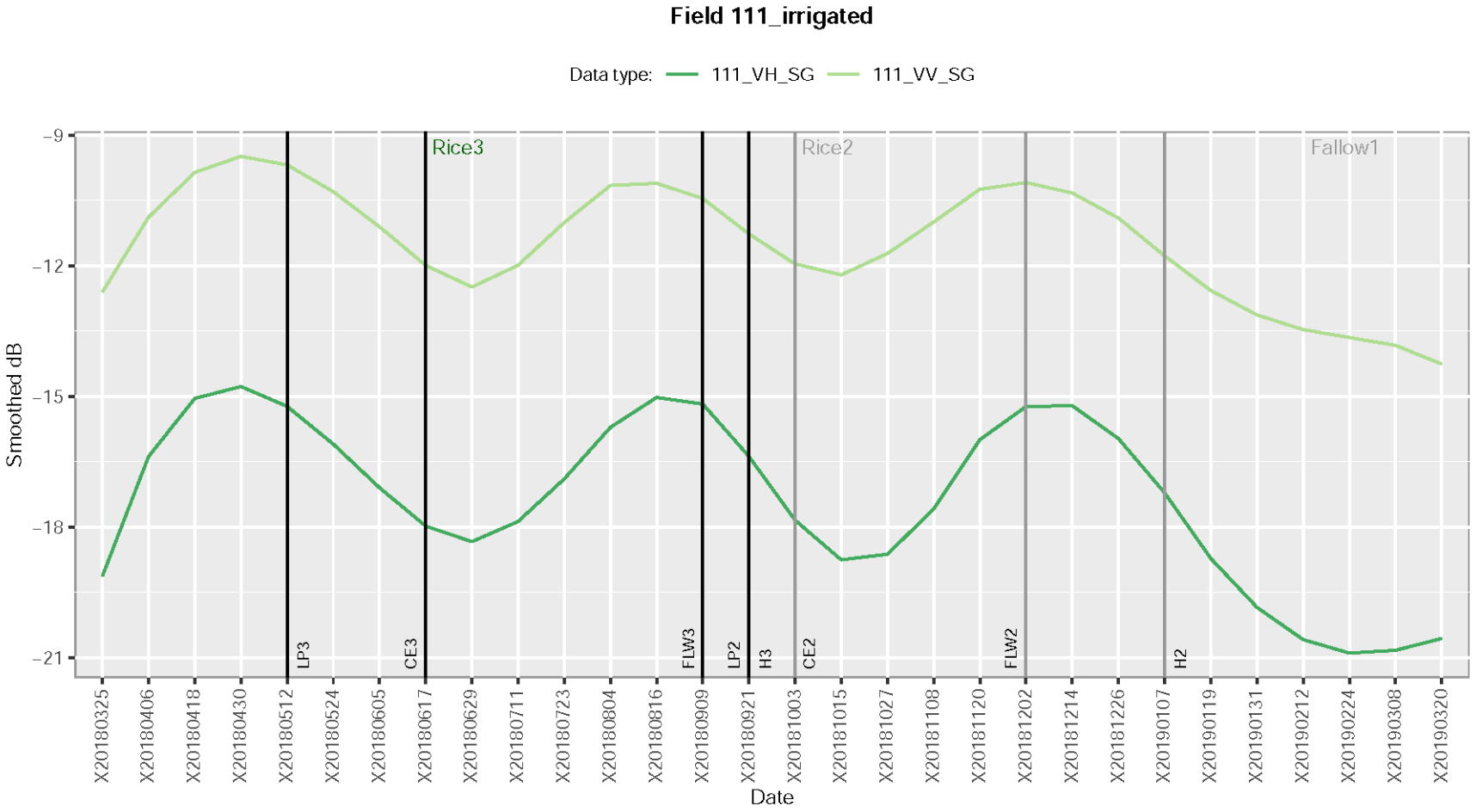
Field 111_irrigated
Data type: 111_VH_SG 111_VV_SG
Rice3
Rice2
Fallow1
Smoothed dB
−9
−12
−15
−18
−21
LP3
CE3
FLW3
LP2
H3
CE2
FLW2
H2
X20180325
X20180406
X20180418
X20180430
X20180512
X20180524
X20180605
X20180617
X20180629
X20180711
X20180723
X20180804
X20180816
X20180909
X20180921
X20181003
X20181015
X20181027
X20181108
X20181120
X20181202
X20181214
X20181226
X20190107
X20190119
X20190131
X20190212
X20190224
X20190308
X20190320
Date

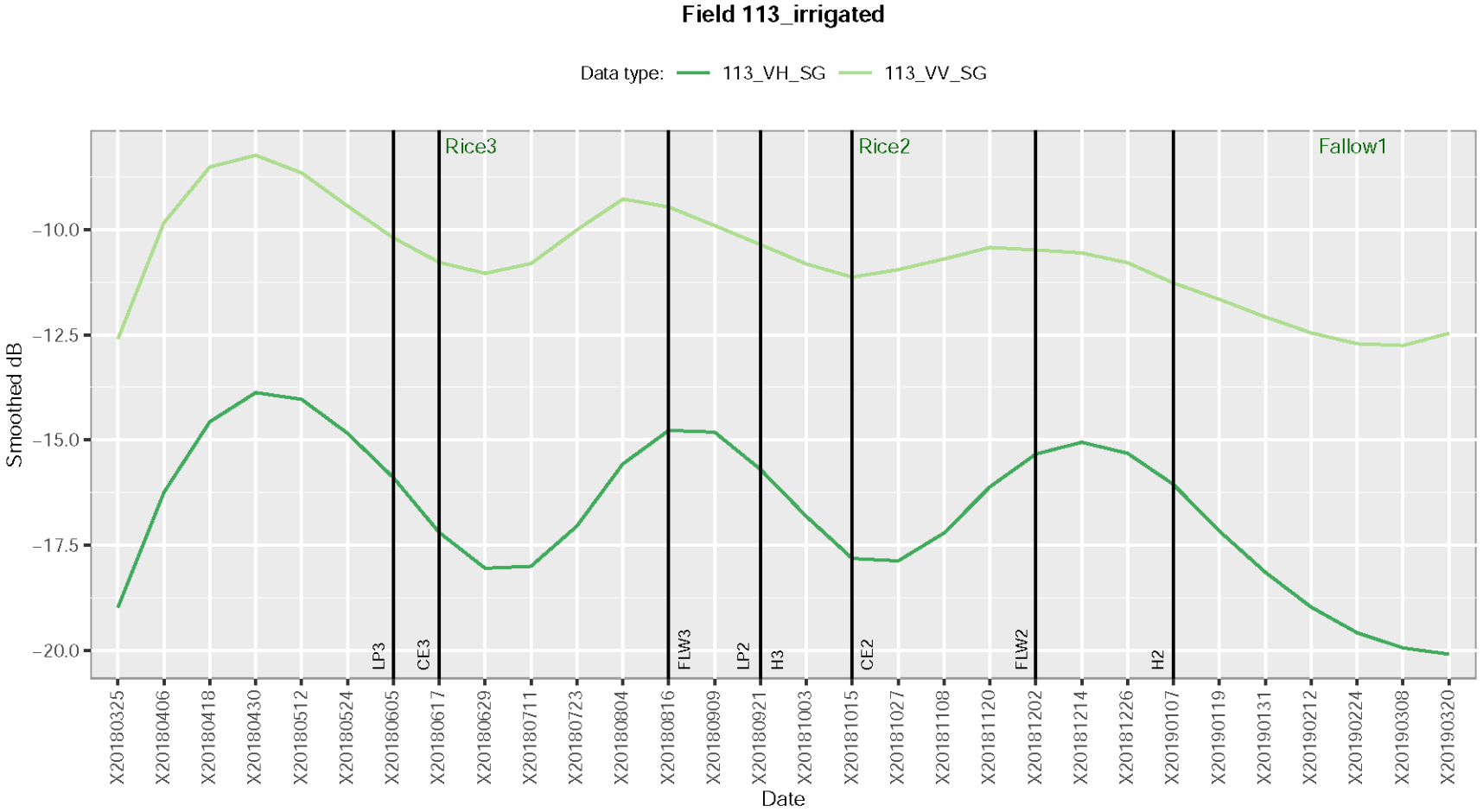
Field 113_irrigated
Data type: 113_VH_SG 113_VV_SG
Rice3
Rice2
Fallow1
Smoothed dB
−10.0
−12.5
−15.0
−17.5
−20.0
LP3
CE3
FLW3
LP2
H3
CE2
FLW2
H2
X20180325
X20180406
X20180418
X20180430
X20180512
X20180524
X20180605
X20180617
X20180629
X20180711
X20180723
X20180804
X20180816
X20180909
X20180921
X20181003
X20181015
X20181027
X20181108
X20181120
X20181202
X20181214
X20181226
X20190107
X20190119
X20190131
X20190212
X20190224
X20190308
X20190320
Date

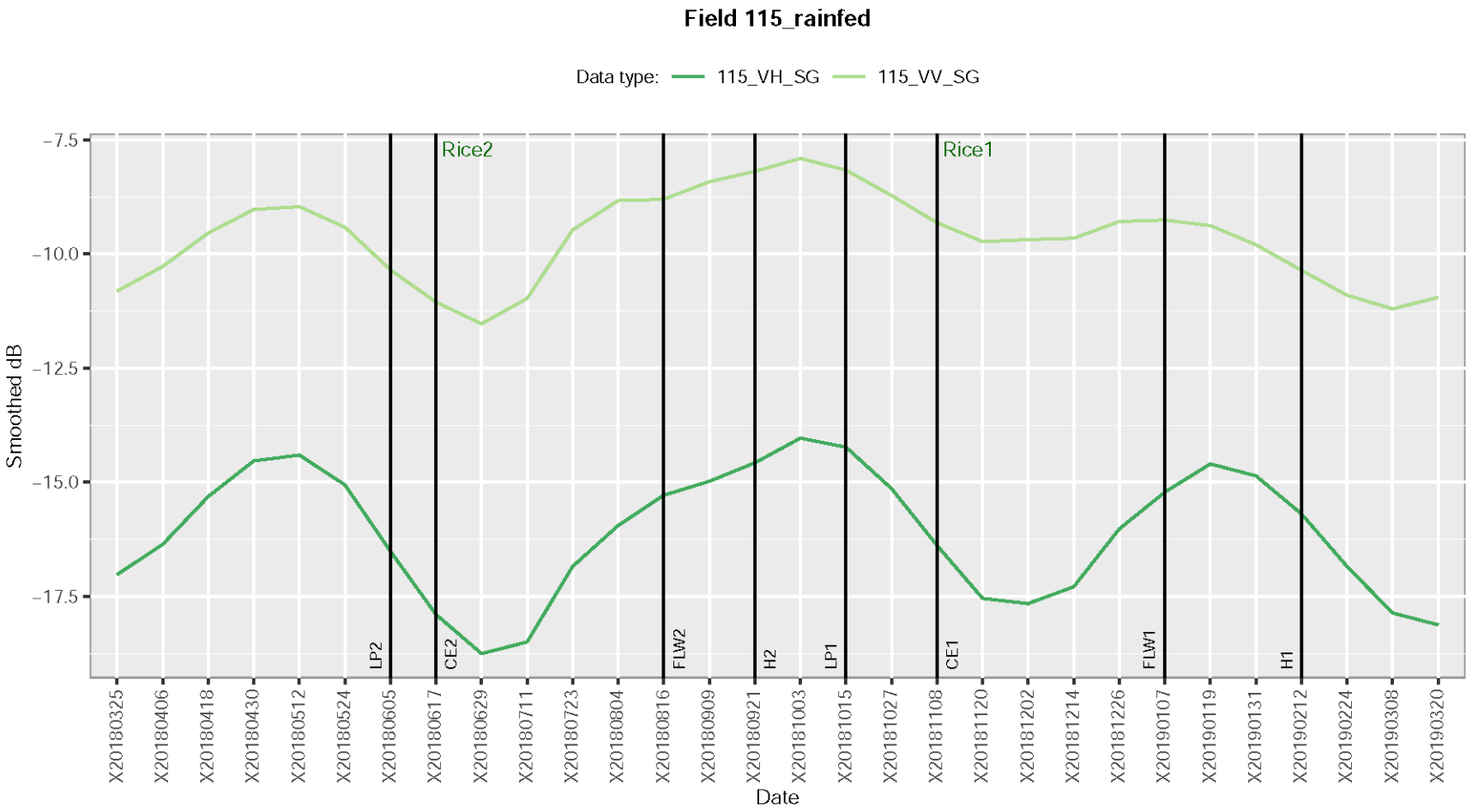
Field 115_rainfed
Data type: 115_VH_SG 115_VV_SG
Smoothed dB
−7.5
−10.0
−12.5
−15.0
−17.5
Rice2
Rice1
LP2
CE2
FLW2
H2
LP1
CE1
FLW1
H1
X20180325
X20180406
X20180418
X20180430
X20180512
X20180524
X20180605
X20180617
X20180629
X20180711
X20180723
X20180804
X20180816
X20180909
X20180921
X20181003
X20181015
X20181027
X20181108
X20181120
X20181202
X20181214
X20181226
X20190107
X20190119
X20190131
X20190212
X20190224
X20190308
X20190320
Date

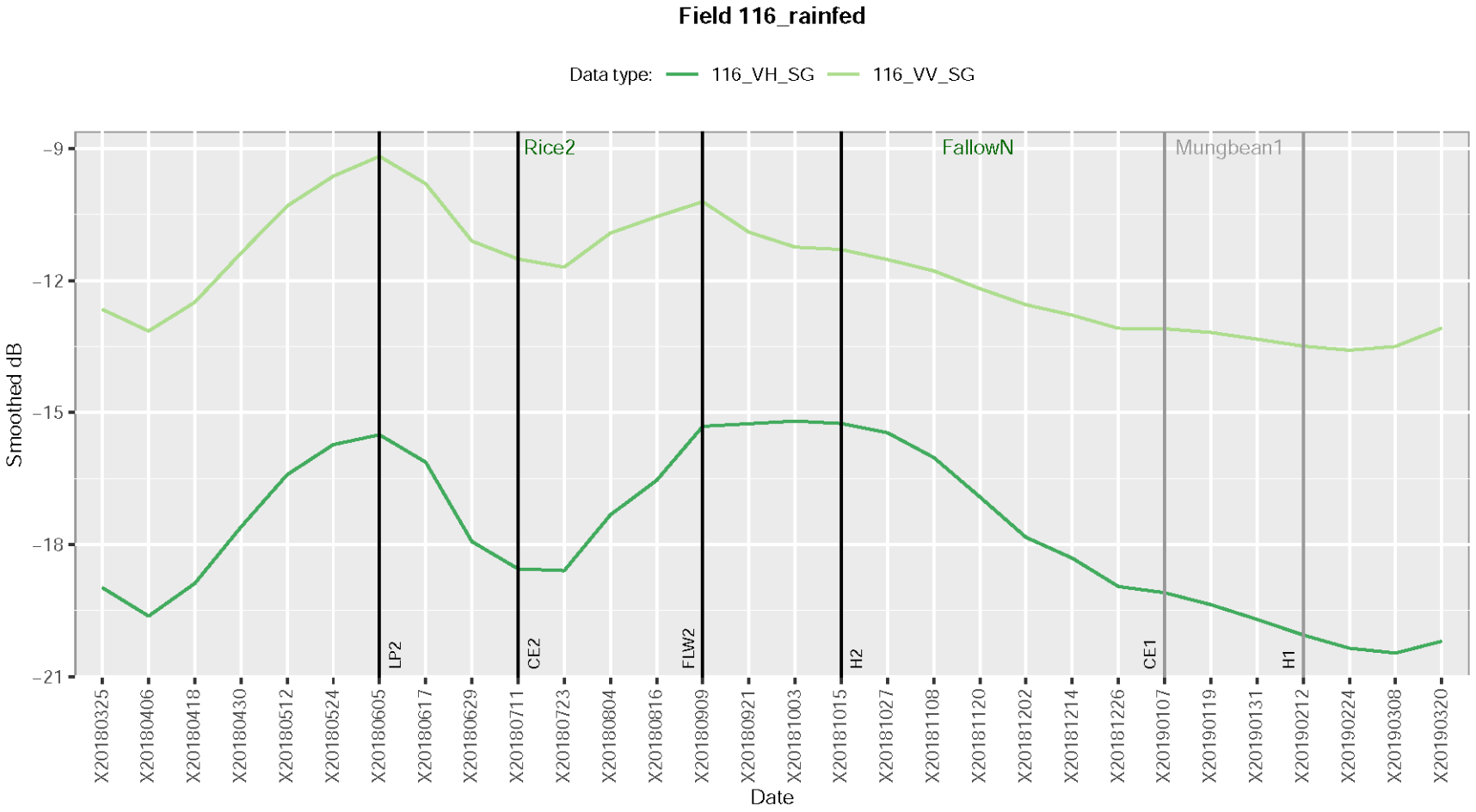
Field 116_rainfed
Data type: 116_VH_SG 116_VV_SG
Rice2
FallowN
Mungbean1
LP2
CE2
FLW2
H2
CE1
H1
Smoothed dB
−9
−12
−15
−18
−21
X20180325
X20180406
X20180418
X20180430
X20180512
X20180524
X20180605
X20180617
X20180629
X20180711
X20180723
X20180804
X20180816
X20180909
X20180921
X20181003
X20181015
X20181027
X20181108
X20181120
X20181202
X20181214
X20181226
X20190107
X20190119
X20190131
X20190212
X20190224
X20190308
X20190320
Date

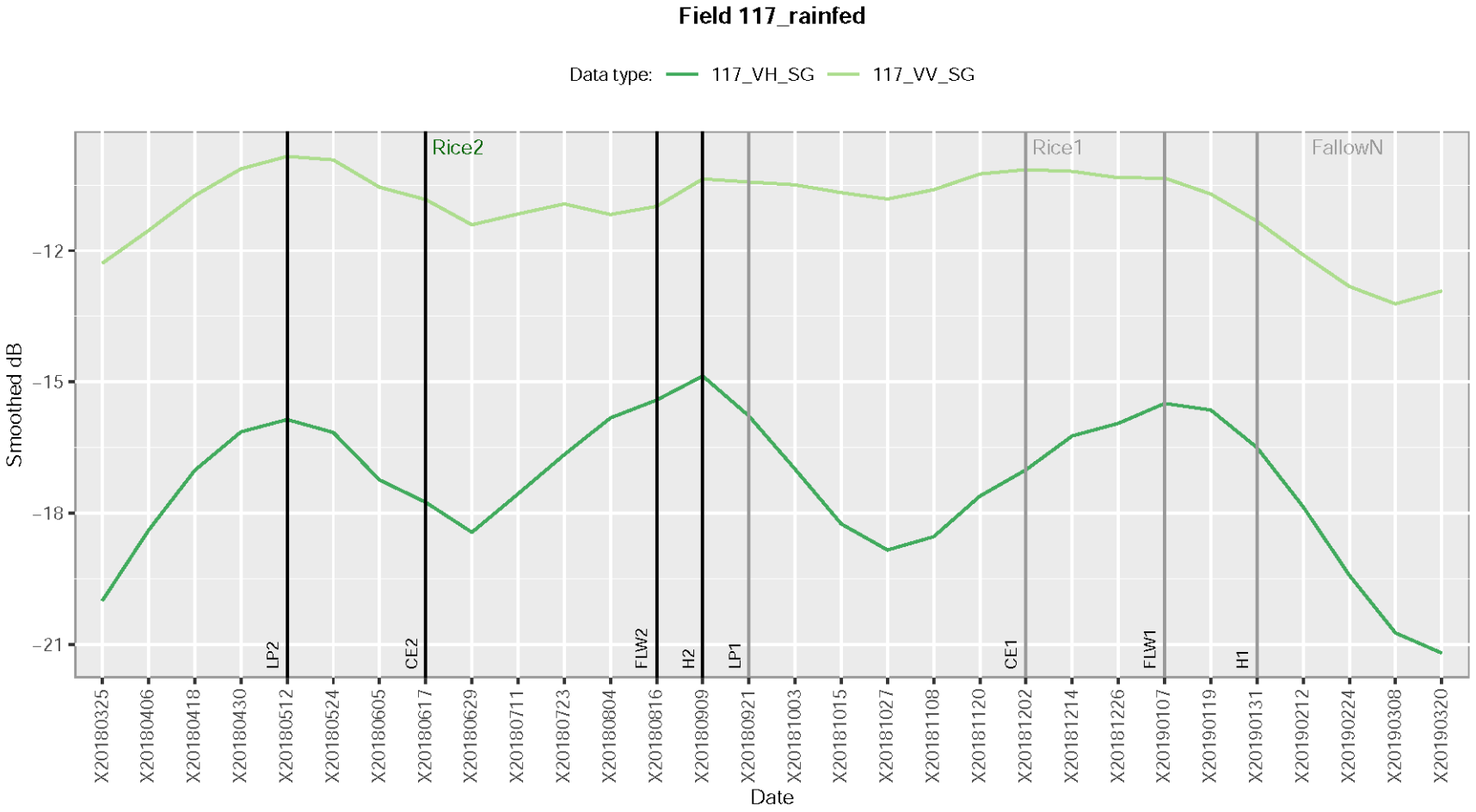
Field 117_rainfed
Data type: 117_VH_SG 117_VV_SG
Rice2
Rice1
FallowN
Smoothed dB
−12
−15
−18
−21
LP2
CE2
FLW2
H2
LP1
CE1
FLW1
H1
X20180325
X20180406
X20180418
X20180430
X20180512
X20180524
X20180605
X20180617
X20180629
X20180711
X20180723
X20180804
X20180816
X20180909
X20180921
X20181003
X20181015
X20181027
X20181108
X20181120
X20181202
X20181214
X20181226
X20190107
X20190119
X20190131
X20190212
X20190224
X20190308
X20190320
Date

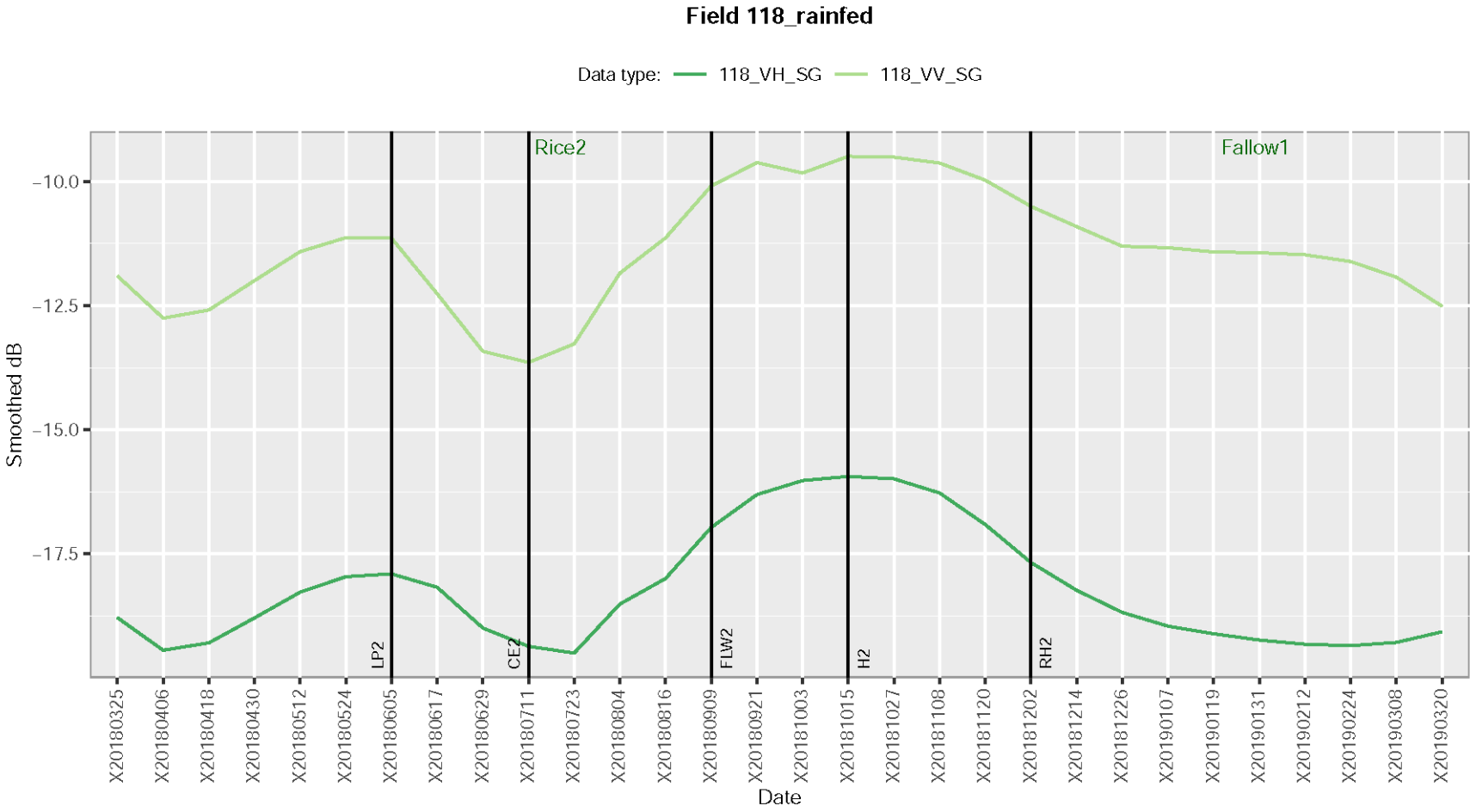
Field 118_rainfed
Data type: 118_VH_SG 118_VV_SG
Rice2
Fallow1
LP2
CE2
FLW2
H2
RH2
Smoothed dB
−10.0
−12.5
−15.0
−17.5
X20180325
X20180406
X20180418
X20180430
X20180512
X20180524
X20180605
X20180617
X20180629
X20180711
X20180723
X20180804
X20180816
X20180909
X20180921
X20181003
X20181015
X20181027
X20181108
X20181120
X20181202
X20181214
X20181226
X20190107
X20190119
X20190131
X20190212
X20190224
X20190308
X20190320
Date

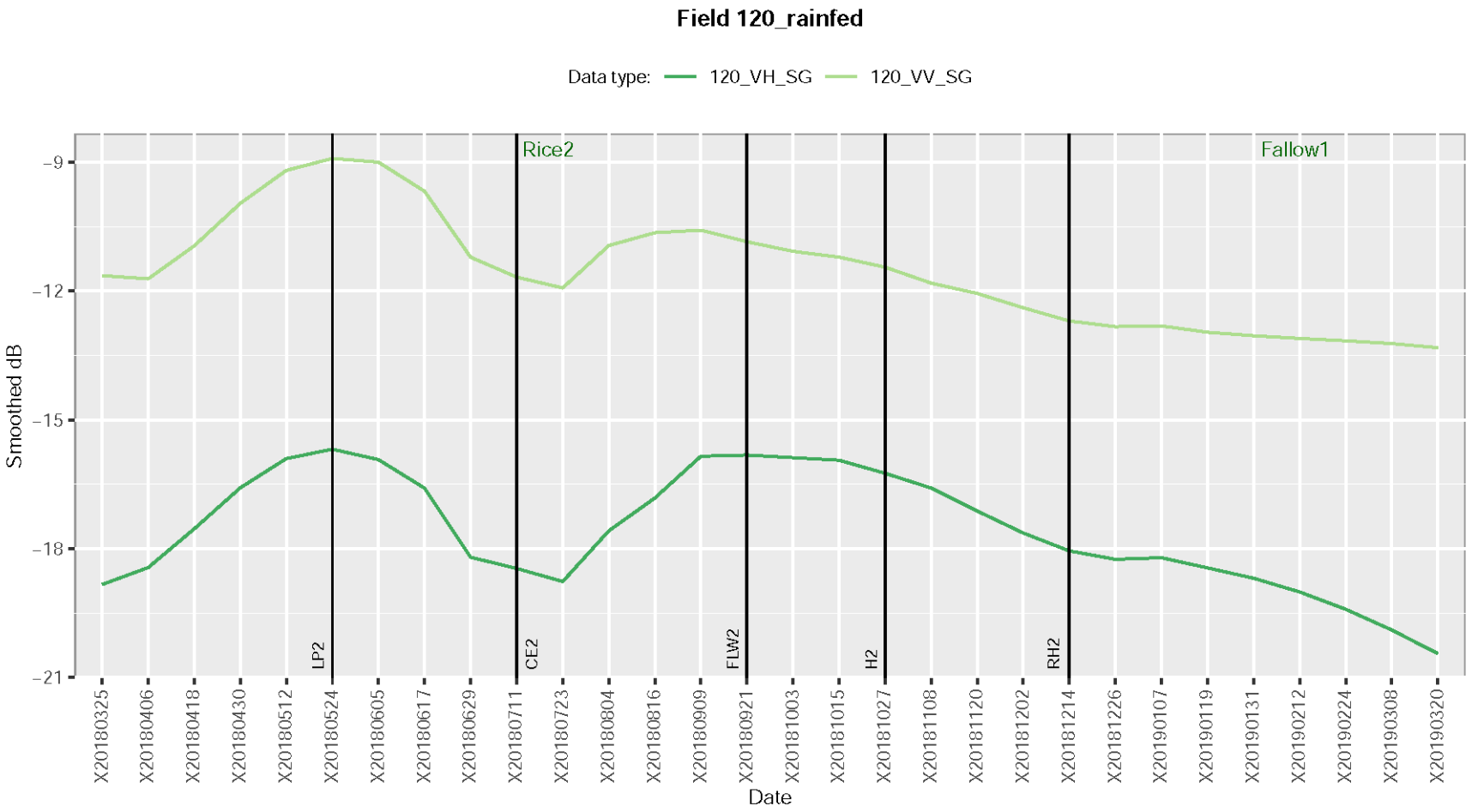
Field 120_rainfed
Data type: 120_VH_SG 120_VV_SG
Rice2
Fallow1
Smoothed dB
−9
−12
−15
−18
−21
LP2
CE2
FLW2
H2
RH2
X20180325
X20180406
X20180418
X20180430
X20180512
X20180524
X20180605
X20180617
X20180629
X20180711
X20180723
X20180804
X20180816
X20180909
X20180921
X20181003
X20181015
X20181027
X20181108
X20181120
X20181202
X20181214
X20181226
X20190107
X20190119
X20190131
X20190212
X20190224
X20190308
X20190320
Date

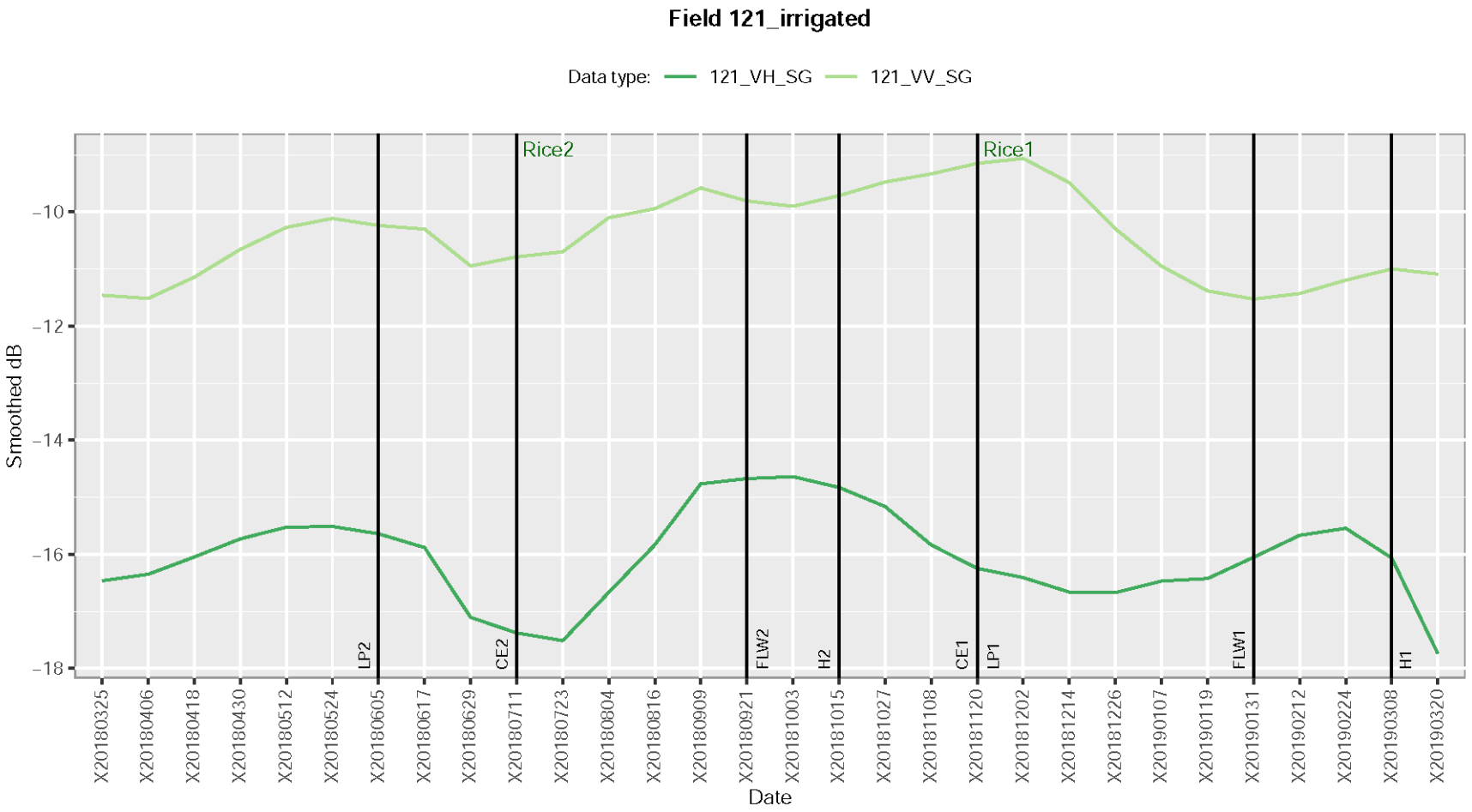
Field 121_irrigated
Data type: 121_VH_SG 121_VV_SG
Rice2
Rice1
Smoothed dB
−10
−12
−14
−16
−18
LP2
CE2
FLW2
H2
CE1
LP1
FLW1
H1
X20180325
X20180406
X20180418
X20180430
X20180512
X20180524
X20180605
X20180617
X20180629
X20180711
X20180723
X20180804
X20180816
X20180909
X20180921
X20181003
X20181015
X20181027
X20181108
X20181120
X20181202
X20181214
X20181226
X20190107
X20190119
X20190131
X20190212
X20190224
X20190308
X20190320
Date

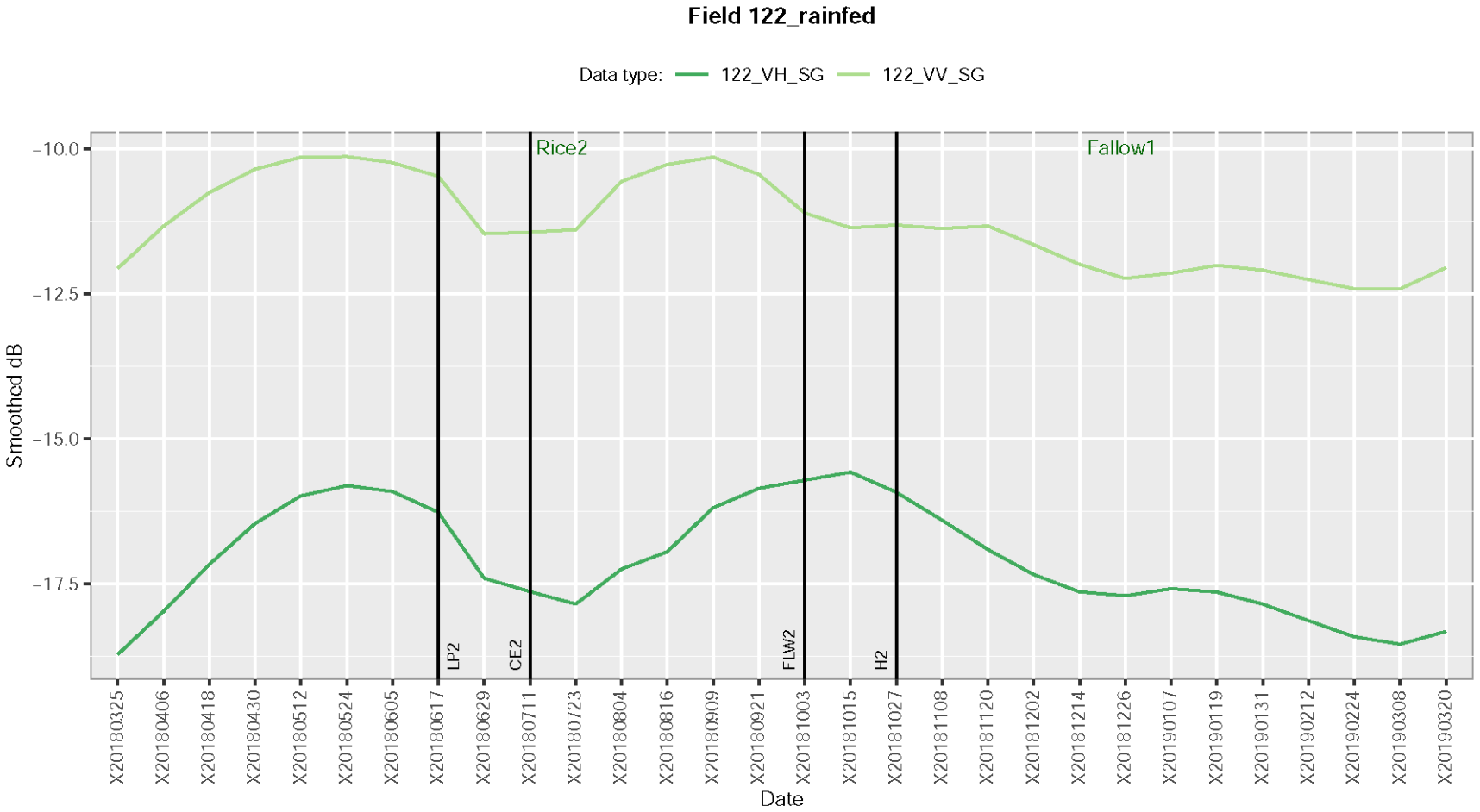
Field 122_rainfed
Data type: 122_VH_SG 122_VV_SG
Rice2
Fallow1
LP2
CE2
FLW2
H2
Smoothed dB
−10.0
−12.5
−15.0
−17.5
X20180325
X20180406
X20180418
X20180430
X20180512
X20180524
X20180605
X20180617
X20180629
X20180711
X20180723
X20180804
X20180816
X20180909
X20180921
X20181003
X20181015
X20181027
X20181108
X20181120
X20181202
X20181214
X20181226
X20190107
X20190119
X20190131
X20190212
X20190224
X20190308
X20190320
Date

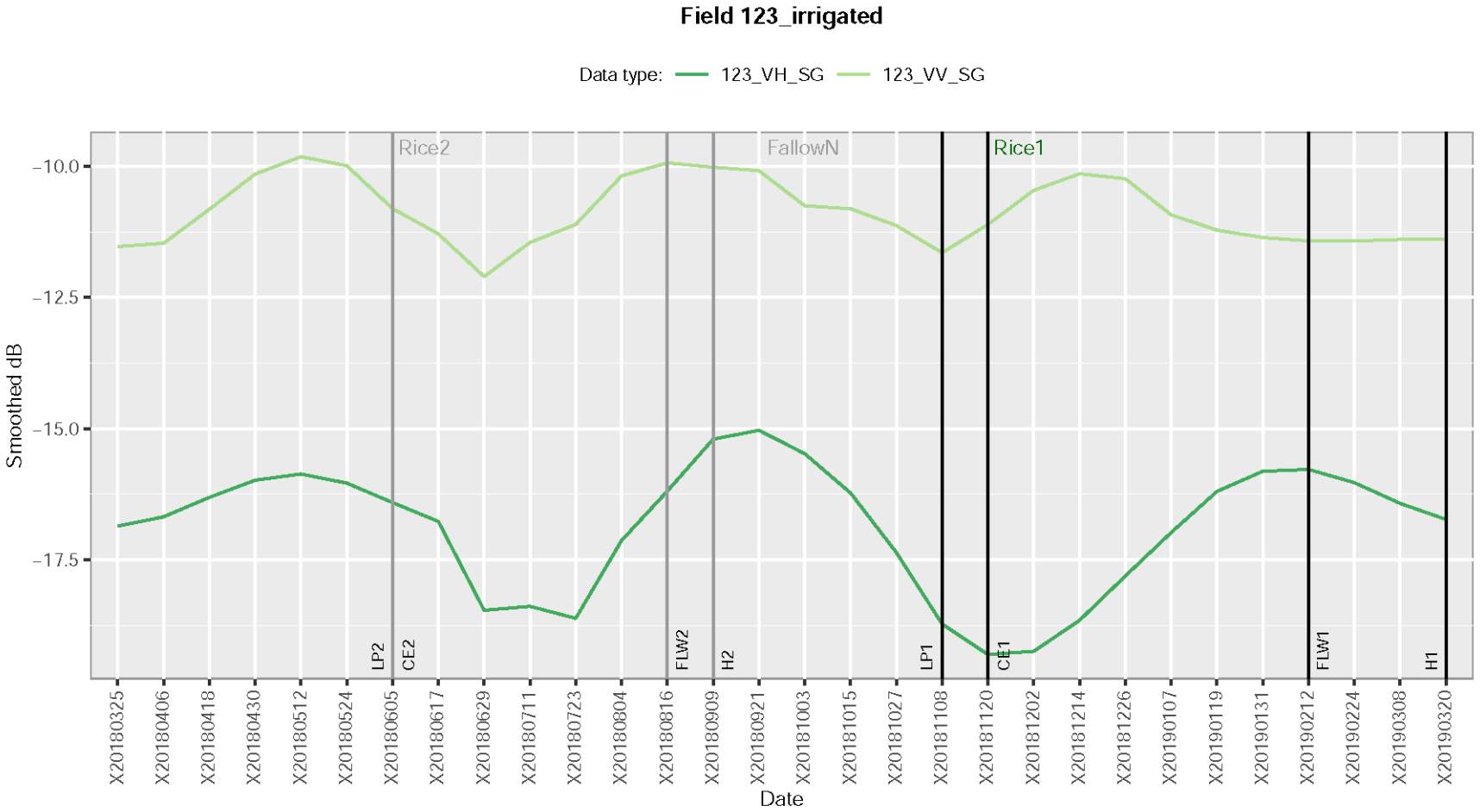
Field 123_irrigated
Data type: 123_VH_SG 123_VV_SG
Rice2
FallowN
Rice1
−10.0
−12.5
−15.0
−17.5
Smoothed dB
LP2
CE2
FLW2
H2
LP1
CE1
FLW1
H1
X20180325
X20180406
X20180418
X20180430
X20180512
X20180524
X20180605
X20180617
X20180629
X20180711
X20180723
X20180804
X20180816
X20180909
X20180921
X20181003
X20181015
X20181027
X20181108
X20181120
X20181202
X20181214
X20181226
X20190107
X20190119
X20190131
X20190212
X20190224
X20190308
X20190320
Date

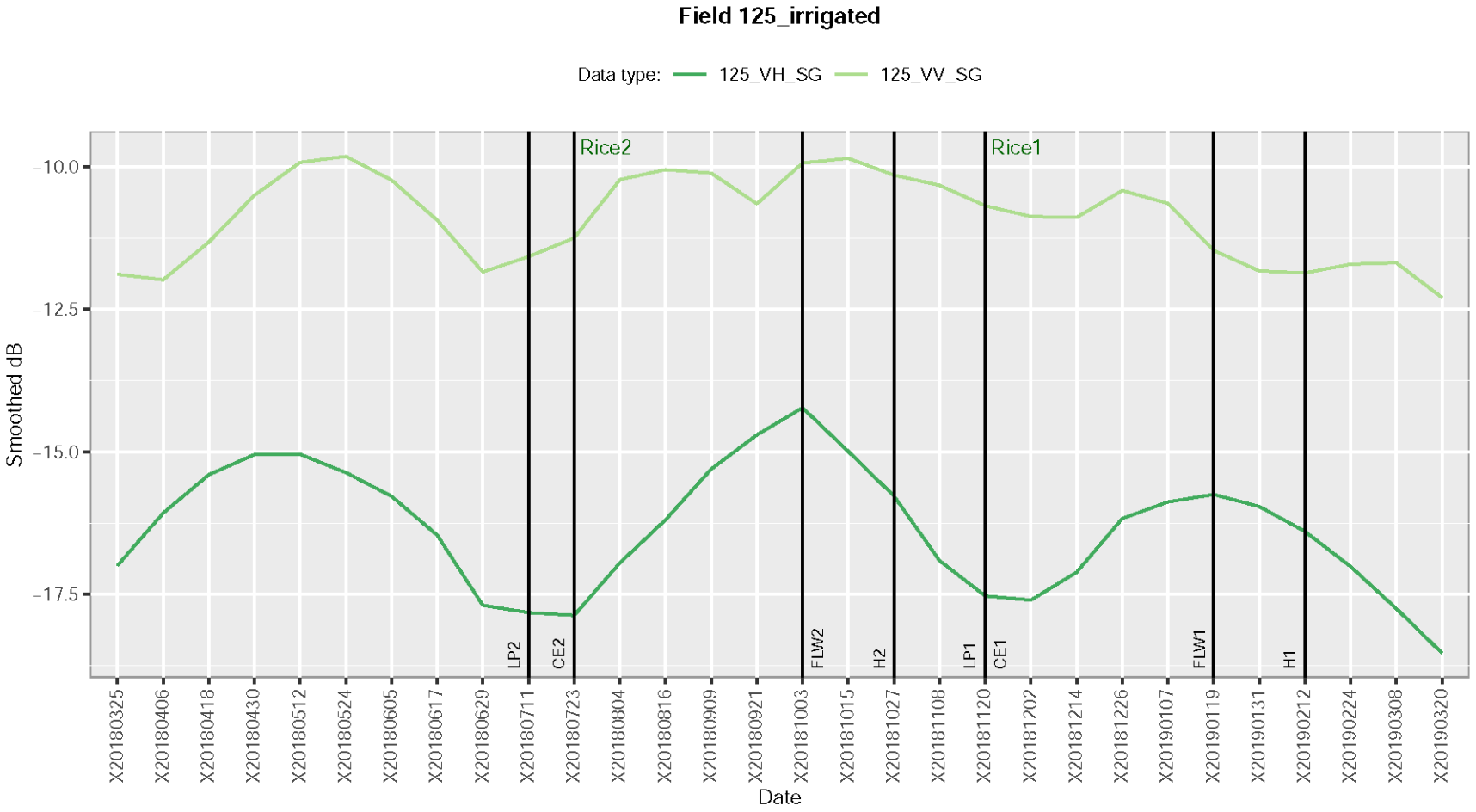
Field 125_irrigated
Data type: 125_VH_SG 125_VV_SG
Rice2
Rice1
−10.0
−12.5
−15.0
−17.5
Smoothed dB
LP2
CE2
FLW2
H2
LP1
CE1
FLW1
H1
X20180325
X20180406
X20180418
X20180430
X20180512
X20180524
X20180605
X20180617
X20180629
X20180711
X20180723
X20180804
X20180816
X20180909
X20180921
X20181003
X20181015
X20181027
X20181108
X20181120
X20181202
X20181214
X20181226
X20190107
X20190119
X20190131
X20190212
X20190224
X20190308
X20190320
Date

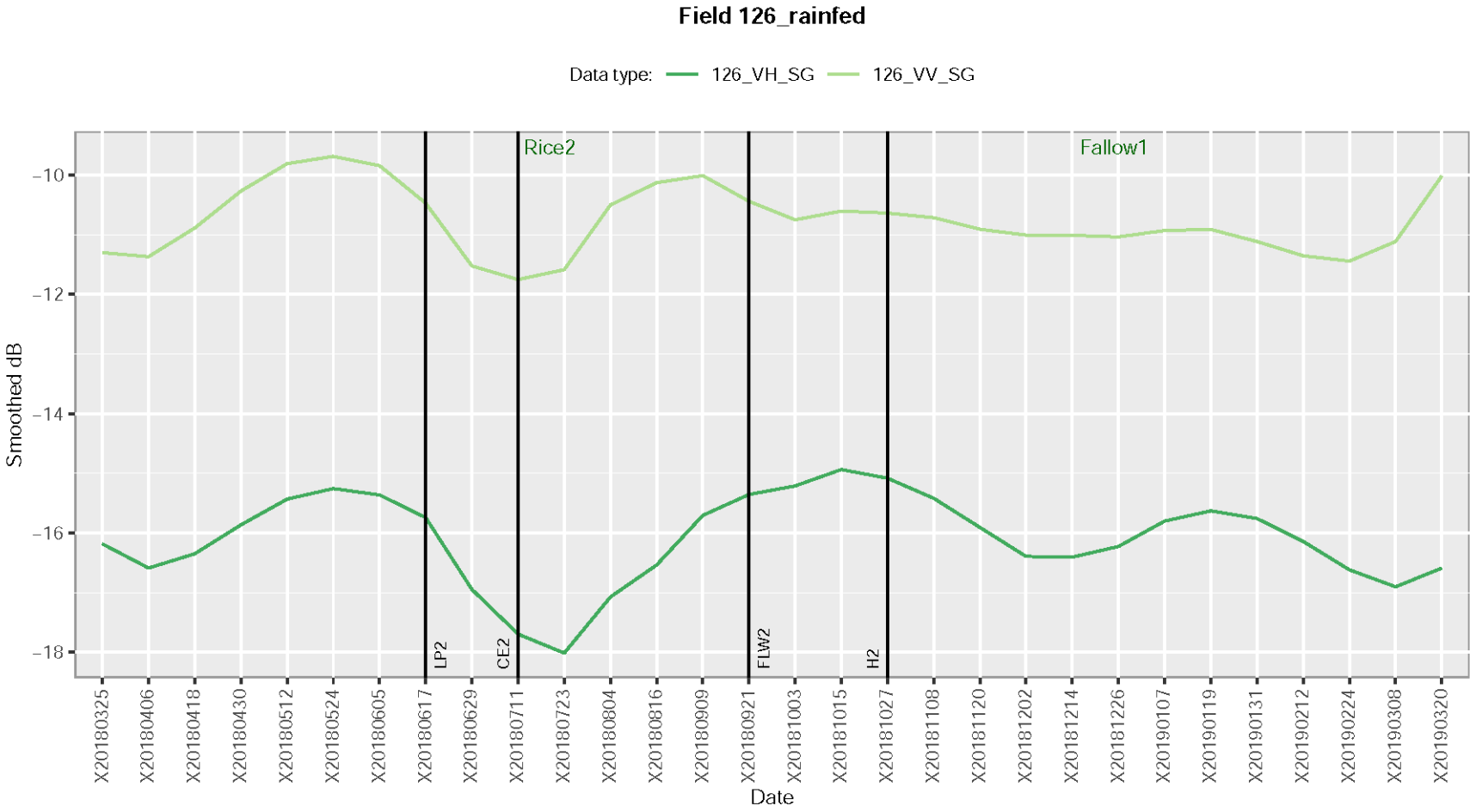
Field 126_rainfed
Data type: 126_VH_SG 126_VV_SG
Rice2
Fallow1
LP2
CE2
FLW2
H2
Smoothed dB
−10
−12
−14
−16
−18
X20180325
X20180406
X20180418
X20180430
X20180512
X20180524
X20180605
X20180617
X20180629
X20180711
X20180723
X20180804
X20180816
X20180909
X20180921
X20181003
X20181015
X20181027
X20181108
X20181120
X20181202
X20181214
X20181226
X20190107
X20190119
X20190131
X20190212
X20190224
X20190308
X20190320
Date

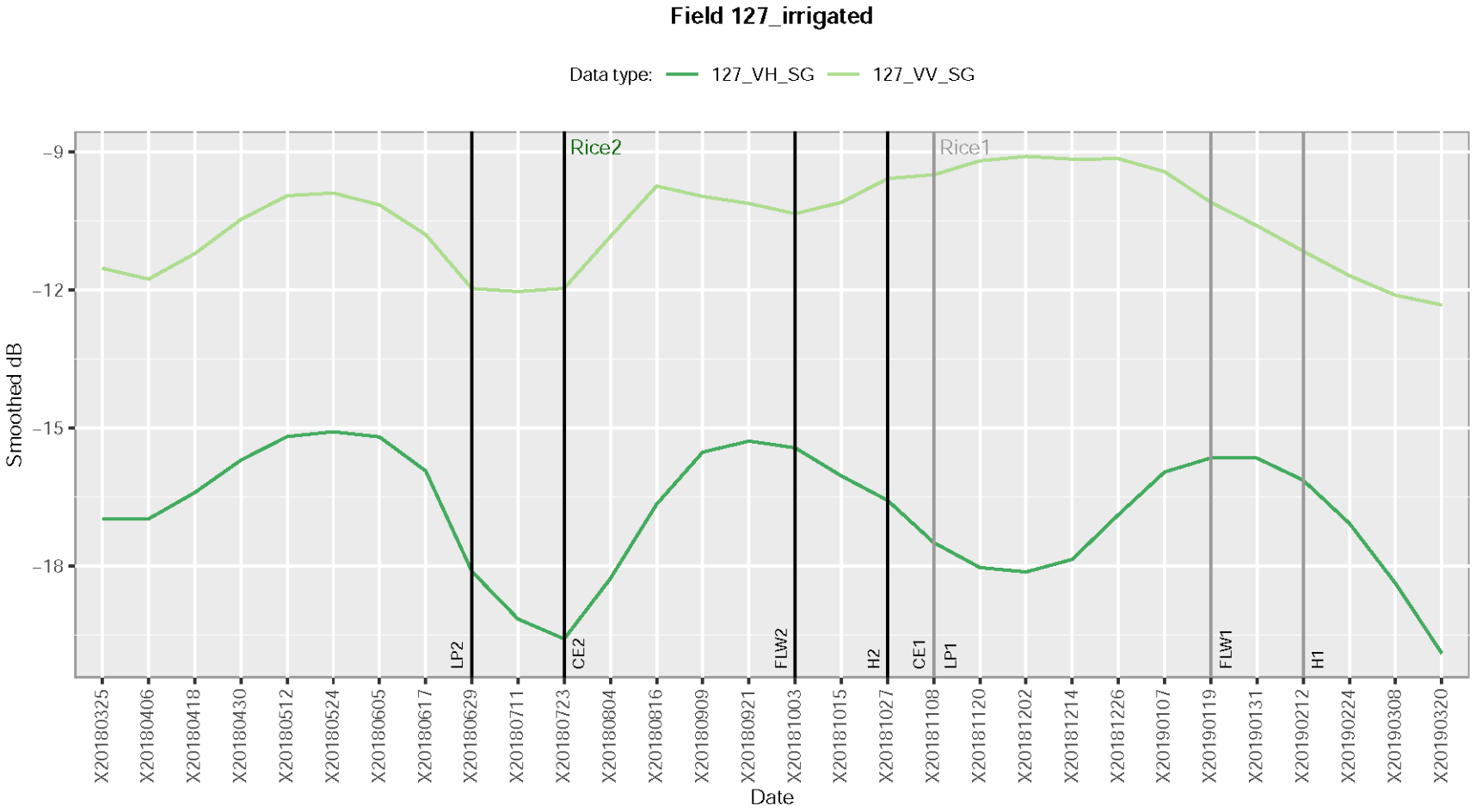
Field 127_irrigated
Data type: 127_VH_SG 127_VV_SG
Rice2
Rice1
−9
−12
−15
−18
Smoothed dB
LP2
CE2
FLW2
H2
CE1
LP1
FLW1
H1
X20180325
X20180406
X20180418
X20180430
X20180512
X20180524
X20180605
X20180617
X20180629
X20180711
X20180723
X20180804
X20180816
X20180909
X20180921
X20181003
X20181015
X20181027
X20181108
X20181120
X20181202
X20181214
X20181226
X20190107
X20190119
X20190131
X20190212
X20190224
X20190308
X20190320
Date

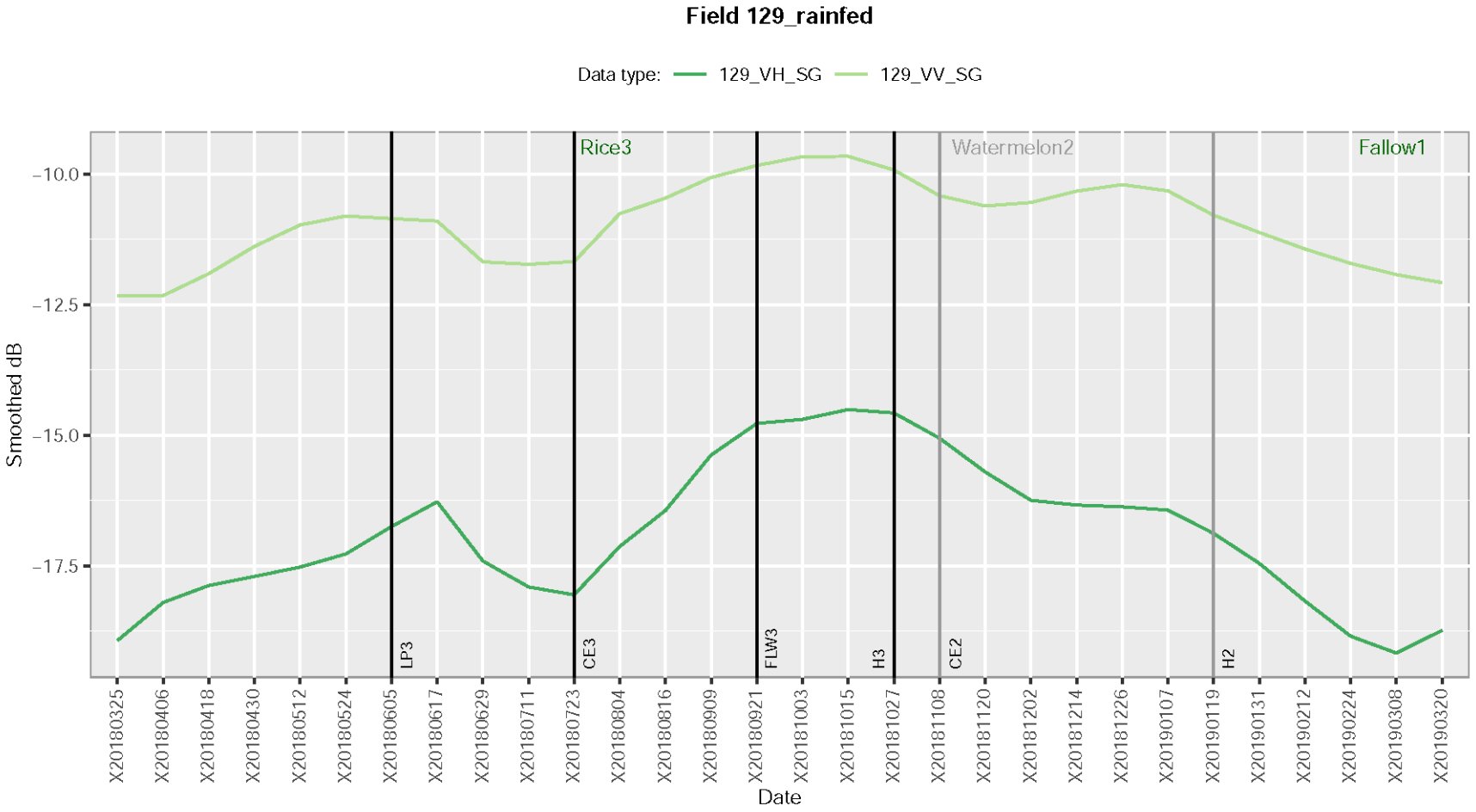
Field 129_rainfed
Data type: 129_VH_SG 129_VV_SG
Rice3
Watermelon2
Fallow1
−10.0
−12.5
−15.0
−17.5
Smoothed dB
LP3
CE3
FLW3
H3
CE2
H2
X20180325
X20180406
X20180418
X20180430
X20180512
X20180524
X20180605
X20180617
X20180629
X20180711
X20180723
X20180804
X20180816
X20180909
X20180921
X20181003
X20181015
X20181027
X20181108
X20181120
X20181202
X20181214
X20181226
X20190107
X20190119
X20190131
X20190212
X20190224
X20190308
X20190320
Date

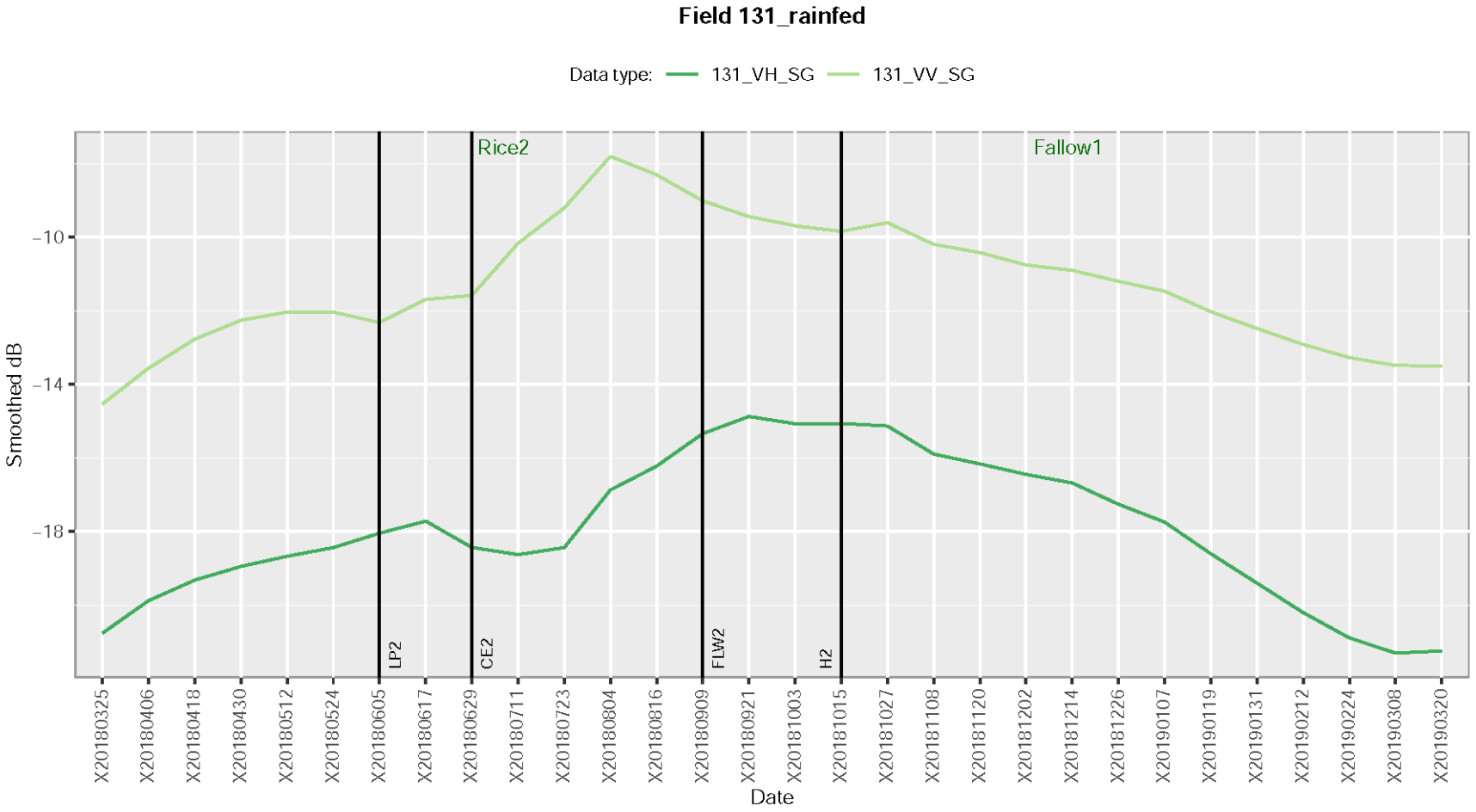
Field 131_rainfed
Data type: 131_VH_SG 131_VV_SG
Rice2
Fallow1
LP2
CE2
FLW2
H2
Smoothed dB
-10
-14
-18
X20180325
X20180406
X20180418
X20180430
X20180512
X20180524
X20180605
X20180617
X20180629
X20180711
X20180723
X20180804
X20180816
X20180909
X20180921
X20181003
X20181015
X20181027
X20181108
X20181120
X20181202
X20181214
X20181226
X20190107
X20190119
X20190131
X20190212
X20190224
X20190308
X20190320
Date

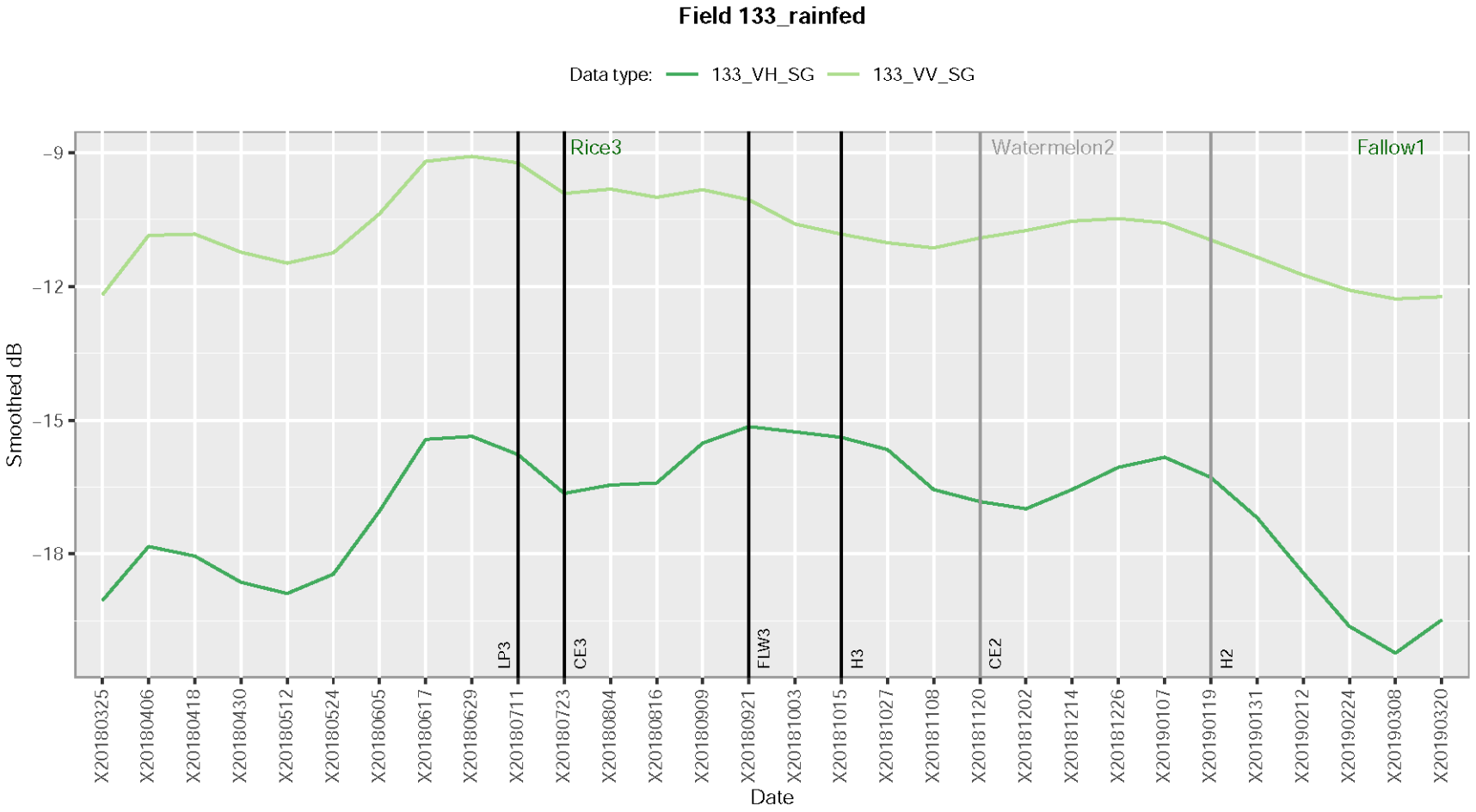
Field 133_rainfed
Data type: 133_VH_SG 133_VV_SG
Rice3
Watermelon2
Fallow1
LP3
CE3
FLW3
H3
CE2
H2
Smoothed dB
-9
-12
-15
-18
X20180325
X20180406
X20180418
X20180430
X20180512
X20180524
X20180605
X20180617
X20180629
X20180711
X20180723
X20180804
X20180816
X20180909
X20180921
X20181003
X20181015
X20181027
X20181108
X20181120
X20181202
X20181214
X20181226
X20190107
X20190119
X20190131
X20190212
X20190224
X20190308
X20190320
Date

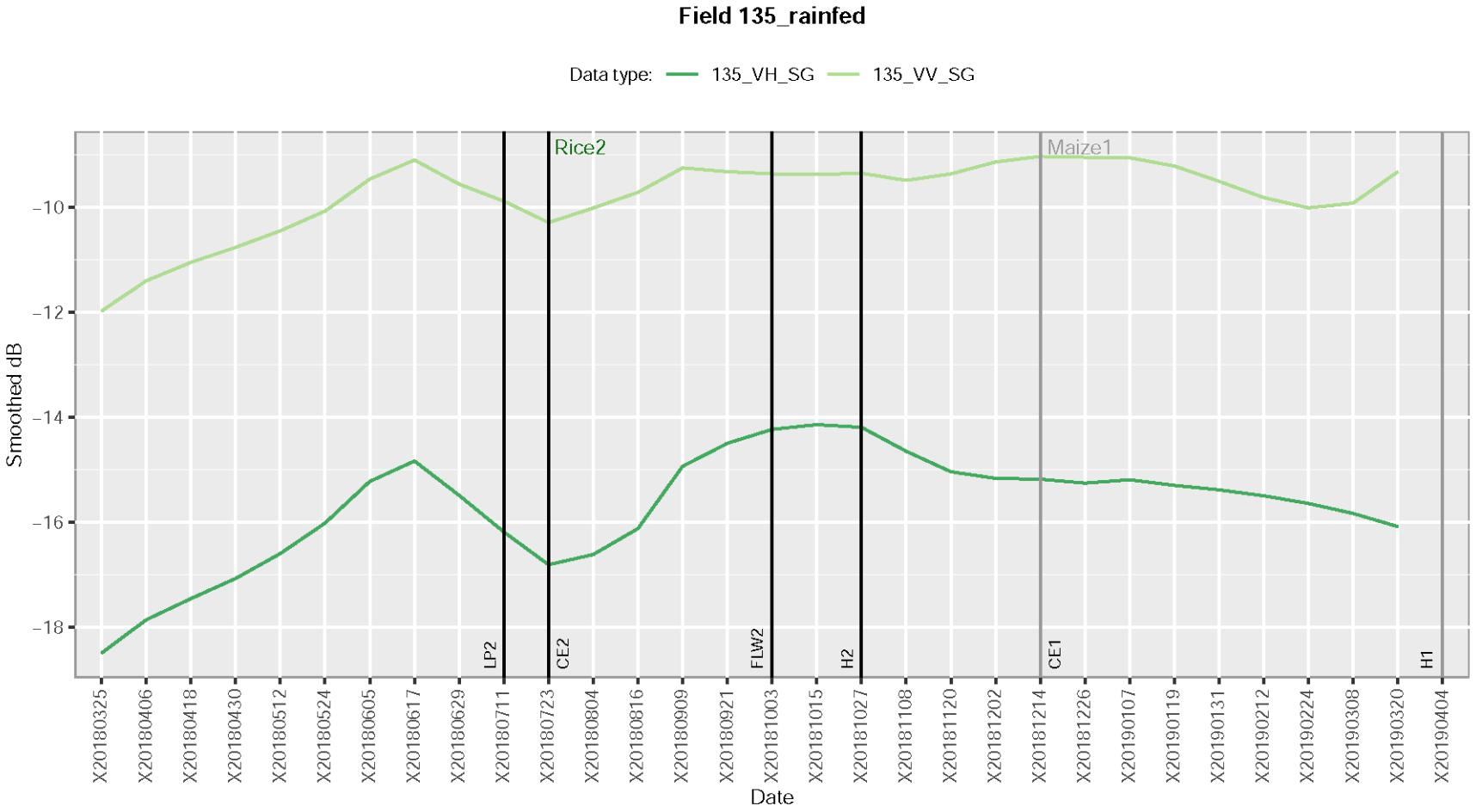
Field 135_rainfed
Data type: 135_VH_SG 135_VV_SG
Rice2
Maize1
LP2
CE2
FLW2
H2
CE1
H1
Smoothed dB
−10
−12
−14
−16
−18
X20180325
X20180406
X20180418
X20180430
X20180512
X20180524
X20180605
X20180617
X20180629
X20180711
X20180723
X20180804
X20180816
X20180909
X20180921
X20181003
X20181015
X20181027
X20181108
X20181120
X20181202
X20181214
X20181226
X20190107
X20190119
X20190131
X20190212
X20190224
X20190308
X20190320
X20190404
Date

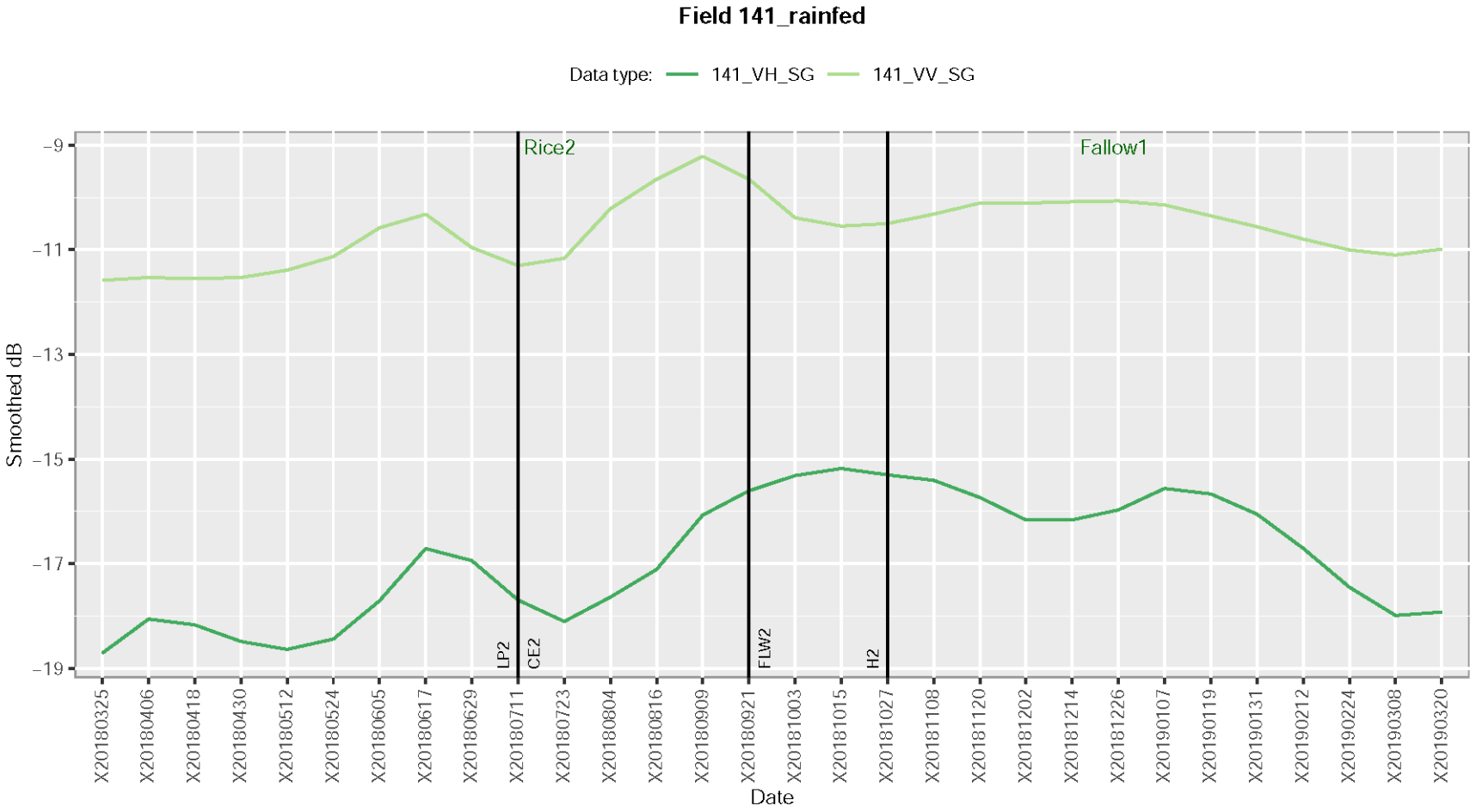
Field 141_rainfed
Data type: 141_VH_SG 141_VV_SG
Rice2
Fallow1
LP2
CE2
FLW2
H2
Smoothed dB
−9
−11
−13
−15
−17
−19
X20180325
X20180406
X20180418
X20180430
X20180512
X20180524
X20180605
X20180617
X20180629
X20180711
X20180723
X20180804
X20180816
X20180909
X20180921
X20181003
X20181015
X20181027
X20181108
X20181120
X20181202
X20181214
X20181226
X20190107
X20190119
X20190131
X20190212
X20190224
X20190308
X20190320
Date

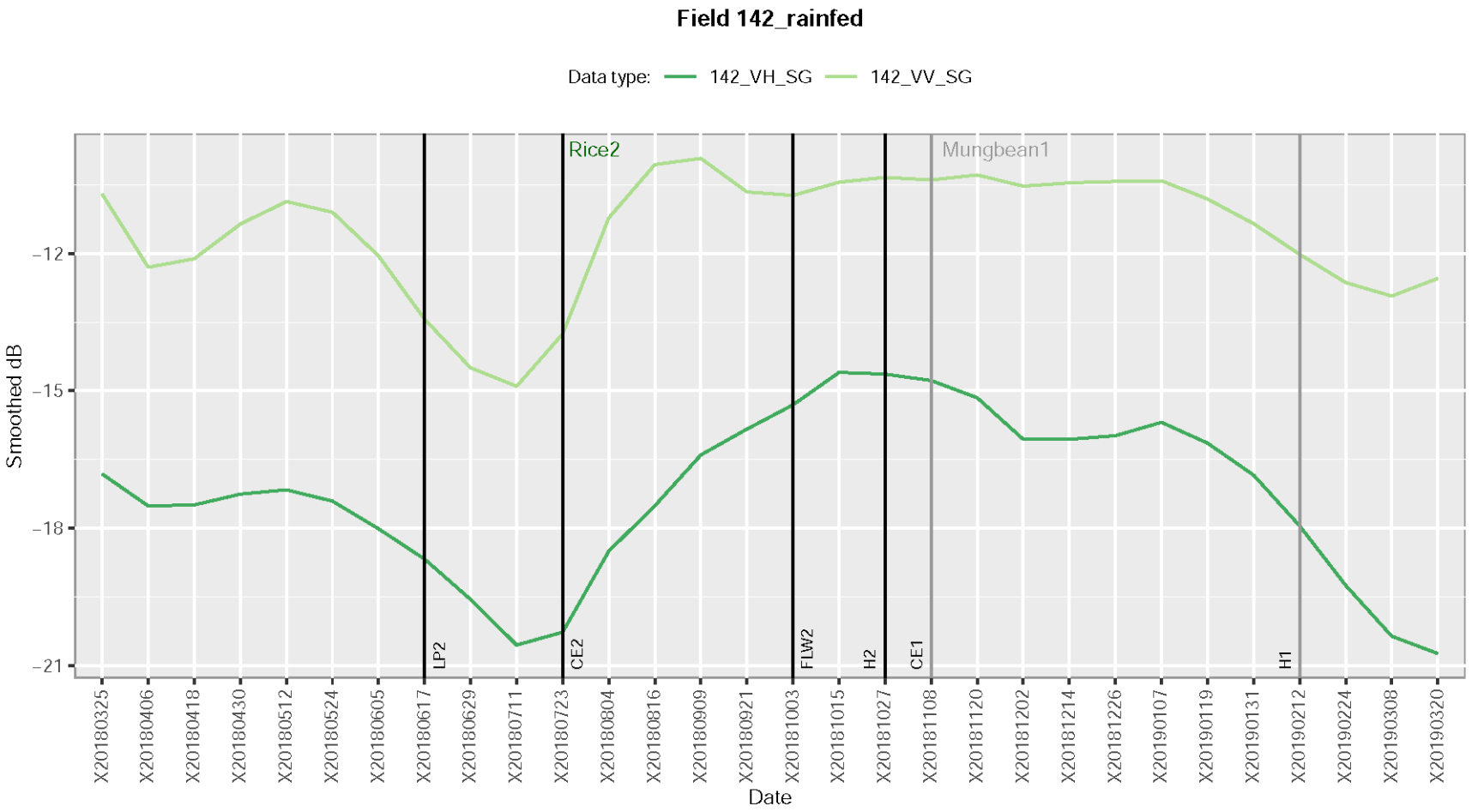
Field 142_rainfed
Data type: 142_VH_SG 142_VV_SG
Rice2
Mungbean1
LP2
CE2
FLW2
H2
CE1
H1
Smoothed dB
-12
-15
-18
-21
X20180325
X20180406
X20180418
X20180430
X20180512
X20180524
X20180605
X20180617
X20180629
X20180711
X20180723
X20180804
X20180816
X20180909
X20180921
X20181003
X20181015
X20181027
X20181108
X20181120
X20181202
X20181214
X20181226
X20190107
X20190119
X20190131
X20190212
X20190224
X20190308
X20190320
Date

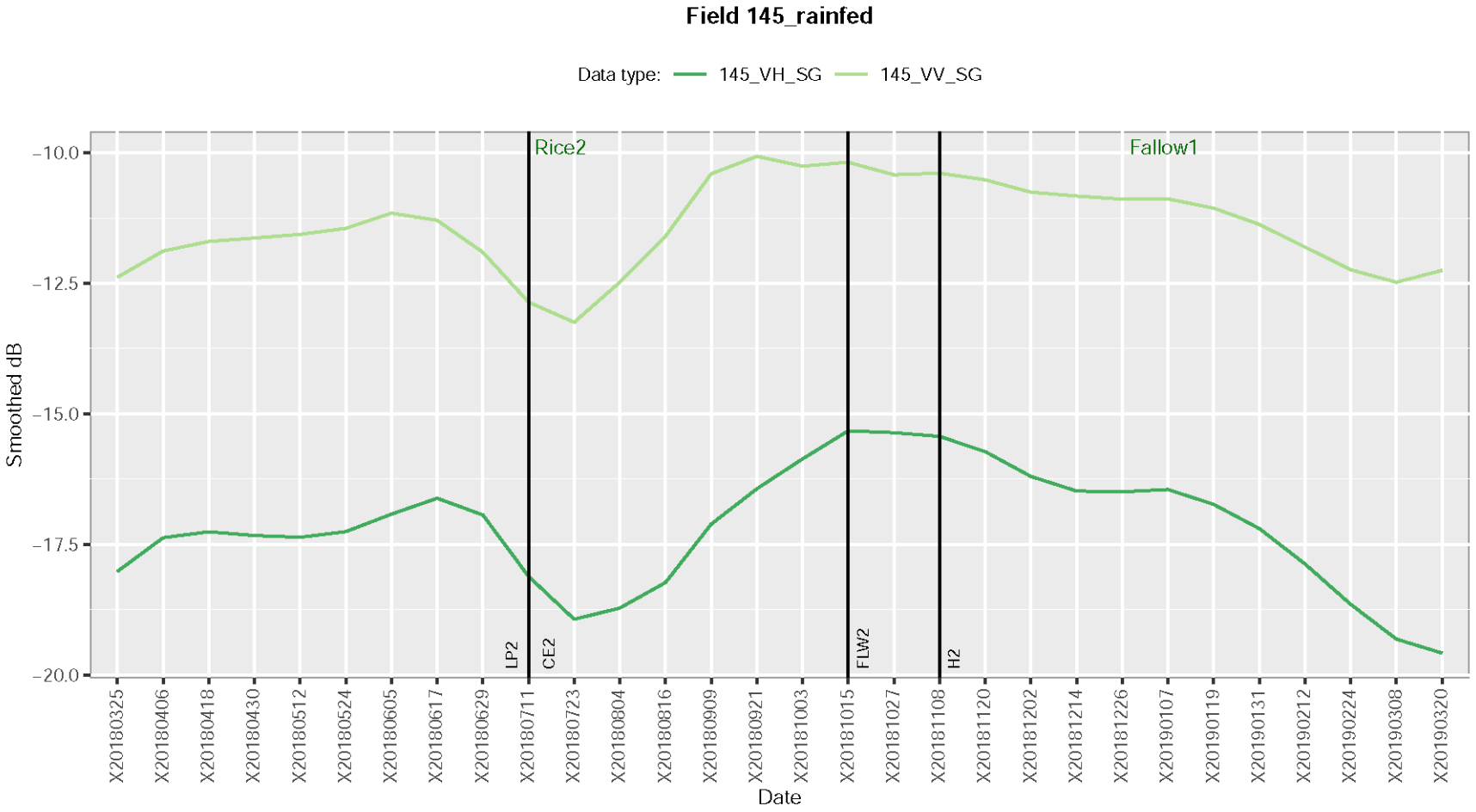
Field 145_rainfed
Data type: 145_VH_SG 145_VV_SG
Rice2
Fallow1
LP2
CE2
FLW2
H2
Smoothed dB
−10.0
−12.5
−15.0
−17.5
−20.0
X20180325
X20180406
X20180418
X20180430
X20180512
X20180524
X20180605
X20180617
X20180629
X20180711
X20180723
X20180804
X20180816
X20180909
X20180921
X20181003
X20181015
X20181027
X20181108
X20181120
X20181202
X20181214
X20181226
X20190107
X20190119
X20190131
X20190212
X20190224
X20190308
X20190320
Date

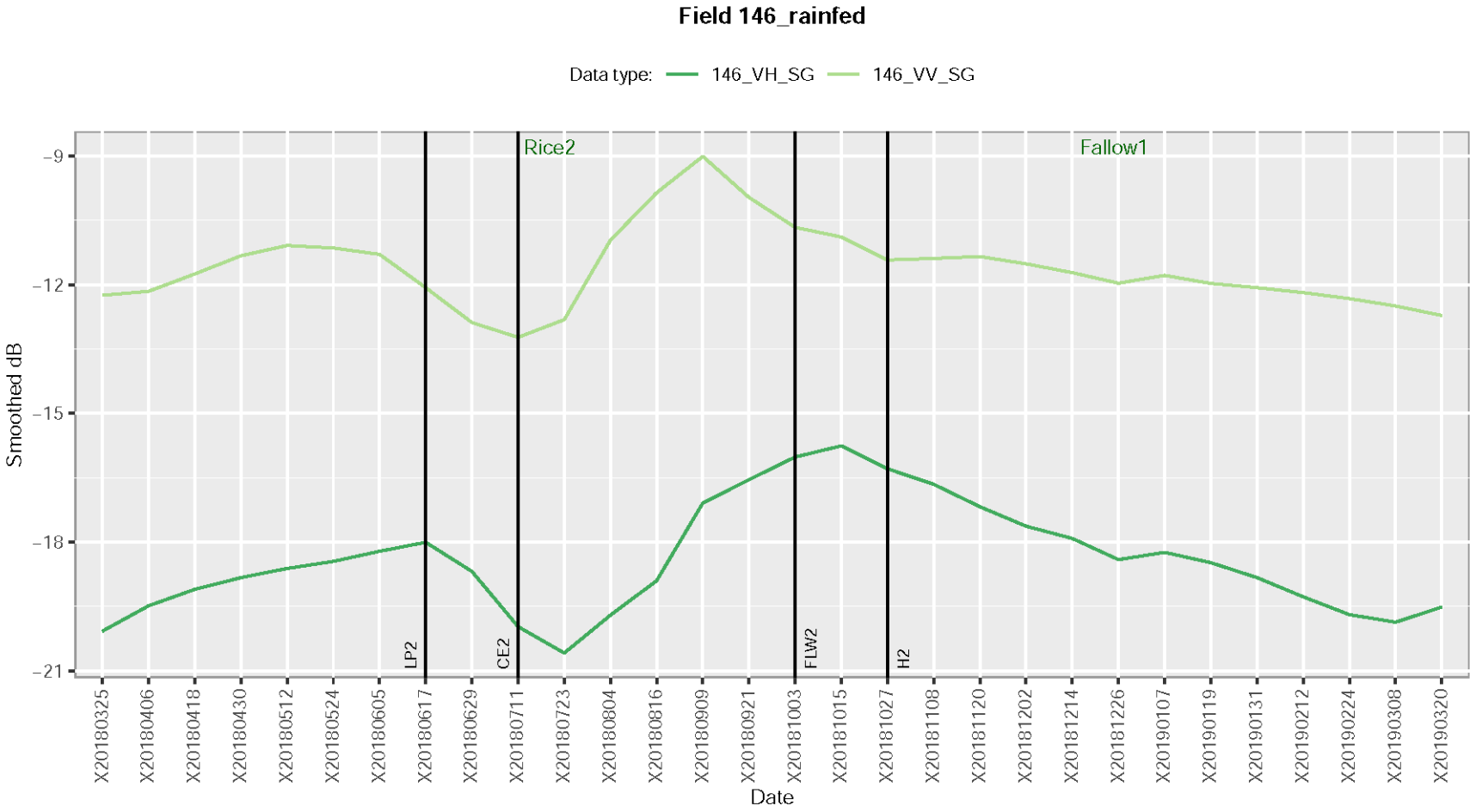
Field 146_rainfed
Data type: 146_VH_SG 146_VV_SG
Rice2
Fallow1
LP2
CE2
FLW2
H2
Smoothed dB
−9
−12
−15
−18
−21
X20180325
X20180406
X20180418
X20180430
X20180512
X20180524
X20180605
X20180617
X20180629
X20180711
X20180723
X20180804
X20180816
X20180909
X20180921
X20181003
X20181015
X20181027
X20181108
X20181120
X20181202
X20181214
X20181226
X20190107
X20190119
X20190131
X20190212
X20190224
X20190308
X20190320
Date

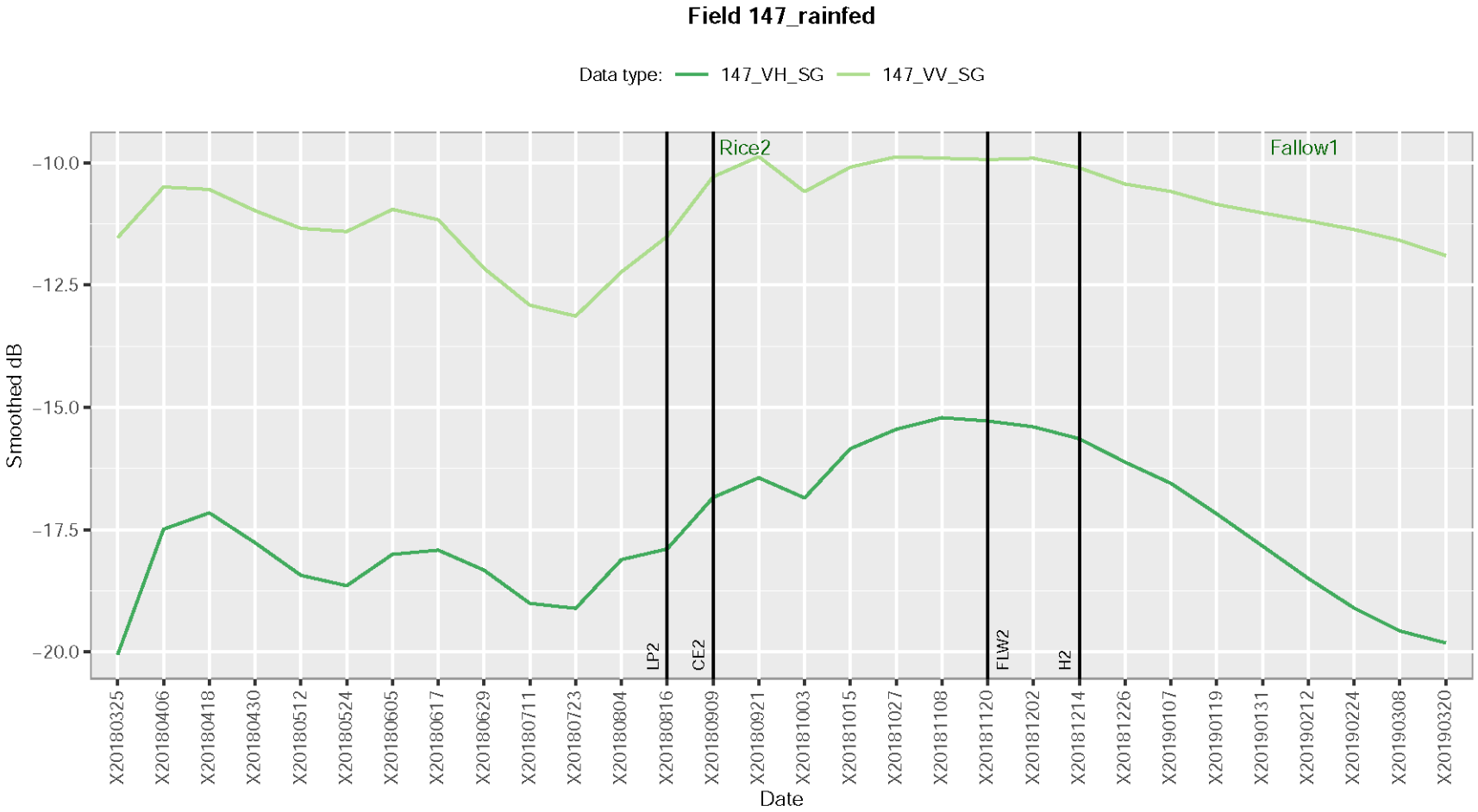
Field 147_rainfed
Data type: 147_VH_SG 147_VV_SG
Rice2
Fallow1
LP2
CE2
FLW2
H2
Smoothed dB
−10.0
−12.5
−15.0
−17.5
−20.0
X20180325
X20180406
X20180418
X20180430
X20180512
X20180524
X20180605
X20180617
X20180629
X20180711
X20180723
X20180804
X20180816
X20180909
X20180921
X20181003
X20181015
X20181027
X20181108
X20181120
X20181202
X20181214
X20181226
X20190107
X20190119
X20190131
X20190212
X20190224
X20190308
X20190320
Date

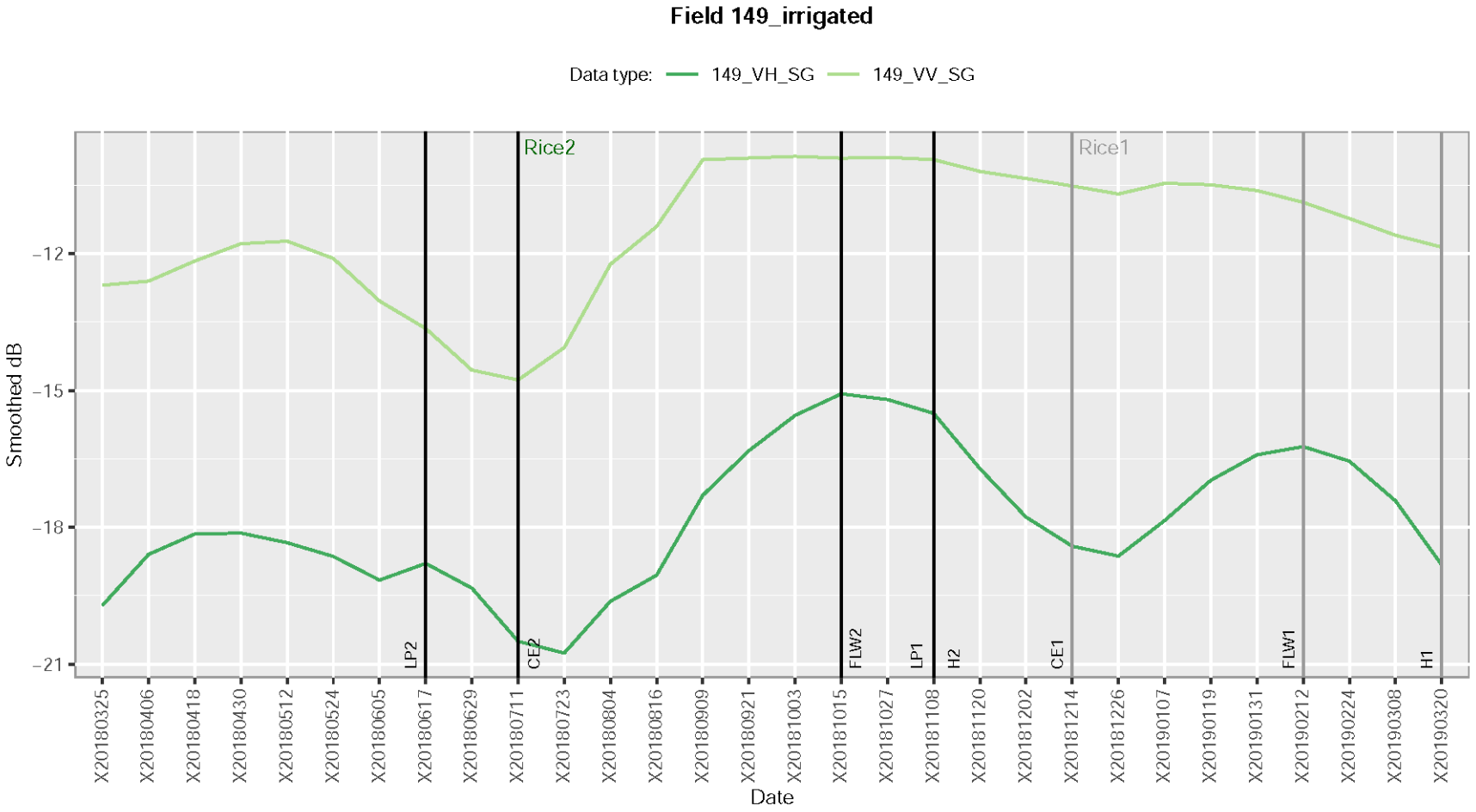
Field 149_irrigated
Data type: 149_VH_SG 149_VV_SG
Rice2
Rice1
Smoothed dB
−12
−15
−18
−21
LP2
CE2
FLW2
LP1
H2
CE1
FLW1
H1
X20180325
X20180406
X20180418
X20180430
X20180512
X20180524
X20180605
X20180617
X20180629
X20180711
X20180723
X20180804
X20180816
X20180909
X20180921
X20181003
X20181015
X20181027
X20181108
X20181120
X20181202
X20181214
X20181226
X20190107
X20190119
X20190131
X20190212
X20190224
X20190308
X20190320
Date

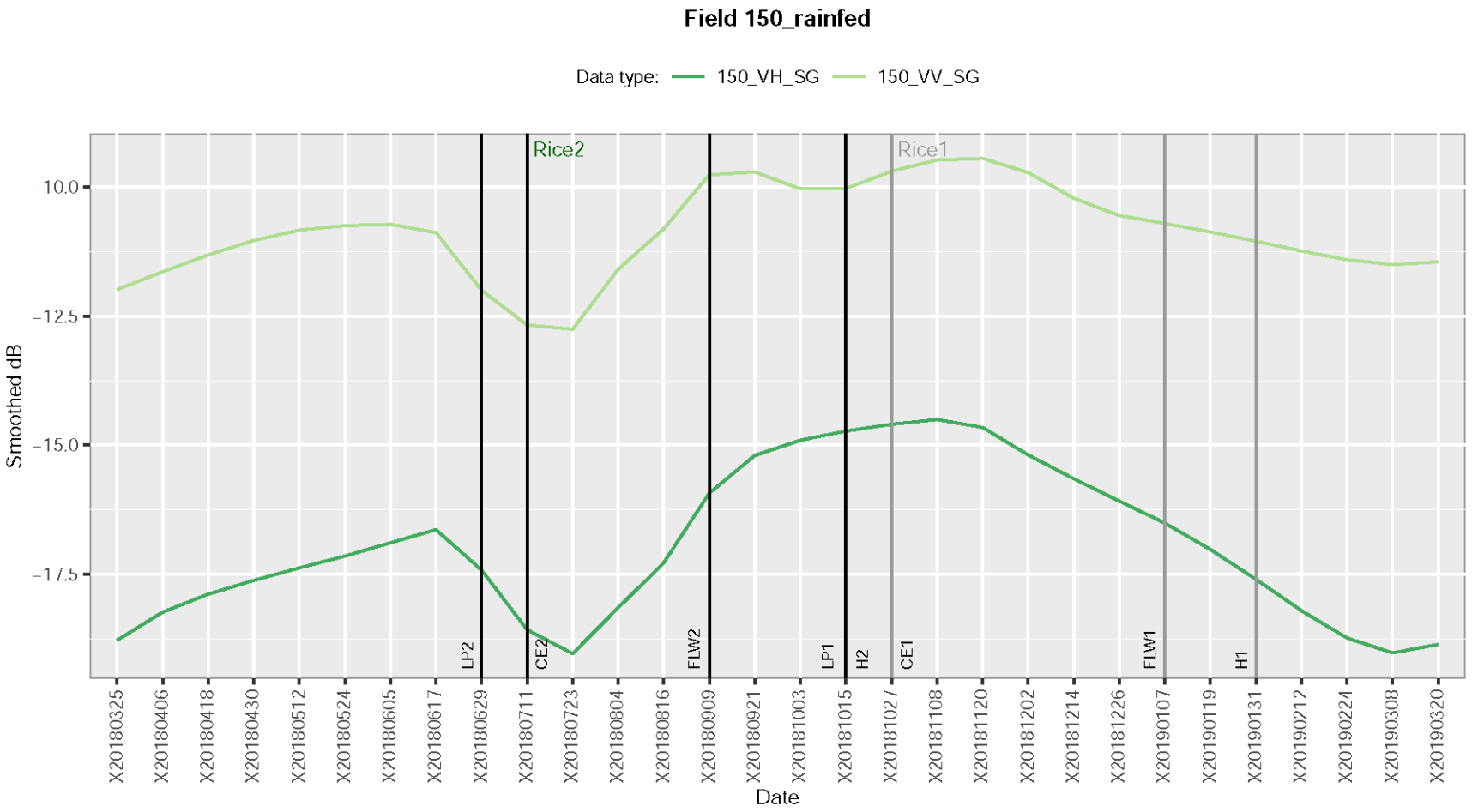
Field 150_rainfed
Data type: 150_VH_SG 150_VV_SG
Rice2
Rice1
−10.0
−12.5
−15.0
−17.5
Smoothed dB
LP2
CE2
FLW2
LP1
H2
CE1
FLW1
H1
X20180325
X20180406
X20180418
X20180430
X20180512
X20180524
X20180605
X20180617
X20180629
X20180711
X20180723
X20180804
X20180816
X20180909
X20180921
X20181003
X20181015
X20181027
X20181108
X20181120
X20181202
X20181214
X20181226
X20190107
X20190119
X20190131
X20190212
X20190224
X20190308
X20190320
Date

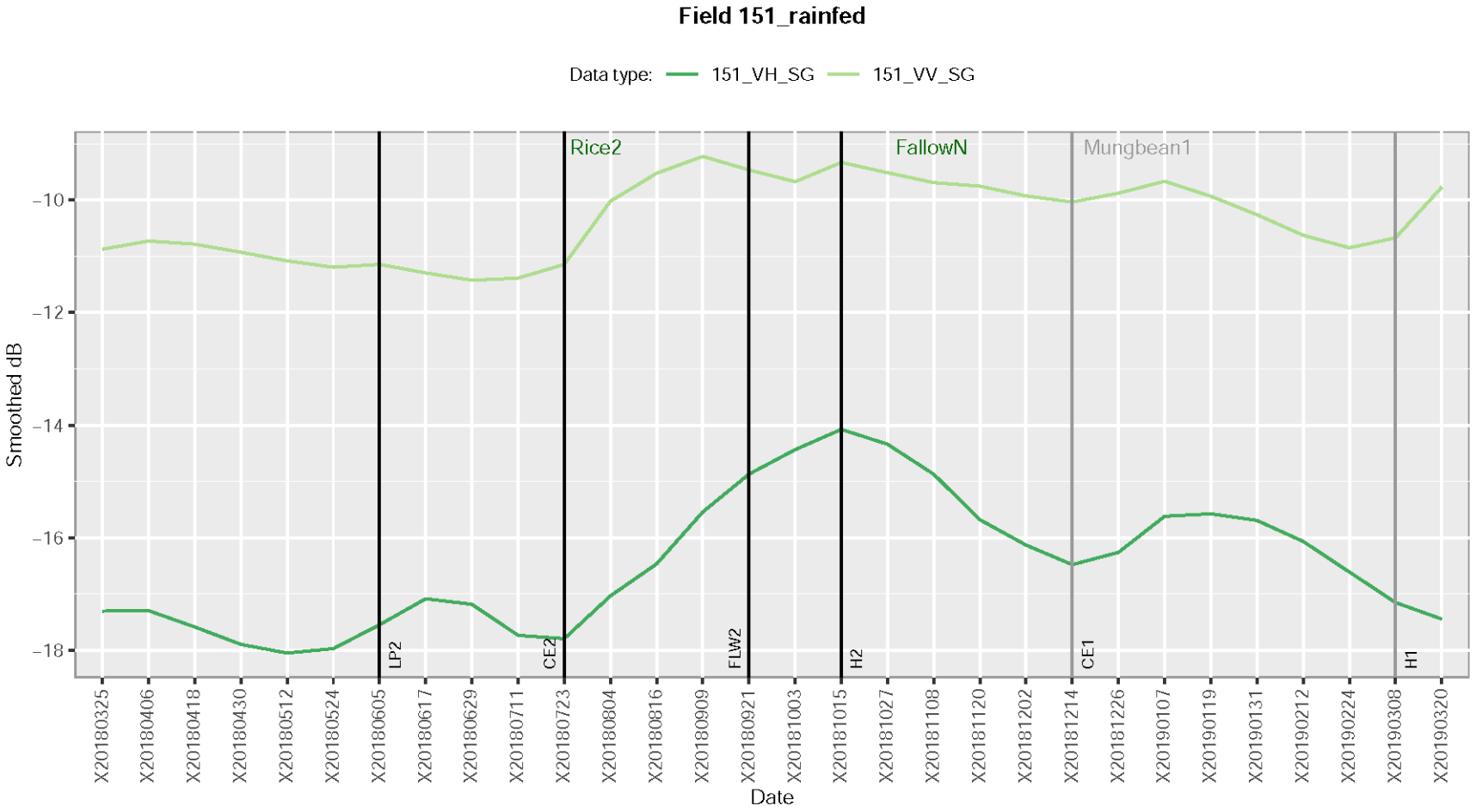
Field 151_rainfed
Data type: 151_VH_SG 151_VV_SG
Rice2
FallowN
Mungbean1
LP2
CE2
FLW2
H2
CE1
H1
Smoothed dB
−10
−12
−14
−16
−18
X20180325
X20180406
X20180418
X20180430
X20180512
X20180524
X20180605
X20180617
X20180629
X20180711
X20180723
X20180804
X20180816
X20180909
X20180921
X20181003
X20181015
X20181027
X20181108
X20181120
X20181202
X20181214
X20181226
X20190107
X20190119
X20190131
X20190212
X20190224
X20190308
X20190320
Date

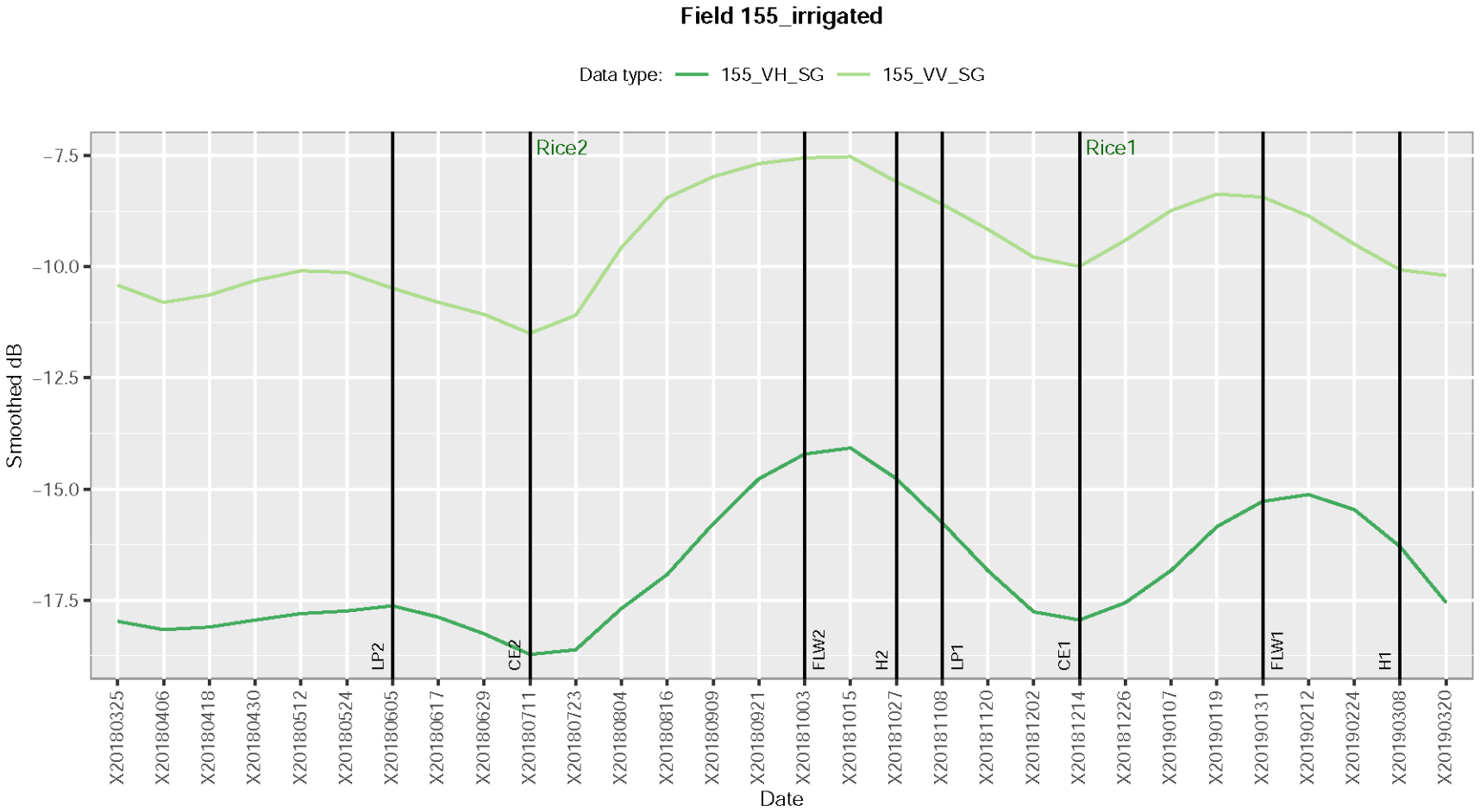
Field 155_irrigated
Data type: 155_VH_SG 155_VV_SG
Rice2
Rice1
Smoothed dB
−7.5
−10.0
−12.5
−15.0
−17.5
LP2
CE2
FLW2
H2
LP1
CE1
FLW1
H1
X20180325
X20180406
X20180418
X20180430
X20180512
X20180524
X20180605
X20180617
X20180629
X20180711
X20180723
X20180804
X20180816
X20180909
X20180921
X20181003
X20181015
X20181027
X20181108
X20181120
X20181202
X20181214
X20181226
X20190107
X20190119
X20190131
X20190212
X20190224
X20190308
X20190320
Date

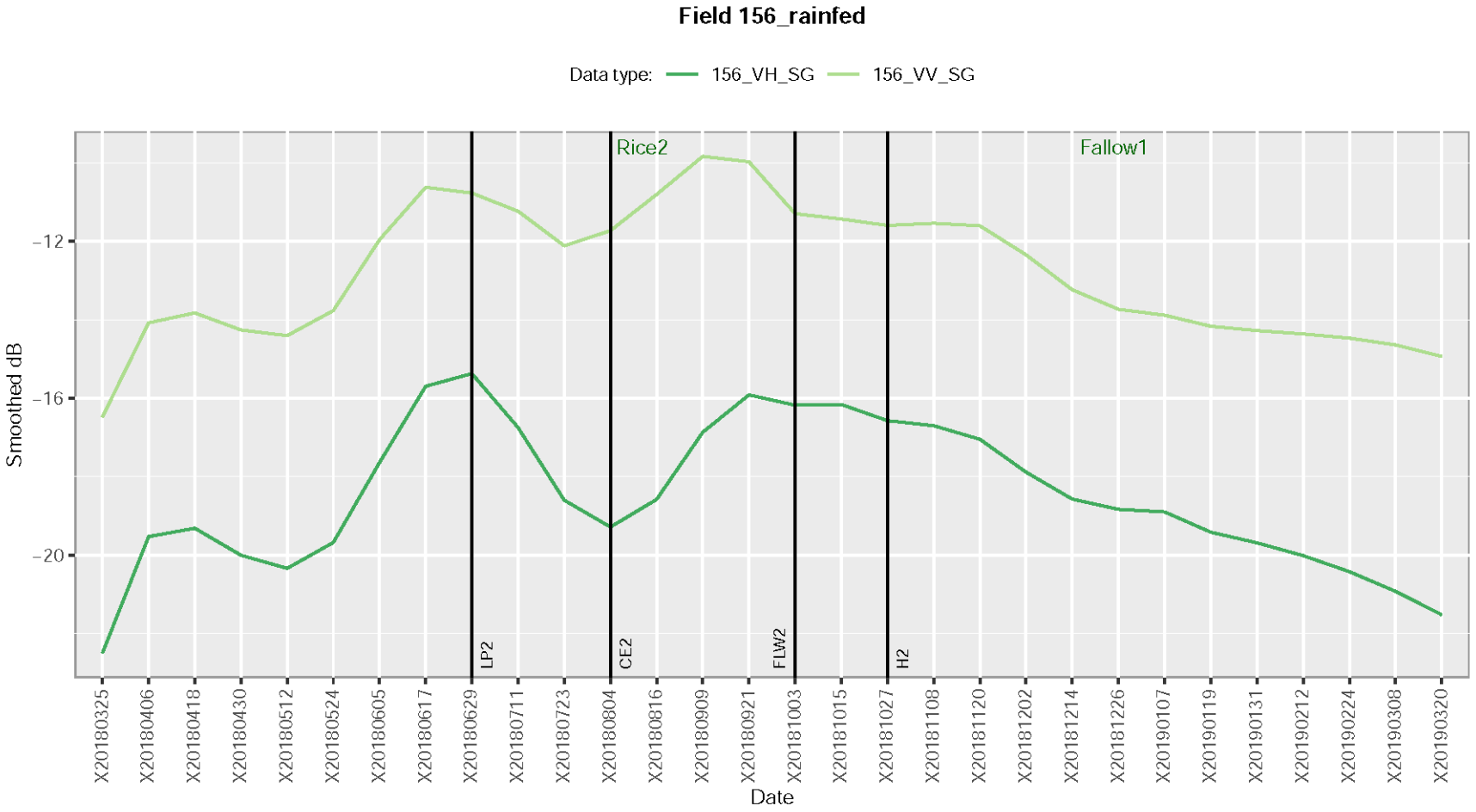
Field 156_rainfed
Data type: 156_VH_SG 156_VV_SG
Rice2
Fallow1
LP2
CE2
FLW2
H2
Smoothed dB
-12
-16
-20
X20180325
X20180406
X20180418
X20180430
X20180512
X20180524
X20180605
X20180617
X20180629
X20180711
X20180723
X20180804
X20180816
X20180909
X20180921
X20181003
X20181015
X20181027
X20181108
X20181120
X20181202
X20181214
X20181226
X20190107
X20190119
X20190131
X20190212
X20190224
X20190308
X20190320
Date

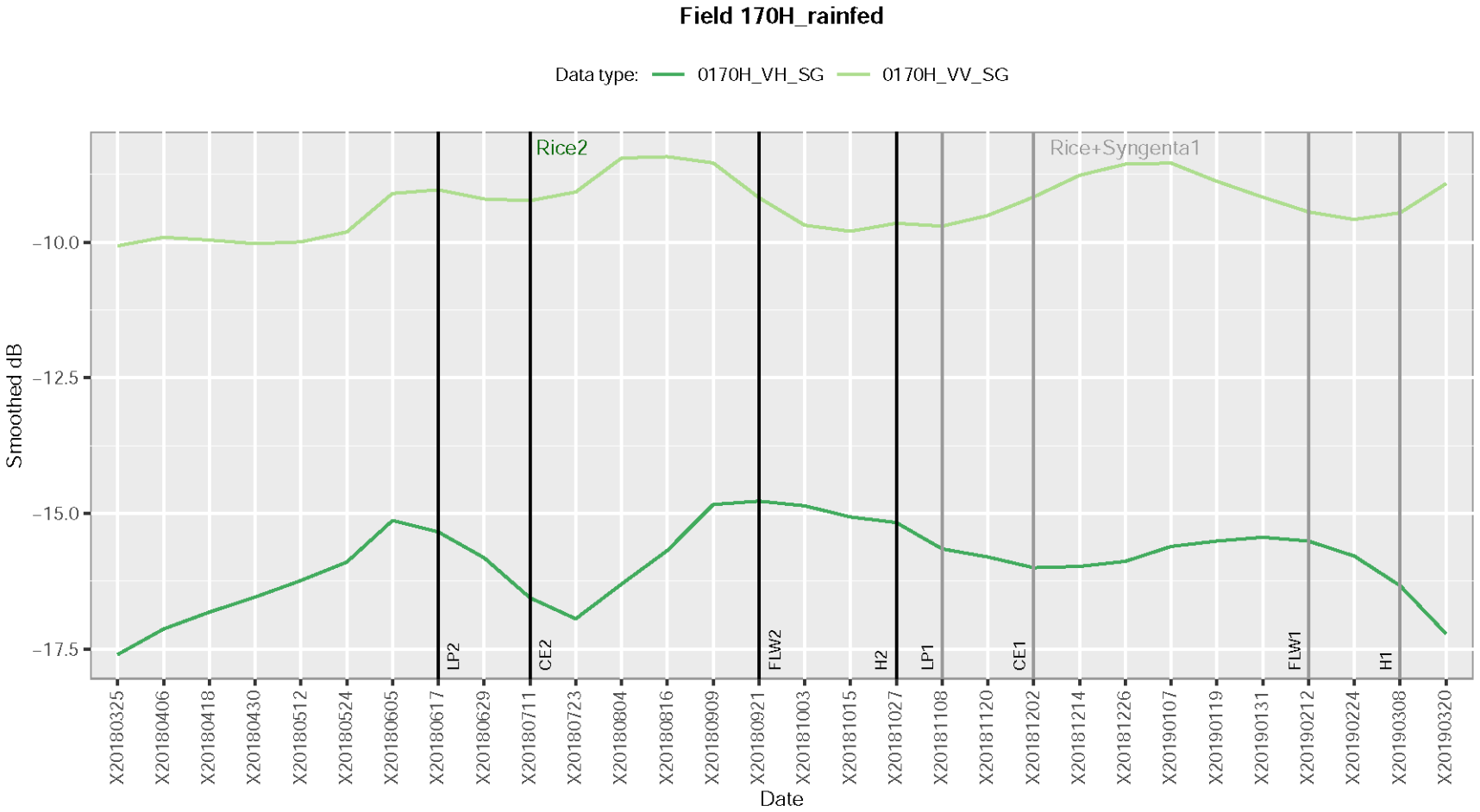
Field 170H_rainfed
Data type: 0170H_VH_SG 0170H_VV_SG
Rice2
Rice+Syngenta1
Smoothed dB
−10.0
−12.5
−15.0
−17.5
LP2
CE2
FLW2
H2
LP1
CE1
FLW1
H1
X20180325
X20180406
X20180418
X20180430
X20180512
X20180524
X20180605
X20180617
X20180629
X20180711
X20180723
X20180804
X20180816
X20180909
X20180921
X20181003
X20181015
X20181027
X20181108
X20181120
X20181202
X20181214
X20181226
X20190107
X20190119
X20190131
X20190212
X20190224
X20190308
X20190320
Date

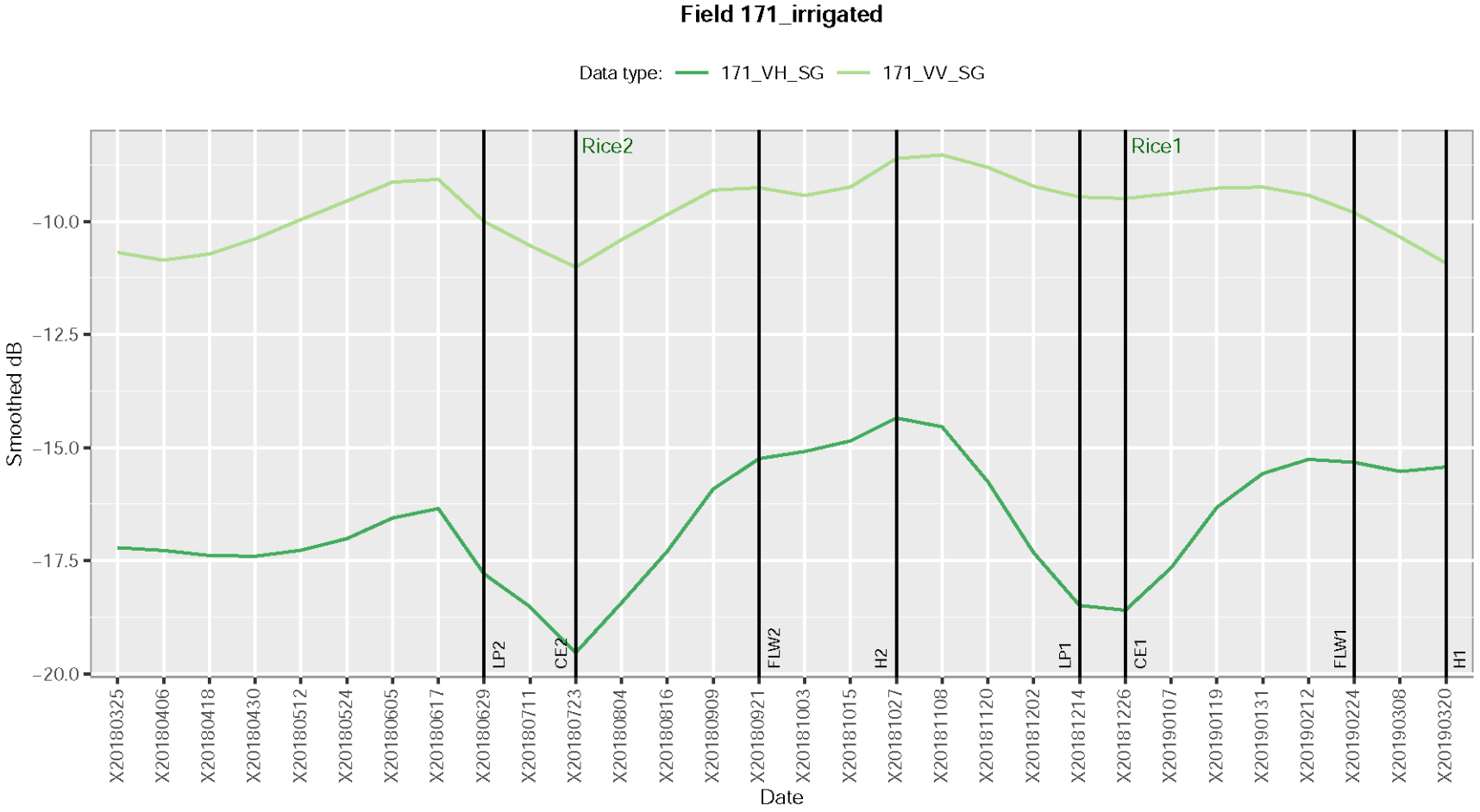
Field 171_irrigated
Data type: 171_VH_SG 171_VV_SG
Rice2
Rice1
LP2
CE2
FLW2
H2
LP1
CE1
FLW1
H1
Smoothed dB
−10.0
−12.5
−15.0
−17.5
−20.0
X20180325
X20180406
X20180418
X20180430
X20180512
X20180524
X20180605
X20180617
X20180629
X20180711
X20180723
X20180804
X20180816
X20180909
X20180921
X20181003
X20181015
X20181027
X20181108
X20181120
X20181202
X20181214
X20181226
X20190107
X20190119
X20190131
X20190212
X20190224
X20190308
X20190320
Date

Time series for Pangasinan VV/VH polarisation ratio:

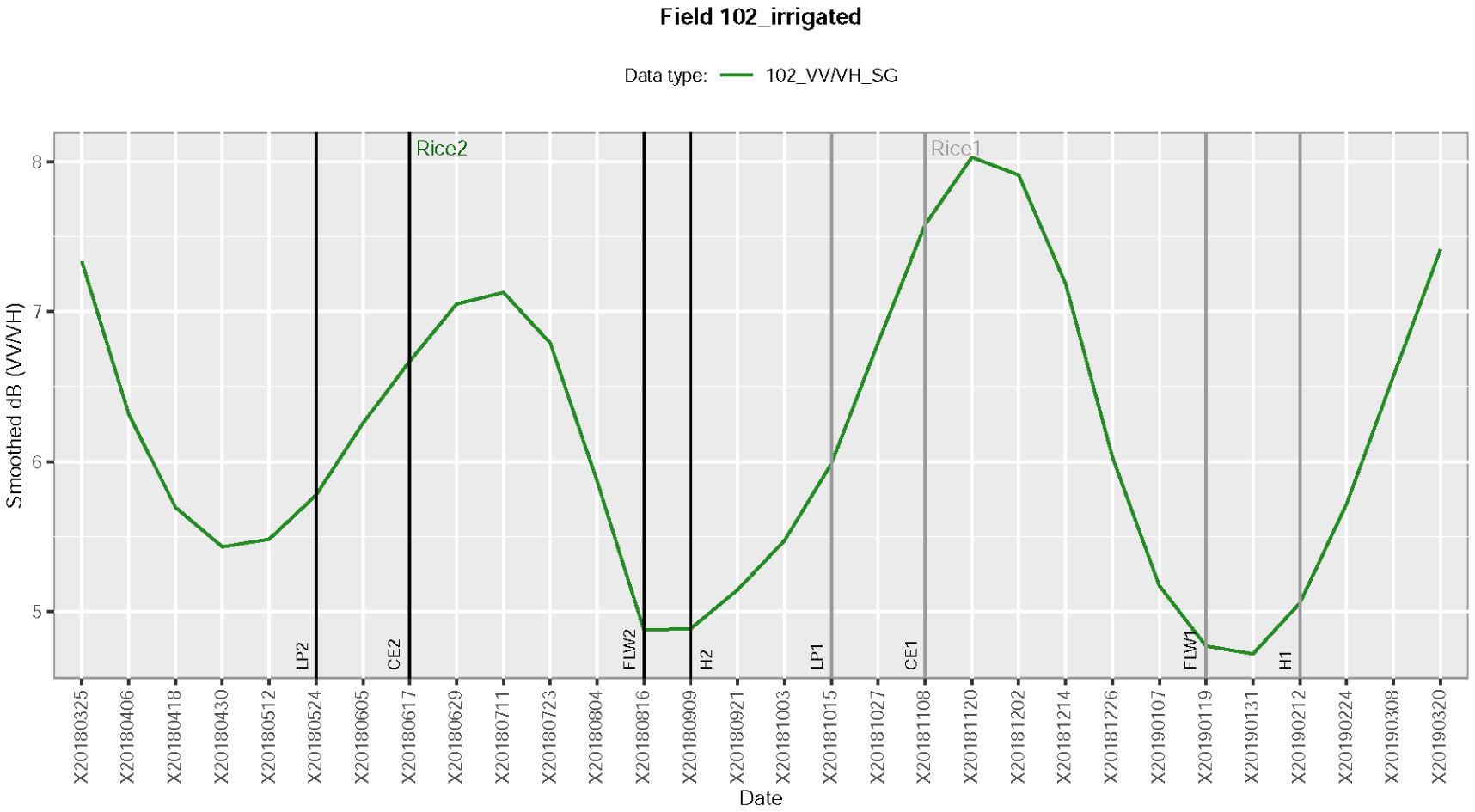

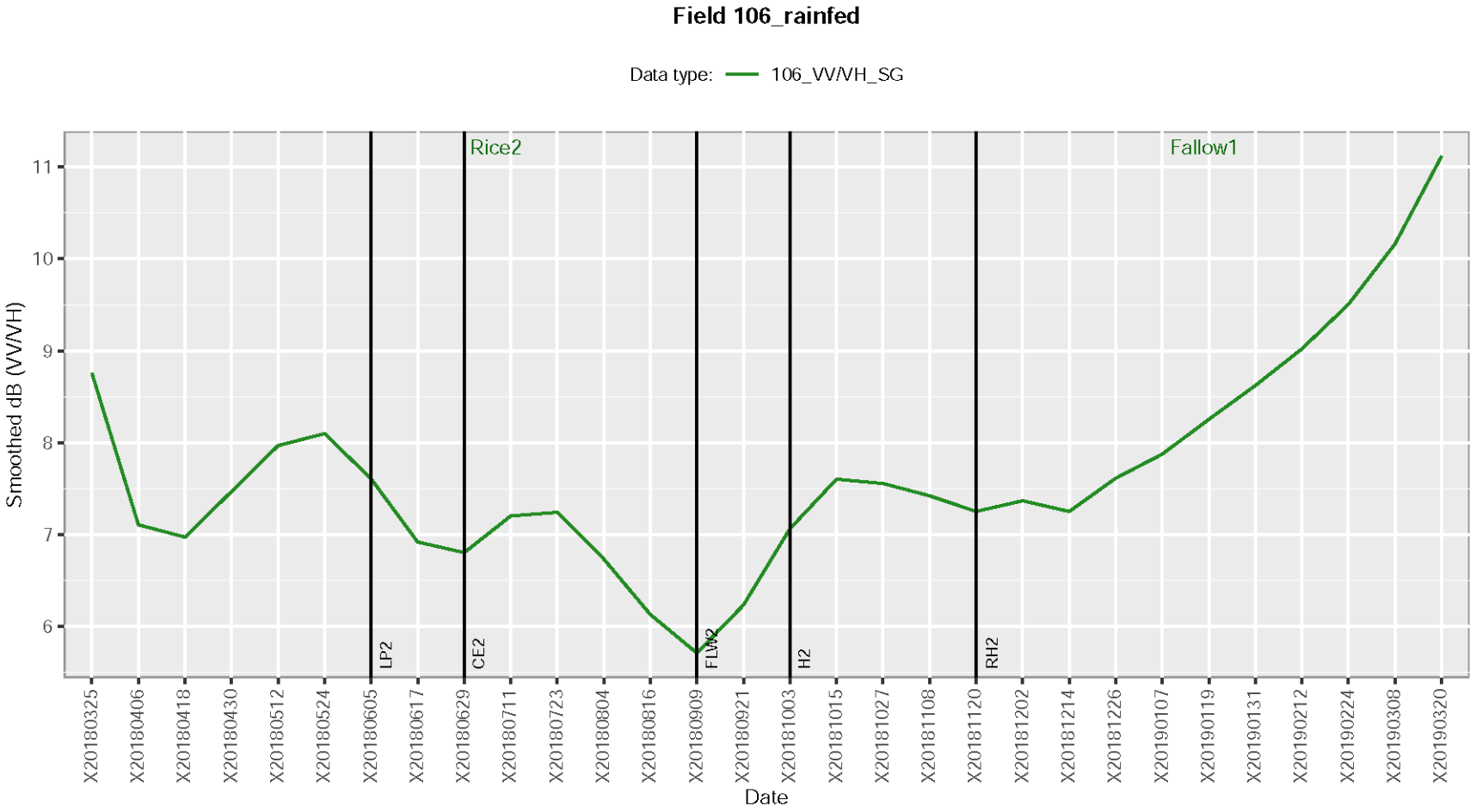
Field 106_rainfed
Data type: 106_VV/VH_SG
Rice2
Fallow1
LP2
CE2
FLW2
H2
RH2
Smoothed dB (VV/VH)
11
10
9
8
7
6
X20180325
X20180406
X20180418
X20180430
X20180512
X20180524
X20180605
X20180617
X20180629
X20180711
X20180723
X20180804
X20180816
X20180909
X20180921
X20181003
X20181015
X20181027
X20181108
X20181120
X20181202
X20181214
X20181226
X20190107
X20190119
X20190131
X20190212
X20190224
X20190308
X20190320
Date

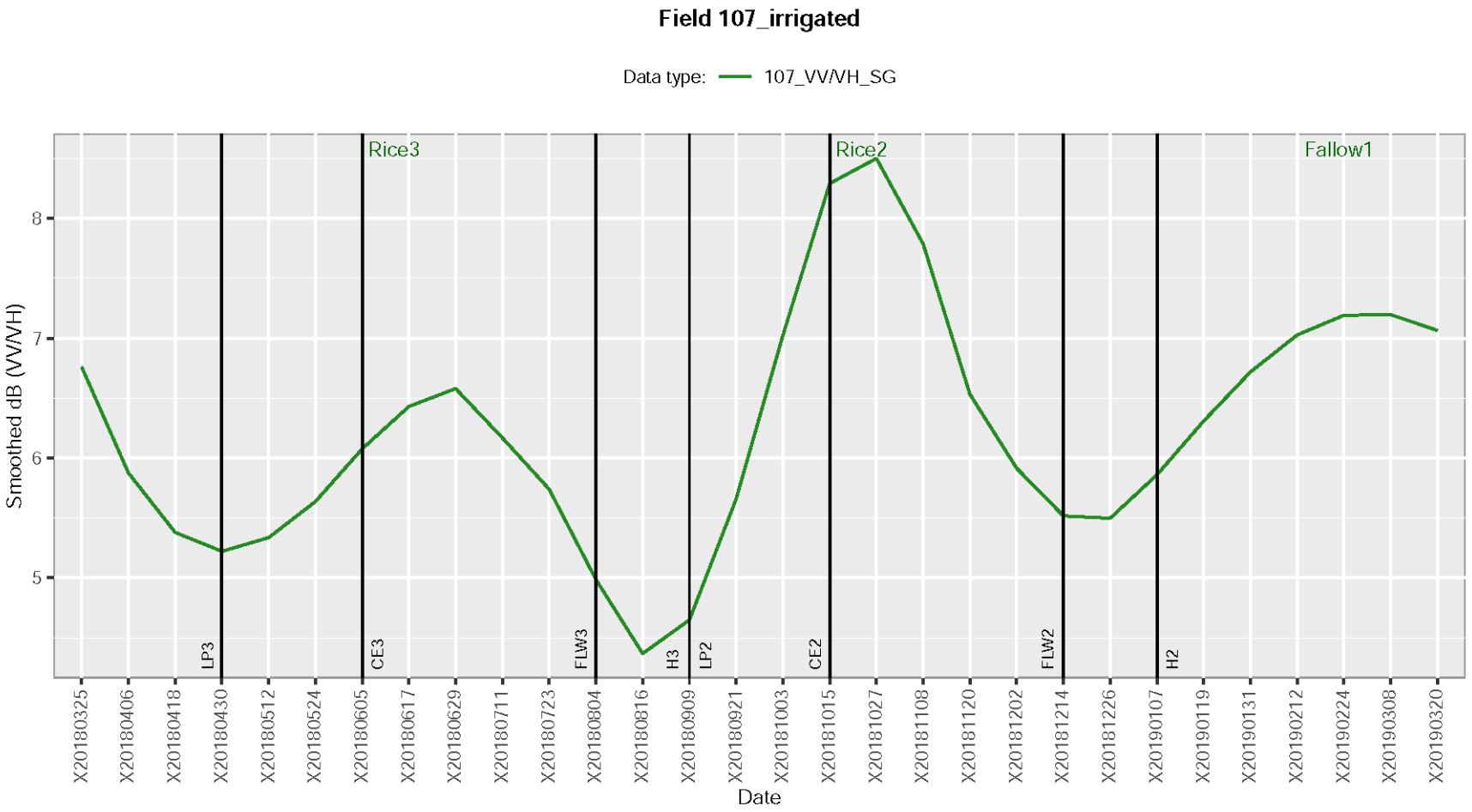
Field 107_irrigated
Data type: 107_VV/VH_SG
Rice3
Rice2
Fallow1
LP3
CE3
FLW3
H3
LP2
CE2
FLW2
H2
Smoothed dB (VV/VH)
8
7
6
5
X20180325
X20180406
X20180418
X20180430
X20180512
X20180524
X20180605
X20180617
X20180629
X20180711
X20180723
X20180804
X20180816
X20180909
X20180921
X20181003
X20181015
X20181027
X20181108
X20181120
X20181202
X20181214
X20181226
X20190107
X20190119
X20190131
X20190212
X20190224
X20190308
X20190320
Date

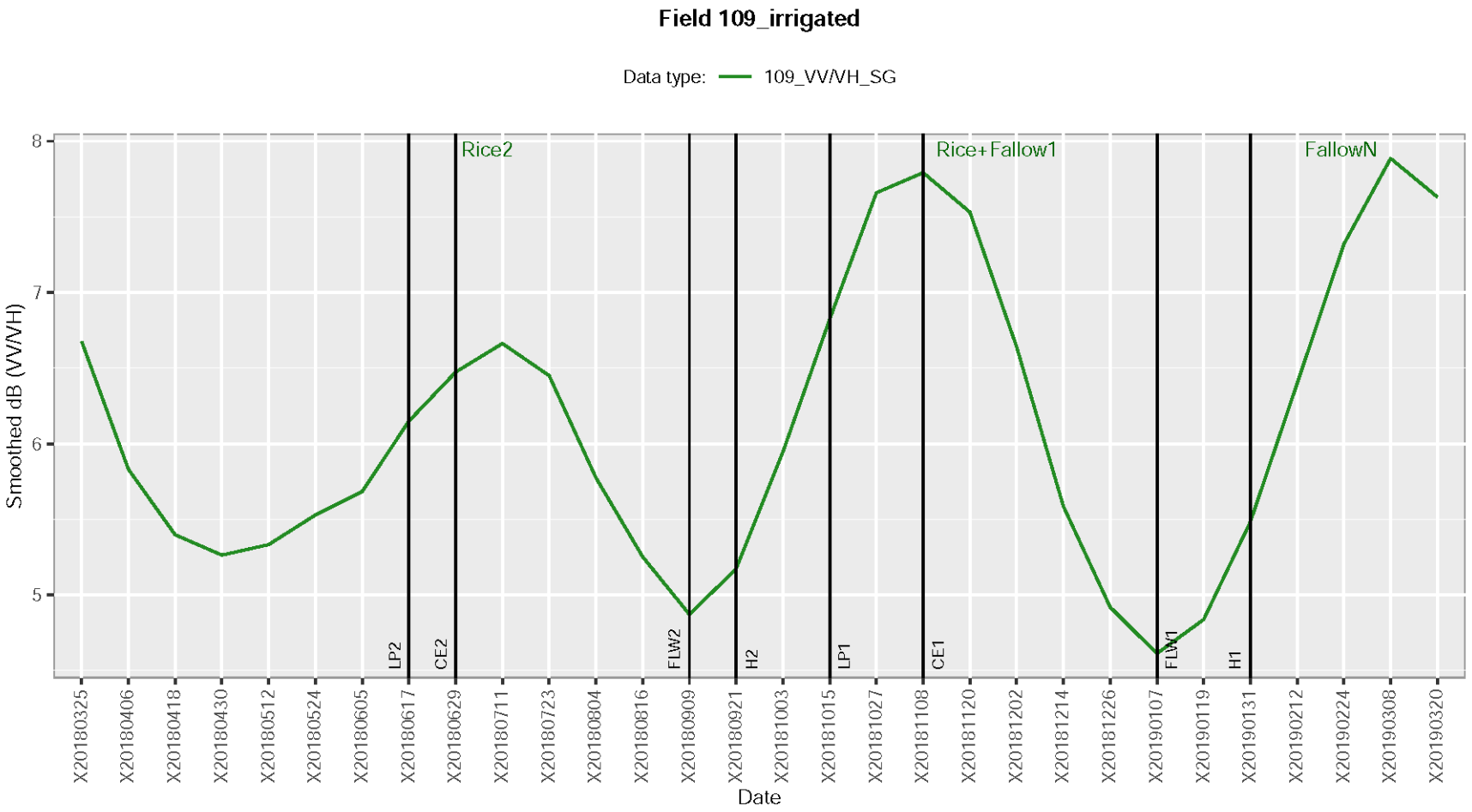
Field 109_irrigated
Data type: 109_VV/VH_SG
Smoothed dB (VV/VH)
8
7
6
5
Rice2
Rice+Fallow1
FallowN
LP2
CE2
FLW2
H2
LP1
CE1
FLW1
H1
X20180325
X20180406
X20180418
X20180430
X20180512
X20180524
X20180605
X20180617
X20180629
X20180711
X20180723
X20180804
X20180816
X20180909
X20180921
X20181003
X20181015
X20181027
X20181108
X20181120
X20181202
X20181214
X20181226
X20190107
X20190119
X20190131
X20190212
X20190224
X20190308
X20190320
Date

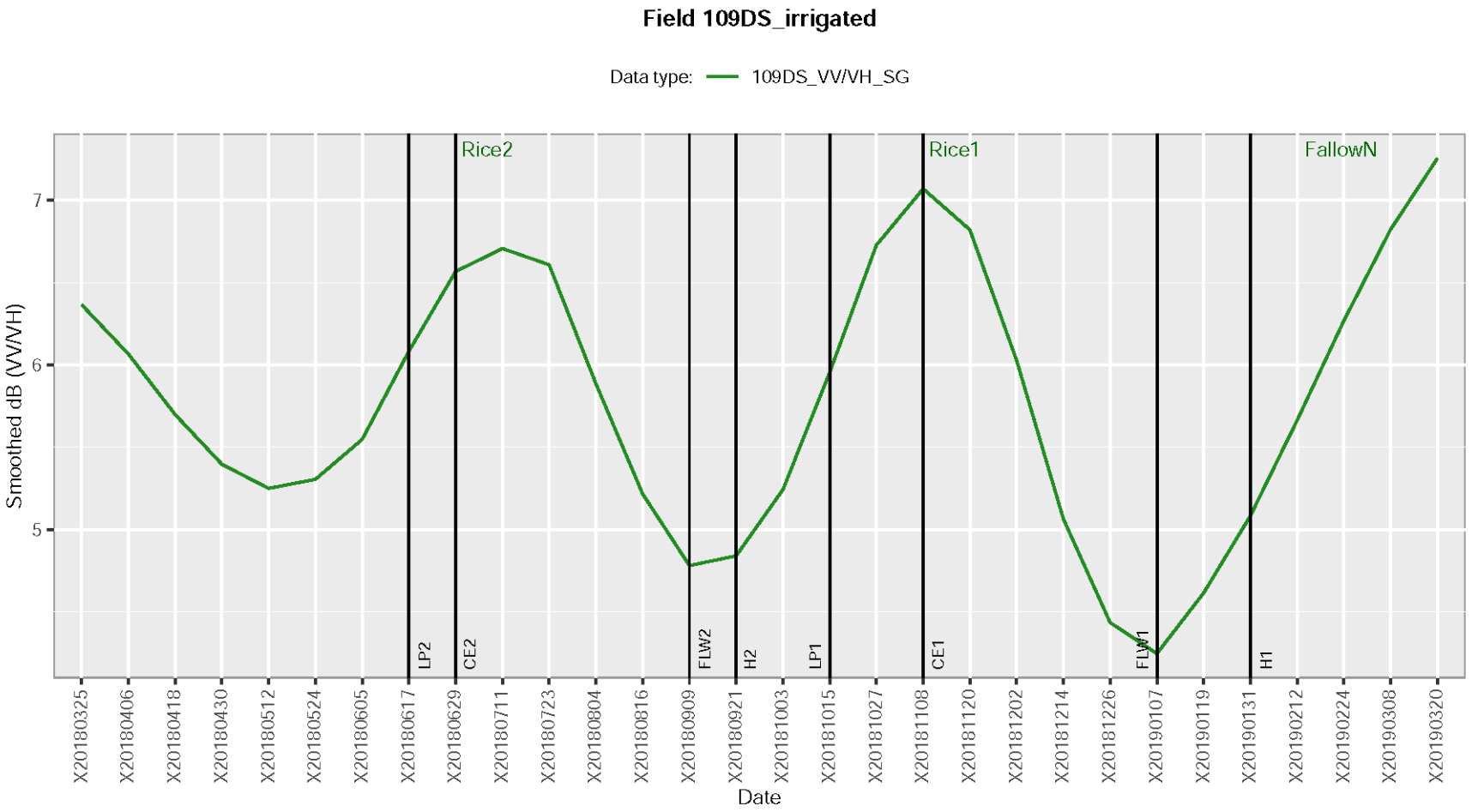
Field 109DS_irrigated
Data type: 109DS_VV/VH_SG
Smoothed dB (VV/VH)
7
6
5
Rice2
Rice1
FallowN
LP2
CE2
FLW2
H2
LP1
CE1
FLW1
H1
X20180325
X20180406
X20180418
X20180430
X20180512
X20180524
X20180605
X20180617
X20180629
X20180711
X20180723
X20180804
X20180816
X20180909
X20180921
X20181003
X20181015
X20181027
X20181108
X20181120
X20181202
X20181214
X20181226
X20190107
X20190119
X20190131
X20190212
X20190224
X20190308
X20190320
Date

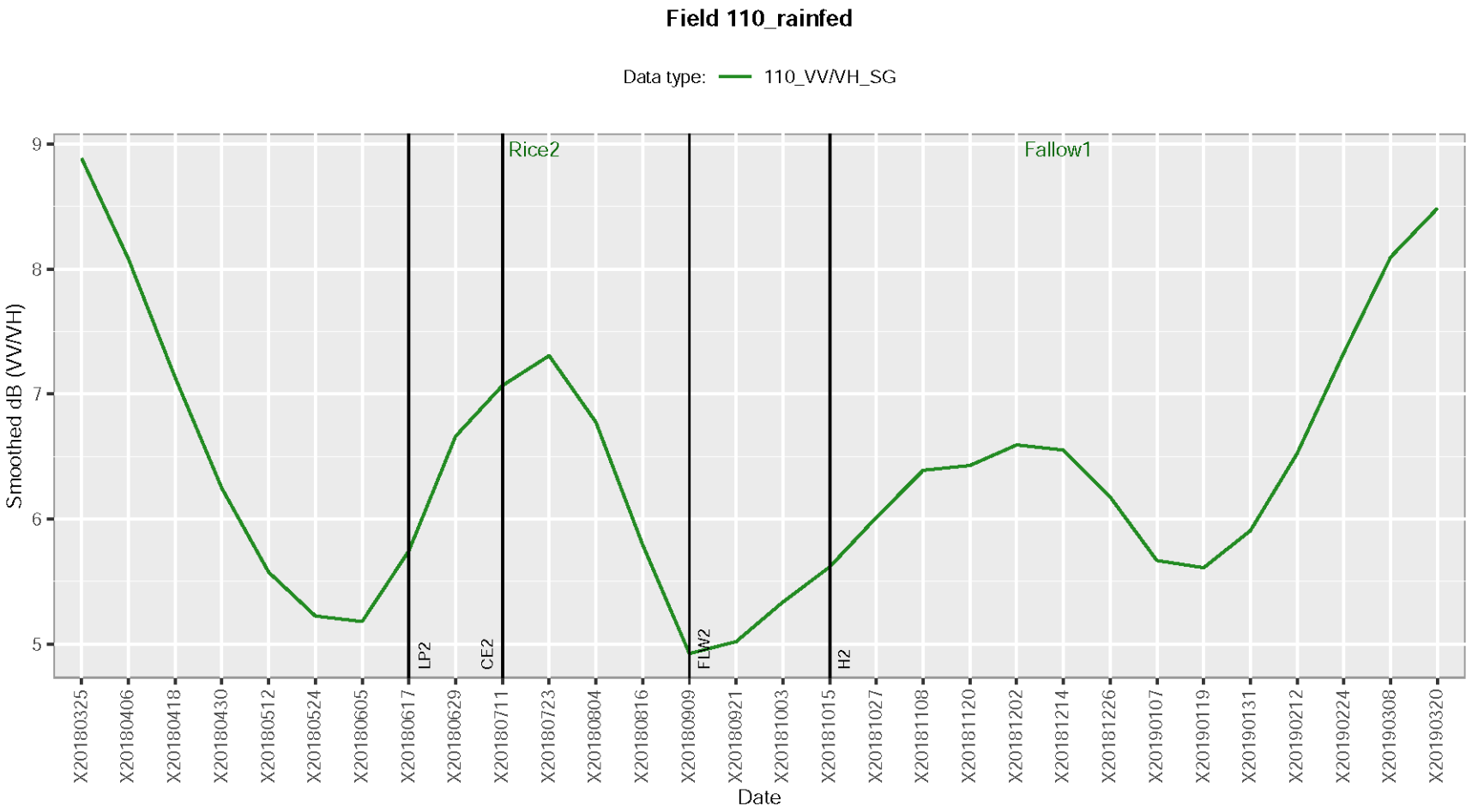
Field 110_rainfed
Data type: 110_VV/VH_SG
Rice2
Fallow1
LP2
CE2
FLW2
H2
Smoothed dB (VV/VH)
9
8
7
6
5
X20180325
X20180406
X20180418
X20180430
X20180512
X20180524
X20180605
X20180617
X20180629
X20180711
X20180723
X20180804
X20180816
X20180909
X20180921
X20181003
X20181015
X20181027
X20181108
X20181120
X20181202
X20181214
X20181226
X20190107
X20190119
X20190131
X20190212
X20190224
X20190308
X20190320
Date

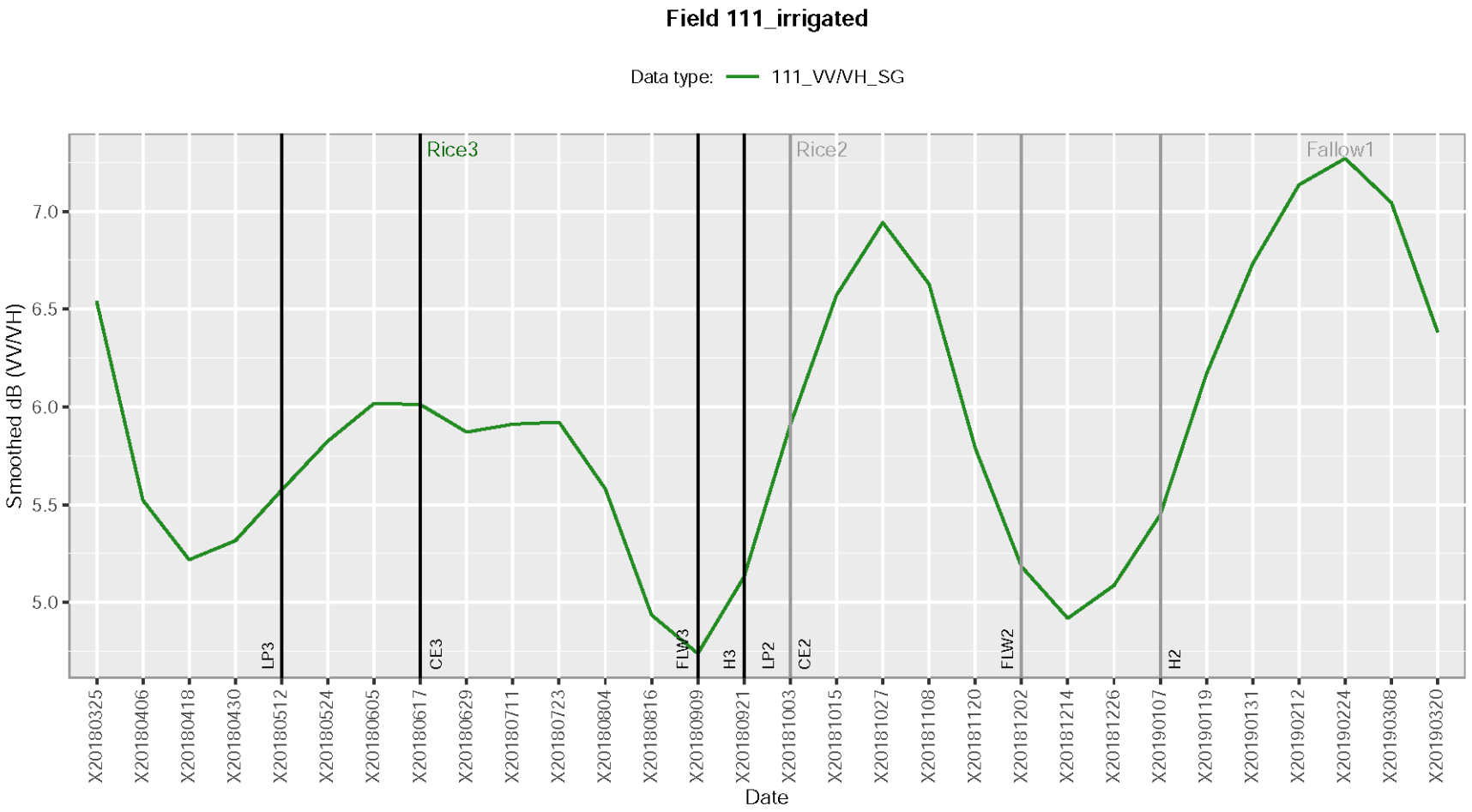
Field 111_irrigated
Data type: 111_VV/VH_SG
Rice3
Rice2
Fallow1
Smoothed dB (VV/VH)
7.0
6.5
6.0
5.5
5.0
LP3
CE3
FLW3
H3
LP2
CE2
FLW2
H2
X20180325
X20180406
X20180418
X20180430
X20180512
X20180524
X20180605
X20180617
X20180629
X20180711
X20180723
X20180804
X20180816
X20180909
X20180921
X20181003
X20181015
X20181027
X20181108
X20181120
X20181202
X20181214
X20181226
X20190107
X20190119
X20190131
X20190212
X20190224
X20190308
X20190320
Date

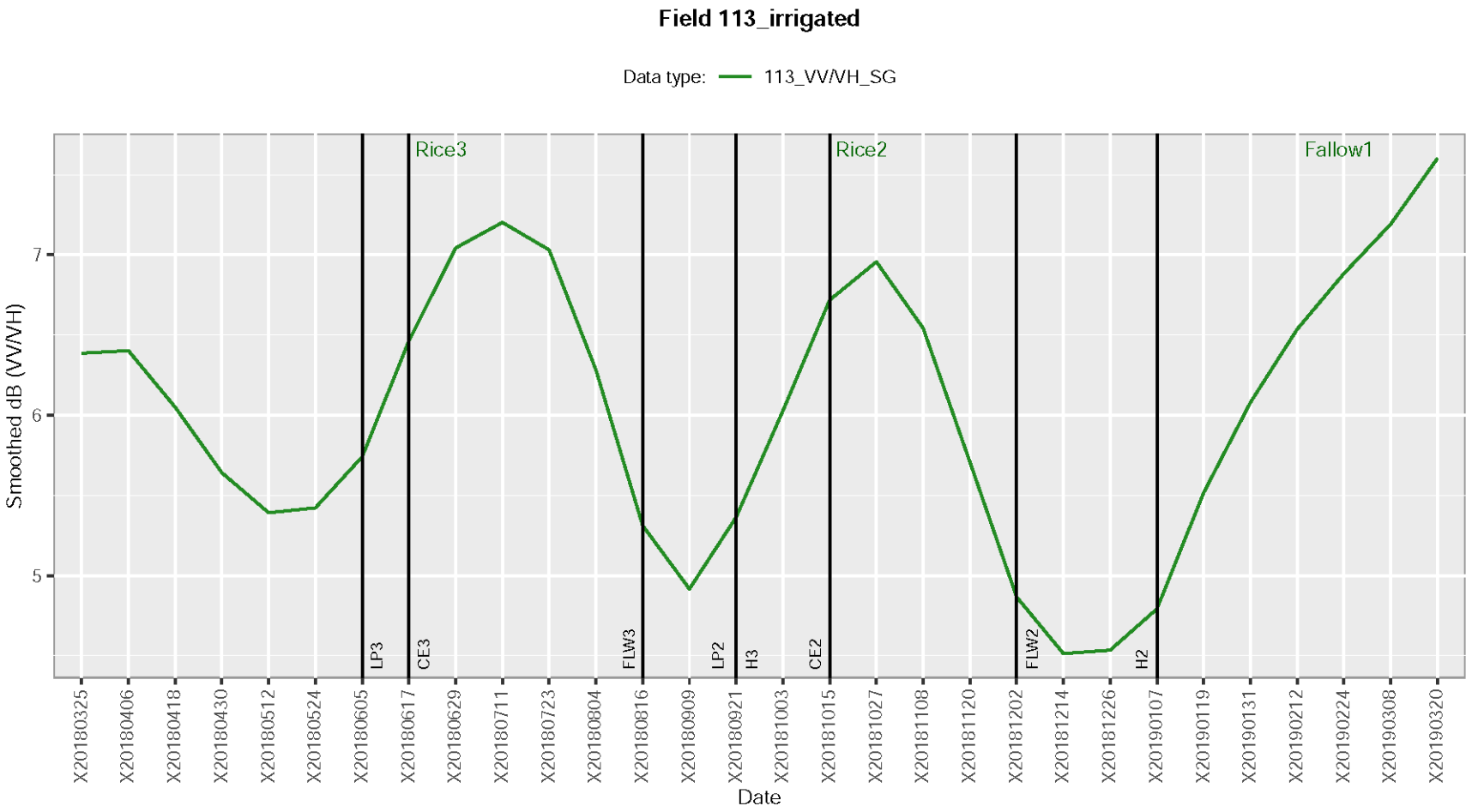
Field 113_irrigated
Data type: 113_VV/VH_SG
Rice3
Rice2
Fallow1
LP3
CE3
FLW3
LP2
H3
CE2
FLW2
H2
Smoothed dB (VV/VH)
7
6
5
X20180325
X20180406
X20180418
X20180430
X20180512
X20180524
X20180605
X20180617
X20180629
X20180711
X20180723
X20180804
X20180816
X20180909
X20180921
X20181003
X20181015
X20181027
X20181108
X20181120
X20181202
X20181214
X20181226
X20190107
X20190119
X20190131
X20190212
X20190224
X20190308
X20190320
Date

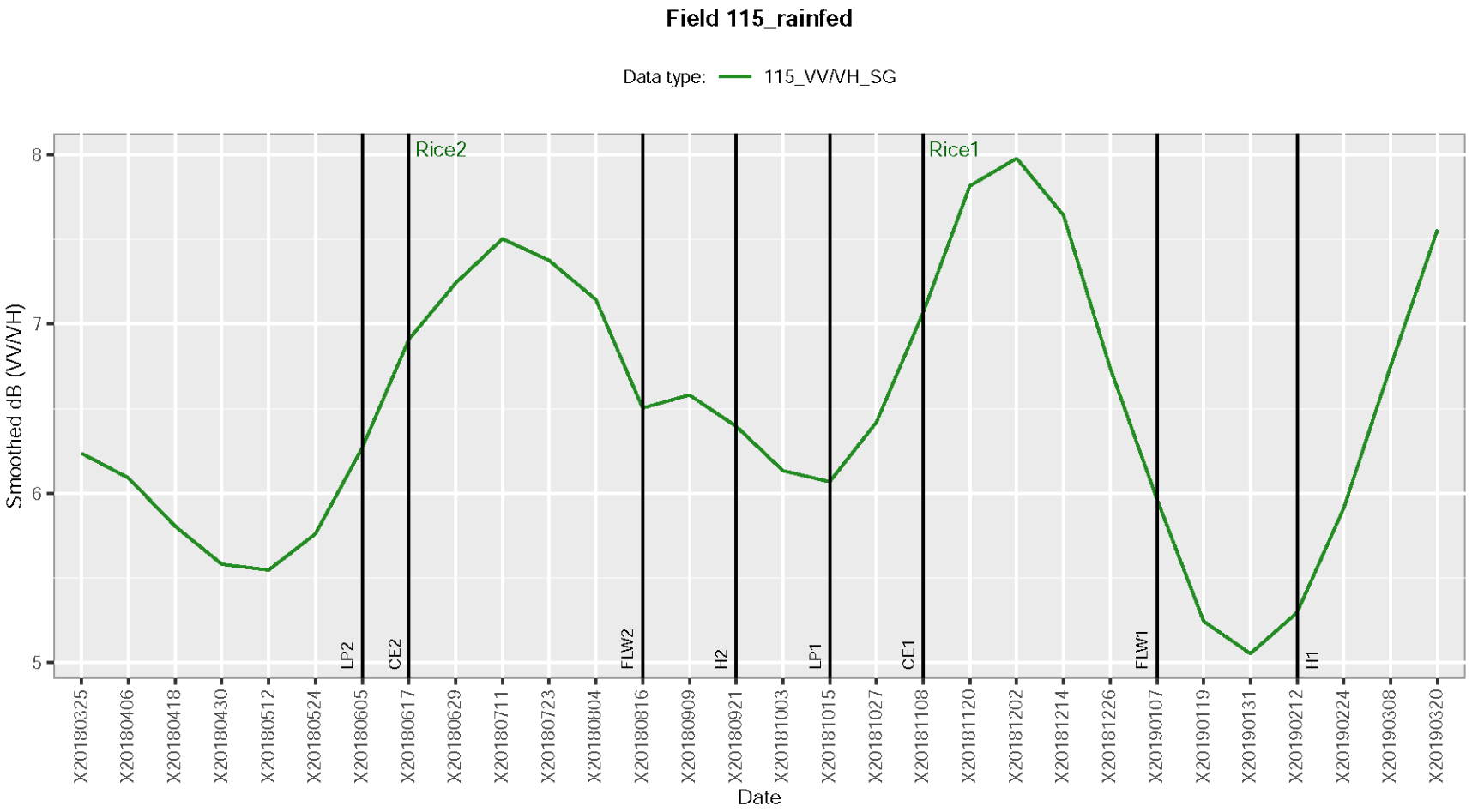
Field 115_rainfed
Data type: 115_VV/VH_SG
Smoothed dB (VV/VH)
8
7
6
5
Rice2
Rice1
LP2
CE2
FLW2
H2
LP1
CE1
FLW1
H1
X20180325
X20180406
X20180418
X20180430
X20180512
X20180524
X20180605
X20180617
X20180629
X20180711
X20180723
X20180804
X20180816
X20180909
X20180921
X20181003
X20181015
X20181027
X20181108
X20181120
X20181202
X20181214
X20181226
X20190107
X20190119
X20190131
X20190212
X20190224
X20190308
X20190320
Date

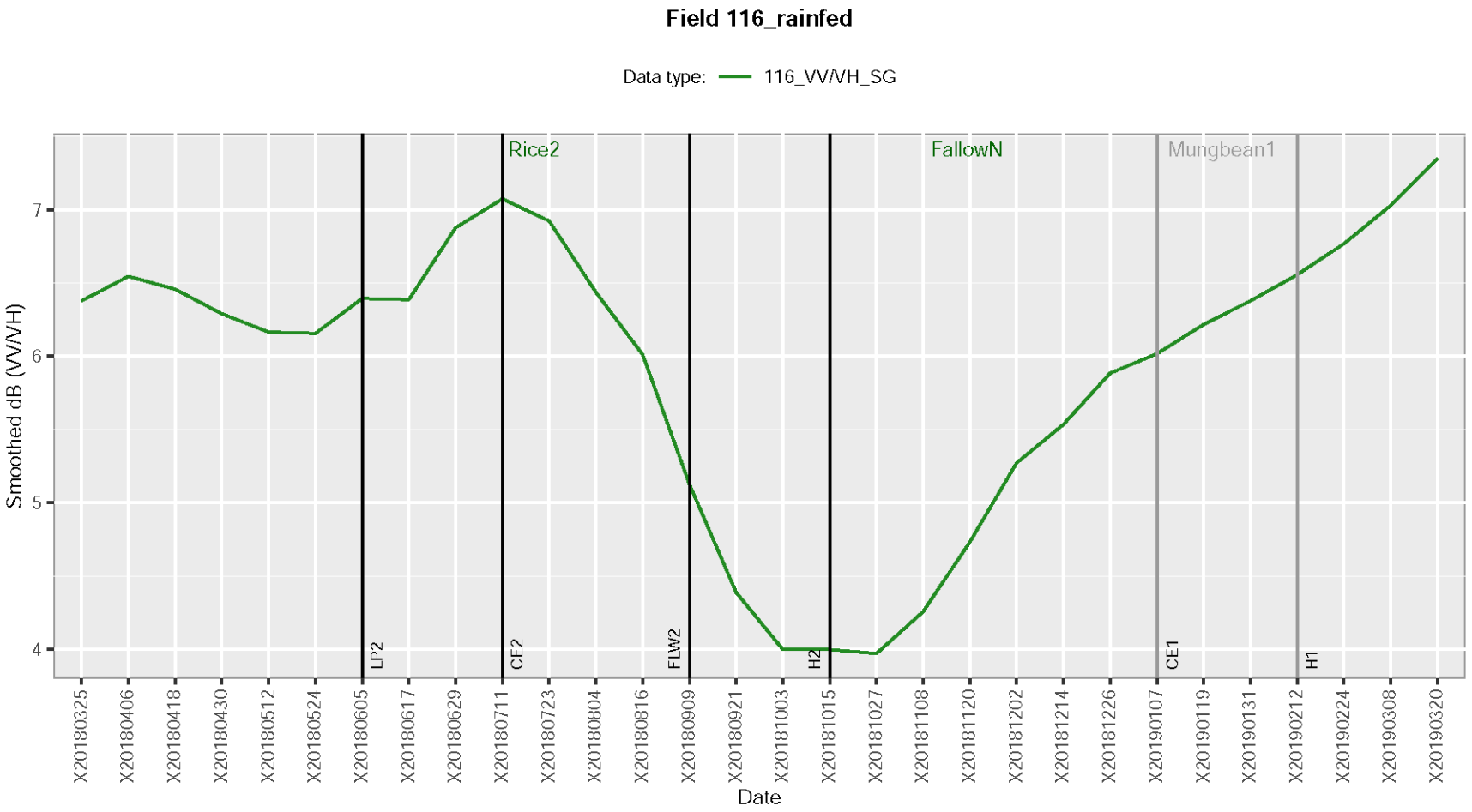
Field 116_rainfed
Data type: 116_VV/VH_SG
Rice2
FallowN
Mungbean1
LP2
CE2
FLW2
H2
CE1
H1
Smoothed dB (VV/VH)
7
6
5
4
X20180325
X20180406
X20180418
X20180430
X20180512
X20180524
X20180605
X20180617
X20180629
X20180711
X20180723
X20180804
X20180816
X20180909
X20180921
X20181003
X20181015
X20181027
X20181108
X20181120
X20181202
X20181214
X20181226
X20190107
X20190119
X20190131
X20190212
X20190224
X20190308
X20190320
Date

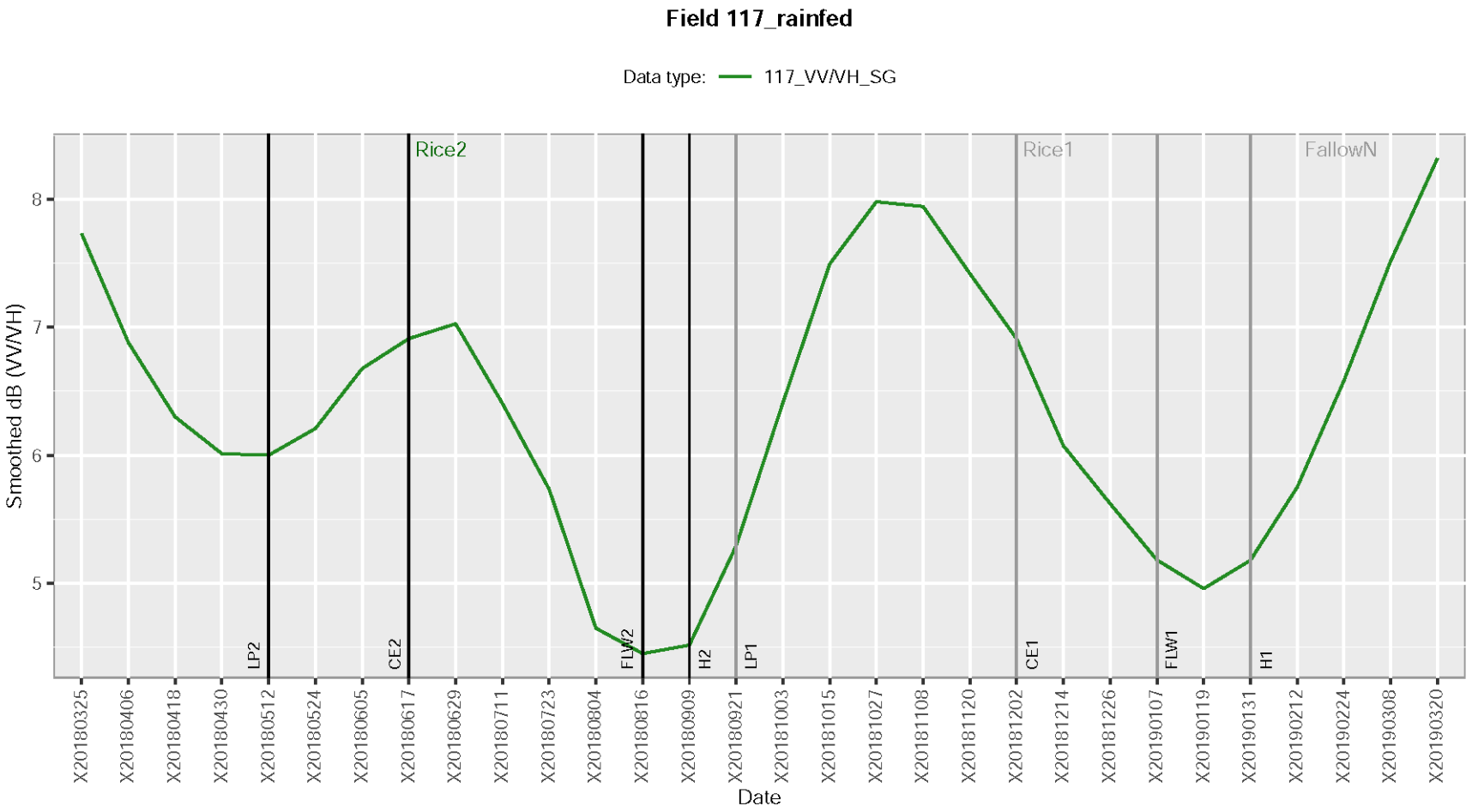
Field 117_rainfed
Data type: 117_VV/VH_SG
Rice2
Rice1
FallowN
Smoothed dB (VV/VH)
8
7
6
5
LP2
CE2
FLW2
H2
LP1
CE1
FLW1
H1
X20180325
X20180406
X20180418
X20180430
X20180512
X20180524
X20180605
X20180617
X20180629
X20180711
X20180723
X20180804
X20180816
X20180909
X20180921
X20181003
X20181015
X20181027
X20181108
X20181120
X20181202
X20181214
X20181226
X20190107
X20190119
X20190131
X20190212
X20190224
X20190308
X20190320
Date

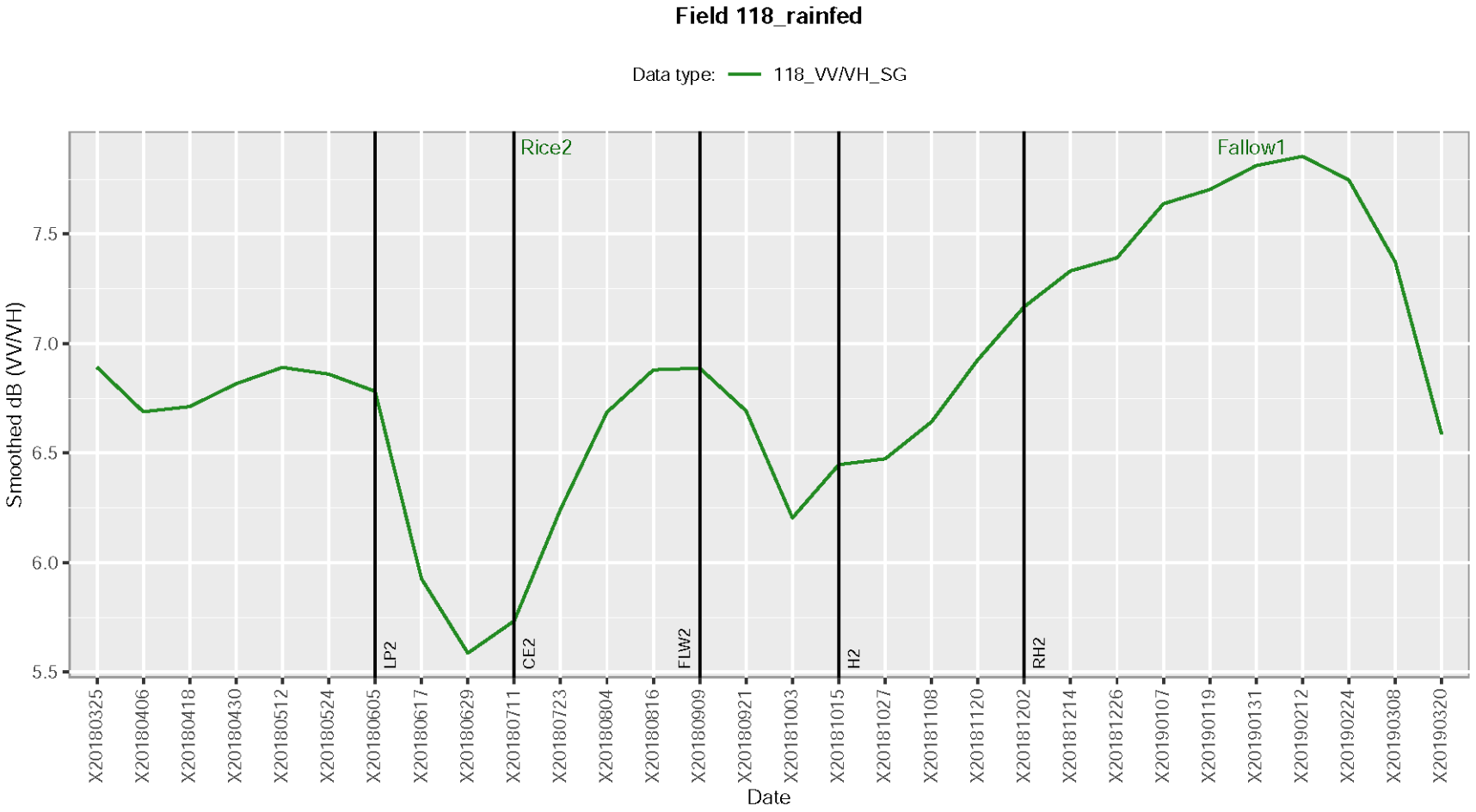
Field 118_rainfed
Data type: 118_VV/VH_SG
Rice2
Fallow1
LP2
CE2
FLW2
H2
RH2
Smoothed dB (VV/VH)
7.5
7.0
6.5
6.0
5.5
X20180325
X20180406
X20180418
X20180430
X20180512
X20180524
X20180605
X20180617
X20180629
X20180711
X20180723
X20180804
X20180816
X20180909
X20180921
X20181003
X20181015
X20181027
X20181108
X20181120
X20181202
X20181214
X20181226
X20190107
X20190119
X20190131
X20190212
X20190224
X20190308
X20190320
Date

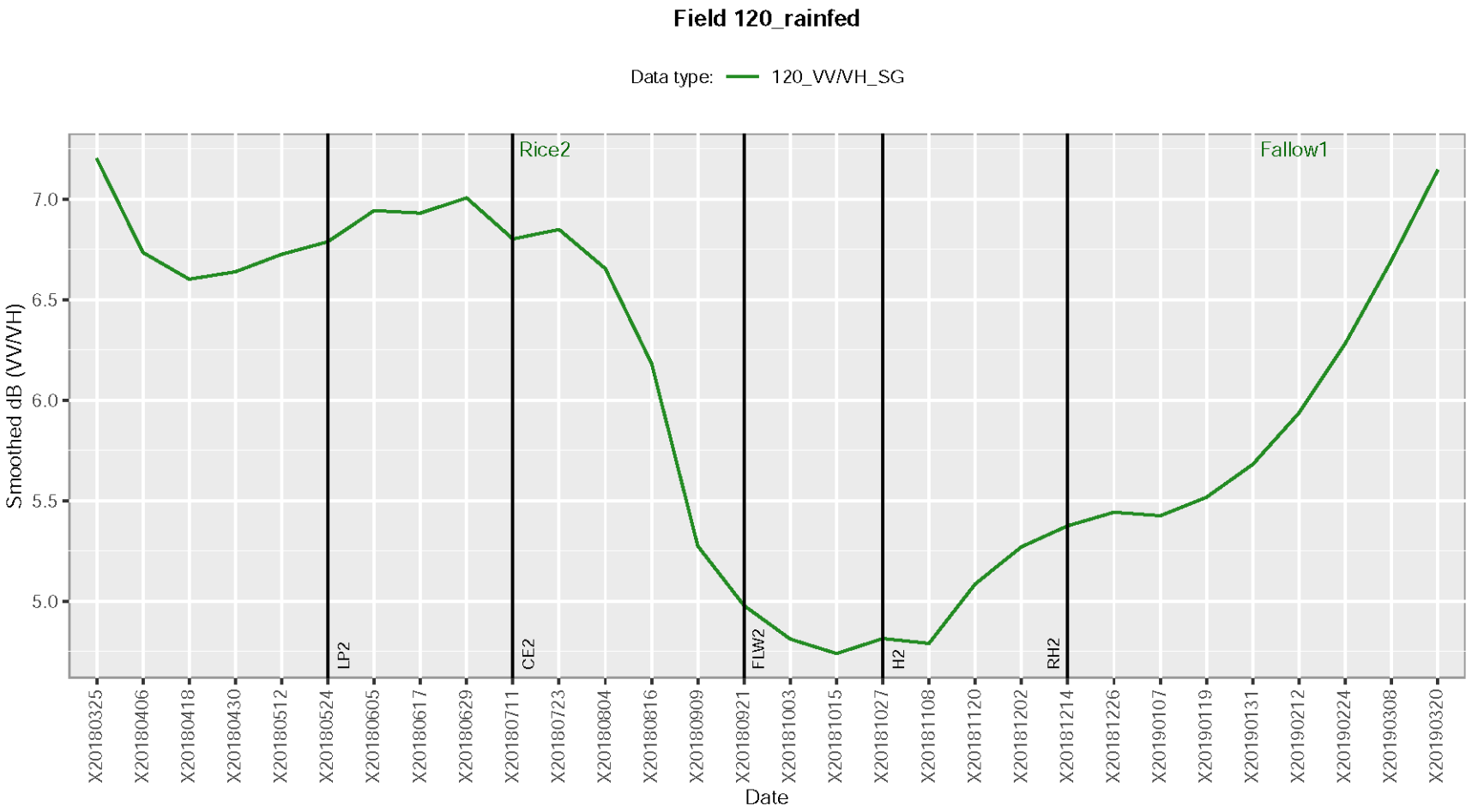
Field 120_rainfed
Data type: 120_VV/VH_SG
Rice2
Fallow1
LP2
CE2
FLW2
H2
RH2
Smoothed dB (VV/VH)
7.0
6.5
6.0
5.5
5.0
X20180325
X20180406
X20180418
X20180430
X20180512
X20180524
X20180605
X20180617
X20180629
X20180711
X20180723
X20180804
X20180816
X20180909
X20180921
X20181003
X20181015
X20181027
X20181108
X20181120
X20181202
X20181214
X20181226
X20190107
X20190119
X20190131
X20190212
X20190224
X20190308
X20190320
Date

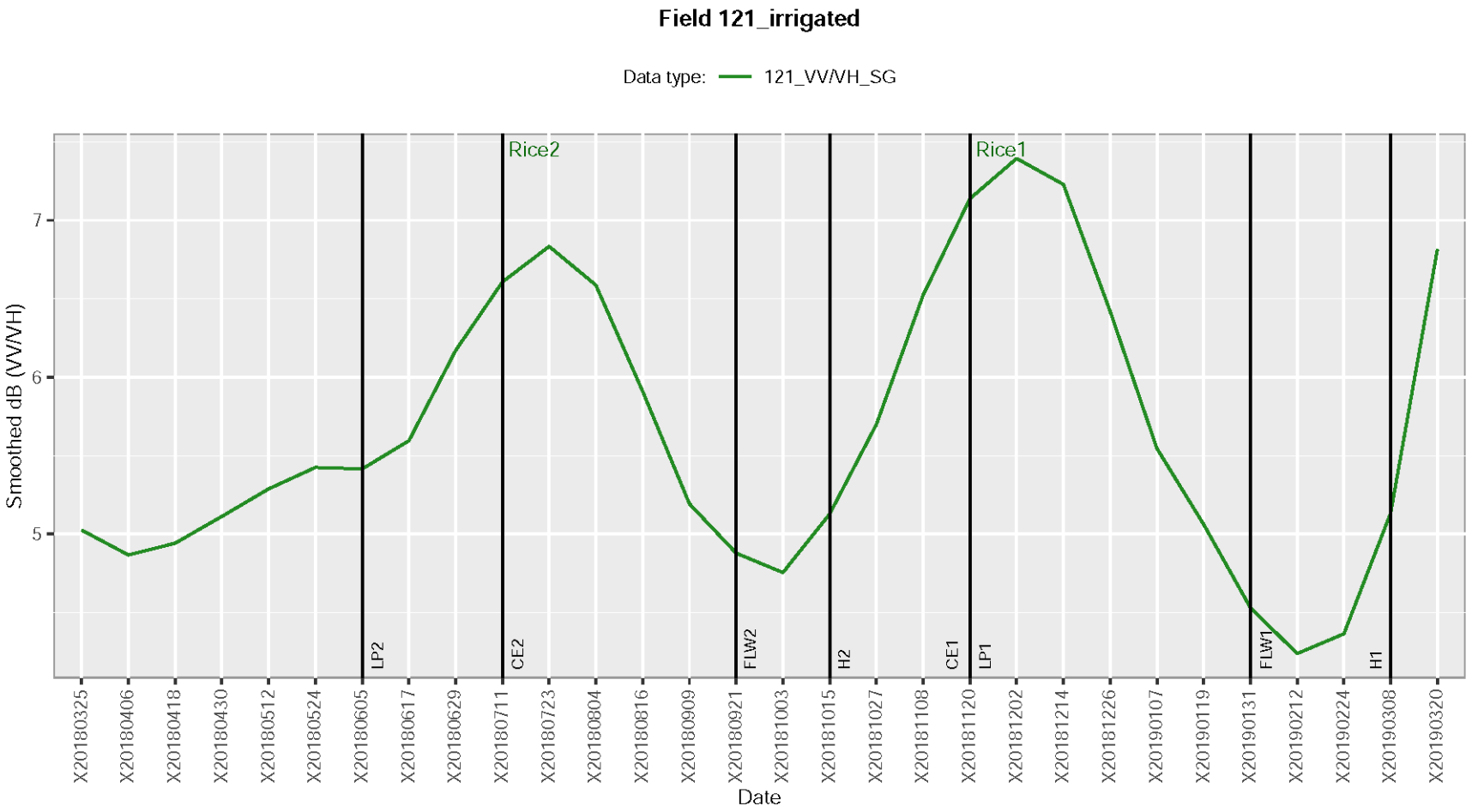
Field 121_irrigated
Data type: 121_VV/VH_SG
Rice2
Rice1
Smoothed dB (VV/VH)
7
6
5
LP2
CE2
FLW2
H2
CE1
LP1
FLW1
H1
X20180325
X20180406
X20180418
X20180430
X20180512
X20180524
X20180605
X20180617
X20180629
X20180711
X20180723
X20180804
X20180816
X20180909
X20180921
X20181003
X20181015
X20181027
X20181108
X20181120
X20181202
X20181214
X20181226
X20190107
X20190119
X20190131
X20190212
X20190224
X20190308
X20190320
Date

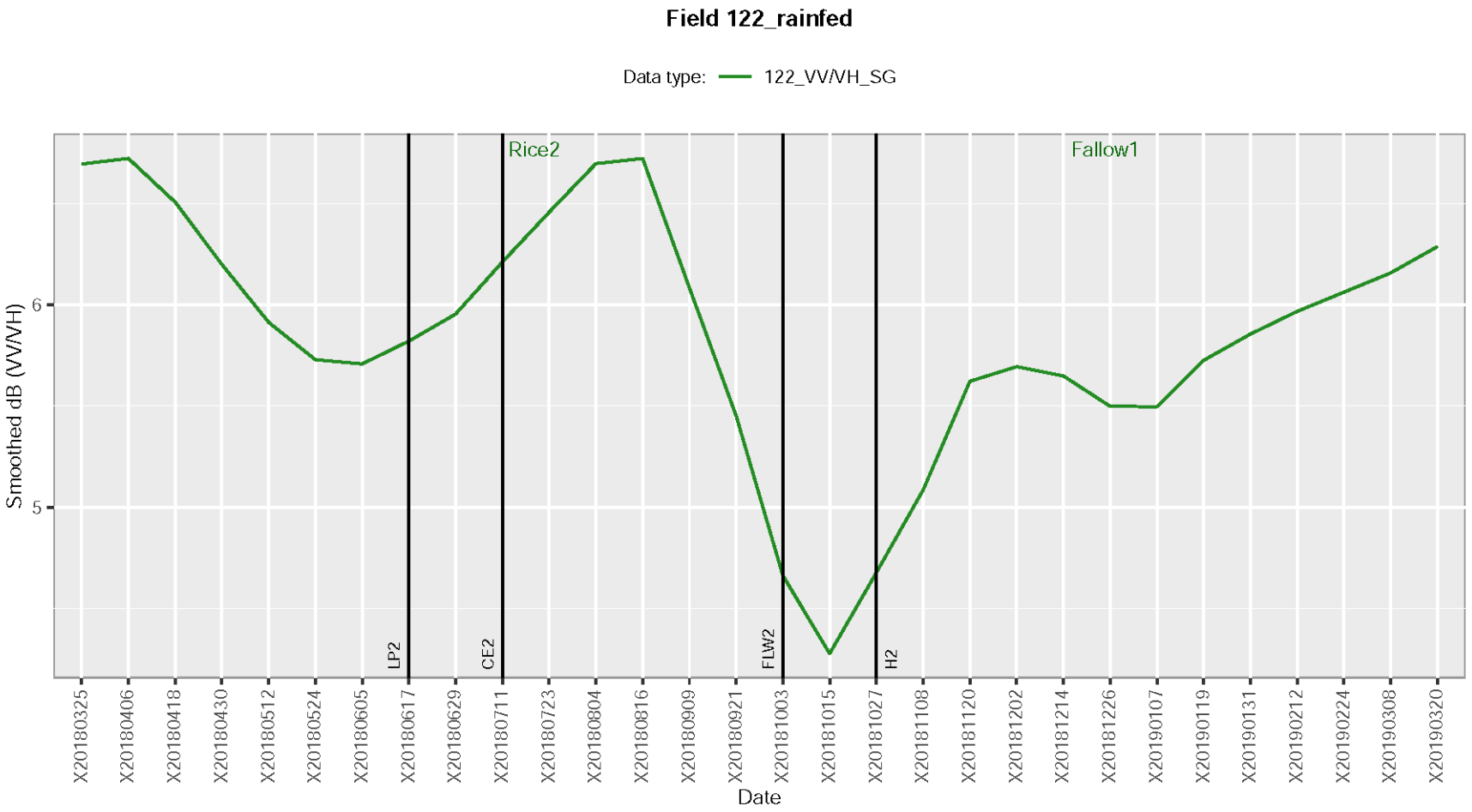
Field 122_rainfed
Data type: 122_VV/VH_SG
Rice2
Fallow1
LP2
CE2
FLW2
H2
Smoothed dB (VV/VH)
6
5
X20180325
X20180406
X20180418
X20180430
X20180512
X20180524
X20180605
X20180617
X20180629
X20180711
X20180723
X20180804
X20180816
X20180909
X20180921
X20181003
X20181015
X20181027
X20181108
X20181120
X20181202
X20181214
X20181226
X20190107
X20190119
X20190131
X20190212
X20190224
X20190308
X20190320
Date

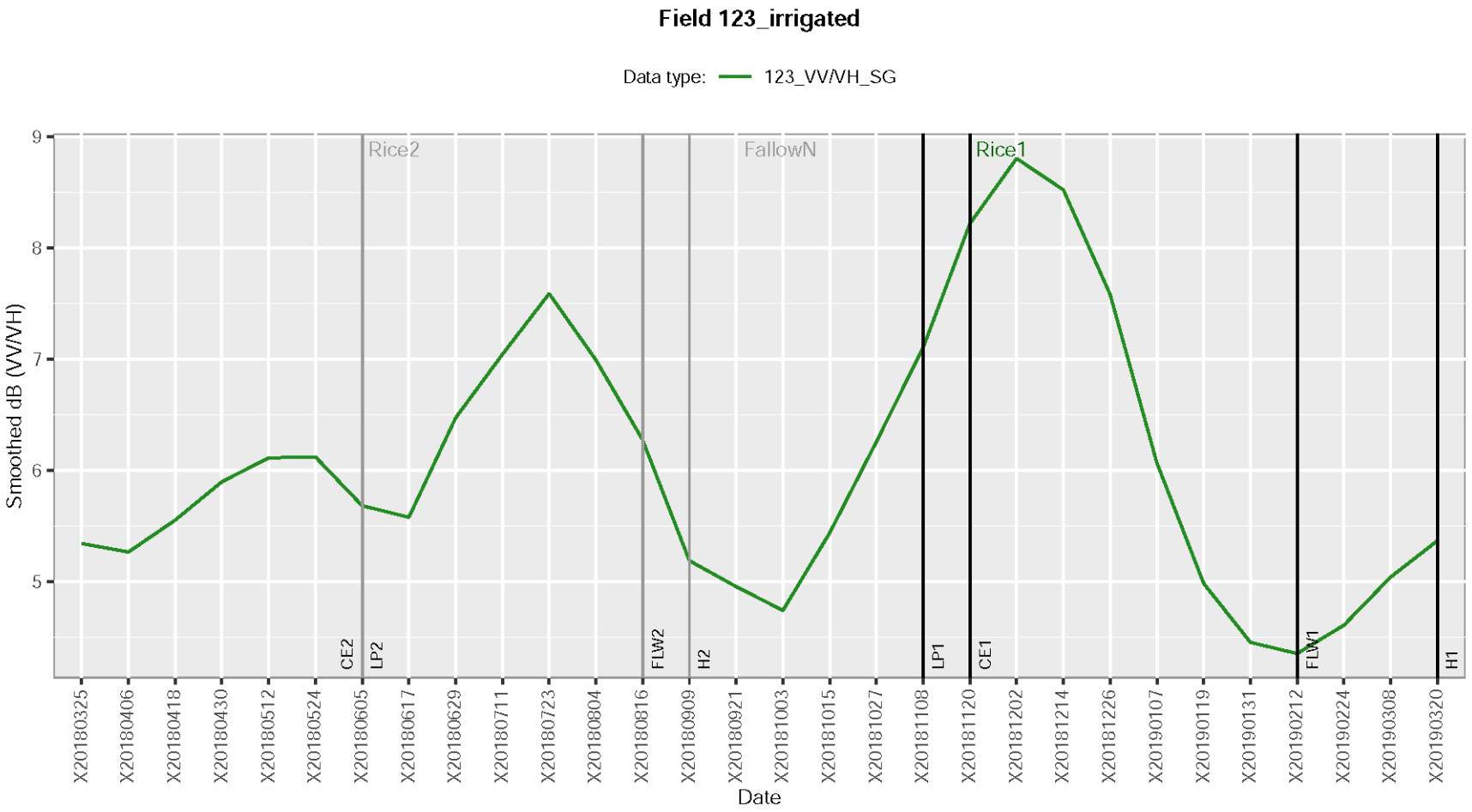
Field 123_irrigated
Data type: 123_VV/VH_SG
Smoothed dB (VV/VH)
9
8
7
6
5
Rice2
FallowN
Rice1
CE2
LP2
FLW2
H2
LP1
CE1
FLW1
H1
X20180325
X20180406
X20180418
X20180430
X20180512
X20180524
X20180605
X20180617
X20180629
X20180711
X20180723
X20180804
X20180816
X20180909
X20180921
X20181003
X20181015
X20181027
X20181108
X20181120
X20181202
X20181214
X20181226
X20190107
X20190119
X20190131
X20190212
X20190224
X20190308
X20190320
Date

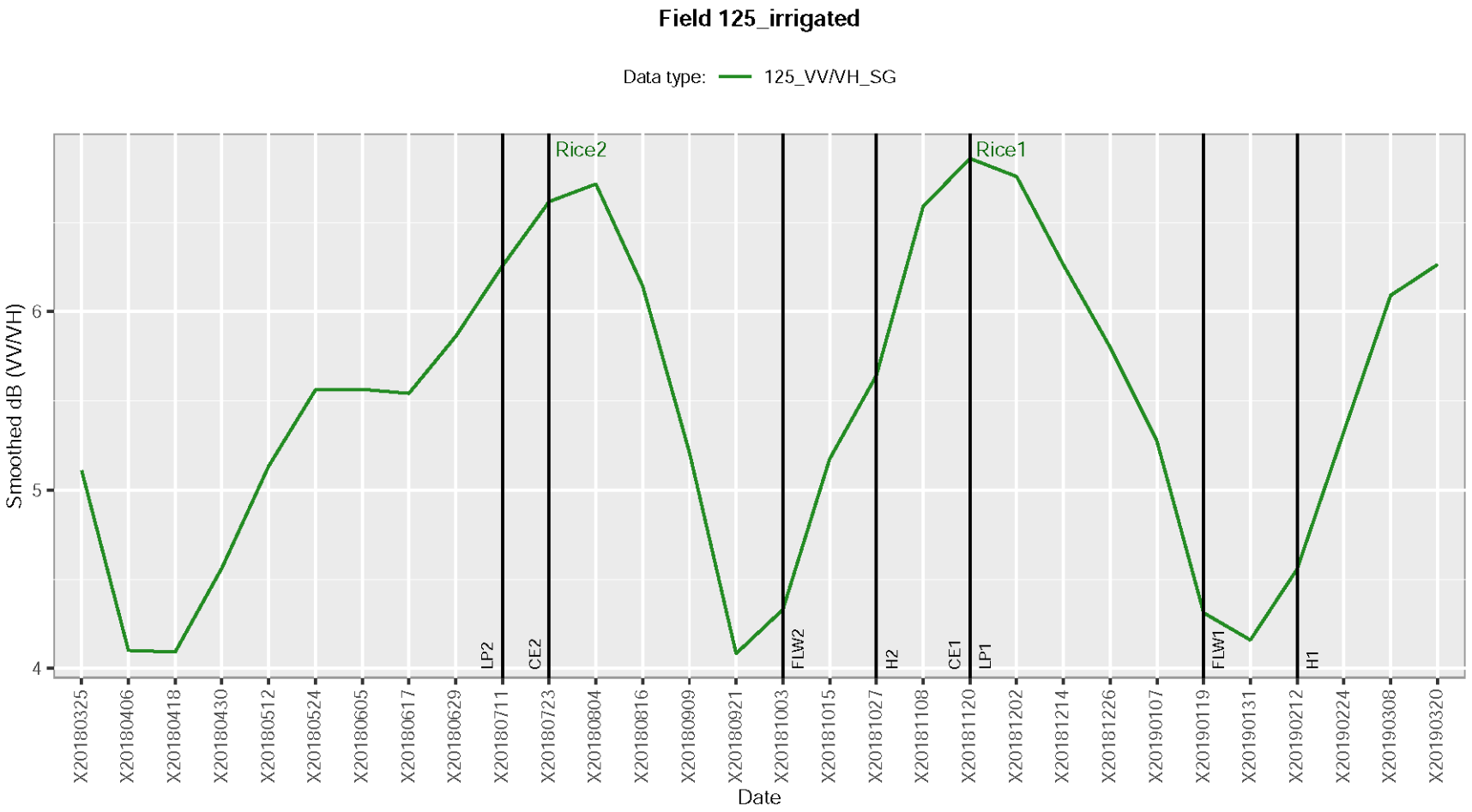
Field 125_irrigated
Data type: 125_VV/VH_SG
Rice2
Rice1
LP2
CE2
FLW2
H2
CE1
LP1
FLW1
H1
Smoothed dB (VV/VH)
6
5
4
X20180325
X20180406
X20180418
X20180430
X20180512
X20180524
X20180605
X20180617
X20180629
X20180711
X20180723
X20180804
X20180816
X20180909
X20180921
X20181003
X20181015
X20181027
X20181108
X20181120
X20181202
X20181214
X20181226
X20190107
X20190119
X20190131
X20190212
X20190224
X20190308
X20190320
Date

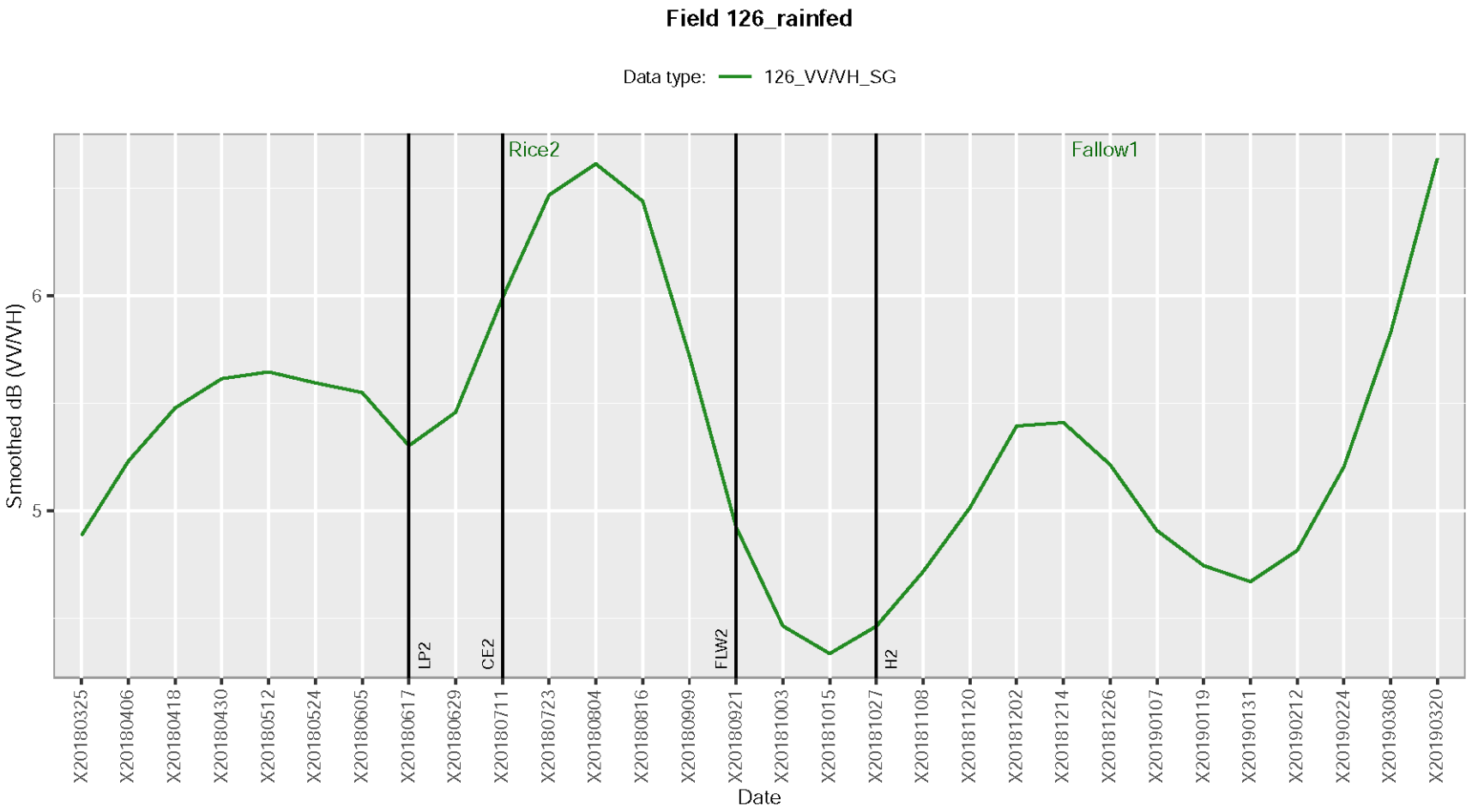
Field 126_rainfed
Data type: 126_VV/VH_SG
Rice2
Fallow1
LP2
CE2
FLW2
H2
Smoothed dB (VV/VH)
6
5
X20180325
X20180406
X20180418
X20180430
X20180512
X20180524
X20180605
X20180617
X20180629
X20180711
X20180723
X20180804
X20180816
X20180909
X20180921
X20181003
X20181015
X20181027
X20181108
X20181120
X20181202
X20181214
X20181226
X20190107
X20190119
X20190131
X20190212
X20190224
X20190308
X20190320
Date

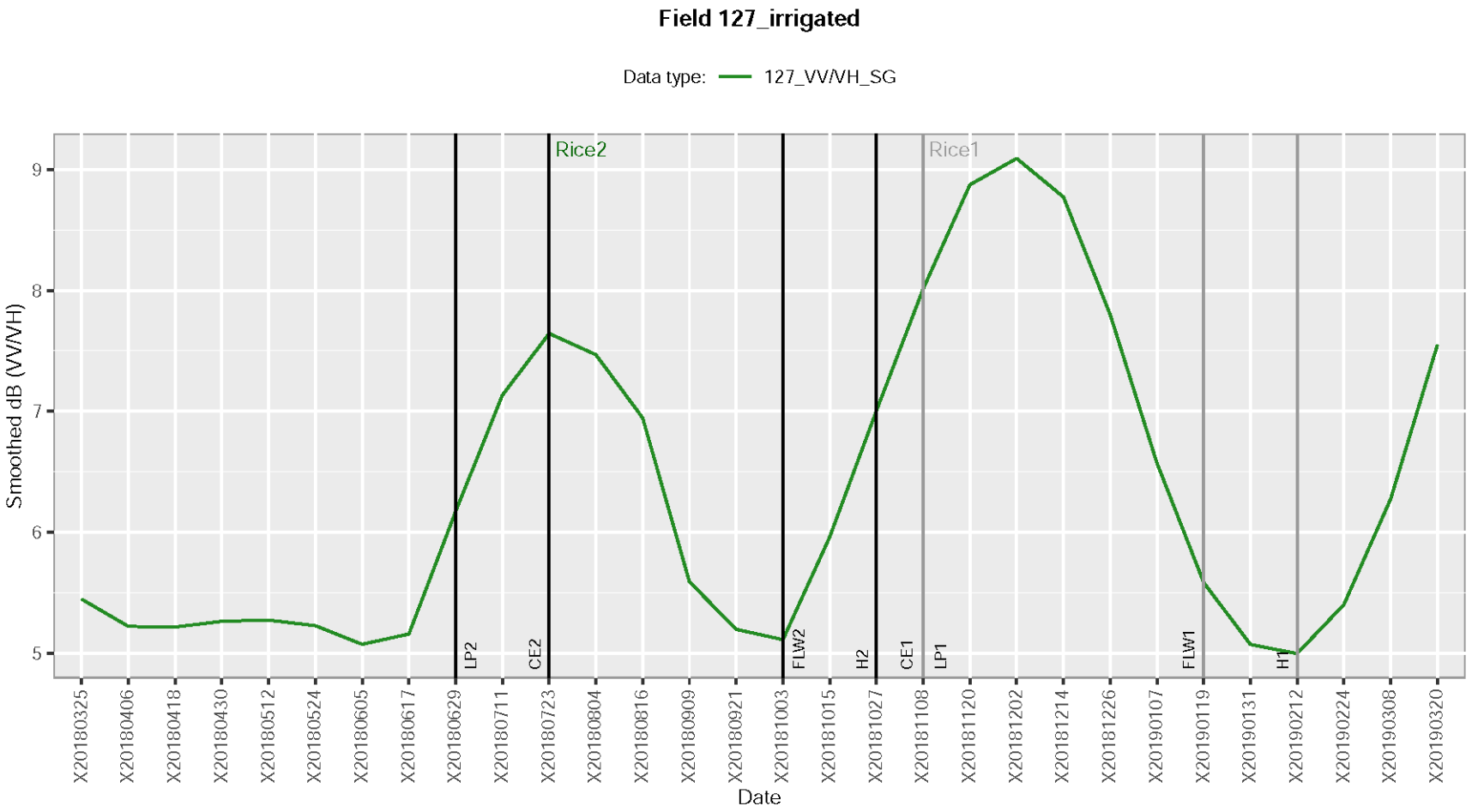
Field 127_irrigated
Data type: 127_VV/VH_SG
Rice2
Rice1
LP2
CE2
FLW2
H2
CE1
LP1
FLW1
H1
Smoothed dB (VV/VH)
9
8
7
6
5
X20180325
X20180406
X20180418
X20180430
X20180512
X20180524
X20180605
X20180617
X20180629
X20180711
X20180723
X20180804
X20180816
X20180909
X20180921
X20181003
X20181015
X20181027
X20181108
X20181120
X20181202
X20181214
X20181226
X20190107
X20190119
X20190131
X20190212
X20190224
X20190308
X20190320
Date

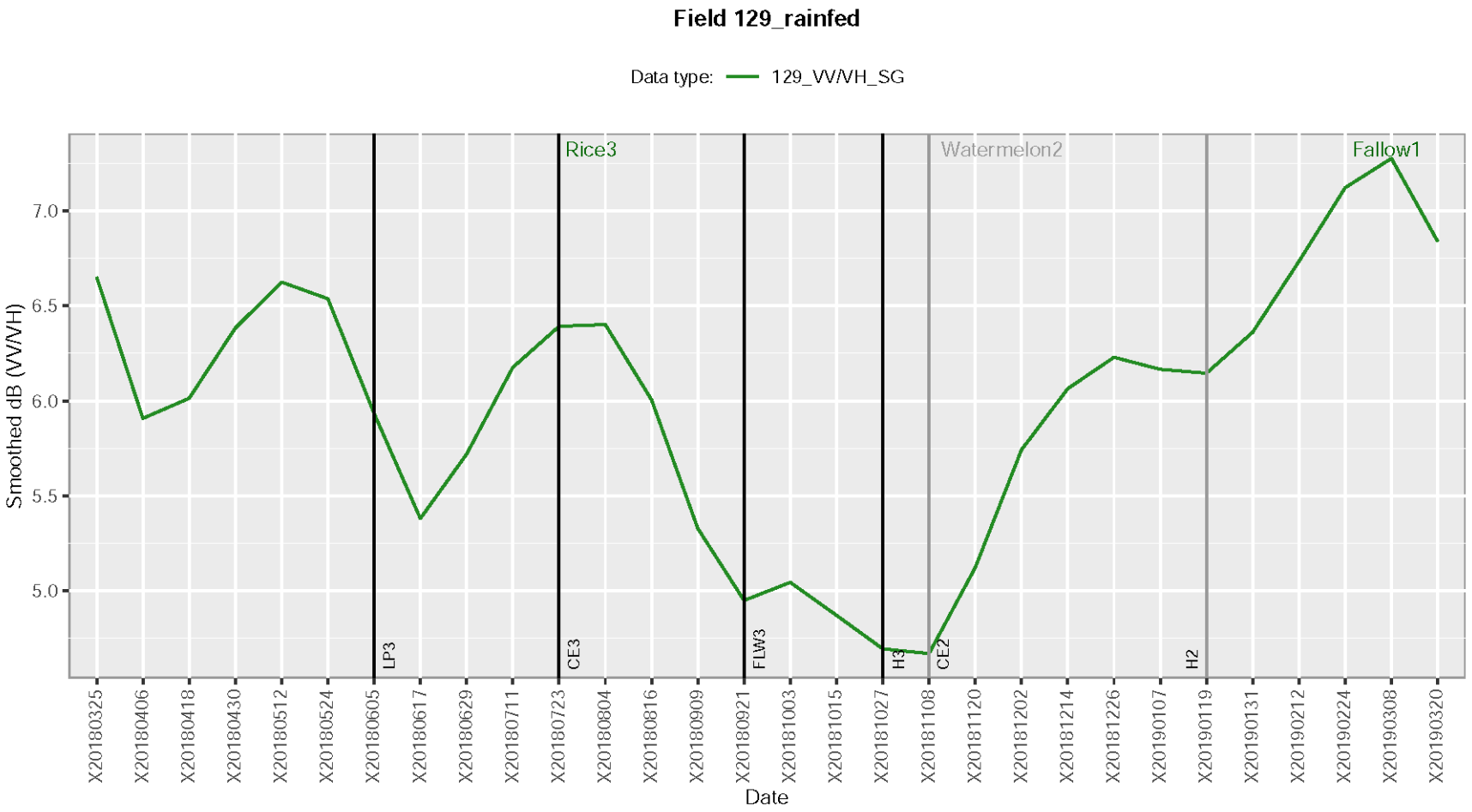
Field 129_rainfed
Data type: 129_VV/VH_SG
Rice3
Watermelon2
Fallow1
LP3
CE3
FLW3
H3
CE2
H2
Smoothed dB (VV/VH)
7.0
6.5
6.0
5.5
5.0
X20180325
X20180406
X20180418
X20180430
X20180512
X20180524
X20180605
X20180617
X20180629
X20180711
X20180723
X20180804
X20180816
X20180909
X20180921
X20181003
X20181015
X20181027
X20181108
X20181120
X20181202
X20181214
X20181226
X20190107
X20190119
X20190131
X20190212
X20190224
X20190308
X20190320
Date

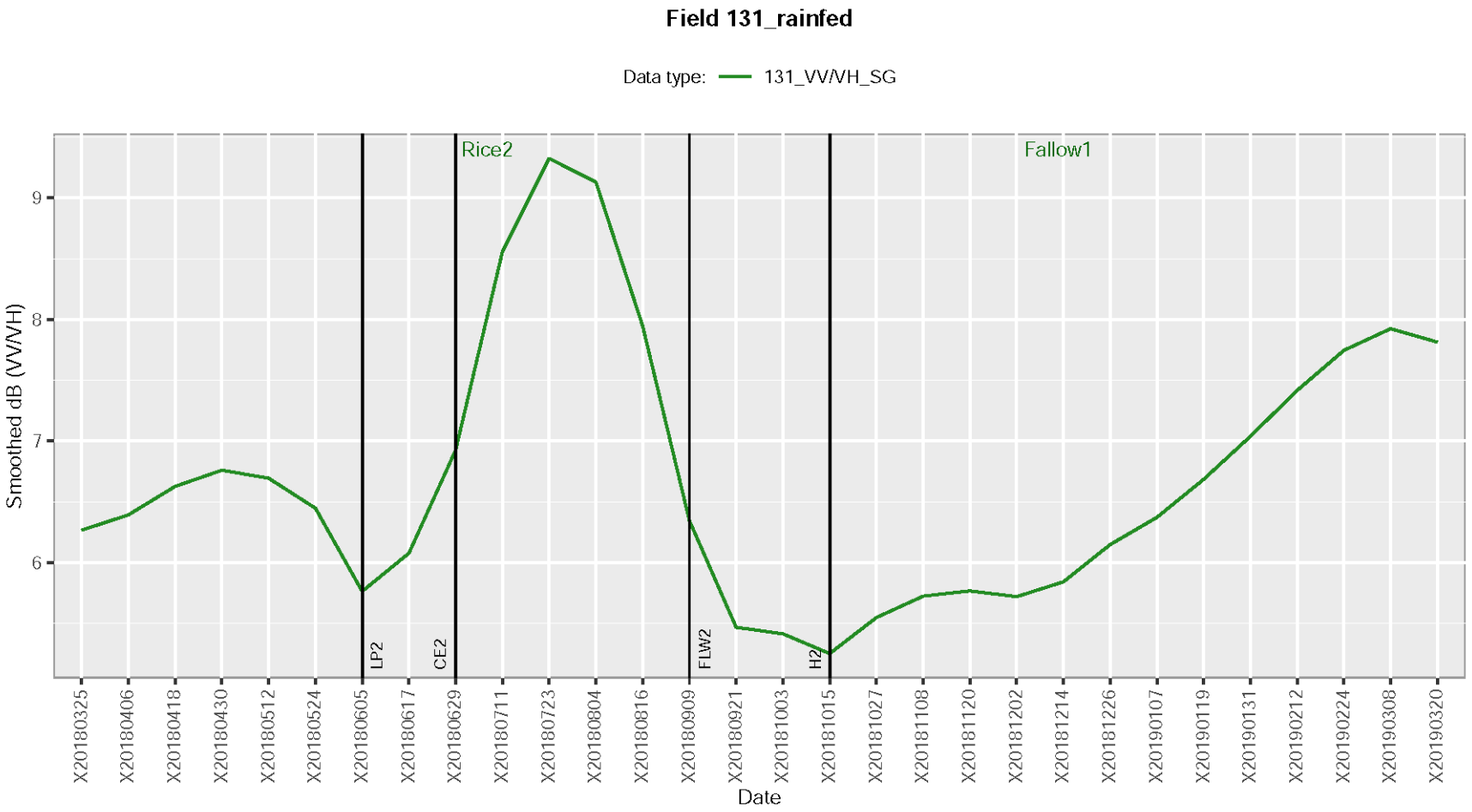
Field 131_rainfed
Data type:
131_VV/VH_SG
Rice2
Fallow1
LP2
CE2
FLW2
H2
Smoothed dB (VV/VH)
9
8
7
6
X20180325
X20180406
X20180418
X20180430
X20180512
X20180524
X20180605
X20180617
X20180629
X20180711
X20180723
X20180804
X20180816
X20180909
X20180921
X20181003
X20181015
X20181027
X20181108
X20181120
X20181202
X20181214
X20181226
X20190107
X20190119
X20190131
X20190212
X20190224
X20190308
X20190320
Date

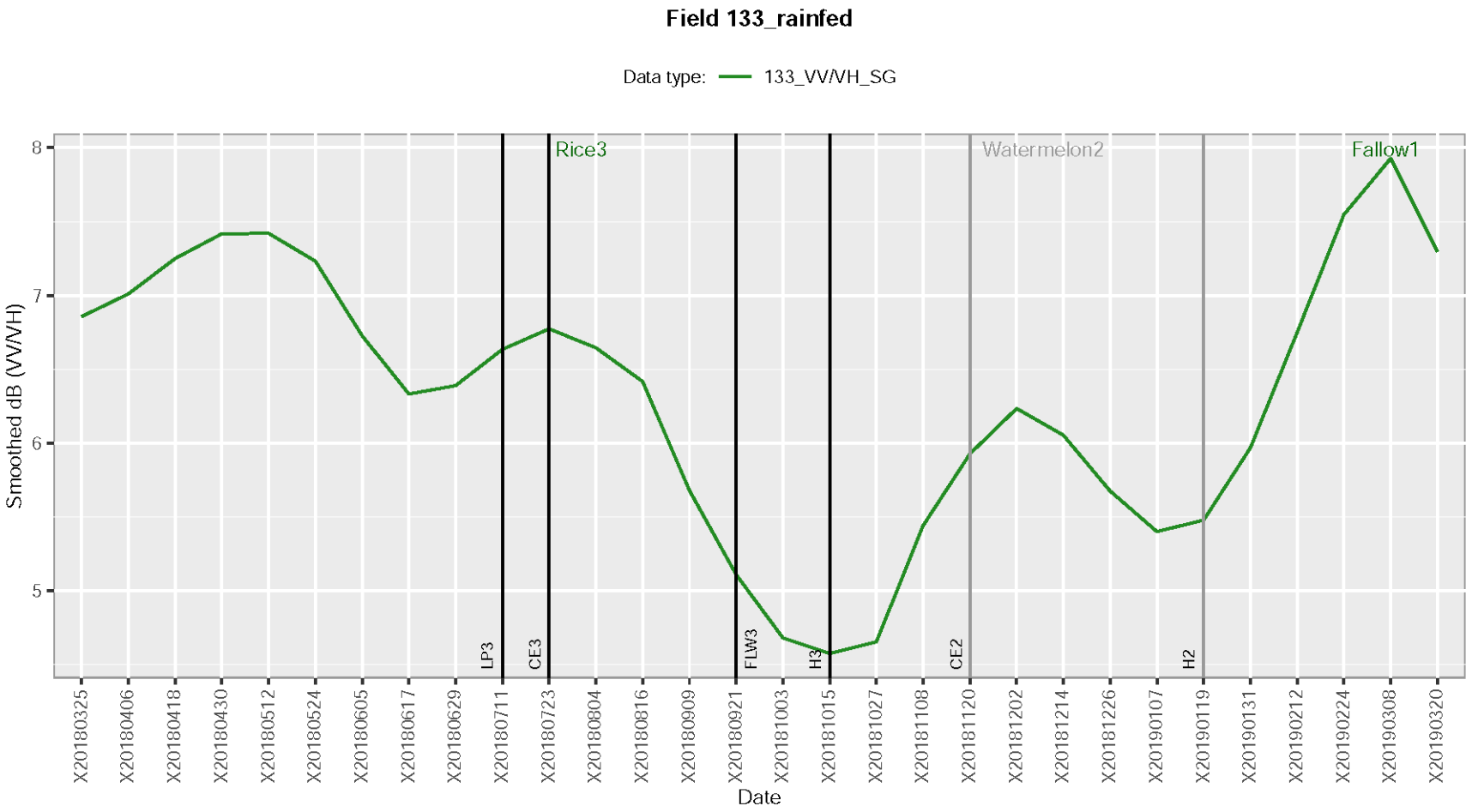
Field 133_rainfed
Data type: 133_VV/VH_SG
Smoothed dB (VV/VH)
8
7
6
5
Rice3
Watermelon2
Fallow1
LP3
CE3
FLW3
H3
CE2
H2
X20180325
X20180406
X20180418
X20180430
X20180512
X20180524
X20180605
X20180617
X20180629
X20180711
X20180723
X20180804
X20180816
X20180909
X20180921
X20181003
X20181015
X20181027
X20181108
X20181120
X20181202
X20181214
X20181226
X20190107
X20190119
X20190131
X20190212
X20190224
X20190308
X20190320
Date

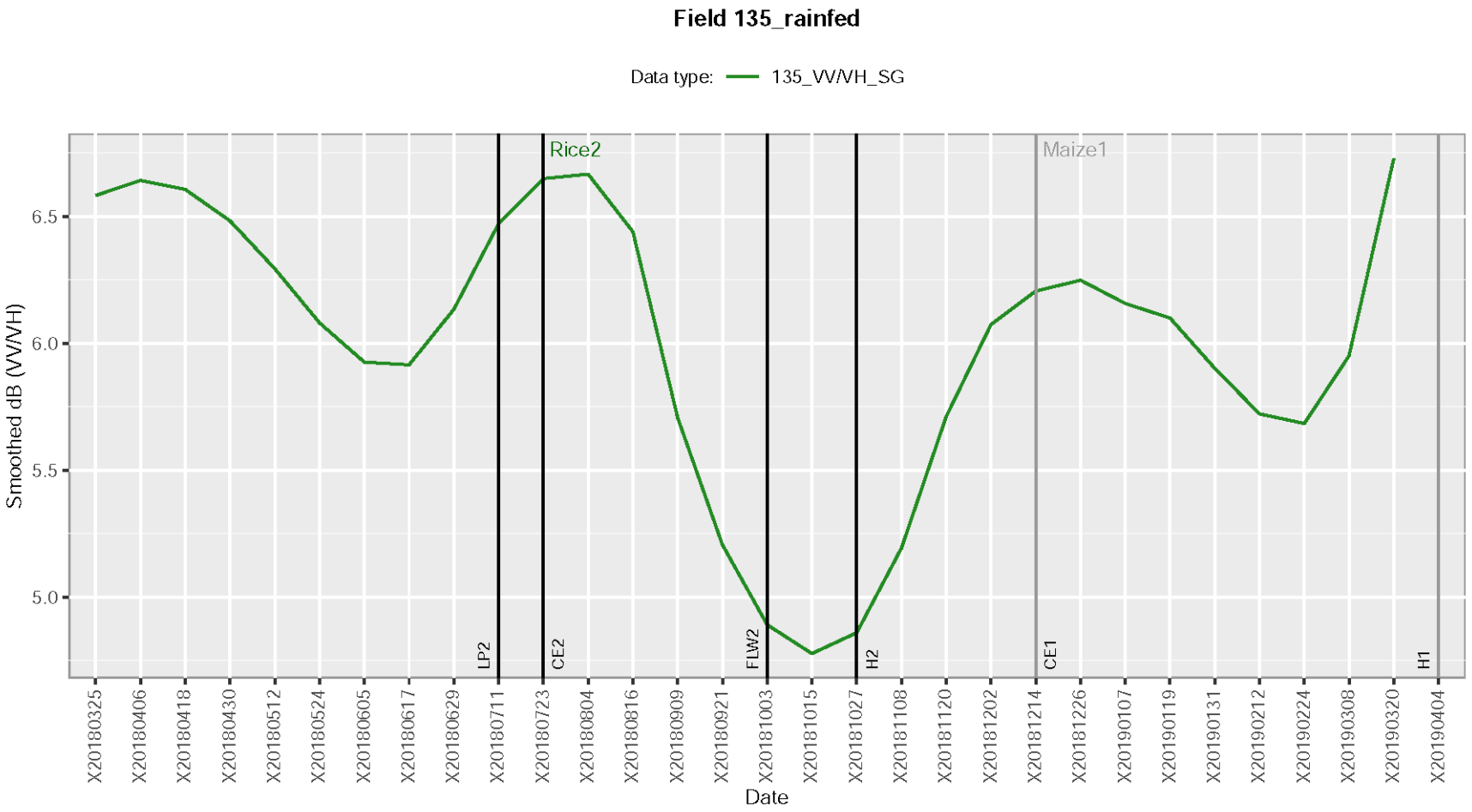
Field 135_rainfed
Data type: 135_VV/VH_SG
Rice2
Maize1
Smoothed dB (VV/VH)
6.5
6.0
5.5
5.0
LP2
CE2
FLW2
H2
CE1
H1
X20180325
X20180406
X20180418
X20180430
X20180512
X20180524
X20180605
X20180617
X20180629
X20180711
X20180723
X20180804
X20180816
X20180909
X20180921
X20181003
X20181015
X20181027
X20181108
X20181120
X20181202
X20181214
X20181226
X20190107
X20190119
X20190131
X20190212
X20190224
X20190308
X20190320
X20190404
Date

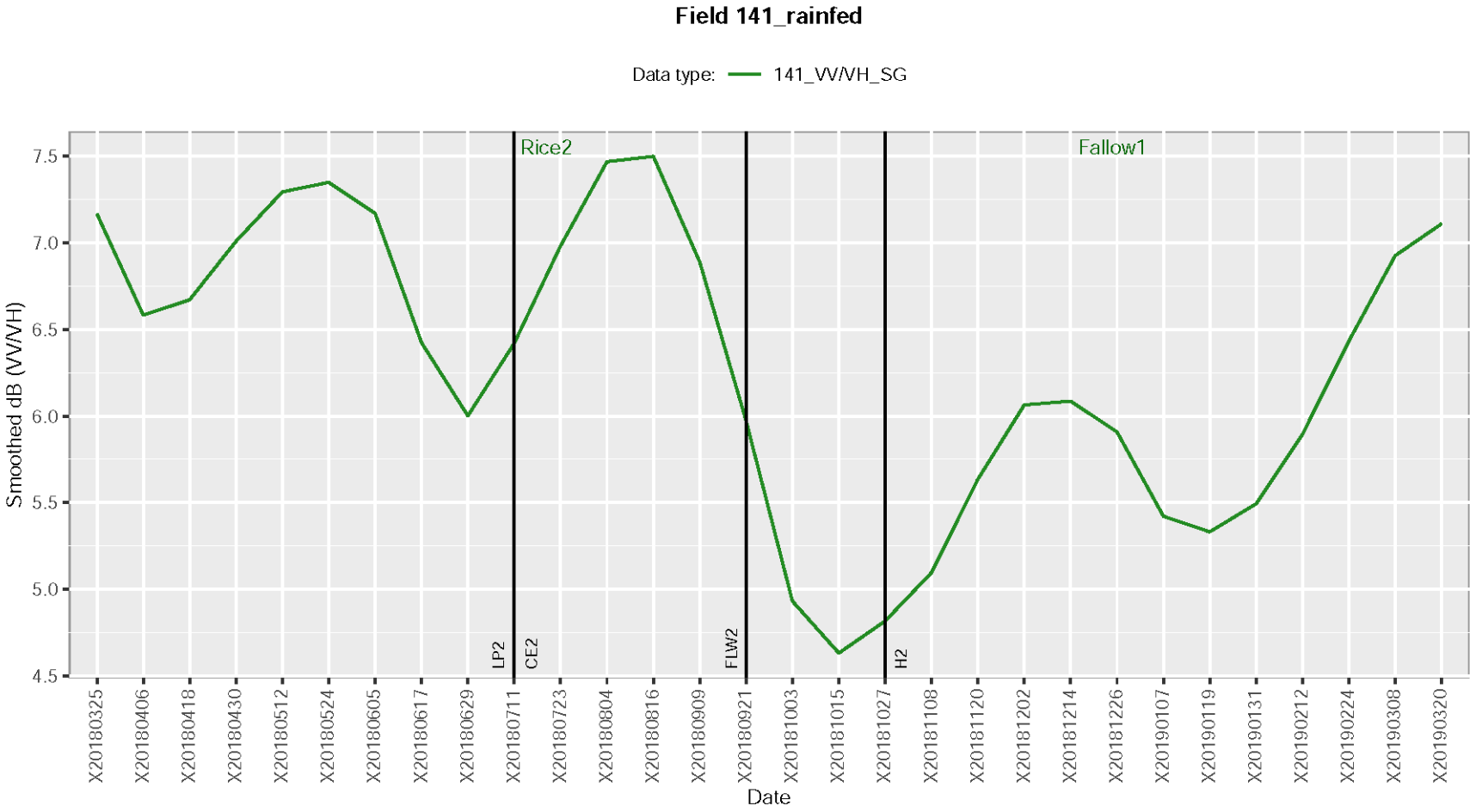
Field 141_rainfed
Data type: 141_VV/VH_SG
Rice2
Fallow1
LP2
CE2
FLW2
H2
Smoothed dB (VV/VH)
7.5
7.0
6.5
6.0
5.5
5.0
4.5
X20180325
X20180406
X20180418
X20180430
X20180512
X20180524
X20180605
X20180617
X20180629
X20180711
X20180723
X20180804
X20180816
X20180909
X20180921
X20181003
X20181015
X20181027
X20181108
X20181120
X20181202
X20181214
X20181226
X20190107
X20190119
X20190131
X20190212
X20190224
X20190308
X20190320
Date

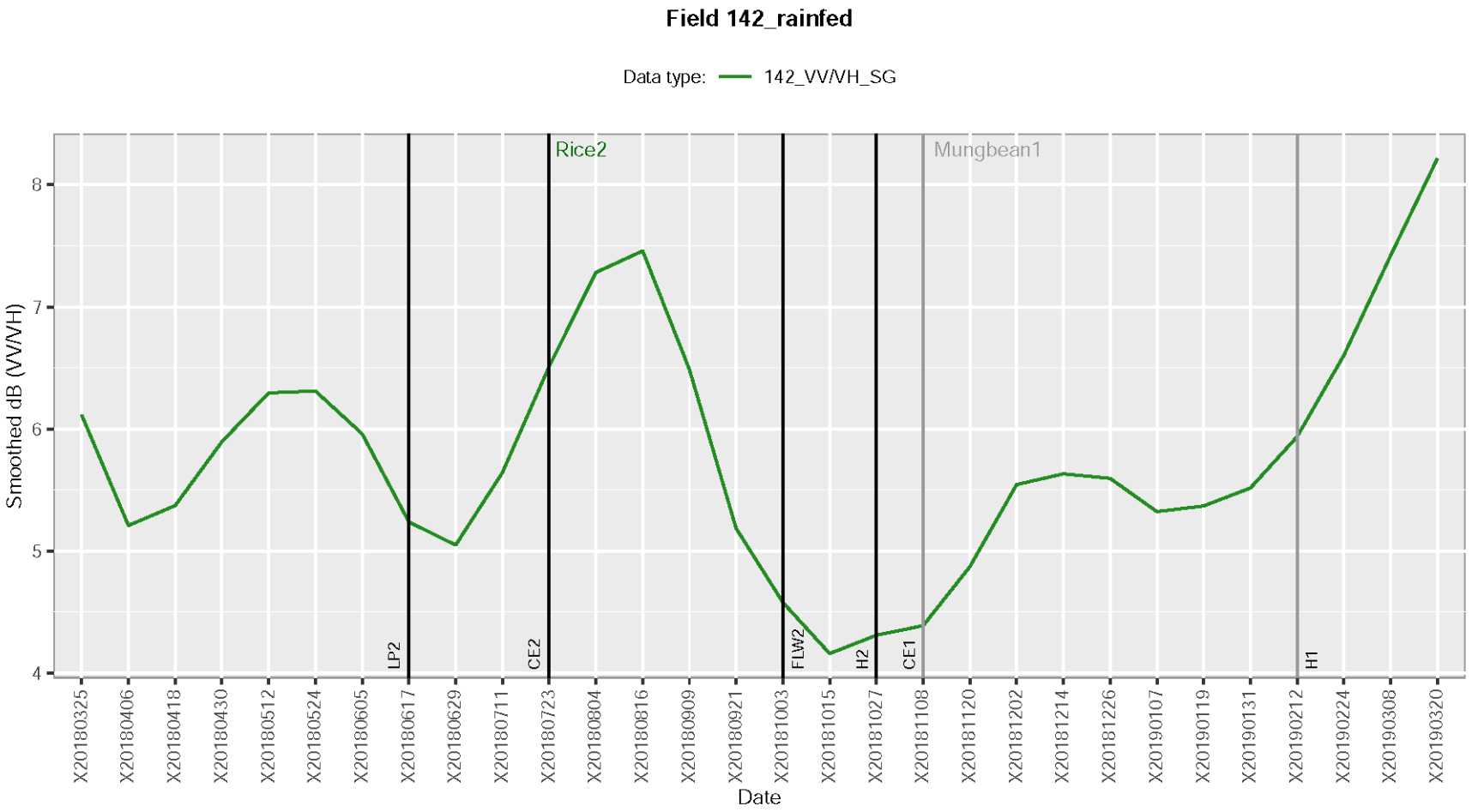
Field 142_rainfed
Data type: 142_VV/VH_SG
Rice2
Mungbean1
LP2
CE2
FLW2
H2
CE1
H1
Smoothed dB (VV/VH)
8
7
6
5
4
X20180325
X20180406
X20180418
X20180430
X20180512
X20180524
X20180605
X20180617
X20180629
X20180711
X20180723
X20180804
X20180816
X20180909
X20180921
X20181003
X20181015
X20181027
X20181108
X20181120
X20181202
X20181214
X20181226
X20190107
X20190119
X20190131
X20190212
X20190224
X20190308
X20190320
Date

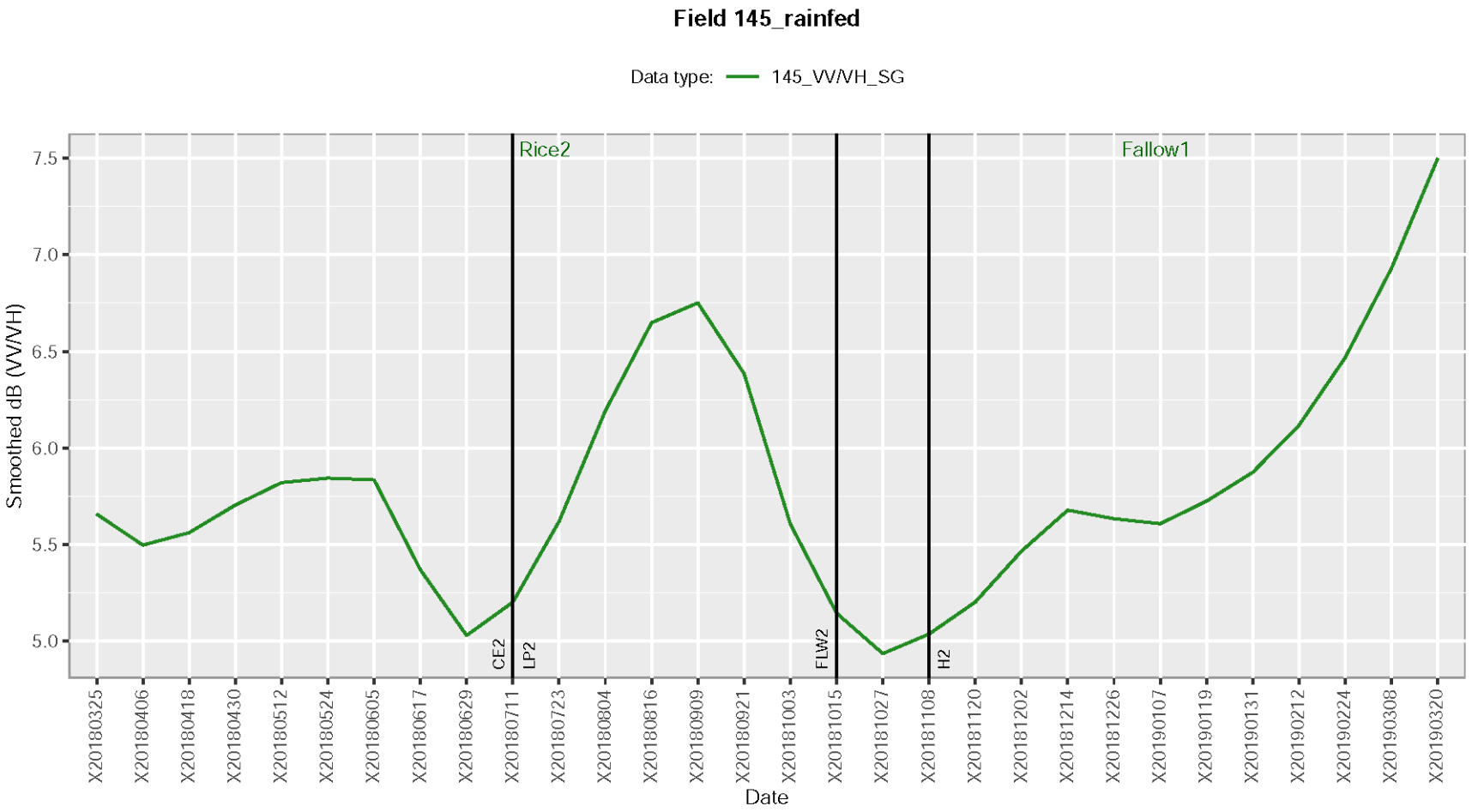
Field 145_rainfed
Data type: 145_VV/VH_SG
Rice2
Fallow1
CE2
LP2
FLW2
H2
Smoothed dB (VV/VH)
7.5
7.0
6.5
6.0
5.5
5.0
X20180325
X20180406
X20180418
X20180430
X20180512
X20180524
X20180605
X20180617
X20180629
X20180711
X20180723
X20180804
X20180816
X20180909
X20180921
X20181003
X20181015
X20181027
X20181108
X20181120
X20181202
X20181214
X20181226
X20190107
X20190119
X20190131
X20190212
X20190224
X20190308
X20190320
Date

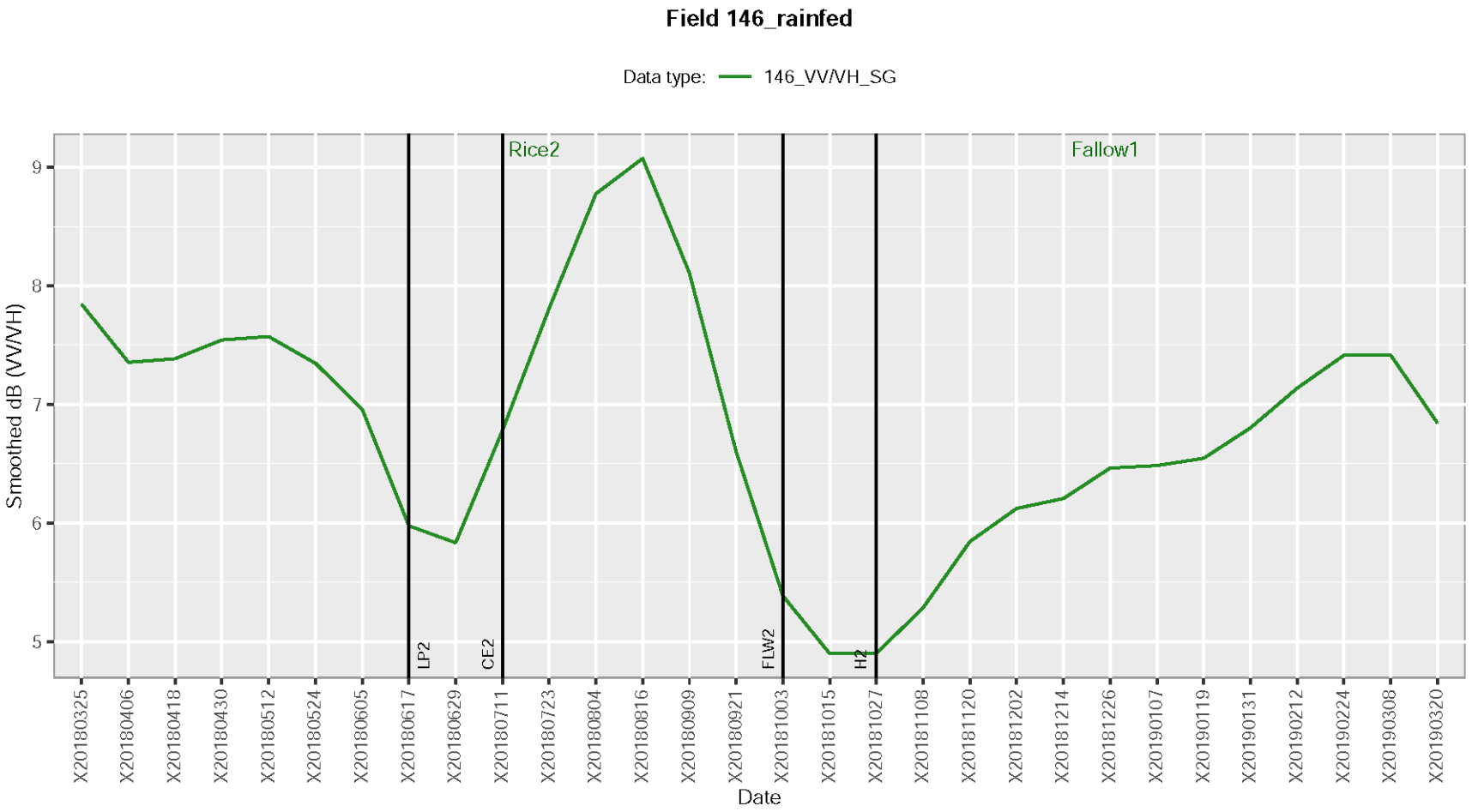
Field 146_rainfed
Data type: 146_VV/VH_SG
Rice2
Fallow1
LP2
CE2
FLW2
H2
Smoothed dB (VV/VH)
9
8
7
6
5
X20180325
X20180406
X20180418
X20180430
X20180512
X20180524
X20180605
X20180617
X20180629
X20180711
X20180723
X20180804
X20180816
X20180909
X20180921
X20181003
X20181015
X20181027
X20181108
X20181120
X20181202
X20181214
X20181226
X20190107
X20190119
X20190131
X20190212
X20190224
X20190308
X20190320
Date

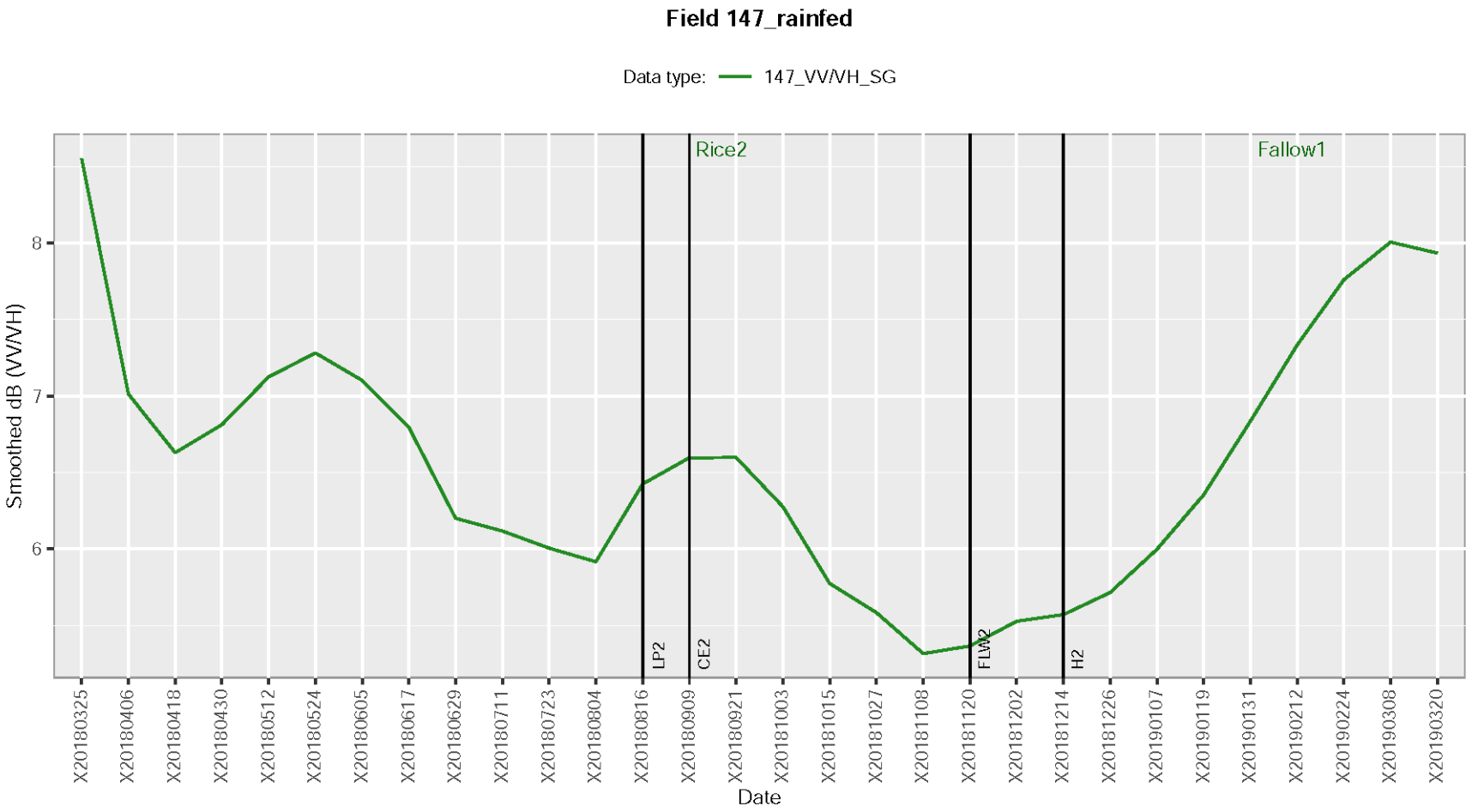
Field 147_rainfed
Data type: 147_VV/VH_SG
Rice2
Fallow1
LP2
CE2
FLW2
H2
Smoothed dB (VV/VH)
8
7
6
X20180325
X20180406
X20180418
X20180430
X20180512
X20180524
X20180605
X20180617
X20180629
X20180711
X20180723
X20180804
X20180816
X20180909
X20180921
X20181003
X20181015
X20181027
X20181108
X20181120
X20181202
X20181214
X20181226
X20190107
X20190119
X20190131
X20190212
X20190224
X20190308
X20190320
Date

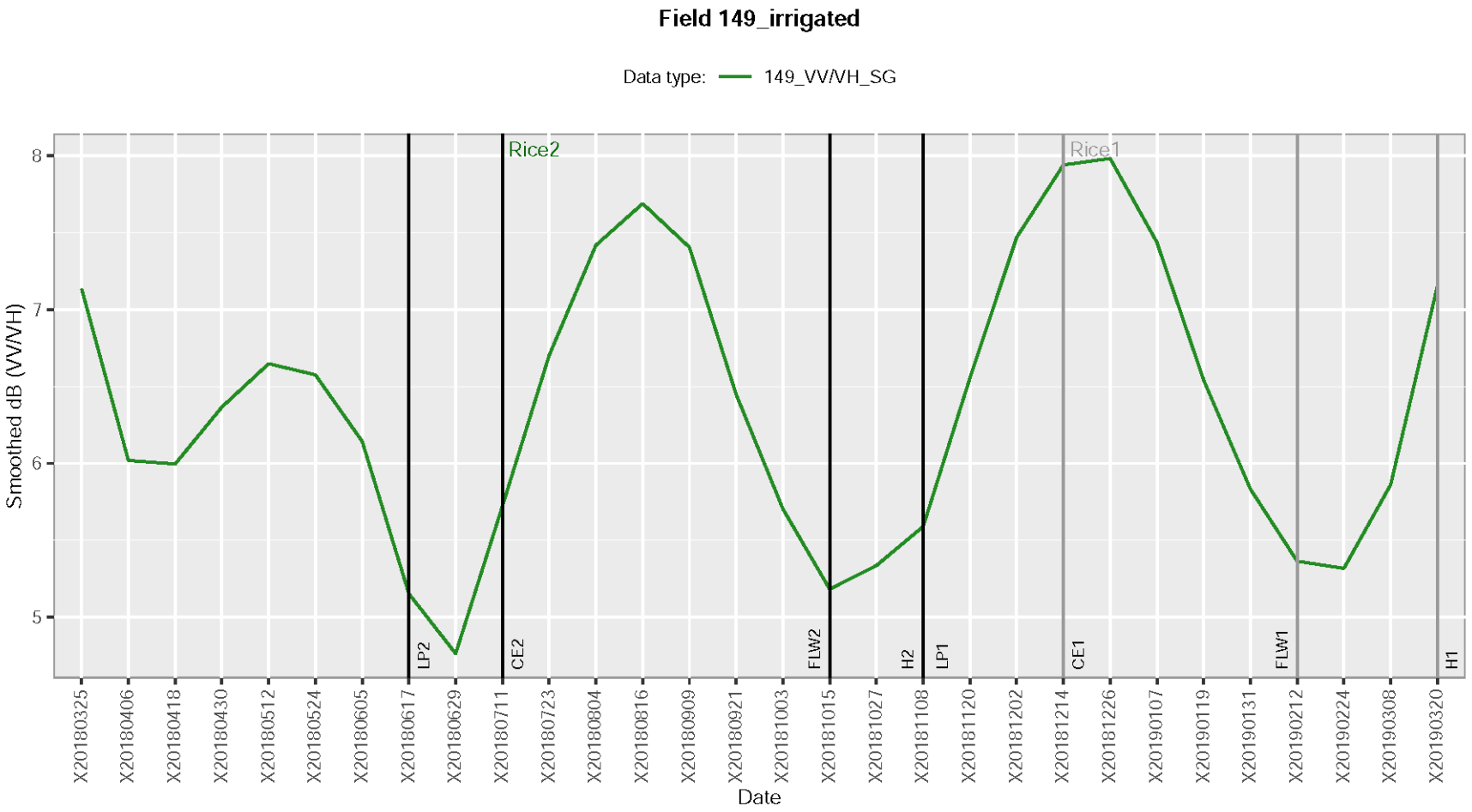
Field 149_irrigated
Data type: 149_VV/VH_SG
Smoothed dB (VV/VH)
8
7
6
5
Rice2
Rice1
LP2
CE2
FLW2
H2
LP1
CE1
FLW1
H1
X20180325
X20180406
X20180418
X20180430
X20180512
X20180524
X20180605
X20180617
X20180629
X20180711
X20180723
X20180804
X20180816
X20180909
X20180921
X20181003
X20181015
X20181027
X20181108
X20181120
X20181202
X20181214
X20181226
X20190107
X20190119
X20190131
X20190212
X20190224
X20190308
X20190320
Date

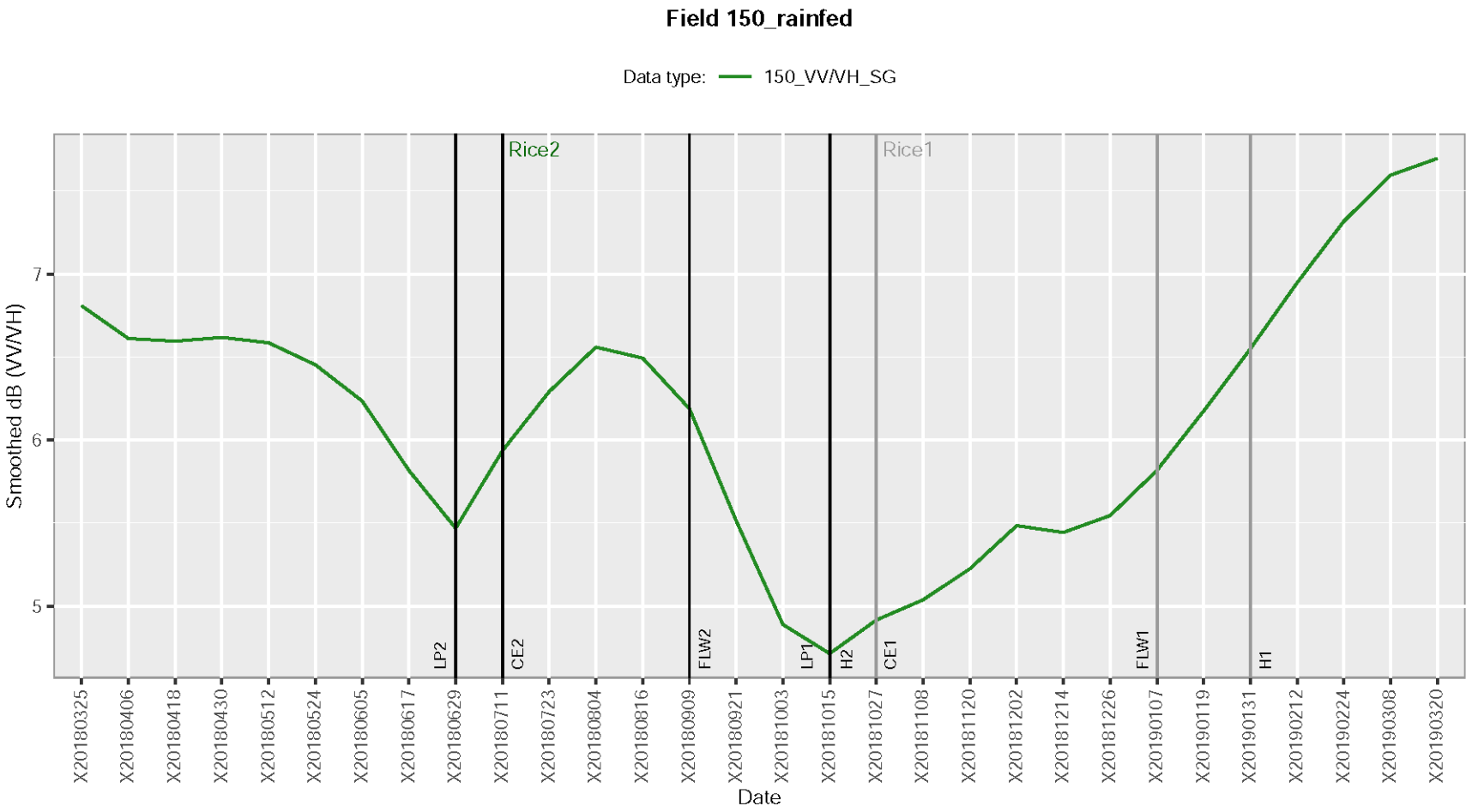
Field 150_rainfed
Data type: 150_VV/VH_SG
Rice2
Rice1
Smoothed dB (VV/VH)
7
6
5
LP2
CE2
FLW2
LP1
H2
CE1
FLW1
H1
X20180325
X20180406
X20180418
X20180430
X20180512
X20180524
X20180605
X20180617
X20180629
X20180711
X20180723
X20180804
X20180816
X20180909
X20180921
X20181003
X20181015
X20181027
X20181108
X20181120
X20181202
X20181214
X20181226
X20190107
X20190119
X20190131
X20190212
X20190224
X20190308
X20190320
Date

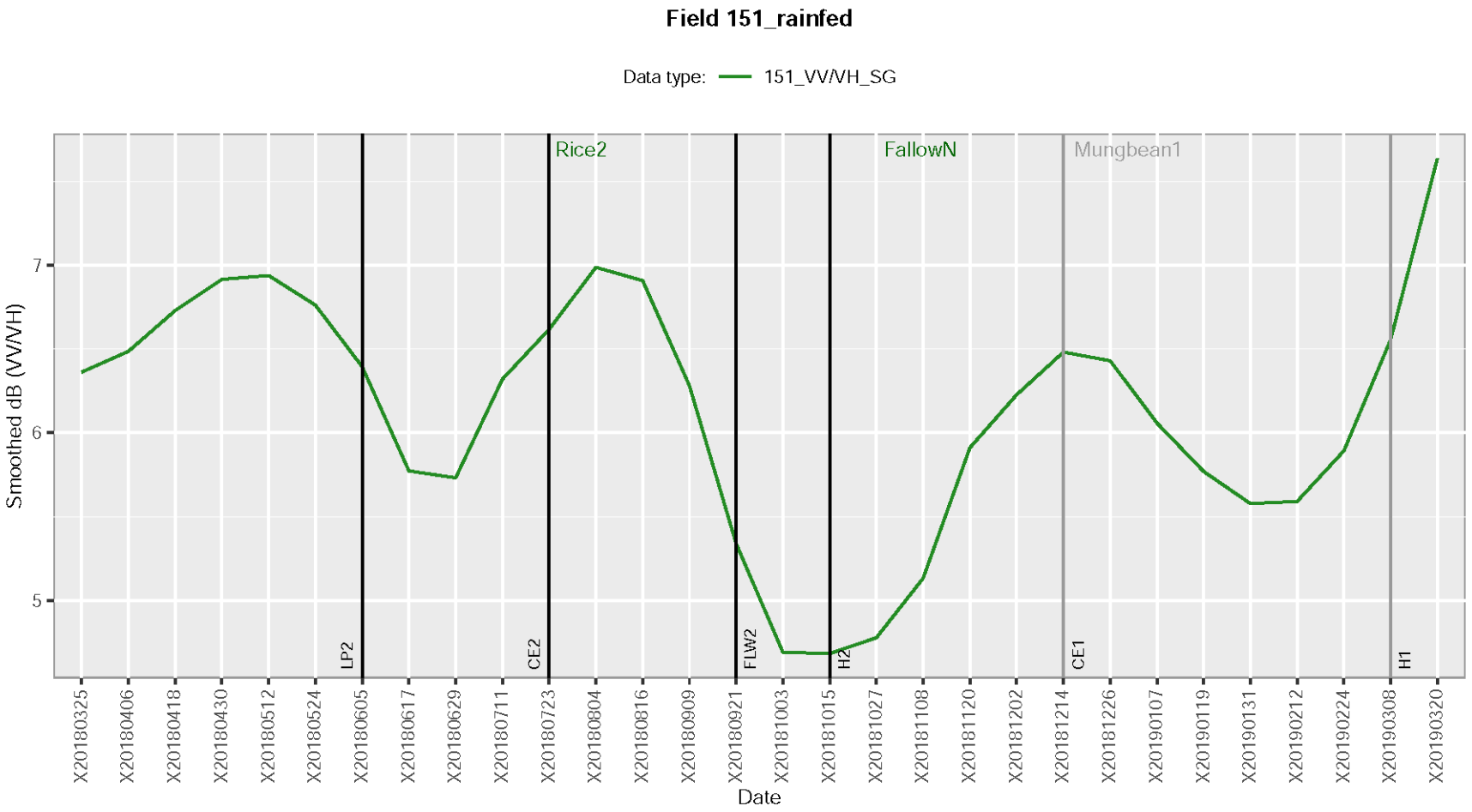
Field 151_rainfed
Data type: 151_VV/VH_SG
Rice2
FallowN
Mungbean1
LP2
CE2
FLW2
H2
CE1
H1
Smoothed dB (VV/VH)
7
6
5
X20180325
X20180406
X20180418
X20180430
X20180512
X20180524
X20180605
X20180617
X20180629
X20180711
X20180723
X20180804
X20180816
X20180909
X20180921
X20181003
X20181015
X20181027
X20181108
X20181120
X20181202
X20181214
X20181226
X20190107
X20190119
X20190131
X20190212
X20190224
X20190308
X20190320
Date

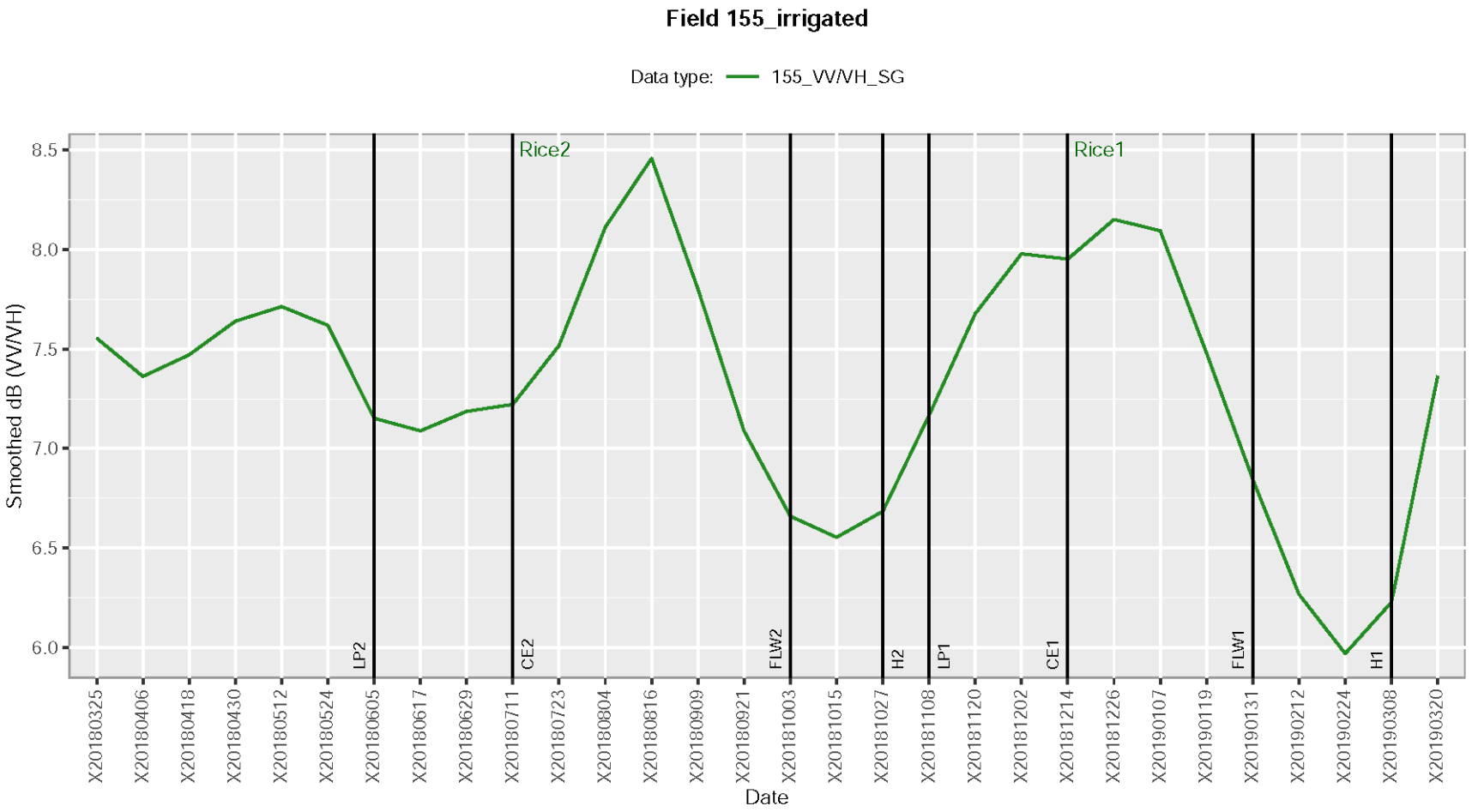
Field 155_irrigated
Data type: 155_VV/VH_SG
Smoothed dB (VV/VH)
8.5
8.0
7.5
7.0
6.5
6.0
Rice2
Rice1
LP2
CE2
FLW2
H2
LP1
CE1
FLW1
H1
X20180325
X20180406
X20180418
X20180430
X20180512
X20180524
X20180605
X20180617
X20180629
X20180711
X20180723
X20180804
X20180816
X20180909
X20180921
X20181003
X20181015
X20181027
X20181108
X20181120
X20181202
X20181214
X20181226
X20190107
X20190119
X20190131
X20190212
X20190224
X20190308
X20190320
Date

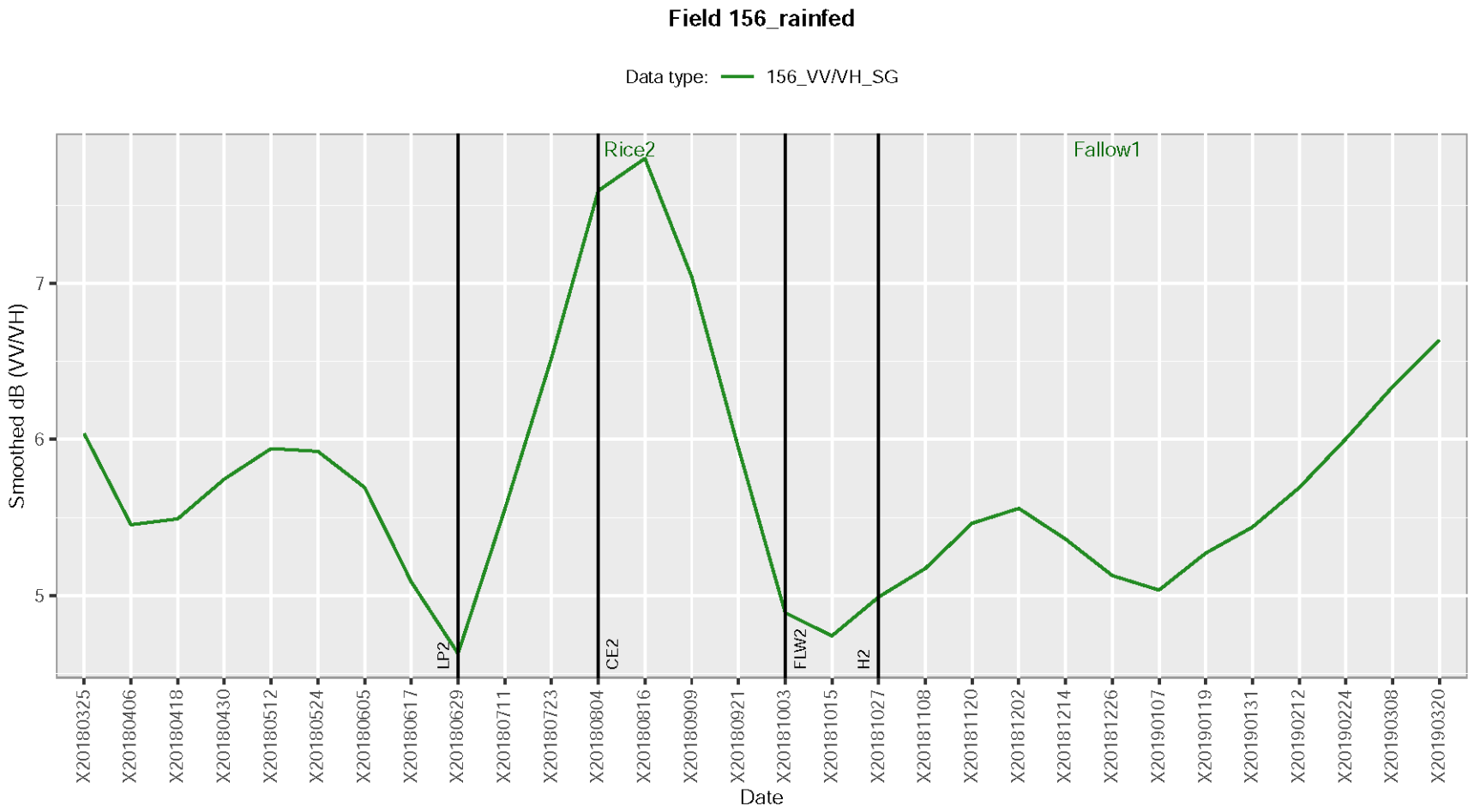
Field 156_rainfed
Data type: 156_VV/VH_SG
Rice2
Fallow1
LP2
CE2
FLW2
H2
Smoothed dB (VV/VH)
7
6
5
X20180325
X20180406
X20180418
X20180430
X20180512
X20180524
X20180605
X20180617
X20180629
X20180711
X20180723
X20180804
X20180816
X20180909
X20180921
X20181003
X20181015
X20181027
X20181108
X20181120
X20181202
X20181214
X20181226
X20190107
X20190119
X20190131
X20190212
X20190224
X20190308
X20190320
Date

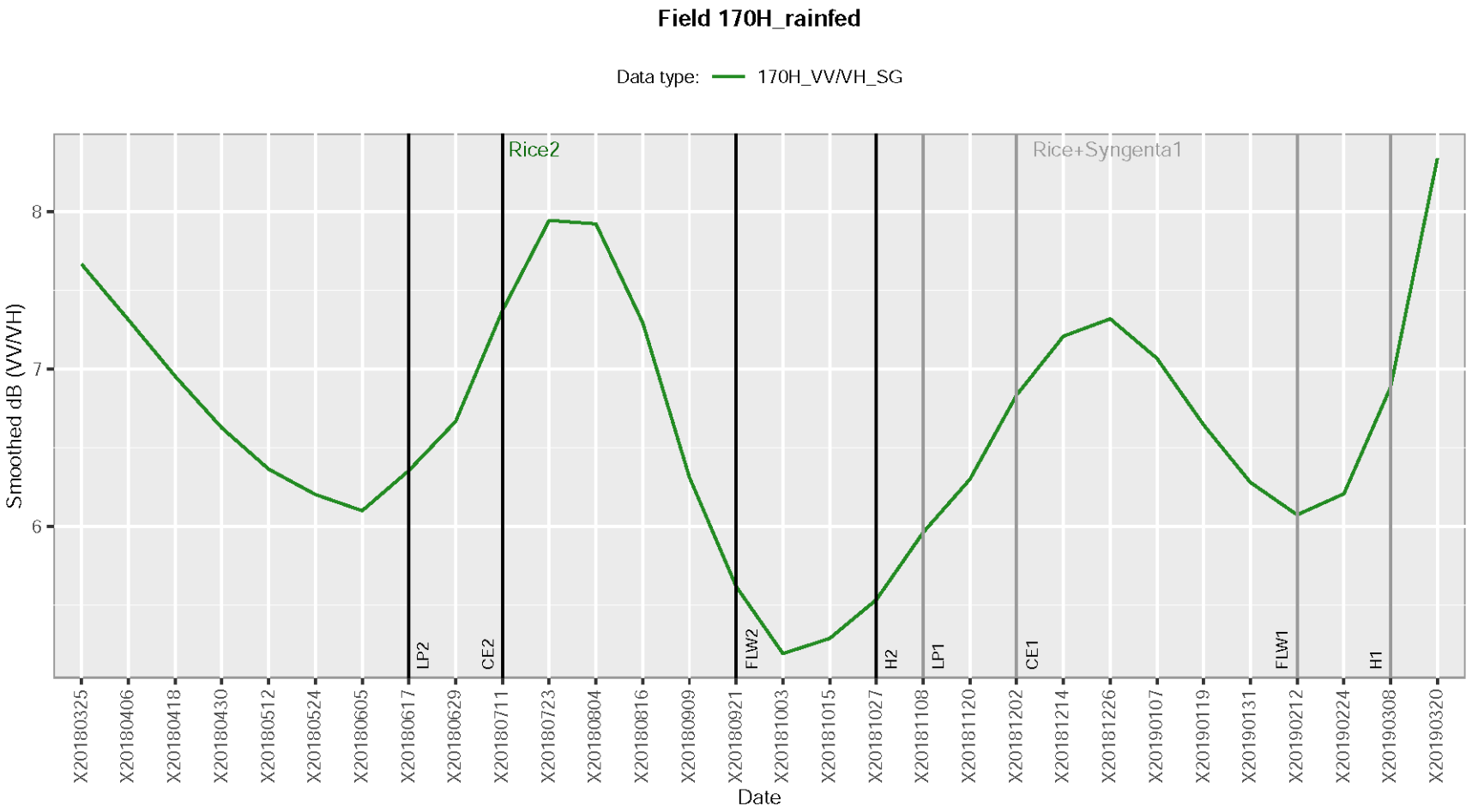
Field 170H_rainfed
Data type: 170H_VV/VH_SG
Rice2
Rice+Syngenta1
Smoothed dB (VV/VH)
8
7
6
LP2
CE2
FLW2
H2
LP1
CE1
FLW1
H1
X20180325
X20180406
X20180418
X20180430
X20180512
X20180524
X20180605
X20180617
X20180629
X20180711
X20180723
X20180804
X20180816
X20180909
X20180921
X20181003
X20181015
X20181027
X20181108
X20181120
X20181202
X20181214
X20181226
X20190107
X20190119
X20190131
X20190212
X20190224
X20190308
X20190320
Date

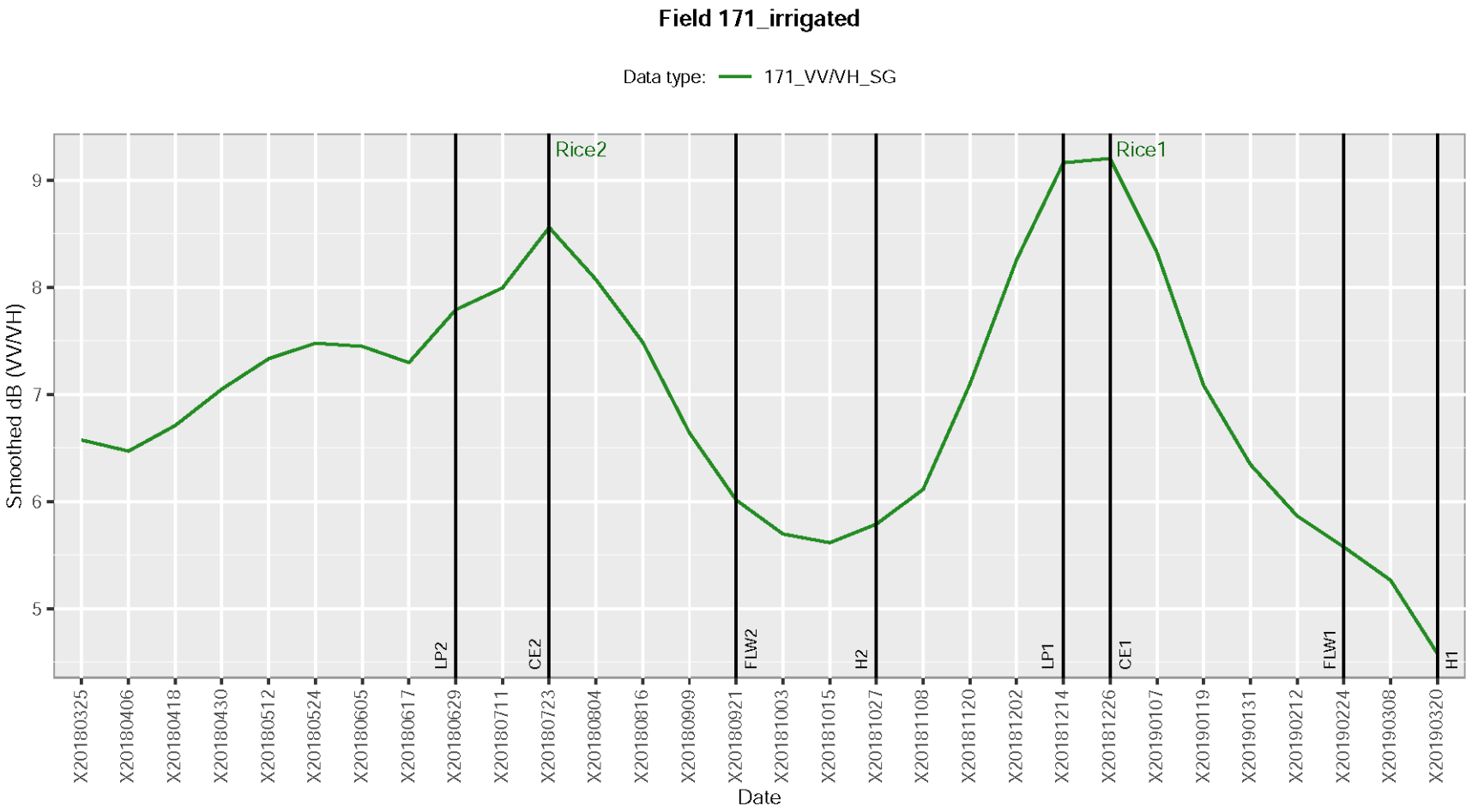
Field 171_irrigated
Data type: 171_VV/VH_SG
Rice2
Rice1
LP2
CE2
FLW2
H2
LP1
CE1
FLW1
H1
Smoothed dB (VV/VH)
9
8
7
6
5
X20180325
X20180406
X20180418
X20180430
X20180512
X20180524
X20180605
X20180617
X20180629
X20180711
X20180723
X20180804
X20180816
X20180909
X20180921
X20181003
X20181015
X20181027
X20181108
X20181120
X20181202
X20181214
X20181226
X20190107
X20190119
X20190131
X20190212
X20190224
X20190308
X20190320
Date

Time series for Iloilo VH and VV polarisations:

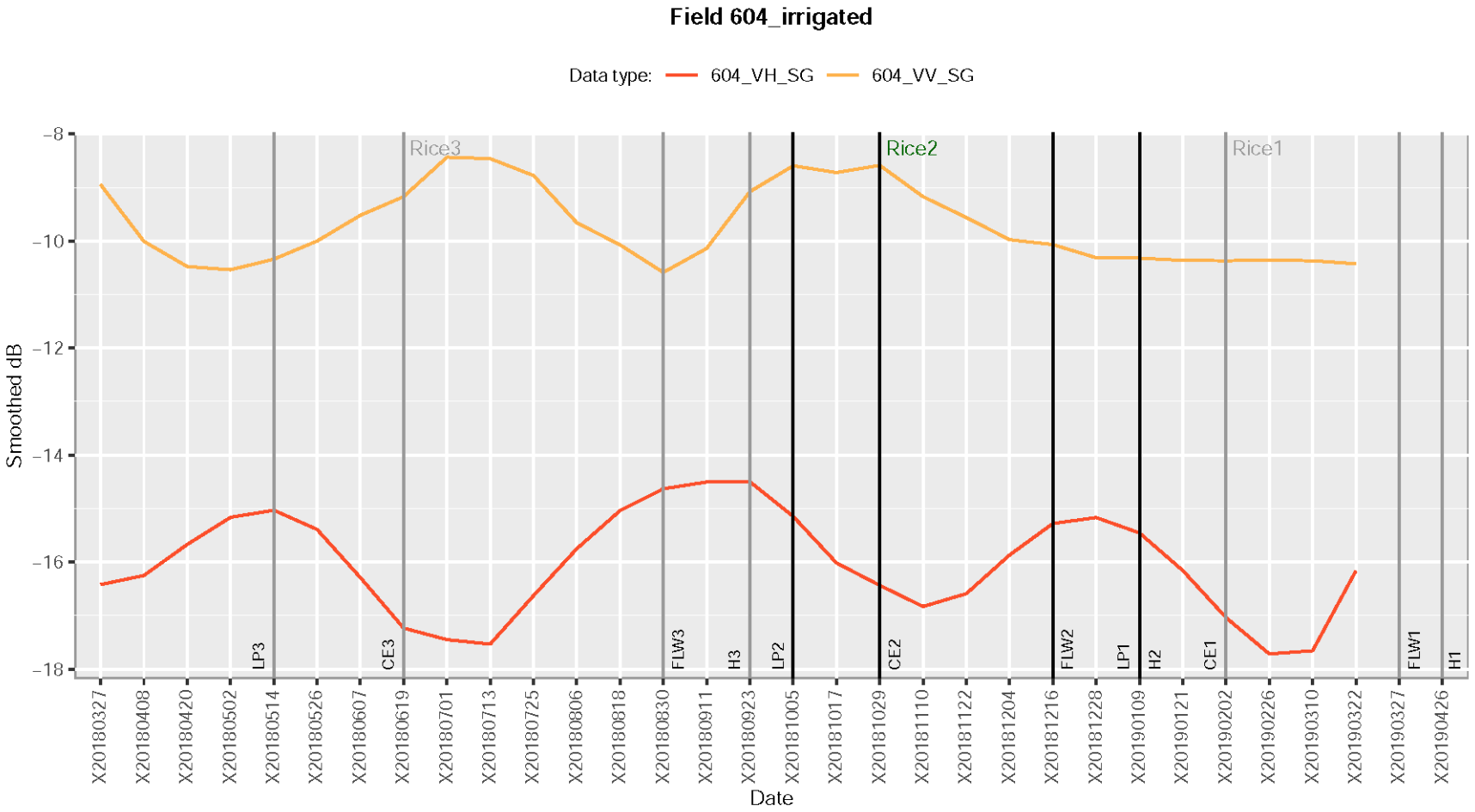

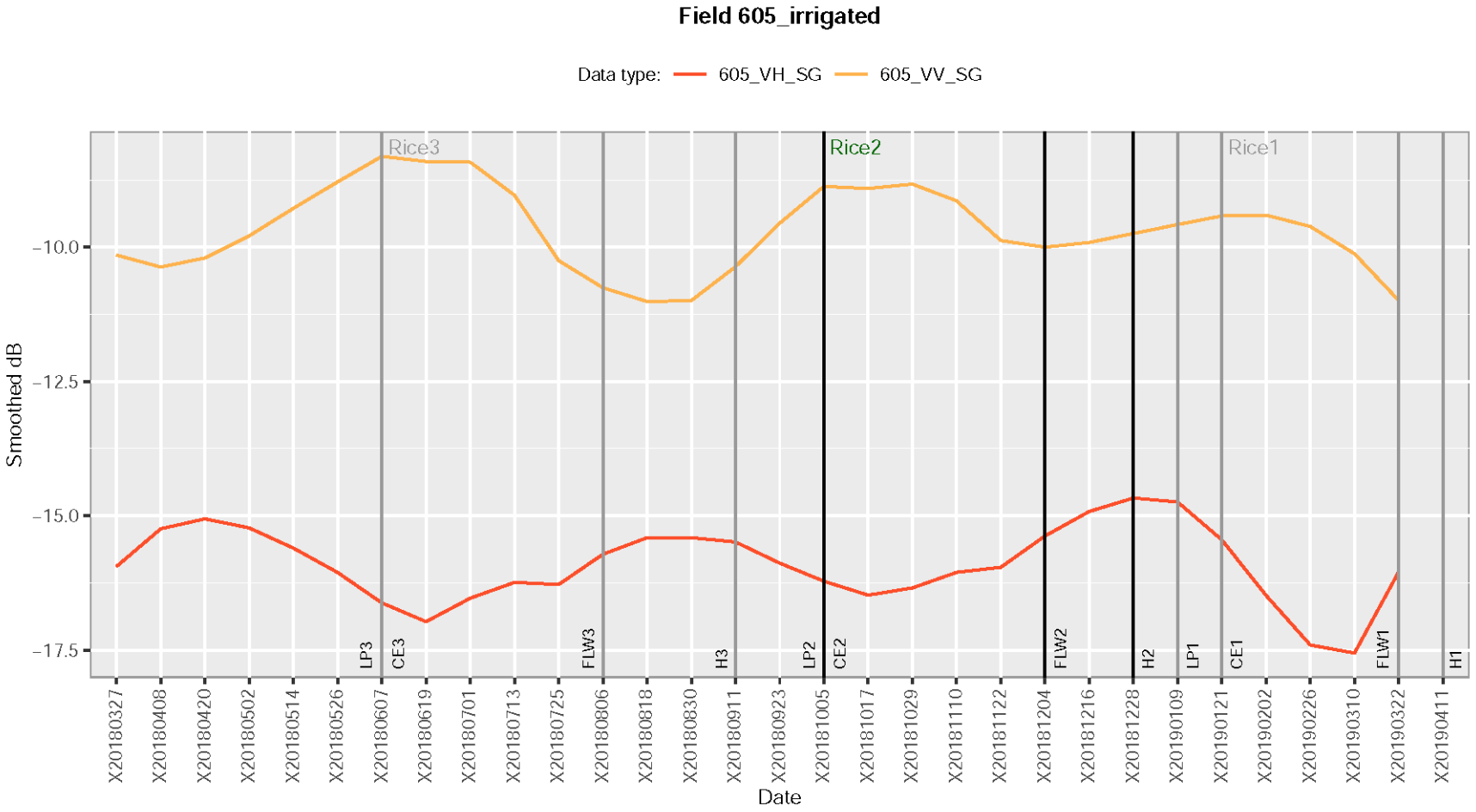
Field 605_irrigated
Data type: 605_VH_SG 605_VV_SG
Rice3
Rice2
Rice1
−10.0
−12.5
−15.0
−17.5
Smoothed dB
LP3
CE3
FLW3
H3
LP2
CE2
FLW2
H2
LP1
CE1
FLW1
H1
X20180327
X20180408
X20180420
X20180502
X20180514
X20180526
X20180607
X20180619
X20180701
X20180713
X20180725
X20180806
X20180818
X20180830
X20180911
X20180923
X20181005
X20181017
X20181029
X20181110
X20181122
X20181204
X20181216
X20181228
X20190109
X20190121
X20190202
X20190226
X20190310
X20190322
X20190411
Date

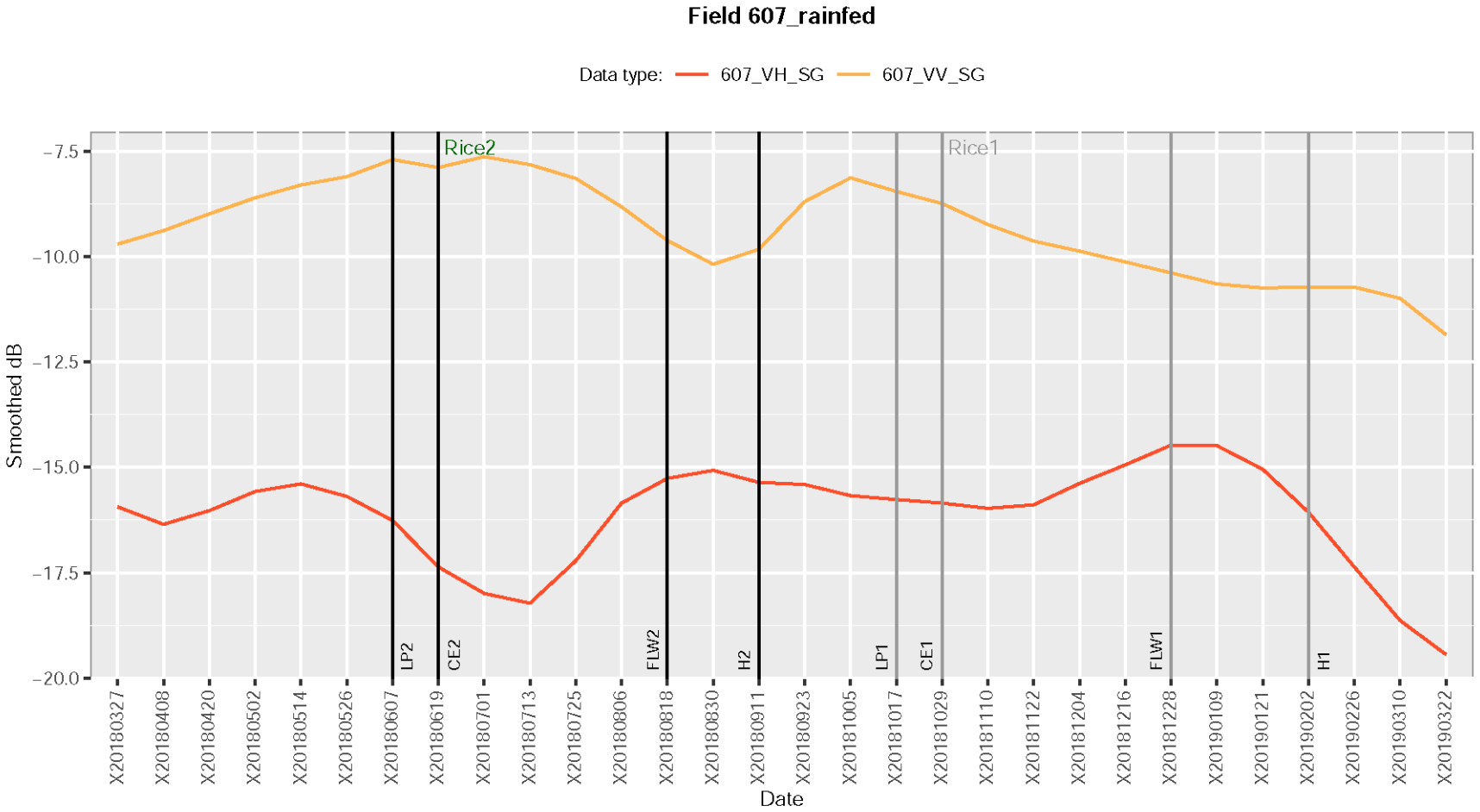
Field 607_rainfed
Data type: 607_VH_SG 607_VV_SG
Rice2
Rice1
LP2
CE2
FLW2
H2
LP1
CE1
FLW1
H1
Smoothed dB
−7.5
−10.0
−12.5
−15.0
−17.5
−20.0
X20180327
X20180408
X20180420
X20180502
X20180514
X20180526
X20180607
X20180619
X20180701
X20180713
X20180725
X20180806
X20180818
X20180830
X20180911
X20180923
X20181005
X20181017
X20181029
X20181110
X20181122
X20181204
X20181216
X20181228
X20190109
X20190121
X20190202
X20190226
X20190310
X20190322
Date

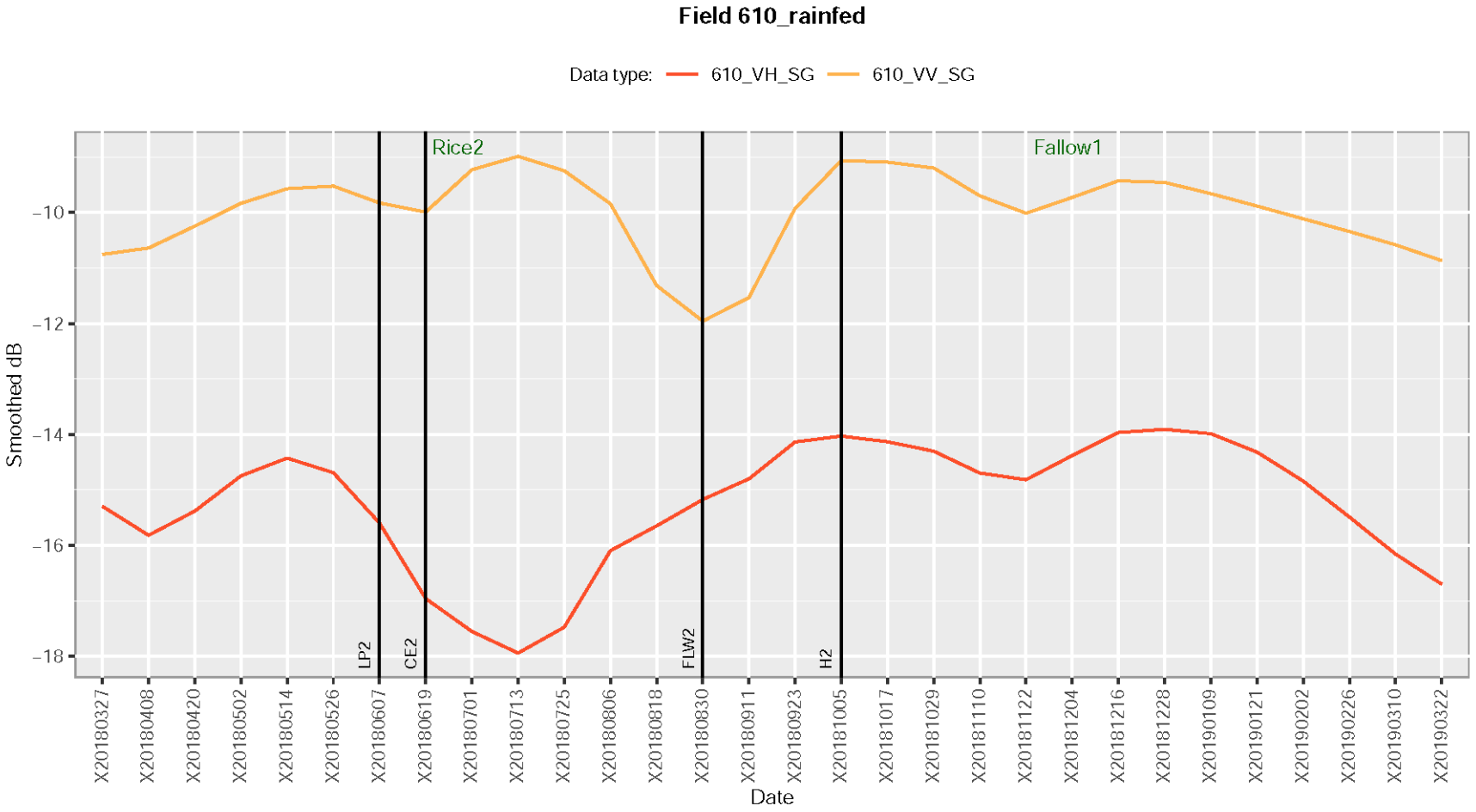
Field 610_rainfed
Data type: 610_VH_SG 610_VV_SG
Rice2
Fallow1
LP2
CE2
FLW2
H2
Smoothed dB
−10
−12
−14
−16
−18
X20180327
X20180408
X20180420
X20180502
X20180514
X20180526
X20180607
X20180619
X20180701
X20180713
X20180725
X20180806
X20180818
X20180830
X20180911
X20180923
X20181005
X20181017
X20181029
X20181110
X20181122
X20181204
X20181216
X20181228
X20190109
X20190121
X20190202
X20190226
X20190310
X20190322
Date

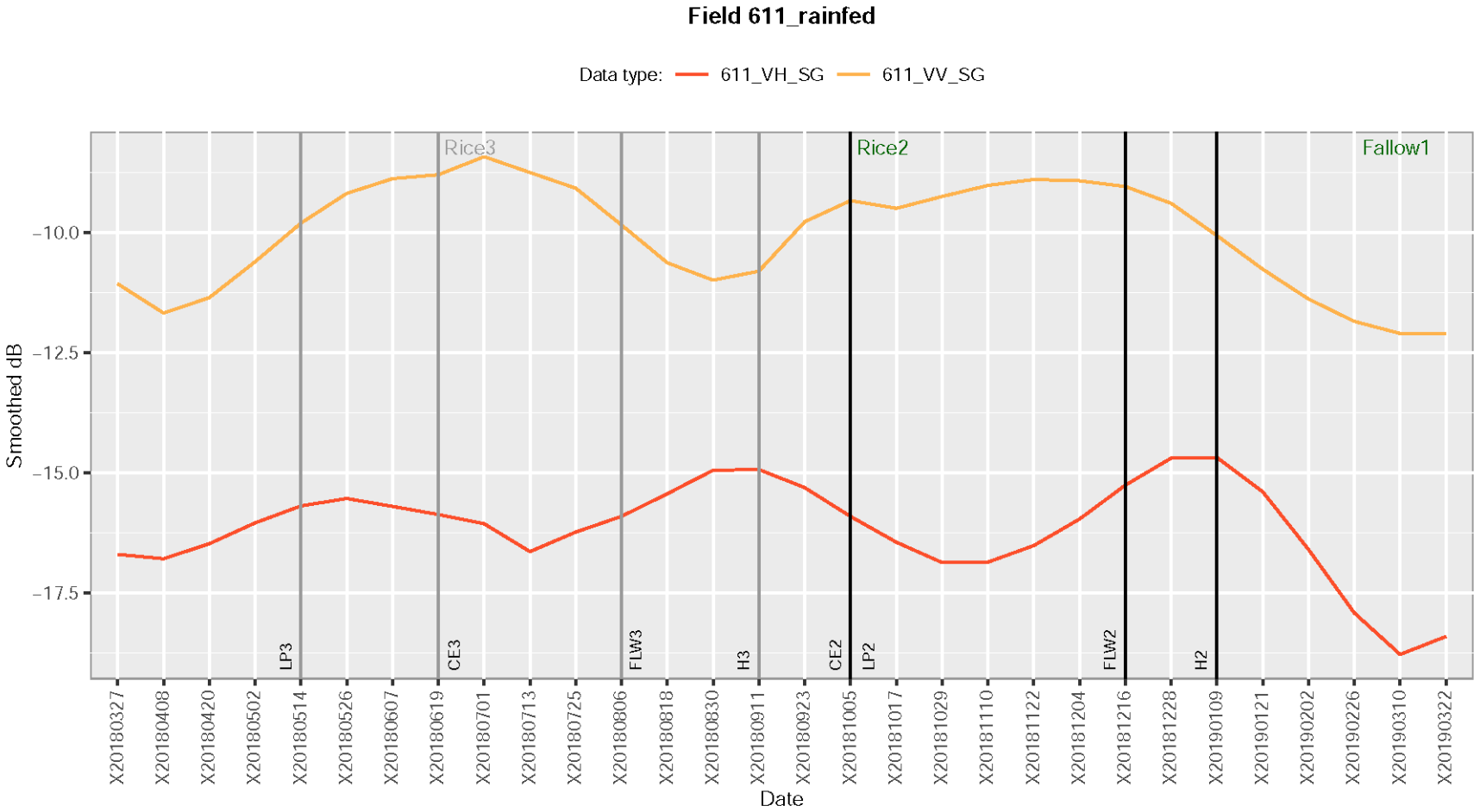
Field 611_rainfed
Data type: 611_VH_SG 611_VV_SG
Rice3
Rice2
Fallow1
Smoothed dB
−10.0
−12.5
−15.0
−17.5
LP3
CE3
FLW3
H3
CE2
LP2
FLW2
H2
X20180327
X20180408
X20180420
X20180502
X20180514
X20180526
X20180607
X20180619
X20180701
X20180713
X20180725
X20180806
X20180818
X20180830
X20180911
X20180923
X20181005
X20181017
X20181029
X20181110
X20181122
X20181204
X20181216
X20181228
X20190109
X20190121
X20190202
X20190226
X20190310
X20190322
Date

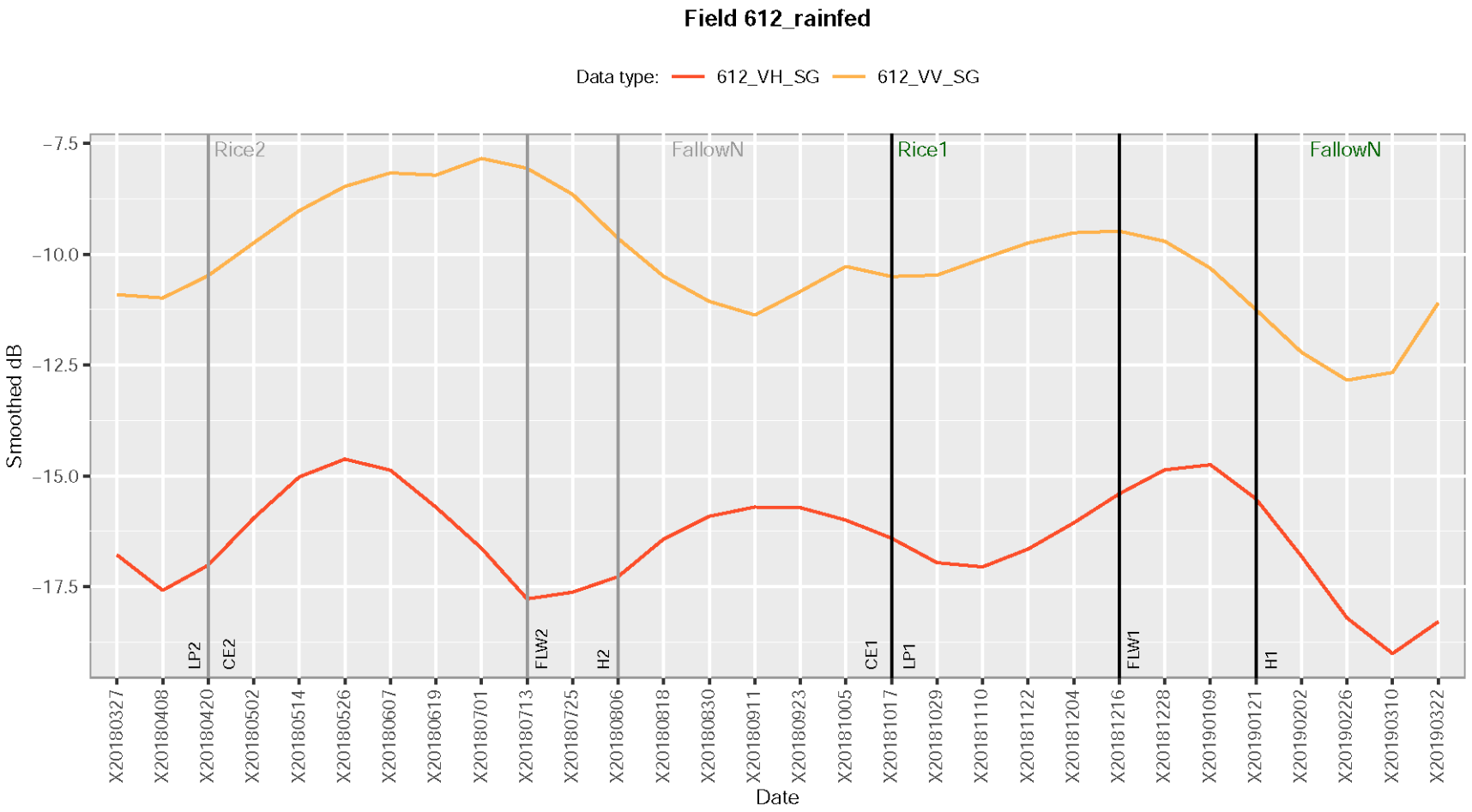
Field 612_rainfed
Data type: 612_VH_SG 612_VV_SG
Smoothed dB
−7.5
−10.0
−12.5
−15.0
−17.5
Rice2
FallowN
Rice1
FallowN
LP2
CE2
FLW2
H2
CE1
LP1
FLW1
H1
X20180327
X20180408
X20180420
X20180502
X20180514
X20180526
X20180607
X20180619
X20180701
X20180713
X20180725
X20180806
X20180818
X20180830
X20180911
X20180923
X20181005
X20181017
X20181029
X20181110
X20181122
X20181204
X20181216
X20181228
X20190109
X20190121
X20190202
X20190226
X20190310
X20190322
Date

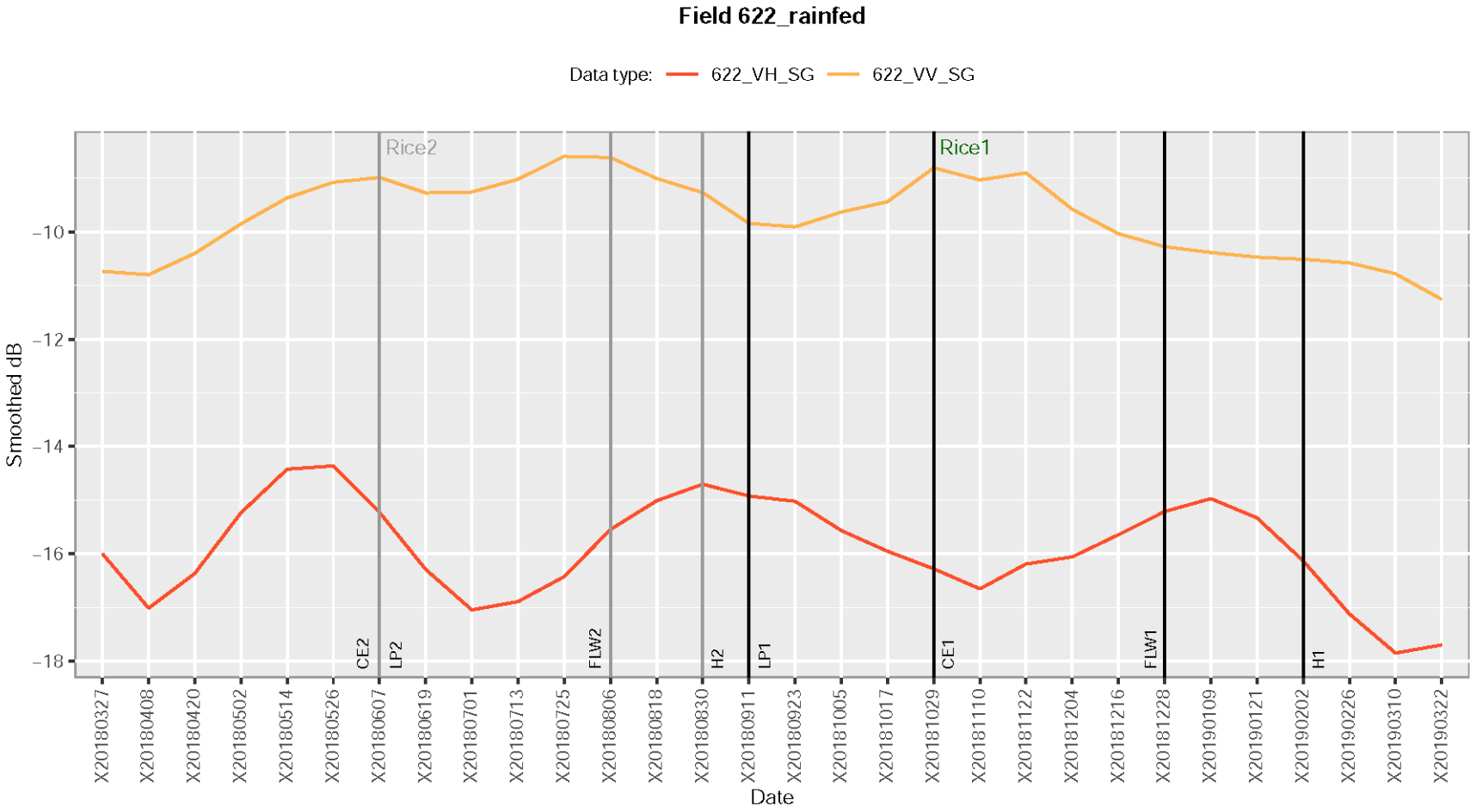
Field 622_rainfed
Data type: 622_VH_SG 622_VV_SG
Rice2
Rice1
Smoothed dB
−10
−12
−14
−16
−18
CE2
LP2
FLW2
H2
LP1
CE1
FLW1
H1
X20180327
X20180408
X20180420
X20180502
X20180514
X20180526
X20180607
X20180619
X20180701
X20180713
X20180725
X20180806
X20180818
X20180830
X20180911
X20180923
X20181005
X20181017
X20181029
X20181110
X20181122
X20181204
X20181216
X20181228
X20190109
X20190121
X20190202
X20190226
X20190310
X20190322
Date

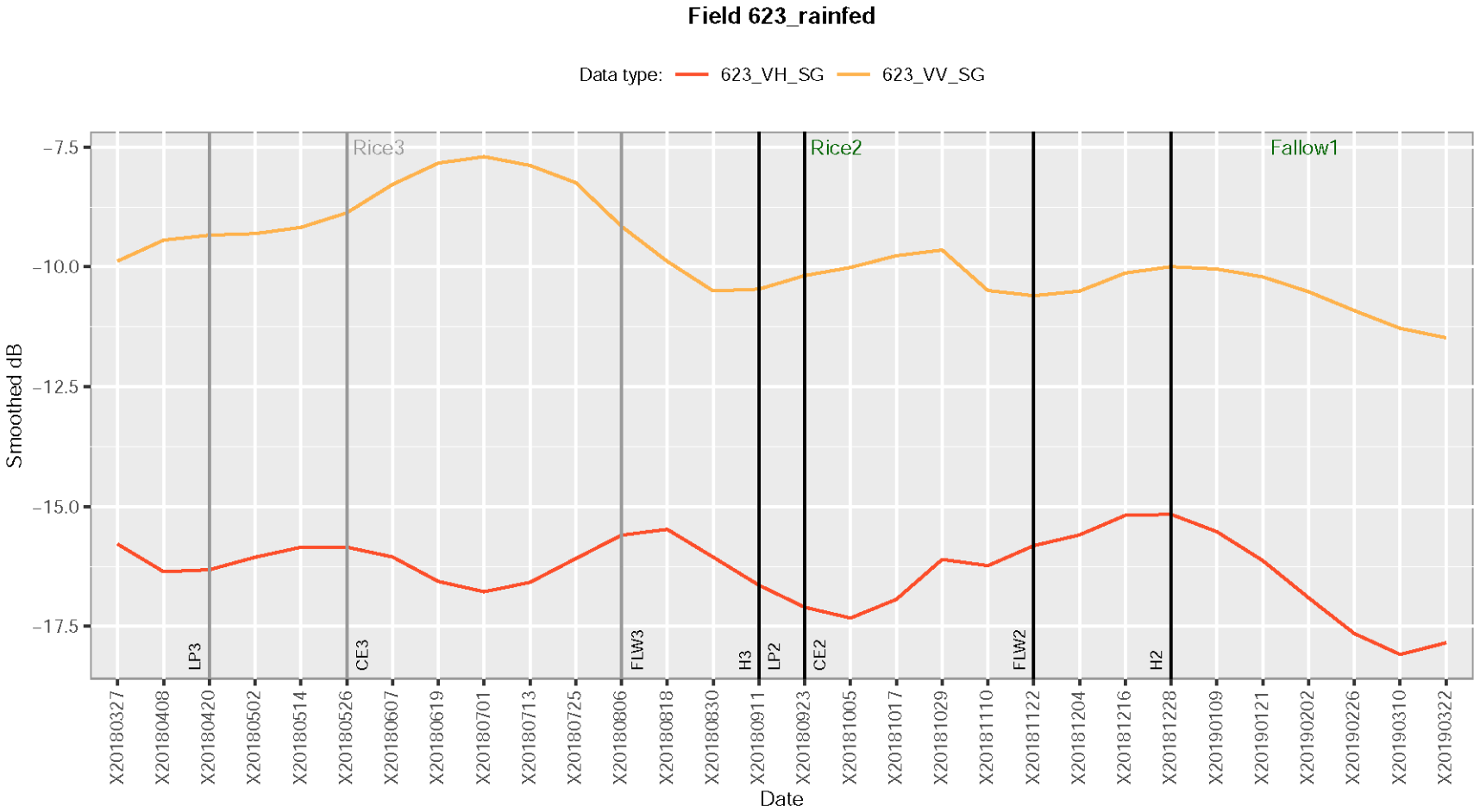
Field 623_rainfed
Data type: 623_VH_SG 623_VV_SG
Smoothed dB
−7.5
−10.0
−12.5
−15.0
−17.5
Rice3
Rice2
Fallow1
LP3
CE3
FLW3
H3
LP2
CE2
FLW2
H2
X20180327
X20180408
X20180420
X20180502
X20180514
X20180526
X20180607
X20180619
X20180701
X20180713
X20180725
X20180806
X20180818
X20180830
X20180911
X20180923
X20181005
X20181017
X20181029
X20181110
X20181122
X20181204
X20181216
X20181228
X20190109
X20190121
X20190202
X20190226
X20190310
X20190322
Date

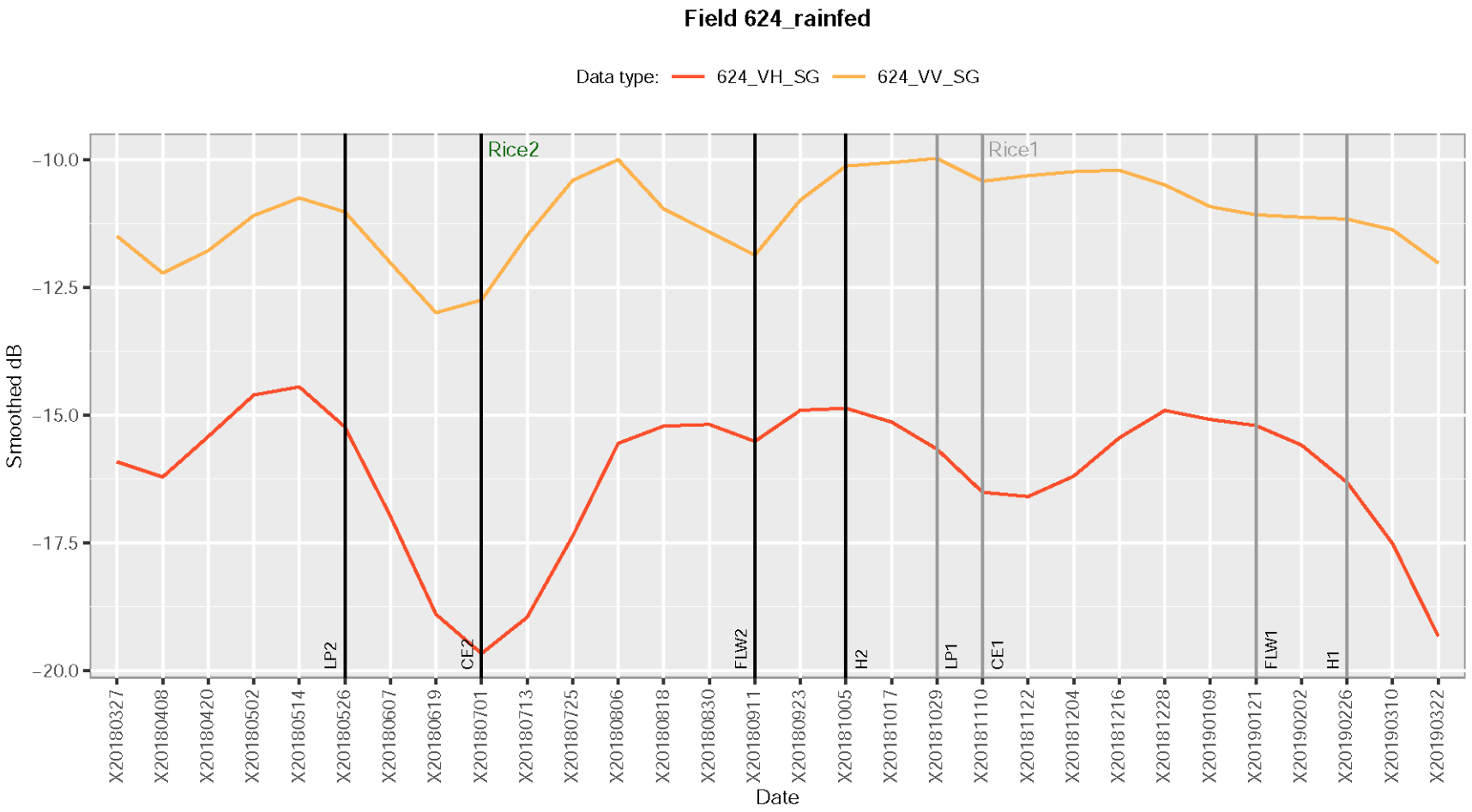
Field 624_rainfed
Data type: 624_VH_SG 624_VV_SG
Rice2
Rice1
−10.0
−12.5
−15.0
−17.5
−20.0
Smoothed dB
LP2
CE2
FLW2
H2
LP1
CE1
FLW1
H1
X20180327
X20180408
X20180420
X20180502
X20180514
X20180526
X20180607
X20180619
X20180701
X20180713
X20180725
X20180806
X20180818
X20180830
X20180911
X20180923
X20181005
X20181017
X20181029
X20181110
X20181122
X20181204
X20181216
X20181228
X20190109
X20190121
X20190202
X20190226
X20190310
X20190322
Date

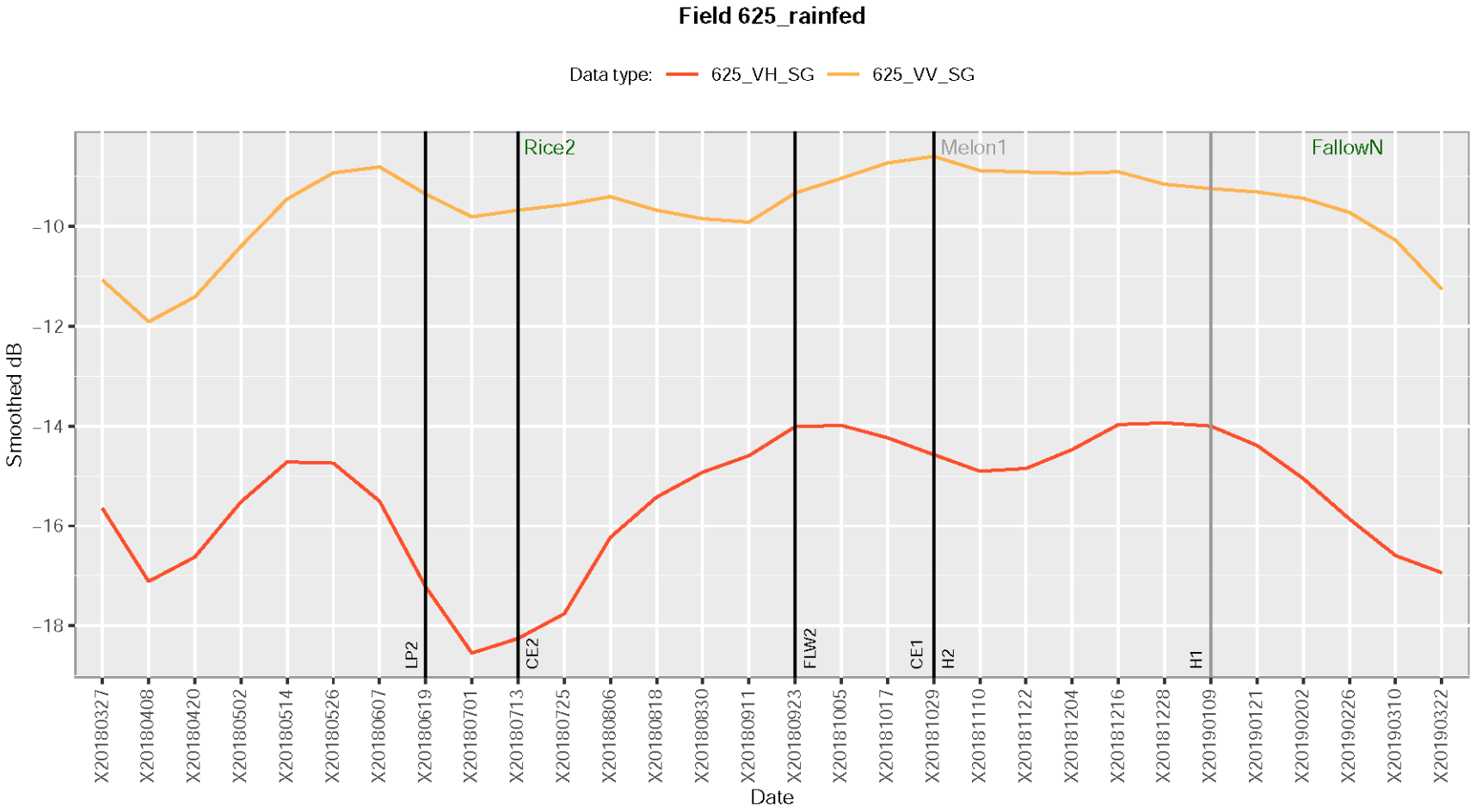
Field 625_rainfed
Data type: 625_VH_SG 625_VV_SG
Rice2
Melon1
FallowN
LP2
CE2
FLW2
CE1
H2
H1
Smoothed dB
−10
−12
−14
−16
−18
X20180327
X20180408
X20180420
X20180502
X20180514
X20180526
X20180607
X20180619
X20180701
X20180713
X20180725
X20180806
X20180818
X20180830
X20180911
X20180923
X20181005
X20181017
X20181029
X20181110
X20181122
X20181204
X20181216
X20181228
X20190109
X20190121
X20190202
X20190226
X20190310
X20190322
Date

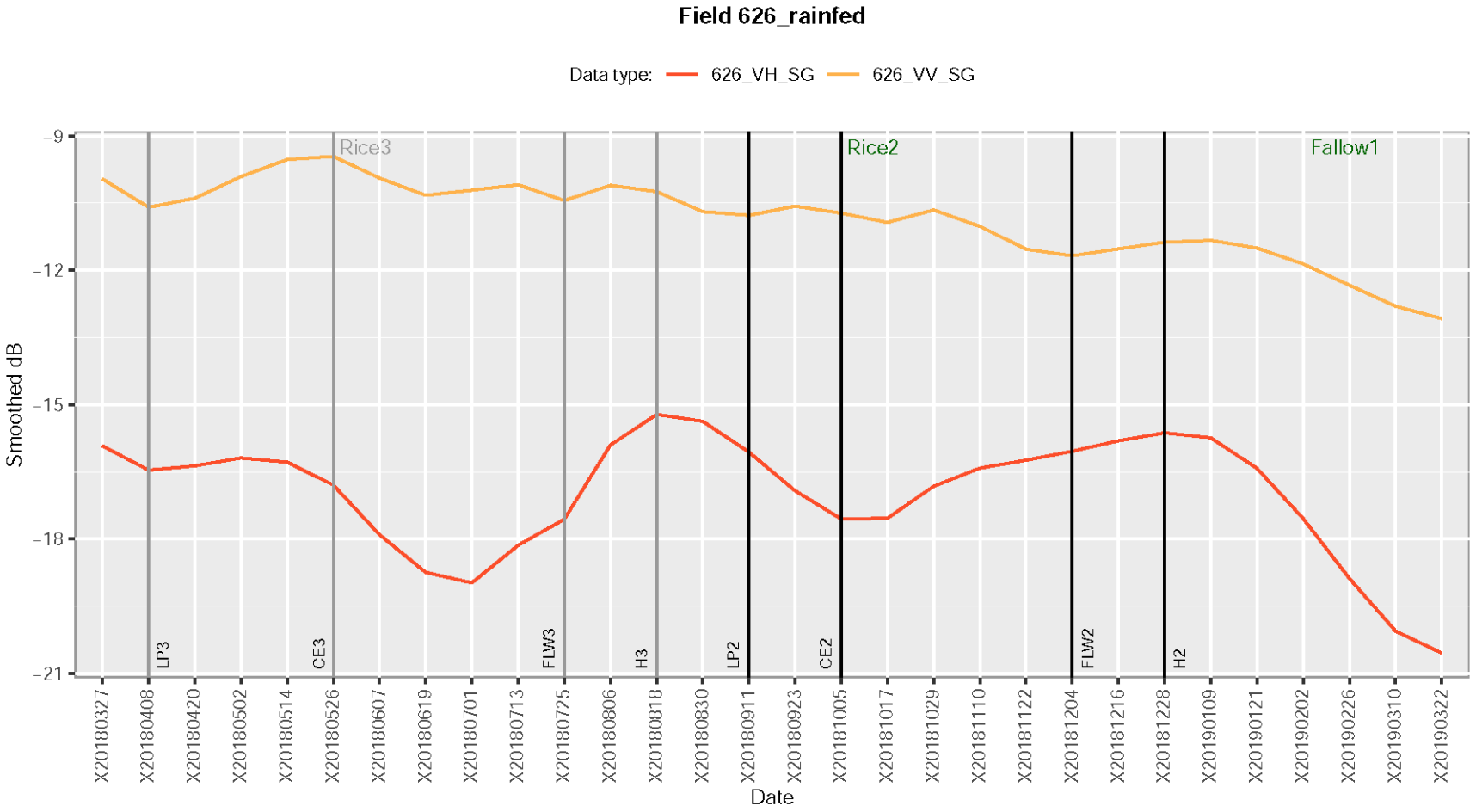
Field 626_rainfed
Data type: 626_VH_SG 626_VV_SG
Rice3
Rice2
Fallow1
Smoothed dB
−9
−12
−15
−18
−21
LP3
CE3
FLW3
H3
LP2
CE2
FLW2
H2
X20180327
X20180408
X20180420
X20180502
X20180514
X20180526
X20180607
X20180619
X20180701
X20180713
X20180725
X20180806
X20180818
X20180830
X20180911
X20180923
X20181005
X20181017
X20181029
X20181110
X20181122
X20181204
X20181216
X20181228
X20190109
X20190121
X20190202
X20190226
X20190310
X20190322
Date

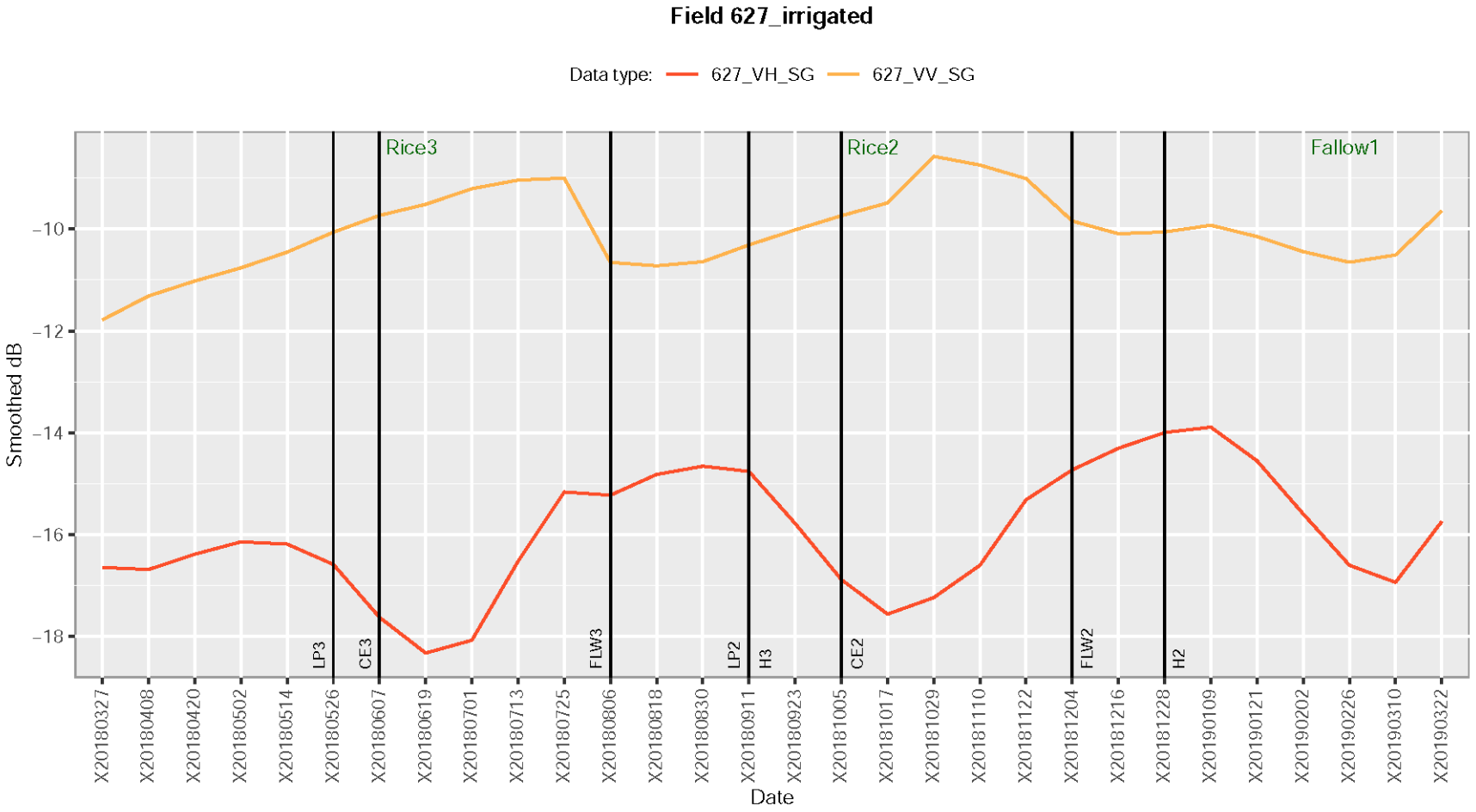
Field 627_irrigated
Data type: 627_VH_SG 627_VV_SG
Rice3
Rice2
Fallow1
LP3
CE3
FLW3
LP2
H3
CE2
FLW2
H2
Smoothed dB
−10
−12
−14
−16
−18
X20180327
X20180408
X20180420
X20180502
X20180514
X20180526
X20180607
X20180619
X20180701
X20180713
X20180725
X20180806
X20180818
X20180830
X20180911
X20180923
X20181005
X20181017
X20181029
X20181110
X20181122
X20181204
X20181216
X20181228
X20190109
X20190121
X20190202
X20190226
X20190310
X20190322
Date

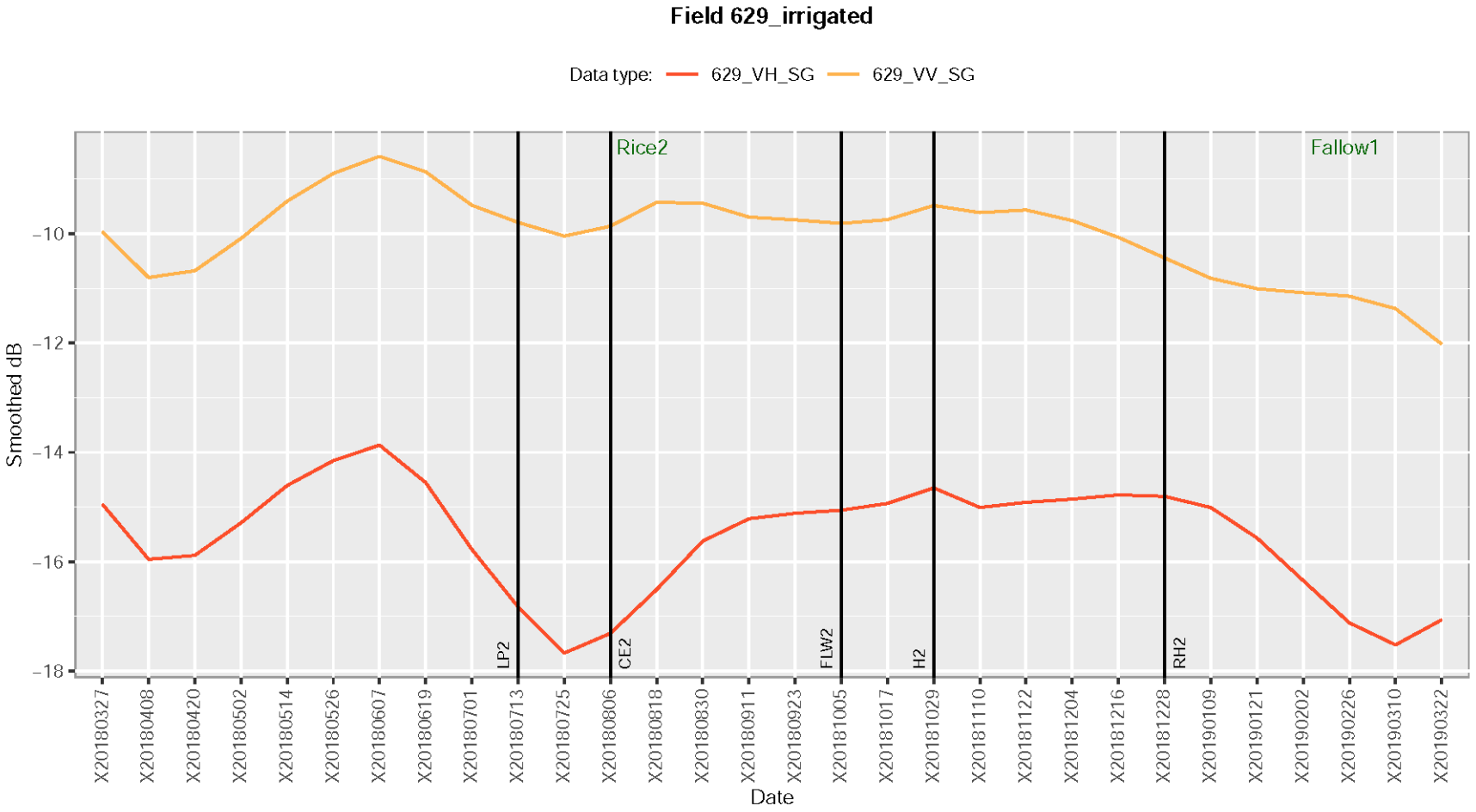
Field 629_irrigated
Data type: 629_VH_SG 629_VV_SG
Rice2
Fallow1
LP2
CE2
FLW2
H2
RH2
Smoothed dB
−10
−12
−14
−16
−18
X20180327
X20180408
X20180420
X20180502
X20180514
X20180526
X20180607
X20180619
X20180701
X20180713
X20180725
X20180806
X20180818
X20180830
X20180911
X20180923
X20181005
X20181017
X20181029
X20181110
X20181122
X20181204
X20181216
X20181228
X20190109
X20190121
X20190202
X20190226
X20190310
X20190322
Date

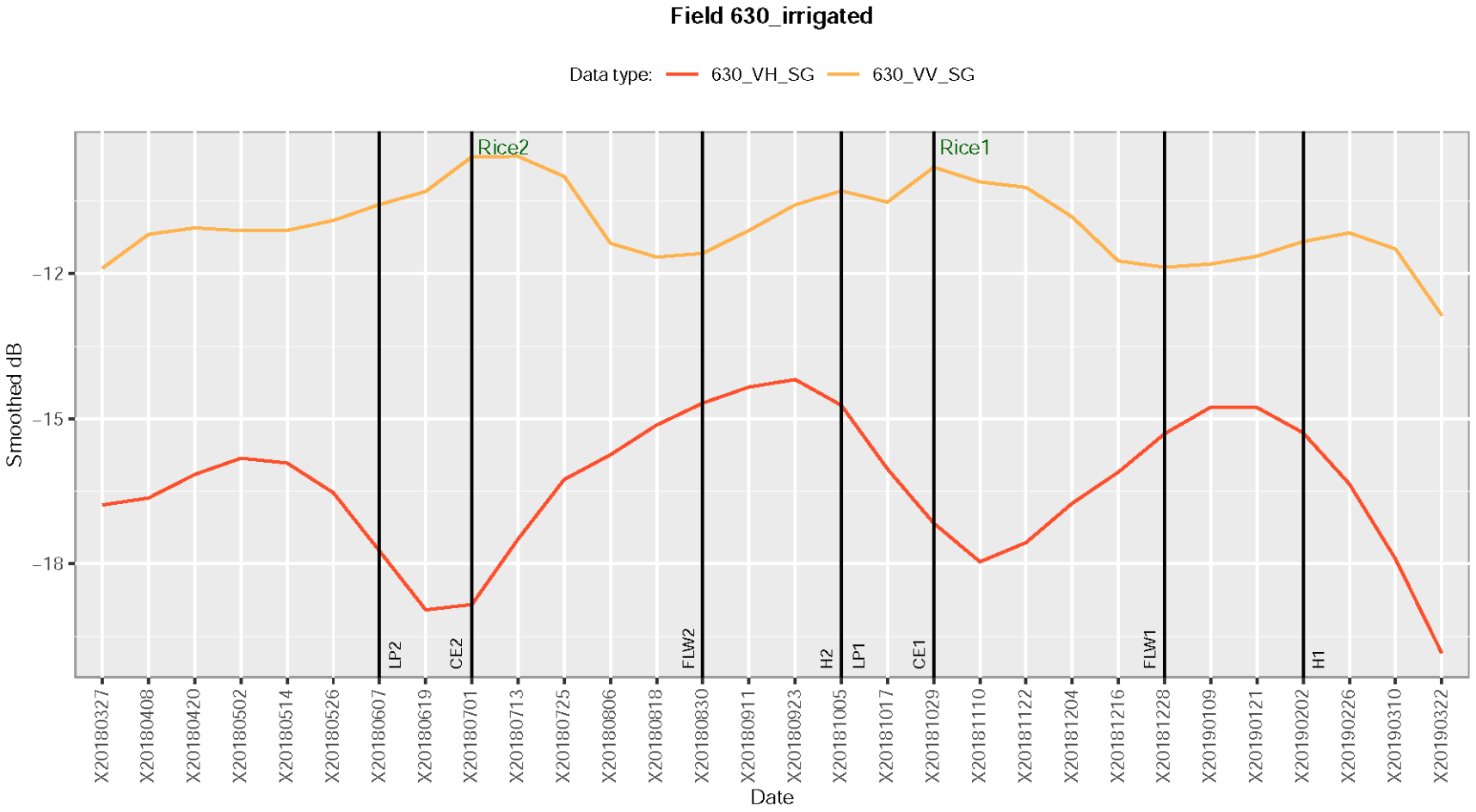
Field 630_irrigated
Data type: 630_VH_SG 630_VV_SG
Rice2
Rice1
LP2
CE2
FLW2
H2
LP1
CE1
FLW1
H1
Smoothed dB
-12
-15
-18
X20180327
X20180408
X20180420
X20180502
X20180514
X20180526
X20180607
X20180619
X20180701
X20180713
X20180725
X20180806
X20180818
X20180830
X20180911
X20180923
X20181005
X20181017
X20181029
X20181110
X20181122
X20181204
X20181216
X20181228
X20190109
X20190121
X20190202
X20190226
X20190310
X20190322
Date

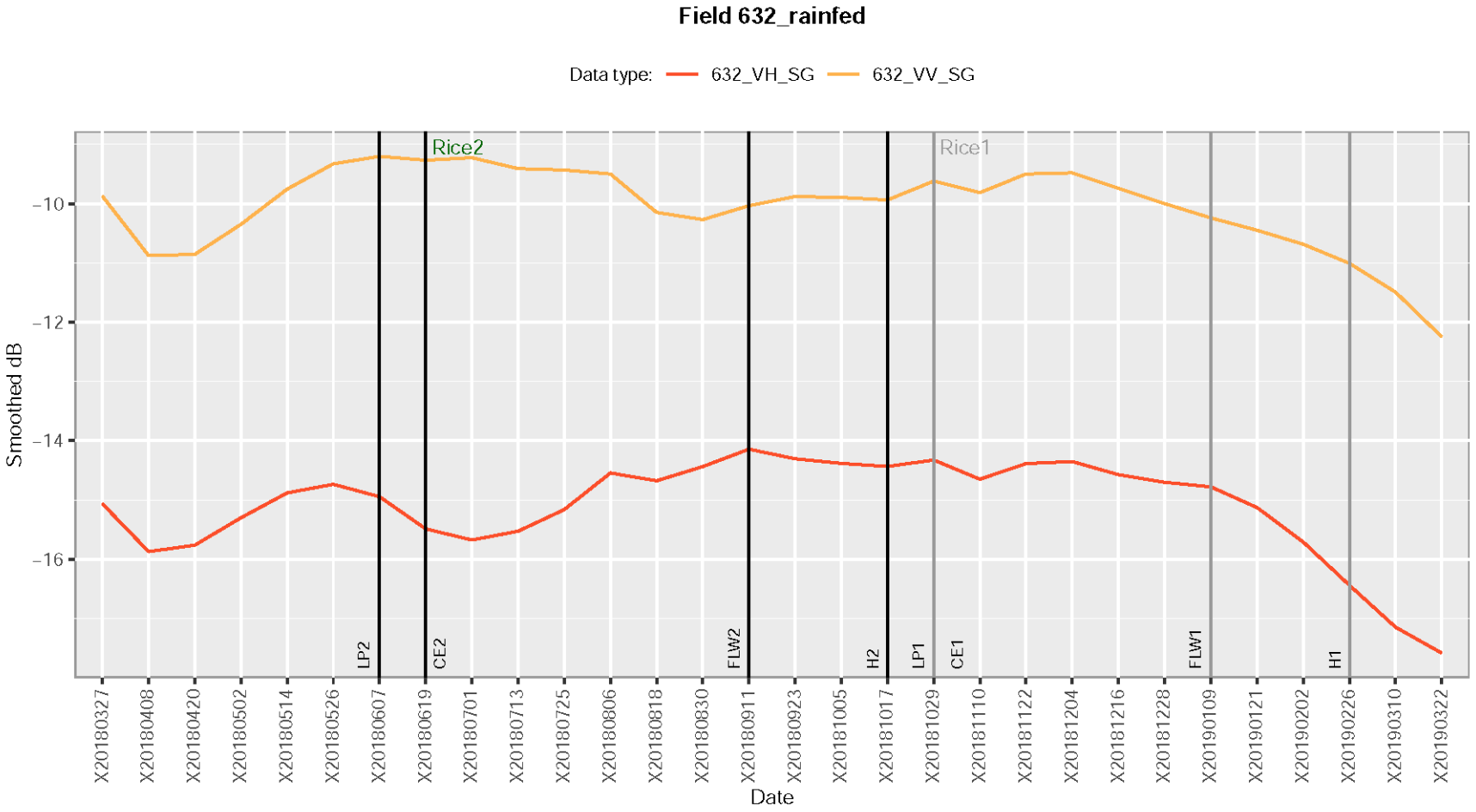
Field 632_rainfed
Data type: 632_VH_SG 632_VV_SG
Rice2
Rice1
Smoothed dB
−10
−12
−14
−16
LP2
CE2
FLW2
H2
LP1
CE1
FLW1
H1
X20180327
X20180408
X20180420
X20180502
X20180514
X20180526
X20180607
X20180619
X20180701
X20180713
X20180725
X20180806
X20180818
X20180830
X20180911
X20180923
X20181005
X20181017
X20181029
X20181110
X20181122
X20181204
X20181216
X20181228
X20190109
X20190121
X20190202
X20190226
X20190310
X20190322
Date

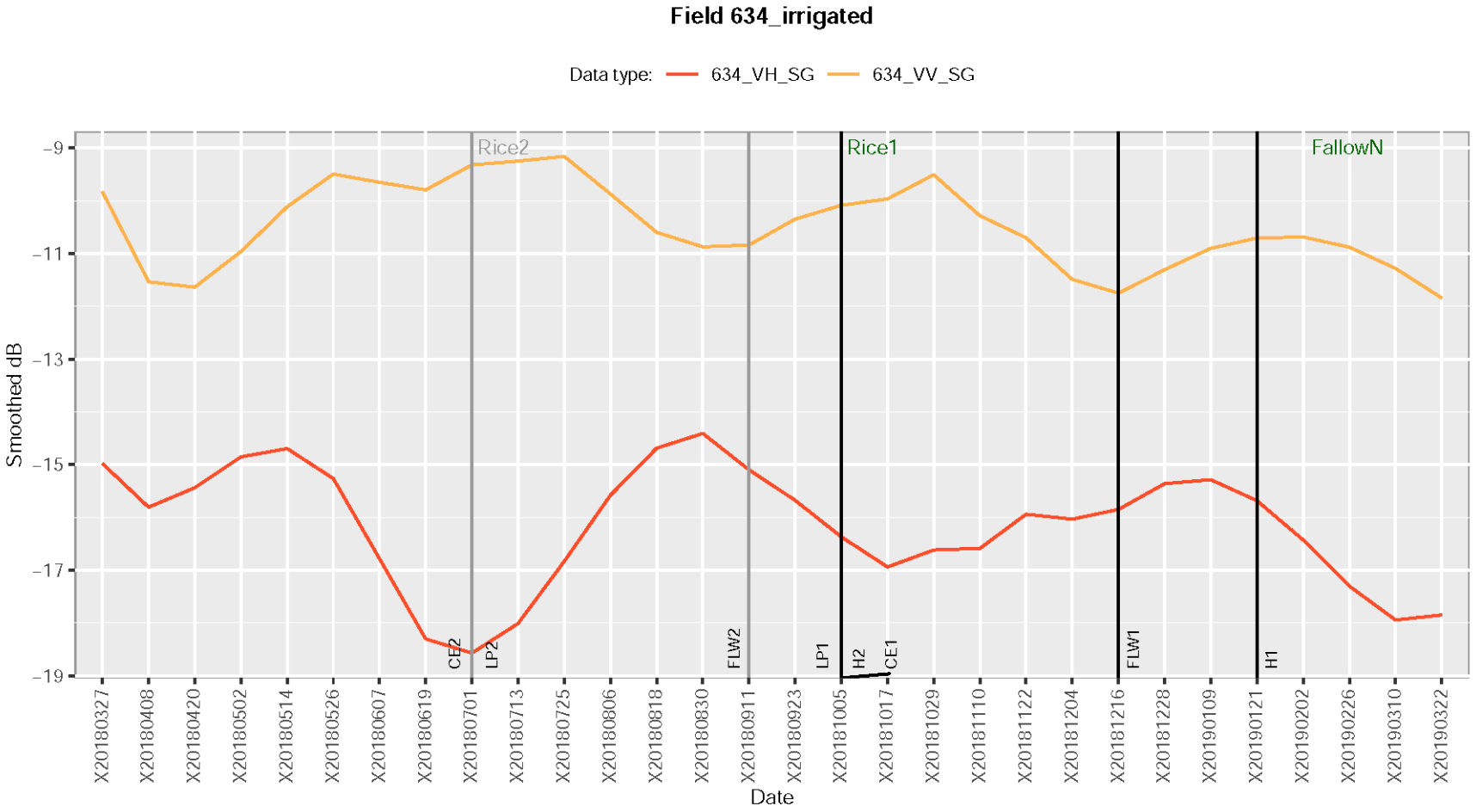
Field 634_irrigated
Data type: 634_VH_SG 634_VV_SG
Rice2
Rice1
FallowN
Smoothed dB
−9
−11
−13
−15
−17
−19
CE2
LP2
FLW2
LP1
H2
CE1
FLW1
H1
X20180327
X20180408
X20180420
X20180502
X20180514
X20180526
X20180607
X20180619
X20180701
X20180713
X20180725
X20180806
X20180818
X20180830
X20180911
X20180923
X20181005
X20181017
X20181029
X20181110
X20181122
X20181204
X20181216
X20181228
X20190109
X20190121
X20190202
X20190226
X20190310
X20190322
Date

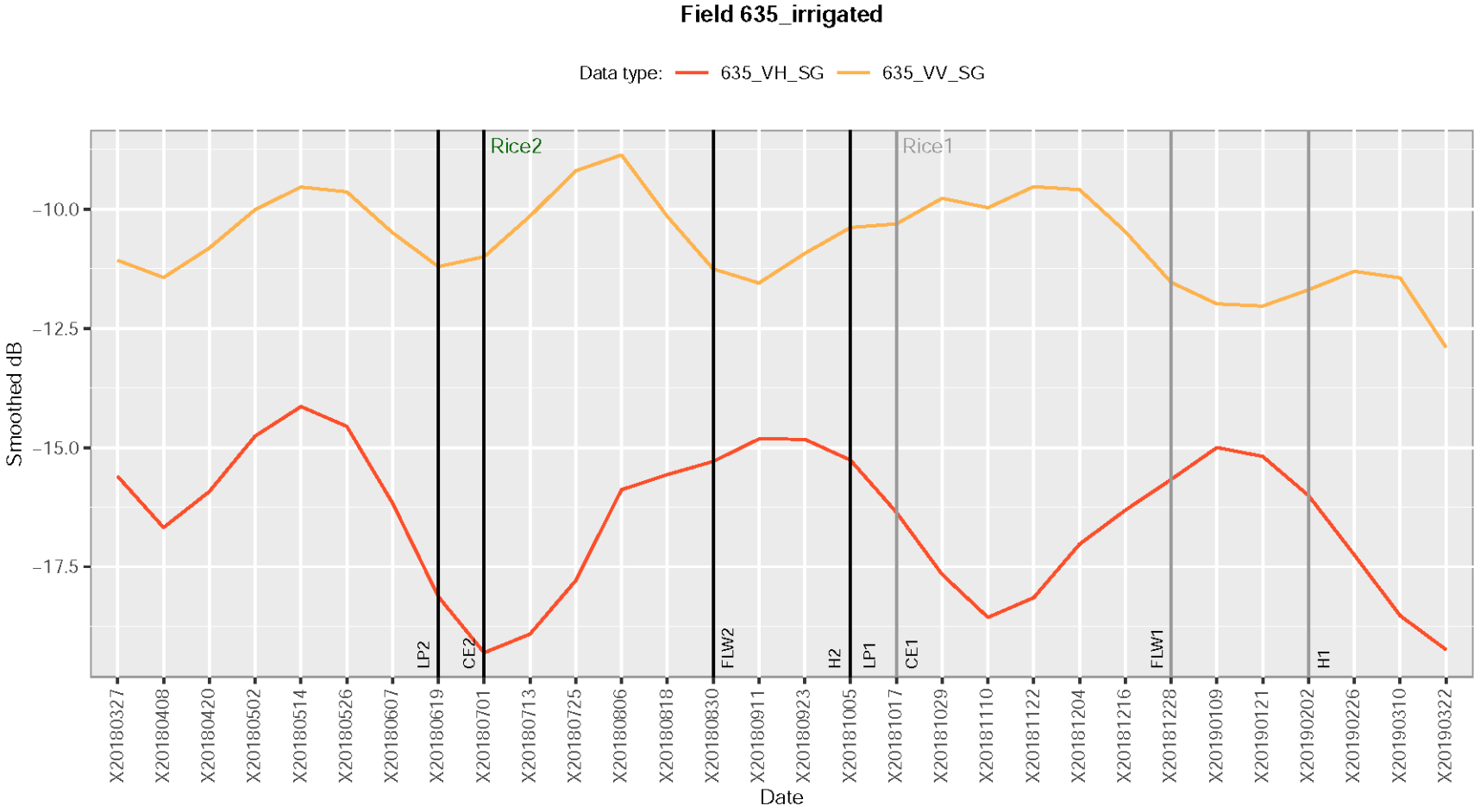
Field 635_irrigated
Data type: 635_VH_SG 635_VV_SG
Rice2
Rice1
−10.0
−12.5
−15.0
−17.5
Smoothed dB
LP2
CE2
FLW2
H2
LP1
CE1
FLW1
H1
X20180327
X20180408
X20180420
X20180502
X20180514
X20180526
X20180607
X20180619
X20180701
X20180713
X20180725
X20180806
X20180818
X20180830
X20180911
X20180923
X20181005
X20181017
X20181029
X20181110
X20181122
X20181204
X20181216
X20181228
X20190109
X20190121
X20190202
X20190226
X20190310
X20190322
Date

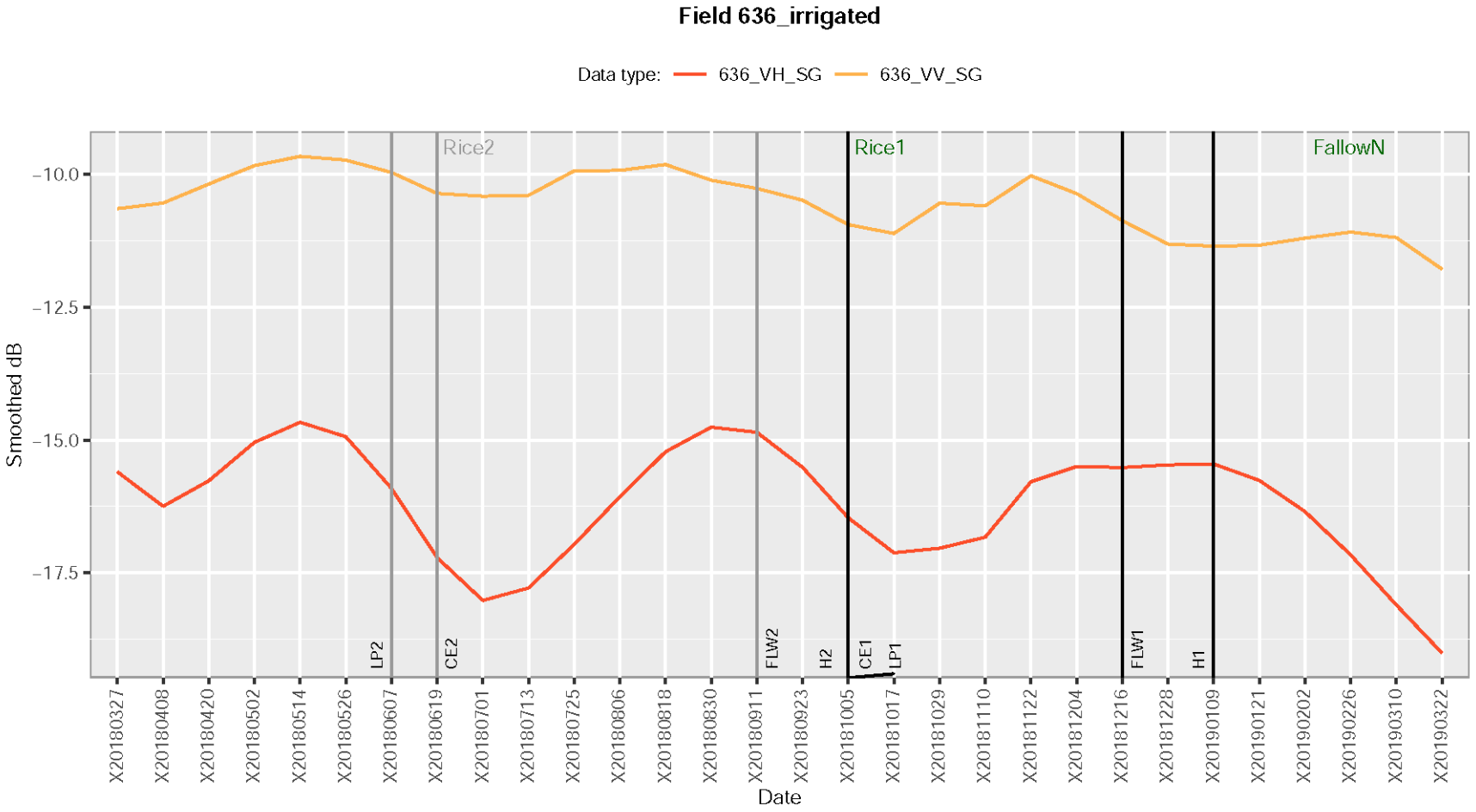
Field 636_irrigated
Data type: 636_VH_SG 636_VV_SG
Rice2
Rice1
FallowN
−10.0
−12.5
−15.0
−17.5
Smoothed dB
LP2
CE2
FLW2
H2
CE1
LP1
FLW1
H1
X20180327
X20180408
X20180420
X20180502
X20180514
X20180526
X20180607
X20180619
X20180701
X20180713
X20180725
X20180806
X20180818
X20180830
X20180911
X20180923
X20181005
X20181017
X20181029
X20181110
X20181122
X20181204
X20181216
X20181228
X20190109
X20190121
X20190202
X20190226
X20190310
X20190322
Date

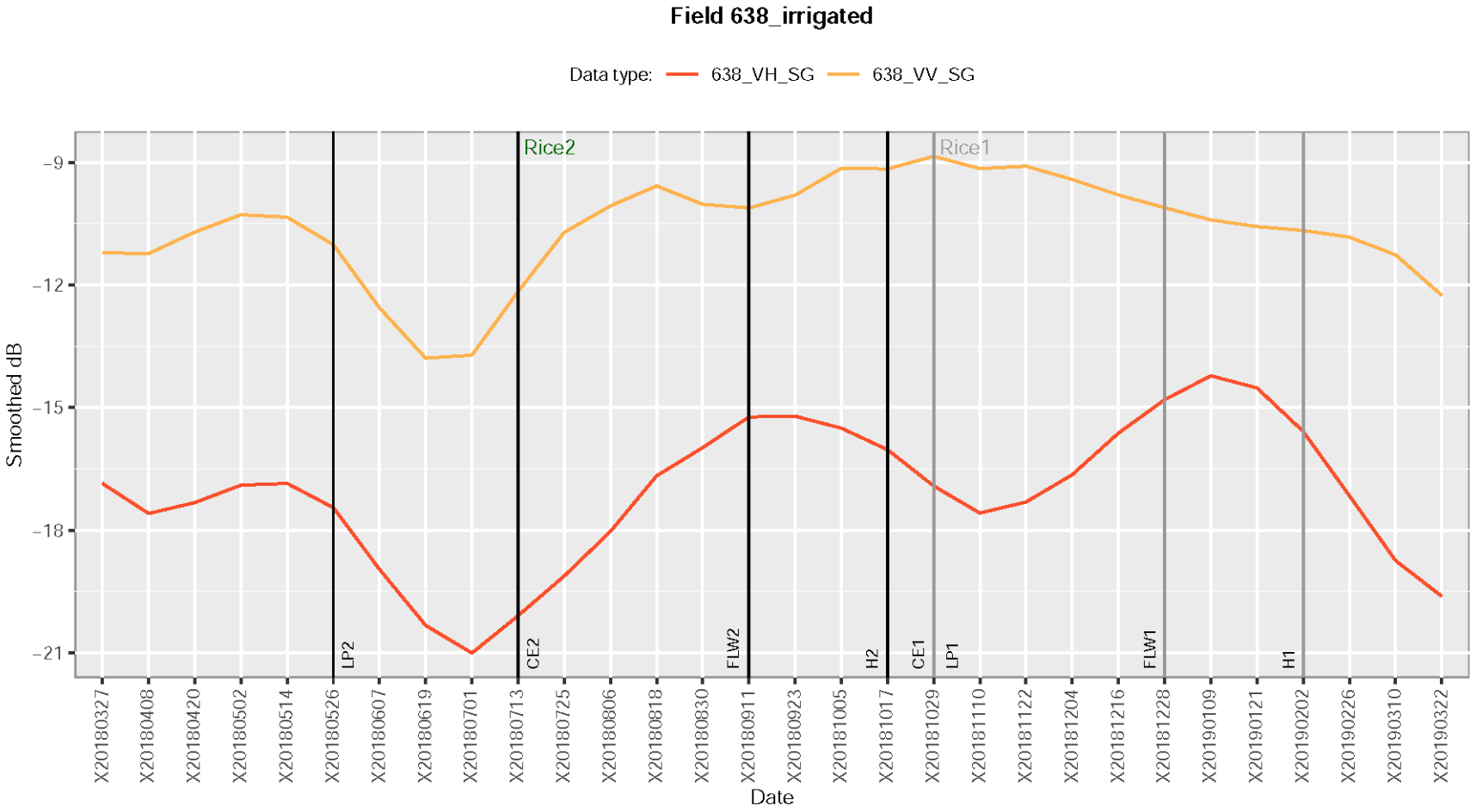
Field 638_irrigated
Data type: 638_VH_SG 638_VV_SG
Rice2
Rice1
Smoothed dB
−9
−12
−15
−18
−21
LP2
CE2
FLW2
H2
CE1
LP1
FLW1
H1
X20180327
X20180408
X20180420
X20180502
X20180514
X20180526
X20180607
X20180619
X20180701
X20180713
X20180725
X20180806
X20180818
X20180830
X20180911
X20180923
X20181005
X20181017
X20181029
X20181110
X20181122
X20181204
X20181216
X20181228
X20190109
X20190121
X20190202
X20190226
X20190310
X20190322
Date

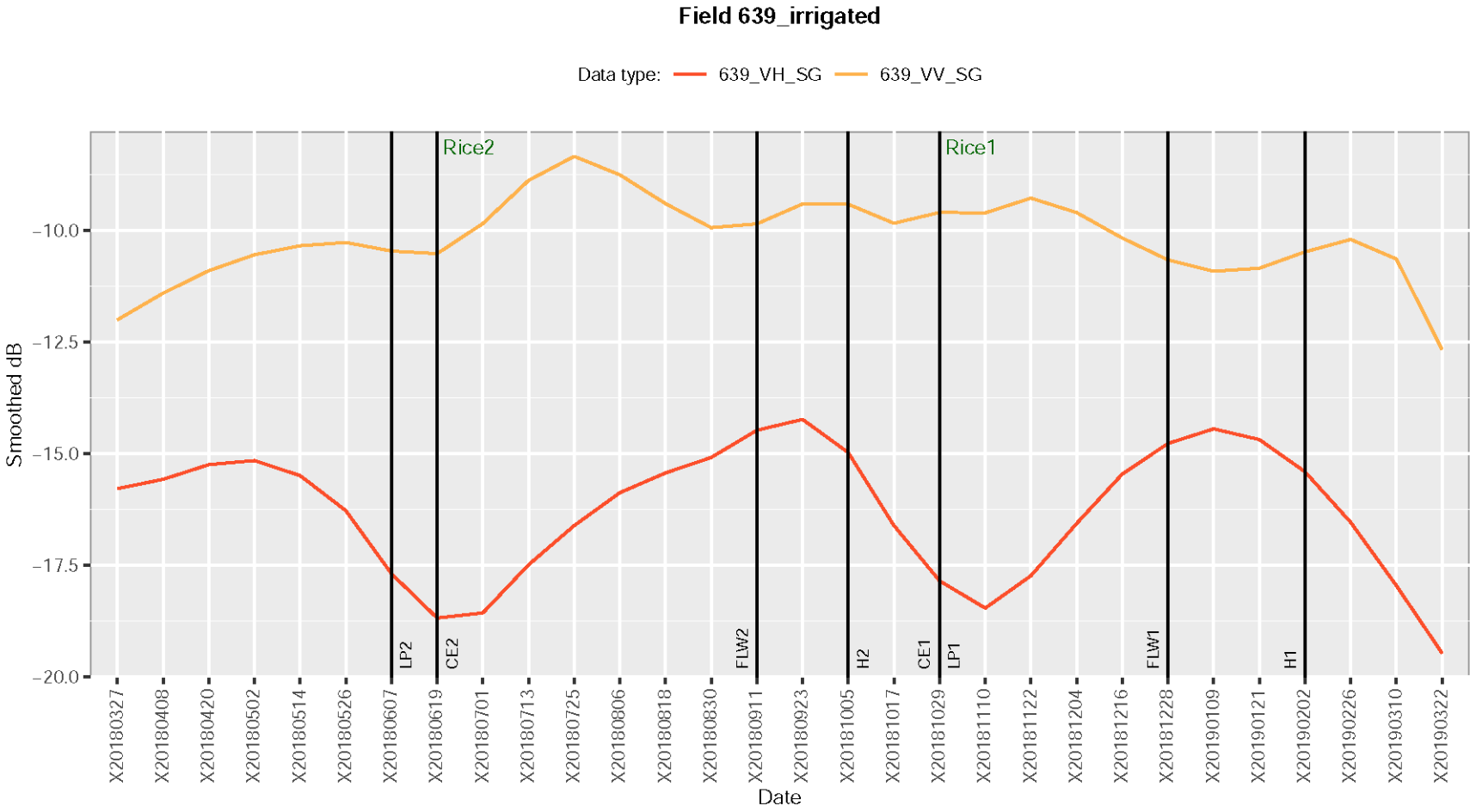
Field 639_irrigated
Data type: 639_VH_SG 639_VV_SG
Rice2
Rice1
LP2
CE2
FLW2
H2
CE1
LP1
FLW1
H1
Smoothed dB
−10.0
−12.5
−15.0
−17.5
−20.0
X20180327
X20180408
X20180420
X20180502
X20180514
X20180526
X20180607
X20180619
X20180701
X20180713
X20180725
X20180806
X20180818
X20180830
X20180911
X20180923
X20181005
X20181017
X20181029
X20181110
X20181122
X20181204
X20181216
X20181228
X20190109
X20190121
X20190202
X20190226
X20190310
X20190322
Date

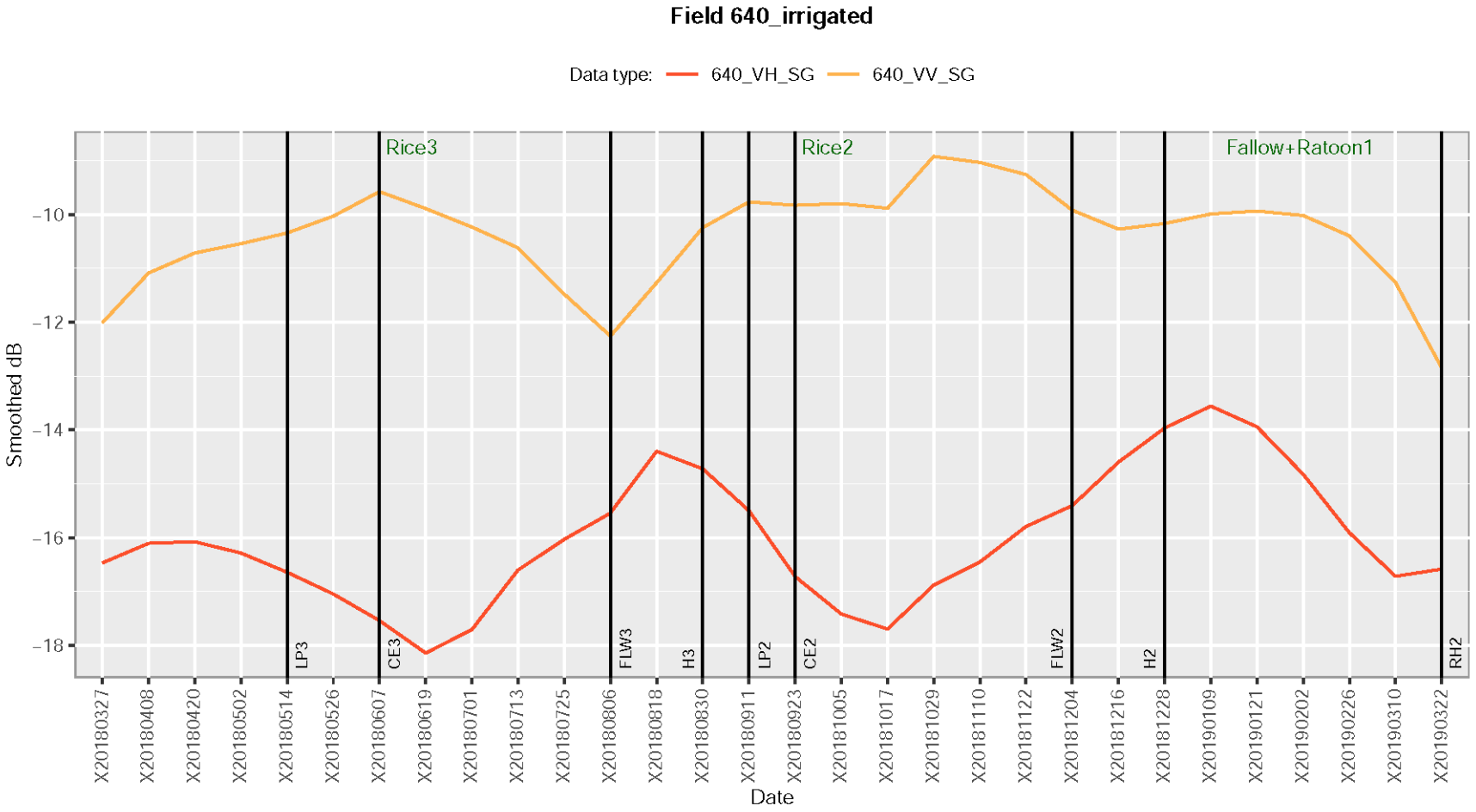
Field 640_irrigated
Data type:
640_VH_SG
640_VV_SG
Rice3
Rice2
Fallow+Ratoon1
Smoothed dB
−10
−12
−14
−16
−18
LP3
CE3
FLW3
H3
LP2
CE2
FLW2
H2
RH2
X20180327
X20180408
X20180420
X20180502
X20180514
X20180526
X20180607
X20180619
X20180701
X20180713
X20180725
X20180806
X20180818
X20180830
X20180911
X20180923
X20181005
X20181017
X20181029
X20181110
X20181122
X20181204
X20181216
X20181228
X20190109
X20190121
X20190202
X20190226
X20190310
X20190322
Date

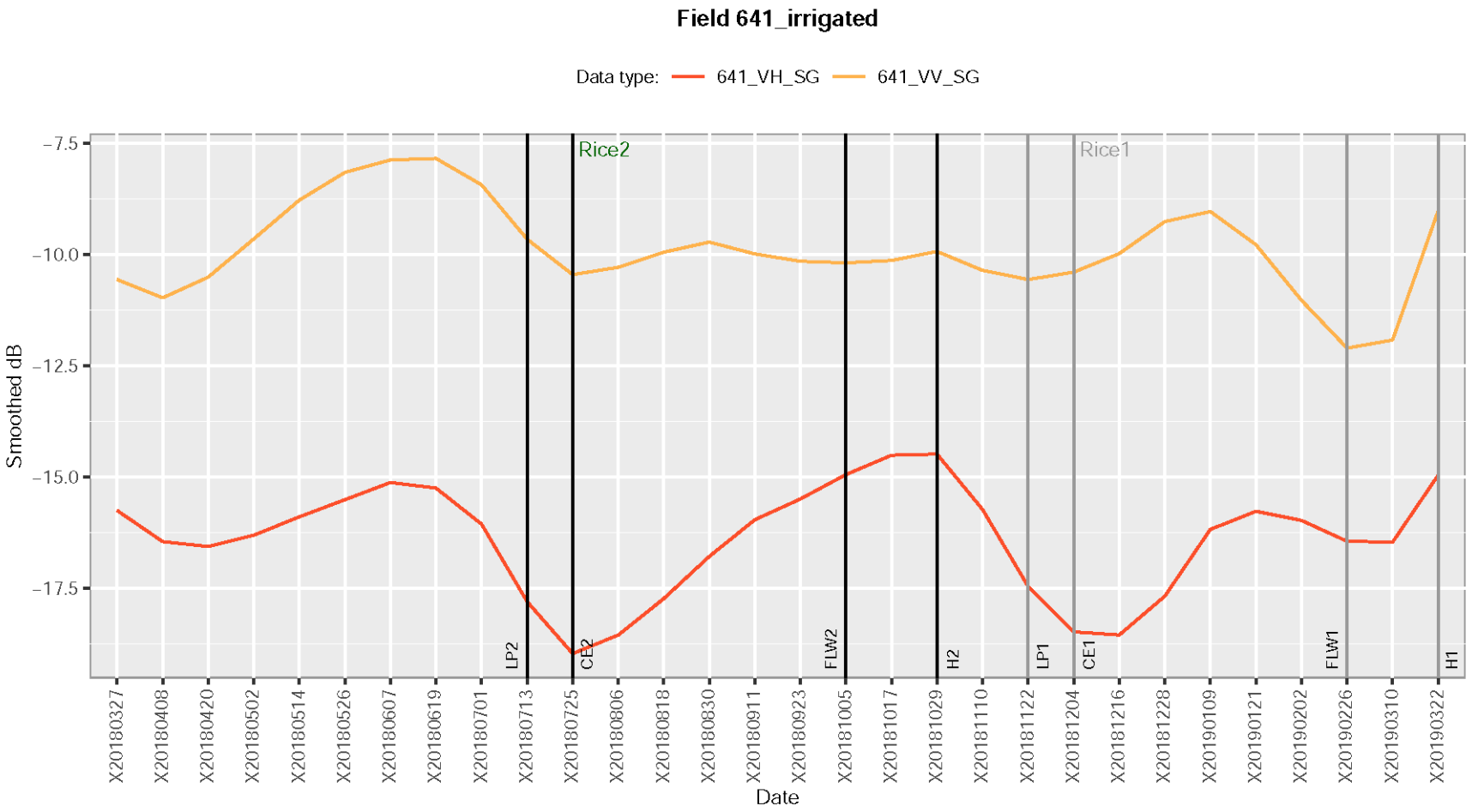
Field 641_irrigated
Data type: 641_VH_SG 641_VV_SG
Rice2
Rice1
Smoothed dB
−7.5
−10.0
−12.5
−15.0
−17.5
LP2
CE2
FLW2
H2
LP1
CE1
FLW1
H1
X20180327
X20180408
X20180420
X20180502
X20180514
X20180526
X20180607
X20180619
X20180701
X20180713
X20180725
X20180806
X20180818
X20180830
X20180911
X20180923
X20181005
X20181017
X20181029
X20181110
X20181122
X20181204
X20181216
X20181228
X20190109
X20190121
X20190202
X20190226
X20190310
X20190322
Date

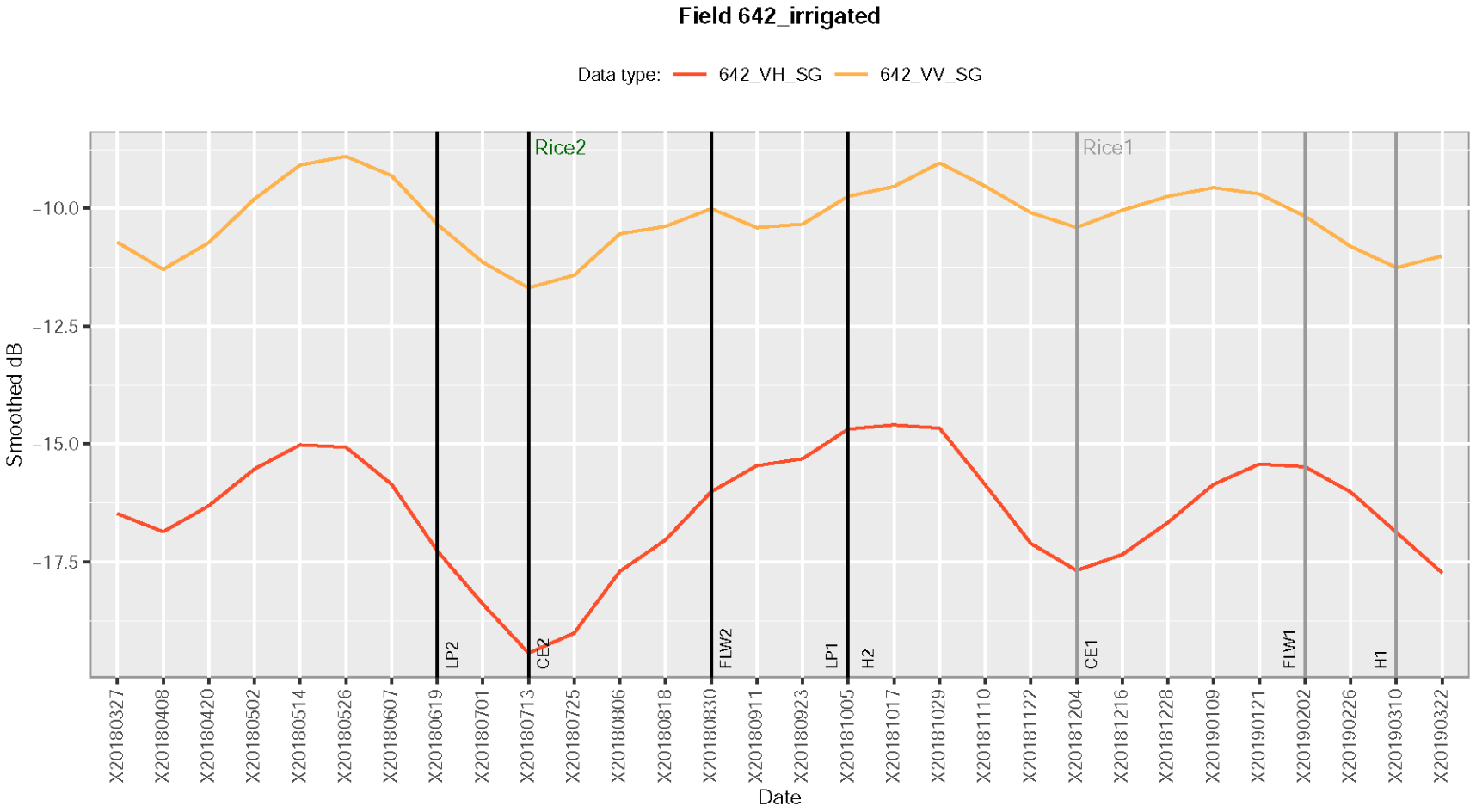
Field 642_irrigated
Data type: 642_VH_SG 642_VV_SG
Rice2
Rice1
−10.0
−12.5
−15.0
−17.5
Smoothed dB
LP2
CE2
FLW2
LP1
H2
CE1
FLW1
H1
X20180327
X20180408
X20180420
X20180502
X20180514
X20180526
X20180607
X20180619
X20180701
X20180713
X20180725
X20180806
X20180818
X20180830
X20180911
X20180923
X20181005
X20181017
X20181029
X20181110
X20181122
X20181204
X20181216
X20181228
X20190109
X20190121
X20190202
X20190226
X20190310
X20190322
Date

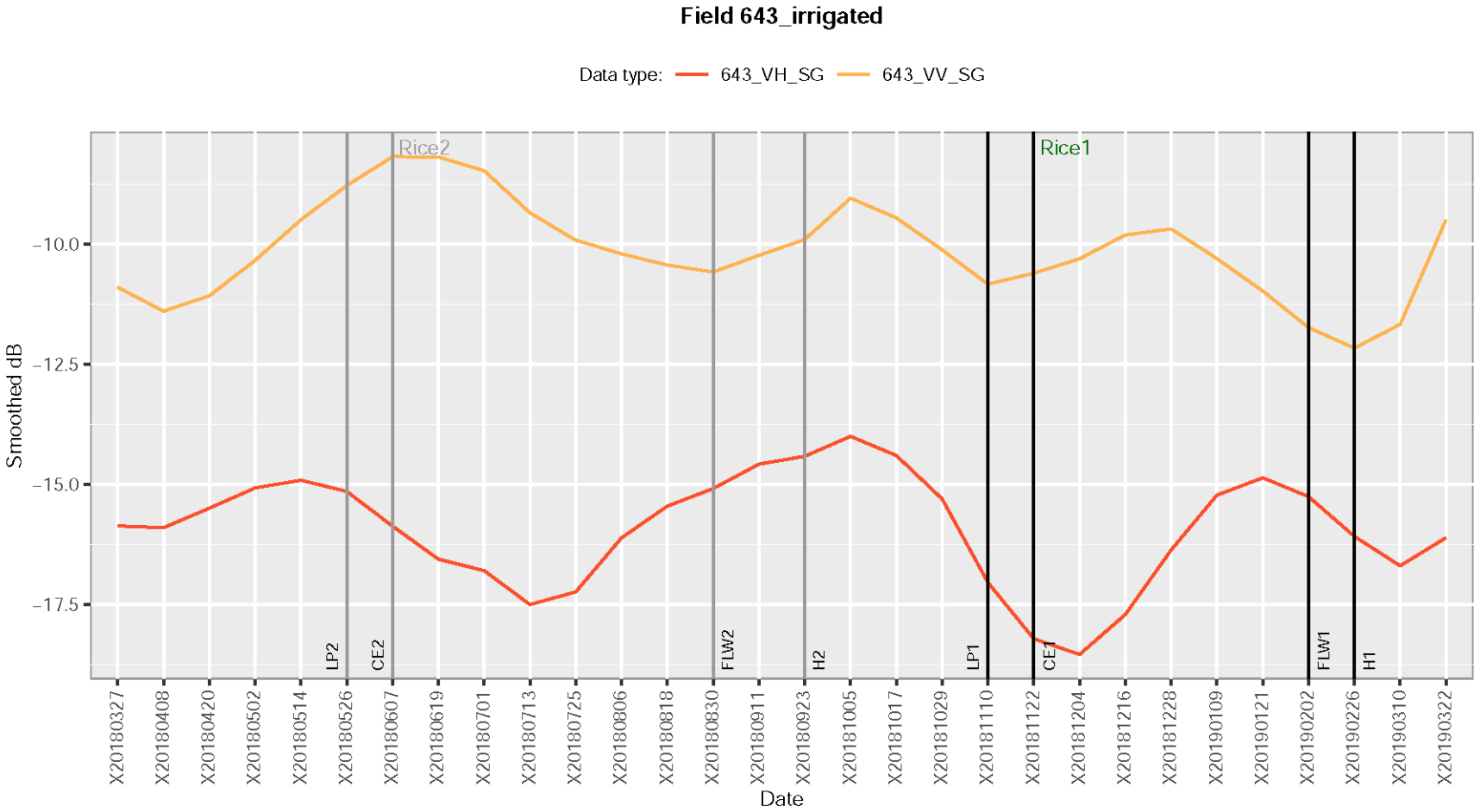
Field 643_irrigated
Data type: 643_VH_SG 643_VV_SG
Smoothed dB
−10.0
−12.5
−15.0
−17.5
Rice2
Rice1
LP2
CE2
FLW2
H2
LP1
CE1
FLW1
H1
X20180327
X20180408
X20180420
X20180502
X20180514
X20180526
X20180607
X20180619
X20180701
X20180713
X20180725
X20180806
X20180818
X20180830
X20180911
X20180923
X20181005
X20181017
X20181029
X20181110
X20181122
X20181204
X20181216
X20181228
X20190109
X20190121
X20190202
X20190226
X20190310
X20190322
Date

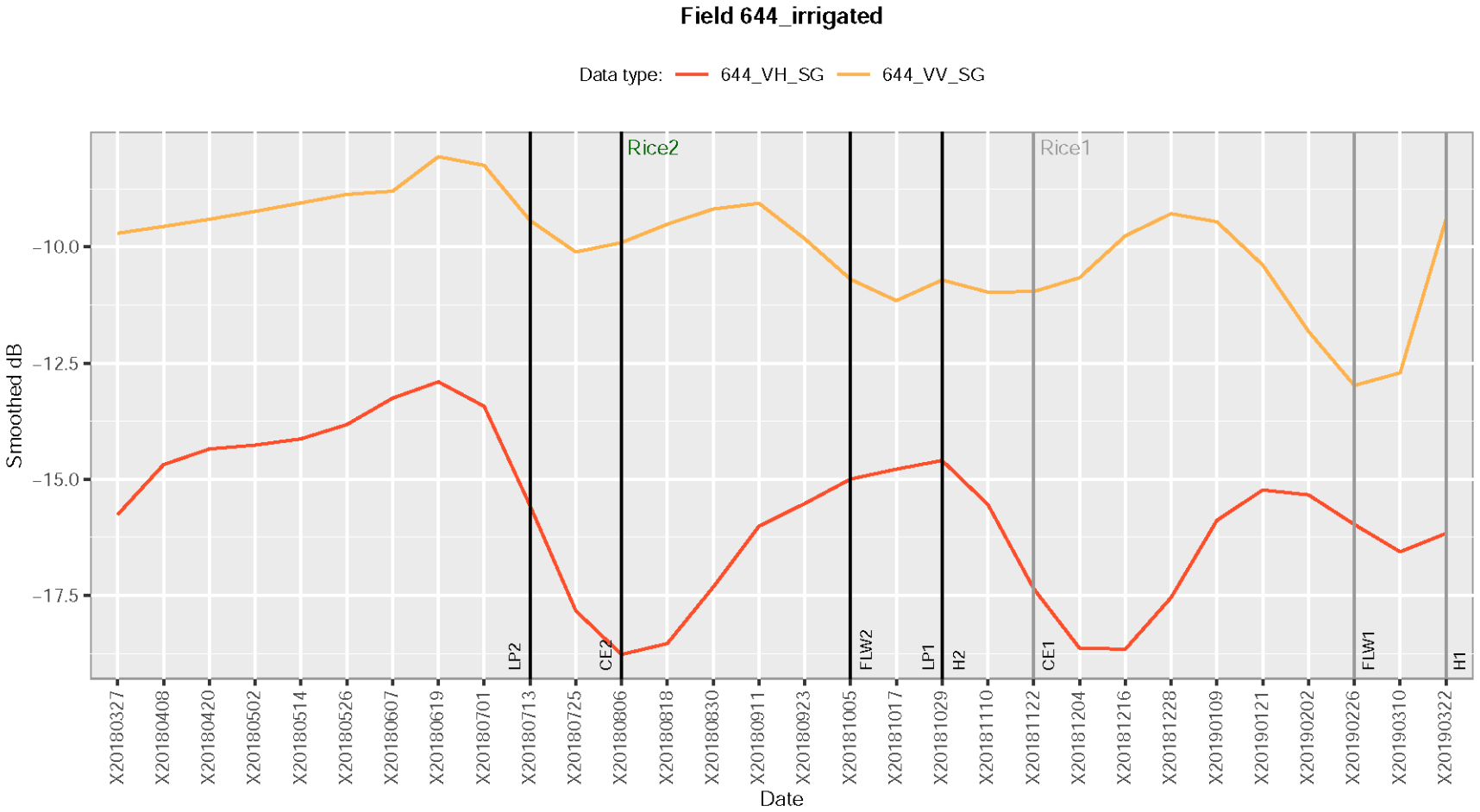
Field 644_irrigated
Data type: 644_VH_SG 644_VV_SG
Rice2
Rice1
−10.0
−12.5
−15.0
−17.5
Smoothed dB
LP2
CE2
FLW2
LP1
H2
CE1
FLW1
H1
X20180327
X20180408
X20180420
X20180502
X20180514
X20180526
X20180607
X20180619
X20180701
X20180713
X20180725
X20180806
X20180818
X20180830
X20180911
X20180923
X20181005
X20181017
X20181029
X20181110
X20181122
X20181204
X20181216
X20181228
X20190109
X20190121
X20190202
X20190226
X20190310
X20190322
Date

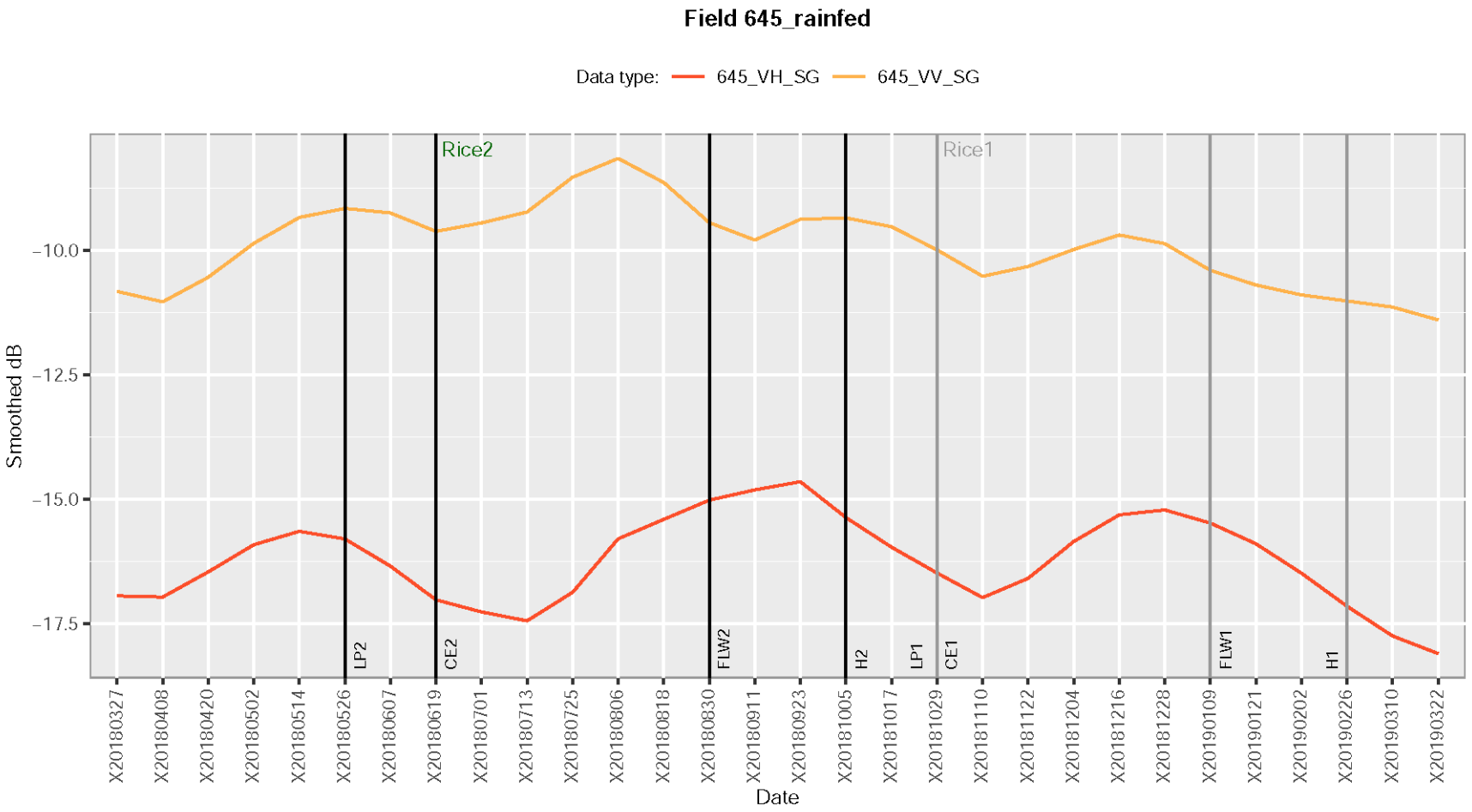
Field 645_rainfed
Data type: 645_VH_SG 645_VV_SG
Rice2
Rice1
Smoothed dB
−10.0
−12.5
−15.0
−17.5
LP2
CE2
FLW2
H2
LP1
CE1
FLW1
H1
X20180327
X20180408
X20180420
X20180502
X20180514
X20180526
X20180607
X20180619
X20180701
X20180713
X20180725
X20180806
X20180818
X20180830
X20180911
X20180923
X20181005
X20181017
X20181029
X20181110
X20181122
X20181204
X20181216
X20181228
X20190109
X20190121
X20190202
X20190226
X20190310
X20190322
Date

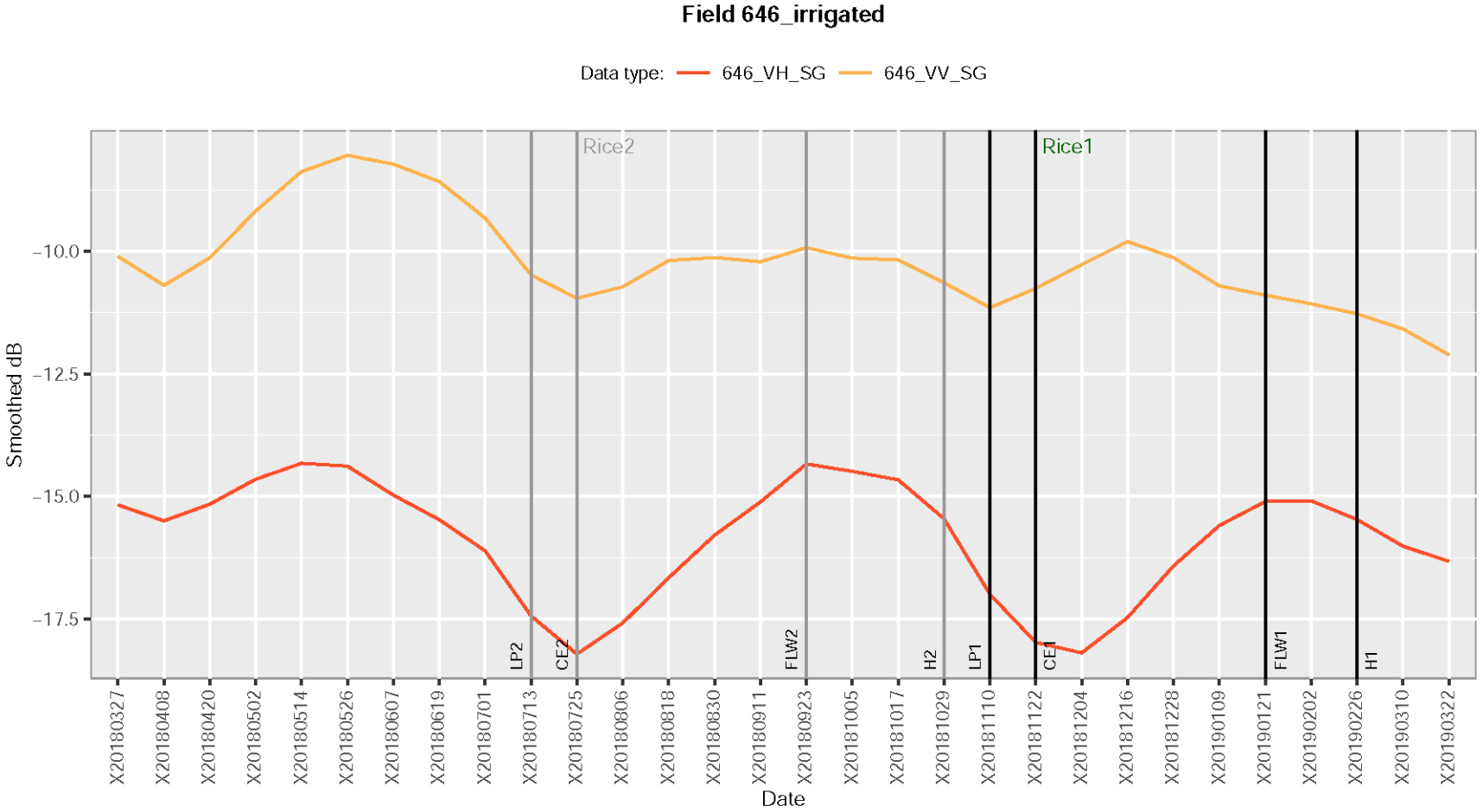
Field 646_irrigated
Data type: 646_VH_SG 646_VV_SG
Rice2
Rice1
−10.0
−12.5
−15.0
−17.5
Smoothed dB
LP2
CE2
FLW2
H2
LP1
CE1
FLW1
H1
X20180327
X20180408
X20180420
X20180502
X20180514
X20180526
X20180607
X20180619
X20180701
X20180713
X20180725
X20180806
X20180818
X20180830
X20180911
X20180923
X20181005
X20181017
X20181029
X20181110
X20181122
X20181204
X20181216
X20181228
X20190109
X20190121
X20190202
X20190226
X20190310
X20190322
Date

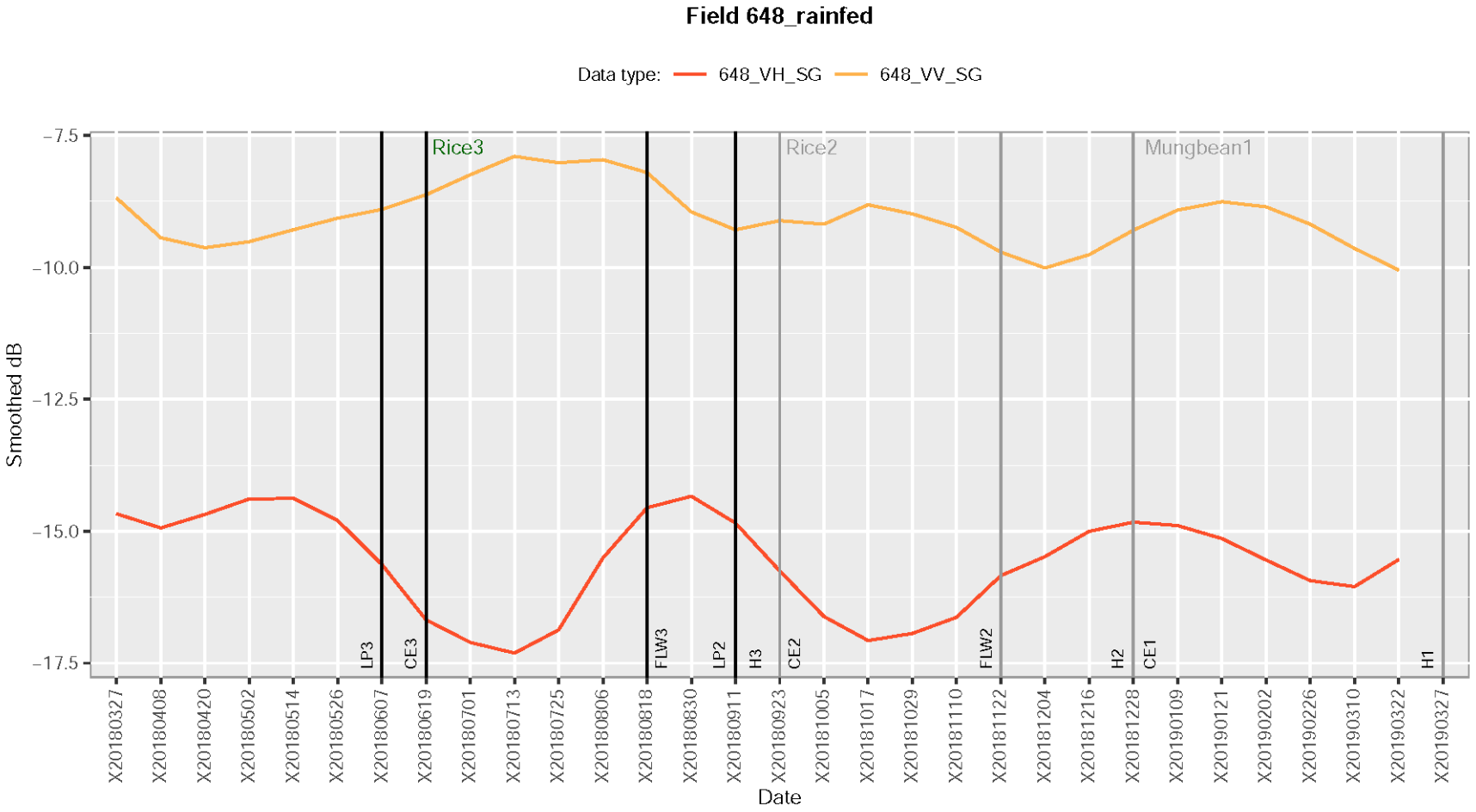
Field 648_rainfed
Data type: 648_VH_SG 648_VV_SG
Smoothed dB
−7.5
−10.0
−12.5
−15.0
−17.5
Rice3
Rice2
Mungbean1
LP3
CE3
FLW3
LP2
H3
CE2
FLW2
H2
CE1
H1
X20180327
X20180408
X20180420
X20180502
X20180514
X20180526
X20180607
X20180619
X20180701
X20180713
X20180725
X20180806
X20180818
X20180830
X20180911
X20180923
X20181005
X20181017
X20181029
X20181110
X20181122
X20181204
X20181216
X20181228
X20190109
X20190121
X20190202
X20190226
X20190310
X20190322
X20190327
Date

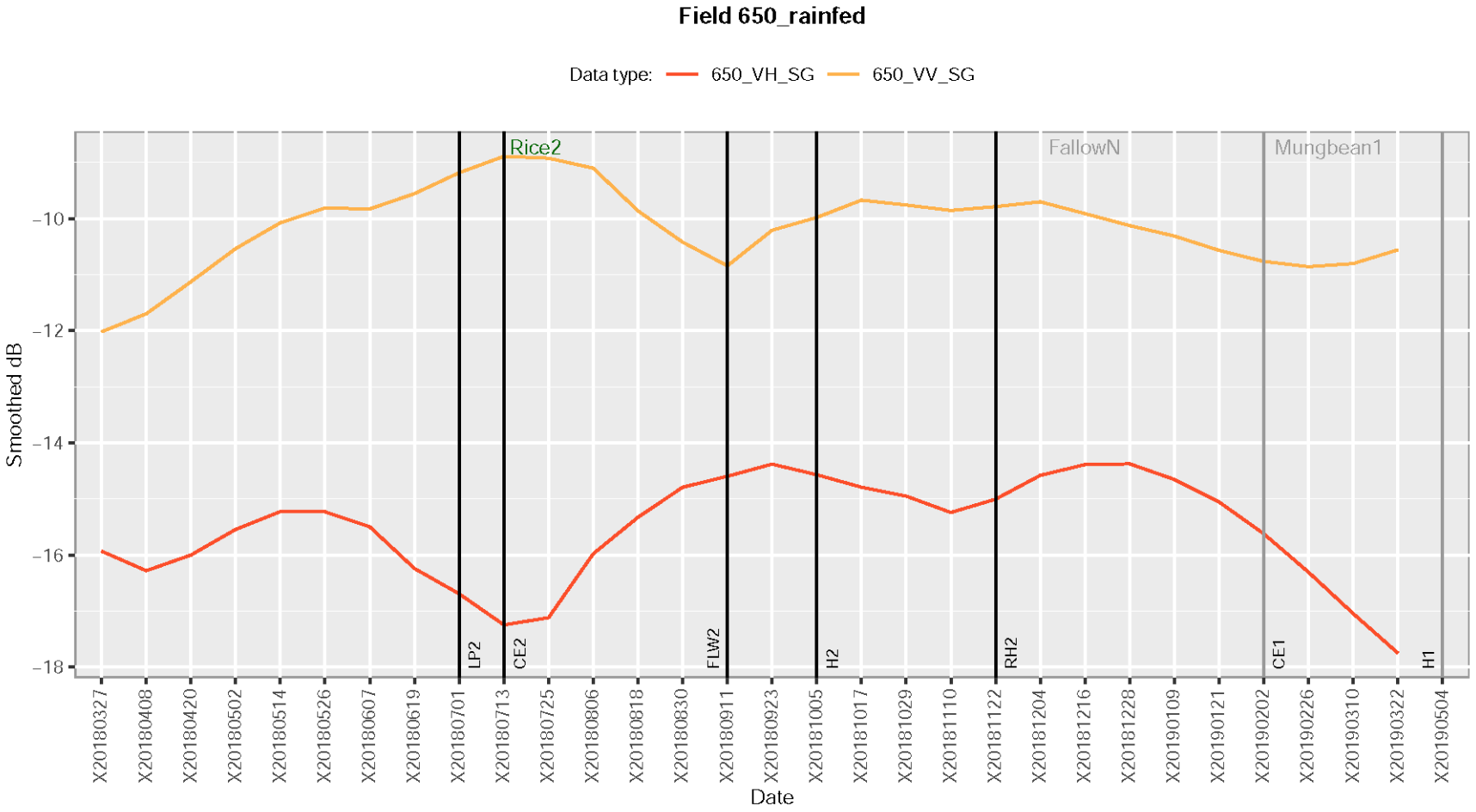
Field 650_rainfed
Data type: 650_VH_SG 650_VV_SG
Rice2
FallowN
Mungbean1
LP2
CE2
FLW2
H2
RH2
CE1
H1
Smoothed dB
−10
−12
−14
−16
−18
X20180327
X20180408
X20180420
X20180502
X20180514
X20180526
X20180607
X20180619
X20180701
X20180713
X20180725
X20180806
X20180818
X20180830
X20180911
X20180923
X20181005
X20181017
X20181029
X20181110
X20181122
X20181204
X20181216
X20181228
X20190109
X20190121
X20190202
X20190226
X20190310
X20190322
X20190504
Date

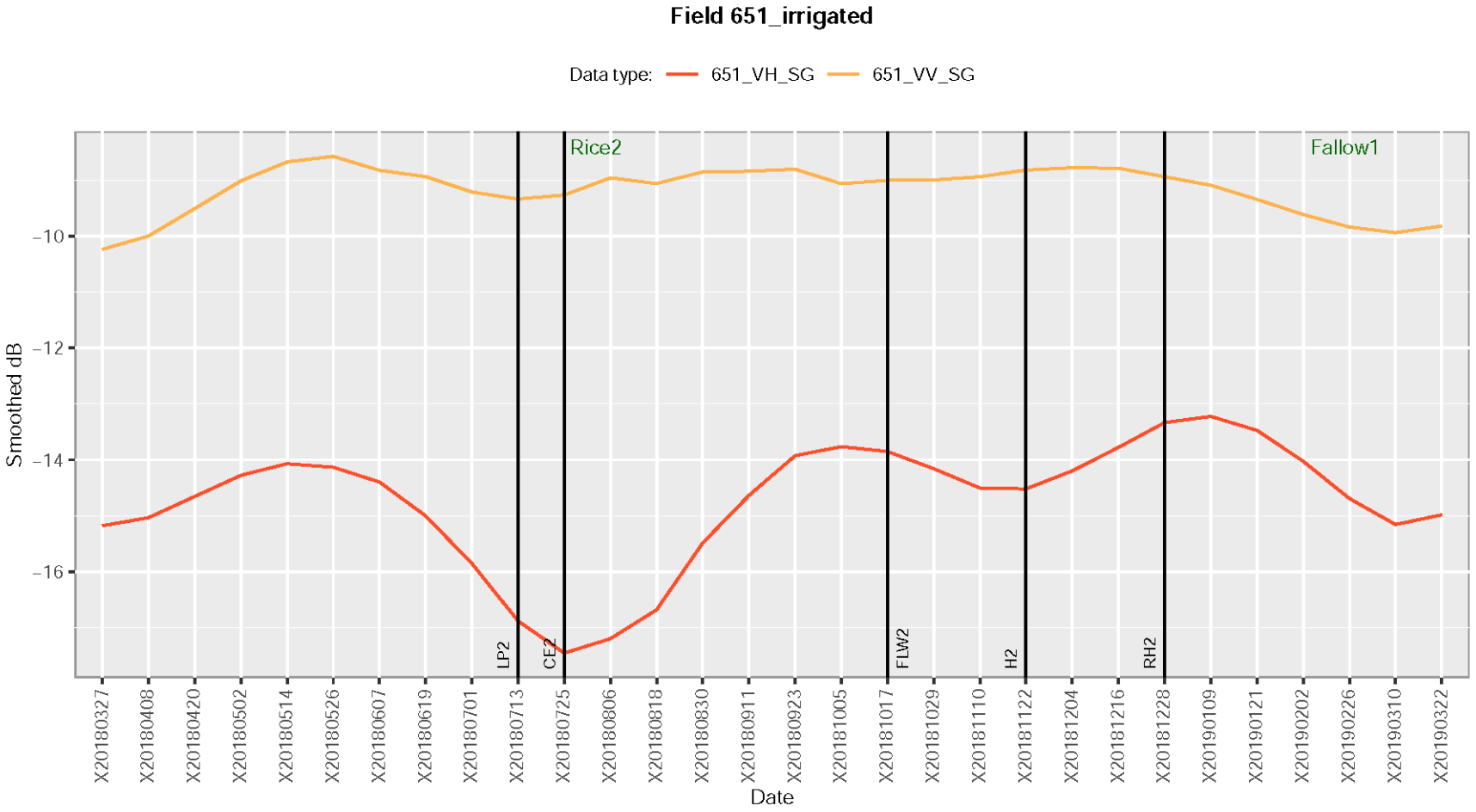
Field 651_irrigated
Data type: 651_VH_SG 651_VV_SG
Rice2
Fallow1
LP2
CE2
FLW2
H2
RH2
Smoothed dB
−10
−12
−14
−16
X20180327
X20180408
X20180420
X20180502
X20180514
X20180526
X20180607
X20180619
X20180701
X20180713
X20180725
X20180806
X20180818
X20180830
X20180911
X20180923
X20181005
X20181017
X20181029
X20181110
X20181122
X20181204
X20181216
X20181228
X20190109
X20190121
X20190202
X20190226
X20190310
X20190322
Date

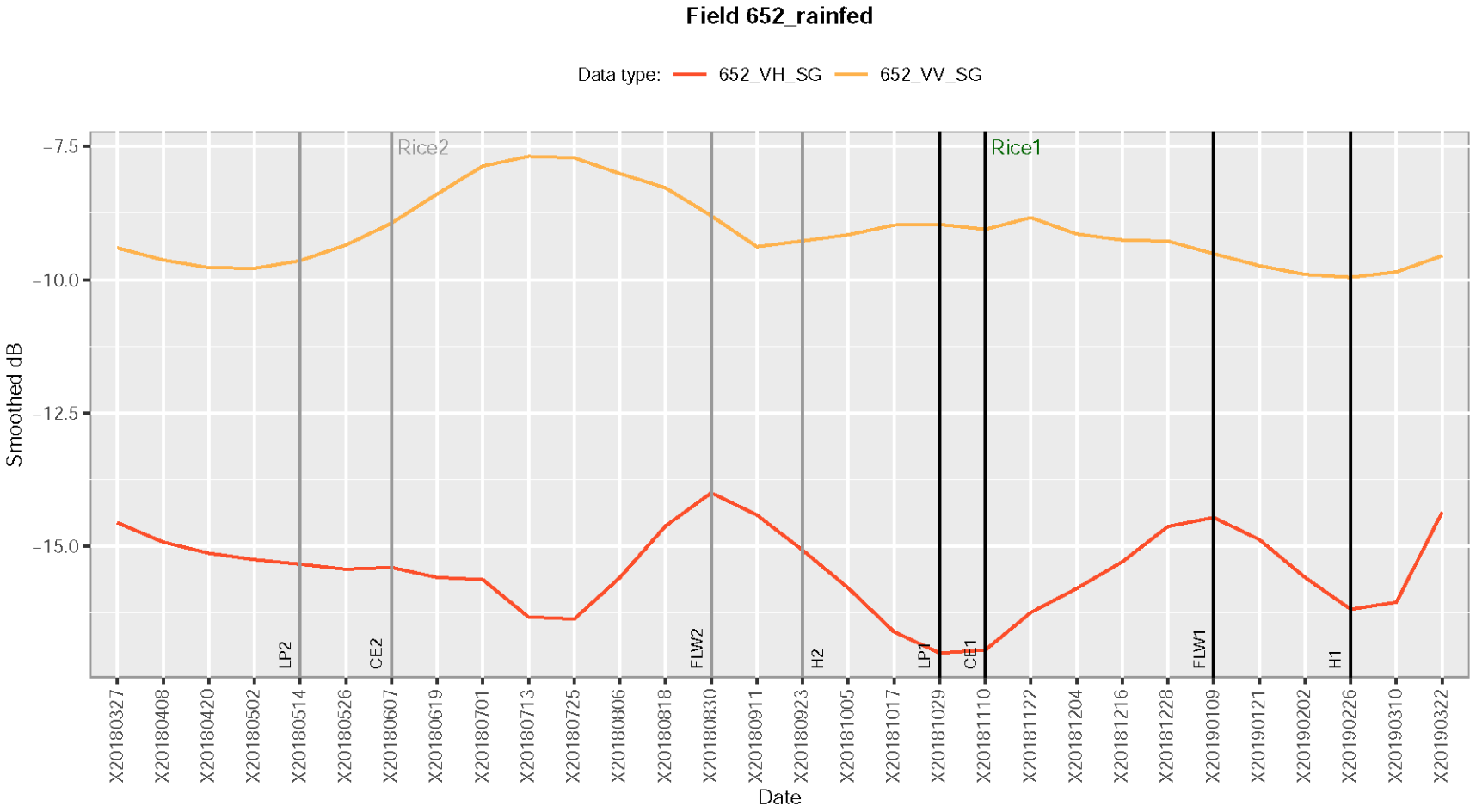
Field 652_rainfed
Data type: 652_VH_SG 652_VV_SG
Smoothed dB
−7.5
−10.0
−12.5
−15.0
Rice2
Rice1
LP2
CE2
FLW2
H2
LP1
CE1
FLW1
H1
X20180327
X20180408
X20180420
X20180502
X20180514
X20180526
X20180607
X20180619
X20180701
X20180713
X20180725
X20180806
X20180818
X20180830
X20180911
X20180923
X20181005
X20181017
X20181029
X20181110
X20181122
X20181204
X20181216
X20181228
X20190109
X20190121
X20190202
X20190226
X20190310
X20190322
Date

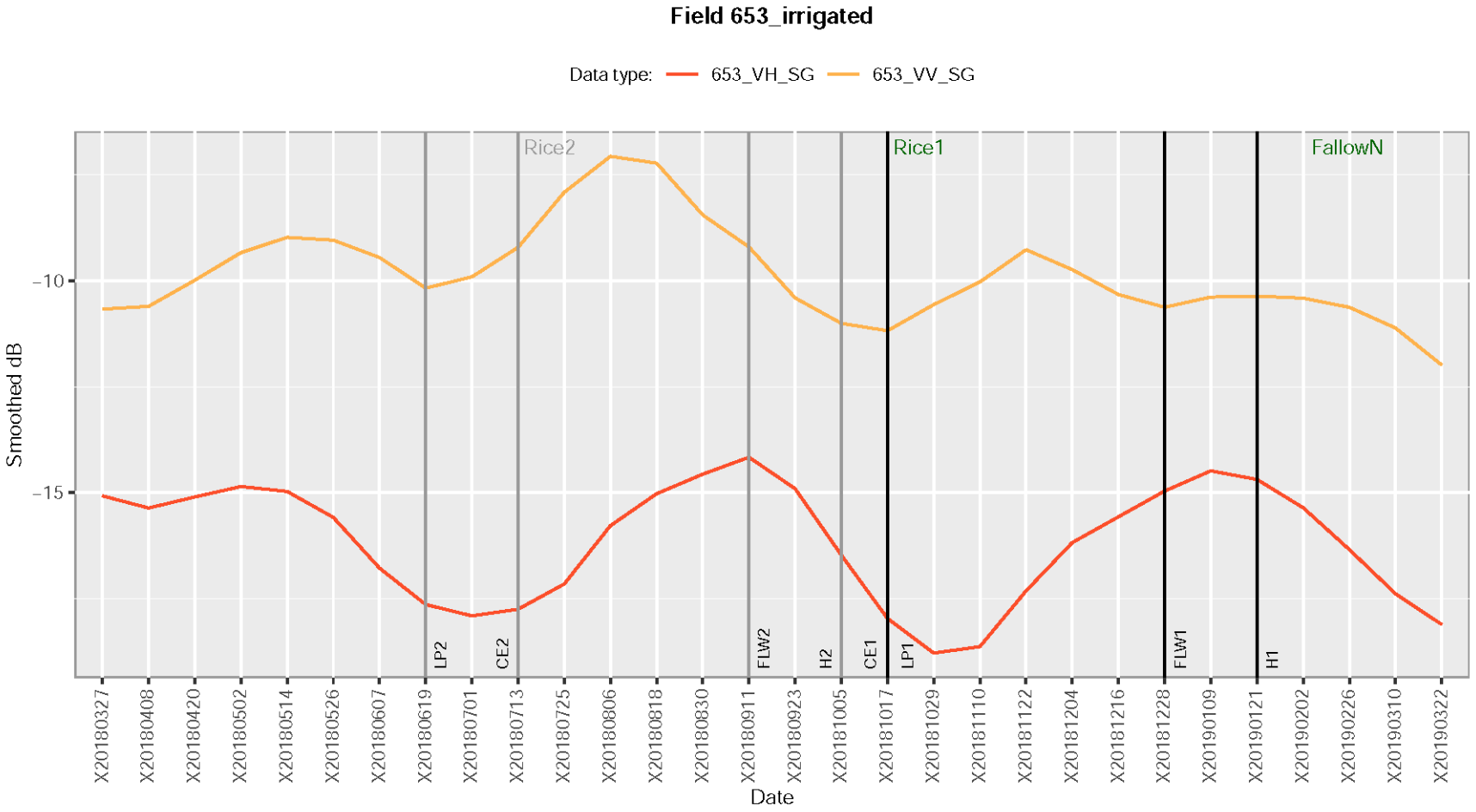
Field 653_irrigated
Data type: 653_VH_SG 653_VV_SG
Rice2
Rice1
FallowN
−10
−15
Smoothed dB
LP2
CE2
FLW2
H2
CE1
LP1
FLW1
H1
X20180327
X20180408
X20180420
X20180502
X20180514
X20180526
X20180607
X20180619
X20180701
X20180713
X20180725
X20180806
X20180818
X20180830
X20180911
X20180923
X20181005
X20181017
X20181029
X20181110
X20181122
X20181204
X20181216
X20181228
X20190109
X20190121
X20190202
X20190226
X20190310
X20190322
Date

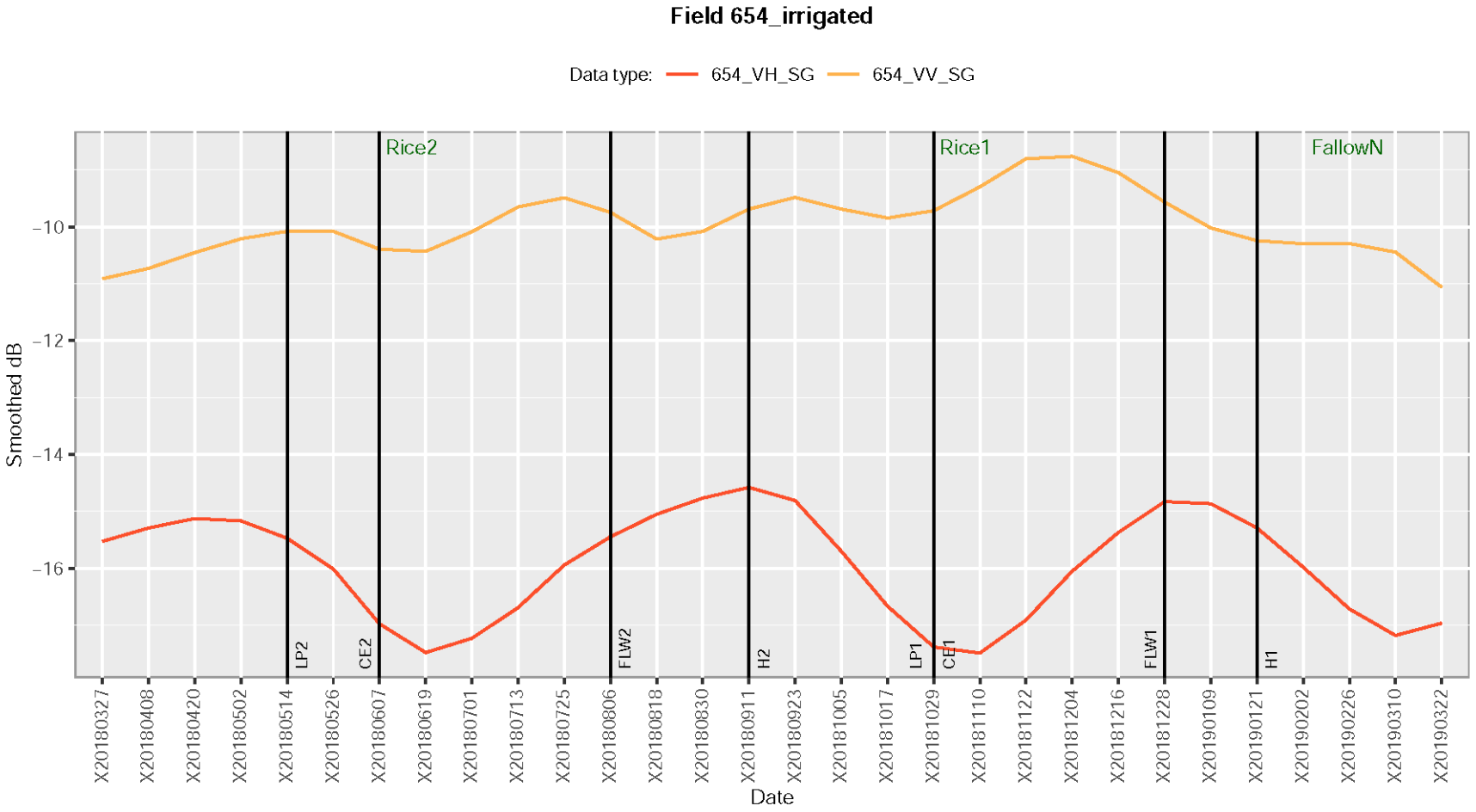
Field 654_irrigated
Data type: 654_VH_SG 654_VV_SG
Rice2
Rice1
FallowN
LP2
CE2
FLW2
H2
LP1
CE1
FLW1
H1
−10
−12
−14
−16
Smoothed dB
X20180327
X20180408
X20180420
X20180502
X20180514
X20180526
X20180607
X20180619
X20180701
X20180713
X20180725
X20180806
X20180818
X20180830
X20180911
X20180923
X20181005
X20181017
X20181029
X20181110
X20181122
X20181204
X20181216
X20181228
X20190109
X20190121
X20190202
X20190226
X20190310
X20190322
Date

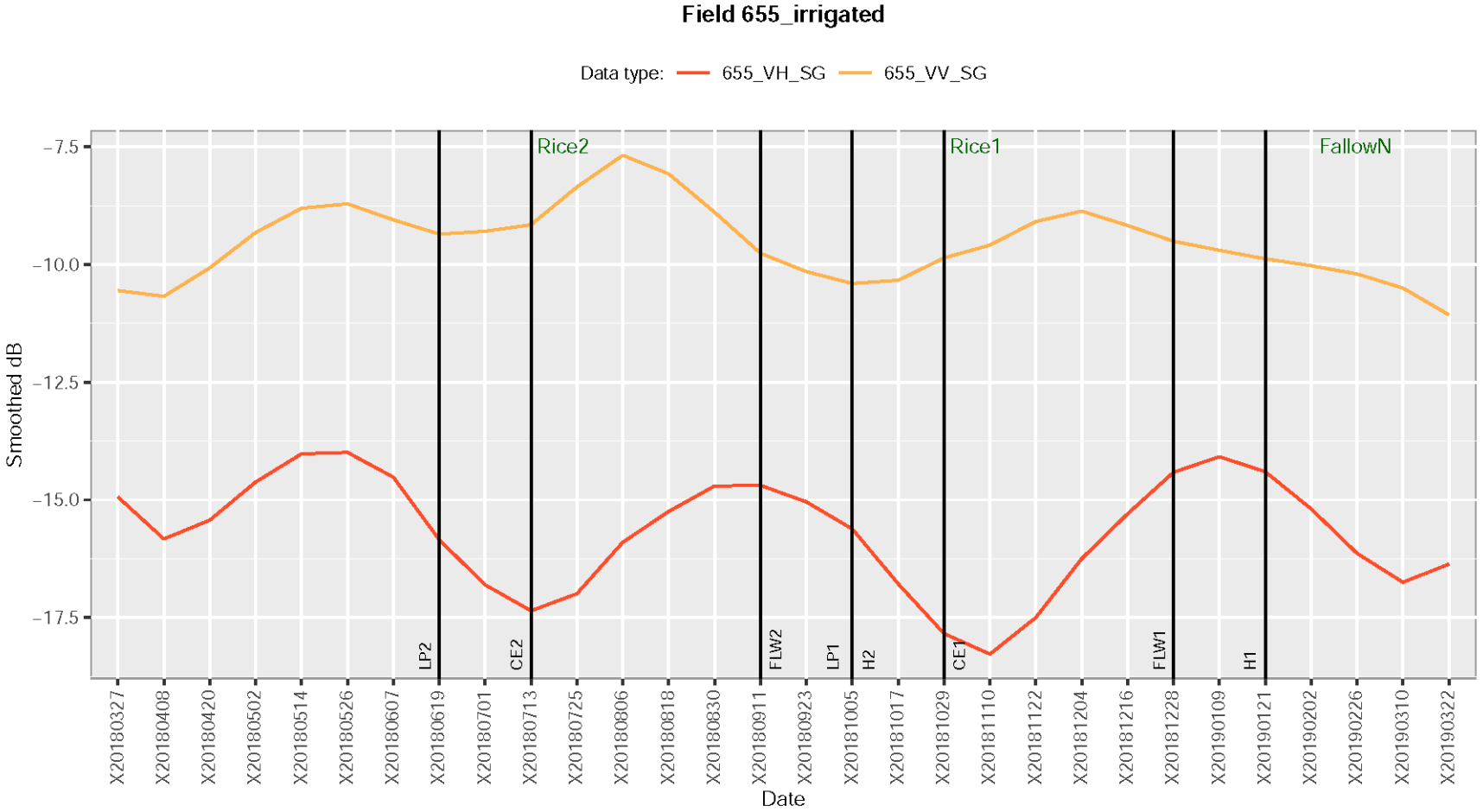
Field 655_irrigated
Data type: 655_VH_SG 655_VV_SG
Smoothed dB
−7.5
−10.0
−12.5
−15.0
−17.5
Rice2
Rice1
FallowN
LP2
CE2
FLW2
LP1
H2
CE1
FLW1
H1
X20180327
X20180408
X20180420
X20180502
X20180514
X20180526
X20180607
X20180619
X20180701
X20180713
X20180725
X20180806
X20180818
X20180830
X20180911
X20180923
X20181005
X20181017
X20181029
X20181110
X20181122
X20181204
X20181216
X20181228
X20190109
X20190121
X20190202
X20190226
X20190310
X20190322
Date

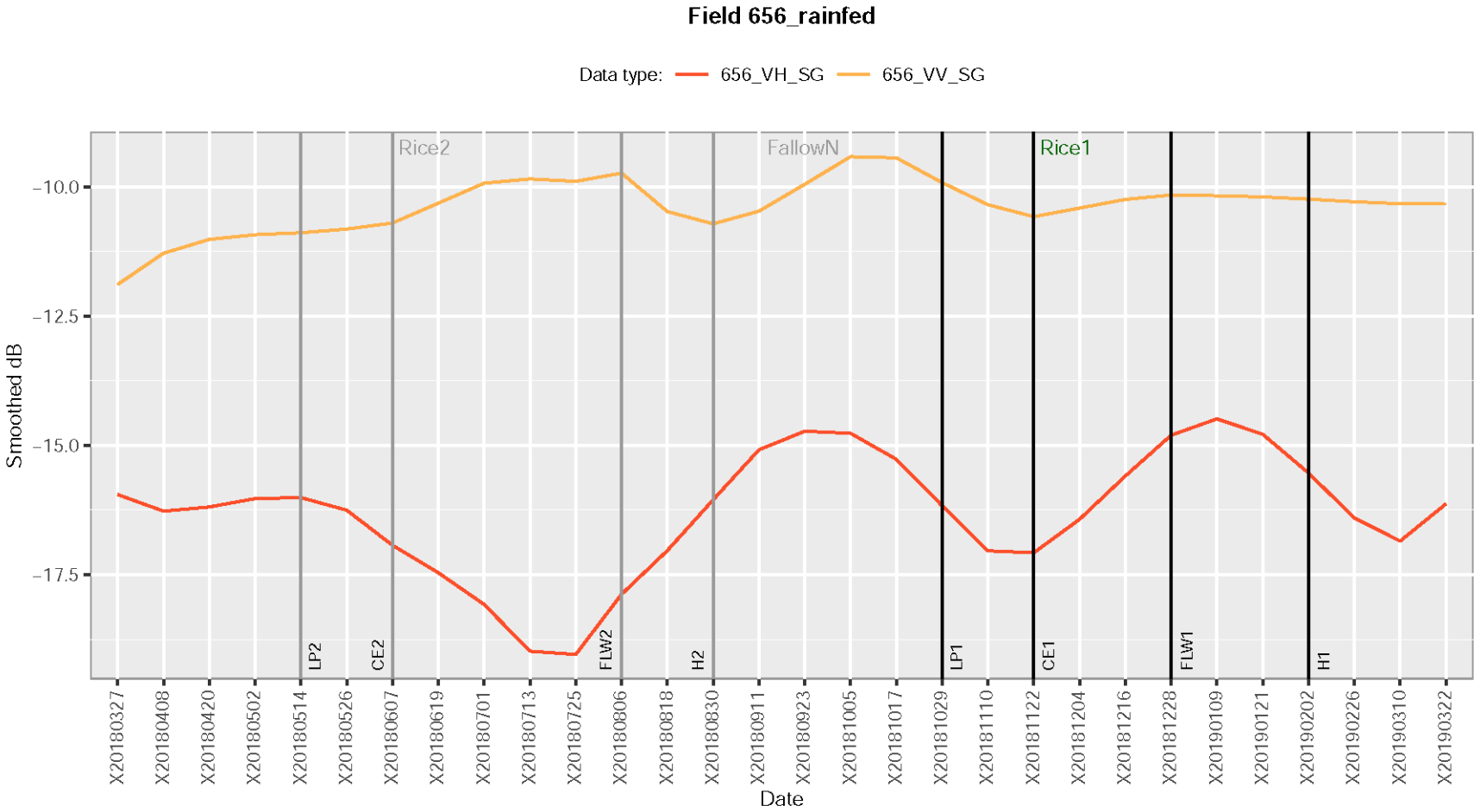
Field 656_rainfed
Data type: 656_VH_SG 656_VV_SG
Rice2
FallowN
Rice1
−10.0
−12.5
−15.0
−17.5
Smoothed dB
LP2
CE2
FLW2
H2
LP1
CE1
FLW1
H1
X20180327
X20180408
X20180420
X20180502
X20180514
X20180526
X20180607
X20180619
X20180701
X20180713
X20180725
X20180806
X20180818
X20180830
X20180911
X20180923
X20181005
X20181017
X20181029
X20181110
X20181122
X20181204
X20181216
X20181228
X20190109
X20190121
X20190202
X20190226
X20190310
X20190322
Date

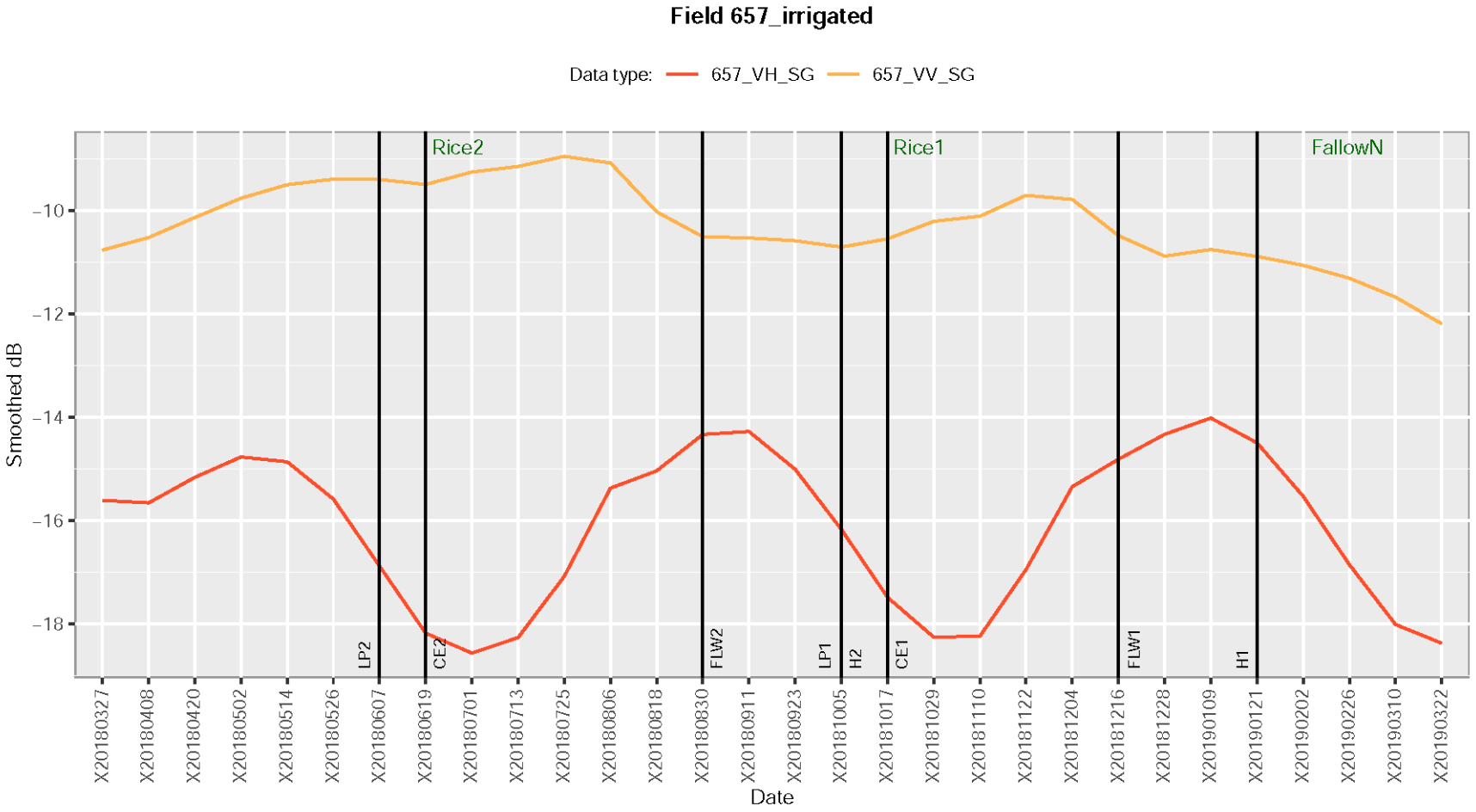
Field 657_irrigated
Data type: 657_VH_SG 657_VV_SG
Rice2
Rice1
FallowN
LP2
CE2
FLW2
LP1
H2
CE1
FLW1
H1
Smoothed dB
−10
−12
−14
−16
−18
X20180327
X20180408
X20180420
X20180502
X20180514
X20180526
X20180607
X20180619
X20180701
X20180713
X20180725
X20180806
X20180818
X20180830
X20180911
X20180923
X20181005
X20181017
X20181029
X20181110
X20181122
X20181204
X20181216
X20181228
X20190109
X20190121
X20190202
X20190226
X20190310
X20190322
Date

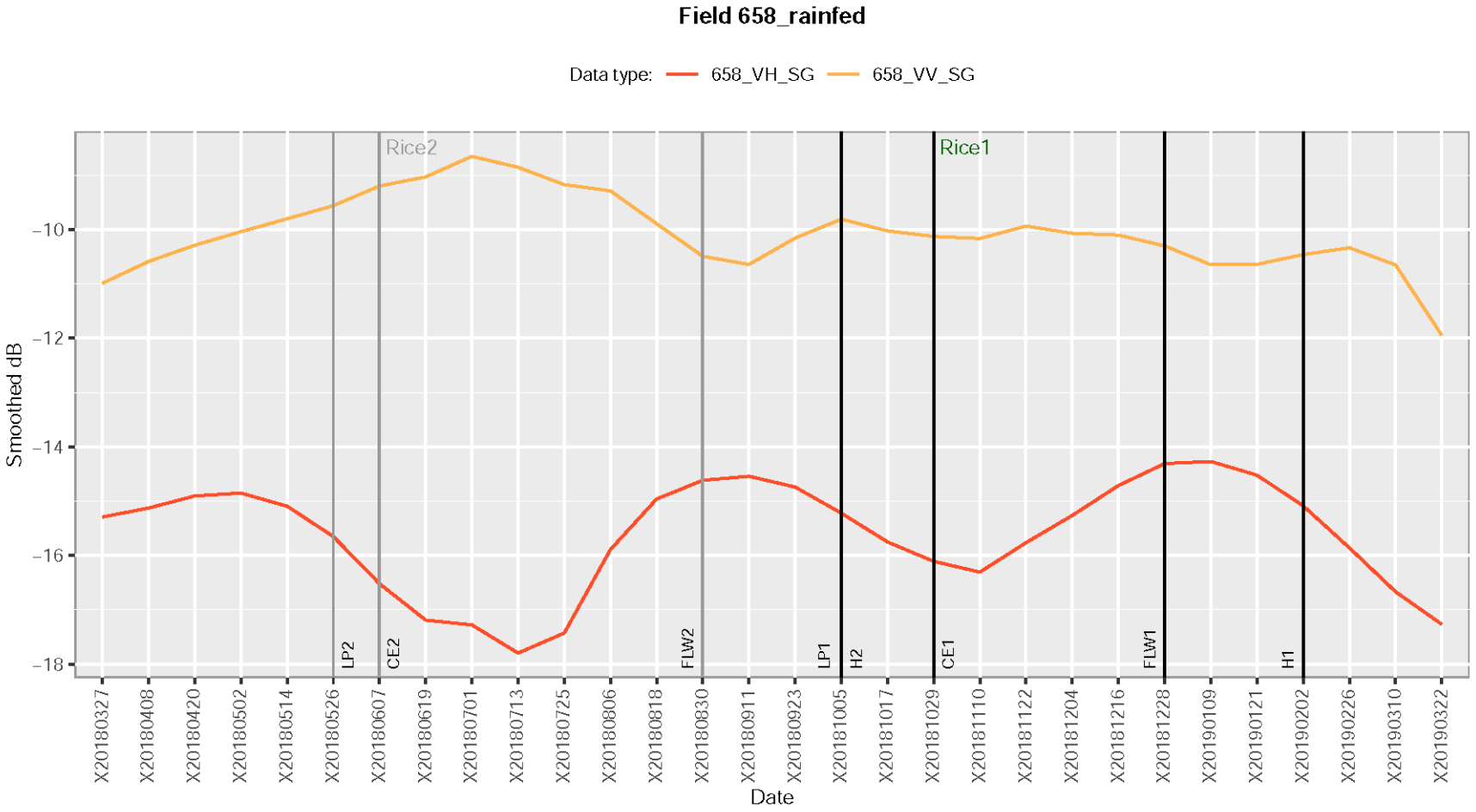
Field 658_rainfed
Data type: 658_VH_SG 658_VV_SG
Rice2
Rice1
Smoothed dB
−10
−12
−14
−16
−18
LP2
CE2
FLW2
LP1
H2
CE1
FLW1
H1
X20180327
X20180408
X20180420
X20180502
X20180514
X20180526
X20180607
X20180619
X20180701
X20180713
X20180725
X20180806
X20180818
X20180830
X20180911
X20180923
X20181005
X20181017
X20181029
X20181110
X20181122
X20181204
X20181216
X20181228
X20190109
X20190121
X20190202
X20190226
X20190310
X20190322
Date

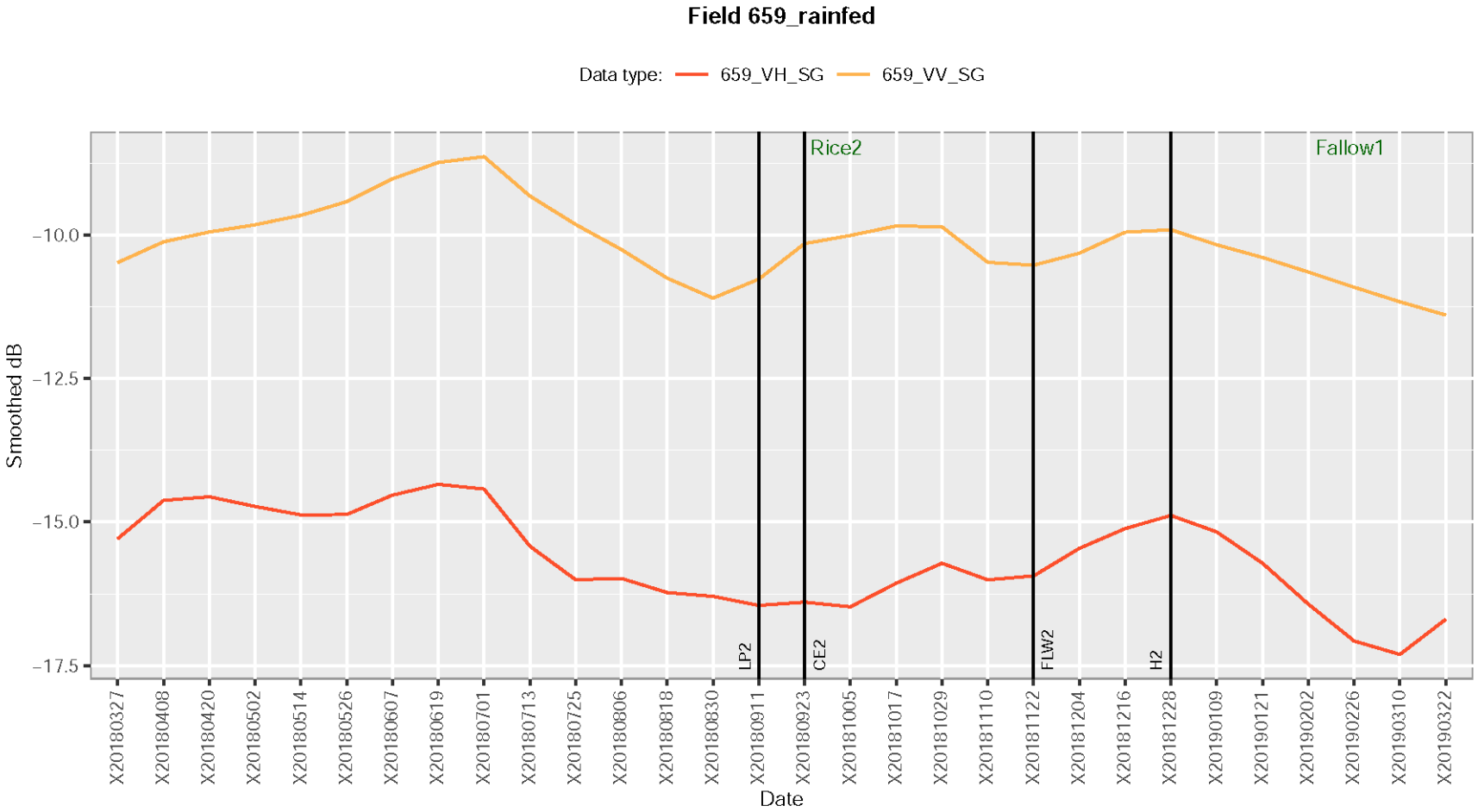
Field 659_rainfed
Data type: 659_VH_SG 659_VV_SG
Rice2
Fallow1
LP2
CE2
FLW2
H2
Smoothed dB
−10.0
−12.5
−15.0
−17.5
X20180327
X20180408
X20180420
X20180502
X20180514
X20180526
X20180607
X20180619
X20180701
X20180713
X20180725
X20180806
X20180818
X20180830
X20180911
X20180923
X20181005
X20181017
X20181029
X20181110
X20181122
X20181204
X20181216
X20181228
X20190109
X20190121
X20190202
X20190226
X20190310
X20190322
Date

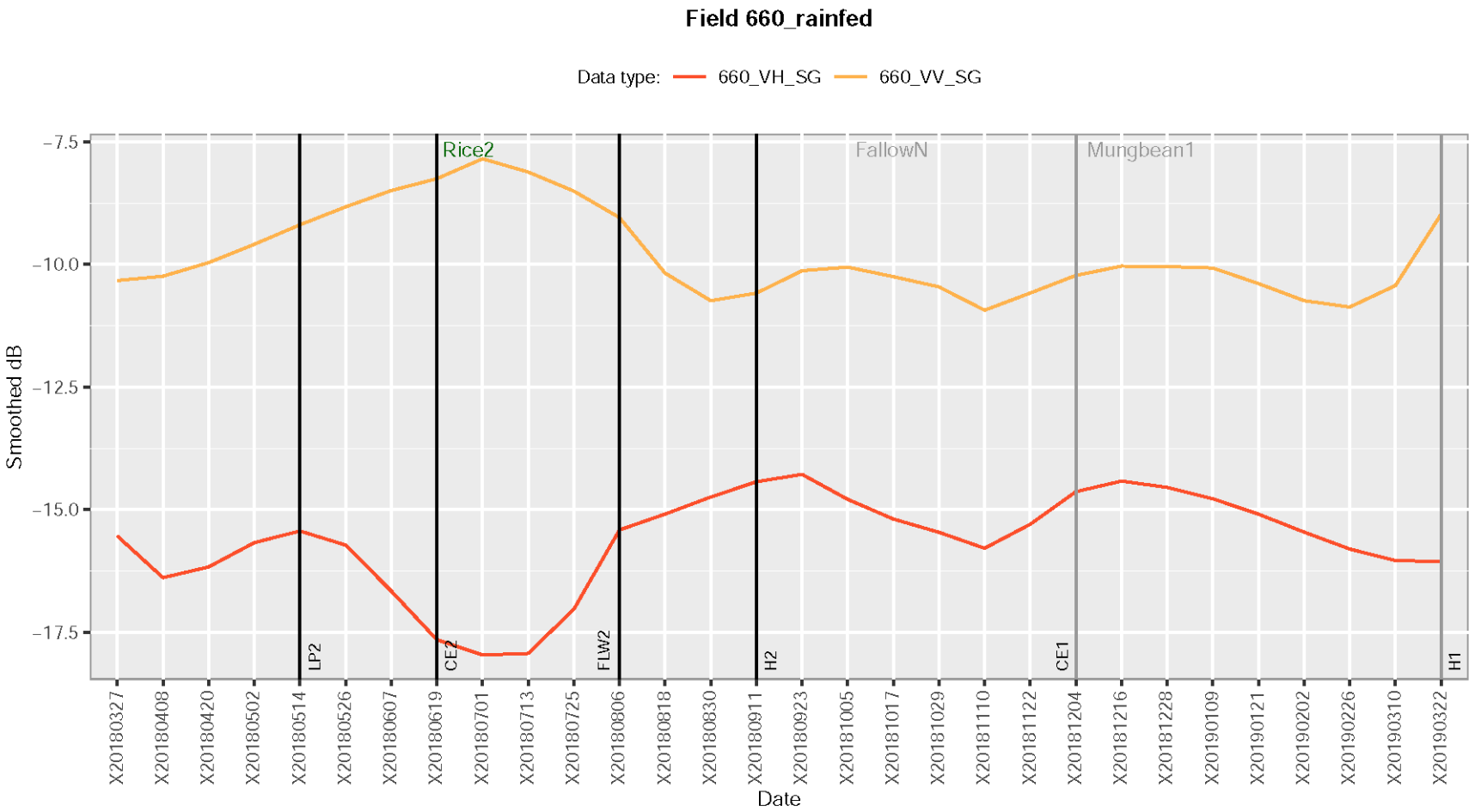
Field 660_rainfed
Data type: 660_VH_SG 660_VV_SG
Rice2
FallowN
Mungbean1
LP2
CE2
FLW2
H2
CE1
H1
Smoothed dB
−7.5
−10.0
−12.5
−15.0
−17.5
X20180327
X20180408
X20180420
X20180502
X20180514
X20180526
X20180607
X20180619
X20180701
X20180713
X20180725
X20180806
X20180818
X20180830
X20180911
X20180923
X20181005
X20181017
X20181029
X20181110
X20181122
X20181204
X20181216
X20181228
X20190109
X20190121
X20190202
X20190226
X20190310
X20190322
Date

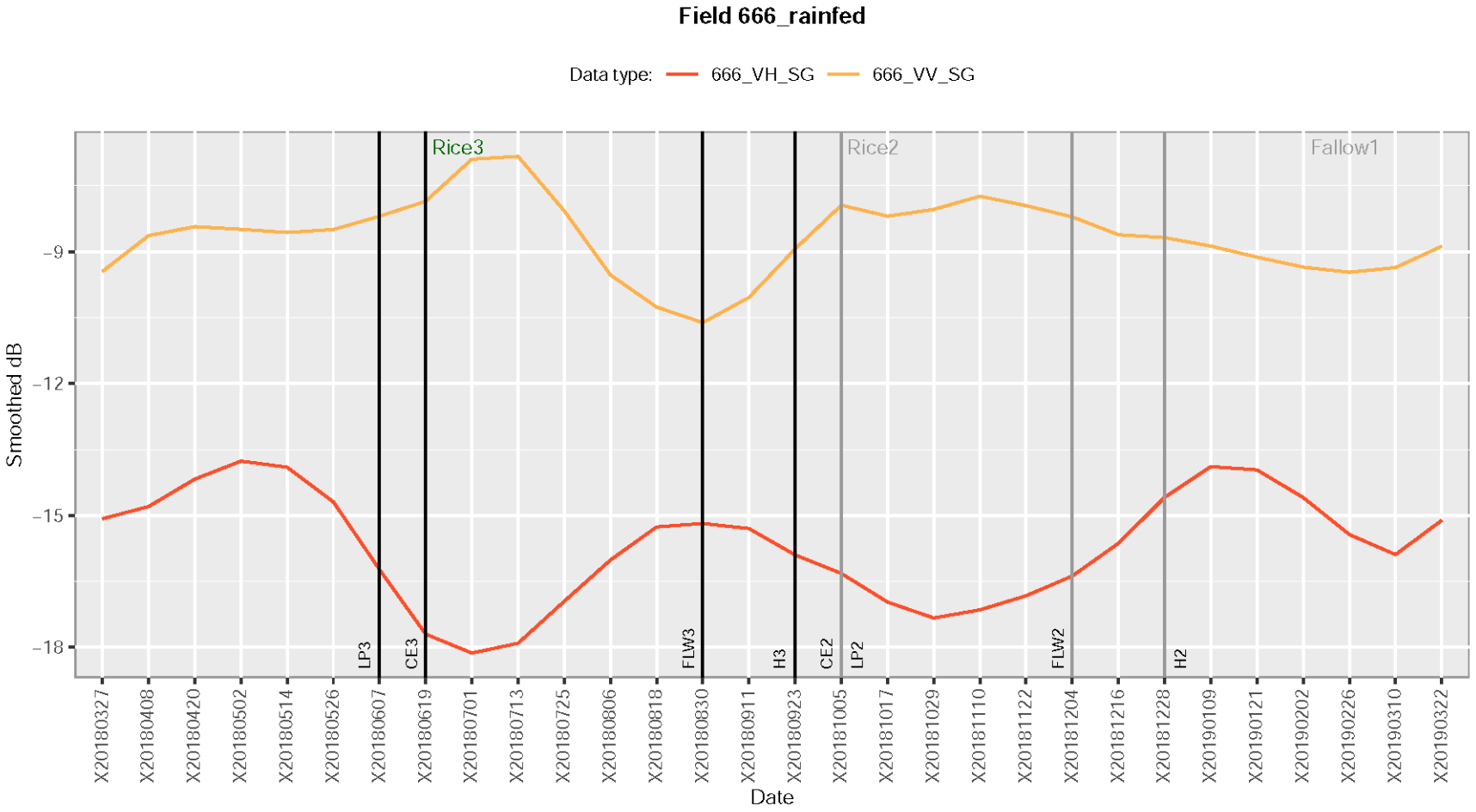
Field 666_rainfed
Data type: 666_VH_SG 666_VV_SG
Rice3
Rice2
Fallow1
Smoothed dB
-9
-12
-15
-18
LP3
CE3
FLW3
H3
CE2
LP2
FLW2
H2
X20180327
X20180408
X20180420
X20180502
X20180514
X20180526
X20180607
X20180619
X20180701
X20180713
X20180725
X20180806
X20180818
X20180830
X20180911
X20180923
X20181005
X20181017
X20181029
X20181110
X20181122
X20181204
X20181216
X20181228
X20190109
X20190121
X20190202
X20190226
X20190310
X20190322
Date

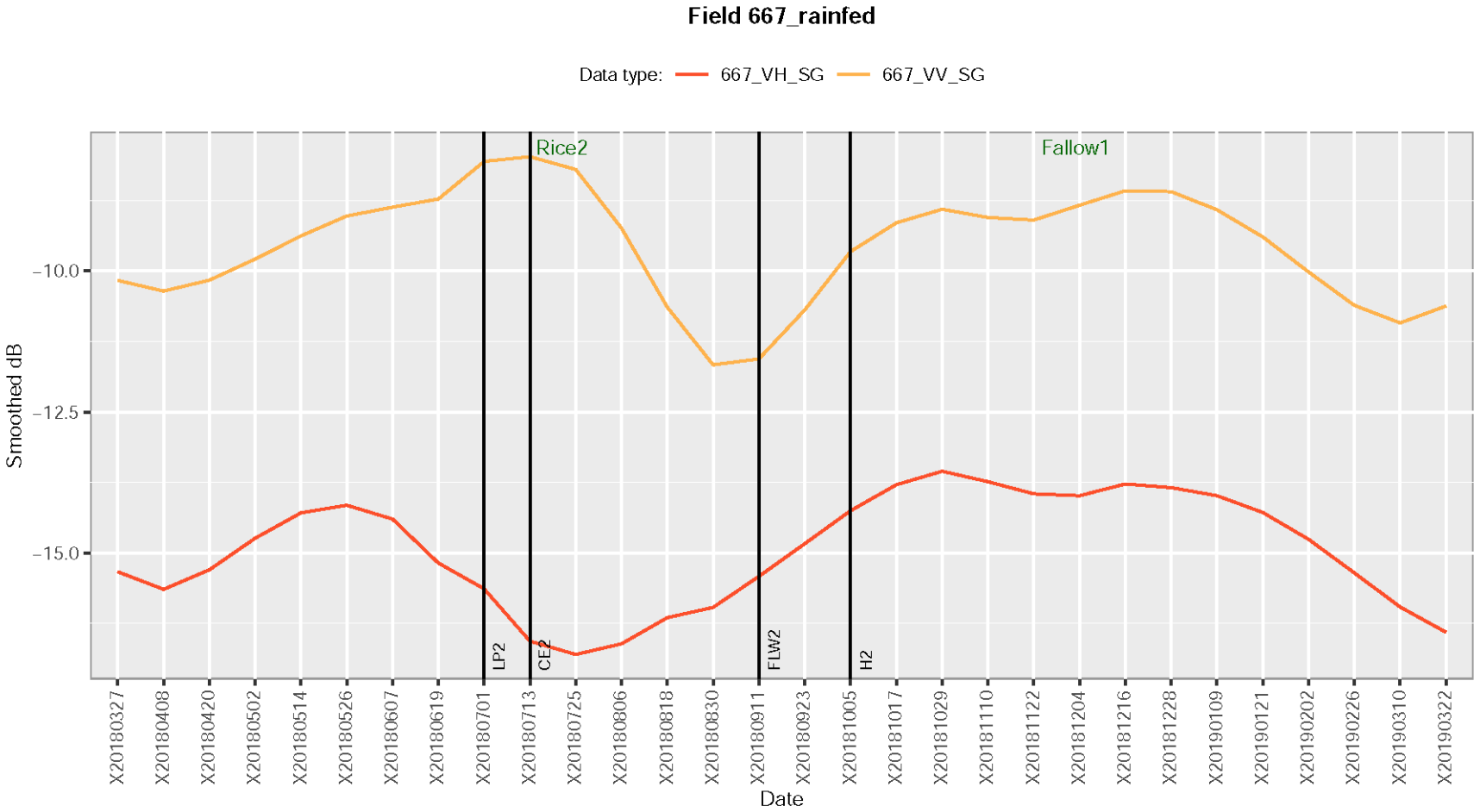
Field 667_rainfed
Data type: 667_VH_SG 667_VV_SG
Rice2
Fallow1
LP2
CE2
FLW2
H2
Smoothed dB
−10.0
−12.5
−15.0
X20180327
X20180408
X20180420
X20180502
X20180514
X20180526
X20180607
X20180619
X20180701
X20180713
X20180725
X20180806
X20180818
X20180830
X20180911
X20180923
X20181005
X20181017
X20181029
X20181110
X20181122
X20181204
X20181216
X20181228
X20190109
X20190121
X20190202
X20190226
X20190310
X20190322
Date

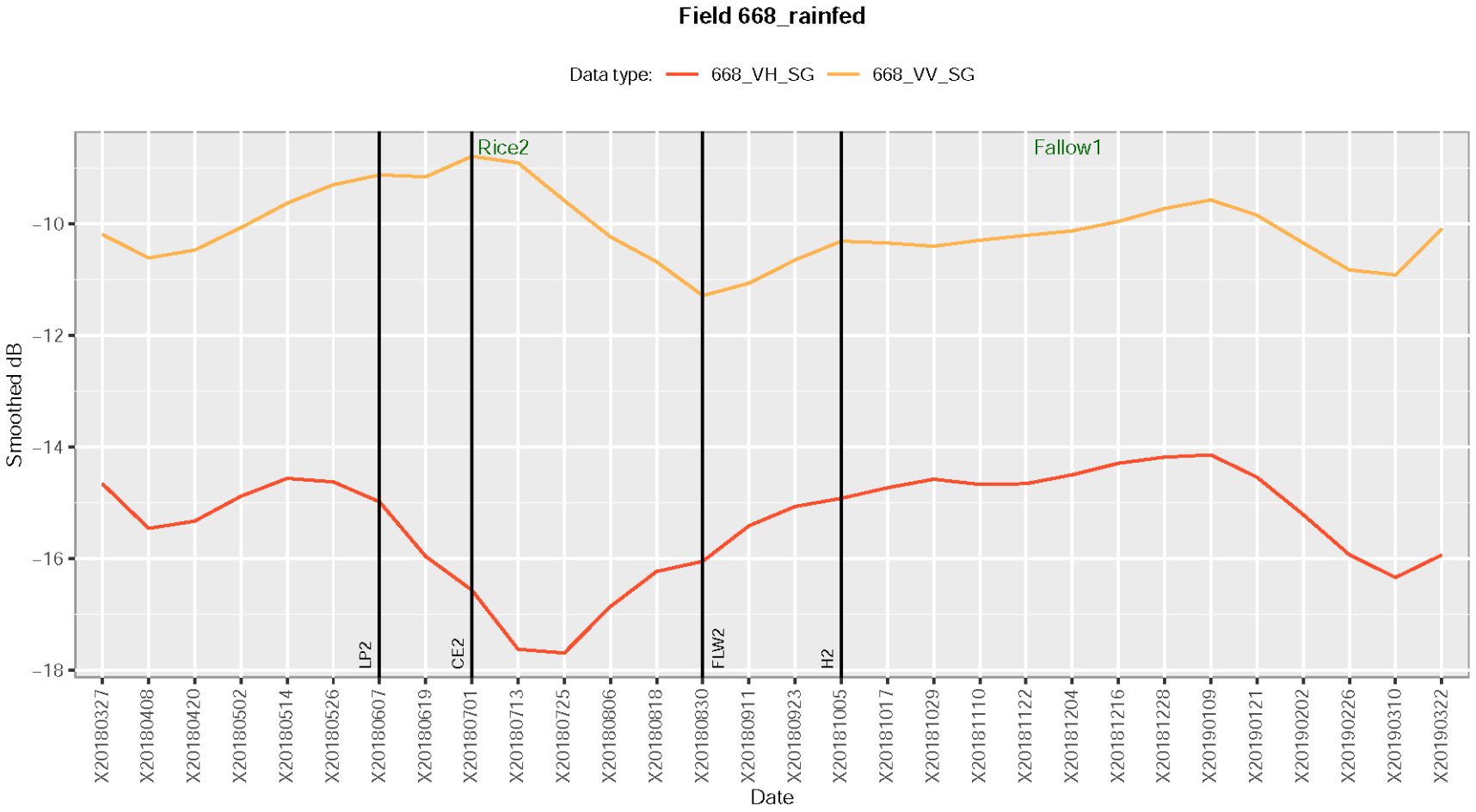
Field 668_rainfed
Data type: 668_VH_SG 668_VV_SG
Rice2
Fallow1
LP2
CE2
FLW2
H2
Smoothed dB
−10
−12
−14
−16
−18
X20180327
X20180408
X20180420
X20180502
X20180514
X20180526
X20180607
X20180619
X20180701
X20180713
X20180725
X20180806
X20180818
X20180830
X20180911
X20180923
X20181005
X20181017
X20181029
X20181110
X20181122
X20181204
X20181216
X20181228
X20190109
X20190121
X20190202
X20190226
X20190310
X20190322
Date

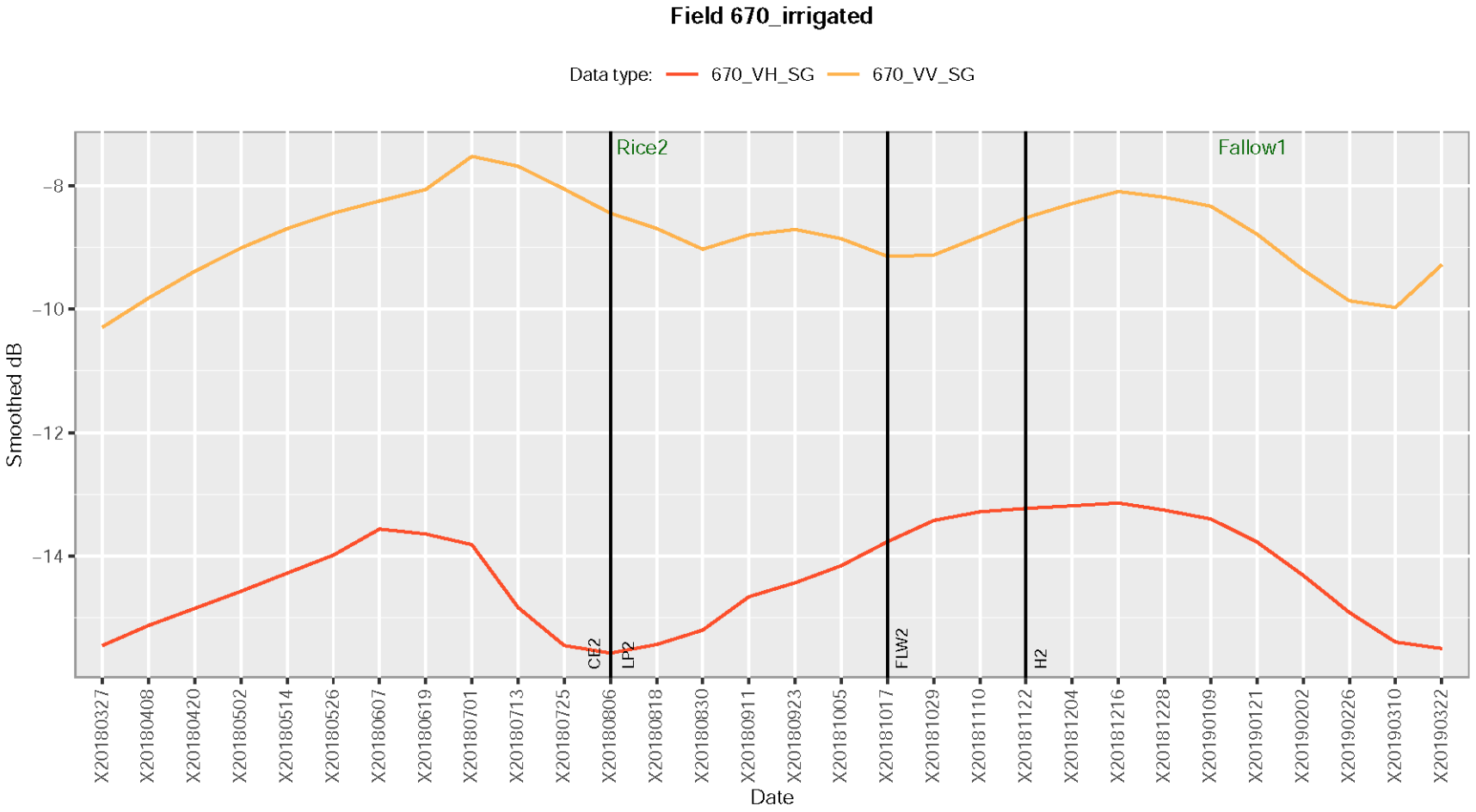
Field 670_irrigated
Data type: 670_VH_SG 670_VV_SG
Rice2
Fallow1
CE2
LP2
FLW2
H2
Smoothed dB
−8
−10
−12
−14
X20180327
X20180408
X20180420
X20180502
X20180514
X20180526
X20180607
X20180619
X20180701
X20180713
X20180725
X20180806
X20180818
X20180830
X20180911
X20180923
X20181005
X20181017
X20181029
X20181110
X20181122
X20181204
X20181216
X20181228
X20190109
X20190121
X20190202
X20190226
X20190310
X20190322
Date

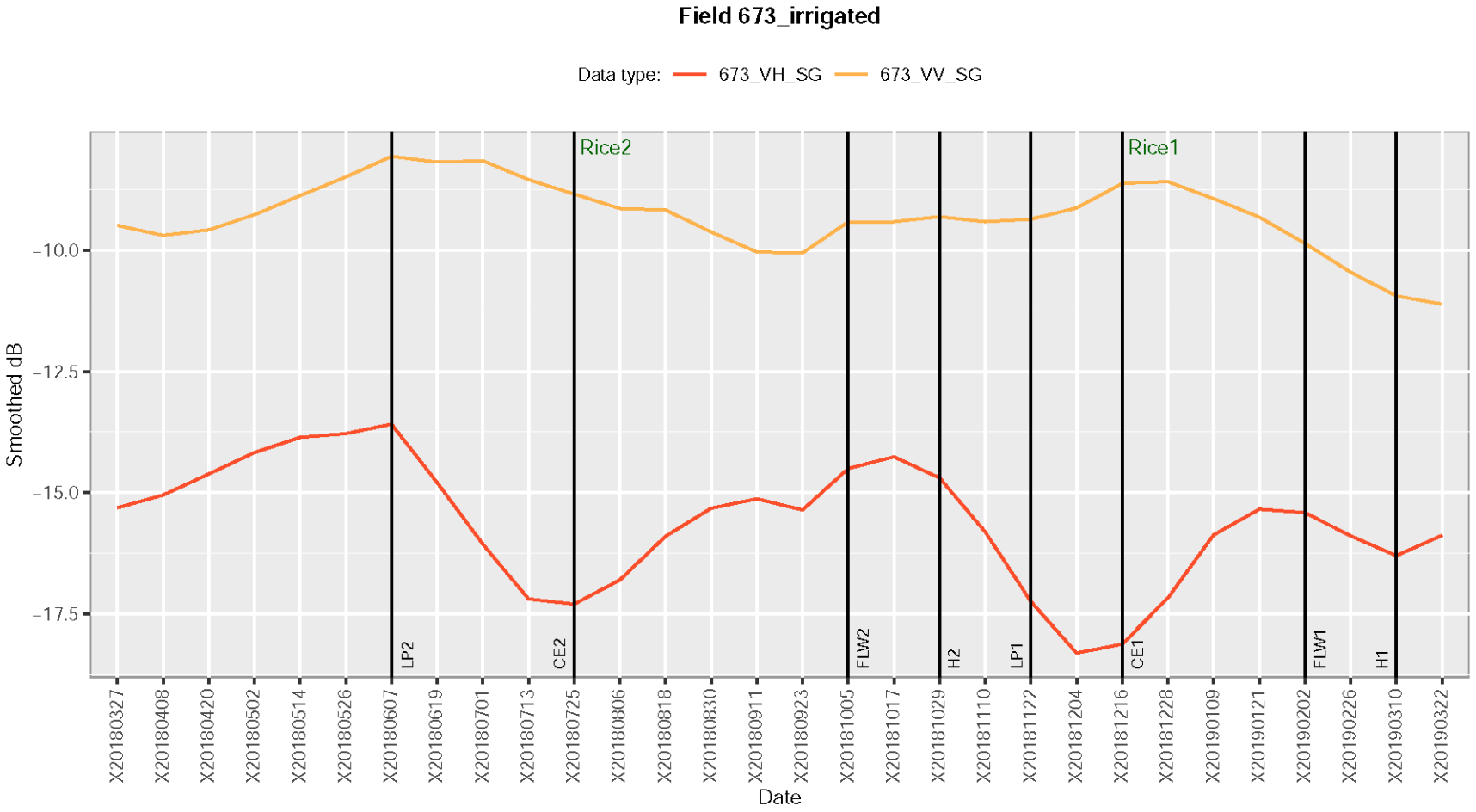
Field 673_irrigated
Data type: 673_VH_SG 673_VV_SG
Rice2
Rice1
LP2
CE2
FLW2
H2
LP1
CE1
FLW1
H1
Smoothed dB
−10.0
−12.5
−15.0
−17.5
X20180327
X20180408
X20180420
X20180502
X20180514
X20180526
X20180607
X20180619
X20180701
X20180713
X20180725
X20180806
X20180818
X20180830
X20180911
X20180923
X20181005
X20181017
X20181029
X20181110
X20181122
X20181204
X20181216
X20181228
X20190109
X20190121
X20190202
X20190226
X20190310
X20190322
Date

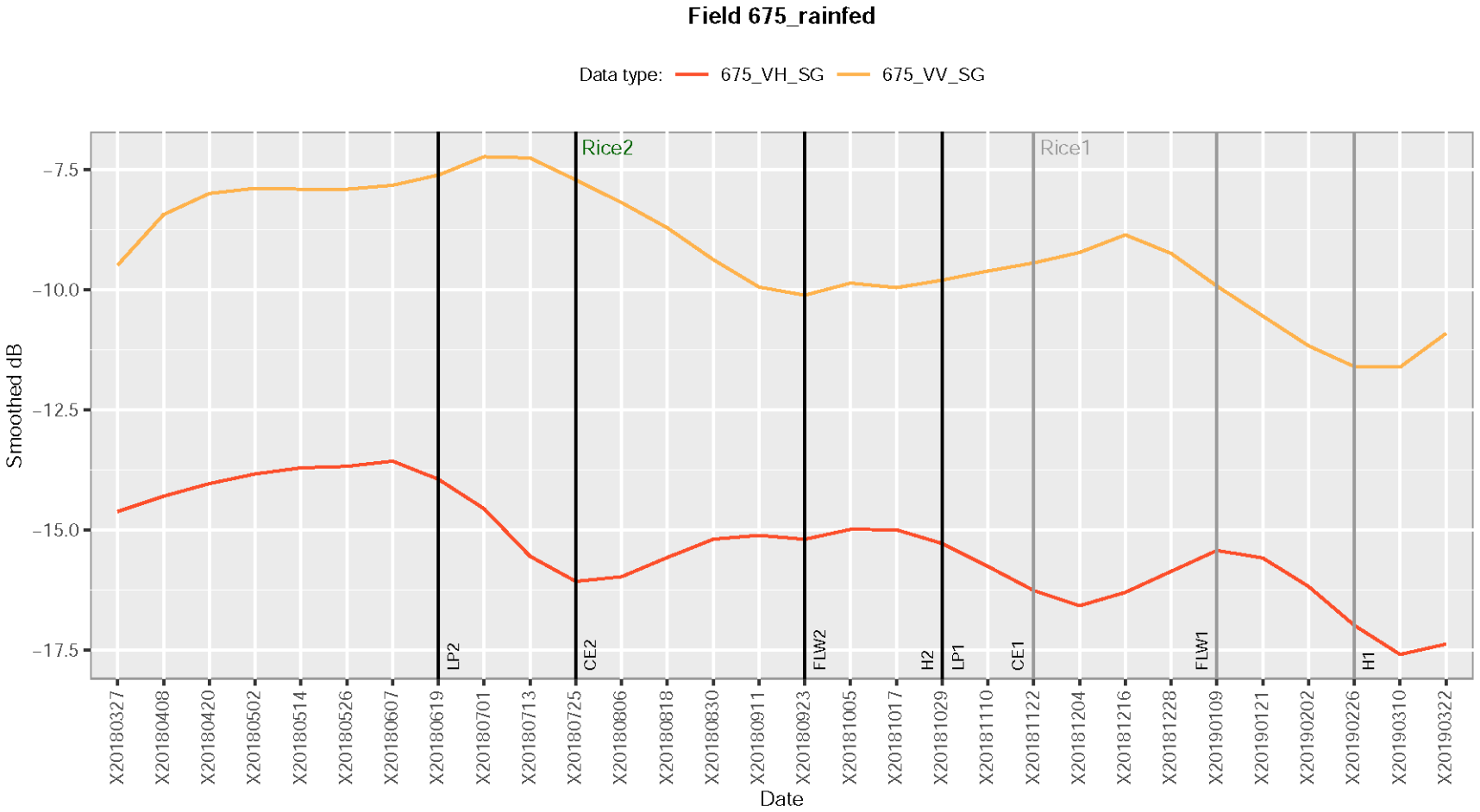
Field 675_rainfed
Data type: 675_VH_SG 675_VV_SG
Rice2
Rice1
LP2
CE2
FLW2
H2
LP1
CE1
FLW1
H1
Smoothed dB
−7.5
−10.0
−12.5
−15.0
−17.5
X20180327
X20180408
X20180420
X20180502
X20180514
X20180526
X20180607
X20180619
X20180701
X20180713
X20180725
X20180806
X20180818
X20180830
X20180911
X20180923
X20181005
X20181017
X20181029
X20181110
X20181122
X20181204
X20181216
X20181228
X20190109
X20190121
X20190202
X20190226
X20190310
X20190322
Date

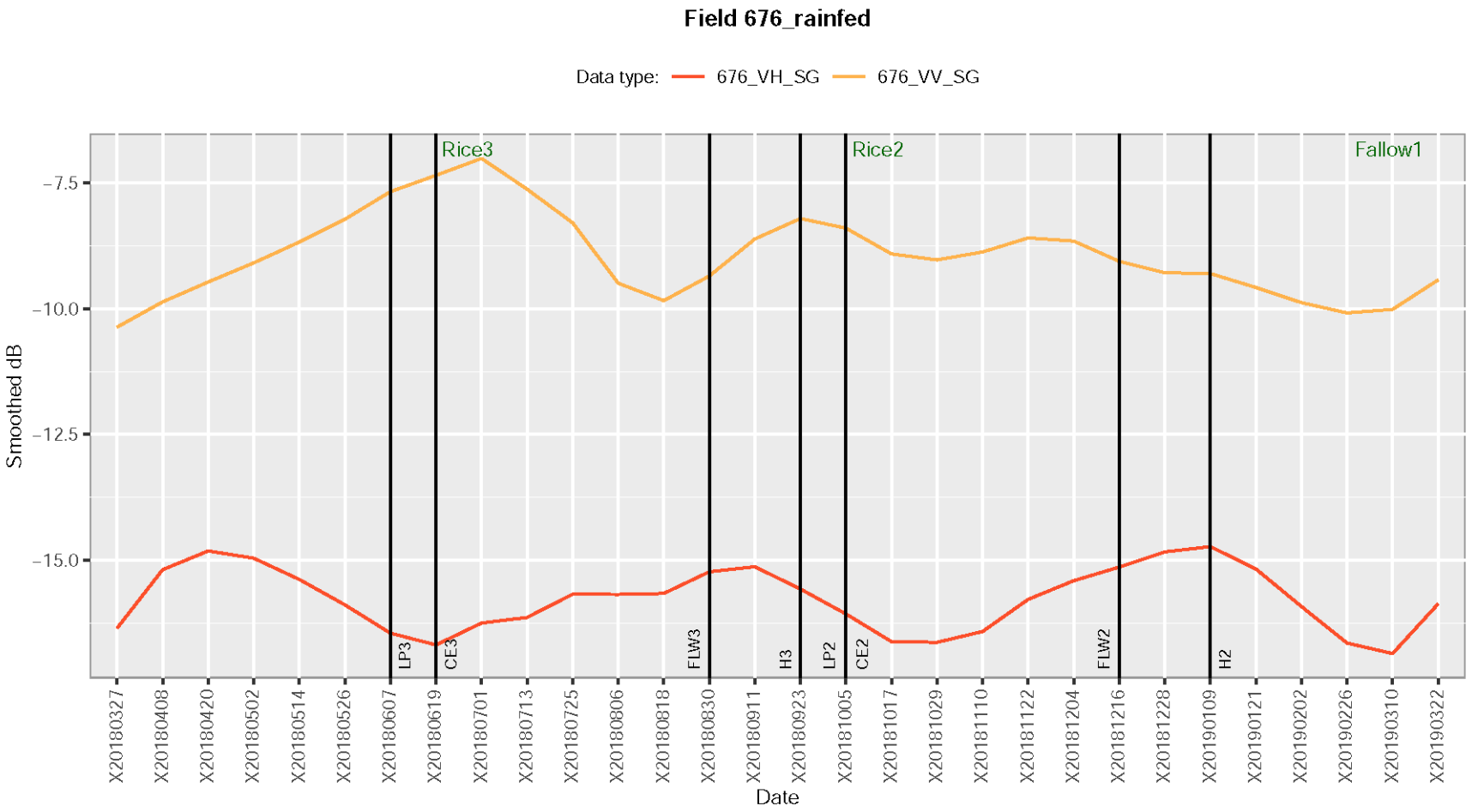
Field 676_rainfed
Data type: 676_VH_SG 676_VV_SG
Rice3
Rice2
Fallow1
Smoothed dB
−7.5
−10.0
−12.5
−15.0
LP3
CE3
FLW3
H3
LP2
CE2
FLW2
H2
X20180327
X20180408
X20180420
X20180502
X20180514
X20180526
X20180607
X20180619
X20180701
X20180713
X20180725
X20180806
X20180818
X20180830
X20180911
X20180923
X20181005
X20181017
X20181029
X20181110
X20181122
X20181204
X20181216
X20181228
X20190109
X20190121
X20190202
X20190226
X20190310
X20190322
Date

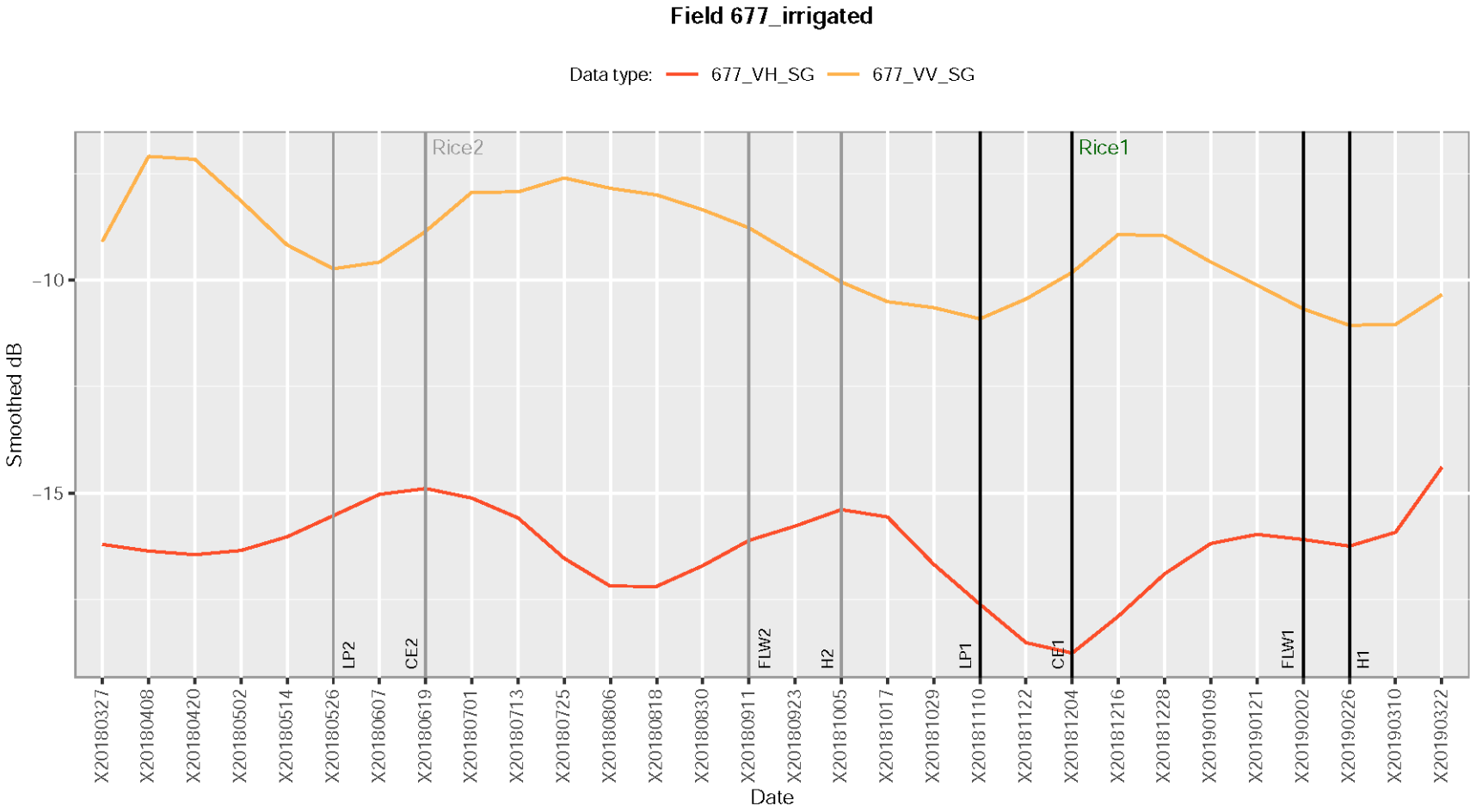
Field 677_irrigated
Data type: 677_VH_SG 677_VV_SG
Rice2
Rice1
−10
−15
Smoothed dB
LP2
CE2
FLW2
H2
LP1
CE1
FLW1
H1
X20180327
X20180408
X20180420
X20180502
X20180514
X20180526
X20180607
X20180619
X20180701
X20180713
X20180725
X20180806
X20180818
X20180830
X20180911
X20180923
X20181005
X20181017
X20181029
X20181110
X20181122
X20181204
X20181216
X20181228
X20190109
X20190121
X20190202
X20190226
X20190310
X20190322
Date

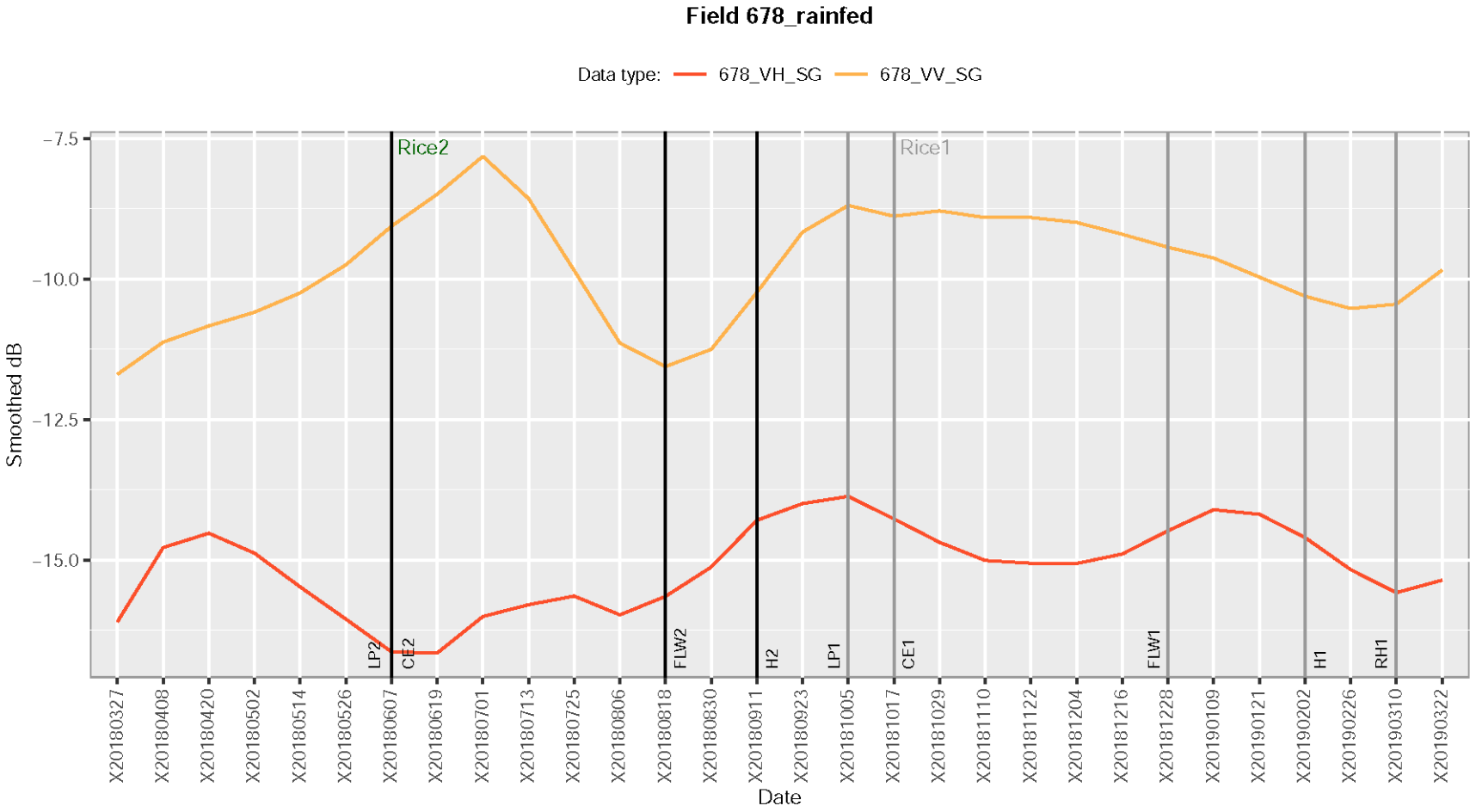
Field 678_rainfed
Data type: 678_VH_SG 678_VV_SG
Smoothed dB
−7.5
−10.0
−12.5
−15.0
Rice2
Rice1
LP2
CE2
FLW2
H2
LP1
CE1
FLW1
H1
RH1
X20180327
X20180408
X20180420
X20180502
X20180514
X20180526
X20180607
X20180619
X20180701
X20180713
X20180725
X20180806
X20180818
X20180830
X20180911
X20180923
X20181005
X20181017
X20181029
X20181110
X20181122
X20181204
X20181216
X20181228
X20190109
X20190121
X20190202
X20190226
X20190310
X20190322
Date

Time series for Iloilo VV/VH polarisation ratio:

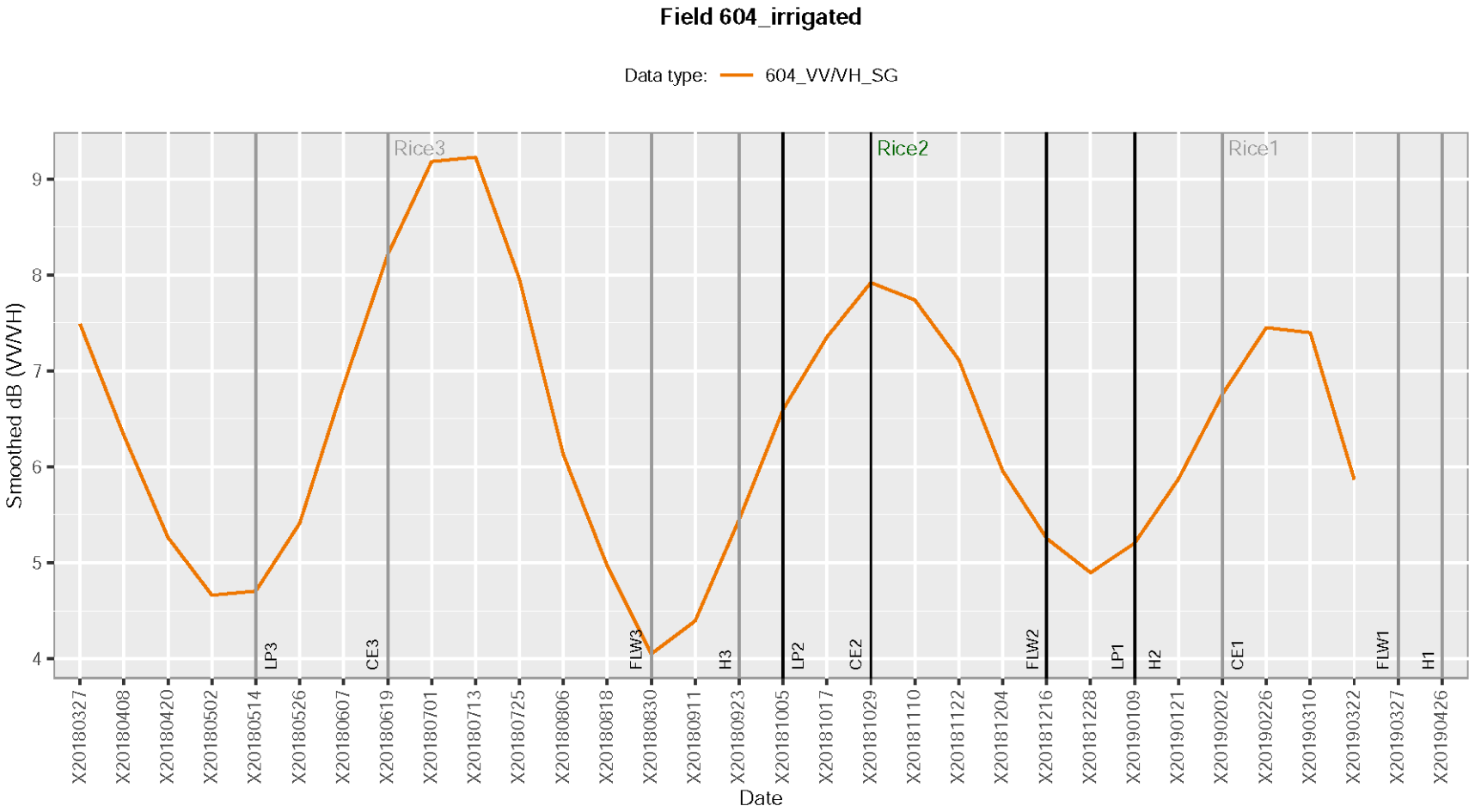

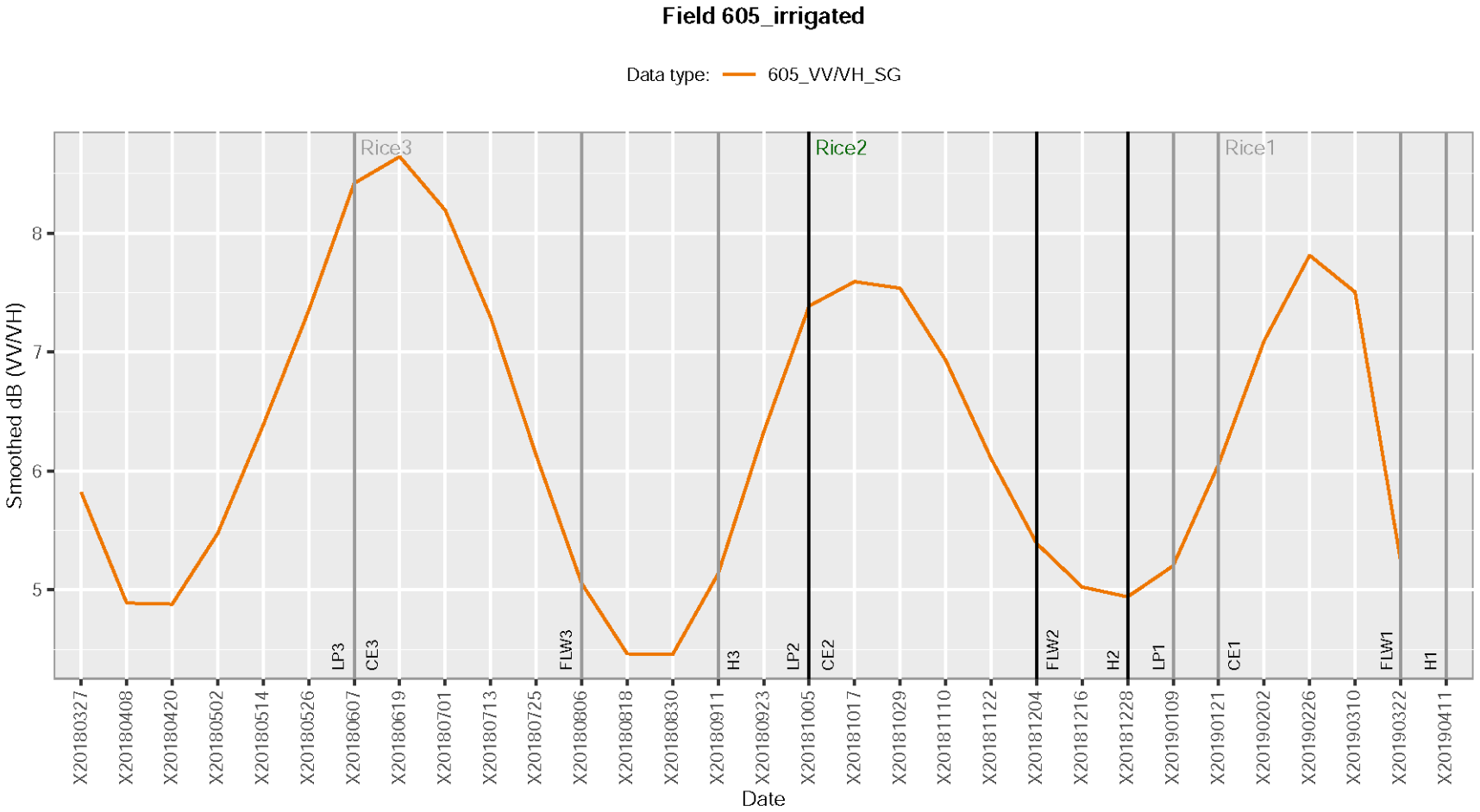
Field 605_irrigated
Data type: 605_VV/VH_SG
Rice3
Rice2
Rice1
Smoothed dB (VV/VH)
8
7
6
5
LP3
CE3
FLW3
H3
LP2
CE2
FLW2
H2
LP1
CE1
FLW1
H1
X20180327
X20180408
X20180420
X20180502
X20180514
X20180526
X20180607
X20180619
X20180701
X20180713
X20180725
X20180806
X20180818
X20180830
X20180911
X20180923
X20181005
X20181017
X20181029
X20181110
X20181122
X20181204
X20181216
X20181228
X20190109
X20190121
X20190202
X20190226
X20190310
X20190322
X20190411
Date

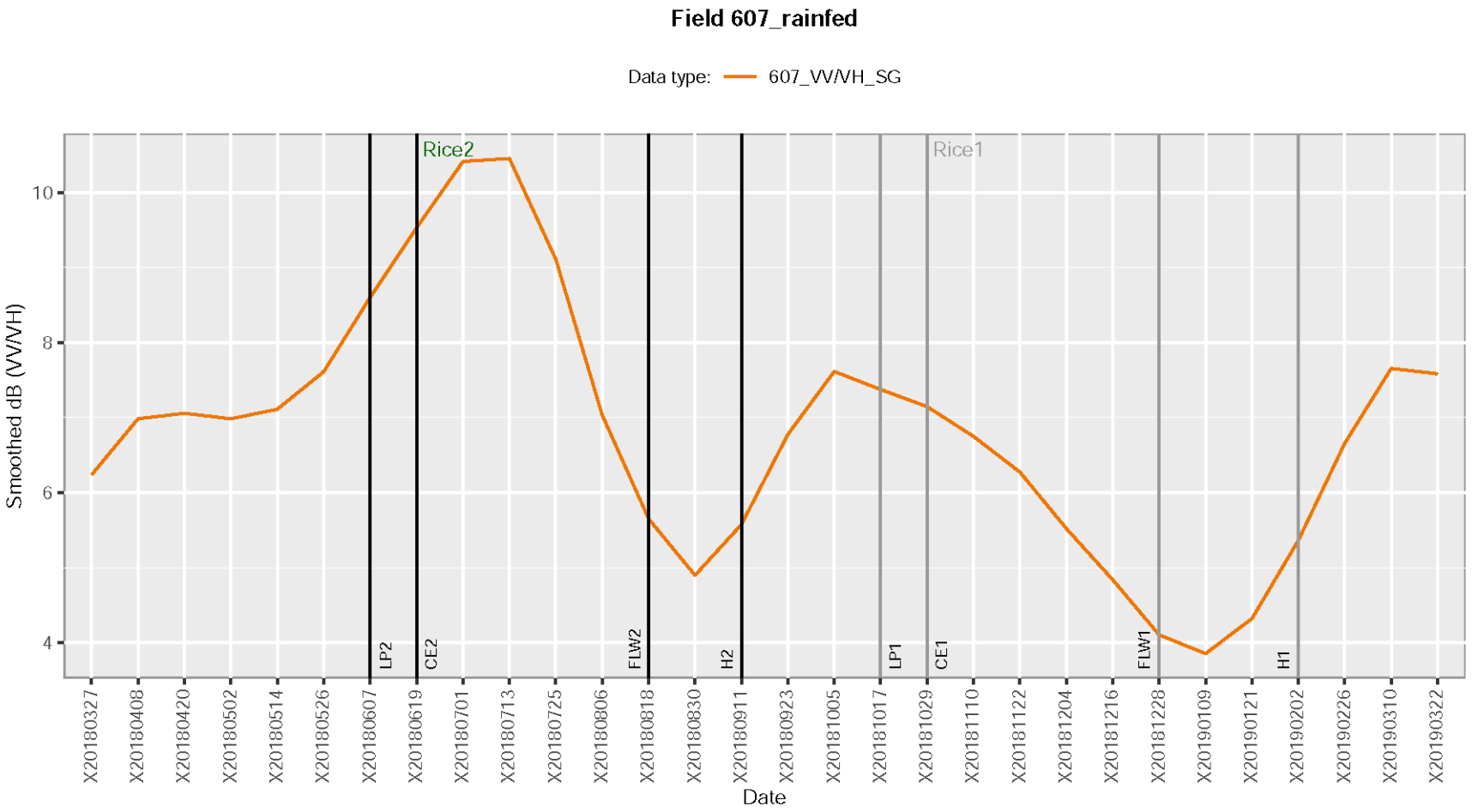
Field 607_rainfed
Data type: 607_VV/VH_SG
Rice2
Rice1
Smoothed dB (VV/VH)
10
8
6
4
LP2
CE2
FLW2
H2
LP1
CE1
FLW1
H1
X20180327
X20180408
X20180420
X20180502
X20180514
X20180526
X20180607
X20180619
X20180701
X20180713
X20180725
X20180806
X20180818
X20180830
X20180911
X20180923
X20181005
X20181017
X20181029
X20181110
X20181122
X20181204
X20181216
X20181228
X20190109
X20190121
X20190202
X20190226
X20190310
X20190322
Date

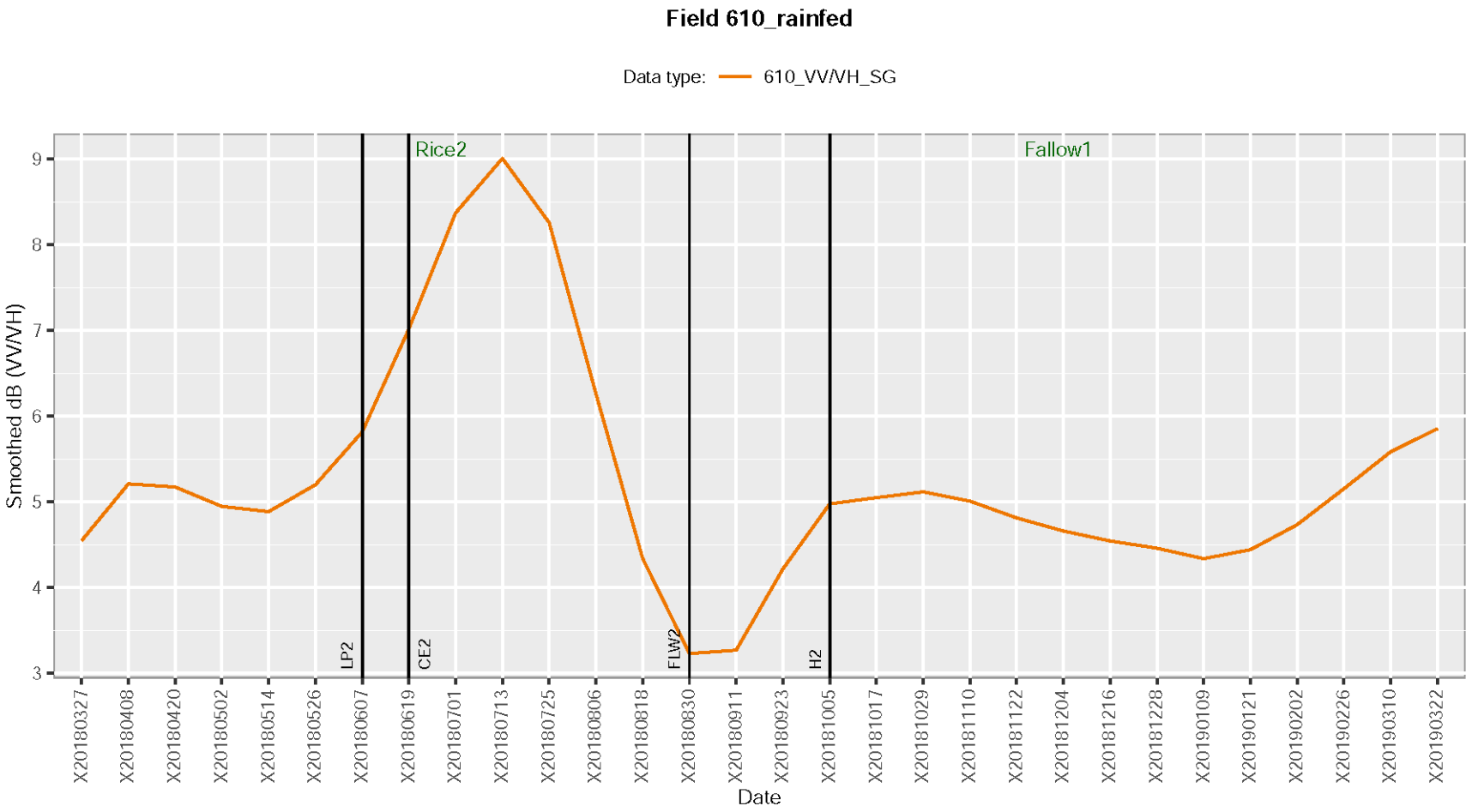
Field 610_rainfed
Data type: 610_VV/VH_SG
Rice2
Fallow1
LP2
CE2
FLW2
H2
Smoothed dB (VV/VH)
Date
X20180327
X20180408
X20180420
X20180502
X20180514
X20180526
X20180607
X20180619
X20180701
X20180713
X20180725
X20180806
X20180818
X20180830
X20180911
X20180923
X20181005
X20181017
X20181029
X20181110
X20181122
X20181204
X20181216
X20181228
X20190109
X20190121
X20190202
X20190226
X20190310
X20190322

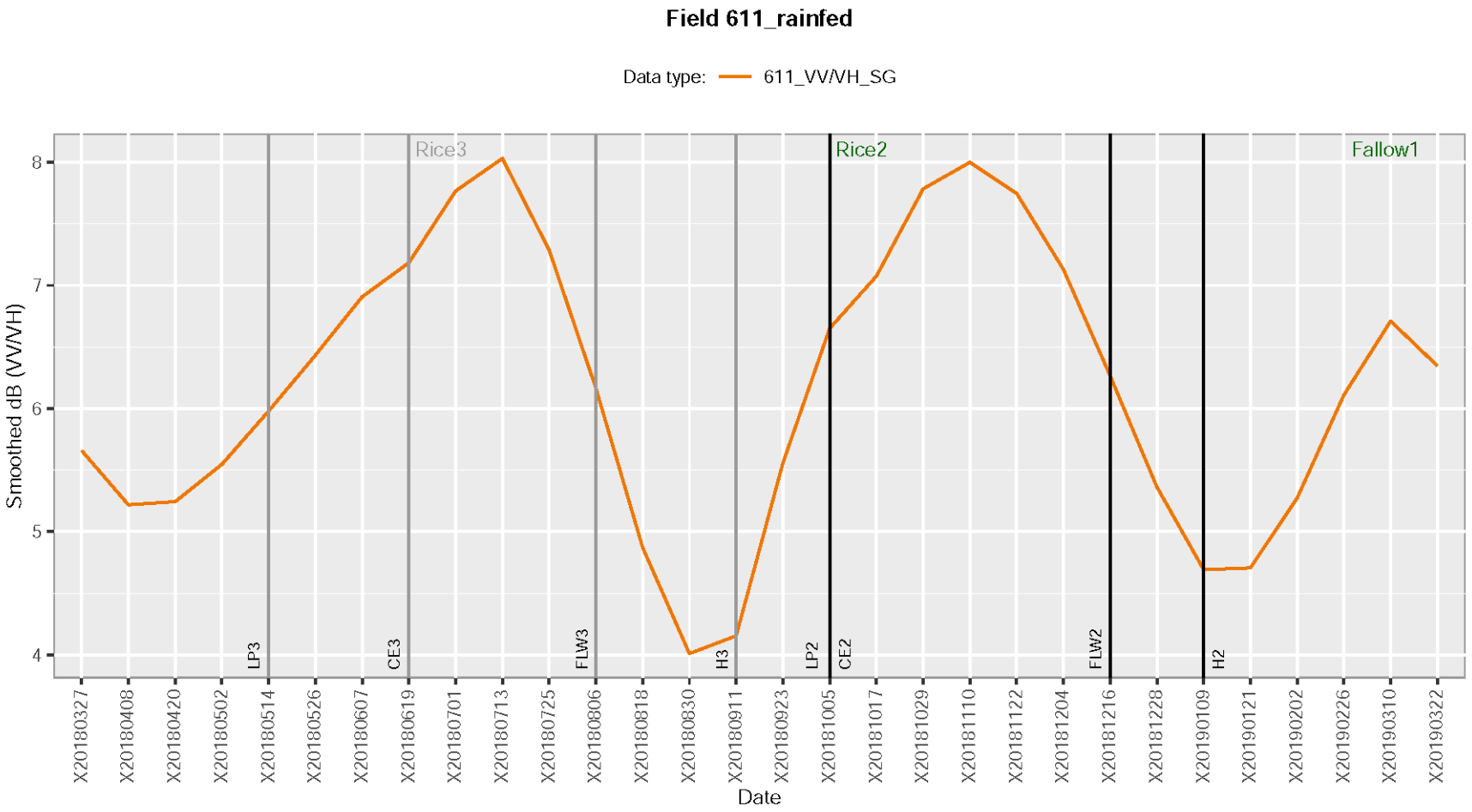
Field 611_rainfed
Data type: 611_VV/VH_SG
Rice3
Rice2
Fallow1
LP3
CE3
FLW3
H3
LP2
CE2
FLW2
H2
Smoothed dB (VV/VH)
8
7
6
5
4
X20180327
X20180408
X20180420
X20180502
X20180514
X20180526
X20180607
X20180619
X20180701
X20180713
X20180725
X20180806
X20180818
X20180830
X20180911
X20180923
X20181005
X20181017
X20181029
X20181110
X20181122
X20181204
X20181216
X20181228
X20190109
X20190121
X20190202
X20190226
X20190310
X20190322
Date

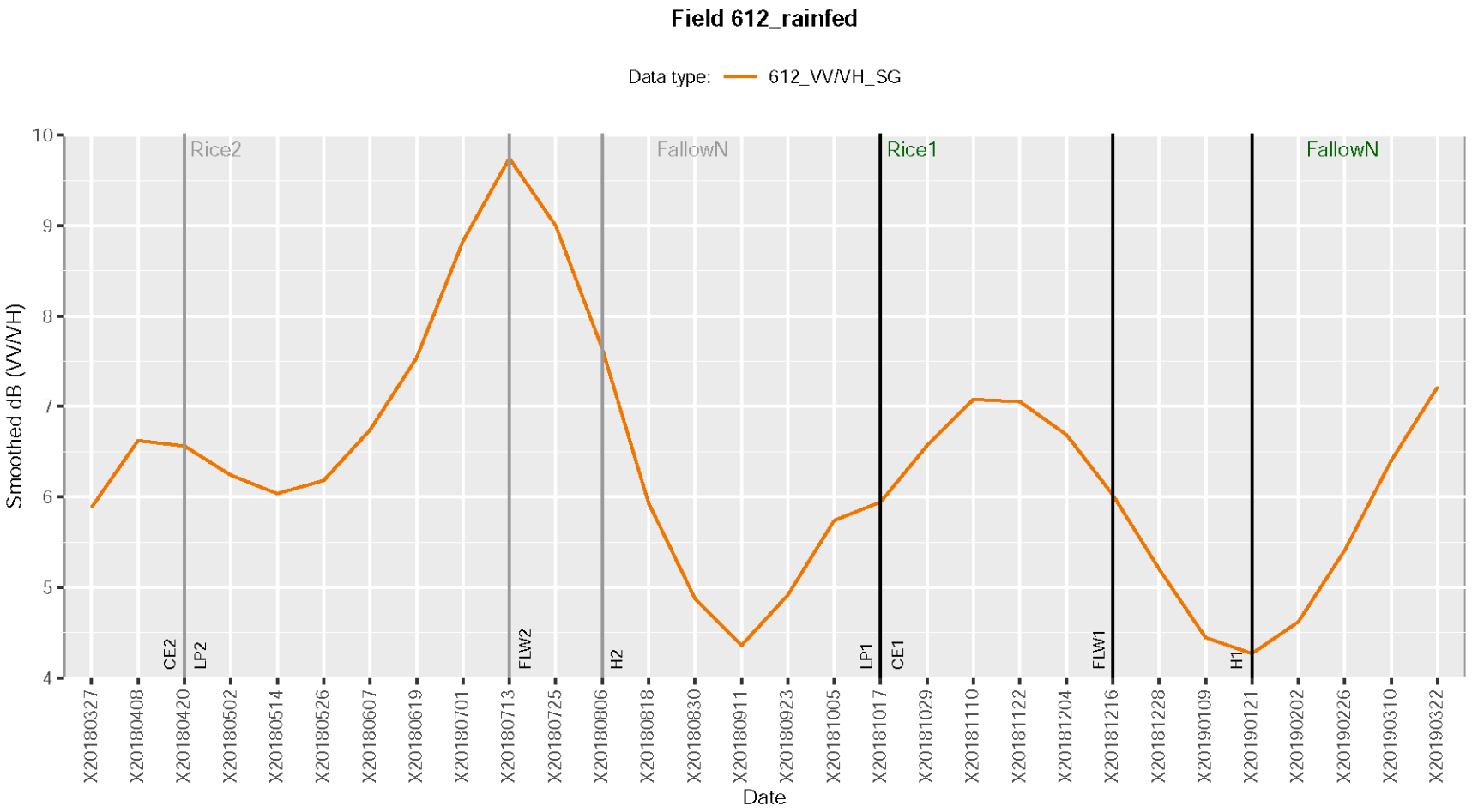
Field 612_rainfed
Data type: 612_VV/VH_SG
Smoothed dB (VV/VH)
10
9
8
7
6
5
4
Rice2
FallowN
Rice1
FallowN
CE2
LP2
FLW2
H2
LP1
CE1
FLW1
H1
X20180327
X20180408
X20180420
X20180502
X20180514
X20180526
X20180607
X20180619
X20180701
X20180713
X20180725
X20180806
X20180818
X20180830
X20180911
X20180923
X20181005
X20181017
X20181029
X20181110
X20181122
X20181204
X20181216
X20181228
X20190109
X20190121
X20190202
X20190226
X20190310
X20190322
Date

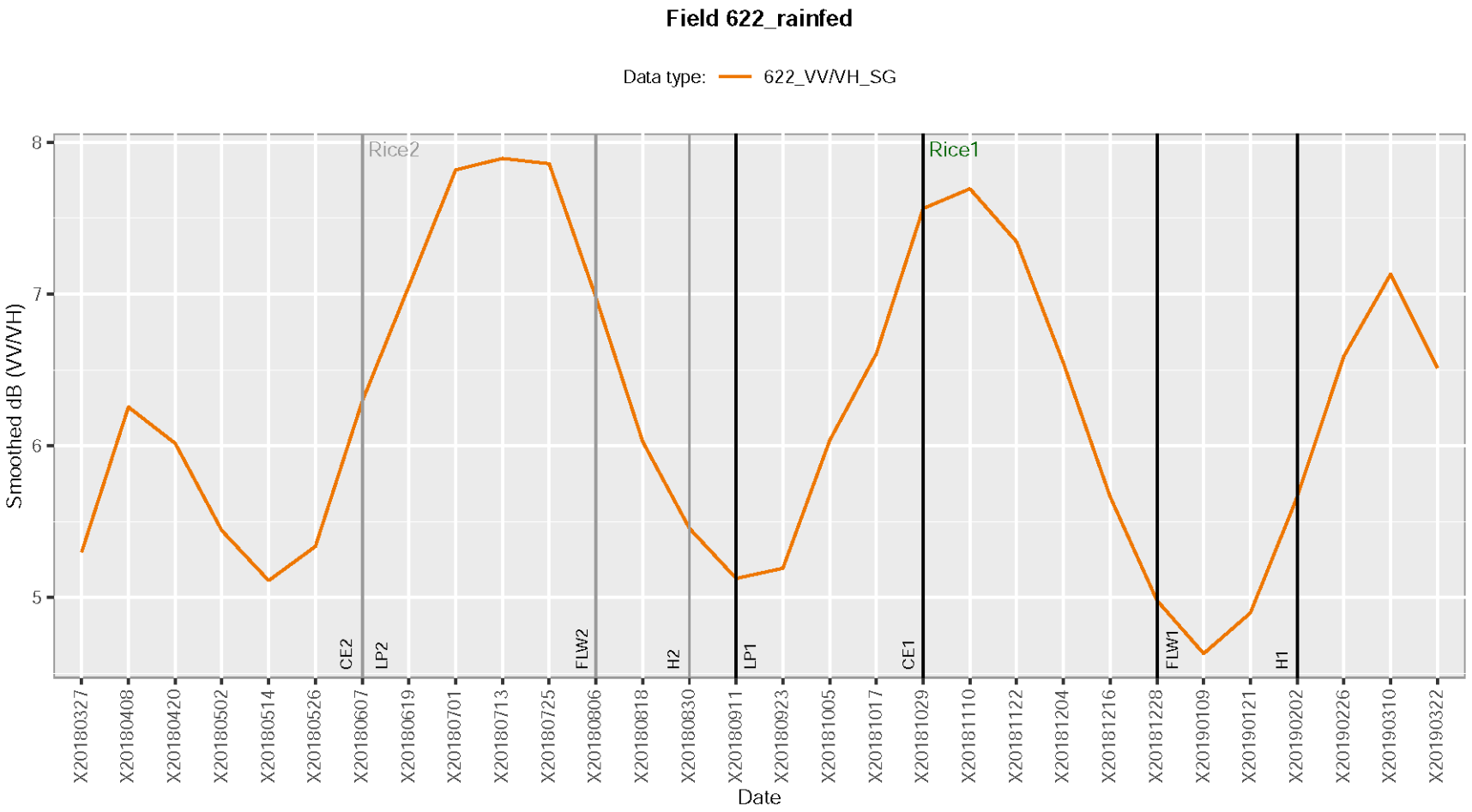
Field 622_rainfed
Data type: 622_VV/VH_SG
Smoothed dB (VV/VH)
8
7
6
5
Rice2
Rice1
CE2
LP2
FLW2
H2
LP1
CE1
FLW1
H1
X20180327
X20180408
X20180420
X20180502
X20180514
X20180526
X20180607
X20180619
X20180701
X20180713
X20180725
X20180806
X20180818
X20180830
X20180911
X20180923
X20181005
X20181017
X20181029
X20181110
X20181122
X20181204
X20181216
X20181228
X20190109
X20190121
X20190202
X20190226
X20190310
X20190322
Date

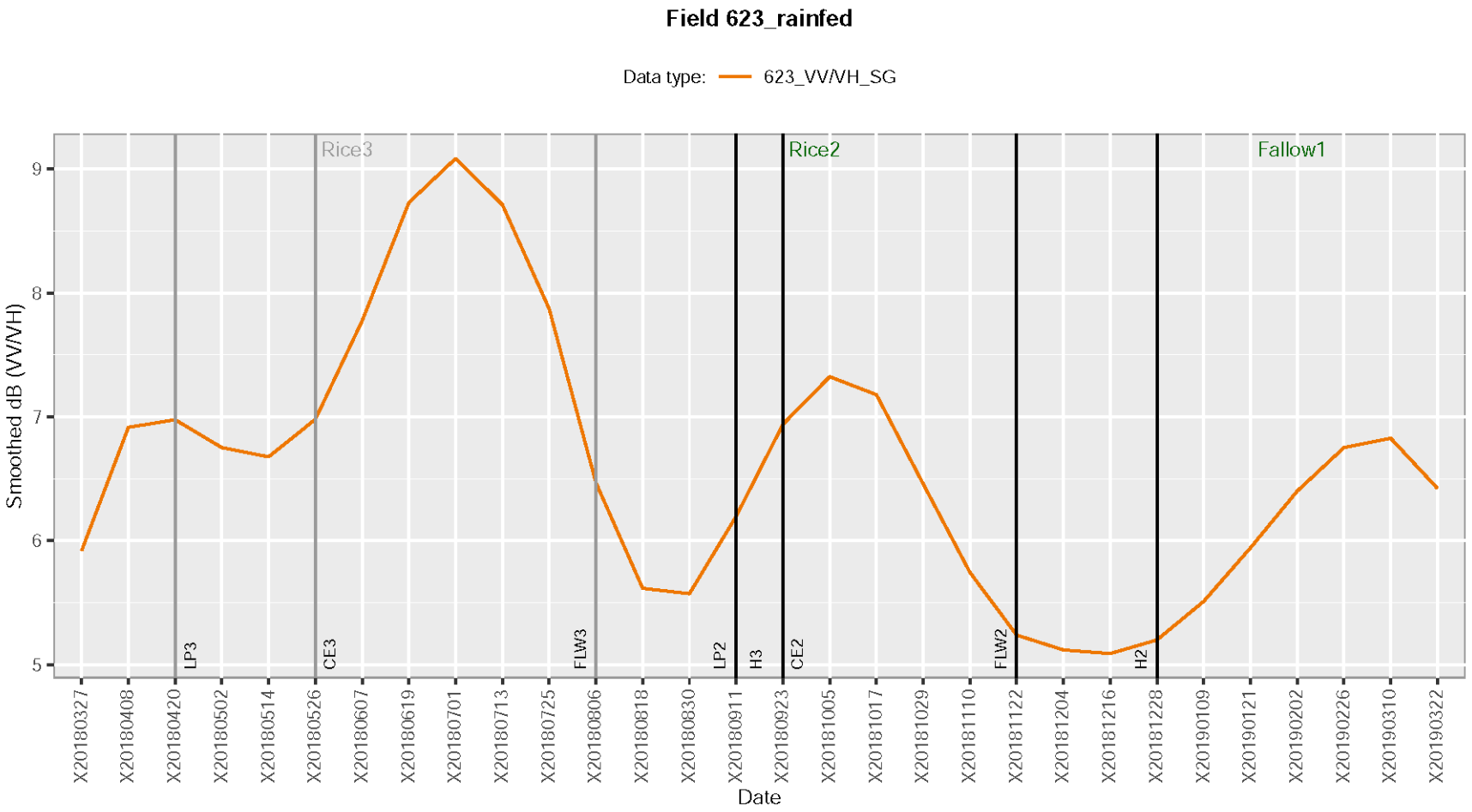
Field 623_rainfed
Data type: 623_VV/VH_SG
Rice3
Rice2
Fallow1
Smoothed dB (VV/VH)
9
8
7
6
5
LP3
CE3
FLW3
LP2
H3
CE2
FLW2
H2
X20180327
X20180408
X20180420
X20180502
X20180514
X20180526
X20180607
X20180619
X20180701
X20180713
X20180725
X20180806
X20180818
X20180830
X20180911
X20180923
X20181005
X20181017
X20181029
X20181110
X20181122
X20181204
X20181216
X20181228
X20190109
X20190121
X20190202
X20190226
X20190310
X20190322
Date

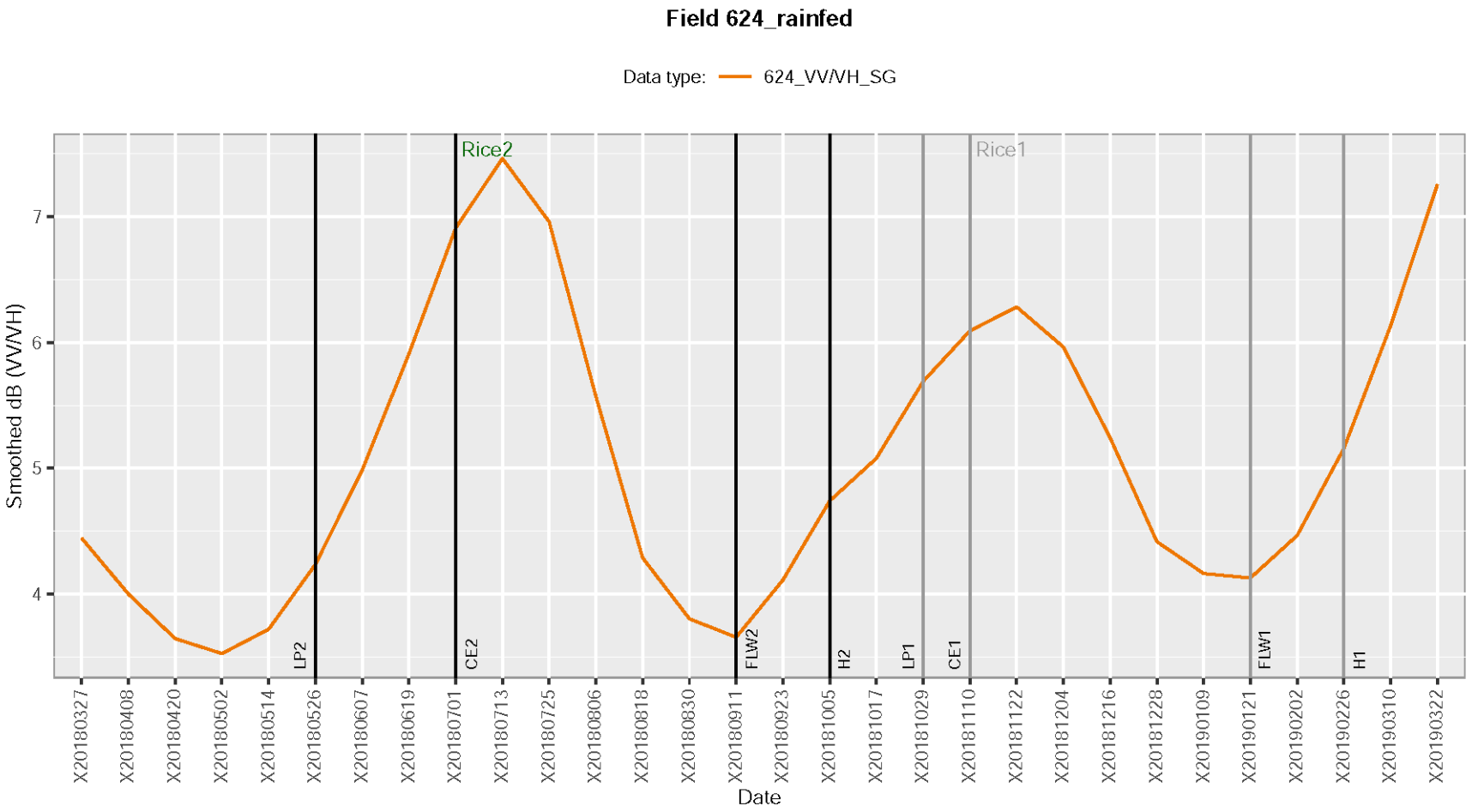
Field 624_rainfed
Data type: 624_VV/VH_SG
Rice2
Rice1
Smoothed dB (VV/VH)
7
6
5
4
LP2
CE2
FLW2
H2
LP1
CE1
FLW1
H1
X20180327
X20180408
X20180420
X20180502
X20180514
X20180526
X20180607
X20180619
X20180701
X20180713
X20180725
X20180806
X20180818
X20180830
X20180911
X20180923
X20181005
X20181017
X20181029
X20181110
X20181122
X20181204
X20181216
X20181228
X20190109
X20190121
X20190202
X20190226
X20190310
X20190322
Date

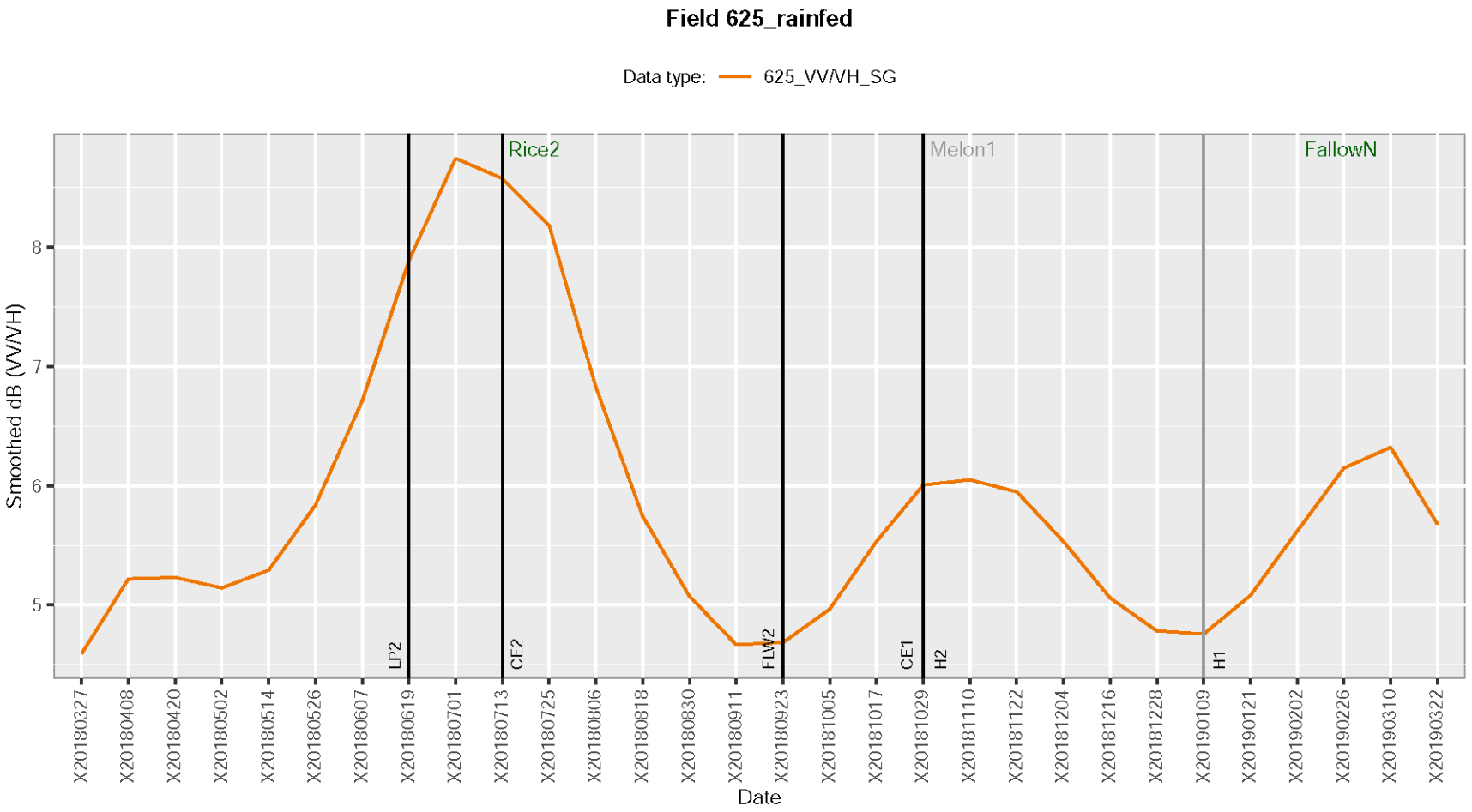
Field 625_rainfed
Data type: 625_VV/VH_SG
Rice2
Melon1
FallowN
LP2
CE2
FLW2
CE1
H2
H1
Smoothed dB (VV/VH)
8
7
6
5
X20180327
X20180408
X20180420
X20180502
X20180514
X20180526
X20180607
X20180619
X20180701
X20180713
X20180725
X20180806
X20180818
X20180830
X20180911
X20180923
X20181005
X20181017
X20181029
X20181110
X20181122
X20181204
X20181216
X20181228
X20190109
X20190121
X20190202
X20190226
X20190310
X20190322
Date

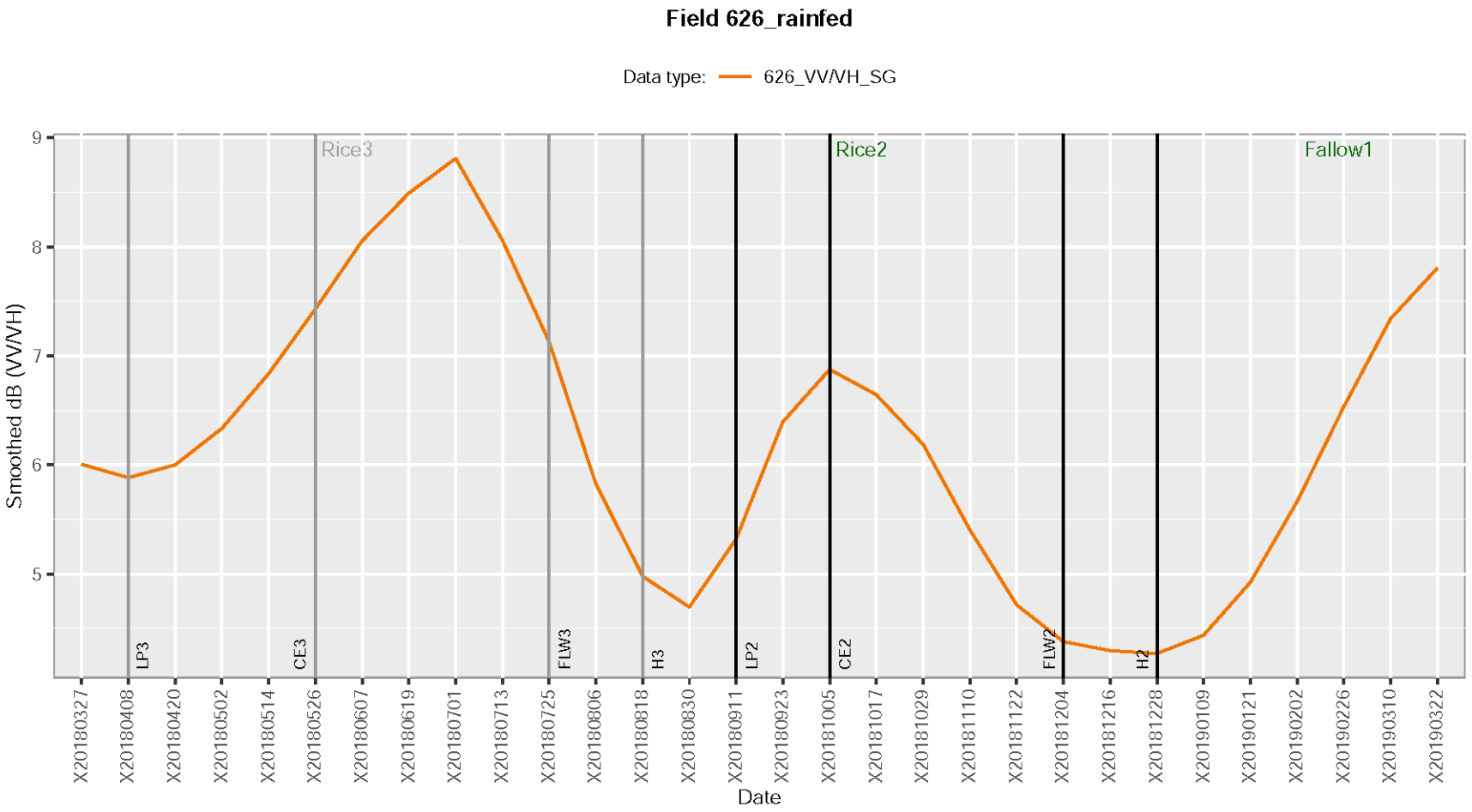
Field 626_rainfed
Data type: 626_VV/VH_SG
Smoothed dB (VV/VH)
9
8
7
6
5
Rice3
Rice2
Fallow1
LP3
CE3
FLW3
H3
LP2
CE2
FLW2
H2
X20180327
X20180408
X20180420
X20180502
X20180514
X20180526
X20180607
X20180619
X20180701
X20180713
X20180725
X20180806
X20180818
X20180830
X20180911
X20180923
X20181005
X20181017
X20181029
X20181110
X20181122
X20181204
X20181216
X20181228
X20190109
X20190121
X20190202
X20190226
X20190310
X20190322
Date

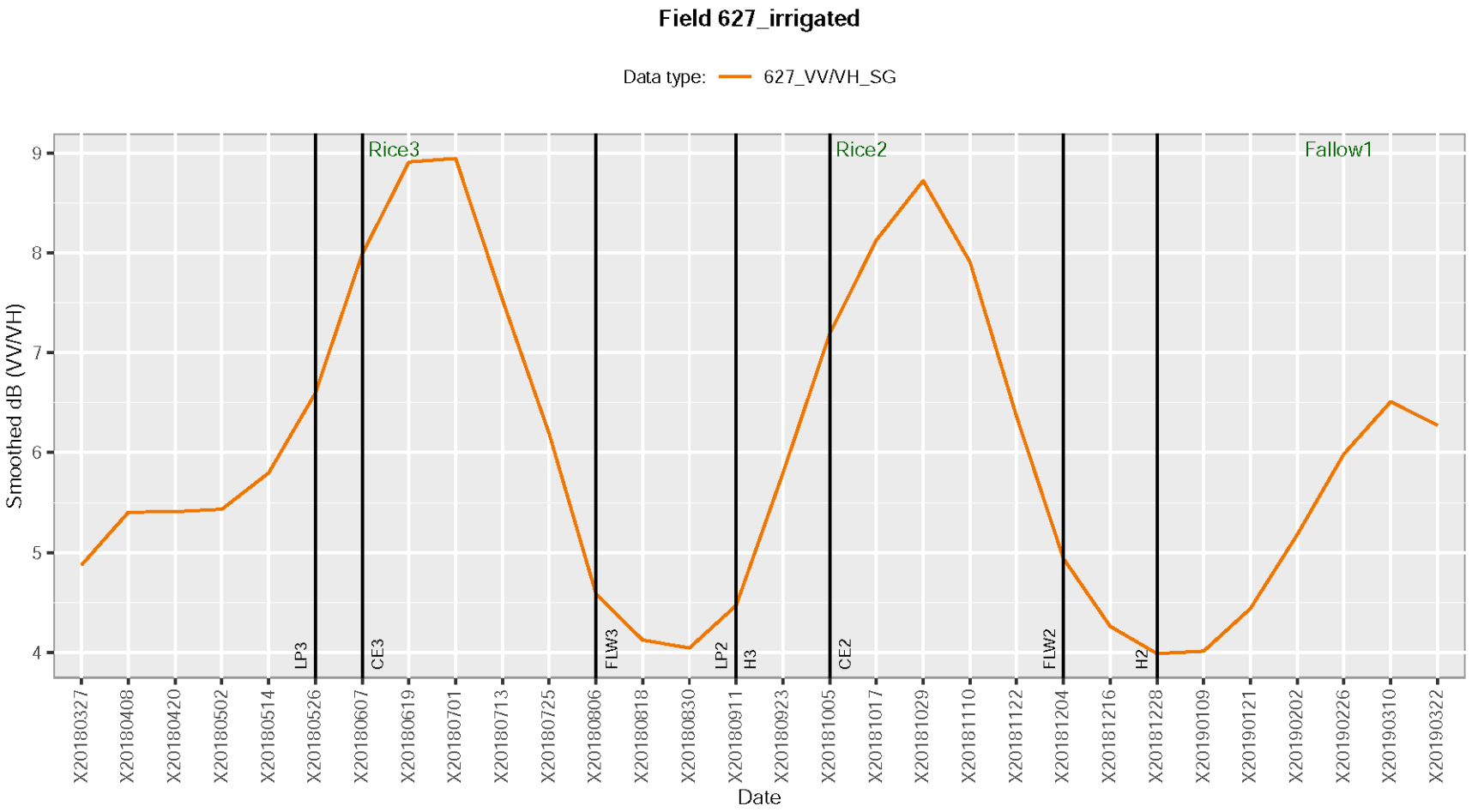
Field 627_irrigated
Data type: 627_VV/VH_SG
Smoothed dB (VV/VH)
9
8
7
6
5
4
Rice3
Rice2
Fallow1
LP3
CE3
FLW3
LP2
H3
CE2
FLW2
H2
X20180327
X20180408
X20180420
X20180502
X20180514
X20180526
X20180607
X20180619
X20180701
X20180713
X20180725
X20180806
X20180818
X20180830
X20180911
X20180923
X20181005
X20181017
X20181029
X20181110
X20181122
X20181204
X20181216
X20181228
X20190109
X20190121
X20190202
X20190226
X20190310
X20190322
Date

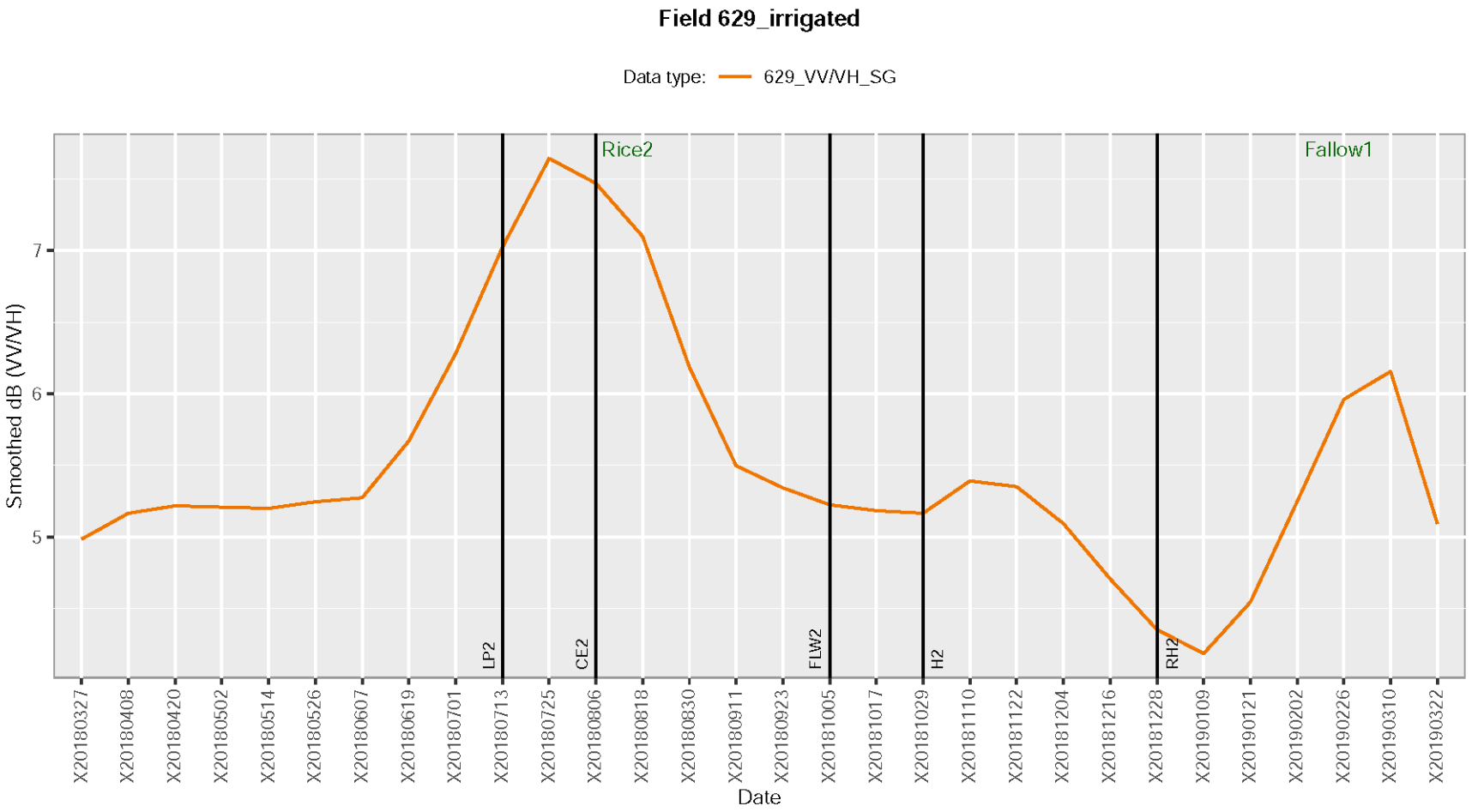
Field 629_irrigated
Data type: 629_VV/VH_SG
Rice2
Fallow1
LP2
CE2
FLW2
H2
RH2
Smoothed dB (VV/VH)
7
6
5
X20180327
X20180408
X20180420
X20180502
X20180514
X20180526
X20180607
X20180619
X20180701
X20180713
X20180725
X20180806
X20180818
X20180830
X20180911
X20180923
X20181005
X20181017
X20181029
X20181110
X20181122
X20181204
X20181216
X20181228
X20190109
X20190121
X20190202
X20190226
X20190310
X20190322
Date

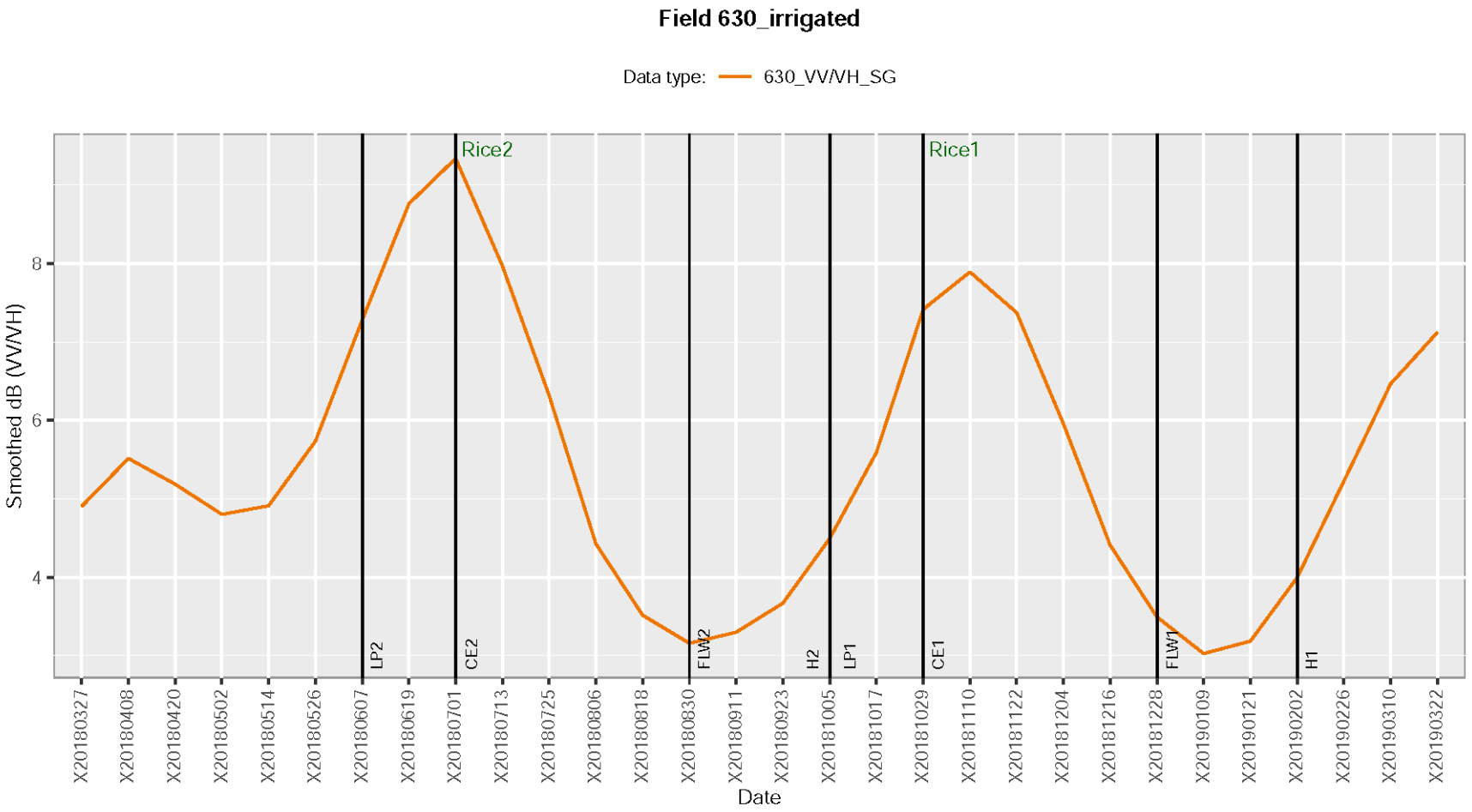
Field 630_irrigated
Data type: 630_VV/VH_SG
Smoothed dB (VV/VH)
8
6
4
Rice2
Rice1
LP2
CE2
FLW2
H2
LP1
CE1
FLW1
H1
X20180327
X20180408
X20180420
X20180502
X20180514
X20180526
X20180607
X20180619
X20180701
X20180713
X20180725
X20180806
X20180818
X20180830
X20180911
X20180923
X20181005
X20181017
X20181029
X20181110
X20181122
X20181204
X20181216
X20181228
X20190109
X20190121
X20190202
X20190226
X20190310
X20190322
Date

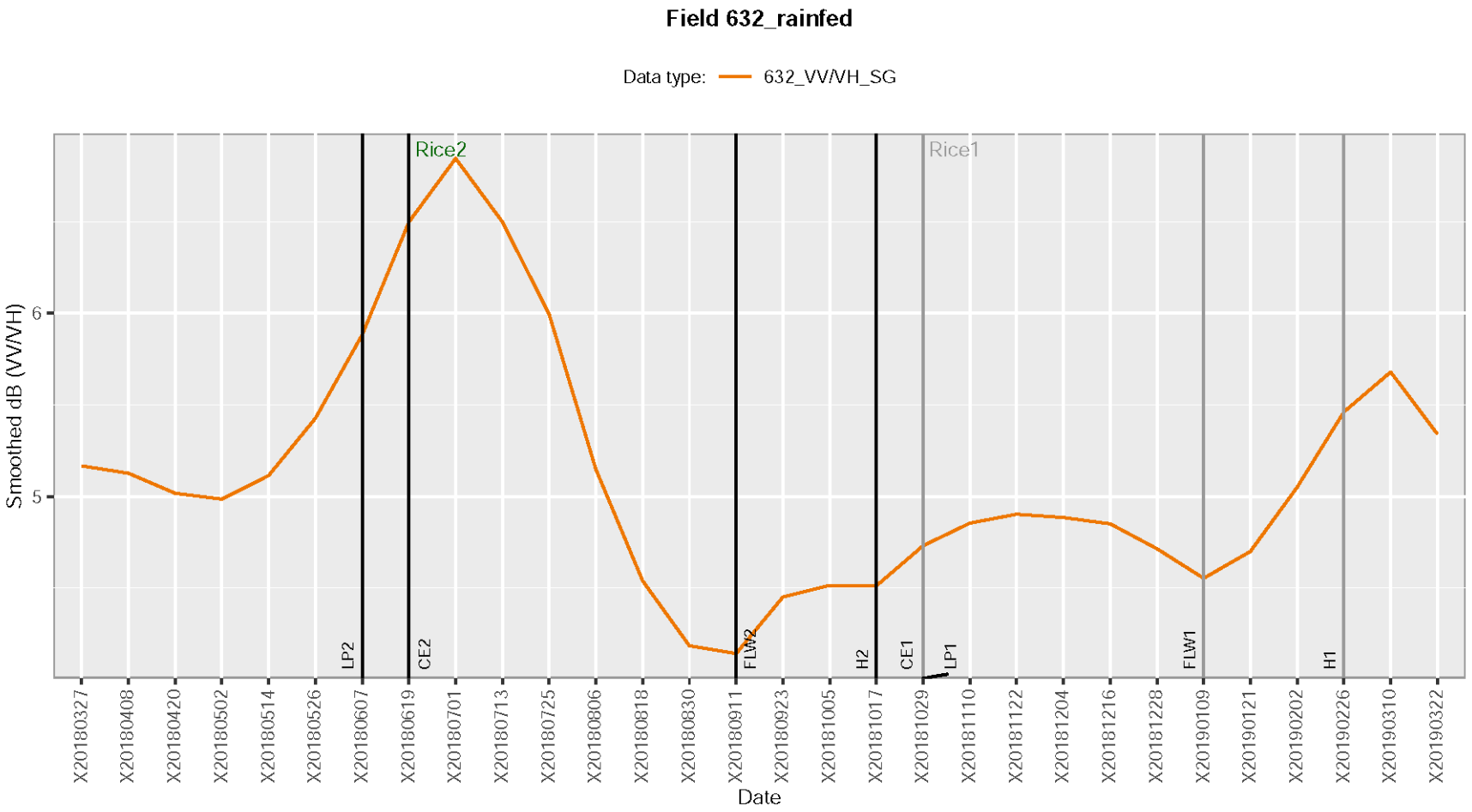
Field 632_rainfed
Data type: 632_VV/VH_SG
Rice2
Rice1
Smoothed dB (VV/VH)
6
5
LP2
CE2
FLW2
H2
CE1
LP1
FLW1
H1
X20180327
X20180408
X20180420
X20180502
X20180514
X20180526
X20180607
X20180619
X20180701
X20180713
X20180725
X20180806
X20180818
X20180830
X20180911
X20180923
X20181005
X20181017
X20181029
X20181110
X20181122
X20181204
X20181216
X20181228
X20190109
X20190121
X20190202
X20190226
X20190310
X20190322
Date

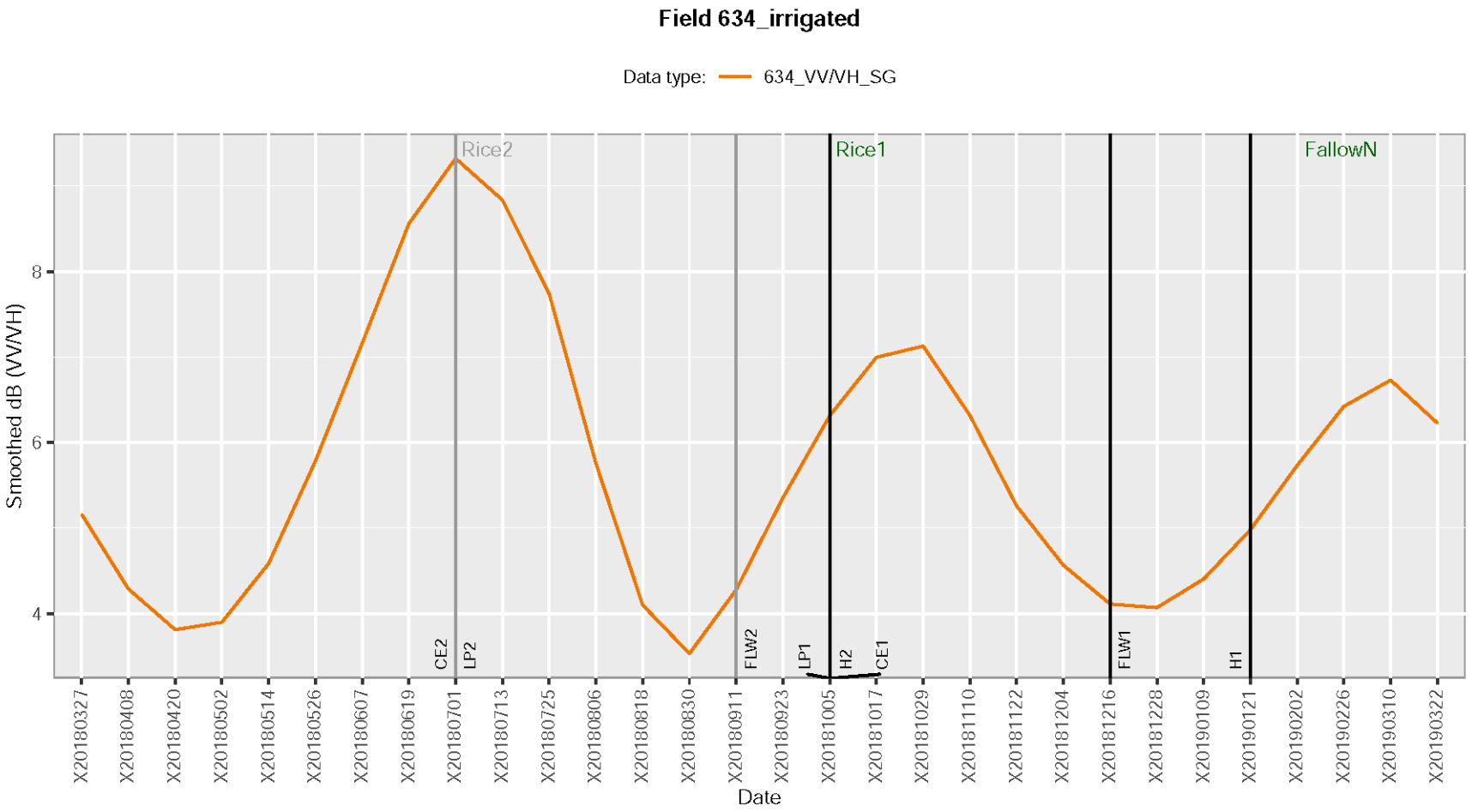
Field 634_irrigated
Data type: 634_VV/VH_SG
Rice2
Rice1
FallowN
Smoothed dB (VV/VH)
8
6
4
CE2
LP2
FLW2
LP1
H2
CE1
FLW1
H1
X20180327
X20180408
X20180420
X20180502
X20180514
X20180526
X20180607
X20180619
X20180701
X20180713
X20180725
X20180806
X20180818
X20180830
X20180911
X20180923
X20181005
X20181017
X20181029
X20181110
X20181122
X20181204
X20181216
X20181228
X20190109
X20190121
X20190202
X20190226
X20190310
X20190322
Date

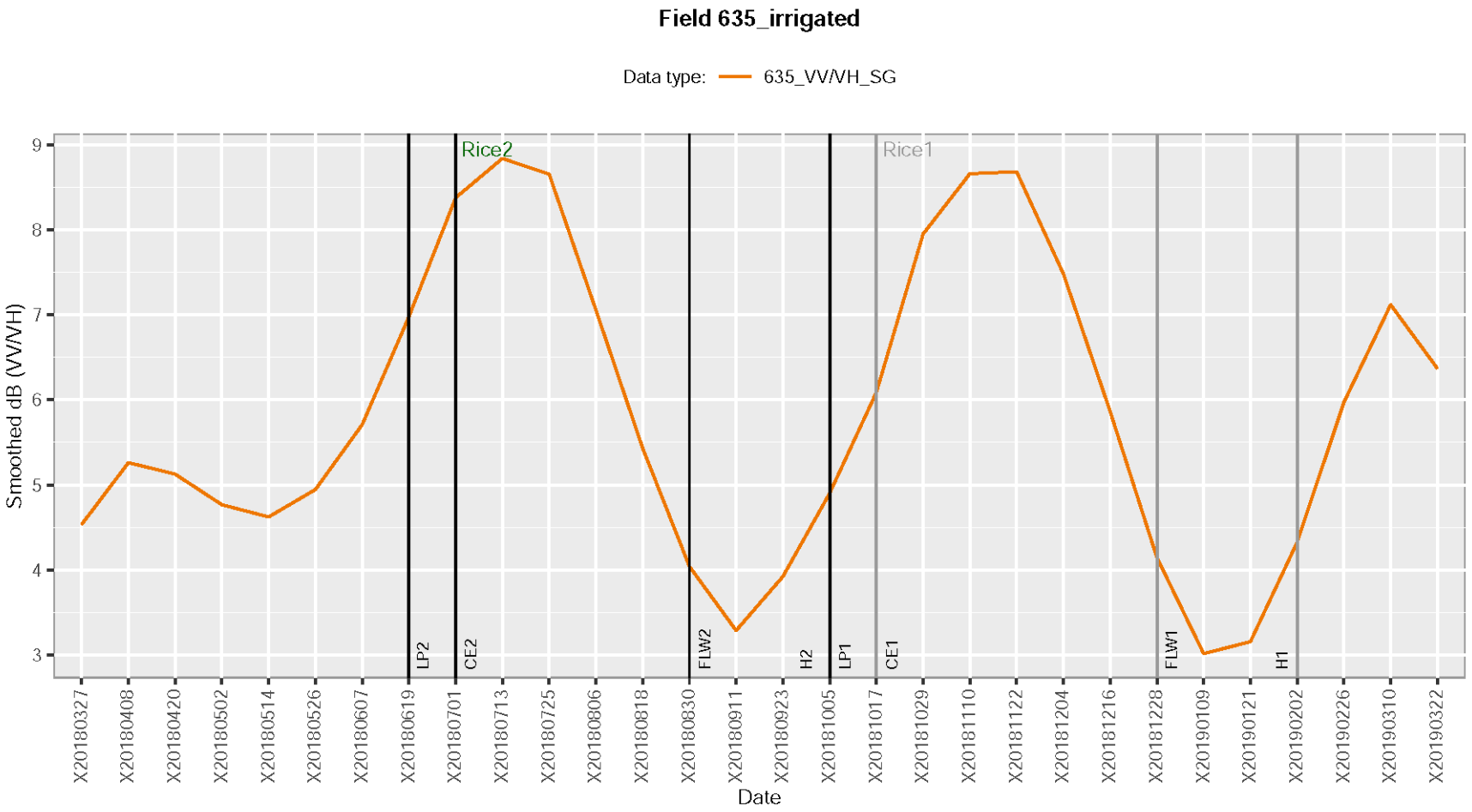
Field 635_irrigated
Data type: 635_VV/VH_SG
Smoothed dB (VV/VH)
9
8
7
6
5
4
3
Rice2
Rice1
LP2
CE2
FLW2
H2
LP1
CE1
FLW1
H1
X20180327
X20180408
X20180420
X20180502
X20180514
X20180526
X20180607
X20180619
X20180701
X20180713
X20180725
X20180806
X20180818
X20180830
X20180911
X20180923
X20181005
X20181017
X20181029
X20181110
X20181122
X20181204
X20181216
X20181228
X20190109
X20190121
X20190202
X20190226
X20190310
X20190322
Date

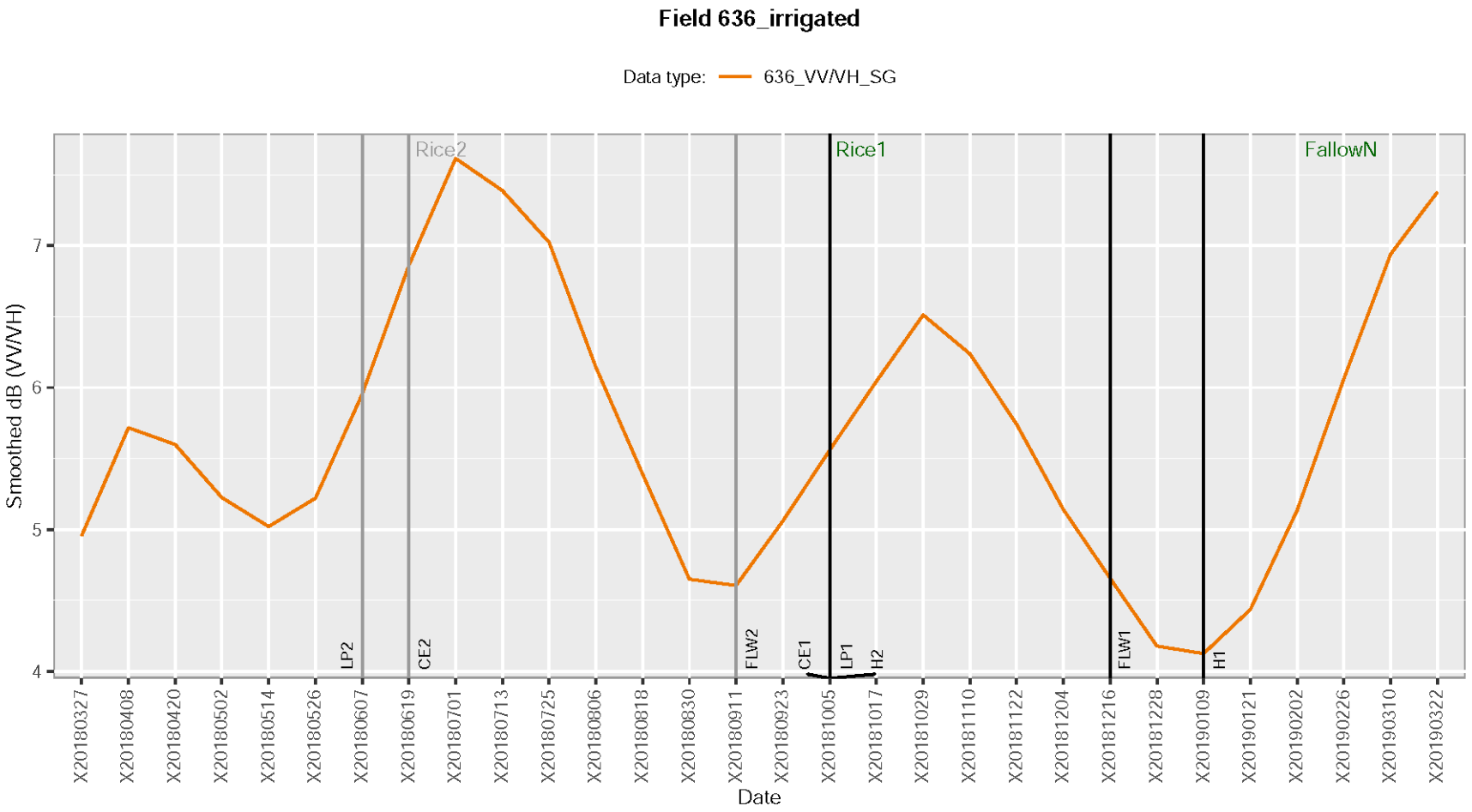
Field 636_irrigated
Data type: 636_VV/VH_SG
Rice2
Rice1
FallowN
Smoothed dB (VV/VH)
7
6
5
4
LP2
CE2
FLW2
CE1
LP1
H2
FLW1
H1
X20180327
X20180408
X20180420
X20180502
X20180514
X20180526
X20180607
X20180619
X20180701
X20180713
X20180725
X20180806
X20180818
X20180830
X20180911
X20180923
X20181005
X20181017
X20181029
X20181110
X20181122
X20181204
X20181216
X20181228
X20190109
X20190121
X20190202
X20190226
X20190310
X20190322
Date

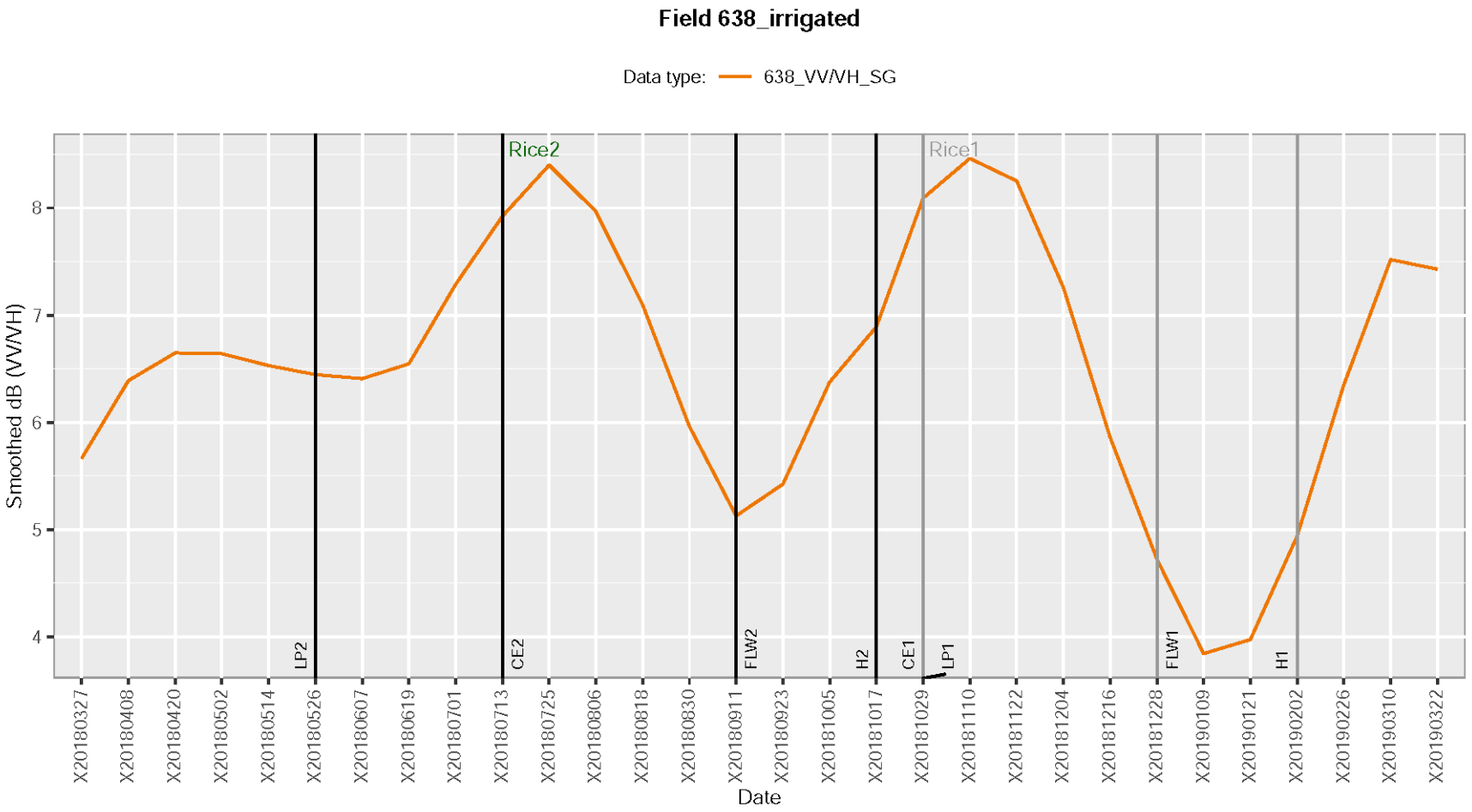
Field 638_irrigated
Data type: 638_VV/VH_SG
Rice2
Rice1
LP2
CE2
FLW2
H2
CE1
LP1
FLW1
H1
Smoothed dB (VV/VH)
4
5
6
7
8
X20180327
X20180408
X20180420
X20180502
X20180514
X20180526
X20180607
X20180619
X20180701
X20180713
X20180725
X20180806
X20180818
X20180830
X20180911
X20180923
X20181005
X20181017
X20181029
X20181110
X20181122
X20181204
X20181216
X20181228
X20190109
X20190121
X20190202
X20190226
X20190310
X20190322
Date

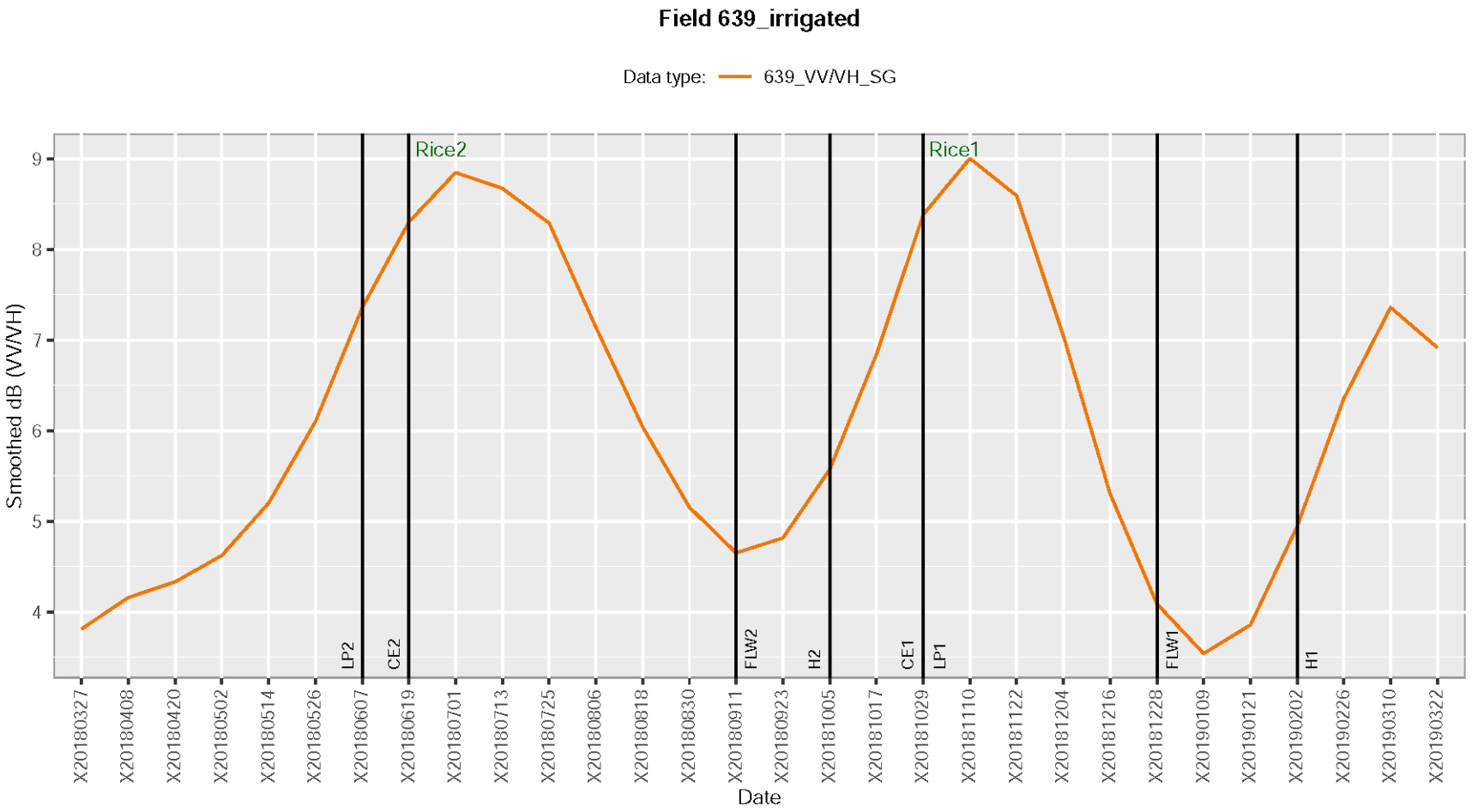
Field 639_irrigated
Data type: 639_VV/VH_SG
Smoothed dB (VV/VH)
9
8
7
6
5
4
Rice2
Rice1
LP2
CE2
FLW2
H2
CE1
LP1
FLW1
H1
X20180327
X20180408
X20180420
X20180502
X20180514
X20180526
X20180607
X20180619
X20180701
X20180713
X20180725
X20180806
X20180818
X20180830
X20180911
X20180923
X20181005
X20181017
X20181029
X20181110
X20181122
X20181204
X20181216
X20181228
X20190109
X20190121
X20190202
X20190226
X20190310
X20190322
Date

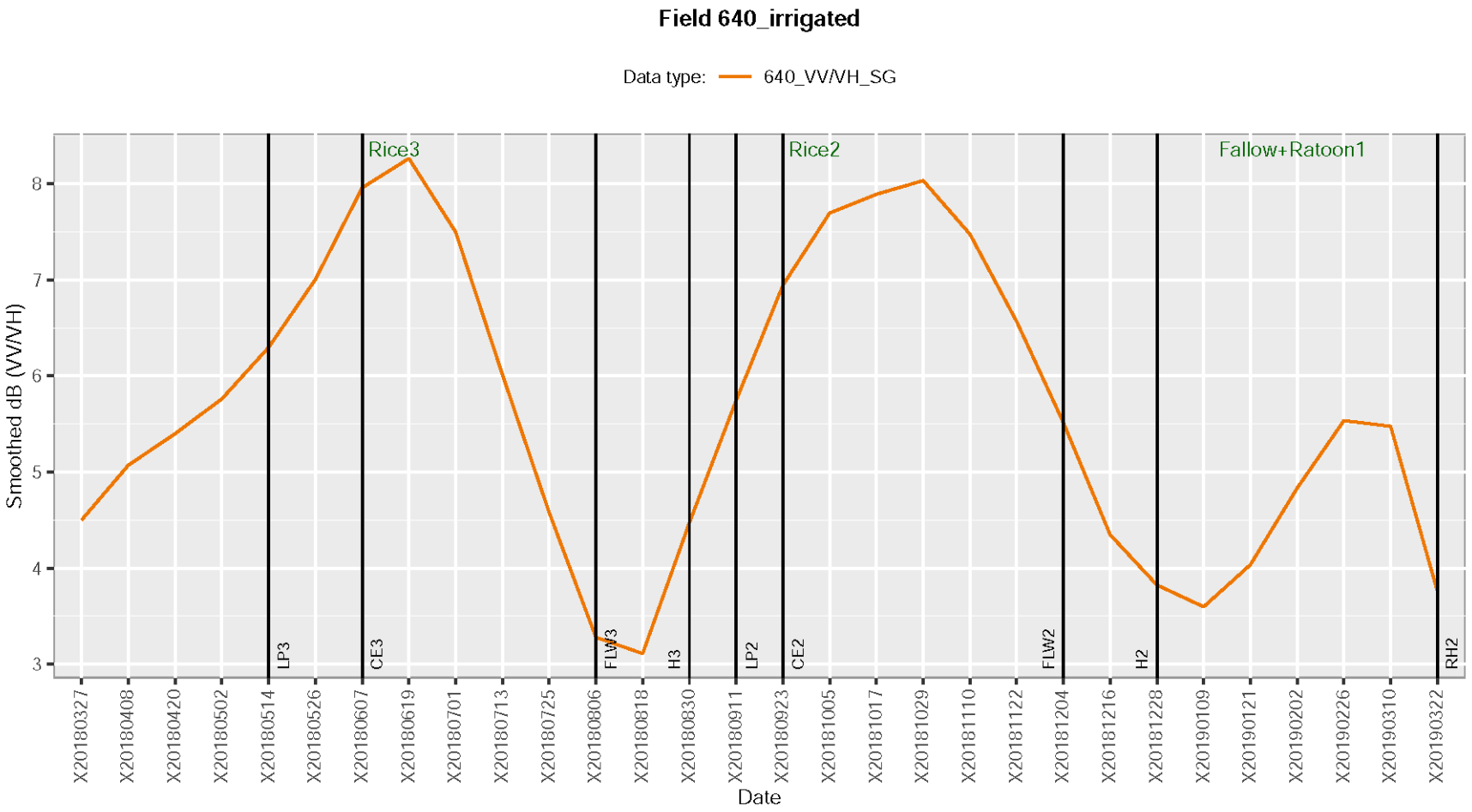
Field 640_irrigated
Data type: 640_VV/VH_SG
Rice3
Rice2
Fallow+Ratoon1
LP3
CE3
FLW3
H3
LP2
CE2
FLW2
H2
RH2
Smoothed dB (VV/VH)
Date
X20180327
X20180408
X20180420
X20180502
X20180514
X20180526
X20180607
X20180619
X20180701
X20180713
X20180725
X20180806
X20180818
X20180830
X20180911
X20180923
X20181005
X20181017
X20181029
X20181110
X20181122
X20181204
X20181216
X20181228
X20190109
X20190121
X20190202
X20190226
X20190310
X20190322

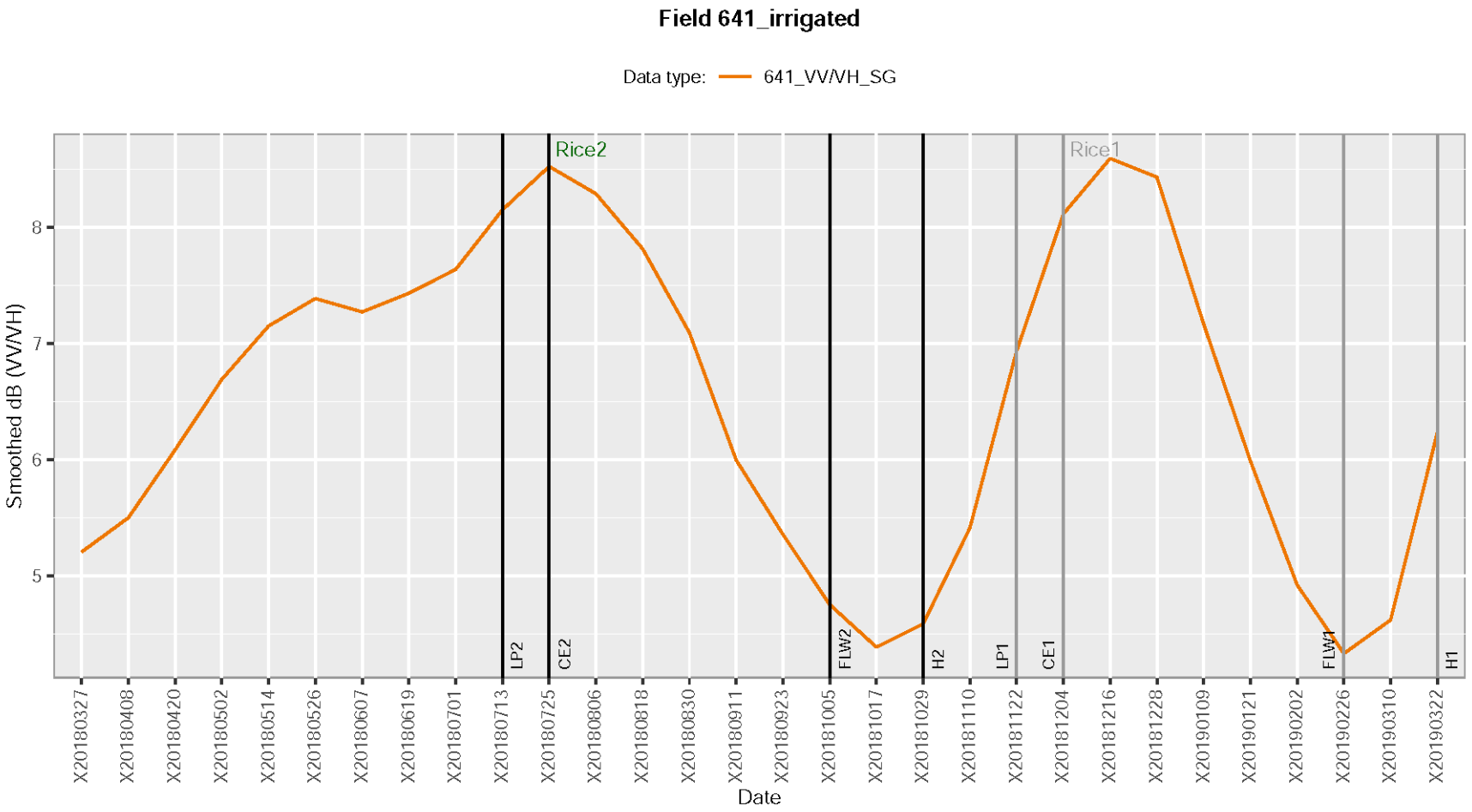
Field 641_irrigated
Data type: 641_VV/VH_SG
Smoothed dB (VV/VH)
8
7
6
5
Rice2
Rice1
LP2
CE2
FLW2
H2
LP1
CE1
FLW1
H1
X20180327
X20180408
X20180420
X20180502
X20180514
X20180526
X20180607
X20180619
X20180701
X20180713
X20180725
X20180806
X20180818
X20180830
X20180911
X20180923
X20181005
X20181017
X20181029
X20181110
X20181122
X20181204
X20181216
X20181228
X20190109
X20190121
X20190202
X20190226
X20190310
X20190322
Date

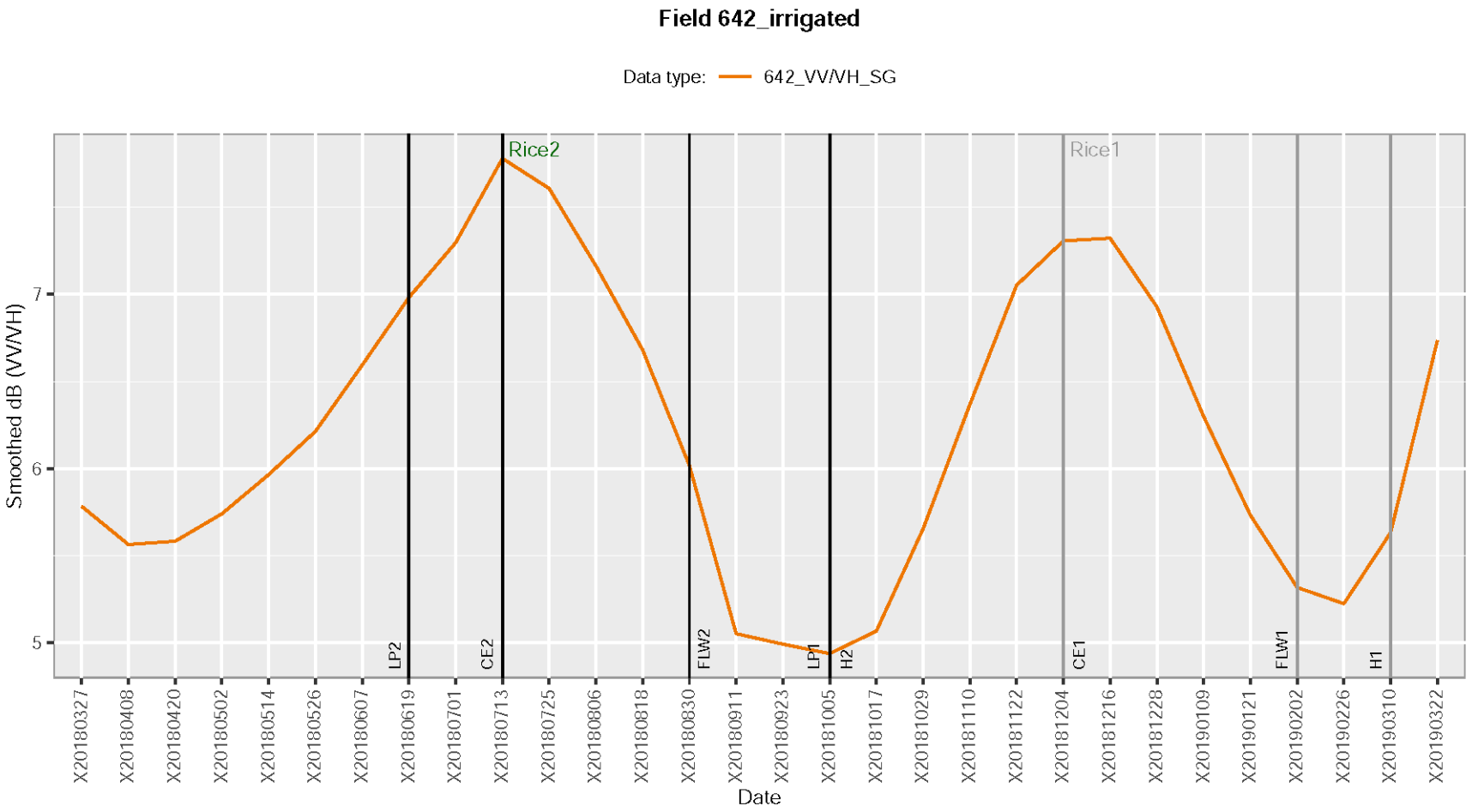
Field 642_irrigated
Data type: 642_VV/VH_SG
Rice2
Rice1
Smoothed dB (VV/VH)
7
6
5
LP2
CE2
FLW2
LP1
H2
CE1
FLW1
H1
X20180327
X20180408
X20180420
X20180502
X20180514
X20180526
X20180607
X20180619
X20180701
X20180713
X20180725
X20180806
X20180818
X20180830
X20180911
X20180923
X20181005
X20181017
X20181029
X20181110
X20181122
X20181204
X20181216
X20181228
X20190109
X20190121
X20190202
X20190226
X20190310
X20190322
Date

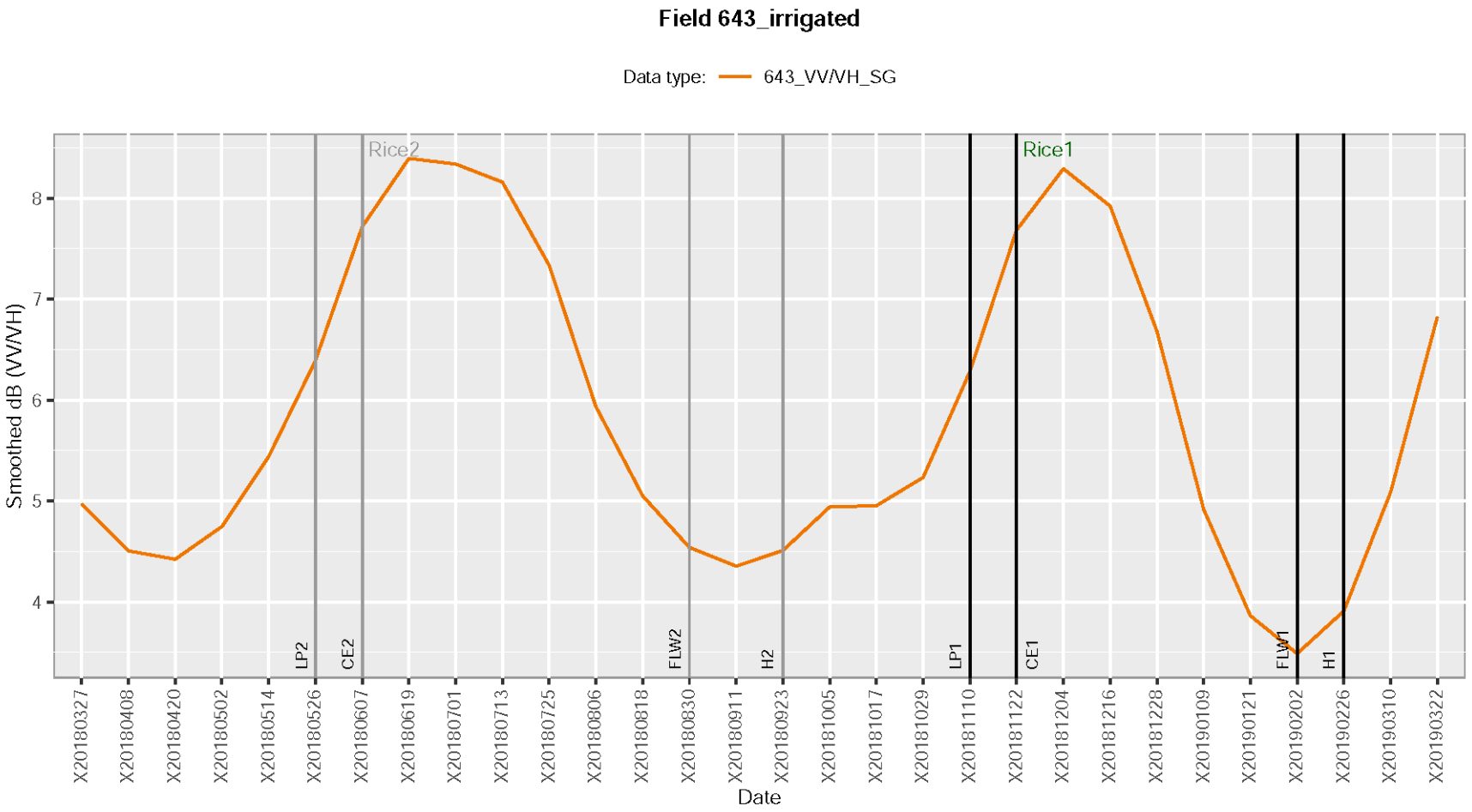
Field 643_irrigated
Data type: 643_VV/VH_SG
Smoothed dB (VV/VH)
8
7
6
5
4
Rice2
Rice1
LP2
CE2
FLW2
H2
LP1
CE1
FLW1
H1
X20180327
X20180408
X20180420
X20180502
X20180514
X20180526
X20180607
X20180619
X20180701
X20180713
X20180725
X20180806
X20180818
X20180830
X20180911
X20180923
X20181005
X20181017
X20181029
X20181110
X20181122
X20181204
X20181216
X20181228
X20190109
X20190121
X20190202
X20190226
X20190310
X20190322
Date

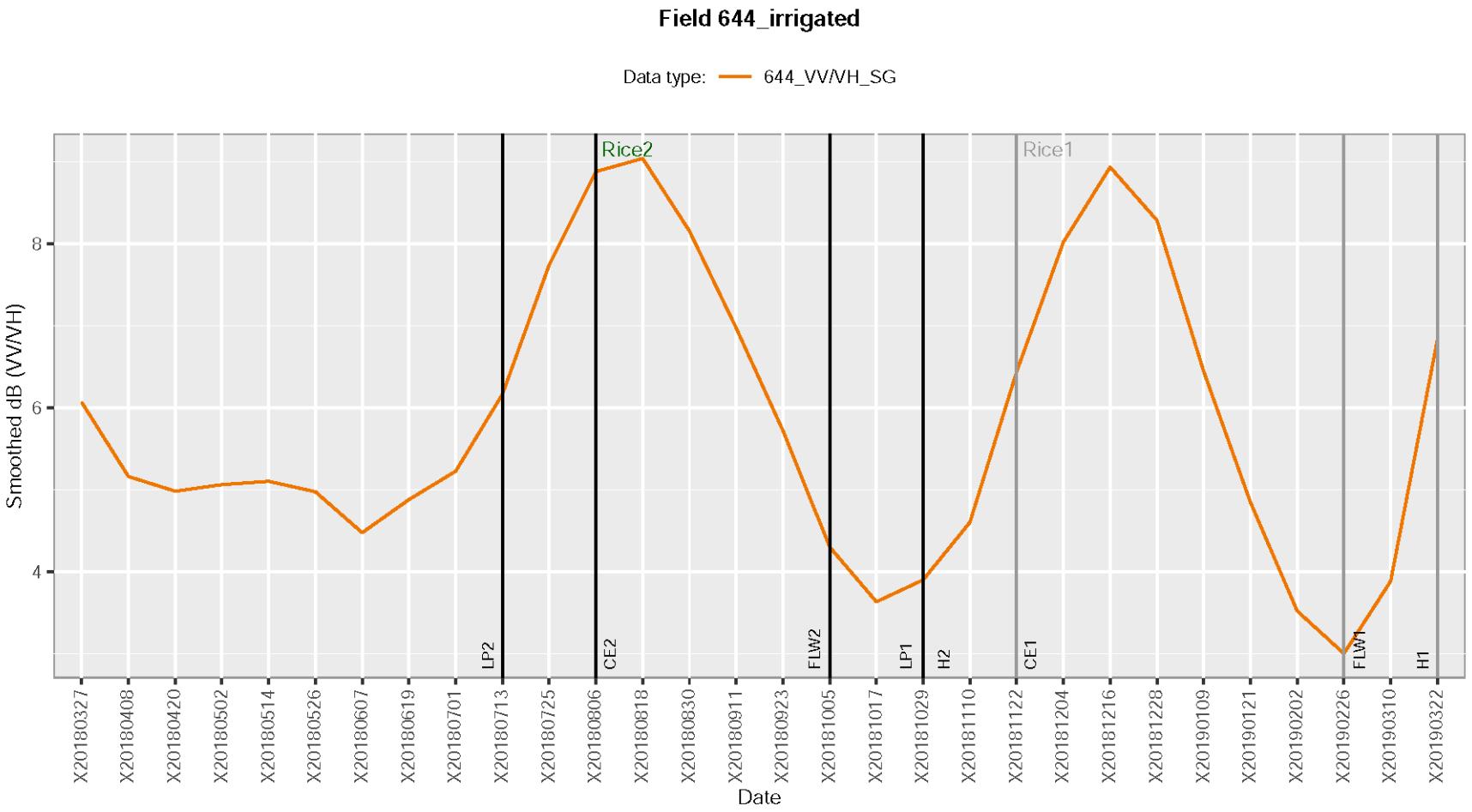
Field 644_irrigated
Data type: 644_VV/VH_SG
Rice2
Rice1
Smoothed dB (VV/VH)
8
6
4
LP2
CE2
FLW2
LP1
H2
CE1
FLW1
H1
X20180327
X20180408
X20180420
X20180502
X20180514
X20180526
X20180607
X20180619
X20180701
X20180713
X20180725
X20180806
X20180818
X20180830
X20180911
X20180923
X20181005
X20181017
X20181029
X20181110
X20181122
X20181204
X20181216
X20181228
X20190109
X20190121
X20190202
X20190226
X20190310
X20190322
Date

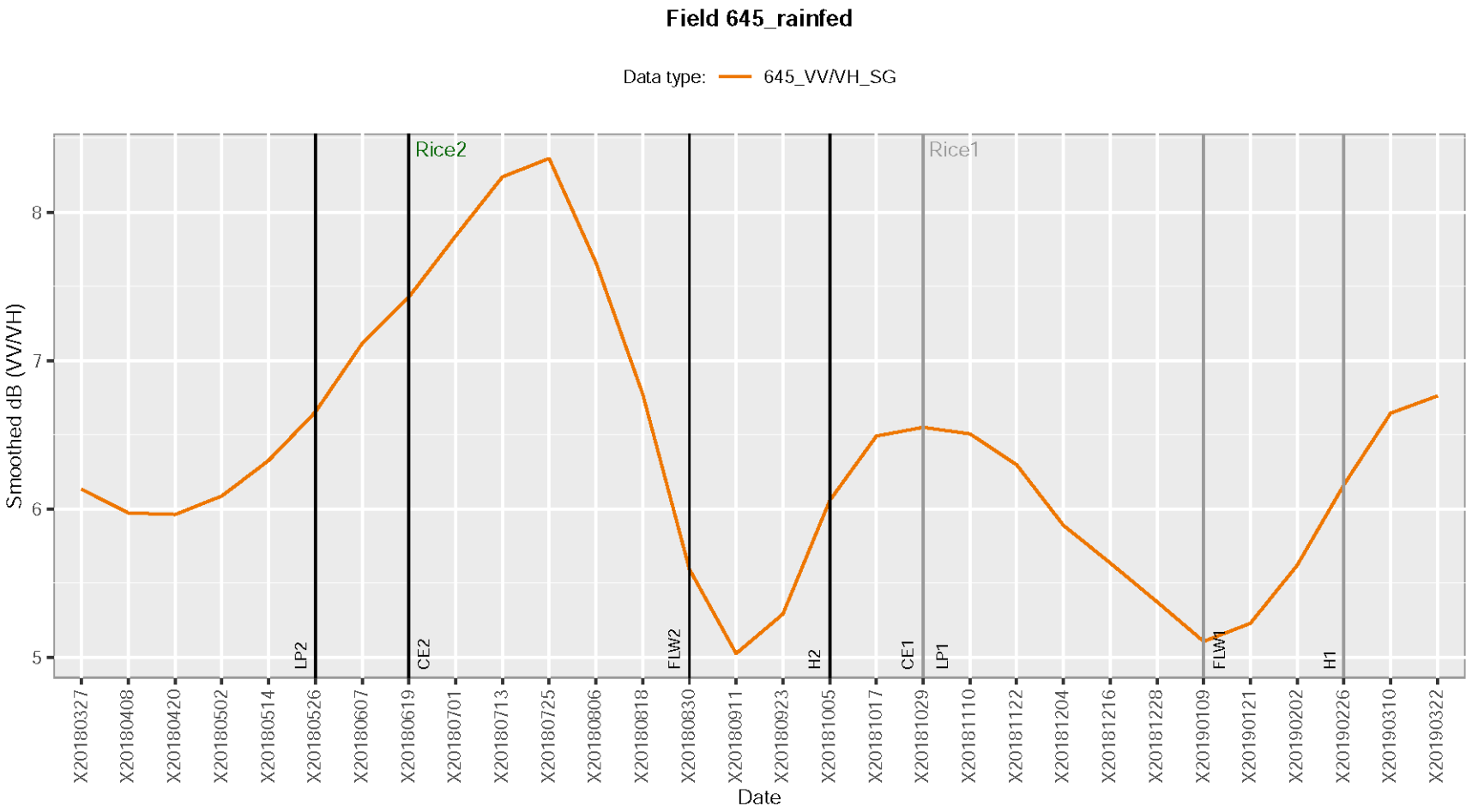
Field 645_rainfed
Data type: 645_VV/VH_SG
Rice2
Rice1
Smoothed dB (VV/VH)
8
7
6
5
LP2
CE2
FLW2
H2
CE1
LP1
FLW1
H1
X20180327
X20180408
X20180420
X20180502
X20180514
X20180526
X20180607
X20180619
X20180701
X20180713
X20180725
X20180806
X20180818
X20180830
X20180911
X20180923
X20181005
X20181017
X20181029
X20181110
X20181122
X20181204
X20181216
X20181228
X20190109
X20190121
X20190202
X20190226
X20190310
X20190322
Date

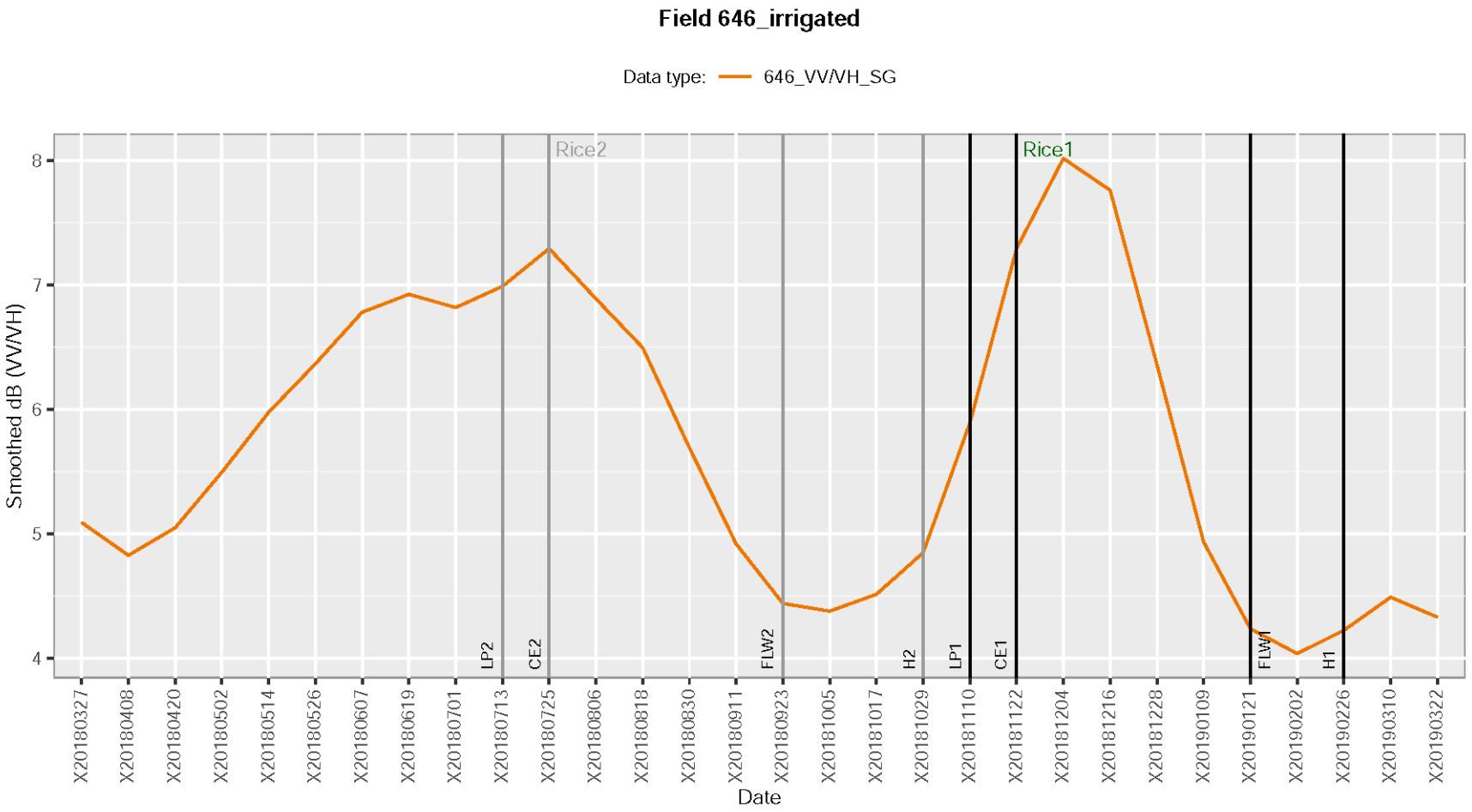
Field 646_irrigated
Data type: 646_VV/VH_SG
Rice2
Rice1
LP2
CE2
FLW2
H2
LP1
CE1
FLW1
H1
Smoothed dB (VV/VH)
8
7
6
5
4
X20180327
X20180408
X20180420
X20180502
X20180514
X20180526
X20180607
X20180619
X20180701
X20180713
X20180725
X20180806
X20180818
X20180830
X20180911
X20180923
X20181005
X20181017
X20181029
X20181110
X20181122
X20181204
X20181216
X20181228
X20190109
X20190121
X20190202
X20190226
X20190310
X20190322
Date

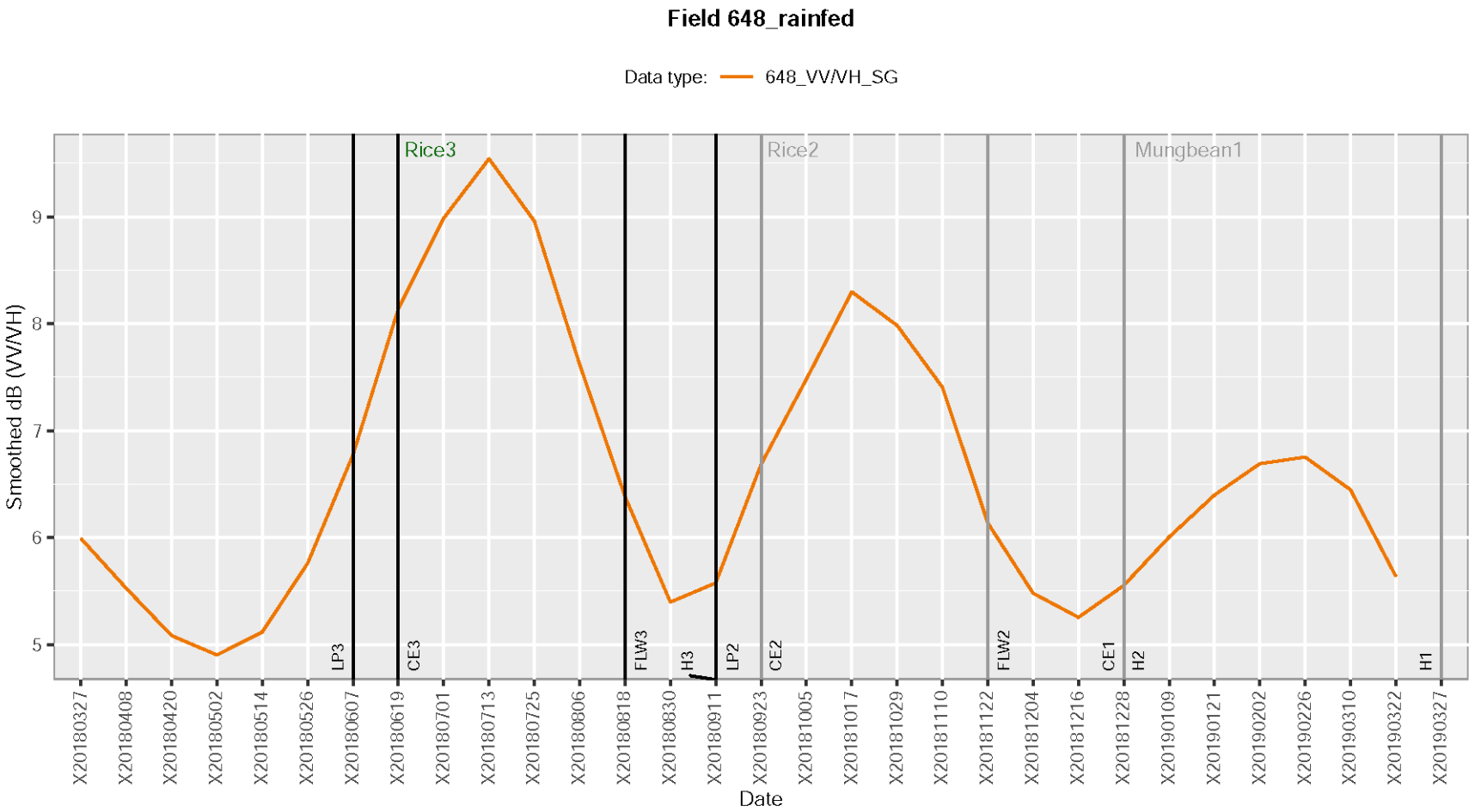
Field 648_rainfed
Data type: 648_VV/VH_SG
Rice3
Rice2
Mungbean1
Smoothed dB (VV/VH)
9
8
7
6
5
LP3
CE3
FLW3
H3
LP2
CE2
FLW2
CE1
H2
H1
X20180327
X20180408
X20180420
X20180502
X20180514
X20180526
X20180607
X20180619
X20180701
X20180713
X20180725
X20180806
X20180818
X20180830
X20180911
X20180923
X20181005
X20181017
X20181029
X20181110
X20181122
X20181204
X20181216
X20181228
X20190109
X20190121
X20190202
X20190226
X20190310
X20190322
X20190327
Date

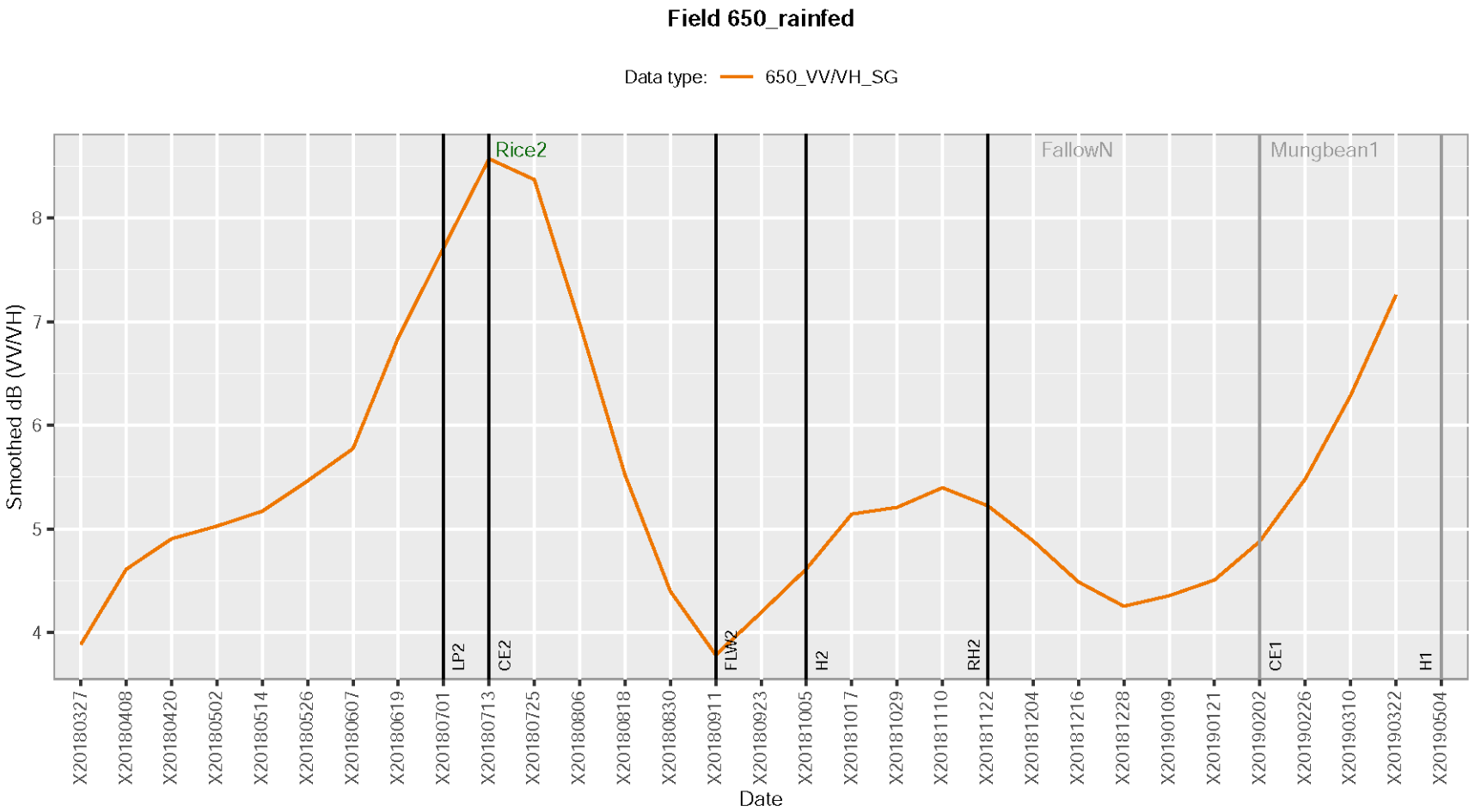
Field 650_rainfed
Data type: 650_VV/VH_SG
Smoothed dB (VV/VH)
8
7
6
5
4
Rice2
FallowN
Mungbean1
LP2
CE2
FLW2
H2
RH2
CE1
H1
X20180327
X20180408
X20180420
X20180502
X20180514
X20180526
X20180607
X20180619
X20180701
X20180713
X20180725
X20180806
X20180818
X20180830
X20180911
X20180923
X20181005
X20181017
X20181029
X20181110
X20181122
X20181204
X20181216
X20181228
X20190109
X20190121
X20190202
X20190226
X20190310
X20190322
X20190504
Date

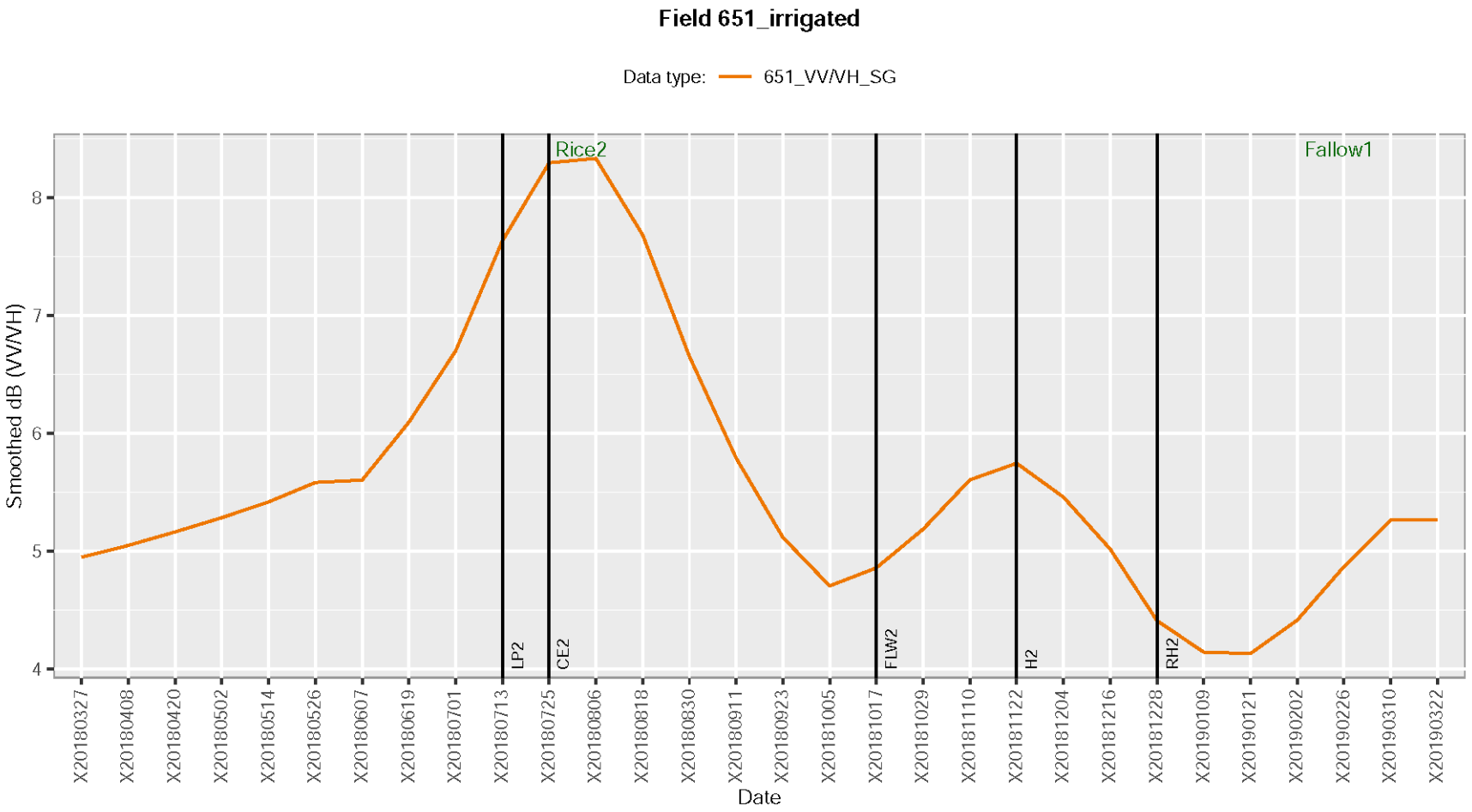
Field 651_irrigated
Data type: 651_VV/VH_SG
Rice2
Fallow1
LP2
CE2
FLW2
H2
RH2
Smoothed dB (VV/VH)
8
7
6
5
4
X20180327
X20180408
X20180420
X20180502
X20180514
X20180526
X20180607
X20180619
X20180701
X20180713
X20180725
X20180806
X20180818
X20180830
X20180911
X20180923
X20181005
X20181017
X20181029
X20181110
X20181122
X20181204
X20181216
X20181228
X20190109
X20190121
X20190202
X20190226
X20190310
X20190322
Date

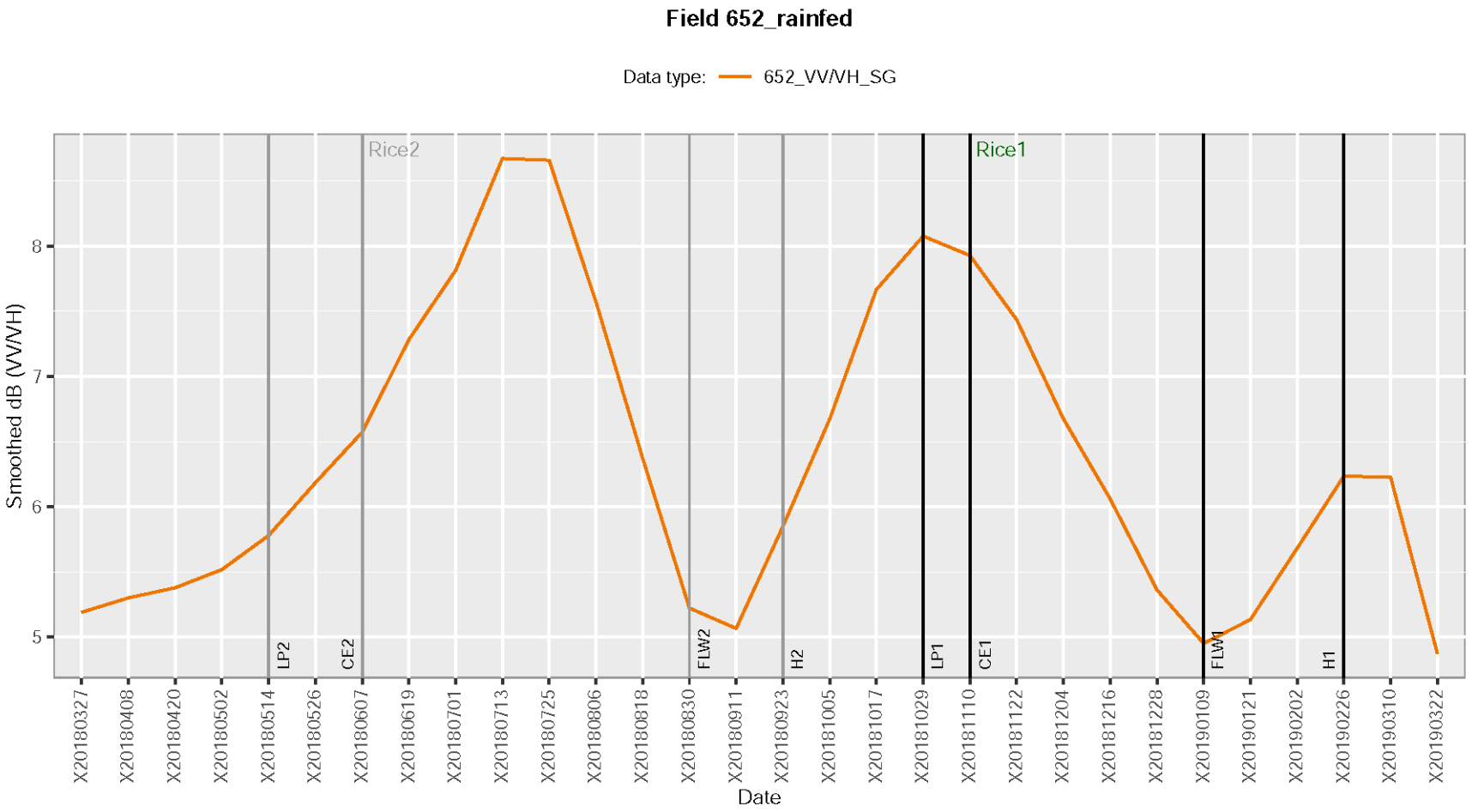
Field 652_rainfed
Data type: 652_VV/VH_SG
Rice2
Rice1
LP2
CE2
FLW2
H2
LP1
CE1
FLW1
H1
Smoothed dB (VV/VH)
5
6
7
8
X20180327
X20180408
X20180420
X20180502
X20180514
X20180526
X20180607
X20180619
X20180701
X20180713
X20180725
X20180806
X20180818
X20180830
X20180911
X20180923
X20181005
X20181017
X20181029
X20181110
X20181122
X20181204
X20181216
X20181228
X20190109
X20190121
X20190202
X20190226
X20190310
X20190322
Date

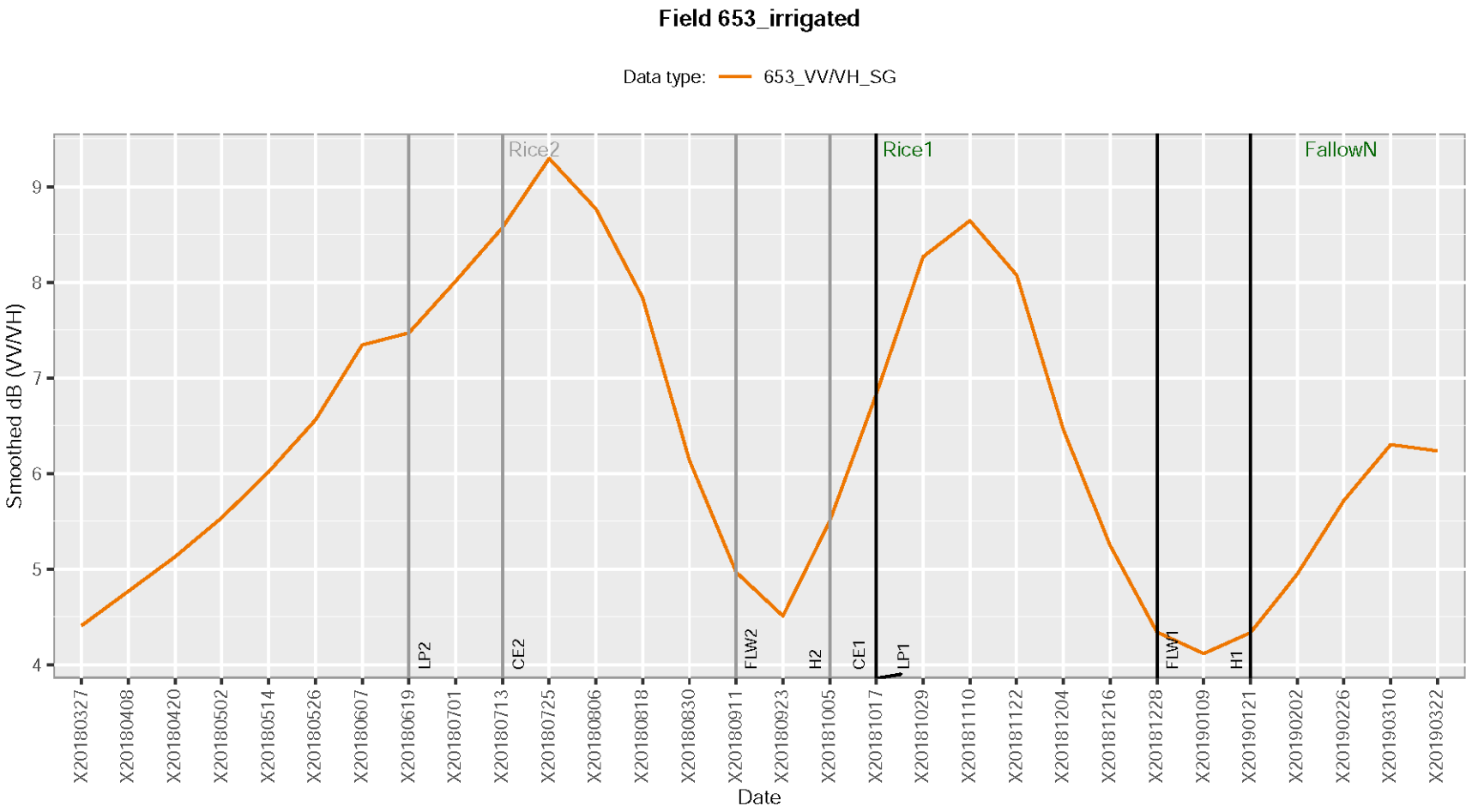
Field 653_irrigated
Data type: 653_VV/VH_SG
Smoothed dB (VV/VH)
Rice2
Rice1
FallowN
LP2
CE2
FLW2
H2
CE1
LP1
FLW1
H1
Date

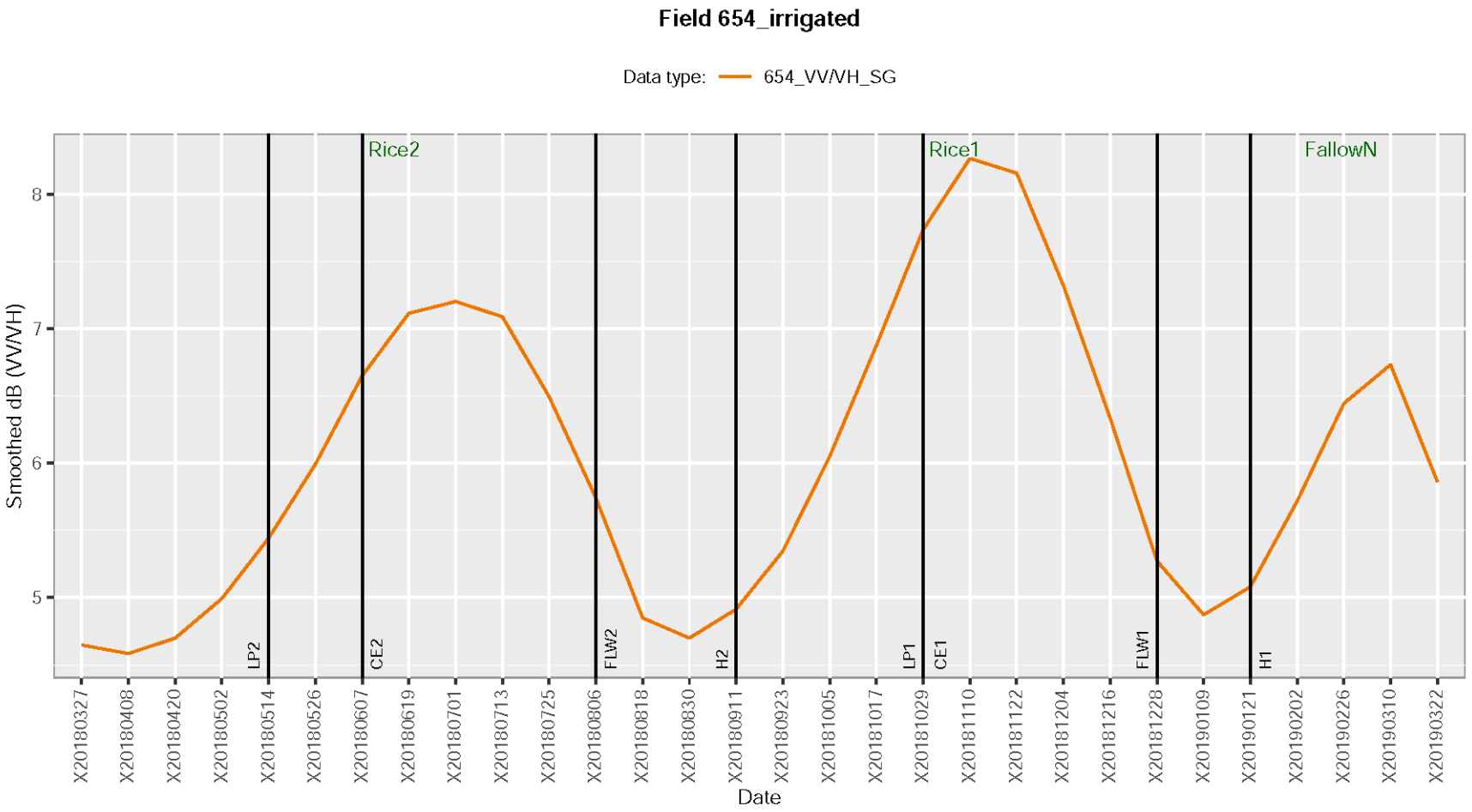
Field 654_irrigated
Data type: 654_VV/VH_SG
Rice2
Rice1
FallowN
LP2
CE2
FLW2
H2
LP1
CE1
FLW1
H1
Smoothed dB (VV/VH)
8
7
6
5
X20180327
X20180408
X20180420
X20180502
X20180514
X20180526
X20180607
X20180619
X20180701
X20180713
X20180725
X20180806
X20180818
X20180830
X20180911
X20180923
X20181005
X20181017
X20181029
X20181110
X20181122
X20181204
X20181216
X20181228
X20190109
X20190121
X20190202
X20190226
X20190310
X20190322
Date

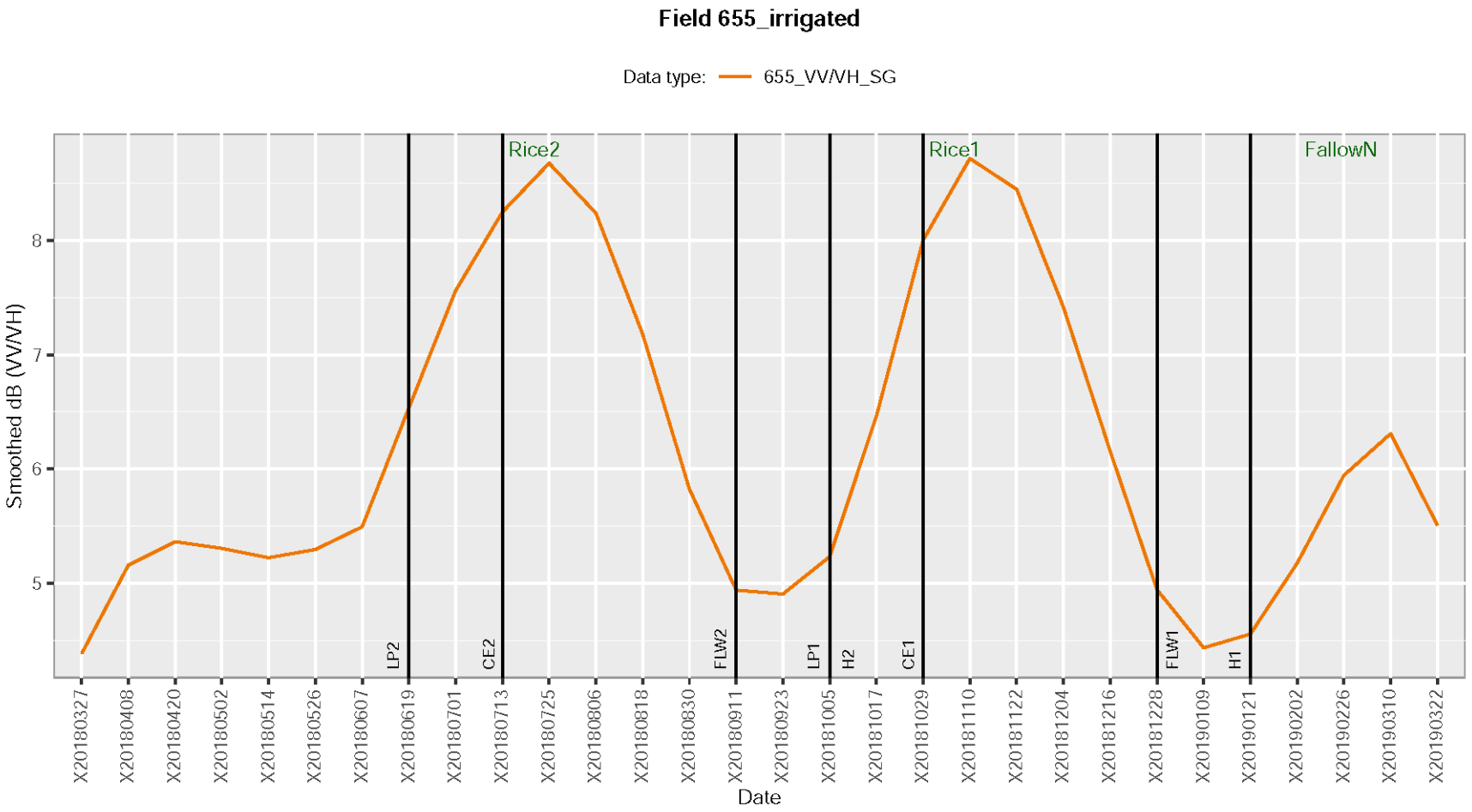
Field 655_irrigated
Data type: 655_VV/VH_SG
Rice2
Rice1
FallowN
LP2
CE2
FLW2
LP1
H2
CE1
FLW1
H1
Smoothed dB (VV/VH)
5
6
7
8
X20180327
X20180408
X20180420
X20180502
X20180514
X20180526
X20180607
X20180619
X20180701
X20180713
X20180725
X20180806
X20180818
X20180830
X20180911
X20180923
X20181005
X20181017
X20181029
X20181110
X20181122
X20181204
X20181216
X20181228
X20190109
X20190121
X20190202
X20190226
X20190310
X20190322
Date

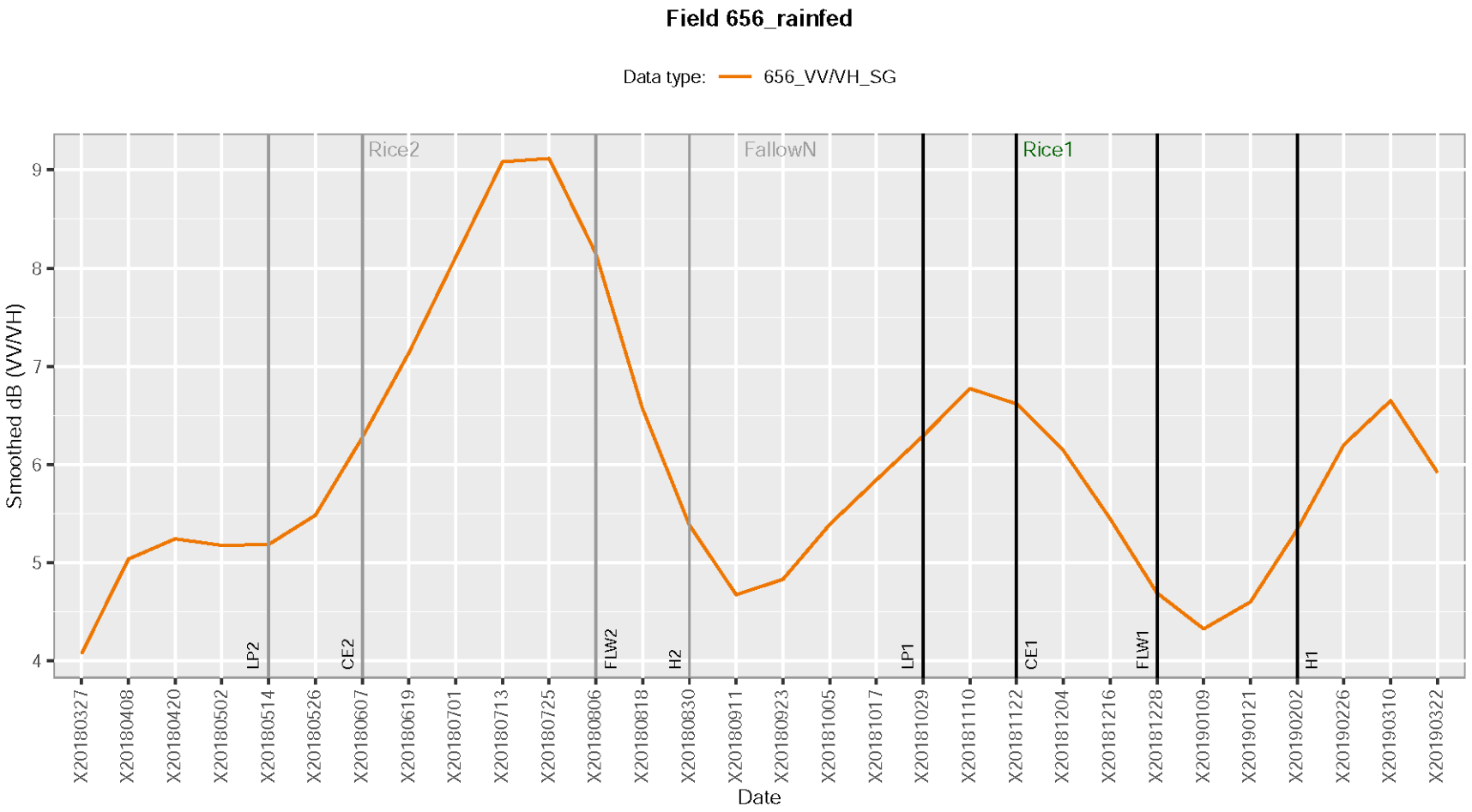
Field 656_rainfed
Data type: 656_VV/VH_SG
Rice2
FallowN
Rice1
Smoothed dB (VV/VH)
9
8
7
6
5
4
LP2
CE2
FLW2
H2
LP1
CE1
FLW1
H1
X20180327
X20180408
X20180420
X20180502
X20180514
X20180526
X20180607
X20180619
X20180701
X20180713
X20180725
X20180806
X20180818
X20180830
X20180911
X20180923
X20181005
X20181017
X20181029
X20181110
X20181122
X20181204
X20181216
X20181228
X20190109
X20190121
X20190202
X20190226
X20190310
X20190322
Date

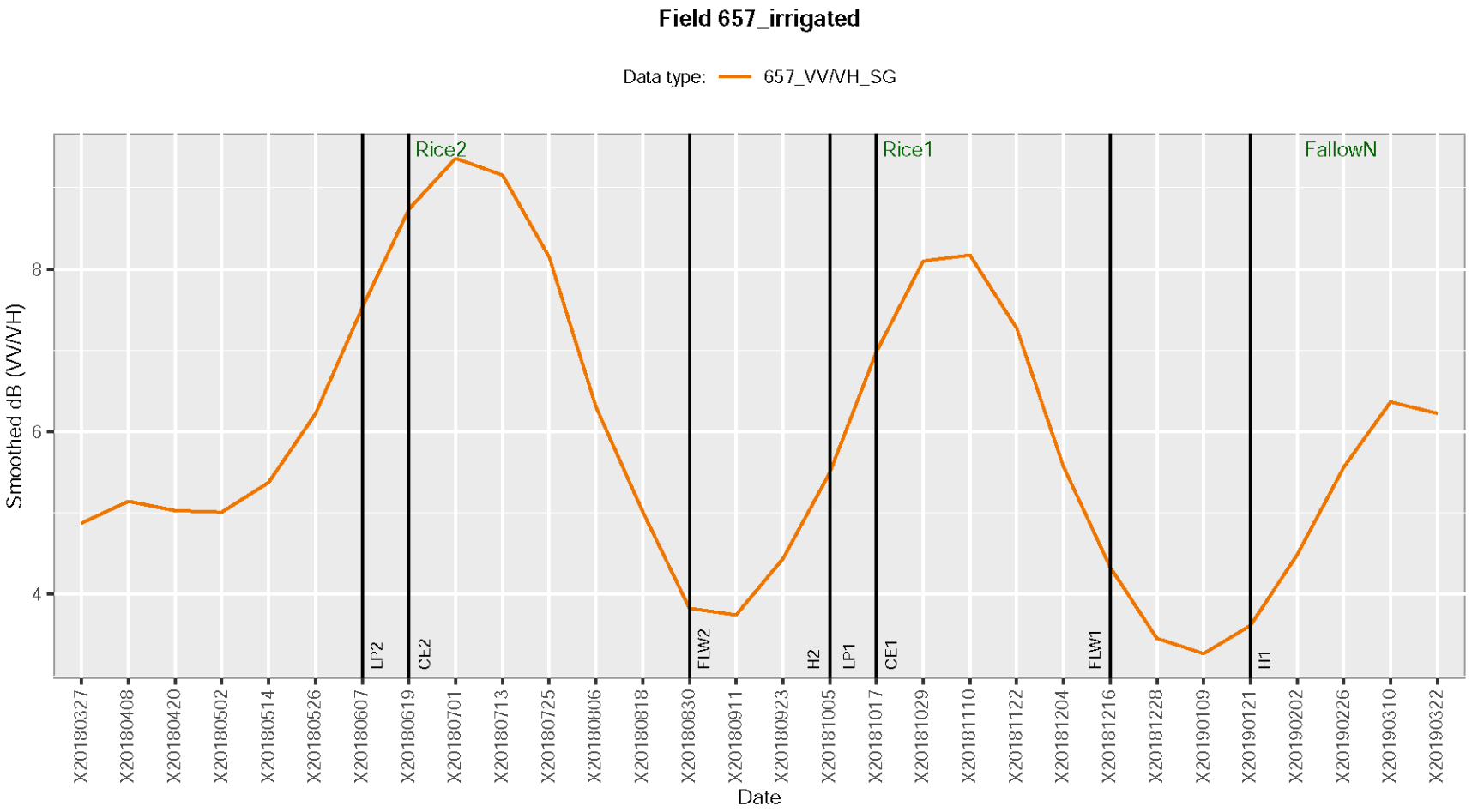
Field 657_irrigated
Data type: 657_VV/VH_SG
Rice2
Rice1
FallowN
Smoothed dB (VV/VH)
8
6
4
LP2
CE2
FLW2
H2
LP1
CE1
FLW1
H1
X20180327
X20180408
X20180420
X20180502
X20180514
X20180526
X20180607
X20180619
X20180701
X20180713
X20180725
X20180806
X20180818
X20180830
X20180911
X20180923
X20181005
X20181017
X20181029
X20181110
X20181122
X20181204
X20181216
X20181228
X20190109
X20190121
X20190202
X20190226
X20190310
X20190322
Date

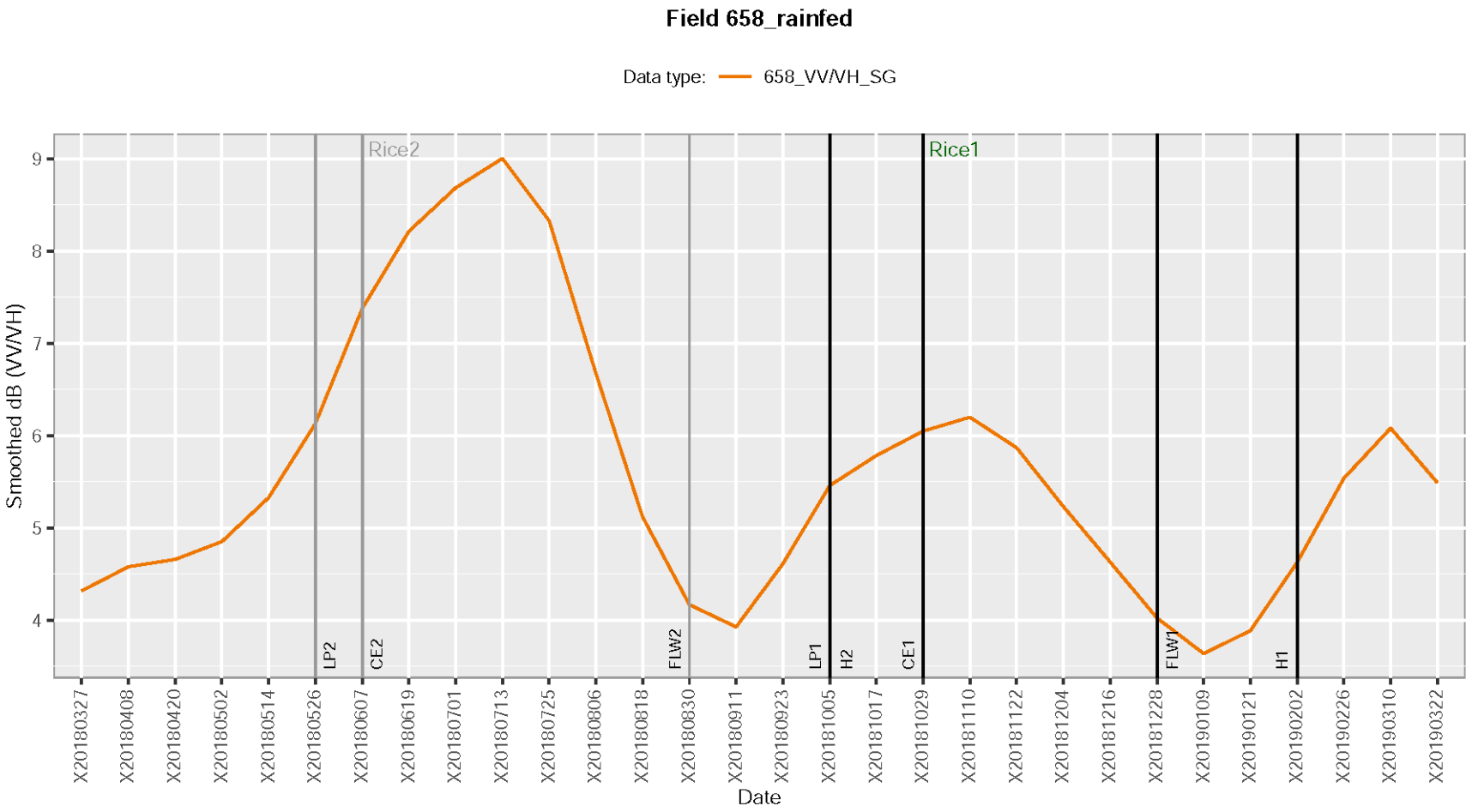
Field 658_rainfed
Data type: 658_VV/VH_SG
Smoothed dB (VV/VH)
9
8
7
6
5
4
Rice2
Rice1
LP2
CE2
FLW2
LP1
H2
CE1
FLW1
H1
X20180327
X20180408
X20180420
X20180502
X20180514
X20180526
X20180607
X20180619
X20180701
X20180713
X20180725
X20180806
X20180818
X20180830
X20180911
X20180923
X20181005
X20181017
X20181029
X20181110
X20181122
X20181204
X20181216
X20181228
X20190109
X20190121
X20190202
X20190226
X20190310
X20190322
Date

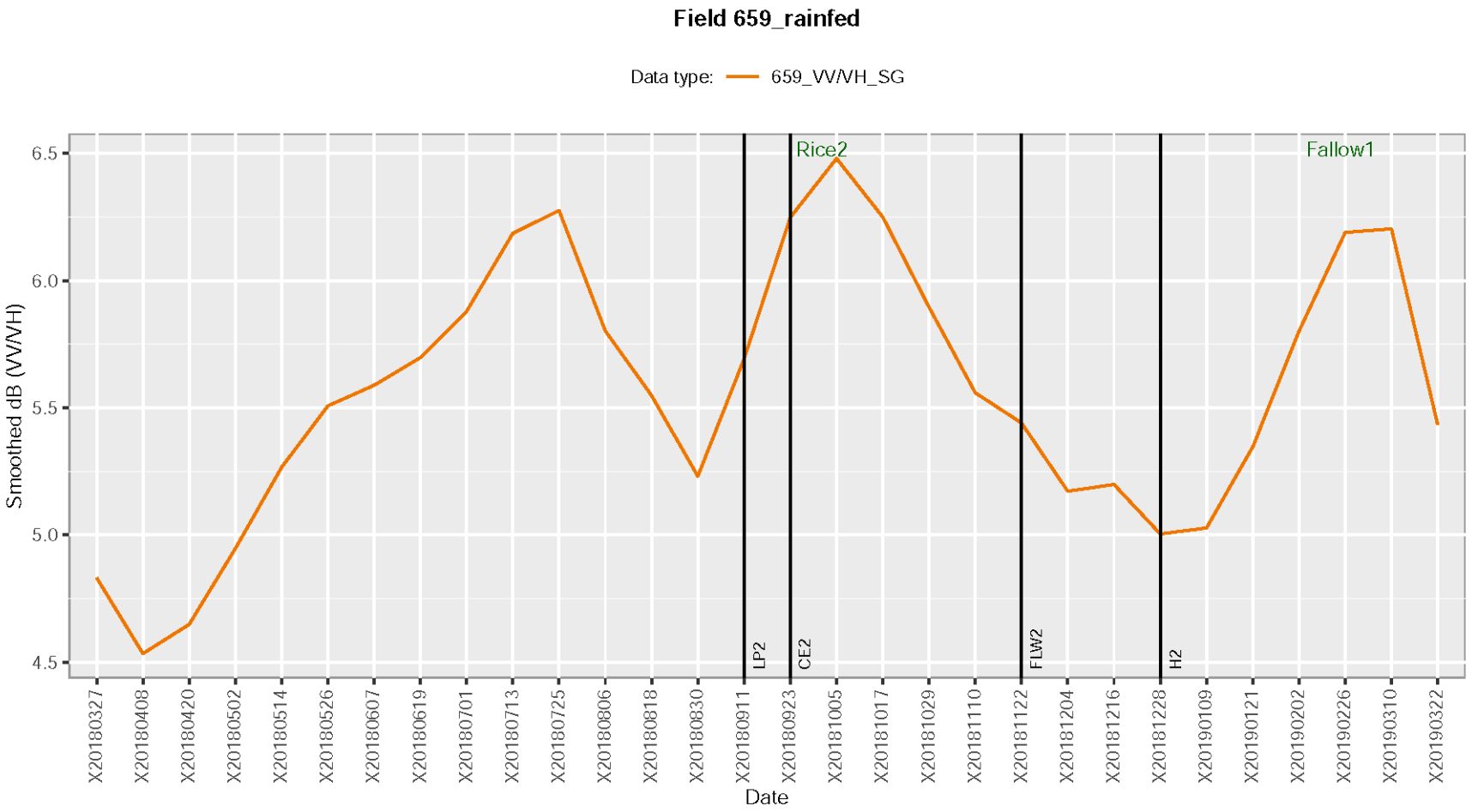
Field 659_rainfed
Data type: 659_VV/VH_SG
Smoothed dB (VV/VH)
6.5
6.0
5.5
5.0
4.5
Rice2
Fallow1
LP2
CE2
FLW2
H2
X20180327
X20180408
X20180420
X20180502
X20180514
X20180526
X20180607
X20180619
X20180701
X20180713
X20180725
X20180806
X20180818
X20180830
X20180911
X20180923
X20181005
X20181017
X20181029
X20181110
X20181122
X20181204
X20181216
X20181228
X20190109
X20190121
X20190202
X20190226
X20190310
X20190322
Date

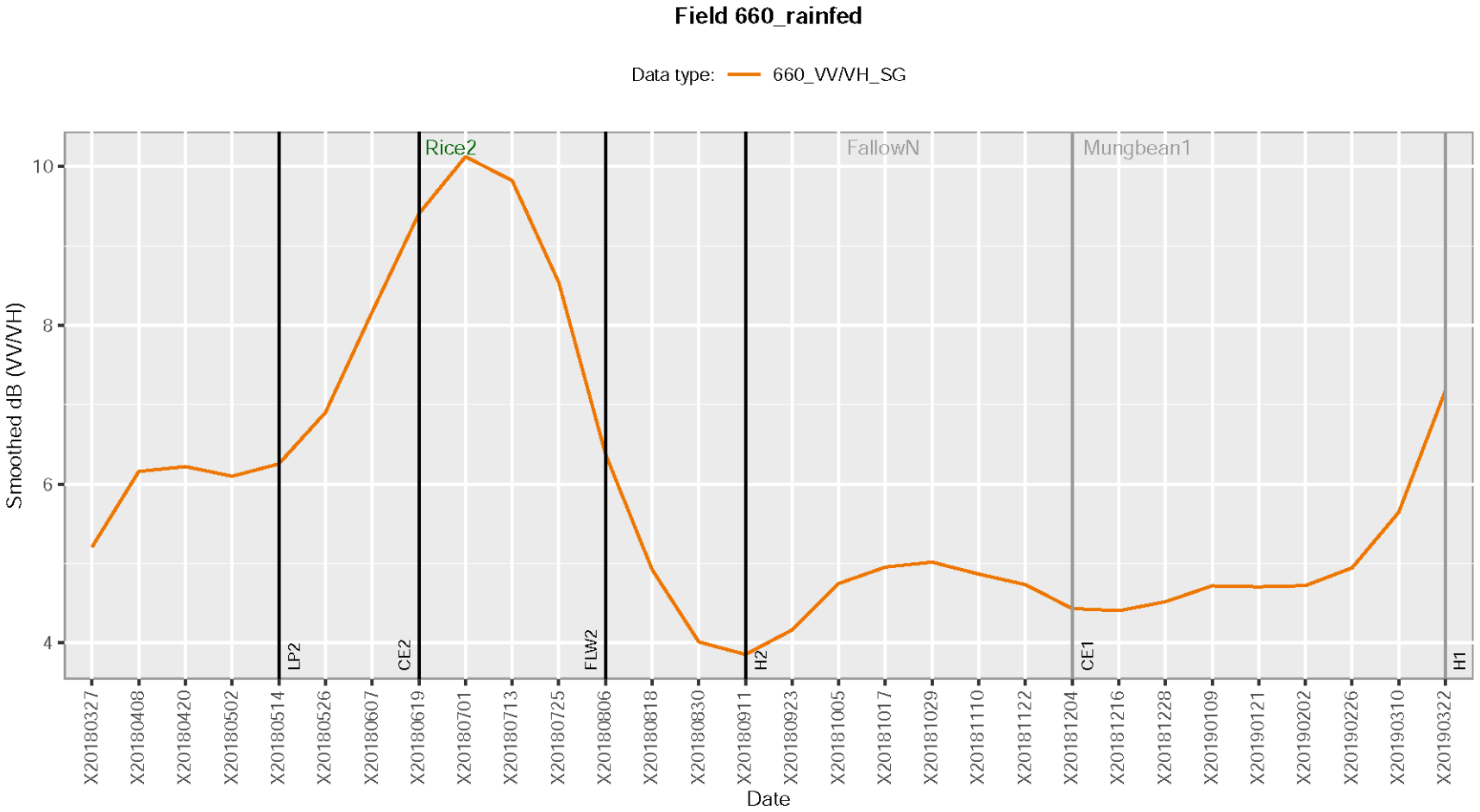
Field 660_rainfed
Data type: 660_VV/VH_SG
Rice2
FallowN
Mungbean1
Smoothed dB (VV/VH)
10
8
6
4
LP2
CE2
FLW2
H2
CE1
H1
X20180327
X20180408
X20180420
X20180502
X20180514
X20180526
X20180607
X20180619
X20180701
X20180713
X20180725
X20180806
X20180818
X20180830
X20180911
X20180923
X20181005
X20181017
X20181029
X20181110
X20181122
X20181204
X20181216
X20181228
X20190109
X20190121
X20190202
X20190226
X20190310
X20190322
Date

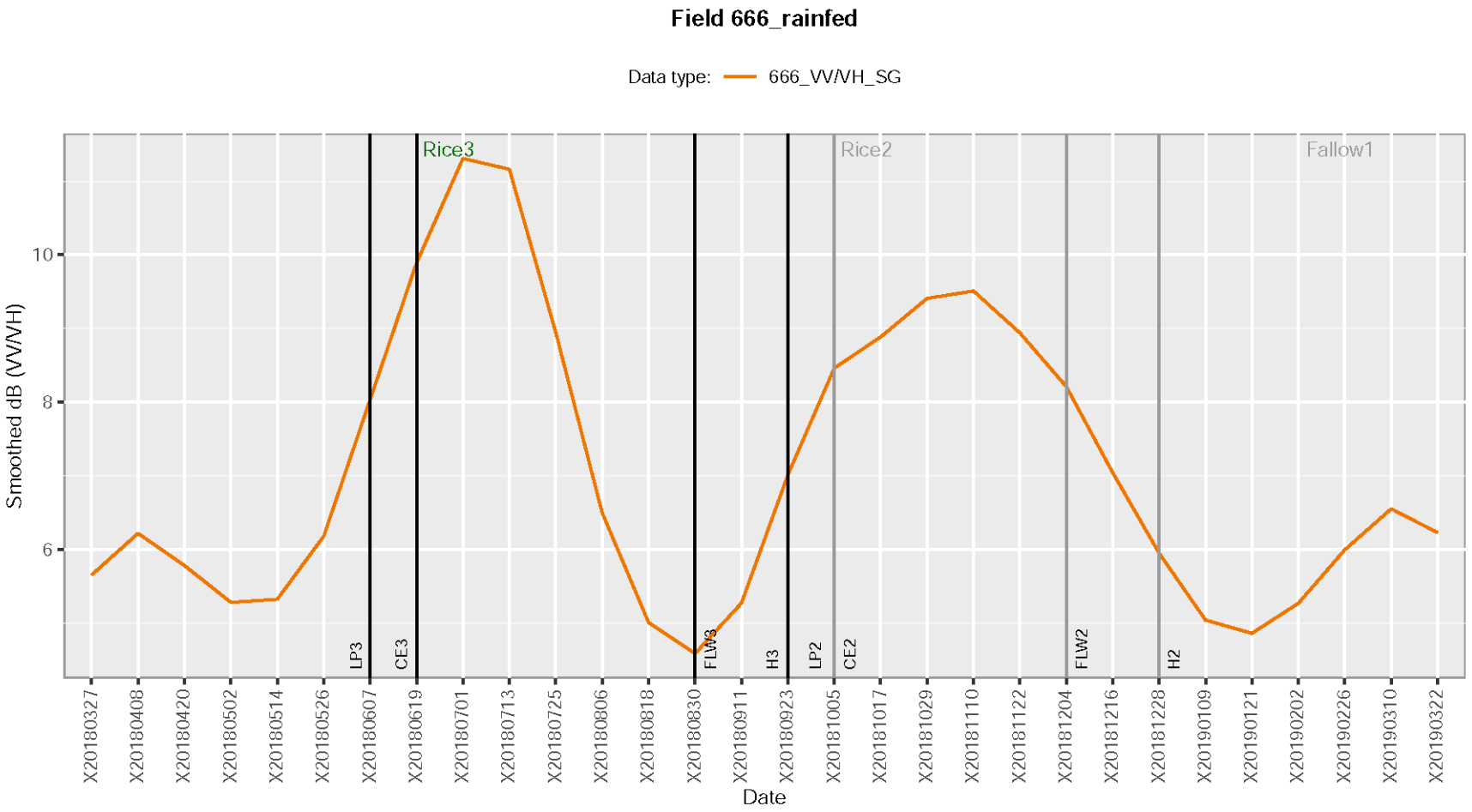
Field 666_rainfed
Data type: 666_VV/VH_SG
Rice3
Rice2
Fallow1
Smoothed dB (VV/VH)
10
8
6
LP3
CE3
FLW3
H3
LP2
CE2
FLW2
H2
X20180327
X20180408
X20180420
X20180502
X20180514
X20180526
X20180607
X20180619
X20180701
X20180713
X20180725
X20180806
X20180818
X20180830
X20180911
X20180923
X20181005
X20181017
X20181029
X20181110
X20181122
X20181204
X20181216
X20181228
X20190109
X20190121
X20190202
X20190226
X20190310
X20190322
Date

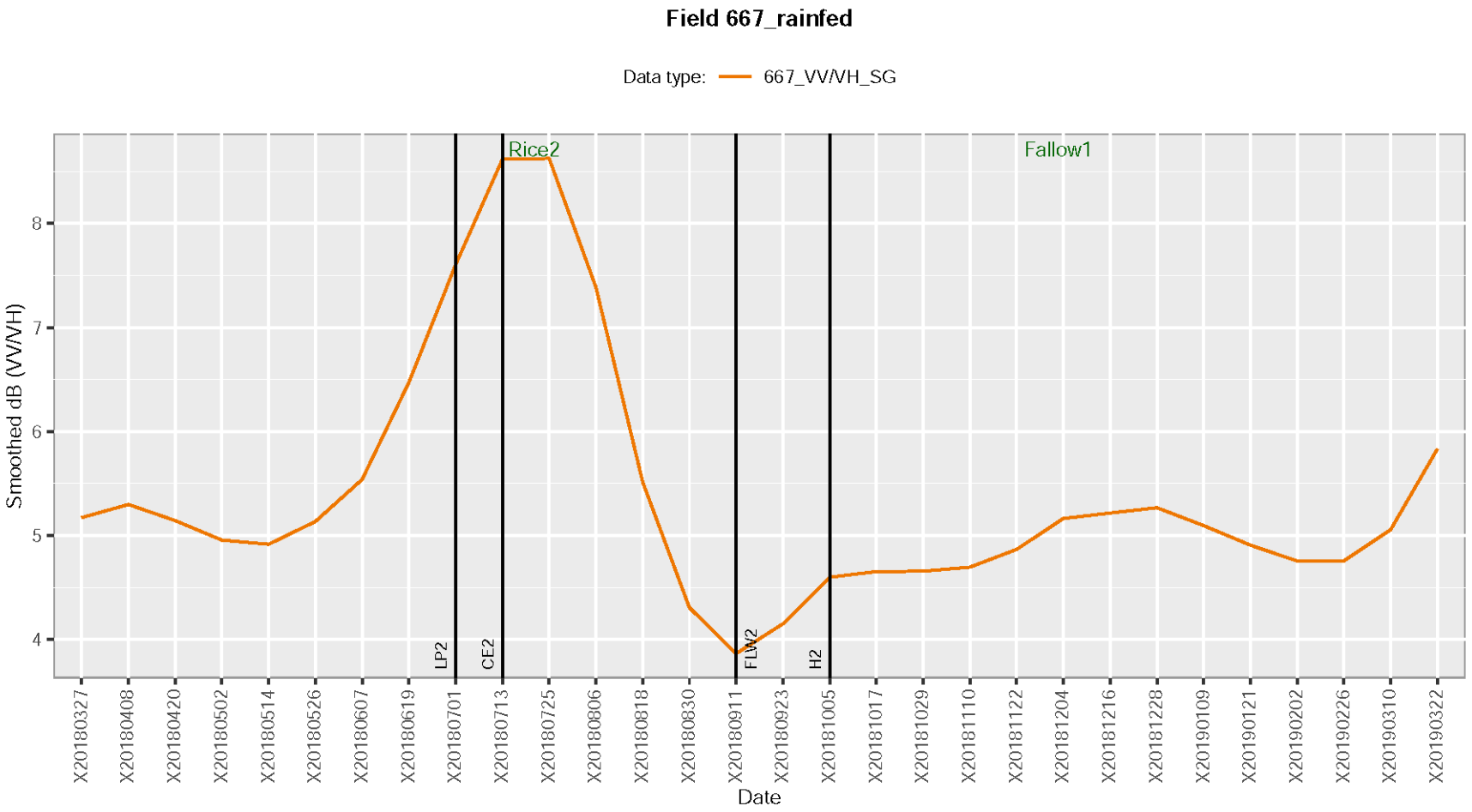
Field 667_rainfed
Data type: 667_VV/VH_SG
Rice2
Fallow1
LP2
CE2
FLW2
H2
Smoothed dB (VV/VH)
8
7
6
5
4
X20180327
X20180408
X20180420
X20180502
X20180514
X20180526
X20180607
X20180619
X20180701
X20180713
X20180725
X20180806
X20180818
X20180830
X20180911
X20180923
X20181005
X20181017
X20181029
X20181110
X20181122
X20181204
X20181216
X20181228
X20190109
X20190121
X20190202
X20190226
X20190310
X20190322
Date

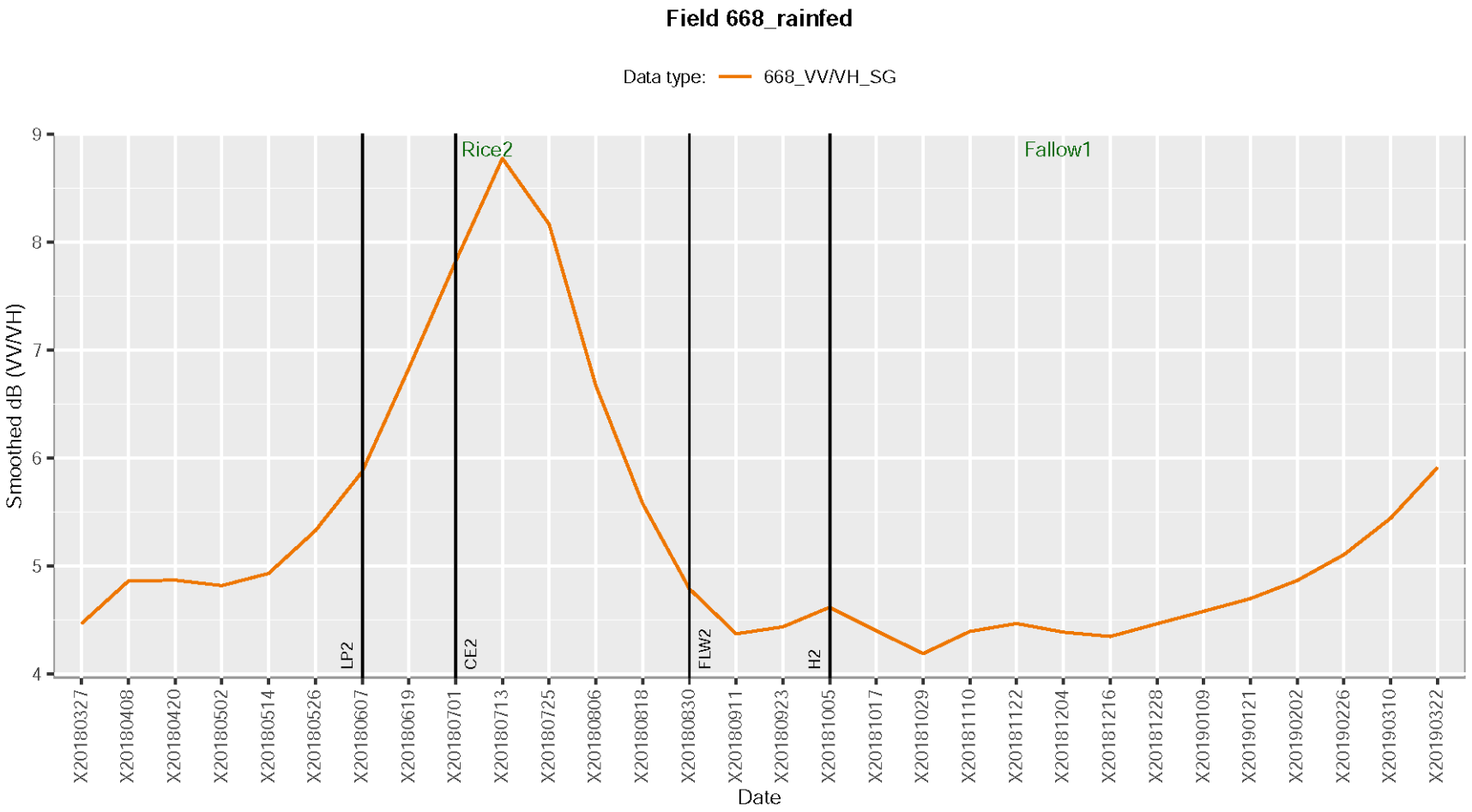
Field 668_rainfed
Data type: 668_VV/VH_SG
Rice2
Fallow1
LP2
CE2
FLW2
H2
Smoothed dB (VV/VH)
Date
9
8
7
6
5
4
X20180327
X20180408
X20180420
X20180502
X20180514
X20180526
X20180607
X20180619
X20180701
X20180713
X20180725
X20180806
X20180818
X20180830
X20180911
X20180923
X20181005
X20181017
X20181029
X20181110
X20181122
X20181204
X20181216
X20181228
X20190109
X20190121
X20190202
X20190226
X20190310
X20190322

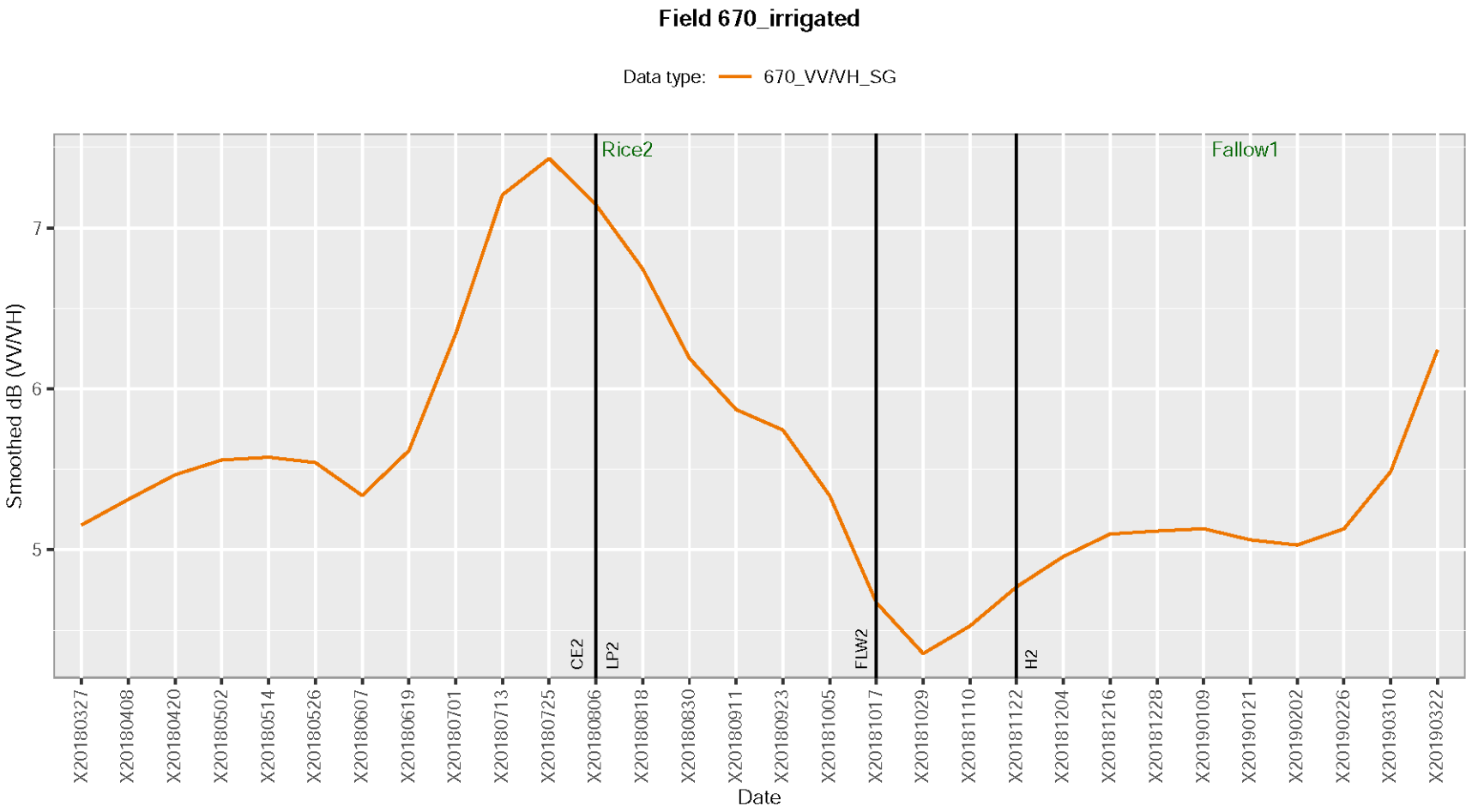
Field 670_irrigated
Data type: 670_VV/VH_SG
Rice2
Fallow1
CE2
LP2
FLW2
H2
Smoothed dB (VV/VH)
7
6
5
X20180327
X20180408
X20180420
X20180502
X20180514
X20180526
X20180607
X20180619
X20180701
X20180713
X20180725
X20180806
X20180818
X20180830
X20180911
X20180923
X20181005
X20181017
X20181029
X20181110
X20181122
X20181204
X20181216
X20181228
X20190109
X20190121
X20190202
X20190226
X20190310
X20190322
Date

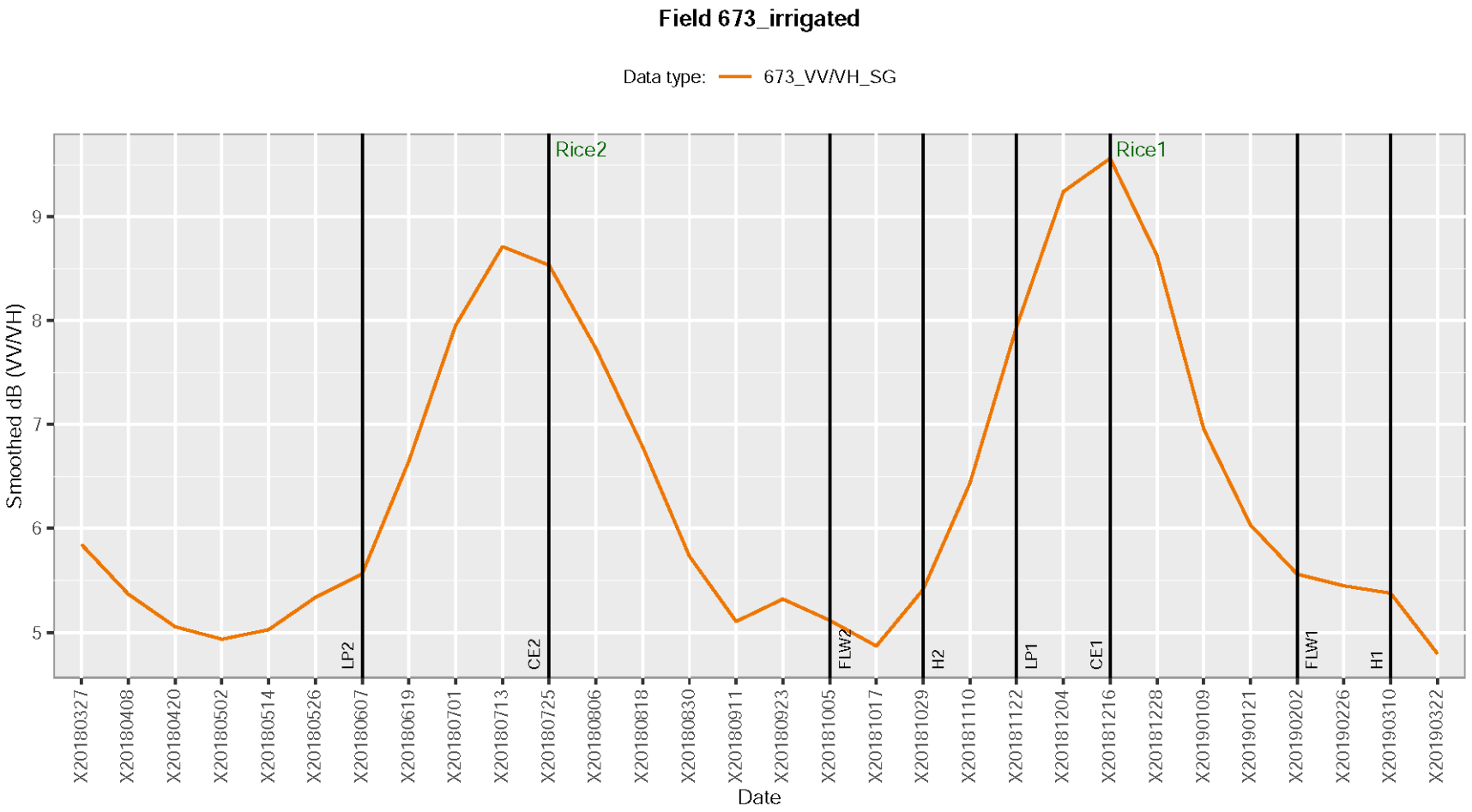
Field 673_irrigated
Data type: 673_VV/VH_SG
Smoothed dB (VV/VH)
9
8
7
6
5
Rice2
Rice1
LP2
CE2
FLW2
H2
LP1
CE1
FLW1
H1
X20180327
X20180408
X20180420
X20180502
X20180514
X20180526
X20180607
X20180619
X20180701
X20180713
X20180725
X20180806
X20180818
X20180830
X20180911
X20180923
X20181005
X20181017
X20181029
X20181110
X20181122
X20181204
X20181216
X20181228
X20190109
X20190121
X20190202
X20190226
X20190310
X20190322
Date

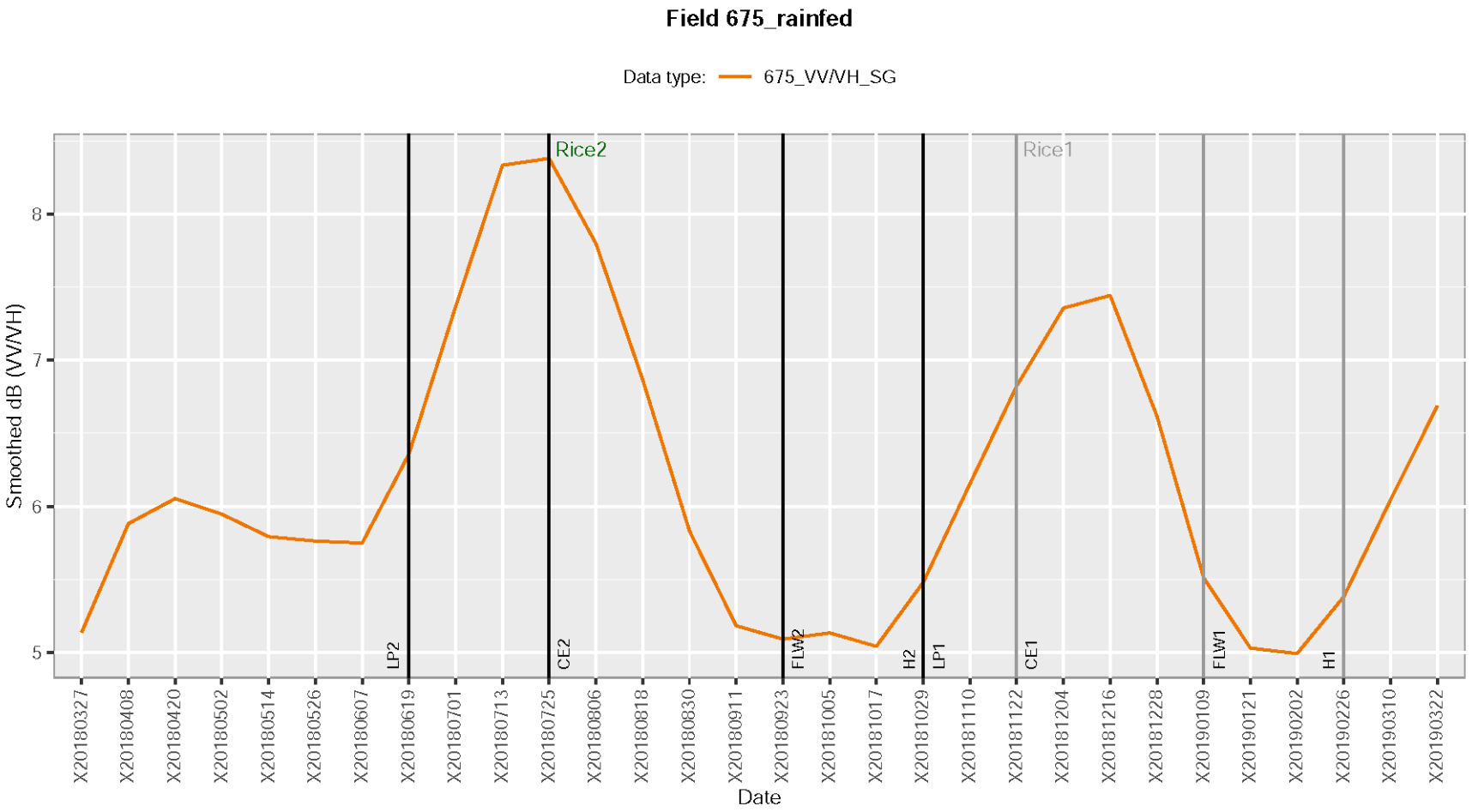
Field 675_rainfed
Data type: 675_VV/VH_SG
Smoothed dB (VV/VH)
8
7
6
5
Rice2
Rice1
LP2
CE2
FLW2
H2
LP1
CE1
FLW1
H1
X20180327
X20180408
X20180420
X20180502
X20180514
X20180526
X20180607
X20180619
X20180701
X20180713
X20180725
X20180806
X20180818
X20180830
X20180911
X20180923
X20181005
X20181017
X20181029
X20181110
X20181122
X20181204
X20181216
X20181228
X20190109
X20190121
X20190202
X20190226
X20190310
X20190322
Date

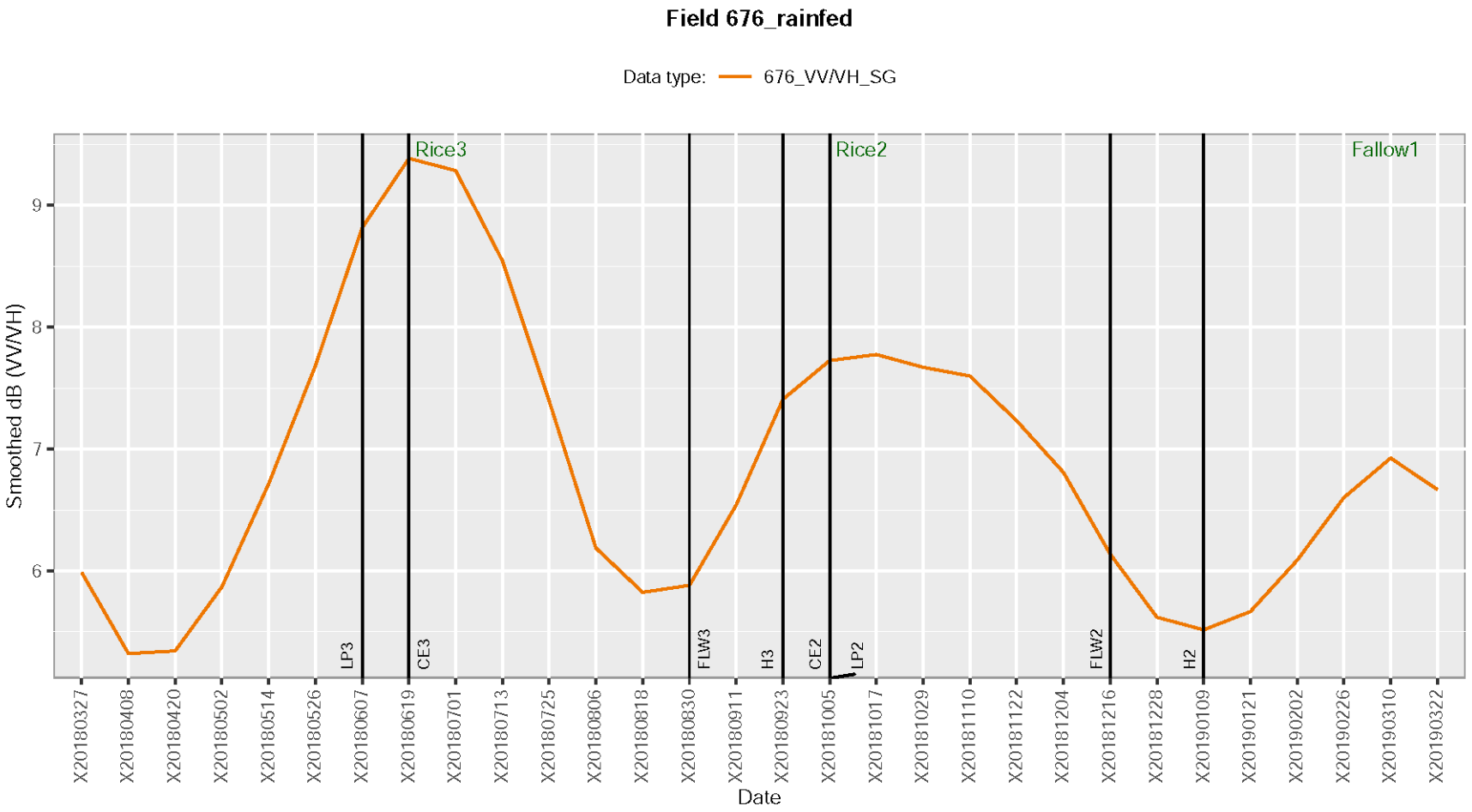
Field 676_rainfed
Data type: 676_VV/VH_SG
Rice3
Rice2
Fallow1
Smoothed dB (VV/VH)
9
8
7
6
LP3
CE3
FLW3
H3
CE2
LP2
FLW2
H2
X20180327
X20180408
X20180420
X20180502
X20180514
X20180526
X20180607
X20180619
X20180701
X20180713
X20180725
X20180806
X20180818
X20180830
X20180911
X20180923
X20181005
X20181017
X20181029
X20181110
X20181122
X20181204
X20181216
X20181228
X20190109
X20190121
X20190202
X20190226
X20190310
X20190322
Date

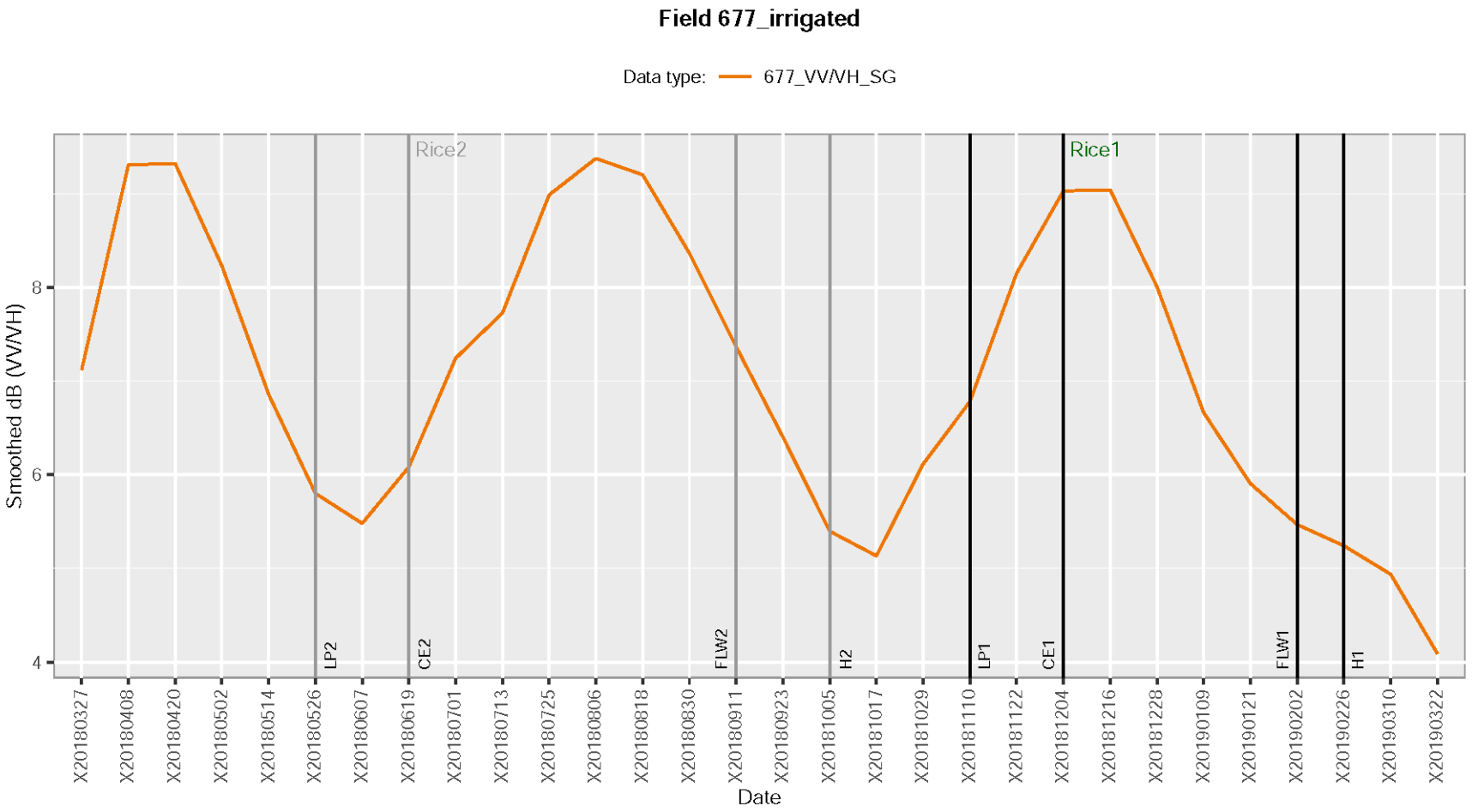
Field 677_irrigated
Data type: 677_VV/VH_SG
Rice2
Rice1
Smoothed dB (VV/VH)
8
6
4
LP2
CE2
FLW2
H2
LP1
CE1
FLW1
H1
X20180327
X20180408
X20180420
X20180502
X20180514
X20180526
X20180607
X20180619
X20180701
X20180713
X20180725
X20180806
X20180818
X20180830
X20180911
X20180923
X20181005
X20181017
X20181029
X20181110
X20181122
X20181204
X20181216
X20181228
X20190109
X20190121
X20190202
X20190226
X20190310
X20190322
Date

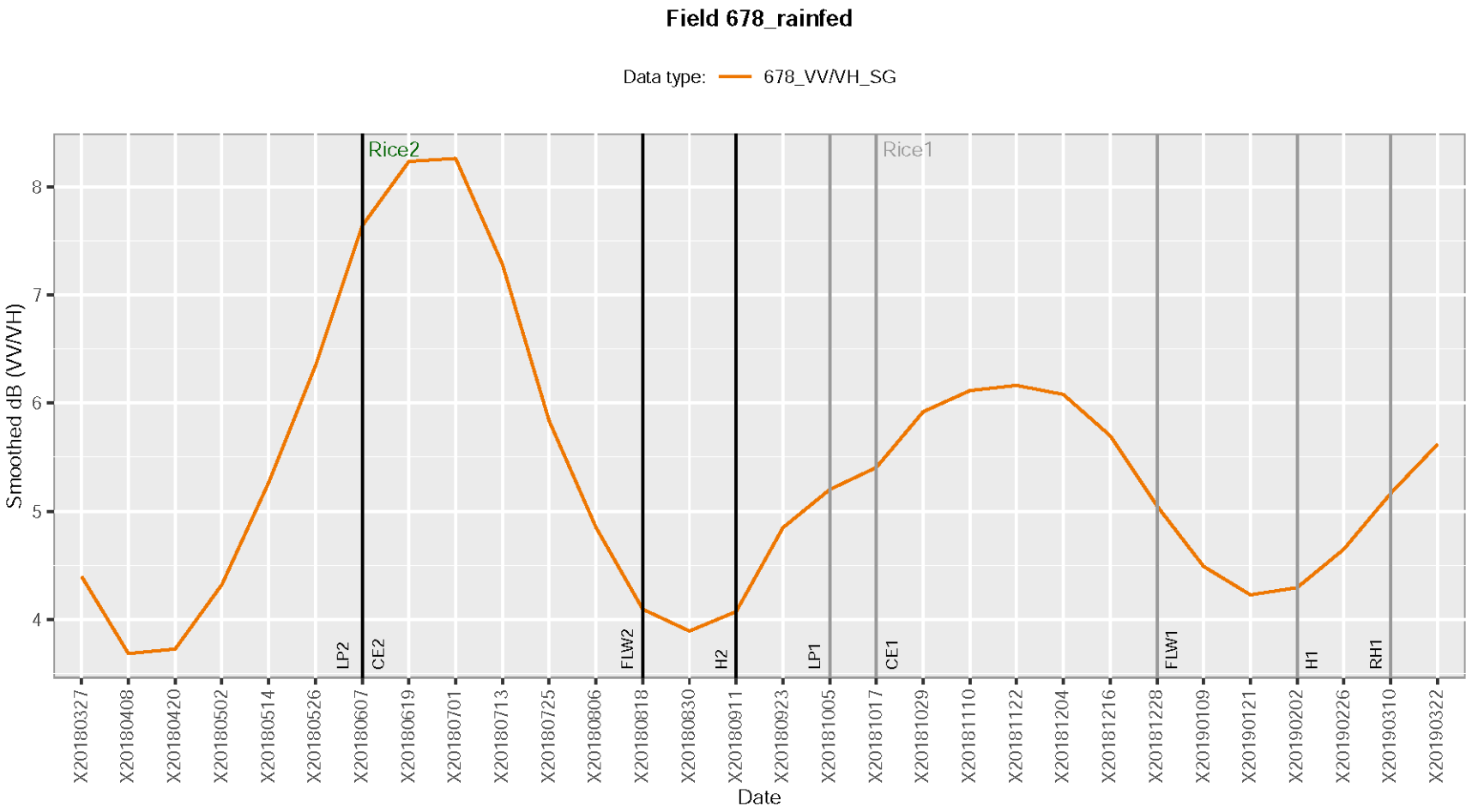
Field 678_rainfed
Data type: 678_VV/VH_SG
Rice2
Rice1
Smoothed dB (VV/VH)
8
7
6
5
4
LP2
CE2
FLW2
H2
LP1
CE1
FLW1
H1
RH1
X20180327
X20180408
X20180420
X20180502
X20180514
X20180526
X20180607
X20180619
X20180701
X20180713
X20180725
X20180806
X20180818
X20180830
X20180911
X20180923
X20181005
X20181017
X20181029
X20181110
X20181122
X20181204
X20181216
X20181228
X20190109
X20190121
X20190202
X20190226
X20190310
X20190322
Date

Series from Lund University

Department of Physical Geography and Ecosystem Science

Master Thesis in Geographical Information Science

1. *Anthony Lawther:* The application of GIS-based binary logistic regression for slope failure susceptibility mapping in the Western Grampian Mountains, Scotland (2008).
2. *Rickard Hansen:* Daily mobility in Grenoble Metropolitan Region, France. Applied GIS methods in time geographical research (2008).
3. *Emil Bayramov:* Environmental monitoring of bio-restoration activities using GIS and Remote Sensing (2009).
4. *Rafael Villarreal Pacheco:* Applications of Geographic Information Systems as an analytical and visualization tool for mass real estate valuation: a case study of Fontibon District, Bogota, Columbia (2009).
5. *Siri Oestreich Waage:* a case study of route solving for oversized transport: The use of GIS functionalities in transport of transformers, as part of maintaining a reliable power infrastructure (2010).
6. *Edgar Pimiento:* Shallow landslide susceptibility – Modelling and validation (2010).
7. *Martina Schäfer:* Near real-time mapping of floodwater mosquito breeding sites using aerial photographs (2010).
8. *August Pieter van Waarden-Nagel:* Land use evaluation to assess the outcome of the programme of rehabilitation measures for the river Rhine in the Netherlands (2010).
9. *Samira Muhammad:* Development and implementation of air quality data mart for Ontario, Canada: A case study of air quality in Ontario using OLAP tool. (2010).
10. *Fredros Oketch Okumu*: Using remotely sensed data to explore spatial and temporal relationships between photosynthetic productivity of vegetation and malaria transmission intensities in selected parts of Africa (2011).
11. *Svajunas Plunge:* Advanced decision support methods for solving diffuse water pollution problems (2011).
12. *Jonathan Higgins:* Monitoring urban growth in greater Lagos: A case study using GIS to monitor the urban growth of Lagos 1990 - 2008 and produce future growth prospects for the city (2011).

13. *Mårten Karlberg:* Mobile Map Client API: Design and Implementation for Android (2011).

14. *Jeanette McBride:* Mapping Chicago area urban tree canopy using color infrared imagery (2011).

15. *Andrew Farina:* Exploring the relationship between land surface temperature and vegetation abundance for urban heat island mitigation in Seville, Spain (2011).

16. *David Kanyari*: Nairobi City Journey Planner: An online and a Mobile Application (2011).

17. *Laura V. Drews:* Multi-criteria GIS analysis for siting of small wind power plants - A case study from Berlin (2012).

18. *Qaisar Nadeem:* Best living neighborhood in the city - A GIS based multi criteria evaluation of ArRiyadh City (2012).

19. *Ahmed Mohamed El Saeid Mustafa:* Development of a photo voltaic building rooftop integration analysis tool for GIS for Dokki District, Cairo, Egypt (2012).

20. *Daniel Patrick Taylor*: Eastern Oyster Aquaculture: Estuarine Remediation via Site Suitability and Spatially Explicit Carrying Capacity Modeling in Virginia's Chesapeake Bay (2013).

21. *Angeleta Oveta Wilson:* A Participatory GIS approach to *unearthing* Manchester's Cultural Heritage '*gold mine'* (2013).

22. *Ola Svensson:* Visibility and Tholos Tombs in the Messenian Landscape: A Comparative Case Study of the Pylian Hinterlands and the Soulima Valley (2013).

23. *Monika Ogden:* Land use impact on water quality in two river systems in South Africa (2013).

24. *Stefan Rova:* A GIS based approach assessing phosphorus load impact on Lake Flaten in Salem, Sweden (2013).

25. *Yann Buhot:* Analysis of the history of landscape changes over a period of 200 years. How can we predict past landscape pattern scenario and the impact on habitat diversity? (2013).

26. *Christina Fotiou:* Evaluating habitat suitability and spectral heterogeneity models to predict weed species presence (2014).

27. *Inese Linuza:* Accuracy Assessment in Glacier Change Analysis (2014).

28. *Agnieszka Griffin:* Domestic energy consumption and social living standards: a GIS analysis within the Greater London Authority area (2014).

29. *Brynja Guðmundsdóttir:* Detection of potential arable land with remote sensing and GIS - A Case Study for Kjósarhreppur (2014).

30. *Oleksandr Nekrasov:* Processing of MODIS Vegetation Indices for analysis of agricultural droughts in the southern Ukraine between the years 2000-2012 (2014).

31. *Sarah Tressel:* Recommendations for a polar Earth science portal in the context of Arctic Spatial Data Infrastructure (2014).

32. *Caroline Gevaert:* Combining Hyperspectral UAV and Multispectral Formosat-2 Imagery for Precision Agriculture Applications (2014).

33. *Salem Jamal-Uddeen:* Using GeoTools to implement the multi-criteria evaluation analysis - weighted linear combination model (2014).

34. *Samanah Seyedi-Shandiz:* Schematic representation of geographical railway network at the Swedish Transport Administration (2014).

35. *Kazi Masel Ullah:* Urban Land-use planning using Geographical Information System and analytical hierarchy process: case study Dhaka City (2014).

36. *Alexia Chang-Wailing Spitteler:* Development of a web application based on MCDA and GIS for the decision support of river and floodplain rehabilitation projects (2014).

37. *Alessandro De Martino:* Geographic accessibility analysis and evaluation of potential changes to the public transportation system in the City of Milan (2014).

38. *Alireza Mollasalehi:* GIS Based Modelling for Fuel Reduction Using Controlled Burn in Australia. Case Study: Logan City, QLD (2015).

39. *Negin A. Sanati:* Chronic Kidney Disease Mortality in Costa Rica; Geographical Distribution, Spatial Analysis and Non-traditional Risk Factors (2015).

40. *Karen McIntyre:* Benthic mapping of the Bluefields Bay fish sanctuary, Jamaica (2015).

41. *Kees van Duijvendijk:* Feasibility of a low-cost weather sensor network for agricultural purposes: A preliminary assessment (2015).

42. *Sebastian Andersson Hylander:* Evaluation of cultural ecosystem services using GIS (2015).

43. *Deborah Bowyer:* Measuring Urban Growth, Urban Form and Accessibility as Indicators of Urban Sprawl in Hamilton, New Zealand (2015).

44. *Stefan Arvidsson:* Relationship between tree species composition and phenology extracted from satellite data in Swedish forests (2015).

45. *Damián Giménez Cruz*: GIS-based optimal localisation of beekeeping in rural Kenya (2016).

46. *Alejandra Narváez Vallejo:* Can the introduction of the topographic indices in LPJ-GUESS improve the spatial representation of environmental variables? (2016).

47. *Anna Lundgren:* Development of a method for mapping the highest coastline in Sweden using breaklines extracted from high resolution digital elevation models (2016).

48. *Oluwatomi Esther Adejoro:* Does location also matter? A spatial analysis of social achievements of young South Australians (2016).

49. *Hristo Dobrev Tomov:* Automated temporal NDVI analysis over the Middle East for the period 1982 - 2010 (2016).

50. *Vincent Muller:* Impact of Security Context on Mobile Clinic Activities A GIS Multi Criteria Evaluation based on an MSF Humanitarian Mission in Cameroon (2016).

51. *Gezahagn Negash Seboka:* Spatial Assessment of NDVI as an Indicator of Desertification in Ethiopia using Remote Sensing and GIS (2016).

52. *Holly Buhler:* Evaluation of Interfacility Medical Transport Journey Times in Southeastern British Columbia. (2016).

53. *Lars Ole Grottenberg*: Assessing the ability to share spatial data between emergency management organisations in the High North (2016).

54. *Sean Grant:* The Right Tree in the Right Place: Using GIS to Maximize the Net Benefits from Urban Forests (2016).

55. *Irshad Jamal:* Multi-Criteria GIS Analysis for School Site Selection in Gorno-Badakhshan Autonomous Oblast, Tajikistan (2016).

56. *Fulgencio Sanmartín:* Wisdom-volkano: A novel tool based on open GIS and time-series visualization to analyse and share volcanic data (2016).

57. *Nezha Acil:* Remote sensing-based monitoring of snow cover dynamics and its influence on vegetation growth in the Middle Atlas Mountains (2016).

58. *Julia Hjalmarsson:* A Weighty Issue: Estimation of Fire Size with Geographically Weighted Logistic Regression (2016).

59. *Mathewos Tamiru Amato:* Using multi-criteria evaluation and GIS for chronic food and nutrition insecurity indicators analysis in Ethiopia (2016).

60. *Karim Alaa El Din Mohamed Soliman El Attar:* Bicycling Suitability in Downtown, Cairo, Egypt (2016).

61. *Gilbert Akol Echelai:* Asset Management: Integrating GIS as a Decision Support Tool in Meter Management in National Water and Sewerage Corporation (2016).

62. *Terje Slinning:* Analytic comparison of multibeam echo soundings (2016).

63. *Gréta Hlín Sveinsdóttir:* GIS-based MCDA for decision support: A framework for wind farm siting in Iceland (2017).

64. *Jonas Sjögren:* Consequences of a flood in Kristianstad, Sweden: A GIS-based analysis of impacts on important societal functions (2017).

65. *Nadine Raska:* 3D geologic subsurface modelling within the Mackenzie Plain, Northwest Territories, Canada (2017).

66. *Panagiotis Symeonidis*: Study of spatial and temporal variation of atmospheric optical parameters and their relation with PM 2.5 concentration over Europe using GIS technologies (2017).

67. *Michaela Bobeck:* A GIS-based Multi-Criteria Decision Analysis of Wind Farm Site Suitability in New South Wales, Australia, from a Sustainable Development Perspective (2017).

68. *Raghdaa Eissa*: Developing a GIS Model for the Assessment of Outdoor Recreational Facilities in New Cities Case Study: Tenth of Ramadan City, Egypt (2017).

69. *Zahra Khais Shahid*: Biofuel plantations and isoprene emissions in Svea and Götaland (2017).

70. *Mirza Amir Liaquat Baig*: Using geographical information systems in epidemiology: Mapping and analyzing occurrence of diarrhea in urban - residential area of Islamabad, Pakistan (2017).

71. *Joakim Jörwall*: Quantitative model of Present and Future well-being in the EU-28: A spatial Multi-Criteria Evaluation of socioeconomic and climatic comfort factors (2017).

72. *Elin Haettner*: Energy Poverty in the Dublin Region: Modelling Geographies of Risk (2017).

73. *Harry Eriksson*: Geochemistry of stream plants and its statistical relations to soil- and bedrock geology, slope directions and till geochemistry. A GIS-analysis of small catchments in northern Sweden (2017).

74. *Daniel Gardevärn:* PPGIS and Public meetings – An evaluation of public participation methods for urban planning (2017).

75. *Kim Friberg:* Sensitivity Analysis and Calibration of Multi Energy Balance Land Surface Model Parameters (2017).

76. *Viktor Svanerud:* Taking the bus to the park? A study of accessibility to green areas in Gothenburg through different modes of transport (2017).

77. *Lisa-Gaye Greene*: Deadly Designs: The Impact of Road Design on Road Crash Patterns along Jamaica's North Coast Highway (2017).

78. *Katarina Jemec Parker*: Spatial and temporal analysis of fecal indicator bacteria concentrations in beach water in San Diego, California (2017).

79. *Angela Kabiru*: An Exploratory Study of Middle Stone Age and Later Stone Age Site Locations in Kenya's Central Rift Valley Using Landscape Analysis: A GIS Approach (2017).

80. *Kristean Björkmann*: Subjective Well-Being and Environment: A GIS-Based Analysis (2018).

81. *Williams Erhunmonmen Ojo*: Measuring spatial accessibility to healthcare for people living with HIV-AIDS in southern Nigeria (2018).

82. *Daniel Assefa*: Developing Data Extraction and Dynamic Data Visualization (Styling) Modules for Web GIS Risk Assessment System (WGRAS). (2018).

83. *Adela Nistora*: Inundation scenarios in a changing climate: assessing potential impacts of sea-level rise on the coast of South-East England (2018).

84. *Marc Seliger*: Thirsty landscapes - Investigating growing irrigation water consumption and potential conservation measures within Utah's largest master-planned community: Daybreak (2018).

85. *Luka Jovičić*: Spatial Data Harmonisation in Regional Context in Accordance with INSPIRE Implementing Rules (2018).

86. *Christina Kourdounouli*: Analysis of Urban Ecosystem Condition Indicators for the Large Urban Zones and City Cores in EU (2018).

87. *Jeremy Azzopardi*: Effect of distance measures and feature representations on distance-based accessibility measures (2018).

88. *Patrick Kabatha*: An open source web GIS tool for analysis and visualization of elephant GPS telemetry data, alongside environmental and anthropogenic variables (2018).

89. *Richard Alphonce Giliba*: Effects of Climate Change on Potential Geographical Distribution of Prunus africana (African cherry) in the Eastern Arc Mountain Forests of Tanzania (2018).

90. *Eiður Kristinn Eiðsson*: Transformation and linking of authoritative multi-scale geodata for the Semantic Web: A case study of Swedish national building data sets (2018).

91. *Niamh Harty*: HOP!: a PGIS and citizen science approach to monitoring the condition of upland paths (2018).

92. *José Estuardo Jara Alvear*: Solar photovoltaic potential to complement hydropower in Ecuador: A GIS-based framework of analysis (2018).

93. *Brendan O'Neill*: Multicriteria Site Suitability for Algal Biofuel Production Facilities (2018).

94. *Roman Spataru*: Spatial-temporal GIS analysis in public health – a case study of polio disease (2018).

95. *Alicja Miodońska*: Assessing evolution of ice caps in Suðurland, Iceland, in years 1986 - 2014, using multispectral satellite imagery (2019).

96. *Dennis Lindell Schettini*: A Spatial Analysis of Homicide Crime's Distribution and Association with Deprivation in Stockholm Between 2010-2017 (2019).

97. *Damiano Vesentini*: The Po Delta Biosphere Reserve: Management challenges and priorities deriving from anthropogenic pressure and sea level rise (2019).

98. *Emilie Arnesten*: Impacts of future sea level rise and high water on roads, railways and environmental objects: a GIS analysis of the potential effects of increasing sea levels and highest projected high water in Scania, Sweden (2019).

99. *Syed Muhammad Amir Raza*: Comparison of geospatial support in RDF stores: Evaluation for ICOS Carbon Portal metadata (2019).

100. *Hemin Tofiq*: Investigating the accuracy of Digital Elevation Models from UAV images in areas with low contrast: A sandy beach as a case study (2019).

101. *Evangelos Vafeiadis*: Exploring the distribution of accessibility by public transport using spatial analysis. A case study for retail concentrations and public hospitals in Athens (2019).

102. *Milan Sekulic*: Multi-Criteria GIS modelling for optimal alignment of roadway by-passes in the Tlokweng Planning Area, Botswana (2019).

103. *Ingrid Piirisaar*: A multi-criteria GIS analysis for siting of utility-scale photovoltaic solar plants in county Kilkenny, Ireland (2019).

104. *Nigel Fox*: Plant phenology and climate change: possible effect on the onset of various wild plant species' first flowering day in the UK (2019).

105. *Gunnar Hesch*: Linking conflict events and cropland development in Afghanistan, 2001 to 2011, using MODIS land cover data and Uppsala Conflict Data Programme (2019).

106. *Elijah Njoku*: Analysis of spatial-temporal pattern of Land Surface Temperature (LST) due to NDVI and elevation in Ilorin, Nigeria (2019).

107. *Katalin Bunyevácz*: Development of a GIS methodology to evaluate informal urban green areas for inclusion in a community governance program (2019).

108. *Paul dos Santos*: Automating synthetic trip data generation for an agent-based simulation of urban mobility (2019).

109. *Robert O' Dwyer*: Land cover changes in Southern Sweden from the mid-Holocene to present day: Insights for ecosystem service assessments (2019).

110. *Daniel Klingmyr*: Global scale patterns and trends in tropospheric NO2 concentrations (2019).

111. *Marwa Farouk Elkabbany*: Sea Level Rise Vulnerability Assessment for Abu Dhabi, United Arab Emirates (2019).

112. *Jip Jan van Zoonen*: Aspects of Error Quantification and Evaluation in Digital Elevation Models for Glacier Surfaces (2020).

113. *Georgios Efthymiou*: The use of bicycles in a mid-sized city – benefits and obstacles identified using a questionnaire and GIS (2020).

114. *Haruna Olayiwola Jimoh*: Assessment of Urban Sprawl in MOWE/IBAFO Axis of Ogun State using GIS Capabilities (2020).

115. *Nikolaos Barmpas Zachariadis*: Development of an iOS, Augmented Reality for disaster management (2020).

116. *Ida Storm*: ICOS Atmospheric Stations: Spatial Characterization of CO2 Footprint Areas and Evaluating the Uncertainties of Modelled CO2 Concentrations (2020).

117. *Alon Zuta*: Evaluation of water stress mapping methods in vineyards using airborne thermal imaging (2020).

118. *Marcus Eriksson*: Evaluating structural landscape development in the municipality Upplands-Bro, using landscape metrics indices (2020).

119. *Ane Rahbek Vierø*: Connectivity for Cyclists? A Network Analysis of Copenhagen's Bike Lanes (2020).

120. *Cecilia Baggini*: Changes in habitat suitability for three declining Anatidae species in saltmarshes on the Mersey estuary, North-West England (2020).

121. *Bakrad Balabanian*: Transportation and Its Effect on Student Performance (2020).

122. *Ali Al Farid*: Knowledge and Data Driven Approaches for Hydrocarbon Microseepage Characterizations: An Application of Satellite Remote Sensing (2020).

123. *Bartlomiej Kolodziejczyk*: Distribution Modelling of Gene Drive-Modified Mosquitoes and Their Effects on Wild Populations (2020).

124. *Alexis Cazorla*: Decreasing organic nitrogen concentrations in European water bodies - links to organic carbon trends and land cover (2020).

125. *Kharid Mwakoba*: Remote sensing analysis of land cover/use conditions of community-based wildlife conservation areas in Tanzania (2021).

126. *Chinatsu Endo*: Remote Sensing Based Pre-Season Yellow Rust Early Warning in Oromia, Ethiopia (2021).

127. *Berit Mohr*: Using remote sensing and land abandonment as a proxy for long-term human out-migration. A Case Study: Al-Hassakeh Governorate, Syria (2021).

128. *Kanchana Nirmali Bandaranayake*: Considering future precipitation in delineation locations for water storage systems - Case study Sri Lanka (2021).

129. *Emma Bylund*: Dynamics of net primary production and food availability in the aftermath of the 2004 and 2007 desert locust outbreaks in Niger and Yemen (2021).

130. *Shawn Pace*: Urban infrastructure inundation risk from permanent sea-level rise scenarios in London (UK), Bangkok (Thailand) and Mumbai (India): A comparative analysis (2021).

131. *Oskar Evert Johansson*: The hydrodynamic impacts of Estuarine Oyster reefs, and the application of drone technology to this study (2021).

132. *Pritam Kumarsingh*: A Case Study to develop and test GIS/SDSS methods to assess the production capacity of a Cocoa Site in Trinidad and Tobago (2021).

133. *Muhammad Imran Khan*: Property Tax Mapping and Assessment using GIS (2021).

134. *Domna Kanari*: Mining geosocial data from Flickr to explore tourism patterns: The case study of Athens (2021).

135. *Mona Tykesson Klubien*: Livestock-MRSA in Danish pig farms (2021).

136. *Ove Njøten*: Comparing radar satellites. Use of Sentinel-1 leads to an increase in oil spill alerts in Norwegian waters (2021).

137. *Panagiotis Patrinos*: Change of heating fuel consumption patterns produced by the economic crisis in Greece (2021).

138. *Lukasz Langowski*: Assessing the suitability of using Sentinel-1A SAR multi-temporal imagery to detect fallow periods between rice crops (2021).